



**University of
Sheffield**

**THE TARGETED DELIVERY OF G3 PEPTIDE DRUG
CONJUGATES IN PROSTATE CANCER**

by

Gisela Martinez Andrade

A thesis submitted in partial fulfilment of the requirements for the degree of
Doctor of Philosophy

The University of Sheffield
School of Biosciences
PhD Biomedical Science

August 2023

*To my dear son, Ricardo
and in memory of my beloved sister,
Lucia*

"Science is the poetry of reality"

-Richard Dawkins

"Nothing in life is to be feared; it is only to be understood"

-Marie Curie

Declaration

I, the author, Gisela Martinez Andrade, confirm that the Thesis is my own work. I am aware of the University's Guidance on the Use of Unfair Means (www.sheffield.ac.uk/ssid/unfair-means). This work has not been previously been presented for an award at this, or any other, university.

Acknowledgements

My PhD voyage has been a unique, revealing, and occasionally overwhelming experience. I am extremely grateful to have had the opportunity to carry out my research project at the University of Sheffield, for the possibility to create new knowledge, for all the experiences that have shaped me, and for all the tools and skills learned along the way. And above all, I am very grateful to all the people who one way or another, have played a part in the completion of my doctorate.

First of all, I want to thank my supervisor, Steve Brown, for his valuable guidance, encouragement, support, and shared knowledge. For granting me the opportunity to perform my research in his laboratory, for his patience and empathy, for his input of creative research ideas and his always full of energy and positive attitude.

I want to thank my advisors, Anestis Tsakiridis, Fredericus J Van, and Prof. Steve Winder, for their useful advice, constructive feedback and critical analysis that broadened my way of viewing my project.

To Dr Simon Turega and Dr Phillip Lane of Sheffield Hallam University for their collaboration with the production of the peptide drug conjugates.

To Chun Guo for his kind support, for all his technical advice and for lending me his equipment and reagents.

To Elena Rainero for sharing her expertise in colocalization analysis and endocytosis.

To Andrew Metcalfe for allowing me to use the Perak Laboratories and the devices and supplies for western blots.

Also, very grateful to Deepa Bliss for her incredible help, time and technical advice.

To all my lab colleagues, for their help and encouragement. To those who were there at the beginning and to those who were at the end of my doctorate; to Roja, Lucie N' Koy, Anas, Keivalin, Christian, and Mac.

To all my network of support, to all my friends in Sheffield and Mexico, especially to Ingrid Saldaña and Regina Solis for always being there for me, for all those long-night talks, encouragement and advices.

To Conacyt for providing the funding for most of my tuition fee and partial maintenance, and to the University of Sheffield for their additional economical support.

Special gratitude to my older brother, Andrés Martínez for his immense financial support during my doctorate, for always believing in me and being an example to follow.

To all my dear family for being my core and for their unconditional love. To my parents who always gave me the best they could and for their immense help with the care of my son, when I started my studies.

To my younger brother Samuel Martínez, for his presence, his listening and openness, words of motivation, and his contribution proofreading some of the sections of my thesis.

To my sister Lucia, that even no longer with us, for reminding me to be more present, to push myself and to enjoy the beauty and the struggle of every experience.

To my partner, Kyle Fixter for being my life companion, for his love, emotional support and time shared, for proofreading parts of my thesis and for his words of motivation and affirmation in times of greatest stress and frustration.

To Sue, Dale and Katya, for their constant support, advices and beautiful shared moments.

And finally to my dear son, Ricardo, for being my greatest strength and pride. For his massive help on those writing days, for his love and moments spend. For existing, being himself, and part of my life.

Abstract

Prostate cancer (PCa) remains a leading global health issue for men, with androgen deprivation therapy and chemotherapy or androgen receptor signalling inhibitors being the main treatments. However, these treatments show peripheral toxicity or resistance. Although therapeutic strategies have arisen in the last decade, there is still a necessity to improve PCa treatments due to limited overall survival. Peptide drug conjugates (PDC) that can selectively deliver drugs to cancer cells using peptides, while reducing the cytotoxicity to healthy cells, represent a valuable option. Due to its cell selectivity for cancer cells and ease of drug conjugation, the cationic G3 peptide is a suitable choice to generate PDC. This thesis aimed to explore the therapeutic capacity of G3 as part of PDC in PCa.

This thesis demonstrates the PCa cell specificity and enhanced uptake of G3. The peptide was non-toxic to PNT2 cells, but had a high-dose-dependent cytotoxic impact in PCa cells. The subcellular localization of G3 was situated in endolysosomal compartments. Our RNA interference (RNAi) and colocalization data suggest that G3 is internalized through scavenger receptors-mediated (SR-F1, SR-F2, and SR-B1) endocytosis, and to our knowledge this is the first time that SR-F1 and SR-F2 have been identified in the entry of CPP. The protein expression analysis corroborated the RNAi KD of target SR genes. G3 PDC coupled with LSD1 inhibitors resulted in PDC-2 and PDC-4 producing cell impairment at low doses. It appears that the PDC escape the endosomes releasing the drugs, since PDC-2 and PDC-4 show signs of LSD1 inhibition via the accumulation of H3K4me2 marks. G3 was successful in delivering functional siRNAs, however it was less efficient than commercial transfection reagents. In conclusion, our research provides the first evidence of the therapeutic delivering capacity of G3, as a PDC, since it shows efficient LSD1-epigenetic inhibition in PCa.

Table of contents

Portrait	1
Declaration	4
Acknowledgements	5
Abstract	7
Table of contents	8
List of figures	12
List of tables	14
Abbreviations	15
CHAPTER 1	23
1. BACKGROUND	23
1.1 Prostate function, structure and cellular components	23
1.2 Prostate cancer: symptoms, risk factors, mortality and incidence	25
1.3 Prostate cancer development	28
1.4 Prostate cancer diagnosis	30
1.5 Genetic landscape in prostate cancer	31
1.6 Current treatments for prostate cancer	36
1.7 Peptide drug conjugates	45
1.7.1 Targeting peptides	49
1.7.2 Linker	50
1.7.3 Payload	51
1.7.4 Current approved PDC for cancer therapy	54
1.8 G3 or G(IKK)3I-NH2 peptide	54
1.9 Project rationale	56
CHAPTER 2	59
2. MATERIALS & METHODS	59
2.1 Cell culture	59
2.1.1 Cell lines	59
2.1.2 Passaging	59
2.1.3 Cryopreservation protocol	60
2.1.4 Thawing protocol	60
2.2 Seeding multi-well plates for High Content Screening	61
2.3 Fixing and staining procedure	61
2.4 High Content Screening (HCS)	62
2.5 High content custom module analysis	62

2.6	Peptide internalization assay.....	63
2.7	Anti-proliferative activity	64
2.8	Prostate cancer spheroids.....	64
2.9	Immunolabeling of endosomal compartments.....	65
2.10	Confocal Microscopy	65
2.10.1	Samples preparation for high resolution imaging	66
2.11	Cell selectivity validation analysis	66
2.12	Co-culture assay	67
2.13	Colocalization analysis of endosomal markers	67
2.14	Macropinocytosis inhibition	69
2.15	Silencing of gene expression using siRNAs.....	69
2.16	Western Blot for siRNA knockdown validation	73
2.16.1	Buffers and solutions.....	73
2.16.2	Protein extraction of whole cell lysates	73
2.16.3	Protein quantification.....	74
2.16.4	Samples preparation	75
2.16.5	Gel run.....	75
2.16.6	Blot transfer run.....	76
2.16.7	Ponceau staining and blocking membrane	76
2.16.8	Antibody probing	77
2.16.9	Blot imaging.....	77
2.16.10	Normalization and semi-quantification	78
2.17	Colocalization analysis of scavenger receptors	78
2.18	Peptide drug conjugates analysis in prostate cancer	78
2.19	Cell viability assay of PDC	80
2.20	Hydrogen peroxide assay.....	80
2.21	Immunolabelling of histone demethylation marks	81
2.22	H3K4me2 protein expression analysis	81
2.22.1	Histones acid extraction	82
2.22.2	Histones sample preparation.....	83
2.22.3	Western Blot of histone marks	83
2.23	LSD1 siRNA knockdown	83
2.24	Targeted delivery of siRNAs using G3 peptide	84
2.25	Statistical Analysis.....	85
CHAPTER 3.....		86
3.	G3 CELL SELECTIVITY & SUBCELLULAR DISTRIBUTION	86
3.1	Introduction: CPPs and PDCs	86

3.1.1	Cell-penetrating peptides	87
3.1.2	Internalization mechanisms of CPPs.....	89
3.1.3	Key factors in the cellular uptake of drug delivery peptides	94
3.2	Results	97
3.2.1	G3 uptake in prostate cancer vs non-cancer prostate cells	97
3.2.2	Cytotoxic analysis.....	101
3.2.3	Co-culture assay	107
3.2.4	Colocalization analysis and endosomal distribution	109
3.2.5	Macropinocytosis Inhibition	120
3.3	Discussion	123
3.3.1	Does G3 have prostate cancer cell selectivity?.....	123
3.3.2	Does G3 exhibit a cytotoxic effect in prostate cancer cells?	125
3.3.3	Is the subcellular localization of G3 in clathrin-associated compartments?	126
CHAPTER 4.....		130
4.	ROLE OF SCAVENGER RECEPTORS IN THE UPTAKE MECHANISM OF G3..	130
4.1	Introduction.....	130
4.2	Scavenger receptors diversity and classification.....	130
4.2.1	SR Class B	131
4.2.2	SR Class F	134
4.3	Scavenger receptors in prostate cancer.....	137
4.4	Targeted receptors for peptides uptake	141
4.5	Targeting SR with peptides in PCa	143
4.6	Results	144
4.6.1	Endocytic proteins siRNA knockdown.....	144
4.6.2	Scavenger receptor siRNA screen	148
4.6.3	Validation of scavenger receptors	150
4.6.4	Protein expression RNAi knockdown validation	153
4.6.5	SR antibody labelling using HCS	153
4.6.6	SR antibody labelling using WB	163
4.6.7	Colocalization analysis of scavenger receptors and FITC-G3	167
4.7	Discussion	170
4.7.1	Could scavenger receptors be involved in the uptake of G3? Scavenger receptor and G3 internalization: A Possible Connection?.....	171
CHAPTER 5.....		177
5.	PEPTIDE DRUG CONJUGATES USING G3 AND LSD1 INHIBITORS.....	177
5.1	Introduction.....	177
5.2	Peptide drug conjugates against prostate cancer	177
5.3	Understanding LSD1 demethylation of histones and non-histone proteins.....	179

5.4	LSD1 structural components	184
5.5	LSD1 demethylation reaction	185
5.6	LSD1 demethylase-independent activity	186
5.7	Role of LSD1 in prostate cancer	187
5.8	Diversity of LSD1 inhibitors	189
5.9	PDC using G3 and TCP-based LSD1 inhibitors	192
5.10	Results	194
5.10.1	Cell viability assays using G3 conjugates	194
5.10.2	Hydrogen peroxide assay	196
5.10.3	Histone demethylation analysis by HCS	198
5.10.4	Histone demethylation analysis by WB	205
5.10.5	Targeted delivery of siRNAs into prostate cancer cells using G3	210
5.11	Discussion	216
5.11.1	Cellular impairment after LSD1 inhibition	216
5.11.2	The limitations of using hydrogen peroxide assay in PCa cells	217
5.11.3	Does the G3 PDC deliver LSD1 inhibitors in prostate cancer cells?	218
5.11.4	G3 facilitates the delivery of siRNAs into prostate cancer cells	220
CHAPTER 6		222
6.	GENERAL DISCUSSION	222
6.1	Factors contributing to prostate cancer cell selectivity and uptake	224
6.2	Future investigations: Beyond scavenger receptor knockdown in G3 uptake	226
6.3	2D Maximum Intensity Projection: A Reliable Approach for Colocalization?	228
6.4	Avoiding lysosomal degradation and embracing endosomal escape in peptide therapeutics	229
6.5	G3 PDC wider implications & G3 therapeutic applications	231
CHAPTER 7		234
7.	CONCLUSION & FUTURE PERSPECTIVES	234
8.	APPENDICES	237
Appendix A. Analysis of non-specific staining removal in High Content Screening.		237
Appendix B. Optimization of siRNA transfections.		240
Appendix C. Optimization of Western Blots		242
9.	REFERENCES	245

List of figures

Fig.1. Anatomical zones of the prostate.....	23
Fig. 2. Schematic representation of the prostate cell diversity.....	24
Fig. 3. Key risk factors in PCa.....	26
Fig. 4. Spectrum of genetic alterations in PCa development.	32
Fig. 5. Overview of PDC configuration.....	47
Fig. 6. G3 peptide main attributes.....	55
Fig. 7. Colocalization analysis.....	69
Fig. 8. Chemical structure of peptide drug conjugates.....	79
Fig. 9. CPP internalization mechanisms.	89
Fig. 10. FITC-G3 uptake in prostate cancer vs non-cancer prostate cells.	98
Fig. 11. Z-stacks of prostate cancer cells after FITC-G3 treatment.	100
Fig. 12. FITC-G3 uptake at increasing concentrations.	101
Fig. 13. FITC-G3 cell viability analysis in PNT2.....	103
Fig. 14. FITC-G3 cytotoxic analysis in LNCaP.....	104
Fig. 15. FITC-G3 cytotoxic analysis in PC-3.	105
Fig. 16. FITC-G3 internalization in PCa spheroids.	106
Fig. 17. CD44 antibody specificity test.....	108
Fig. 18. Cell selectivity analysis in co-culture system.	108
Fig. 19. Colocalization analysis of FITC-G3 and key markers of endocytosis in LNCaP....	110
Fig. 20. Colocalization analysis of FITC-G3 and key markers of endocytosis in PC-3	111
Fig. 21. Colocalization analysis of FITC-G3 and early markers of endocytosis in LNCaP..	113
Fig. 22. Colocalization analysis of FITC-G3 and early markers of endocytosis PC-3.....	114
Fig. 23. Colocalization analysis of FITC-G3 and late markers of endocytosis LNCaP.	116
Fig. 24. Colocalization analysis of FITC-G3 and late markers of endocytosis in PC-3.	117
Fig. 25. Colocalization analysis of FITC-G3 and LAMP1 in LNCaP.	118
Fig. 26. Colocalization analysis of FITC-G3 and LAMP1 in PC-3.....	119
Fig. 27. Macropinocytosis inhibition analysis in LNCaP.....	121
Fig. 28. Macropinocytosis inhibition analysis in PC-3.	122
Fig. 29. Representation of SR class B and F structure.....	134
Fig. 30. Scavenger receptors involved in prostate cancer.....	137
Fig. 31. Endocytic genes knockdown in LNCaP.	146
Fig. 32. Endocytic genes knockdown in PC-3.....	147
Fig. 33. Scavenger receptors pool knockdown in LNCaP.....	149
Fig. 34. Scavenger receptors pool knockdown in PC-3.....	149
Fig. 35. SR hits knockdown in LNCaP.	151
Fig. 36. SR hits knockdown in PC-3.	152
Fig. 37. MYO5C antibody labelling after siRNA knockdown in LNCaP.....	155
Fig. 38. MYO5C antibody labelling after siRNA knockdown in PC-3.	156
Fig. 39. SR-B1 antibody labelling after siRNA knockdown in LNCaP.....	157
Fig. 40. SR-B1 antibody labelling after siRNA knockdown in PC-3.....	158
Fig. 41. SR-F1 antibody labelling after siRNA knockdown in LNCaP.....	159
Fig. 42. SR-F1 antibody labelling after siRNA knockdown in PC-3.	160
Fig. 43. SR-F2 antibody labelling after siRNA knockdown in LNCaP.....	161
Fig. 44. SR-F2 antibody labelling after siRNA knockdown in PC-3.	162
Fig. 45. Analysis of SR-B1 protein levels and knockdown using siRNA in PCa cells.	164

Fig. 46. Analysis of SR-F1 protein levels and knockdown using siRNA in PCa cells.	165
Fig. 47. Analysis of SR-F2 protein levels and knockdown using siRNA in PCa cells.	166
Fig. 48. Colocalization of scavenger receptors and FITC-G3 in LNCaP.	168
Fig. 49. Colocalization of scavenger receptors and FITC-G3 in PC-3.	169
Fig. 50. Colormap colocalization analysis of scavenger receptors and FITC-G3.	170
Fig. 51. Hypothetical models of SR phenotypes.	176
Fig. 52. LSD1 serves as an epigenetic regulator.	180
Fig. 53. LSD1 structure.	185
Fig. 54. LSD1 demethylation reaction.	186
Fig. 55. Cell viability impairment after TCP treatment.	194
Fig. 56. LNCaP cell viability analysis using PDC.	195
Fig. 57. PC-3 cell viability analysis using PDC.	196
Fig. 58. HRP-coupled assay in LNCaP.	197
Fig. 59. HRP-coupled assay in PC-3.	197
Fig. 60. H3K4me antibody labelling after TCP treatment in LNCaP.	199
Fig. 61. H3K4me2 antibody labelling after TCP treatment in LNCaP.	199
Fig. 62. H3K4me antibody labelling after TCP treatment in PC-3.	200
Fig. 63. H3K4me2 antibody labelling after TCP treatment in PC-3.	201
Fig. 64. H3K4me2 labelling after PDC treatment in LNCaP.	203
Fig. 65. H3K4me2 labelling after PDC treatment in PC-3.	204
Fig. 66. H3K4me2 and HKP linear range detection in LNCaP lysates.	205
Fig. 67. H3K4me2 and HKP linear range detection in PC-3 lysates.	206
Fig. 68. H3K4me2 protein levels after PDC treatment in LNCaP.	208
Fig. 69. H3K4me2 protein levels after PDC treatment in PC-3.	209
Fig. 70. G3 siGLO targeted delivery in LNCaP.	211
Fig. 71. G3 siRNAs targeted delivery in PC-3.	212
Fig. 72. LSD1 siRNA targeted delivery by G3 in LNCaP.	214
Fig. 73. LSD1 siRNA targeted delivery by G3 in PC-3.	215
Fig. 74. G3 PDC inhibition of LSD1 in PCa.	219
Fig. A1. Visual representation of CuME steps for non-specific staining removal.	239
Fig. B1. Red-siGLO transfection optimization in LNCaP.	240
Fig. B2. Red-siGLO transfection optimization in PC-3.	241
Fig. C1. SR-B1 and HKP linear range detection in LNCaP lysates.	242
Fig. C2. SR-B1 and HKP linear range detection in PC-3 lysates.	242
Fig. C3. SR-F1 and HKP linear range detection in LNCaP lysates.	243
Fig. C4. SR-F1 and HKP linear range detection in PC-3 lysates.	243
Fig. C5. SR-F2 and HKP linear range detection in LNCaP lysates.	244
Fig. C6. SR-F2 and HKP linear range detection in PC-3 lysates.	244

List of tables

Table 1. Current therapies for PCa.....	38
Table 2. PDC vs ADC.....	49
Table 3. Endocytosis-related siRNA controls	72
Table 4. Scavenger receptor siRNA library	73
Table 5. BSA standard dilutions	75
Table 6. Peptide drug conjugates using G3 and modified LSD1 inhibitors	80
Table 7. Cancer cell specific peptides	97
Table 8. Peptide-binding Scavenger receptors	143
Table 9. LSD1 non-histone substrate partners	184
Table 10. G3 PDC-2 and PDC-4	218

Abbreviations

ACE2	Angiotensin converting enzyme-2
AcBSA	Acetylated BSA
AcLDL	Acetylated low-density lipoprotein
ADC	Antibody drug conjugates
ADT	Androgen deprivation therapy
AGO2	Argonaute RISC catalytic component 2
AKT	Protein kinase B
AMACR	Alpha-methylacyl-CoA racemase
AOF2	Flavin-containing amine oxidase domain-containing protein 2
AOL	Amine oxidase-like domain
APC	Adenomatous polyposis coli protein
AP-2	Adaptor protein complex 2
AR	Androgen receptor
ARSI	Androgen receptor signalling inhibitors
AR-V7	Androgen receptor splice variant 7
α-SMA	Alpha-smooth muscle actin
ATCC	American Type Culture Collection
ATM	Ataxia-telangiectasia mutated
ATRA	All-trans retinoic acid
bFGF	Basic fibroblast growth factor
BLT-1	Block lipid transport-1
BNCT	Boron neutron capture therapy
BRCA1	Breast cancer gene 1
BRCA2	Breast cancer gene 2
BRD4	Bromodomain-containing protein 4
BSA	Bovine serum albumin
CAPRA	Cancer of the Prostate Risk Assessment
CAV1	Caveolin 1
CBP	cAMP response element-binding protein-binding protein
Cdc42	Cell division cycle 42
CD44	Cluster of differentiation 44
CD44v6	CD44 splice form variant 6
CD44v9	CD44 splice form variant 9
CD13	Cluster of differentiation 13

CD57	Cluster of differentiation 57
CD63	Cluster of differentiation 63
CD81	Cluster of differentiation 81
CENPE	Centrosome-associated protein E
CgA	Chromogranin A
CHEK2	Checkpoint kinase 2
CK5	Cytokeratin 5
CK8	Cytokeratin 8
CK14	Cytokeratin 14
CK18	Cytokeratin 18
CLSM	Confocal laser scanning microscope
CME	Clathrin-mediated endocytosis
CNAs	Copy number alterations
CNS	Central nervous system
CoREST	Co-repressor for element-1-silencing transcription factor
CPP	Cell penetrating peptide
CREB	cAMP-response element-binding protein
cRGD-Lipep-Ms	cRGD-functionalized lipophilic peptide micelles
CRPC	Castration Resistant Prostate Cancer
CRT	Calreticulin
CST	Cell Signalling Technology
CtBP	C-terminal-binding protein 1
CTNNB1	Catenin beta 1
CuAAC	C-terminal using a Cu(I)-catalyzed azide–alkyne 1,3-dipolar cycloaddition
CuME	Custom Module Editor
CvME	Caveolae-mediated endocytosis
CXCR4	C-X-C Motif Chemokine Receptor 4
CXCR6	C-X-C Motif Chemokine Receptor 6
CYP17A1	Cytochrome P450 17A1
DAMPs	Damage-associated molecular patterns
DB	Dodecaborates
DDR	DNA damage response
DF1	DharmaFect1
DHT	Dihydrotestosterone
DMEM	Dulbecco's Modified Eagle's Medium
DMSO	Dimethyl sulfoxide
DNMT1	DNA methyltransferase 1

DNM1	Dynamin 1
dsRNA	Double-stranded RNA
DTPA	Diethylenetriamine pentaacetate
DXT	Dextran
EBRT	External beam radiation therapy
EDB-FN	Extra-domain B fibronectin
EEA1	Early endosomal autoantigen 1
EGF-like	Epidermal growth factor-like
EGFR	Epidermal growth factor receptor
EIPA	Ethyl-isopropyl amiloride
EMT	Epithelial-mesenchymal transition
ERα	Estrogen receptor alpha
ERG	ETS-related gene
ERRα	Estrogen-related receptor α
ESBL	Extended spectrum beta-lactamase resistant
ETS	Erythroblast transformation specific
ETV1	ETS translocation variant 1
E2F1	Transcription factor E2 promoter binding factor 1
FAD	Flavin adenine dinucleotide
FBS	Foetal bovine serum
FBXW7	F-box and WD repeat domain-containing 7
FDA	Food and Drug Administration
FITC	Fluorescein isothiocyanate
FITC-G3	FITC-labelled G(IKK)3I-NH ₂ peptide
FOV	Fields of view
GAPDH	Glyceraldehyde 3-phosphate dehydrogenase
GATA2	GATA-binding factor 2
GEEC	GPI-enriched endosomal compartment
GLP-1	Glucagon-like peptide 1
GnRH	Gonadotropin releasing hormone
GnRH-R	Gonadotropin releasing hormone-receptor
GP2	Granule protein 2
Gp96	Glycoprotein 96
GRPR	Gastrin-releasing peptide receptor
GRP170	Glucose-regulated protein 170
GTP	Guanosine-5'-triphosphate
G3	G(IKK)3I-NH ₂ peptide
HBSS	Hanks Balance Salt Solution

HCL	Hydrochloric acid
HCS	High Content Screening
HCV	Hepatitis C virus
HDAC	Histone deacetylases
HDL	High-density lipoprotein
HER2	Human epidermal growth factor receptor 2
HGPIN	High-grade prostatic intraepithelial neoplasia
HIF-1α	Hypoxia-inducible factor 1-alpha
HKP	Housekeeping protein
HOXB13	Homeobox protein Hox-B13
HRP	Horseradish peroxidase
HSP	Heat shock proteins
HV	High voltage
H2O2	Hydrogen peroxide
H3	Histone 3
H3K4me1	Histone 3 mono methyl lysine 4
H3K4me2	Histone 3 dimethyl lysine 4
H3K9me1	Histone 3 mono lysine 9
H3K9me2	Histone 3 dimethyl lysine 9
H4K20me2	Histone 4 dimethyl lysine 20
IC50	Half-maximal inhibitory concentration
Icorr	Index of correlation
IDCP	Intraductal carcinoma of the prostate
IIC	Cellular integrated intensity
INF	Interferon
KD	Knockdown
KDM1A	Lysine-specific demethylase 1A
Ki	Inhibitory constant
LAMP1	Lysosomal-associated membrane protein 1
LBD	Ligand binding domain
LDL	Low-density lipoprotein
lncRNAs	Long coding RNAs
LPAR6	Lysophosphatidic acid receptor 6
LPS	Lipopolysaccharide
LRP1	Low density lipoprotein receptor-related protein 1
LSD1	Lysine-specific demethylase 1
LSD1n	Neuronal isoform of LSD1
LSD2	Lysine-specific demethylase 2

LTA	Lipoteichoic acid
LMWC	Low molecular weight chitosan
LMWP	Low molecular weight protamine
MAO	Monoamine oxidases
MaIBSA	maleylated BSA
mCRPC	Metastatic castration resistant prostate cancer
mCSPC	Metastatic castration sensitive prostate cancer
MEF2	Myocyte enhancer factor 2
MEFD2	Myocyte enhancer factor 2D
MEGF10	Multiple EGF like domains 10
MHC	Major histocompatibility complex
mHSPC	Metastatic hormonal sensitive prostate cancer
MIP	Maximum intensity projection
MLH1	MutL homolog 1
MMAE	Monomethyl auristatin E
MMP-2	Matrix metalloproteinase 2
MMP-9	Matrix metalloproteinase 9
MMR	Mismatch repair
mpMRI	Multiparametric magnetic resonance imaging
MRSA	Methicillin-resistant Staphylococcus aureus
MSH2	MutS homolog 2
MSH6	MutS homolog 6
MSKCC	Memorial Sloan Kettering Cancer Center
MTA1	Metastatic tumor antigen 1
MWCS	Multi Wavelength Cell Scoring
MYC	MYC proto-oncogene, bHLH transcription factor
MYO5A	Myosin Va
MYO5B	Myosin Vb
MYO5C	Myosin Vc
MYPT1	Myosin phosphatase targeting subunit1
NaN3	Sodium azide
NaOH	Sodium hydroxide
NEPC	Neuroendocrine prostate cancer
NF-κB	Nuclear factor kappa-light-chain-enhancer of activated B
NF1-pDNA	NickFect1-pDNA
NF51-pDNA	NickFect51-pDNA
NGR	Neovasculature-specific peptide
NKX3.1	NK3 Homeobox 1

NLS	Nuclear localization sequences
nmCRPC	non-metastatic castration resistant prostate cancer
nMDP	Normalized mean deviation product
NSE	Neuron-specific enolase
NS3	Non-structural Protein 3
NuRD	Nucleosome remodelling and deacetylase
NURF	Nucleosome remodelling factor
OCT4	Octamer-binding transcription factor 4
OLR1	Oxidized low density lipoprotein receptor 1
oxLDL	Oxidized LDL
PALB2	Partner and localizer of BRCA2
PAMPs	Pathogen-associated molecular patterns
PAP	Prostatic acid phosphatase
PARPi	Poly (ADP ribose) polymerase inhibitors
PARP1/2	Poly (ADP ribose) polymerase 1 or 2
PBS	Phosphate Buffered Saline
PCa	Prostate Cancer
PDC	Peptide drug conjugates
PD-L1	Programmed death-ligand
pDNA	Plasmid DNA
PD-1	Programmed cell death protein 1
PF32-pDNA	PepFect32-pDNA
PIK3C3	Phosphatidylinositol 3-kinase catalytic subunit type 3
PIN	Prostatic intraepithelial neoplasia
PI3K	Phosphoinositide 3-kinase
PI3Kβ	Phosphoinositide 3-kinase β
PI(3)P	Phosphatidylinositol 3-phosphate
PMSF	Phenylmethylsulfonyl fluoride
PMS2	Postmeiotic segregation increased 2
PRR	Pattern recognition receptors
PSMA	Prostate-specific membrane antigen
PSMA-PET	Prostate-specific membrane antigen positron emission tomography
PSA	Prostate-specific antigen
PTEN	Phosphatase and tensin homolog
PXN	Focal adhesion protein paxillin
p62	Autophagy receptor p62
p63	Tumour protein 63
RAB5	Ras-related protein Rab-5

RAB7	Ras-related protein Rab-7
RAB14	Ras-Related Protein Rab-14
RAC	Ras-related C3 botulinum toxin substrate 1
RACK1	Receptor for activated C kinase 1
RANKL	Receptor activator of nuclear factor kappa-B ligand
RB	Running Buffer
RB1	Retinoblastoma tumour suppressor gene 1
RIPA	Radio-Immunoprecipitation Assay
RISC	RNA-induced silencing complex
RNAi	RNA interference
ROI	Region of interest
RT	Room temperature
SD	Standard deviation
SEM	Standard error mean
SERCA	Sarcoplasmic or endoplasmic reticulum calcium adenosine triphosphatase
SETD7	SET domain containing 7, histone lysine methyltransferase
siRNA	Small interference RNA
SNAIL1	Snail family transcriptional repressor 1
SPOP	Speckle type BTB/POZ protein
SR	Scavenger receptor
SR-A1	Scavenger receptor class A member 1
SR-A3	Scavenger receptor class A member 3
SR-A5	Scavenger receptor class A member 5
SR-B1	Scavenger receptor class B member 1
SR-B2	Scavenger receptor class B member 2
SR-B3	Scavenger receptor class B member 3
SR-E1	Scavenger receptor class E member 1
SR-F1	Scavenger receptor class F member 1
SR-F2	Scavenger receptor class F member 2
SR-F3	Scavenger receptor class F member 3
SR-G1	Scavenger receptor class G member 1
SR-H2	Scavenger receptor class H member 2
SR-K1	Scavenger receptor class K member 1
SR-L1	Scavenger receptor class L member 1
STAT3	Signal transducers and activators of transcription 3
SUVs	Small unilamellar vesicles
SV40	Simian Virus 40

SYN	Synaptophysin
TAM	Tumour associated macrophages
TBS	Tris-Buffer Saline
TBST	Tris-Buffer Saline Tween
TCP	Trans-2-phenylcyclopropylamine
TEB	Triton extraction buffer
TEM	Transmission electron microscopy
TF	Transferrin
TLR	Toll-like receptors
TMPRSS2-ERG	Transmembrane protease serine 2:v-ets erythroblastosis virus E26 oncogene homolog
TNF	Tumour necrosis factor
TP53	Tumour protein p53
TRAMP	Transgenic adenocarcinoma of mouse prostate
TRT	Targeted radionuclide therapy
UBB	Ubiquitin B
UBE2C	Ubiquitin conjugating enzyme E2 C
UHRF1	Ubiquitin like with PHD and ring finger domains 1
VEGF	Vascular endothelial growth factor
VEGF-A	Vascular endothelial growth factor A
VIM	Vimentin
WB	Western blot
ZNF217	Zinc finger protein 217

CHAPTER 1

1. BACKGROUND

1.1 Prostate function, structure and cellular components

The prostate is an exocrine male gland that is situated under the bladder. It is responsible for producing a protective liquid that enhances the durability of the sperm and corresponds to approximately the 30% of the seminal fluid (Duncan & Thompson, 2007; Verze et al., 2016). It has an endodermal origin and its development and function are well documented to be governed by androgens (Kellokumpu-Lehtinen & Pelliniemi, 1988; Kellokumpu-Lehtinen et al., 1981). The anatomical structure of the prostate is classified in 4 areas, from which 3 of them have a glandular composition, namely central, peripheral and transitional zones, while the fourth one, called anterior zone is formed mainly of fibrovascular stroma (Figure 1) (McNeal, 1981).

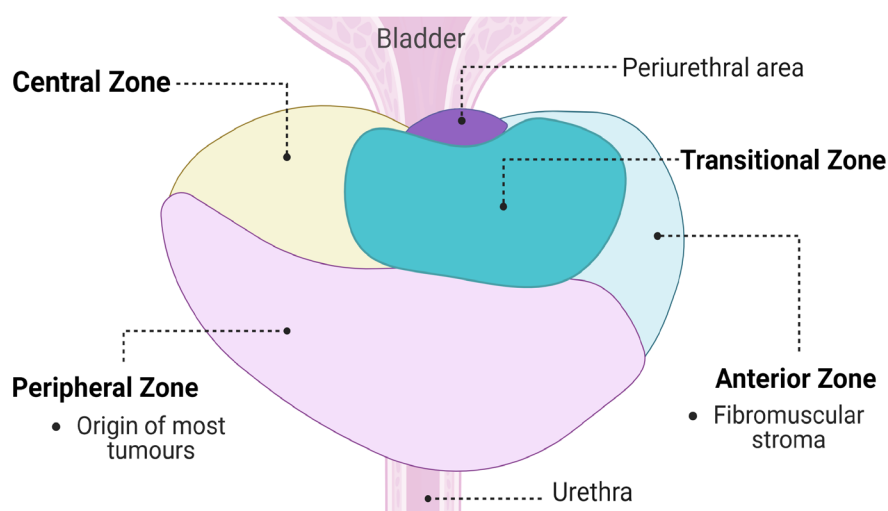


Fig.1. Anatomical zones of the prostate. The gland is divided in 4 zones: central, peripheral, transitional and anterior. PCa initiates usually in the peripheral zone. The periurethral area corresponds to the small glandular section surrounding the urethra. Based on McNeal's anatomical model. Created with BioRender.com

Figure 2 illustrates the 3 cellular lineages present in the prostatic epithelium, namely basal, luminal and a limited quantity of neuroendocrine cells, which is bordered by stroma (McNeal, 1988; Van Leenders & Schalken, 2003). Each cell type is characterized by specific differentiation markers including the presence of specific cytokeratin (CK) or cluster of differentiation (CD) proteins. Basal cells have a high rate of proliferation and are outlined by the expression of tumour protein 63 (p63), CK5, CK14 and CD44 (Bonkhoff et al., 1994b; Liu et al., 1997; Okada et al., 1992; Signoretti et al., 2000; Terpe et al., 1994). Luminal cells have secretory functions and are distinguished by very high amounts of androgen receptor (AR), as well as by the presence of CK8, CK18, prostate-specific antigen (PSA) and CD57 (Liu et al., 1997; Okada et al., 1992). Whereas the luminal layer requires androgens, especially dihydrotestosterone (DHT) to survive, the basal layer is not reliant on them.

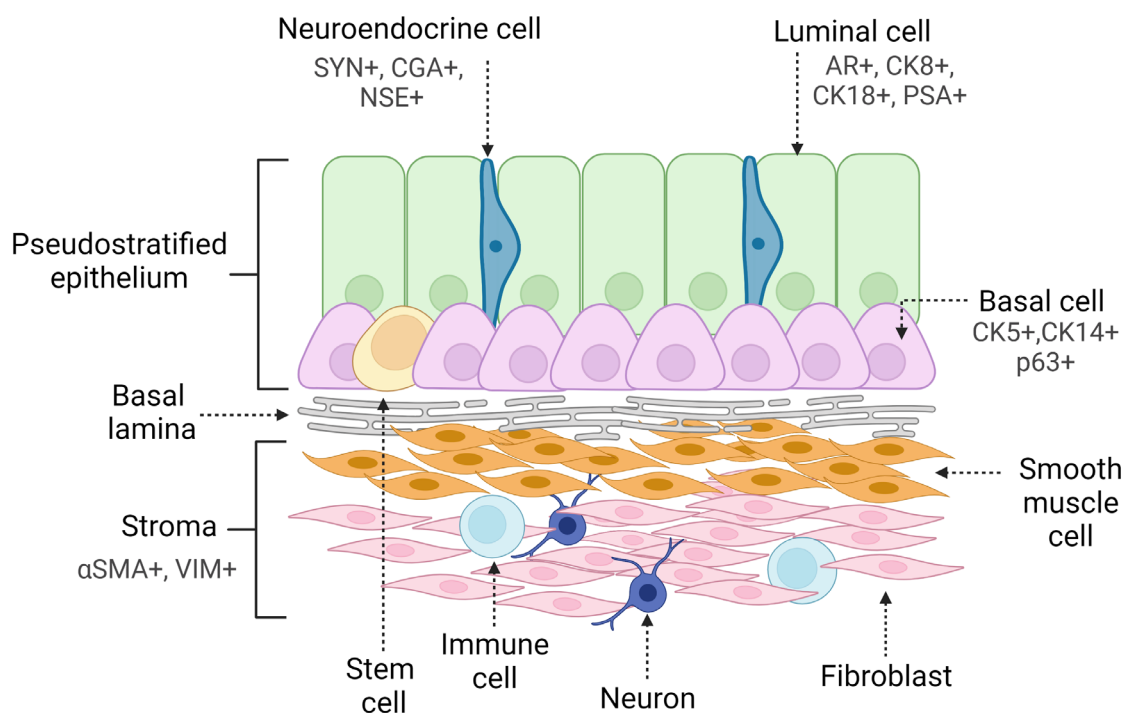


Fig. 2. Schematic representation of the prostate cell diversity. The pseudostratified epithelium is arranged in a luminal layer and a basal layer with neuroendocrine cells scarcely scattered, followed by the basement membrane and the stroma. The biomarkers of each cell type are indicated: tumour protein 63 (p63), cytokeratin 5/8/14/18 (CK5/CK8/CK14/CK18), androgen receptor (AR), prostate-specific antigen (PSA), synaptophysin (SYN), neuron-specific enolase (NSE), chromogranin A (CgA), α -Smooth muscle actin (α -SMA) and vimentin (VIM) Created with BioRender.com

The small population of neuroendocrine cells that constitute approximately 1% of the prostatic epithelium, are located slightly more in the transitional and peripheral zone of the gland, however they are distributed at random sites as single cells in the luminal and basal layers of all zones (Santamaría et al., 2002). Synaptophysin (SYN), neuron-specific enolase (NSE) and chromogranin A (CgA) are the most common differentiation markers for neuroendocrine cells, which are specialized cells with non-proliferative profiles that lack AR and PSA (Bonkhoff et al., 1994a; Huang et al., 2006; Huttner et al., 1991; Krijnen et al., 1993). Among the diversity of peptides that neuroendocrine cells produce, some of them are bombesin, calcitonin, serotonin, somatostatin and vasoactive intestinal peptide (Abdul et al., 1994; Abrahamsson et al., 1987; Aprikian et al., 1997; Di Sant'Agnese & De Mesy Jensen, 1984; Di Sant'Agnese et al., 1989; Gkonos et al., 1996; Shah et al., 1994; Solano et al., 1996).

The cellular diversity in the prostatic stroma comprises large amounts of smooth muscle cells, as well as, vascular cells, fibroblasts, myofibroblasts, nerve cells, lymphocytes, macrophages and neutrophils (Farnsworth, 1999). The cellular diversity within the gland is preserved via a complex dynamic of hormonal regulation, adhesion attachments with the basement membrane and growth factors. It is thought that stromal fibroblasts produce specific paracrine signals that contribute to the development of the duct's patterning, however their main function in the adult prostate is to sustain the ducts (Hayward & Cunha, 2000; Prins & Putz, 2008; Timms, 2008).

1.2 Prostate cancer: symptoms, risk factors, mortality and incidence

After lung cancer, prostate cancer (PCa) has the most global incidence in men, with approximately 1.4 million diagnosed cases, and the fifth place in worldwide mortality rates (Sung et al., 2021). Considering the past 30 years, the urological cancer that has had the most worldwide incidence growth is PCa (Zi et al., 2021). In American male populations, PCa represents the most common diagnosed tumour, and it occupies the second place regarding cancer-associated mortality estimations, accounting for 11% of fatalities per year (Siegel et al., 2023). The UK displays similar trends in prostate cancer-associated death rates, as PCa is the second most frequent reason for male cancer fatalities. Although the incidence of PCa varies among ethnic groups and

geographical locations, it is estimated that annually 1 of 25 men all over the world will have been diagnosed with PCa at some point (Bray et al., 2018; Culp et al., 2020).

Clinically, PCa is a very heterogeneous illness; many individuals manifest an aggressive disease with metastasis, whilst other patients exhibit a reluctant disease with modest progression (Testa et al., 2019). Although the national guidelines often associate urinary symptoms, such as slow urinary flow, frequency, nocturia, and a feeling of incomplete bladder emptying, with PCa, research over the past 30 years does not support this connection (Gnanapragasam et al., 2022). Some studies have even suggested an inverse association between urinary symptoms and the disease (Engel et al., 2020; Collin et al., 2008; Franlund et al., 2012). Recognizing that PCa is frequently asymptomatic in its curable stages is necessary since relying only on these urine symptoms might result in a diagnosis of late-stage disease (Gnanapragasam et al., 2022). Furthermore, the etiology of PCa is not entirely defined, but numerous epidemiological studies have identified some of the most important risk triggers, including age, diet, family history, genetic predisposition, and ethnicity (Figure 3) (Giri & Beebe-Dimmer, 2016; Pernar et al., 2018).

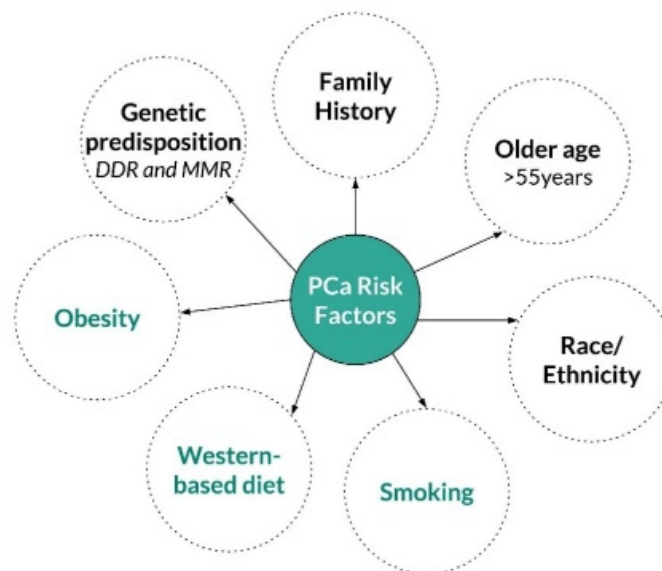


Fig. 3. Key risk factors in PCa. The main components that contribute towards the onset in the disease. Germline mutations in DNA damage response (DDR) and mismatch match repair (MMR) are associated to PCa predisposition.

The occurrence of PCa rises with age independently of living in high-income and low-income countries. Men younger than 40 years have less probability of acquiring PCa, while the incidence rate augments drastically for males older than 55 years (Bray et al., 2018; Ferlay et al., 2015). The intrinsic mechanism for aging's role in PCa predisposition is unresolved, however several theories have been stated, such as impairments in the DNA damage response that are unique to the prostate (Kiviharju-af Hällström et al., 2007).

It has been reported that the highest heritable cancer in male populations is PCa (Rebbeck, 2017). Accordingly, in a Nordic Twin Study of Cancer, they revealed that PCa displayed the largest projection of heritability, accounting for approximately 57% of the total population (Mucci et al., 2016). The chance of acquiring PCa is more for men that have a direct relative who suffers from the disease, the more members in the family are diagnosed, and if relatives are affected before the age of 55 (Barber et al., 2018; Chen et al., 2008; Nelson et al., 2013). Associated-genes of the Lynch syndrome or the hereditary breast and ovarian cancer syndrome, have been correlated to the risk of developing PCa (Bhanji et al., 2021; Dominguez-Valentin et al., 2020; Ren et al., 2019). Precisely, over 160 single nucleotide polymorphisms and mutations in key genes, such as Ataxia-telangiectasia mutated (ATM), breast cancer genes 1 or 2 (BRCA1/2), checkpoint kinase 2 (CHEK2), partner and localizer of BRCA2 (PALB2), and homeobox protein Hox-B13 (HOXB13); as well as genes involved in mismatch repair (MMR) signalling, including postmeiotic segregation increased 2 (PMS2), MutL homolog 1 (MLH1), MutS homolog 2 (MSH2), and MutS homolog 6 (MSH6), have been linked to PCa susceptibility (Daly et al., 2021; Vietri et al., 2021).

According to studies, it has been proposed that at least partly, the differences in PCa incidence and mortality estimates in different geographical territories, is associated with ethnicity and race. It has been identified that Asians present the lowest rate of PCa, exhibiting a 3 fold difference from African-Americans, who have been reported to have the highest disease prevalence (Lloyd et al., 2015). In contrast to European and Asian males, the onset of hereditary PCa is 2 and 3 times greater in cohorts of African Americans (Kohaar et al., 2019; Zhen et al., 2018). However, social variables like racial discrimination and economic disadvantages, as well as coexistent medical

problems, like heart disease; or environmental factors including obesity and diet, may all influence to obtain less favourable results for African American males (Dess et al., 2019; Zhen et al., 2018).

Other non-genetic factors that impact the probability of PCa initiation have been recognized. One of them is obesity, which has been proposed to cause predisposition to lethal PCa, as well as to reduce chances of biochemical efficacy after standard therapies and hence increasing mortality rates (Wilson et al., 2022). Another factor is tobacco smoking, which has been suggested to enhance PCa mortality and relapse; however, it is considered to have a negative association with PCa prevalence (Al-Fayez & El-Metwally, 2023; Darcey & Boyle, 2018; Rohrmann et al., 2013). Western-based diet has also been correlated to PCa emergence (Lin et al., 2015).

1.3 Prostate cancer development

PCa is a complex condition that involves a multifocal and multistep progression. Over 80% of malignant tumours initiate in the peripheral zone, which corresponds to the 70% of the whole organ (Haffner et al., 2009; McNeal, 1981; Zlotta et al., 2013). PCa neoplasms normally develop from prostate gland cells, most typically at late age (Attard et al., 2016). Controversial studies have postulated either basal or luminal cells as tumour-originating cells (Chua et al., 2014; Goldstein et al., 2010; Lee & Shen, 2015). The main drivers of PCa are acquired mutations and environmental influences at a micro and macro scale, that together facilitate the shift from benign to malignant state in the prostatic epithelium, along with a sequence of morphological alterations and intrinsic tumorigenic signalling pathways (He et al., 2022; Sandhu et al., 2021; Sfanos et al., 2018).

It is well-known that the oncogenesis and development of PCa is substantially regulated by AR signalling (Tindall & Lonergan, 2011). PCa induction is hypothesized to be influenced by long-term infection and sustained inflammation, particularly through the production of reactive oxygen species and oxidative stress reaction, that causes harm to the DNA and mutagenesis (Sfanos et al., 2018). In general terms, PCa starts with a malignant transformation of the gland into a condition known as prostatic

intraepithelial neoplasia (PIN), that is characterized by lower quantities of basal cells and excessive amounts of luminal cells (Shen & Abate-Shen, 2010). PIN is categorized as low or high-grade, and the latter develops into an androgen-dependent adenocarcinoma that is initially dormant, but over time gets activated, giving rise to local invasion in the immediate vicinity, due to the absence of the basal cell stratum. From this stage, the oncogenic tumour may either continue enclosed in the prostate or might start proliferating and migrating beyond the gland, ending up in metastasis (Rebello et al., 2021; Testa et al., 2019). The adenocarcinoma can be recognized from the high-grade PIN (HGPIN), by the lack of basal markers, including p63, CK5 and CK14; as well as the expression of the luminal markers CK8 and CK18, and elevated expression of alpha-methylacyl-CoA racemase (AMACR) (Hameed & Humphrey, 2005b, 2005a; Shen & Abate-Shen, 2010).

Some PCa subtypes display diverse morphological characteristics and atypical cytological profiles, that implicate a different clinical relevance than HGPIN (Kweldam, van Leenders, & van der Kwast, 2019). PIN-like carcinoma, ductal adenocarcinoma, and intraductal carcinoma of the prostate (IDCP) are some of these malignant lesions that present a "large gland" pattern (Zhou, 2018). The structural architecture of PIN-like carcinoma is similar to HGPIN as it is lined with pseudostratified cells, however the cells are more closely packed together with flat and tufted patterns, and complete absence of basal cells (Hameed & Humphrey, 2006). Both, ductal adenocarcinoma and IDCP, occur rarely and descend from a shared cellular clone ancestor with adenocarcinoma, and present elevated genetic variability, encompassing DNA damage response (DDR) mutated genes (Chua et al., 2017; Schweizer et al., 2019). Basal cell density is low in ductal adenocarcinomas, which are identified by papillary, cribriform, solid formations, and necrosis, as well as frequent haemorrhage and inflammation as signs of stromal response (Zhou, 2018). Loose or dense cribriform formations or solid tumour deposits sometimes with necrotic core, and sparse surrounding basal cells, are characteristics of IDCP (Zhou, 2018). Neuroendocrine prostate cancer (NEPC) is another severe AR-independent PCa subtype conformed mostly of neuroendocrine cells, that is characterized by the expression of synaptophysin and chromogranin A, as well as presenting a pure small cell carcinoma phenotype and mixed histopathology (Beltran et al., 2014; Parimi et al., 2014). Rare

prostate sarcomas have also been identified, largely constituted by myofibroblasts populations (Sexton et al., 2001; Sohn et al., 2014).

1.4 Prostate cancer diagnosis

There is no specialised single test for diagnosis of PCa, but rather a combination of tools are used. Disease diagnosis initially consists of a digital rectal examination in conjunction with a laboratory test to determine PSA levels (Catalona et al., 1991). Despite PSA amounts in human serum typically fluctuate and augment with age, it has been suggested that there is around 25% chance of developing PCa, if PSA readings range from 4 to 10 ng/mL; and more than 50%, if the levels are higher than 10 ng/mL (Mohler et al., 2010). However, a biopsy of the prostate can provide a stronger diagnosis, followed by grading of the tumour stage using the standardized Gleason Scoring System (Munjal & Leslie, 2023). This useful grading platform employs a system that rates the level of differentiation of the glandular tissue based on histological features and general architecture of the PCa cells (Gleason, 1966).

In addition, nomograms have been developed to improve the assessment of risk severity, taking into account the Gleason score, PSA screening, and tumour staging; for reinforcement on patient advice, especially in ambiguous cases. These nomograms are available at no cost through academic institutions, such as the Cancer of the Prostate Risk Assessment (CAPRA) score, the Partin tables, and the Memorial Sloan Kettering Cancer Center (MSKCC) nomogram (Basourakos et al., 2021; Stephenson et al., 2005; Zhao et al., 2008).

Currently, more individual-tailored strategies are improving the field of diagnosis and management of PCa, encompassing molecular indicators exams and next-generation imaging techniques, such as prostate-specific membrane antigen positron emission tomography (PSMA-PET) scans and multiparametric magnetic resonance imaging (mpMRI) (Kasivisvanathan et al., 2018; Porzycki & Ciszkowicz, 2020). In patients that have had a confirmed diagnosis, further commercial tissue-derived biomarkers tests can be performed, to contribute in treatment stratification and risk classification (Basourakos et al., 2021). The generation of artificial intelligence software to support

and enhance the reliability and quality of PCa scoring already exists, however its employment is not open to the general public (Steiner et al., 2020).

1.5 Genetic landscape in prostate cancer

The genetic component of initial and advanced PCa is vastly diverse. It is characterized by the progressive build-up of somatic mutations throughout a patient's lifespan (Figure 4) (Rebello et al., 2021). The spectrum of genetic alterations involves the dysregulation of several molecular pathways, including those common in other human cancers such as DDR, cell cycle control, cell proliferation, and apoptosis, but also some pathways that are tissue specific, like the androgen signalling and chromatin regulation (Abeshouse et al., 2015; Robinson et al., 2015).

The majority of early genetic modifications are rearrangements of gene organization and copy number alterations (CNAs), while the mutational landscape corresponds to a 3 to 6% of the primary cancer genetic composition (Baca et al., 2013; Ciriello et al., 2013; Hieronymus et al., 2014). A high frequency of gene fusions among AR-regulated promoters and erythroblast transformation specific (ETS) transcription factors, such as ETS-related gene (ERG) and ETS translocation variant 1 (ETV1) genes, is common in early stages of PCa (Carver et al., 2009). Specifically, transmembrane protease serine 2:v-ets erythroblastosis virus E26 oncogene homolog (TMPRSS2-ERG) fusions make for 40 to 60% of the initial genetic profile, whereas forkhead box A1 (FOXA1) gain-of-function mutations for 3 to 5% of them, and speckle type BTB/POZ protein (SPOP) loss-of-function mutations account for 5% to 15% of the cases (Armenia et al., 2018; Fraser et al., 2017). In fact, mutations in the AR gene are unusual in the onset of the disease (Fraser et al., 2017). The genetic variability of localised PCa presents the following 3 features in nearly a third of them: chromothripsis, which is a process that results in chromosome shattering, kataegis, that refers to contained gene hypermutations, and chromoplexy, which refers to intricate patterns of rearrangements (Hieronymus et al., 2014; Lalonde et al., 2014; Rubin & Demichelis, 2018).

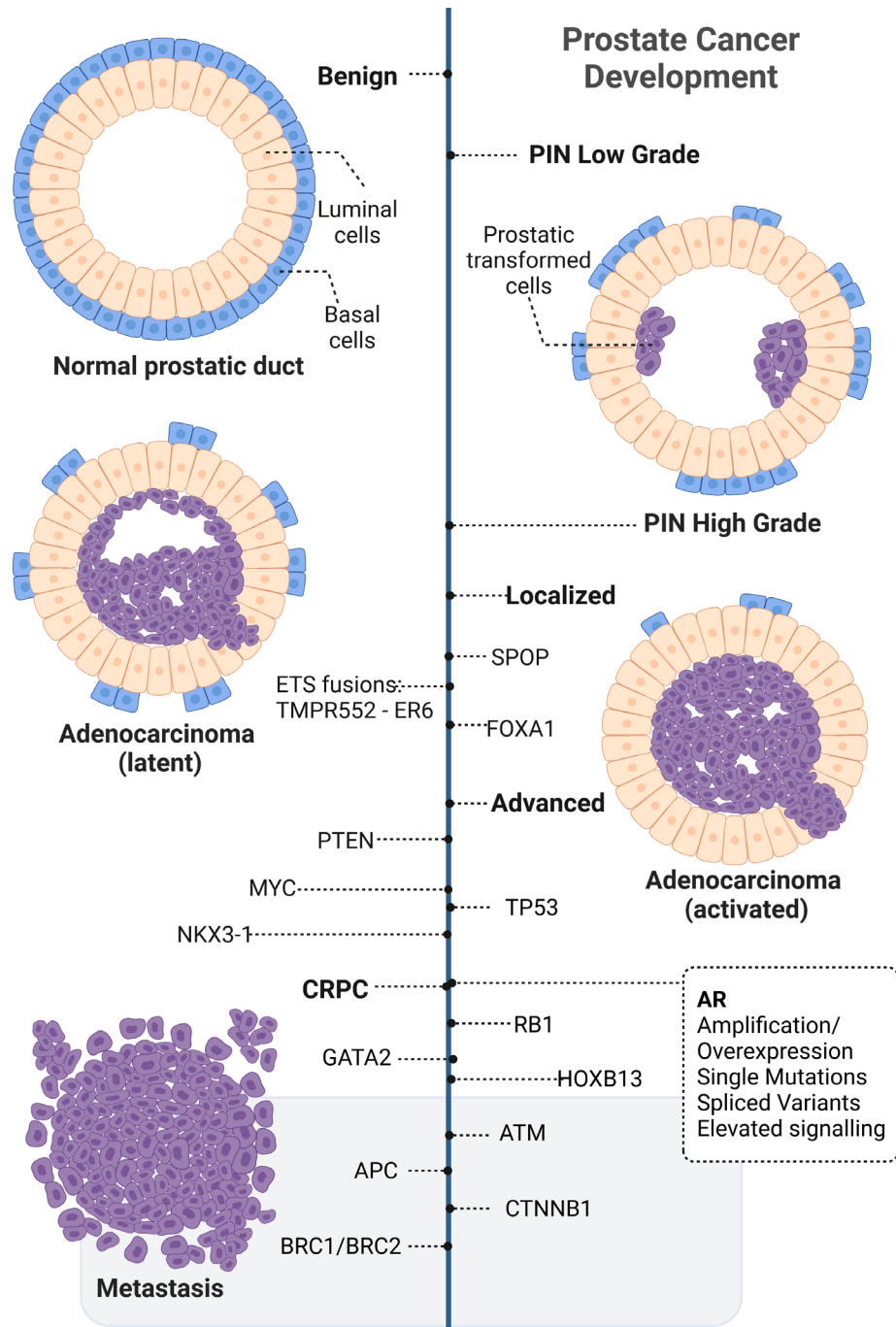


Fig. 4. Spectrum of genetic alterations in PCa development. Starting from a benign prostate, a precancerous state is induced via malignant transformation into a prostatic intraepithelial neoplasia (PIN), that evolves from low to high grade, and eventually into an adenocarcinoma that gets activated. In confined PCa, the main genetic profile is distinguished by TMPRSS2-ERG fusions, mutation in FOXA1 and deletion of SPOP. In advanced stages, tumour suppressors (TP53 and RB1 mutations, MYC amplification, and PTEN loss) and transcription factors (GATA2 mutations and HOXB13 overexpression) are disturbed. AR overexpression/amplification, mutations, AR splicing are common in castrate resistant prostate cancer (CRPC). At mCRPC, aberrations in ATM, BRC1 and BRC2, as well as CTNNB1 amplification and loss of APC are characteristic (Rebello et al., 2021). Created with BioRender.com.

Abnormal alterations of the AR signalling axis contribute to the progression of PCa. In 50% of castration-resistant tumours, it has been reported that the AR is overexpressed, accounting for an increase in receptor numbers by a factor of three to five (Feldman & Feldman, 2001; Gelmann, 2002). Approximately in 20 to 30% of castration resistant prostate cancer (CRPC), gene amplification of the AR has been detected, causing a doubling of AR mRNA levels, protein stabilization, and a rise in sensitivity towards testosterone (Bubendorf et al., 1999; Harris et al., 2009; Visakorpi et al., 1995). More than 150 mutations in the AR have been identified in the disease, comprising deletions, insertions, pre-termination and mostly single point mutations in its ligand binding domain (LBD), which consequently impairs ligand selectivity and promotes trans-activation (Fujita & Nonomura, 2019). Among them, the most predominant mutations are W742C, W743L, L702H, T878A, and H875Y (Ledet et al., 2020).

Also as a result of single or accumulated mutations and rearrangements, PCa exhibits AR alternative splicing, including more than 20 variants, the majority of which are truncated versions missing LBD (Brooke & Bevan, 2009; Van der Steen et al., 2013). The androgen receptor splice variant 7 (AR-V7), highly prevalent in CRPC, has been recognized to stimulate the expression of cell cycle genes, such as ubiquitin conjugating enzyme E2 C (UBE2C), as well as to block the transcription of tumour suppressor genes (Cato et al., 2019; Hu et al., 2009; Hu et al., 2012). Likewise, in metastases of CRPC patients, several studies have detected elevated expression of AR-V7, in contrast to less than 1% of its expression in primary PCa (Hörnberg et al., 2011; Qu et al., 2015; Sharp et al., 2018). As LBD is the main target of AR-based therapies, the truncated variants of AR that do not have a functional LBD (e.g. AR-V7) have demonstrated sustained activity, as they induce ligand-independent AR signalling, causing resistance to androgen receptor signalling inhibitors (ARSI) in CRPC (Antonarakis et al., 2014). All these anomalies in the AR axis, including AR point mutations, AR amplification and truncated variants, as well as, the substitution of androgens supplies through intratumoral synthesis and AR-independent processes, such as overstimulation of additional signalling pathways, such as phosphoinositide 3-kinase and protein kinase B (PI3K/AKT) or nuclear factor kappa-light-chain-enhancer of activated B (NF- κ B) and neuroendocrine differentiation, are all regarded as

resistance mechanisms to AR-targeted drugs (Galletti et al., 2017; Nakazawa et al., 2017).

Genetic modifications in several transcription factors of the AR have been linked to advancement to metastatic CRPC, which are involved in genetic stability and tumour growth regulation. Among them, mutations in tumour suppressors are recurrent in PCa, such as the loss or deletions of phosphatase and tensin homolog (PTEN), that promotes resistance and metastasis via the stimulation of the PI3K-AKT pathway (Mulholland et al., 2012; Wang et al., 2012). In fact, PTEN mutations have been identified in approximately 60% of CRPC, while in 30% of primary PCa (Batra & Winkler, 2018). Mutations in tumour protein p53 (TP53) and retinoblastoma tumour suppressor gene 1 (RB1), which are tumour suppressors that control cell cycle arrest, have been reported in 20 to 50% of metastatic CRPC (Abida et al., 2019; Armenia et al., 2018). Early stages of PCa often exhibit enhanced MYC proto-oncogene, bHLH transcription factor (MYC) expression, which triggers the production of genes that disrupt cell growth and proliferation and its overexpression is retained until metastasis (Gurel et al., 2008; Quigley et al., 2018). Mutations in the AR transcription factor, FOXA1 also persists in late stages of the disease, which enriches the transactivation of AR and development of CRPC (S. Gupta et al., 2017). Specifically, the WNT signalling gets activated as a result of the increased DNA affinity that mutated FOXA1 exhibits (Parolia et al., 2019).

The enhanced expression of the transcription factor HOXB13 has been reported in PCa (Edwards et al., 2005). The reprogramming of the AR cisome in transformed prostate epithelial cells, into a tumour-mimicking configuration is mediated through HOXB13 and FOXA1 (Pomerantz et al., 2015). HOXB13 has been recognized to restrain p21 expression causing activation of RB-E2F pathway, that in turn stimulates androgen-independent PCa proliferation (Y.-R. Kim et al., 2010). In addition, HOXB13 suppression has been revealed to prevent CRPC cell proliferation via an AR-V7-dependent mechanism, since the transactivation of AR-V7 key genes need HOXB13 (Chen et al., 2018). There is a genetic variation of HOXB13 that codes for the substitution G84E that increases the risk of developing PCa (Ewing et al., 2012).

Poor prognosis for patients was initially associated with enriched expression of the transcription factor GATA-binding factor 2 (GATA2), in tissues derived from metastatic PCa (Chiang et al., 2014; He et al., 2014). Furthermore, the crucial functions of GATA2 in different stages of the disease has been demonstrated. In early PCa, it was identified that GATA2 increase tumour motility and invasiveness by stimulating androgen responsive gene expression, while in late stages it is involved in the regulation of androgen-independent signalling pathways that contribute to the disease progression (Rodriguez-Bravo et al., 2017). Also, the androgen-regulated NK3 Homeobox 1 (NKX3.1) has been found consistently down-regulated or even completely lost in 78% of metastases, while 6 to 22% was recognized in primary PCa (Bowen et al., 2000).

WNT pathway has been extensively investigated in PCa. In localized PCa, WNT signalling is not commonly disturbed, however WNT-associated mutations have been detected in approximately 18% of mCRPC tumours, including gene amplification in catenin beta 1 (CTNNB1) and loss of function in adenomatous polyposis coli protein (APC) (Robinson et al., 2015).

DDR and MMR genes are involved in PCa. ATM, BRCA1, BRCA2, and checkpoint kinase 2 (CHK2) are amongst the most common DDR genetic aberrations in metastatic stages of CRPC (Abida et al., 2017; Robinson et al., 2015). Even though these mutations can have a somatic origin, there is a germline-based prostate cancer risk and lethal phenotype linked to BRCA1, BRCA2, and ATM mutations (Mijuskovic et al., 2018; Na et al., 2017; Y. Wei et al., 2020). Increased microsatellite instability and hypermutation can be caused by loss of function in MMR genes, due to the disruption in the preservation of genomic integrity throughout DNA replication and recombination (Beltran, 2013; Sedhom & Antonarakis, 2019). Although MMR mutations have a hereditary component related to PCa susceptibility, these alterations are scarce in PCa, accounting for 2 to 5% of the cancers, being MSH2 and MSH6 the most prevalent (Guedes et al., 2017; Pritchard et al., 2014; Vietri et al., 2021). For the small subset of mCRPC that exhibit microsatellite instability and MMR deficiency, immune checkpoint blockade (PD-1 inhibitors) has been exploited to profit these patients, however more research is required in the subsequent resistance routes (Abida et al., 2019; Antonarakis et al., 2019; Le et al., 2017).

The chromatin remodelling factor known as, chromodomain helicase DNA binding protein 1 (CHD1), mainly supports DNA transcription and replication, and participates in the adjustment of nucleosome placement (Farnung et al., 2017). CHD1 is considered a tumour suppressor in PCa and its deletion (8%) has been identified through large-scale cancer genome studies, in initial and metastatic PCa (Burkhardt et al., 2013; Grasso et al., 2012; Huang et al., 2012; Liu et al., 2012). Interestingly, PTEN inactivation and TMPRSS-ERG translocations are not commonly presented in subjects that harbour CHD1 loss, instead SPOP mutations are typically prevalent in this genetic profile (Abeshouse et al., 2015; Zhao et al., 2017). The induction of chromatin instability, DNA repair disturbances, transcriptional plasticity, AR redistribution and malfunction are events produced by CHD1 deletion in PCa (Augello et al., 2019; Kari et al., 2016; Shenoy et al., 2017; Zhang et al., 2020). Conversely, the stabilization of CDH1 is promoted in tumours that have PTEN deletion, influencing cancer evolution, drug resistance and reconfiguration of the tumour microenvironment (Li et al., 2022; Zhao et al., 2017; Zhao et al., 2020).

1.6 Current treatments for prostate cancer

The clinical and pathological criteria, including PSA results, cancer staging, and tissue morphology classification, based on the latest standardization of the Gleason Score; as well as, the patient's own situation, comprising family history, projected lifespan, age, overall health and predilections, have an impact on how PCa is therapeutically managed (Epstein et al., 2016; Rao et al., 2018; Rebello et al., 2021). Additionally, taking into consideration crucial variables, like the number of biopsies yielding a positive result, the size of the neoplasm in the biopsy samples, molecular biomarkers and imaging outcomes, the disease is categorized into low, intermediate and high risk (Eggerer et al., 2020). Although, the therapeutic strategies for PCa have progressed in the last 10 years, the habitual treatments for low-risk cancerous stages are still active surveillance, surgery and radiotherapy, sometimes accompanied with androgen deprivation therapy (ADT); while advanced and metastatic PCa are always treated with ADT in co-therapy with chemotherapy or next generation hormonal medications (Rebello et al., 2021; Sandhu et al., 2021; Sekhoacha et al., 2022). In Table 1, a brief list of the current therapies against different stages of PCa is provided.

Table 1. Current therapies for PCa

Treatment	Stage	Main features/types	Main adverse effects	References
Prostatectomy	Localized	Surgical removal of the prostate	Inability to control urination and erectile dysfunction	(Donovan et al., 2016; Kesch et al., 2021)
Radiotherapy (In some cases with ADT)	Localized	<u>Brachytherapy</u> : employs radioactive seeds <u>External beam radiation therapy (EBRT)</u> : uses high doses of radiation beams	Chronic bowel irritability, including mucus or blood, urinary discomfort and/or frequent urges to urinate, and hematuria	(Baskar et al., 2012; Donovan et al., 2016)
ADT (with chemotherapy or ARSIs)	Intermediate to advanced; mHSPC, CRPC/mCRPC	Chemical inhibition of androgens: 1. <u>GnRH agonists</u> : leuprolide, goserelin, and triptorelin 2. <u>GnRH antagonists</u> : degarelix 3. <u>Anti-androgens (First generation)</u> : Bicalutamide, flutamide, and nilutamide	Cardiovascular disease, stroke, heart failure, myocardial infarction, hypertension, arrhythmia, diabetes, metabolic syndrome, anaemia, osteoporosis, fatigue, impotence and loss of muscle	(Cornford et al., 2021; Grossmann & Zajac, 2011; Hu et al., 2020)
Chemotherapy	Advanced; mHSPC, CRPC/mCRPC	Taxane-based treatments: Docetaxel and cabazitaxel	Alopecia, neuropathy, anaemia, nail changes, chronic fatigue, diarrhoea, nausea, vomiting and taste dysfunction	(James et al., 2016; Omlin et al., 2015; Sweeney et al., 2015)
Cryotherapy	Localized	Focal cryoablation	Potency and lower urinary tract obstruction	(Kotamarti & Polascik, 2023)

Next-generation treatments

ARSI (with ADT)	Advanced; mHSPC, nmCRPC and mCRPC	<u>Anti-androgens (2nd generation):</u> Enzalutamide, apalutamide, and darolutamide <u>Androgen synthesis inhibitor:</u> Abiraterone	Seizures, cognitive dysfunction, falls, pathological fractures, skin itchiness, joint pain, constipation and fatigue Abiraterone: Cardiovascular events, low potassium levels in blood, fluid retention, enhanced liver activity and hypertension	(Armstrong et al., 2019; Chi et al., 2019; Davis et al., 2019; Fizazi et al., 2017; Graff et al., 2015; James et al., 2016; Smith et al., 2022; von Klot et al., 2014) (McKay et al., 2019)
PARP inhibitors	Advanced and mCRPC	<u>DNA repair inhibitor:</u> Olaparib Rucaparib	Fatigue, nausea, and anemia	(Abida et al., 2020; De Bono et al., 2020; Fizazi et al., 2023)
Immunotherapy	mCRPC	Sipuleucel-T vaccine <u>Immune checkpoint inhibitor:</u> Pembrolizumab (PD-1)	Cell-based vaccine: Fatigue, chills, nausea, fever, back pain, diarrhea, and anemia PD-1: Immune-related adverse events, e.g. immune-mediated skin reactions or endocrinopathies	(Kantoff et al., 2010; Marcus et al., 2019)
Targeted radionuclide therapy	mCRPC	Bone-targeting Radium-223 177Lu-PSMA	Bone pain flare, fatigue, constipation, diarrhea, anemia, nausea, thrombocytopenia, and neutropenia	(Parker et al., 2013) (Sartor et al., 2021; Violet et al., 2019)
Bone-targeting agents	mCRPC	Zoledronic acid and Denosumab (anti-RANKL)	Bone pain, anaemia, reduced appetite, nausea, fatigue, back pain, and constipation	(Fizazi et al., 2011; Saad et al., 2002; Stopeck et al., 2010)

Patients with reduced risk are normally subjected to active surveillance. The management of PCa through this passive strategy implicates constant monitoring, anticipated intervention, repeated biopsies, additional PSA screenings and/or digital rectal inspections, to minimize overtreatment (Choo et al., 2002; Mottet et al., 2017). Men with confined PCa, who receive an early diagnosis have almost a 100% probability of surviving for at least 5 years (Siegel et al., 2020; Wang et al., 2021). For enclosed neoplasms, treatment choices are usually radiotherapy or radical prostatectomy. Although the surgical removal of the prostate and adjacent tissues is effective for localized PCa, it is usually accompanied by severe effects, mainly erectile dysfunction and urinary incontinence (Kesch et al., 2021). Radiotherapy is a suitable treatment for affected men that are not eligible for surgery (Baskar et al., 2012). Three main types of radiotherapy exist for PCa. Brachytherapy consists in the insertion of radioactive agents into the affected gland via a catheter into the rectum or urethra; while external beam radiation therapy (EBRT) targets the cancer tissue with potent X-ray laser. Targeted radionuclide therapy (TRT), which consists in the employment of radionuclides in conjugation to cancer-targeting molecules, is relatively new and still in development (Muralidhar et al., 2023). In patients with local intermediate and high-risk PCa, it has been reported that surgery or EBRT paired with ADT, offers a more effective response; nonetheless more standardization and considerations are required (Mottet et al., 2021; Ventimiglia et al., 2019).

Cryotherapy is another contemporary option to treat focal PCa, that has offered optimistic functional results, however there is a lack of long-term tracking studies to evaluate the overall clinical impact (Kotamarti & Polascik, 2023).

In order to proliferate, grow and survive, prostate cells, whether benign or oncogenic, crucially rely on androgens (Tindall & Lonergan, 2011). Thus, for patients with intermediate to high risk PCa, including advance and recurrent disease, hormonal therapy or ADT is still the most conventional treatment, however administered in combination with other therapies (Cornford et al., 2021). Hormonal therapy was initiated by Huggins research in the 1940s (Huggins & Hodges, 1941). The basic mechanism in ADT is to decline testosterone levels via surgical or chemical suppression, using gonadotropin-releasing hormone (GnRH) agonists (e.g. leuprolide, goserelin, and triptorelin) or antagonists (e.g. degarelix), anti-androgens or a mixture

of them, in order to diminish tumour growth and delay disease progression (K. Desai et al., 2021; Huggins & Hodges, 1941). The disruption of endocrine-associated pathways intrinsic to ADT therapy promotes a vast range of adverse effects, comprising severe cardiovascular events, such as cardiovascular disease, stroke, heart failure, myocardial infarction, hypertension and arrhythmia, as well as other complications such as diabetes, metabolic syndrome, anaemia, osteoporosis, fatigue, impotence and loss of muscle (Grossmann & Zajac, 2011; Hu et al., 2020).

ADT accomplishes castrate testosterone levels, that in turn declines tumour burden and enhance survival and mitigation of the symptoms for several months up to 2 or 3 years (Sumanasuriya & De Bono, 2018; Tucci et al., 2015). Unfortunately, most tumours will become resistant to ADT through underlying mechanisms that adapt or re-activate AR signalling, leading to the development of CRPC (Klotz et al., 2015; Scher & Sawyers, 2005; Wadosky & Koochekpour, 2016). Patients treated with prolonged ADT, that suddenly present biochemical and radiological deterioration, as a reflection of 3 continuous PSA upsurges with a gap of at least a week, along with castrate serum levels of testosterone lower than 50 ng/dL, are considered in CRPC stage (Cornford et al., 2021). Death rates related to PCa are mostly consequence of CRPC (Feldman & Feldman, 2001). In rare cases, similar to CRPC, NEPC can develop following ADT due to an androgen resistance mechanism, although it can also develop spontaneously (Beltran et al., 2014).

CRCP is normally divided in metastatic CRPC (mCRPC) and non-metastatic CRPC (nmCRPC), while the term metastatic hormonal sensitive prostate cancer (mHSPC) or also known metastatic castration sensitive prostate cancer (mCSPC), refers to a phenotype that is responsive to androgens but either has developed de novo metastases or presents disease recurrence following confined treatment, typically with radiotherapy or radical surgery (Hofmann et al., 2021; Kenrick et al., 2020).

Taxane-based treatments are the main chemotherapeutic drugs used for metastatic CRPC, such as docetaxel and cabazitaxel. Taxanes cause microtubule stability, which leads to cell cycle arrest followed by cell death (Kraus et al., 2003; Kroon et al., 2016). Since 2004, the most ad hoc treatment for metastatic PCa was prolonged ADT with GnRH agonists/antagonists all throughout disease advancement, in combination with

periodic docetaxel and prednisone (Tannock et al., 2004). After docetaxel resistance, cabazitaxel has been proposed for patients with mCRPC as a follow up treatment (Crawford et al., 2015). In dual therapy with ADT, docetaxel is still used to treat mCRPC or mHSPC, since it has demonstrated for more than 20 years to provide adequate effectiveness (James et al., 2016; Sweeney et al., 2015). However, in terms of overall survival for mCRPC de novo patients, cabazitaxel did not provide a better overall survival outcome in initial-line treatment when compared to docetaxel, as revealed in the FIRSTANA trial (Oudard et al., 2017).

In the previous ten years, the therapeutic approaches for metastatic PCa have diversified. Flutamide, nilutamide, and bicalutamide were the first generation of Food and Drug Administration (FDA)-approved AR antagonists, and their use started as monotherapy in the late 1980s and early 1990s (Airhart et al., 1978; Cockshott et al., 1990; Eri & Tveter, 1993; Jacobo et al., 1976; Namer et al., 1988; Navratil, 1987). Novel second-generation ARSIs were developed, including enzalutamide, abiraterone, apalutamide, and darolutamide, to overcome the challenges in CRPC (Crawford et al., 2018). While the first-generation of anti-androgens worked by directly associating to the AR to block testosterone or DHT, ARSIs not only exhibit stronger binding affinity to AR, but also suppress the translocation of AR to the nucleus, prevent its DNA binding, and inhibit the recruitment of transcription co-activators (K. Desai et al., 2021). From a mutagenic screen of the non-steroidal agonist RU59063, enzalutamide was the first ARSI discovered (Tran et al., 2009). The administration of enzalutamide is normally well accepted, and it has been confirmed to avoid androgen withdrawal syndrome in patients, however it also induces adverse events including constipation, fatigue, arthralgia, and enhanced risk of seizures (Graff et al., 2015; von Klot et al., 2014).

Similar in functionality to enzalutamide, apalutamide displays higher binding efficacy to the LBD of the AR than other anti-androgens, and has several favourable features, such as reduced systemic elimination, long serum half-life, effective oral absorption, and elevated tumour to plasma balance (Clegg et al., 2012). Through the production of a synthetic molecule library, Darolutamide was created as a distinctive ARSI, that has higher AR binding potency than enzalutamide and apalutamide (Moilanen et al., 2015).

Other types of ARSIs disrupt the AR axis by targeting intertumoural androgen production. Abiraterone is an irreversible inactivator of the androgen synthesis, that promotes the suppression of androgens in the adrenal glands, cancer cells and the testes, via the inhibition of cytochrome P450 17A1 (CYP17A1) (Rehman & Rehman, 2012). It was granted approval by the FDA in 2011, and recommended in combination with prednisone for patients with mCRPC (Caffo et al., 2018).

In immunotherapy, novel therapeutic options are recently available for the treatment of mCRPCa. In 2010, the cell-based sipuleucel-T vaccine (Provenge) was given approval by the FDA (Kantoff et al., 2010). In order to induce PCa cell clearance by T cell recognition, the basic mechanism of the sipuleucel-T vaccine involves the administration of the patient's dendritic cells, that were immunized with recombinant prostatic acid phosphatase (PAP) (Fong et al., 2001). Although, the dendritic-based vaccine provides a 4-month overall survival increase in the IMPACT trial, the treatment did not provide a benefit in terms of delaying the advancement of illness (Kantoff et al., 2010).

Another immunotherapeutic tactic that has been developed is immune checkpoint therapy. This treatment is based on controlling receptors or ligands that have a negative regulatory immune role, commonly called immune checkpoints, such as the programmed cell death protein 1 (PD-1) and programmed death-ligand (PD-L1) (Claps et al., 2020; Elia et al., 2018; Jiao et al., 2019). Multiple checkpoint inhibitory antibodies have been assessed in clinical trials, however the general outcomes of monotherapies have been poor (H. Liang et al., 2023; Maselli et al., 2023). For specific mCRPC patients treated unsuccessfully with recommended therapies, and that have high microsatellite instability and MMR malfunction, as well as elevated tumour mutational load, the FDA has granted their approval for the anti-PD-1 immunotherapy, named pembrolizumab (Marcus et al., 2019). Since the results from single immunotherapies trials have been ineffective, ongoing trials are evaluating diverse mixtures of immune checkpoint inhibitors or other immune-based strategies with other therapies, including ARSIs, cryotherapy, radiotherapy, chemotherapy, and others (Fong et al., 2021; Graff et al., 2021; Petrylak et al., 2021; Ross et al., 2020).

In metastatic PCa, there have been dramatic improvements in TRT. Strontium-89 and Samarium-153 were the first TRT-approved radionuclides exclusively for palliative use. These radionuclides did not improve survival but have the capacity to target metastatic bone illness (Reddy et al., 1986; Sartor et al., 2004). A α -emitting bone-targeting radionuclide, radium-223 was exposed to imitate calcium as it was internalized by osteoblasts within the bone metastasis (Parker et al., 2013). Radium-223 therapy has proven to enhance overall survival in the ALSYMPCA trial over traditional treatments in cohorts of men with mCRPC (Hoskin et al., 2014). Conversely, in the ERA 223 trial it was demonstrated that Radium-223 therapy administered as monotherapy was more efficient, than when given as dual medication with abiraterone or prednisone, resulting in a bone-associated incident delay in mCRPC subjects (Smith et al., 2019). The imaging biomarker strategy PSMA-PET used for PCa diagnosis to visualize PSMA-positive tumour cells, for instance the ^{68}Ga -PSMA PET-CT, led to the further investigation of different TRT using varied small molecules, including antibodies or small molecules with radionuclides. Among them, the FDA-approved ^{177}Lu -labelled PSMA-617 (^{177}Lu -PSMA), stands out for its clinical effects in mCRPC patients following chemotherapy and ARSI, by targeting PSMA in PCa cells and delivering beta-particle radiation (Sartor et al., 2021; Violet et al., 2019). Additionally, a meta-analysis comprising 6 small trials in mCRPC, testing an α -emitting actinium-225 (^{225}Ac) radionuclide instead of the beta-emitting ^{177}Lu with PSMA-617 molecule, indicated an efficient and relatively safe profile, however further randomized trials are necessary for ^{225}Ac -PSMA-617 (Ma et al., 2022).

A couple of bone-targeting molecules have had FDA approval, particularly for the prevention of skeletal-related events and to mitigate bone density depletion, in metastatic CRPC that has migrated to the bones. Zoledronic acid represents a third-generation bisphosphonate, that has demonstrated inhibition of osteoclastic activity delaying skeletal-related events for patients with mCRPC (Saad et al., 2002). Among the principal adverse events that bisphosphonates generate are enhanced risk of renal damage, hypocalcemia, osteonecrosis of the jaw, esophagitis, gastrointestinal bleeding, or ulcers (Bartl et al., 2008; Gartrell et al., 2014). Another bone-targeting agent, denosumab, that has proven beneficial effects in mCRPC via targeting the receptor activator of nuclear factor kappa-B ligand (RANKL) in osteoclasts (Fizazi et al., 2011; Stopeck et al., 2010).

Furthermore, other innovative therapeutic strategies have emerged that target DNA repair signalling. The family of 17 repair enzymes known as Poly (ADP ribose) polymerase (PARP) are key to preserve DNA integrity, specially PARP1 and PARP2 (S. Lang et al., 2019). In cells with a preexisting DDR genetic mutation, PARP inhibitors (PARPi) can trigger synthetic lethality interaction by blocking PARP and hence causing impairment of the DNA response (Kaelin, 2005; Lord & Ashworth, 2017). As mentioned in a preceding section, around 20% of subjects with mCRPC have mutations in DDR genes (Robinson et al., 2015). First proposed in 2005 as a potential approach to treating patients with BRCA-mutant cancers (Bryant et al., 2005; Farmer et al., 2005). At this time, two PARPi, namely olaparib and rucaparib are available for treatment of mCRPC exclusively for patients that carry BRCA1 or BRCA2 mutations. Both PARPi were approved by the FDA in 2020, supported by their clinical trials success (Abida et al., 2020; De Bono et al., 2020).

Multiple co-therapies have been investigated in recent clinical trials. Even though second generation of antiandrogens are more efficient and potent than traditional ADT, patients still developed resistance mechanisms. Specifically, the trials of synergistic treatments between ADT and enzalutamide, ADT and apalutamide, ADT and abiraterone plus prednisone, ADT and darolutamide plus docetaxel, have supported a beneficial gain from the therapy amplification in patients suffering from mHSPC (Armstrong et al., 2019; Chi et al., 2019; Davis et al., 2019; Fizazi et al., 2017; James et al., 2016; Smith et al., 2022). Triple treatment combinations are being tested in ongoing trials (Hahn et al., 2018). Combinatorial approaches are under current investigation for the use of PARPi (A. Taylor et al., 2023). Other randomised clinical trials are evaluating precise molecular therapies in PCa that haven't had FDA approval, such as PI3K/AKT inhibitors. For example, in the IPAtential150, the mixture of ipatasertib, an effective AKT inhibitor, plus abiraterone, showing some early indications of potential application for patients with PTEN-deletion and mCRPC, however it requires further assessment (Sweeney et al., 2021).

There are no specific treatments for rare PCa histological subtypes, such as PIN-like carcinoma, ductal adenocarcinoma, IDCP, and NEPC. Intraductal carcinoma and ductal adenocarcinoma are more aggressive and have worse oncological results than PIN-like carcinoma, which has a better prognosis and is regarded as a histological

variant of acinar prostate carcinoma (Marra et al., 2023; Varma, 2023). Under the Gleason grading system, PIN-like carcinoma is designated as a pattern 3, while ductal adenocarcinoma is classified as a pattern 4 or 5 (Amin, 2018; Zhou, 2018). Their therapeutic management generally follows the conventional guidelines for acinar PCa depending on their risk classification (Cozzi et al., 2022; Zhou, 2018). In contrast, major international urological societies have made controversial recommendations on the diagnosis and management of IDCP. There is also an ongoing debate about its incorporation into the Gleason scoring system (Epstein et al., 2021; van Leenders et al., 2020). Although IDCP frequently denotes a high-grade PCa development pattern, it occasionally occurs as a precursor to aggressive PCa that lacks an invasive component (Cohen et al., 2007; Guo & Epstein, 2006; Surinrspanont & Zhou, 2023). Based on histological and radiological characteristics, it has been proposed that the treatment for IDCP should be patient-specific and determined in a multidisciplinary setting (Varma, 2023). In the case of NEPC, the most widely used treatment has been platinum-based chemotherapy, typically in conjunction with etoposide and cisplatin or carboplatin (Aparicio et al., 2013).

1.7 Peptide drug conjugates

More than a century ago, a scientist called Paul Ehrlich, who won the Nobel Prize in Medicine in 1908, first proposed the concept of targeted therapy. Ehrlich coined the term “magic bullet”, which represented a molecule that could potentially avoid damaging the body and eliminate pathogens at the same time (Ehrlich, 1901). Nonetheless, it took many decades for the field of targeted therapeutics to emerge.

Since conventional drugs against cancer, such as doxorubicin or cisplatin, are hindered by their lack of specificity towards malignant cells, displaying high cytotoxicity in benign tissues, and subsequent physiological adverse events, selective drug delivery therapies initiated in the area of cancer therapeutics (Chabner & Roberts, 2005; DeVita & Chu, 2008; Tzakos et al., 2013). Currently, molecular targeted therapy comprises heterogeneous pioneering strategies, that use biological transporting agents, such as, small molecules, antibodies, peptides, and other molecules, that deliver drugs or other compounds to work at a cellular and molecular level (Lee et al.,

2018). Among these therapeutics, peptide drug conjugates (PDC) are molecular drug delivery complexes that employ small peptides as drug carriers to target specific sites (Wang et al., 2017; Zhu et al., 2021). PDC are mostly applied to cancer management, however they have been developing for the application of other conditions or diseases, including diabetes, COVID-19, inflammation, rheumatoid arthritis, malaria, analgesia and bacterial infections (Aguiar et al., 2019; Brankiewicz et al., 2022; Eberle et al., 2022; Eiselt et al., 2020; Han et al., 2020; Heh et al., 2023; Moreira et al., 2020; Zaazouee et al., 2022).

In 1972, a series of chlorambucil N mustard peptides were used to create the first PDC to inhibit hormone receptors, by Freer and Stewart (Freer & Stewart, 1972). Their work laid the groundwork of the enormous potential of PDC. It was until 1994, when the first PDC was widely use on the market, as a diagnostic tool to track tumours, known as ^{111}In -DTPA-octreotide, which utilizes octreotide peptide to target the somatostatin receptor, conjugated with a Diethylenetriamine pentaacetate (DTPA) chelator linker to the radioactive payload ^{111}In (Weckbecker et al., 1993). Globally, more than 100 peptide-based drugs are currently in use for clinical applications (Cooper et al., 2021; Lau & Dunn, 2018). The FDA approved the first PDC for cancer treatment in 2018, specifically to manage gastroenteropancreatic neuroendocrine tumours by targeting the somatostatin receptor with ^{177}Lu -DOTA-TATE (Das et al., 2019).

PDC are characterized by 3 main modules that function synergistically: 1) the peptide targeting unit, that guides the drug to the site of interest, 2) the linker, which conjugates the other two elements, and 3) the payload, that executes the desired therapeutic effect (Figure 5) (Fu et al., 2023; Heh et al., 2023; Hoppenz et al., 2020; Li & Roberts, 2003; Vrettos et al., 2018).

PDC share similar features and functions with another selective drug delivery system, known as antibody drug conjugates (ADC), which uses antibodies instead of peptides as targeting unit (He et al., 2021; Wang et al., 2017). Both of them have the same 3 mayor components, targeting unit, payload and linker. The principal differences between ADC and PDC are explained in Table 2.

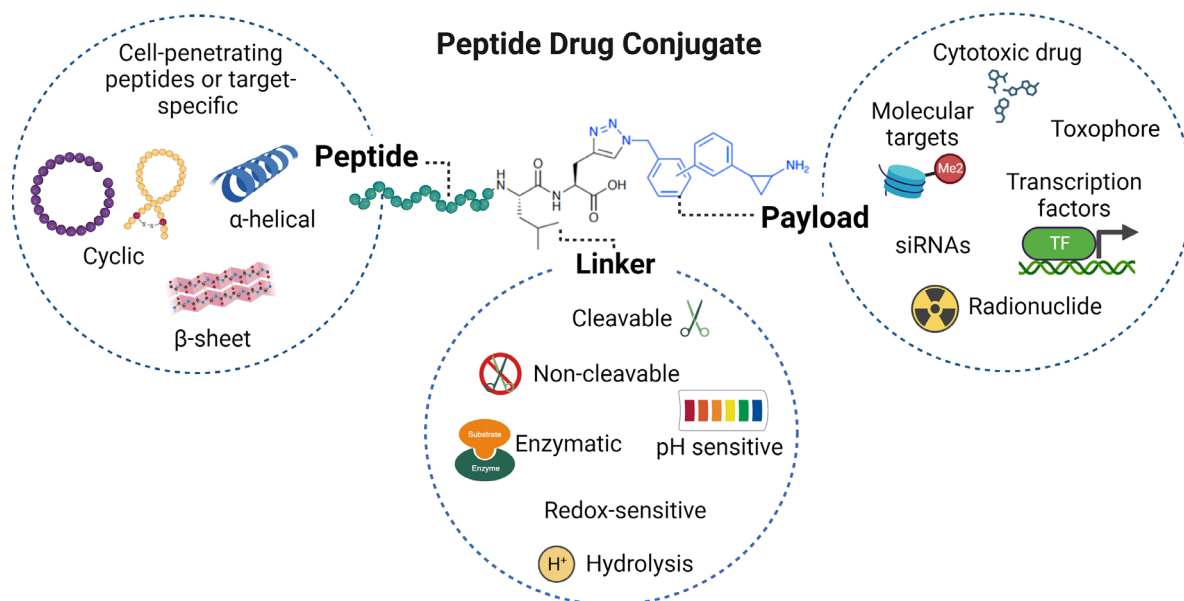


Fig. 5. Overview of PDC configuration. The structure of PDCs is divided in 3 modules, the peptide targeting unit, the linker and payload. The diversity of each type of components is illustrated. The PDC used as an example is represented by an alpha helical peptide, conjugated with click chemistry to a LSD1 inhibitor as payload. Created with BioRender.com.

PDC offer multiple benefits over ADC, involving reduced intrinsic immunogenicity, enhanced penetration to solid tumours and their microenvironment, due to their smaller size, and faster elimination rate (Ahrens et al., 2012; Hoppenz et al., 2020; Weiss & Chamberlin, 2003). ADC are known for their extended circulatory half-life and increased specificity to antigens, however they are often absorbed in the liver or reticuloendothelial system, potentially causing cytotoxicity. Additionally, their large size makes infiltration into tumours and adjacent stroma inefficient (Dreher et al., 2006; Jain & Stylianopoulos, 2010; Pettinato, 2021; Wagh et al., 2018). Although monoclonal antibodies are humanized, they usually accumulate in organs such as the liver or kidney, that may trigger immunogenic reactions (Borsi et al., 2002; Carrasco-Triguero et al., 2013; van Schouwenburg et al., 2010). PDC can be synthesized in mass quantities with relative ease and at a lower cost and their structure enables simple customization with synthetic aa. In contrast, ADC manufacture is more expensive, requires more certifications, and longer periods of time (Firer & Gellerman, 2012; Mäde et al., 2014; Nejadmoghammad et al., 2019). Furthermore, PDC are more flexible in terms of modification and conjugation to a huge range of payloads, while ADC are

hindered by their lack of ability to transport several cytotoxic molecules and poor penetration capacity. Their payload must satisfy specific criteria, like having super cytotoxicity to exert an effect even with limited cargo release (Fu et al., 2023; Wagh et al., 2018)

Table 2. PDC vs ADC

Feature	PDC	ADC	References
Tumour and stromal penetration	High penetration and diffusion due to their small size (2 to 20 kDa)	They are restricted by their large sizes (~150 kDa), that affects penetration into solid tumours	(Dreher et al., 2006; Hoppenz et al., 2020; Jain & Stylianopoulos, 2010; Pettinato, 2021)
Specificity	It depends, however peptides targeting receptors have high specificity to cancer cells	Higher specificity to antigens on the surface of tumour cells	(He et al., 2021; Wang et al., 2017)
Immunogenicity	Low intrinsic immunogenicity	May have elevated immunogenicity, and they have the tendency of accumulating in excretory organs	(Ahrens et al., 2012; Borsi et al., 2002; Carrasco-Triguero et al., 2013; van Schouwenburg et al., 2010)
Manufacture	Easy modification and mass production is less expensive	Expensive, time-demanding and require more validations	(Firer & Gellerman, 2012; Mäde et al., 2014; Nejadmoghammad et al., 2019)
Pharmacokinetics	Short half-life, rapid clearance and less probability of cytotoxicity in the kidneys	Extended half-life circulation. Dose-limiting toxicity to the liver and bone marrow could occur due to non-specific internalization	(Hoppenz et al., 2020; Pettinato, 2021)
Payload	Easy conjugation and multiple options of cytotoxic or varied molecules	Fewer options of cytotoxic molecules that meet super cytotoxicity criteria	(Fu et al., 2023; Wagh et al., 2018)

1.7.1 Targeting peptides

A targeting peptide is the first element of the structure of a PDC. Peptides have demonstrated outstanding capacity of transporting cargos (Chatzisideri et al., 2018; Gronewold et al., 2018). Selecting the peptide is key for the generation of an effective PDC, because it determines the specificity to the site of interest, the efficacy of endocytosis and internal unloading, the overall pharmacokinetic profile and therapeutic outcome (Fu et al., 2023).

Commonly, the peptide component in PDC can be categorized as cell-penetrating peptides (CPP) or tumour-targeting peptide (Fu et al., 2023; Heh et al., 2023; Hoppenz et al., 2020). CPP are regarded as small-sized peptides that enter cells via endocytosis or direct penetration and are capable of exerting intracellular effects either directly or indirectly by carrying other molecules to the desired region (Langel, 2015; Langel, 2019; Zorko & Langel, 2022). These two classifications tend to overlap; however the concept of tumour-targeting peptides refers to peptides that bind with high affinity to cell surface receptors that have elevated expression in oncogenic cells, and hence may be exploited in cancer therapeutics (Ma et al., 2017b; Reubi, 2003; Vhora et al., 2014). Numerous receptors have been postulated as molecular targets of peptides, including integrins, scavenger receptors, somatostatin receptors, epidermal growth factor receptor (EGFR), syndecans, bombesin receptors, vasoactive intestinal peptide, PSMA, gonadotropin releasing hormone-receptor (GnRH-R), chemokines and others (Vrettos et al., 2018; Worm et al., 2020; Zhu et al., 2021). Peptide targeting receptors in cancer cells present binding affinities comparable to those of monoclonal antibodies, but with greater tumoral access (Hoppenz et al., 2020). The targeting peptide requires a potent binding potential, negligible immunogenicity, stability, a long-lasting half-life in circulation and efficient uptake (Fu et al., 2023). One favourable attribute of peptides is that their pharmacodynamic profile can be improved easily through simple modifications that provide more stabilization, such as lipidation (Vlieghe et al., 2010; Zhang & Bulaj, 2012). Peptide adjustments can also boost the binding affinity. For instance, multimerization can allow more peptide-receptor contacts by connecting two or more monomers. Other modifications can enhance the resistance of the peptide towards enzyme degradation, such as cyclization (Vivès et al., 2008).

1.7.2 Linker

In the PDC, the linker basically unifies the peptide and the payload. To guarantee that the highest amount of drug dose reaches the target site, the linker requires to provide stability to the conjugate (Alas et al., 2021). Factors, such as the whole length of the conjugate, the polarity, the desired mode of action, and delivery mechanism influence the type of bonding molecule that could benefit the whole drug delivery system (Alas et al., 2021; Böhme & Beck-Sickinger, 2015). The unloading of the payload can be mediated by linker technologies that take advantage of the biological discrepancies inside the tumour and its surroundings (Bildstein et al., 2011; Joubert et al., 2017). Based on this, the most typical types of linkers are non-cleavable and cleavable, which the latter can be pH-sensitive, redox-sensitive or enzyme-based (Alas et al., 2021; Heh et al., 2023).

Linkers that enter the category of non-cleavable are less prone to break down in circulation than cleavable linkers, ultimately avoiding early drug delivery. Although non-cleavable linkers retain higher stability in plasma, the usual preference is for cleavable linkers (Bargh et al., 2019). Amide or ester bonds are commonly used as non-cleavable linkers (Finan et al., 2012; Ma et al., 2017a).

One strategy for cleavable linkers is to use the shifts of pH in cellular settings. The intrinsic acidity of tumours is consequence of metabolic demands as the malignant cells proliferate. The lack of oxygen and nutrients leads the cancer cells to adopt anaerobic glycolysis, which produces lactic acid, resulting in an acidification of the tumour microenvironment (Zhang et al., 2010). At physiological pH of 7.4 in the bloodstream, linkers that are sensitive to pH remain stable, while the bonds of the linker will undergo hydrolyzation at acidic pH, such as the pH in the tumour surroundings of 6.5 to 6.8, or at lysosomal pH of 4.5–5.0 (Alas et al., 2021; Bargh et al., 2019). Imines, acetals, hydrazine, and hemiacetals are examples of the chemical bonds employed in pH-sensitive linkers, but the most used is the hydrazone bond (Bargh et al., 2019; Langer et al., 2001).

The way redox-based linkers function is by means of the dramatic differences between intracellular and extracellular concentrations of antioxidants. For instance, glutathione

has concentrations inside the cells that exceed those in the plasma by a factor of 4, and this disparity is even more pronounced in tumours due to hypoxic settings (Bansal & Simon, 2018; Böhme & Beck-Sickinger, 2015). Disulfide bonds are used to link the drug to the peptide, that once inside the cell, cleavage will be induced by the variations in glutathione concentrations (Alas et al., 2021). Other chemical bonds can be cleaved by glutathione gradients including metal thiols, thioethers-selenium-tellurium and ferrocene (Fu et al., 2023).

Linkers that are enzyme-sensitive utilize mostly lysosomal enzymes in cancer cells for their cleavage. They incorporate specific amino acid sequences to ester or amide bonds, that facilitates the targeting of esterase, amidases or proteases (Alas et al., 2021). An example of enzyme-sensitive linkers is the cleavable unit (SSKYQ), used in a PDC named KCC-TGX, which gets dissociated upon interaction with PSA, a serine protease that is overexpressed in PCa cells (W. Tai et al., 2011; Watt et al., 1986).

1.7.3 Payload

The active molecule that can cause biological functions in the PDC, is the payload or cargo. For cancer therapy the most frequent payloads are chemotherapeutic drugs, including doxorubicin and camptothecin, which both function by interfering with DNA replication, to induce apoptosis (Z. Chen et al., 2014; Hoppenz et al., 2020; P. Zhang et al., 2013). According to their mechanism of action, chemotherapeutic agents are often categorized in different groups (Malhotra & Perry, 2003). Other cytotoxic drugs that exhibit toxophores, are often integrated as cargos in PDC, which induce their cytotoxicity by suppressing DNA biosynthesis, such as gemcitabine or the folate derivative methotrexate (Böhme et al., 2016; Galmarini et al., 2002). Paclitaxel is also frequently used as payload in PDC, like a PDC that was loaded with 3 paclitaxel molecules to a blood brain barrier infiltrating peptide called angiopep-2 (Régina et al., 2008). This chemotherapeutic drug belongs to the group of taxanes that work by obstruction of microtubule depolymerization (Xiao et al., 2006). The cytotoxic cargo in PDC should have a precise mechanism of action, elevated cellular toxicity, low molecular weight, and preserved anti-tumour action after chemically merging with the peptide (Zhu et al., 2021).

Another common cargo are radionuclides. They are often employed as part of PDC for either diagnosis, such as ^{111}In -DTPA-octreotide, or for therapeutic purposes like ^{177}Lu -DOTA-TATE (Das et al., 2019; Kwekkeboom et al., 2010). For PDC production, the most frequently employed radionuclides are lutetium-177 (^{177}Lu), indium-111 (^{111}In), and yttrium-90 (^{90}Y) (Thundimadathil, 2012).

An alternative type of non-radioactive payload to generate PDC is to use boron-10 (^{10}B) isotopes for boron neutron capture therapy (BNCT). The underlying mechanism behind BNCT is that ^{10}B will be transformed into an active state in cancer cells, via exposure to local irradiation of thermal neutrons (X. Cheng et al., 2022). For instance, two peptides that target mitochondria, namely KLA and RLA, were coupled to dodecaborates (DB), which provided the boron. Notably, DB-RLA showed higher boron concentrations in glioblastoma cells, and post-neutron irradiation, a substantial increase in cell death was obtained (Nakase et al., 2019).

PDC have been primarily investigated to improve the activity of toxic chemicals and radionuclides, however, there are new venues to oncogenic molecular targets by targeting altered signalling mechanisms in cancer cells, novel transcription factors with altered activity, dysregulated epigenetic mechanisms or upregulated enzymes (Bhat et al., 2015; DeBerardinis & Chandel, 2016; Hanahan & Weinberg, 2011; Pfister & Ashworth, 2017). In addition, small interfering RNA (siRNA) have been employed as payload in PDC to impede translation in tumour cells. For example, a PDC conjugated to siRNAs was targeted to bind to $\alpha\beta3$ integrins in glioblastoma cells and release the siRNA to knockdown (KD) the expression of EGFR (He et al., 2017).

Furthermore, next generation drugs are arising as novel payload options for PDC. Among them, protein-based medications can yield effective anti-cancer effects by restraining intracellular protein synthesis and stimulating apoptosis (Gong et al., 2023). Interferon (INF) and tumour necrosis factor (TNF) are the best examples under investigation. Peptides linked to protein-based drugs could provide to the payload higher in vivo stability, increased bioavailability and target specificity (Gong et al., 2023).

The cytokine IFN has a variety of therapeutic uses due to its antiproliferative, antiviral, and immune response-modulating properties, but these uses are restricted by its low stability, lack of cancer cell selectivity, and adverse effects, which include immunological dysfunction, hepatic effects and neural toxicity (Jonasch & Haluska, 2001). The fusion of the tumour neovasculature-specific peptide NGR with IFN α 2a, has led to the production of the PDC known as IFN- α 2a-NGR. The targeting efficiency of IFN α 2a was not only enhanced, with activated apoptosis in vascular epithelial cells and a substantial decline in microvessel density, but also vascular endothelial growth factor (VEGF) and basic fibroblast growth factor (bFGF) expression were suppressed by IFN α 2a in cancer cells, preventing tumour invasion, metastasis, and angiogenesis (Li et al., 2015).

Additionally, the NGR peptide that specifically recognizes overexpressed cluster of differentiation 13 (CD13) in new tumour vessels, was also conjugated to TNF- α , to evaluate the PDC, NGR-hTNF. Enhanced concentrations of the pro-inflammatory cytokine were delivered by NGR-hTNF, provoking cell death in tumours (Arap et al., 2000). Subsequently, a combinatorial method was applied in the clinical trial phase II and NGR-hTNF was merged with doxorubicin, resulting in elevated anti-tumour activity in recurrent small cell lung cancer patients, as well as median survival of 3.2 months without disease progression (Gregorc et al., 2018).

Peptide drugs as cargo in PDC pose another novel therapeutic option and several studies have been published. For example, the anti-mitotic peptide medication monomethyl auristatin E (MMAE) was loaded into cRGD-functionalized lipophilic peptide micelles (cRGD-Lipep-Ms) that target integrins, which proved stronger tolerance in mice and efficiently minimized the development of colorectal tumours with negligible systemic toxicity (Qiu et al., 2018). The exendin-4 peptide imitating the glucagon-like peptide 1 (GLP-1) was coupled to the low molecular weight chitosan (LMWC), to generate the LMWC-exendin-4 conjugate, which demonstrated high hypoglycemic efficacy in a type 2 diabetes mouse model and is expected to be used as an orally administered drug (Ahn et al., 2013).

1.7.4 Current approved PDC for cancer therapy

Until now, the FDA has granted its authorization for cancer therapy to only two PDC, namely ^{177}Lu -DOTA-TATE and melflufen (Das et al., 2019; Fu et al., 2023). Even though melflufen was approved for the treatment of refractory multiple myeloma, its production was discontinued in 2021. This happened due to unsatisfactory results in the phase III clinical trials, in terms of not lowering the risk of mortality (Flanagan et al., 2022; Mateos et al., 2020).

Regarding radioactive PDC for imaging and diagnosis, some PDC have already been granted approval following the development of ^{111}In -DTPA-octreotide, comprising ^{68}Ga -DOTATATE, ^{68}Ga -DOTATOC, and ^{177}Lu -DOTATATE (Pauwels et al., 2018). At the present moment, several PDC are under evaluation at different stages in clinical trials, including ^{77}Lu -PSMA-617 for mCRPC, ANG1005 for several solid tumours and treatment, CBP-1018 for lung cancer, among others (Gong et al., 2021; Kind et al., 2022; Kumthekar et al., 2020; O'Sullivan et al., 2016).

1.8 G3 or G(IKK)3I-NH2 peptide

G(IKK)3I-NH2 (G3) is an α -helix peptide that was engineered as an analogue of the natural peptide, magainin. It belongs to a group of small synthetic peptides containing the sequence repeats of G(IKK)nI-NH2 ($n = 1-4$), which are characterized by their cationic and amphipathic attributes (Hu et al., 2011). Their amphipathic feature is caused by the 1:1 recurrence index of hydrophobic isoleucine and cationic lysine in their sequence (Figure 6). The N-terminus of the peptide is coated with a glycine, while an amide group occupies the C-terminus. This arrangement is expected to confer more resistance to peptidases and preserve α -helical formation (Tossi et al., 1997; 2000). The simple structure of G3, which is only 14 aa long, facilitates aa modifications at the side chains or in the N-/C-terminals, along with conjugation of other molecules, including fluorescent probes (Chen et al., 2016a; Chen et al., 2016b; Cirillo et al., 2020). Although G3 presents an undefined configuration in aqueous medium like other α -helical peptides, it acquires its archetypal α -helical structure upon contact with negatively charged mimicking membranes (Gong et al., 2019; Gong et al., 2020; Hu et al., 2011).

G3 has been proven to exhibit strong antibacterial effects. Gram-positive bacteria including, *Staphylococcus aureus*, methicillin-resistant *Staphylococcus aureus* (MRSA) and *Bacillus subtilis*; as well as gram-negative bacteria, like *Pseudomonas aeruginosa*, *Escherichia coli*, and extended spectrum beta-lactamase resistant (ESBL) *E. coli*, were all demonstrated targets of G3's antibacterial action in several studies. They also reported that G3 caused minimal cytotoxicity against mammalian host, such as human dermal fibroblasts and NIH 3T3 cells (Chen et al., 2015; Gong et al., 2019; Gong et al., 2020; Hu et al., 2011).

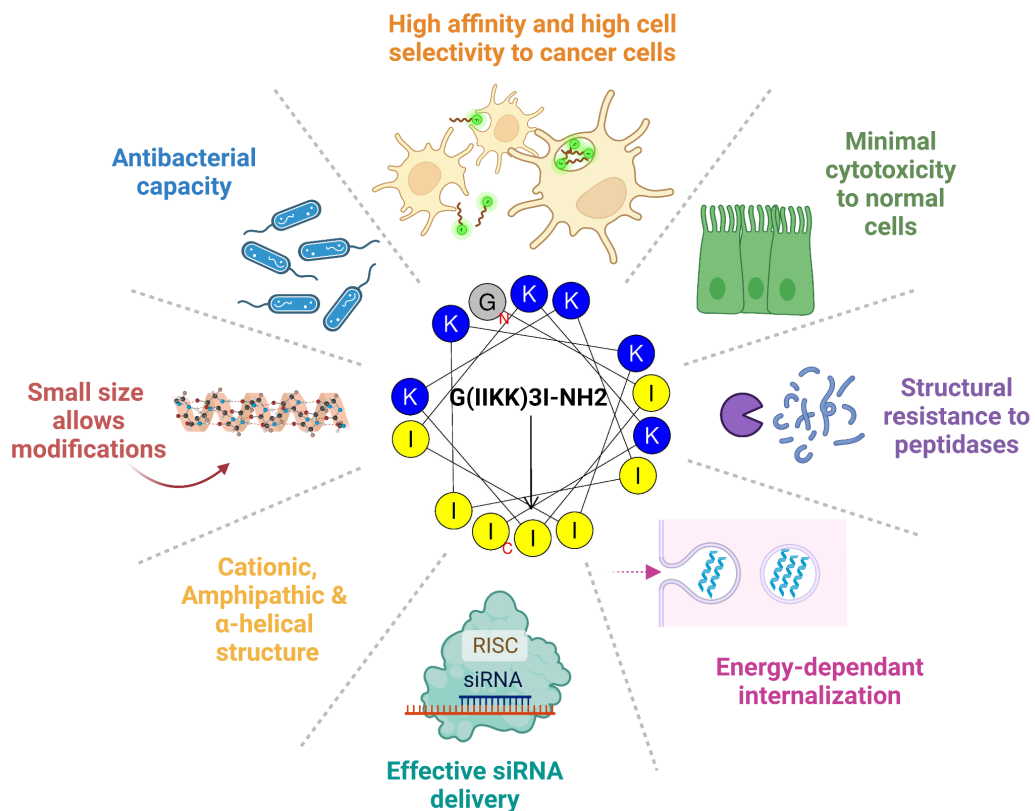


Fig. 6. G3 peptide main attributes. In the middle, a Schiffer-Edmundson wheel projection of the alpha-helical structure of the G(IKK)3I-NH₂ peptide is represented (created in <http://heliquest.ipmc.cnrs.fr/cgi-bin/ComputParams.py>) (Based on Hu et al., 2011). Blue circles indicate hydrophilic aa and yellow ones denote the hydrophobic aa. The principal features of G3 peptide are illustrated, from structural characteristics, potential uptake mechanism, key activity and drug delivery. Created with BioRender.com.

Further to its antimicrobial capacity, G3 revealed high affinity and elevated cancer cell selectivity, specifically towards HeLa, HL60 and HCT-116 cells (Chen, et al., 2014a; Chen et al., 2014b; Cirillo et al., 2021; Hu et al., 2011). Additionally, it was demonstrated that G3 induced an anti-proliferative effect on HeLa cell xenografts in nude mice displaying minor toxicity to the host (Chen et al., 2014b). Initially it was postulated that the selectivity of G3 to cancer cells could be attributed to the negative surface charges and high unsaturated lipid chains in the membranes (Hu et al., 2011; Chen et al., 2016). Yet, in our lab it was established using RNAi and scanning electron microscopy, that G3 is internalized into cells via energy-dependent endocytosis (Cirillo et al., 2021).

In congruence with the drug delivery potential demonstrated by other CPP, it was revealed that G3 could fusion with siRNAs and facilitate their transport and release into colon cancer cells, resulting in the downregulation of gene transcription. In addition, the siRNA targeting delivery was also achieved in cancer spheroids (Cirillo et al., 2021).

1.9 Project rationale

Currently, PCa has no cure and still represents a major health concern for men in most countries (Sung et al., 2021). The orthodox treatments for this disease have evolved in the last decade, shifting from monotherapy to a synergistic approach. For advanced PCa, the most common co-therapy is ADT plus a second generation ARSI and/or with taxane-based chemotherapy (Cornford et al., 2021). Commonly, 2 to 3 years receiving ADT/ARSI treatment, patients will develop underlying resistance and occurrence of CRPC (Klotz et al., 2015; Scher & Sawyers, 2005; Wadosky & Koochekpour, 2016). It has been reported that CRPC has an estimated survival period of 8 to 19 months (Vellky & Ricke, 2020). In fact, the vast majority of PCa death rates are predominantly an outcome of CRPC (Feldman & Feldman, 2001). The therapeutic management of CRPC and mCRPC has also improved in the last years and is moving forward to combinatorial approaches, including the development of next generation ARSI, PARP inhibitors, bone-specific Radium-223, cell-based sipuleucel-T vaccine and immune checkpoint inhibitors, however their impact on overall survival has been limited and

linked to additional mechanisms of resistance (Chen et al., 2022; Cornford et al., 2021; Kantoff et al., 2010; Liang et al., 2023).

Following this rationale, more research into selective drug delivery is crucial. PDC are emerging as an advanced targeted therapy that exploits small peptides for smart drug delivery directed to malignant sites (He et al., 2021; Wang et al., 2017). PDC have a wide range of advantages over conventional treatments including, reduced cytotoxicity to non-cancer tissues, enhanced drug efficacy, improved biocompatibility, excellent tumour infiltration, and control of drug unloading to target site (Fu et al., 2023; Heh et al., 2023; Hoppenz et al., 2020; Zhu et al., 2021).

Therefore, PDCs could be potentially employed to enhance the effectivity of standard drugs for PCa, like androgen inhibitors and taxanes; or to take them a step further to target altered signalling mechanisms in the disease (PI3K–AKT, DDR, WNT) or dysregulated epigenetic mechanisms, using molecular-based drugs (Bhat et al., 2015; Gong et al., 2023; Pfister & Ashworth, 2017). G3 is a CPP that has the key qualities to be used as a targeting unit in PDC, including small size, ease for modification and conjugation, the capacity of delivering small molecules such as siRNAs, and elevated cell selectivity towards some cancer cells (Chen et al., 2014a; Chen et al., 2014b; Cirillo et al., 2021; Hu et al., 2011).

Thus, in this PhD research project, G3 peptide was selected to investigate its therapeutic potential as part of PDC, specifically on the treatment for PCa. A comprehensive examination was conducted from different perspectives and presented in Chapters 3 to 5. Chapter 3 tests the hypothesis that the peptide can be internalized by PCa cells. Additionally, it is evaluated whether G3 has cell specificity towards PCa cells rather than benevolent prostate cells, and in which subcellular compartments G3 is internalized. In Chapter 4, the idea that scavenger receptors (SR) may actively participate in the receptor-mediated endocytosis of G3 in PCa cells is investigated. Chapter 5 analyses whether PDC using G3 as a drug carrier of lysine-specific demethylase 1 (LSD1) inhibitors, could be more effective than commercial LSD1 inhibitors for the treatment of PCa. Secondly, it studies G3's potential for siRNA delivery to PCa cells.

The following main aims were covered:

- To analyse the uptake and cell selectivity of G3 in prostate cancer cells in contrast to normal prostate cells
- To investigate the internal distribution of G3 in prostate cancer cells
- To evaluate if G3 is internalized by prostate cancer cells via receptor-mediated endocytosis and to analyse the role of scavenger receptors in the uptake mechanism
- To assess the effectivity of peptide drug conjugates using G3 as targeting unit and LSD1 inhibitors as payload against prostate cancer
- To analyse the targeted delivery of siRNA using G3 peptide in prostate cancer cells

CHAPTER 2

2. MATERIALS & METHODS

2.1 Cell culture

All sterile work was completed in a Esco Airstream Class II Biological Safety Cabinet. Cell passaging and live cell experiments were completed in the Esco laminar flow cell culture hoods. Briefly, hoods were UV irradiated for 20 minutes, then wiped down with 70% industrial methylated spirits (Fisher Scientific, #11412884).

2.1.1 Cell lines

The metastatic and androgen negative PC-3 cell line (#CRL-1435) and the androgen dependent LNCaP cell line (#1740) were acquired from American Type Culture Collection (ATCC). The normal prostate PNT2 cell line was a kind gift from Prof. Steve Winder. PNT2 cells were used at early passages (p10) in all assays.

2.1.2 Passaging

Prostate cancer cell lines and PNT2 cell line were cultured in Dulbecco's Modified Eagle Medium (DMEM) (GIBCO, Thermo Fisher Scientific, #11965092), complemented with 10% heat inactivated fetal bovine serum (FBS) (GIBCO, Thermo Fisher Scientific, #10082-147) and 1% antibiotics (GIBCO, Thermo Fisher Scientific, #15140122). Cells were held in an incubator (MCO-20AIC, Sanyo) at standard conditions (37 °C, 95% humidity and 5 % CO₂). Harvesting was made

at 70 to 80% of cell confluency by removing the media, washing them once with phosphate buffered saline 1X (PBS 1X) (GIBCO, Thermo Fisher Scientific, #20012-019) and adding 2 ml of Trypsin-EDTA (GIBCO, Thermo Fisher Scientific, #25300-096) for 5 min at 37 °C. The activity of Trypsin-EDTA was stopped by the addition of the double amount of DMEM and floating cells were seeded in T-75 flasks (Nunc, #156499) at a 1:10 or 1:12 dilutions.

2.1.3 Cryopreservation protocol

Batches of frozen prostate cancer and non-cancer cells were prepared at low passages. For the freezing procedure, the cells were trypsinized and the cell suspension was collected into a 15 ml tube (BD Falcon, #352096), and centrifuged at 130 rpm for 5 min in a benchtop centrifuge (Eppendorf, #5427000060). Next, the cellular pellet was carefully mixed in 1 ml of freezing media, which consisted of 7% of sterile dimethyl sulfoxide (DMSO) (Santa Cruz, #sc-358801) in FBS. Once resuspended all the content was transferred into a cryovial (Starlab, #E3110-6112). The concentration of cells in each cryovial was approximately 1×10^6 cells/ml. All cryovials were carefully labelled with the number of passage and cell type, and kept in a freezing box (Fisher Scientific, Corning 432001, #15552771) at -80 °C for at least 24 hours. Afterwards, the cryovials were relocated to the liquid nitrogen tank at -180 °C for longer periods of storage.

2.1.4 Thawing protocol

The frozen cryovials were transported from the liquid nitrogen to the cell culture lab in a freezing box. Before starting the thawing process, a sterile 15 ml tube was filled with 4 ml of pre-warm complete media. The frozen cryovial was thawed in a 37 °C water bath for a maximum of 2 min, followed by a thorough cleansing of the cryovial with 70% ethanol and detergent (Starlab, Chemgene HLD4L, #XTM309) to

avoid any contamination. The cryovial was opened and the cellular content was gradually dispensed into the 15 ml tube with the pre-warm complete media. The cells were spun in the centrifuge at a speed of 130 rpm for 5 min. The pellets were resuspended with 5 ml of full media and placed into a T-25 flask (Falcon, #353014). The flasks were maintained in the incubator at 37 °C, with 5% of CO₂ and cell attachment was monitored the next day. Cells were split into T-75 flasks when high confluency was reached.

2.2 Seeding multi-well plates for High Content Screening

Cells were seeded manually using a multichannel pipette or by employing a Microplate dispenser (Multidrop Combi, Thermo Fisher Scientific) into clear 96-well plates (Greiner Bio One, #655088) or 384-well plates (Perkin Elmer, #6007460). Optimal seeding concentrations were chosen, depending the cell type and the days required for each experiment. Cell counts per ml were quantified using the Countess II Automated Cell Counter (Thermo Fisher Scientific). To accomplish this, the counting slide (Invitrogen, Thermo Fisher Scientific, #C10313) had 10 µl of a 1:1 mixture of cell suspension and Trypan Blue Solution (Invitrogen, Thermo Fisher Scientific, #T10282) and was inserted into the cell counter. The optimal cell density selected for LNCaP cells was 6,500 cells per well for 96-well plates and 3,500 cells per well for 384-well plates. PC-3 and PNT2, cell density for 96-well plates was 5,000 cells per well and for 384-well plates was 2,500 cells for each well. Before placing in the incubator, plates were incubated for 20 min at room temperature (RT) and then incubated at 37 °C in the cell incubator. Sterilizing of the multidrop was done prior and after each experiment, rinsing the 8 channels of the cassette with water, then 70% ethanol and then sterile distilled water.

2.3 Fixing and staining procedure

Living cells in plates had their media discarded, followed by an incubation of 15 min with 4% formaldehyde (Sigma-Aldrich, #50-00-00) in 1xPBS and 2 µg/ml

Hoechst 333420 (Invitrogen, Thermo Fisher Scientific, # 62249). To prevent photobleaching, the cells were incubated and shielded from light during the fixation procedure. After removal of the fixation solution using either the Plate washer (BioTek, ELx405 Select), or with the multichannel pipette (for the LNCaP cells, which were easily detached between washes), plates were washed twice with 1X PBS using a Multidrop bulk liquid handling dispenser (Thermofisher).

For the G3 peptide uptake experiments, Flash Phalloidin Red 594 (BioLegend, #424203) was used as an actin staining at a concentration of 1:100 in PBS 1X. The cytoplasmic staining was done for 30 min in the absence of light followed by two washes with PBS 1X. Fixed plates were covered with foil and stored at 4 °C until imaging.

2.4 High Content Screening (HCS)

Plates were left at room temperature for at least 15 minutes before acquiring the images in the High Content Microscope (ImageXpress Micro, Molecular Devices) using the MetaXpress Software (version 6.2.3.733, Molecular Devices). The exposure time and imaging settings were selected depending on the number of fluorescent channels and intensity of the fluorescent molecules. The objective used for all plates was 20X and 6 or 9 sites per well were collected, depending upon cell density. The exposure time for the DAPI/Hoechst channel ranged from 50 to 150 ms and for all the other channels ranged from 1,000 to 3,000 ms depending on the intensity of each fluorophore. The target maximum intensity was set between 1,000 to 3,000 ms.

2.5 High content custom module analysis

Images were processed using MetaXpress software (version 6.2.3.733). Custom modules were created using the Multi Wavelength Cell Scoring (MWCS) algorithm, to measure cell number and the cellular integrated intensity (IIC) or average intensity per well. The cell number was quantified as objects in

the blue channel by defining the minimum and maximum nuclei sizes of each prostate cancer cell type.

Average intensity refers to the mean of the total object's pixel intensities, while integrated intensity denotes the sum of all the intensity values for all pixels included in an item. The background fluorescence value was selected in each experiment and removed from the scored values.

To avoid measuring clumps of non-specific staining, algorithms were developed using the Custom Module Editor (CuME) (version 2.0.33.3, Molecular Devices). The CuMEs were designed by creating masks of the cells, peptide, and nuclei objects, as presented in Figure A1 in the Appendices. The detailed analysis script of the CuME is included in the Appendix A. This approach enabled the identification of non-specific clumps by assigning a size threshold in the wavelength of interest (green), thereby generating a "clump mask". The positive pits in the green channel were defined using the "transfluor objects" tool, creating a "FITC pits" mask. Subsequently, the "logical operations" tool was applied to remove the "clump mask" from the "FITC pits" mask, creating a new mask designated as the "FITC G3" mask. Finally, to obtain the IIC values, the positive puncta or pits inside the cells were selected as the objects to measure in the "FITC G3 mask".

To ensure the accuracy of clump removal using the CuME, some of the images were visually inspected, although the process was predominantly automated. Challenges such as overlapping cells and varying intensities of staining were addressed by refining the algorithm parameters based on these visual inspections.

2.6 Peptide internalization assay

The cellular internalization of the fluorescein isothiocyanate (FITC) labelled G3 peptide was investigated to compare prostate cancer cells versus non-cancer prostate cells. LNCaP, PC-3 and PNT2 cells were seeded into 384 well plates

in triplicates and incubated at 37 °C with 5% CO₂ for 24 hours. The stock of FITC-labelled G(IKK)3I-NH₂ peptide (FITC-G3) (GL Biochem, #874564) was prepared in molecular biology grade water (Sigma, Life Science, #W4502-1L). Cells were treated with 4 µM FITC-G3 per well for 24 hours. Cells were fixed and stained as previously described and images acquired using the ImageXpress Micro.

2.7 Anti-proliferative activity

Briefly, LNCaP, PC-3, and normal PNT2 prostate cells were added to 384 well plates in triplicate one day before treatment. A concentration curve was created by incubating the cells with the following concentrations of FITC-G3: 0.5 µM, 1 µM, 2.5 µM, 5 µM, 10 µM, 15 µM, 25 µM and 50 µM. After 24 hours incubation, the plates were fixed and stained as explained in section 2.3. The anti-proliferative activity was analysed by measuring cell survival using HCS, by automatically counting cells attached to the plates at the end of the assay. Cell populations were normalised to the non-treated cells and all experiments were done once with 3 replicates for each condition.

2.8 Prostate cancer spheroids

LNCaP and PC-3 cells were seeded in a suspension of 1×10^5 cells/ml in 20 ml in a Nunclon Sphera 96 U-shape plate (Thermo Scientific, #174925), using the Multidrop. The plate was centrifuged at 1,500 rpm for 10 min at 4 °C and placed in the incubator for 10 to 14 days. Spheroid generation was monitored daily after the third day until the form and size was homogenous in each well. FITC-G3 was added at 4 µM per well for 24 hours before fixing and staining with Hoechst and Red Phalloidin. PC-3 spheroids were visualised using ImageXpress Micro and the LNCaP spheroids by using an AMG EVOS FL inverted microscope.

2.9 Immunolabeling of endosomal compartments

Endosomal antibodies were optimized using HCS to examine the internal cellular distribution of FITC-G3 in prostate cancer cells, followed by confocal microscopy. Cells were seeded in triplicates in a 384 well plate and once the cells were attached, the plates were fixed and stained with Hoechst. Plates or dishes (for confocal analysis) were blocked with bovine serum albumin (BSA) 1% for 30 min. The following early endosomal primary antibodies were used at 1:100: anti-EEA1 (#9367S) and anti-Rab5 (#C8B1) from Cell Signalling Technology (CST). Two late endosomal primary antibodies were used: anti-Rab7 (CST, #9367S) at 1:100, and anti-CD63 (Novus Biotechnne, #NBP2-42225) at 1:200 concentration. Anti-LAMP1, (antibody D2D11 CST, #9091) was used as a lysosomal marker at a dose of 1:200. Fixed cells were blocked then incubated overnight at 4 °C with the primary antibody. Thereafter, cells were washed twice with BSA 1% and incubated for 2 hours in the dark using either anti-rabbit IgG (H+L), Fab2 Alexa Fluor 594 (CST, #8889) anti-mouse IgG (H+L) or Fab2 Alexa Fluor 594 (CST, #8890). Both secondary antibodies were used at 1:500 concentration. Finally, plates or dishes were rinsed 3 times with PBS 1X and stored in the cold room.

2.10 Confocal Microscopy

The cellular uptake and internal distribution of the FITC-G3 peptide was assessed using confocal laser scanning microscope (CLSM, Nikon Instruments Europe B.V.) and the images of the z-stacks were obtained using the NIS Element software.

Samples were imaged in the 60X objective of the Nikon 2 Confocal Microscope. Images were acquired using 359 nm, 488 nm and 594 nm or 633 nm wavelengths. Microscopy was completed using the following settings and were applied to all images: control by 1.1, size 1024 and pinhole 1.2 AU. The high voltage (HV) and offset settings were determined in every biological repeat to adjust the light in the detection of the image. A set of 6 to 12 z-stacks were obtained for each control and treated samples. The size of a single z-stack was

assigned as 0.15 μm . For the FITC-G3 internalization experiments in PCa cells, 10 fields of view (FOVs) were analysed per condition, while in the colocalization analyses, 6 FOVs were examined.

2.10.1 Samples preparation for high resolution imaging

Cells were passaged and counted as usual and a suspension of 9×10^5 cell/ml was prepared. An amount of 400 μl of cell suspension was added into the interior section of a 35 mm high μ -Dish (Ibidi, #81156). The μ -Dishes were left for 20 min at RT without disturbing to let the cells distribute evenly on the surface of the well. After cells were attached, 1.5 ml of complete DMEM was added to each μ -Dish. Dishes were maintained in the cellular incubator until required.

2.11 Cell selectivity validation analysis

Confocal microscopy was used to validate the cellular uptake of FITC-G3 of prostate cancer cells (LNCaP and PC-3) versus normal prostate epithelial cells (PNT2) as explained in previous section. Cells were attached to the μ -Dishes one day prior to the assay, FITC-G3 was added to each μ -Dish at a final concentration of 4 μM and incubated overnight at 37 $^{\circ}\text{C}$, followed by standard fixation and phalloidin staining. After imaging, the superimposed images of 10 Z-stacks were analysed using ImageJ. Cell objects were selected using the cytoplasm staining of Red phalloidin by using the region of interest (ROI) selection tools, and the FITC integrated intensity values were measured per image within each cell object. The average of the integrated intensity of 3 random areas of each image without any cells were considered as background fluorescence and subtracted from the total integrated intensity values. The average of each integrated intensity values per image was calculated and data was normalised as percentages.

2.12 Co-culture assay

A co-culture experiment was designed to analyse the uptake selectivity of FITC-G3 peptide in CD44+ cell populations. An antibody against CD44 (CST, #3570S) was tested in PC-3 and PNT2 cells using HCS. Then, a co-culture of PC-3 and PNT2 cells was prepared in a 1:1 ratio and seeded into an Ibidi μ -Dish. Approximately a total of 6,000 cells were added per dish and left in the incubator for one day. FITC-G3 was added to the co-culture at a final concentration of 4 μ M and incubated for 24 hours at 37 °C, before fixing with 4% formaldehyde and nuclear staining solution. The dishes were washed with PBS 1X several times and then blocked with BSA 1% solution for 30 min. Then, the dishes were incubated with anti-CD44 for 24 hours at 4 °C, without adding any permeabilization reagent. The secondary antibody anti-mouse IgG (H+L), Fab2 Alexa Fluor 594 was prepared at 1:1000 dilution in BSA 1%. The dishes were rinsed 3 times with BSA 1% and the secondary antibody solution was added for 2 hours incubation in the absence of light. Lastly, the samples were washed twice with BSA 1% and 3 times with PBS 1X and stored at 4 °C until imaging by confocal microscopy. The maximum projection of all the Z-stacks were analysed using ImageJ. The total number of cells and the percentage of CD44+ and CD44- cells were calculated per superimposed image. Data was analysed as the percentage of FITC+/CD44+ and FITC+/CD44- cell populations.

2.13 Colocalization analysis of endosomal markers

The same antibodies used in section 2.9 were selected as early and late endosomal markers to analyse their degree of colocalization with FITC-G3 in PC-3 and LNCaP cells. Cells were plated in μ -Dishes as explained in section 2.10.1 and FITC-G3 was added at 4 μ M at 37 °C for different time expositions, depending on the endosomal compartment that was going to be assessed. In the samples for early endosomes labelling, the peptide was incubated for 2 hrs. For the late endosomes labelling the peptide was added for 6 hrs. Dishes were exposed to the peptide for a total of 18 hrs for the lysosomes labelling assessment.

Transferrin (TF) (Biotium, CF 568) was selected as a positive control of endocytosis and Dextran (DXT) was tested as a marker for macropinocytosis. Positive control and negative control cells were treated with 4 μ M FITC-G3 for a total of 1 hr and 30 min incubation. TF was given to the cells at 5 μ g/ml for 22 min, then the cells were exposed to FITC-G3 for 1h and 8 min. Negative control cells were treated with DXT at 0.25 μ g/ml for 40 min incubation after the cells have been incubated with FITC-G3 for 50 min. Samples were imaged using Confocal Microscopy as explained on section 2.10.

The images were analysed using ImageJ with the Colocalization Colormap plugin, to measure colocalization ratio of both channels (Figure 7) (Gorlewicz et al., 2020; Jaskolski, Mulle, & Manzoni, 2005). All the z-stack images were superimposed using the Maximum projection option in ImageJ. Then, the ROI were determined in each Maximum intensity projection (MIP) image by selecting the area within cells, removing fluorescent debris from the image. The threshold values for both channels (red and green) were defined using the Jacob ImageJ plugin that allows to generate a mask of the area of interest. The Colocalization Colormap algorithm measures the network of correlation between the pixels of the two images using a qualitative and a quantitative approach. It automatically applies the following mathematical formula to estimate the normalized mean deviation product (nMDP) that gives values from -1 to 1:

$$nMDP = \frac{(A_i - \bar{A})(B_i - \bar{B})}{(A_{max} - \bar{A})(B_{max} - \bar{B})}$$

A_i/B_i = values of particular "i" pixel
 \bar{A}/\bar{B} = means
 A_{max}/B_{max} = highest pixel intensities
in the given A and B signals

In parallel, the Colormap plugin computes the index of correlation (Icorr), that indicates the percentage of colocalized values according the nMDP. The mean of all Icorr values per condition were calculated for further statistical analysis.

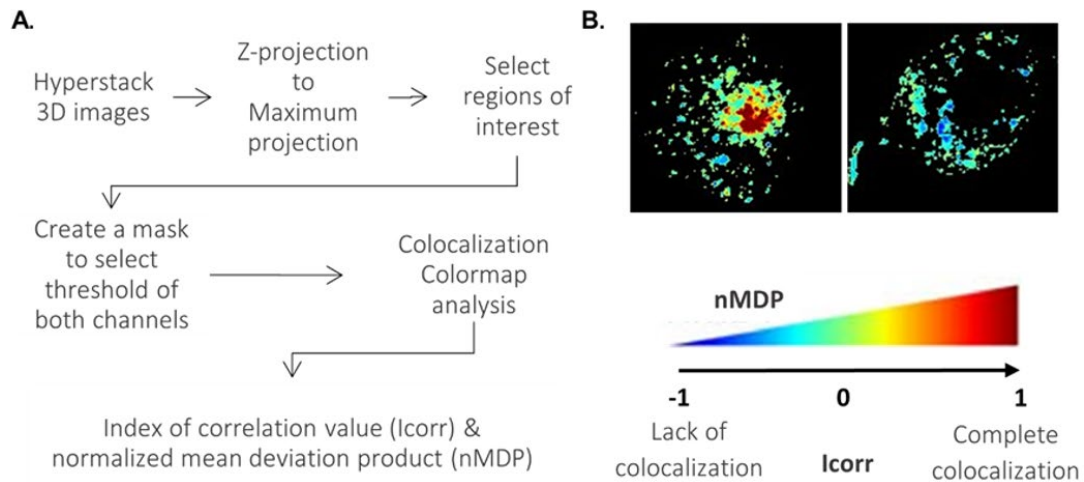


Fig. 7. Colocalization analysis. (A) Workflow diagram of the colocalization steps using z-stacks to create MIP 2D images. (B) Representative images show the nMDP values of a PC-3 prostate cancer cell displaying high colocalization of FITC-G3 and transferrin (left), as well as low colocalization of FITC-G3 and dextran red (right). The nMDP colour scale is represented, indicating the Icorr colocalization values, which range from -1 to 1.

2.14 Macropinocytosis inhibition

Macropinocytosis was blocked using Ethylisopropyl amiloride (EIPA) (Sigma Aldrich, # A3085). Cells exposed to FITC-G3 at 4 μ M for 1hr and 40 min were used as control. DXT was used as an indicator of activated or inactivated macropinocytosis. Cells were incubated with EIPA at 25 μ M for 30 min at RT, followed by the addition of FITC-G3 at 4 μ M for 1 hr incubation at RT and DXT was added at 0.25 mg/ml for 40 min before fixing. Samples were imaged by confocal microscopy as described in section 2.10. The FITC and DXT integrated intensity values of the confocal images were determined using ImageJ. The average of the background measurements were calculated and deducted from the integrated intensity values.

2.15 Silencing of gene expression using siRNAs

A reverse transfection protocol was optimized using siGLO Red (Dharmacon, #D-001630-02-20) as a fluorescent transfection indicator and all experiments were done in triplicates in 384-well plates. The ubiquitin B (UBB) pooled siRNA (siGenome, #M-013382-01-0005) was selected as a functional positive control,

and a combination of non-targeted single siRNAs (siGenome siRNA 2, #D-001206-14-05; siGenome siRNA 3, #D-001210-03-20; ON-Target siRNA 2, #D-001810-02-05; ON-Target siRNA 4, #D-001810-04-20) were used as negative controls.

All siRNA stocks were prepared at 150 nM in molecular grade water to achieve a final concentration of 30 nM per well. The transfection solution was prepared maintaining a proportion of 0.06 μ l of DharmaFECT 1 (DF1) (GE, Dharmacon, #T-2001-03) + 4.94 μ l of basal DMEM for each well. Either the siGLO or the siRNAs were complexed in a 1:1 ratio with the DF1 solution and incubated for 25 minutes at RT. Next, 10 μ l of DF1-siRNA complex solution was added to each well. Prostate cancer cells were prepared at their respective optimal seeding concentration using DMEM with 10% FBS but without antibiotics. To achieve a total volume of 25 μ l, 15 μ l of cell suspension were dispensed in every well. Plates were left at RT for 30 min and then kept in the cell incubator for 48 hrs.

All the control, primary and secondary siRNA knockdowns were done exactly the same as for the siGLO transfection except that after 48 hours, FITC-G3 was added to the siRNA treated wells at a final concentration of 4 μ M, and the assay was left for 72 hrs in the cell incubator. The positive control of the siRNA knockdowns was determined by assessing the decrease of FITC-G3 internalization after silencing the following set of genes that are important in endocytosis: Myosin Vb (MYO5B) (siGenome, #M-023431-01), Myosin Vc (MYO5C) (siGenome, #M-031960-01), Myosin Va (MYO5A) (siGenome, #M-019321-01) and Caveolin 1 (CAV1) (siGenome, #M-003467-01) (Table 3).

Table 3. Endocytosis-related siRNA controls

Gene symbol	Name	Cat. number	Format	Gene ID	Other names
MYO5A	Myosin VA	M-019321-01	Pooled	4644	GS1; MYO5; MYH12; MYR12
MYO5B	Myosin VB	M-023431-01	Pooled	4645	MVID1; PFIC10; DIAR2
MYO5C	Myosin VC	M-031960-01	Pooled	55930	NA
CAV1	Caveolin 1	M-003467-01	Pooled	857	CGL3; PPH3; BSCL3; LCCNS; VIP21; MSTP085

*NA not applicable

A primary KD in High Content Screening was done using a siGenome siRNA library targeting scavenger receptors (SR), as listed in Table 4. SRs were selected based on publications. Hits were defined where the FITC integrated intensity values were significantly reduced when compared with the integrated intensity values in the siRNA non-targeted controls. The FITC integrated intensity values were normalised to percentages using the siRNA non-targeted controls. The decrease of the FITC integrated intensity percentages was taken as a measurement of peptide internalization in the cells. A repeat high content KD screenings were done to validate the chosen SR hits. Experiments were done in triplicates and with 3 biological repeats.

Table 4. Scavenger receptor siRNA library

Gene symbol	Name	Cat. number	Format	Gene ID	Other names
CXCL16	SR-G1	D-007876-01	Single	58191	CXCLG16; SR-PSOX; SRPSOX
OLR1	SR-E1	D-003804-03	Single	4973	LOX1
SCARB2	SR-B3	D-012087-01	Single	950	AMRF; EPM4; LGP85; CD36L2; HLG85; LIMP-2; LIMP2; SR-BII
CD163L1	SR-I2	D-008024-01	Single	283316	WC1; M160; CD163B; SCAR12
CD6	SR-I4	D-007850-01	Single	923	TP120
MARCO	SR-A6	D-008025-01	Single	8685	SR-A6; SCARA2
STAB1	SR-H1	D-014103-01	Single	23166	FEX1; FEEL-1; FELE-1; SCARH2; STAB-1; CLEVER-1
SCARA3	SR-A3	D-013241-01	Single	51435	CSR; APC7; CSR1; MSLR1; MSRL1
CD36	SR-B2	D-010206-03	Single	948	FAT; GP4; GP3B; GPIV; CHDS7; PASIV; SCARB3; BDPLT10
MSR1	SR-A1	D-008035-01	Single	4481	CD204; SCARA1; SR-A; phSR1
CD163	SR-I1	D-007847-01	Single	9332	M130; MM130; SCAR11
CD5	SR-I3	D-007848-02	Single	921	T1; LEU1
SCARF2	SR-F2	D-017502-01/ M-017502-01	Single/ Pooled	91179	NSR1; SREC2; VDEGS; SREC- II; SRECRP-1
SCARB1	SR-B1	D-010592-01/ M-010592-01	Single/ Pooled	949	CLA1; SRB1; CLA-1; SR-BI; CD36L1; HDLQTL6
SCARF1	SR-F1	M-017405-00	Pooled	8578	SREC-I
COLEC12	SR-A4	M-013240-01	Pooled	81035	CLP1; NSR2; SRCL; SCARA4
CD68	SR-D1	M-011236-01	Pooled	968	GP110; LAMP4; SCARD1
STAB2	SR-H2	M-015260-01	Pooled	55576	FEX2; HARE; FEEL2; FELL2; FELE-2; SCARH1
SCARA5	SR-A5	M-018056-02	Pooled	286133	Tesr; NET33

2.16 Western Blot for siRNA knockdown validation

The siRNA knockdown was adapted to T-75 flasks instead of 384-well plates and repeated 3 times. One T-75 flask was used per treatment and non-targeted controls. A mix of a 1:1 ratio of 500 µl of siRNA (150nM) and 500 µl of DF1 were incubated at RT for 25 min and subsequently transfer to a sterile T75 flask to cover the whole surface. Cells were harvested and centrifuged at 130 rpm for 5 min. Pellets were dissolved in 1.5 ml of DMEM with 10% FBS without antibiotics. The 1.5 ml of cell suspension were dispensed to each of the T-75flask and incubated at RT for 30 min. Cells were maintained in the incubator for 3 days ready for protein extraction.

2.16.1 Buffers and solutions

Buffers and solutions that were required for western blot (WB) were prepared as follows. Run Buffer 1X was diluted in sterile distilled water from 10X stock Tris/Glycine/SDS Buffer (Bio-rad, #1610772). The 10X TBS (Tris-Buffer Saline) was prepared with 2.42g TRIS (20mM), 8g NaCl (137mM) and 3.8ml HCl (1M) in 1 L of distilled water maintaining a pH of 7.6. A 5% BSA blocking solution was prepared using 1X TBS with 0.1% Tween 20 detergent (TBST) (Thermo Scientific, #85114) and mixed in a tube roller for around an hour before using. A 0.1% (w/v) Ponceau solution was prepared under the fume hood with 5% (v/v) glacial acetic acid in distilled water.

2.16.2 Protein extraction of whole cell lysates

T-75 flasks at 80% confluency were trypsinized and centrifuged at 130 rpm for 5 min. The cellular pellet with approximately 7×10^6 cells/ml was resuspended in 1 ml of lysis solution composed of Radio-Immunoprecipitation Assay (RIPA) buffer (SERVA, #39244.02) and Complete Mini protease inhibitor cocktail solution EDTA-free (Roche, #11836170001). Tubes were incubated on ice in the shaker for 30 min.

Samples were centrifuged at 14,000 rpm at 4 °C for 20 min. The clear lysates were aliquoted on ice into sterile tubes and kept at -20 °C.

2.16.3 Protein quantification

The protein lysates were quantified using the Bradford assay. Serial dilutions of BSA were prepared in PBS 1X using Quick Start BSA Standard (BIO-RAD, Cat. #5000206) following manual instructions as shown in Table 5. The Quick Start Bradford 1X Dye Reagent (BIO-RAD, Cat. #5000205) was kept at RT for 1 hour before use and 250 µl were added to each well in triplicates of a 96 well plate. Next 5 µl of either BSA dilutions, or Blank or protein lysates were added respectively to each well and incubated for 30 min at RT in the shaker. The absorbance was measured at 595 nM in the Skanti software using a Microplate Reader (Varioskan Flash™, Thermo Fisher Scientific).

Table. 5 BSA standard dilutions

Dilution	Concentration (µg/ml)
1	2000
2	1500
3	1000
4	750
5	500
6	250
7	125
8	0

The quantification analysis of the lysates was done in Excel. The average of the 3 absorbance values of all samples was calculated and the average of the Blank corresponding to background values was

deducted from all. A BSA standard curve was created, where the linear trendline and R equation were calculated to substitute the “x” for the average absorbance values of each unknown sample, to obtain the protein concentration per well. If required, the concentrations were multiplied by the dilution factor to calculate the final protein concentration in each tube.

2.16.4 Samples preparation

The whole lysates were thawed on ice and then diluted in RIPA buffer at a concentration of 20 µg/µl. The Laemmli buffer 2X (SERVA, #42526.01) plus 10% β-mercaptoethanol (Sigma, #M3148-25ML) was prepared in the fume hood. The required volume of protein lysate and Laemmli+ β-mercaptoethanol buffer were mixed together to achieve a final concentration of 10 µg/µl. Tubes were heated at 95 °C for 5 min on a hot block (Techne, Dri-Block, #DB100/2). The samples were centrifuged at 6,000 rpm in a mini centrifuge (Fisher Scientific, #12-006-901) for a duration of 1 to 2 min and stored at – 20 °C until required.

2.16.5 Gel run

Lysate samples and the EZ run protein ladder (Fisher Scientific, #10638393) were thawed on ice. The Mini Protean TGX precast gels (Bio-rad, #456-1093) and the Mini Protean Tetra System (Bio-rad, #1658004EDU) were used for all WBs.

The running cassette was assembled with 2 gels and the inner chamber was filled up with 1X Running Buffer (RB), avoiding leaking from the base. The comb was gently removed from the pre-made gels and the samples were loaded into the wells with a P10 micropipette. The protein ladder was loaded into the first lane at 5 µg/µl concentration. A linear range between the house keeping protein (HKP) and the target protein was defined by loading a series of

increasing concentrations of lysates up to 100 µg. The gels were run at 100 V for 15 min and subsequently at 120 V for approximately 1 hour and 30 min.

2.16.6 Blot transfer run

The gels were taken out of the running unit and carefully separated from the plastic holder with a lever (Bio-Rad, #956-0000). Gels were maintained humid during the transfer manipulation. The Trans-Blot Turbo Transfer System (Bio-Rad, #1704150) was used for all the transfers from the gel to the membranes. The Trans-Blot Turbo Mini 0.2 µm Nitrocellulose Transfer Pack (Bio-Rad, #1704158) was opened and the anode stack was placed in the cassette. The gel was gently laid on top of the blot and a wet 15 ml tube was used instead of a roller to eliminate any bubbles. The electrode stack was positioned on top of the gel, the cassette was closed and inserted into the transfer device. All transfers were run at 25 V, a constant current (const A) of 1.3 for 7 min.

2.16.7 Ponceau staining and blocking membrane

The blots were recovered and moved to a plastic container and covered with 0.1% Ponceau solution for 5 to 10 min incubation in a shaker at RT. The stacks and gels were discarded and the transfer cassettes were rinsed with distilled water. The 0.1% Ponceau solution was recovered in a 50 ml tube for re-use. The Ponceau staining of the blots was done to verify the presence of the proteins of the whole lysate in each lane by the observation of clear red bands. This step also allowed to label each blot accordingly with pencil and to cut the top and side-edges of the membranes. The blots were rinsed with distilled water and subsequently washed 3 to 4 times with 1X TBST for 5 to 10 min at RT. Next, the blots were moved to a 50 ml tube

containing 15 ml of a 5% BSA-TBST blocking solution and left to incubate on a tube roller for one hour at RT.

2.16.8 Antibody probing

The blocking solution was removed from the tubes and the blots were washed in 3 intervals of 5 to 10 min with TBST 1X in a roller, and at RT. The following primary antibodies were utilized and diluted in 3 ml of blocking solution: anti-SCARF1 (Proteintech, #13702-AP) 1:1000, anti-SCARF2 (Novus biologicals, #NBP1-8340) at 1:800, anti-SRB1 (Origene, #TA301489) at 1:1000, anti-MYO5C (Antibodies.com, #A7597) at 1:1000 and anti-GAPDH (Origene, #TA802519) at 1:1200 as HKP. The blots were carefully transferred to a new 50 ml tubes with the primary antibody solution and incubated overnight in a roller at 4 °C.

The primary antibody solution was removed and the membranes were washed 3 times with 1X TBST for 5 to 10 min in a roller at RT. The secondary antibodies goat anti-Rabbit 680 (LICOR, IRDye680RD) and goat anti-Mouse 800 (LICOR, IRDye800CW) were diluted at 1:10,000 concentration in TBST 1X. The blots were incubated in the dark with the 10 ml of secondary solutions for 2 hours at RT. The blots were exposed to four last washes with 1X TBST at RT for 5 to 10 min in a roller. Finally, the blots were dried out at RT in white wipes (Kimberly-Clark Kimcare, #3020, and then stored protected from the light until imaging.

2.16.9 Blot imaging

The blots were imaged using Image Studio software (version is 5.2.5) and LICOR Odyssey XF equipment. The blot was situated on the imaging tray with the protein side-up and inserted in the imaging chamber. In the programme, the western option was chosen, the 700 and 800 channels were selected and the standard time integration was

set at 2. Settings were adjusted according each blot and images were exported as TIFF images.

2.16.10 Normalization and semi-quantification

In order to semi-quantify the target protein bands in each membrane, the HKP was used as a reference for normalization following Licor protocol. Initially, a WB of a serial dilution of each protein lysate was performed to calculate the linear range of the HKP and the target protein. The overlapping of both linear range was considered as the working linear range and the median of each protein concentration was selected as the ideal concentration for all WBs.

2.17 Colocalization analysis of scavenger receptors

A second colocalization analysis was performed using the Colocalization Colormap plugin in ImageJ and the same principles as explained in section 2.13. To test the degree of colocalized signals between FITC-G3 and the next antibodies of scavenger receptors: anti-SRB1, anti-SCARF1 and anti-SCARF2, Transferrin (TF) and Dextran (DXT) were used as positive and negative controls respectively. Cells were treated with FITC-G3 at 4 μ M for a total of 85 min and then fixed and labelled as described previously. Only DXT control was treated with FITC-G3 (4 μ M) for 1 hour and then exposed to DXT for 40 min. The mean of the Icorr values of 6 replicates were analysed per condition.

2.18 Peptide drug conjugates analysis in prostate cancer

A series of 5 peptide drug conjugates (PDC) were produced using click chemistry to bind customised LSD1 inhibitors to the C-terminal of the G3 peptide, by Dr Philip Eduard Lane, under the supervision of Dr Simon Turega from Sheffield Hallam University. The new LSD1 inhibitors were designed by modifying the TCP scaffold by attaching alkyne or azide tags in the para or meta positions as illustrated in Figure 8. In Table 6, the peptide drug conjugates employing LSD1 inhibitors, named PDC-1 to 5 are listed and associated to their

type of LSD1 inhibitors, type of modification and inhibitory activity (IC₅₀), reported by Phillip Lane in his PhD thesis. PDCs 1 to 5 were evaluated in this thesis.

Table 6. Peptide drug conjugates using G3 and modified LSD1 inhibitors

Assigned name	Previous name	LSD1 inhibitor	Modification	*IC ₅₀ (μM)
PDC-1	PP1	Probe 4	Alkyl-alkyne	46
PDC-2	PP2	Probe 5	Alkyl-azide	14 ± 2
PDC-3	PP3	Probe 6	Alkyl-azide	22 ± 14
PDC-4	PP4	Probe 7	Alkyl-azide	8 ± 3
PDC-5	PP5	Probe 8	Alkyl-azide	5 ± 1

*The LSD1 inhibitory values (IC₅₀) correspond to the LSD1 inhibitors without conjugation of the peptide.

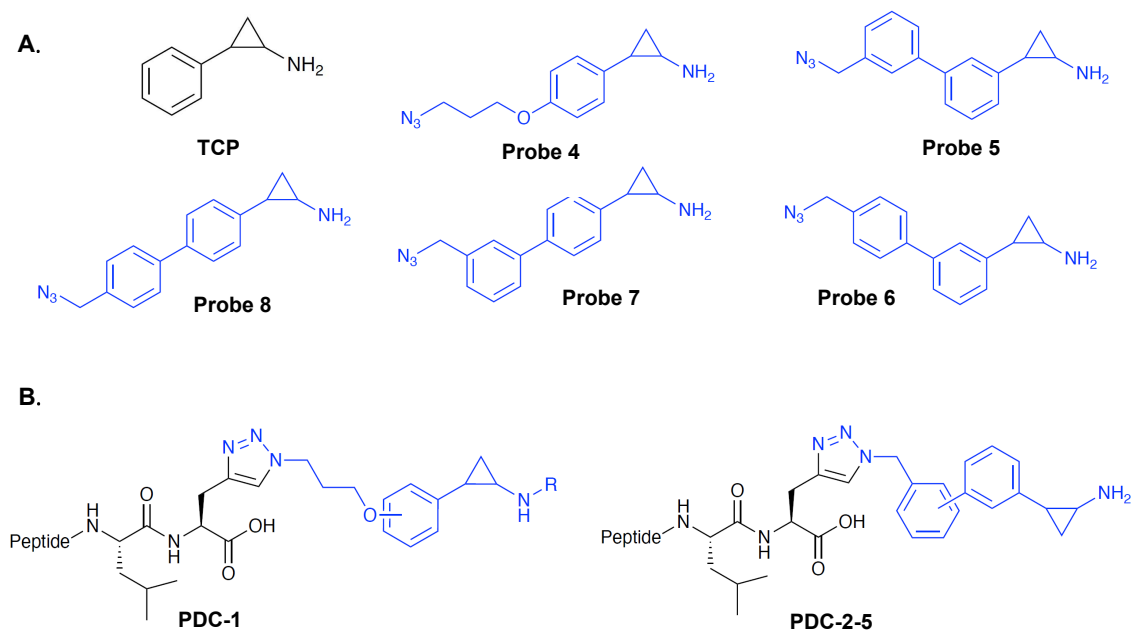


Fig. 8. Chemical structure of peptide drug conjugates. (A) TCP (black) or modified LSD1 inhibitors 4 to 8 (blue) chemical representations. (B) Chemical structure of peptide drug conjugate with LSD1 inhibitors plus alkyne tag (left) and peptide drug conjugates with LSD1 inhibitors plus azide tags (right). Inhibitors are shown in blue. Image adapted from Lane, 2021.

2.19 Cell viability assay of PDC

The cell number was assessed after PDC-1 to 5 using trans-2-phenylcyclopropylamine hydrochloride (TCP) (Sigma, #P8511) as positive control. A pilot assessment was conducted in LNCaP and PC-3 using increasing concentrations of TCP from 100 μ M to 1 mM for 24 hours. The cell number was analysed in LNCaP and PC-3 cells after treatment for 24 hours with the PDC1-5 at the following concentrations: 0.25, 0.5, 1, 2.5 and 5 μ M. Cells treated with the G3 peptide alone at the same concentrations were used as negative controls. Cell number was assessed by High Content Screening and High Content Data Analysis as explained in section 2.5.

2.20 Hydrogen peroxide assay

The Amplex Red Hydrogen Peroxide Assay (Molecular Probes, Invitrogen, #A22188) was adapted from the manufacturer to measure hydrogen peroxide (H_2O_2) from living cells following the protocol used by Wagner et al. 2005.

One day before the experiment, cells were left to attached in triplicates in a 96 well plate at 7×10^4 cells/ml. Cells were treated with the PDC-5 at 5 μ M per well for 24 hrs. TCP was used at 250 μ M as positive control and the G3 peptide at 5 μ M as negative control.

All reagents of the kit were warmed up at RT and a stock of Amplex Red reagent at 10 mM was prepared in DMSO. The Amplex Red reagent was used on the same day of preparation because it is prone to oxidation. The 5X Reaction Buffer was diluted to 1X in molecular biology water. The 10 U/ml of horseradish peroxidase (HRP) stock solution was prepared in Reaction Buffer 1X and aliquots of 50 μ l were kept at -20°C . A 2.5 μ M stock of H_2O_2 solution was made to use as a positive control of the experiment.

The media from wells was disposed and cells were washed twice with 1X Hanks Balance Salt Solution (HBSS) (Gibco, Thermo Fisher, #14025092). Next, 100 μ M Amplex Red plus 0.2 U/ml HRP were prepared in HBSS and 50

μl of the Amplex red solution were disposed in each well to start the reactions. The plates were incubated at 37°C for 10 min and 25 μl of H_2O_2 solution was added to the control wells. The fluorescence was measured at 595 nm in the Varioskan microplate reader at 30 min, 60 min, 120 min and 180 min. The average of the background values was subtracted from the fluorescence averages from each condition.

2.21 Immunolabelling of histone demethylation marks

The effectivity of the LSD1 inhibitors that were coupled to the PDCs was evaluated by immunolabelling of histone demethylation signatures: histone 3 mono methyl lysine 4 (H3K4me) and histone 3 dimethyl lysine 4 (H3K4me₂). 384-well plates were used to seed the cells in triplicates. Cells with no treatment and cells treated with G3 at 5 μM were examined as negative controls. For the positive control, the TCP inhibitor was used at 250 μM . Plates were fixed after 24 hrs and blocked with BSA 1% for 30 min. Plates were treated with 0.3% triton solution for 12 min and stained with the primary antibodies H3K4me (1:400) and H3K4me₂ (1:500) for 24 hrs at 4°C . The next day, plates were washed with BSA 1% and exposed to 1:500 of secondary antibody for 2 hours in the dark. Plates were washed with PBS1X 3 times and kept at 4°C until image acquisition.

2.22 H3K4me₂ protein expression analysis

Histone demethylation protein levels were assessed by western blot in LNCaP and PC-3 cells after treatment with PDC-2 and PDC-4 conjugates at 5 μM or with LSD1 commercial inhibitor TCP at 250 μM as a positive control, for 24 hrs incubation. Cells exposed to native G3 at 5 μM and non-treated cells were used as negative controls. WBs were performed as described in the previous section, but with the following differences:

- a. An acid histone extraction protocol was performed instead of RIPA extraction, that is usually used to obtain whole or cytoplasmic extracts (section 2.22.1).
- b. A neutralization step of the acid samples was executed (section 2.22.2).
- c. A higher percentage of SDS gels was due to the small size of histones (section 2.22.3).
- d. An extended incubation period with the secondary antibodies (section 2.22.3).

2.22.1 Histones acid extraction

The triton extraction buffer (TEB) was made as reported before with 0.5% Triton X-100 (v/v) (Sigma-Aldrich, #T8787), 0.02% (w/v) sodium azide (NaN₃) (Sigma-Aldrich, #71290-10G), 2 mM/L phenylmethylsulfonyl fluoride (PMSF) (Thermo Scientific, #36978), in PBS 1X. A confluent T-75 flask with approximately 7x10⁶ cells/ml were trypsinized and centrifuged at 130 rpm for 5 min. Cell pellets were resuspended in ice cold PBS and centrifuged again at the same conditions two times. The supernatant was discarded and pellets were resuspended in 1 ml of TEB buffer for 10 min and kept on ice with mild stirring. Tubes were centrifuged at 4,000 rpm for 10 min at 4 °C in the Eppendorf centrifuge 5417R rotor F45-30-11.

Following the initial centrifugation and removal of the supernatant, half the amount of TEB was introduced, and the tubes were centrifuged again under the same settings. Then, the acid histone extraction was executed by adding 250µl of 0.2N hydrochloric acid (HCL) (Thermo scientific, #463965000) for 24 hrs at 4 °C in a tube inversion machine. The following day, tubes were centrifuged at the same conditions and the supernatant with the histone fraction was recovered, aliquoted and stored at -20 °C.

2.22.2 Histones sample preparation

The histone extracts were thawed on ice and diluted in Laemmli 2X buffer with 10% β -mercaptoethanol at a final concentration of 10 $\mu\text{g}/\mu\text{l}$. Samples were neutralised with approximately 5 μl of 1M sodium hydroxide (NaOH) per approximately 250 μl of lysate. The neutralization of the HCL acid is important for the Laemmli buffer to work effectively and for the samples to be visualised while running, as the colour of the lysates changed from clear to yellow when adding the Laemmli buffer but recovered the blue colour after neutralizing the HCL acid.

2.22.3 Western Blot of histone marks

Lysates were loaded onto 4-20% precast gels (BIO-RAD, #456-8093) at 4 μg per well, as determined after identifying the optimal working concentration from testing the linear range of both, HKP and target protein increasing concentrations. The running of the gel was done at 90 V for 1 hr. The transfer of the gel to a Trans-Blot 0.2 μm nitrocellulose was set at 25 V, 1.3 const A for 7 min. After the Ponceau staining, blocking of the blot and in between washes, the blots were probed with H3K4me2 (CST, #9725S) and the antibody histone 3 (H3) (Cusabio, #CSB-RA010418A0HU) as loading protein control. Blots were incubated for at least 3 hrs in the absence of light with the Licor secondary antibodies, goat anti-Rabbit 680 and goat anti-Mouse 800. Same settings and equipment were used to image the blots as reported.

2.23 LSD1 siRNA knockdown

LSD1 was knocked down using a pooled LSD1 siRNA in prostate cancer cells (siGenome, #M-009223-01-0005) following the reverse transfection protocol as previously described in section 2.17. A mix of scrambled siRNA 2, 3 and 4 were used as negative controls and UBB siRNA as positive control.

The KD was analysed by antibody labelling using the anti-rabbit LSD1 (C69G12, CST, #2184S). Before antibody probing, plates were blocked with BSA at 1% for 30 min and cell permeabilization was done by exposing the fixed cells to 0.3% Triton X-100 in PBS 1X for 12 min. Plates were incubated with the primary antibody overnight at 4 °C. The following day, wells were washed twice with 1% BSA and incubated with the secondary antibody for 2 hours at RT covered from light. Plates were washed several times with PBS 1X. Both, primary and secondary antibody were used at 1:500 concentration. Finally, plates were stored at 4 °C until imaging.

2.24 Targeted delivery of siRNAs using G3 peptide

The targeted delivery of the siGLO red marker using G3 as a drug vehicle was tested in prostate cancer cells. Cells were plated at optimal density concentrations a day prior the experiment. The following ratios of siGLO and G3 were tested: 1:1 (100 nM siGLO and 100 nM G3), 2:1 (200 nM siGLO and 100 nM G3) and 1:1 (200 nM siGLO and 200 nM G3) concentrations. Both molecules were complexed for 60 min at RT and DF1 plus siGLO were used as positive control. The siGLO-G3 or DF1-siGLO were incubated with the cells for 24 hours in the cell incubator. Next day, the plates were fixed and stored as usual.

Once the most effective condition for complexing G3 peptide and siGLO was detected, the targeted delivery of LSD1 siRNA was assessed in triplicates in PC-3 and LNCaP cells. The UBB siRNA was used as a functional positive control and the same mix of non-targeted siRNAs employed in the previous transfections were designated as negative controls. The ratio used for the LSD1 siRNA and G3 complexes was 2:1, being 200 nM of siRNA and 100 nM of G3 incubated for 1 hr at RT. At the same time, DF1 was used with the same siRNAs as a control for transfection. The G3-siRNA or DF1-siRNA complexes were added to each well in a total volume of 10 µl, and then, 15 µl of cells were

seeded into each well. Plates were incubated for 30 min at RT and then at 37 °C for 72 hrs, followed by standard fixation.

In the LSD1 siRNA delivery experiments, the wells corresponding to DF1 controls and G3-siRNA treatments were labelled with the LSD1 antibody, following the same protocol described in section 2.23. The fixed plates remained at 4 °C until the siRNA KD was assessed by HCS.

2.25 Statistical Analysis

All quantitative data was graphed and statistically analysed using GraphPad Prism 9.5.1 software unless specified otherwise. The mean and standard deviation (SD) or standard error mean (SEM) values were calculated for all assays. Student's t-test ($p < 0.05$) for two statistical comparisons or one way ANOVA analysis ($p < 0.05$) for 3 or more statistical comparisons were calculated for all data sets, except for the Scavenger Receptor Library Screening where the median was calculated and the non-parametric Kruskal-Wallis analysis ($p < 0.05$) with multiple comparisons was applied followed by Benjamini, Krieger and Yekutieli test correction.

CHAPTER 3

3. G3 CELL SELECTIVITY & SUBCELLULAR DISTRIBUTION

3.1 Introduction: CPPs and PDCs

Small peptides are defined by being 4 to 40 aa long and include a group called cell-penetrating peptides (CPPs), defined by their capacity to enter cells. An interesting feature is their ability to induce intracellular effects directly by themselves, or indirectly, by delivering active molecules to the site of interest (Langel, 2015; Langel, 2019; Zorko et al., 2022). Using aspects of CPPs, PDCs are produced as a single targeted complex in which a payload is conjugated to the CPP by means of a linking molecule (Feni & Neundorf, 2017; Gayraud et al., 2021; Klimpel et al., 2019; Vrettos et al., 2018).

It has been proven that PDCs can deliver a spectrum of cargos into the cells including other peptides, proteins, siRNAs, cytotoxic drugs, and radionuclides (Fu et al., 2023; Gong et al., 2023; Heh et al., 2023; Hoppenz et al., 2020). Selection of the peptide is important, because it is the vehicle that is going to transport the active molecule to specific cell types. That in turn could allow a more effective therapeutic effect and a better pharmacokinetic profile along with lower levels of cytotoxicity because the drug is in the right place at a higher concentration. Qualities to consider for a suitable peptide are increased stability, extended plasma half-life, powerful binding affinity, weak immunogenicity and high internalization index (Fu et al., 2023).

One of the most frequent applications of PDCs is in the treatment of cancer (Heh et al., 2023; Vrettos et al., 2018), which is the main goal of my work, to upgrade prostate cancer therapies through targeted delivery using the G3 peptide. Understanding cell selectivity, uptake mechanism, and the underlying internal subcellular distribution of

the drug delivery peptide represents the first crucial steps for the development of safe and competent PDCs. Chapter 3 investigates if the G3 peptide displays affinity towards prostate cancer cells and its subcellular location.

3.1.1 Cell-penetrating peptides

CPPs have been a subject of study in the last 30 years. Details of validated CPPs can be found in a free database, CPPsite 2.0 (<https://webs.iitd.edu.in/raghava/cppsite>) (Agrawal et al., 2016). Due to the diversity within CPPs, it has been difficult to categorize them, however the most common classifications are defined by their origin and physicochemical features (Agrawal et al., 2016; Derakhshankhah & Jafari, 2018; Zorko et al., 2022).

Depending on their origin, CPPs are grouped into protein-derived, synthetic and chimeric (Lindgren et al., 2000). The first ones refer to peptides that originate from a portion of a natural protein, e.g. the Tat peptide, which was the earliest CPP identified, that was derived from HIV-1 transcriptional activator protein (Frankel & Pabo, 1988; Green & Loewenstein, 1988); and in comparison, synthetic CPPs are usually designed based in aa sequences of natural peptides, e.g. G3 and MAP, from the alpha helical amphipathic peptide family (Hu et al., 2011; Oehlke et al., 1998). Chimeric peptides, such as Transportan, include protein-derived sequences with engineered modifications (Pooga et al., 1998).

CPPs are also classed as cationic, amphipathic or hydrophobic depending on their physicochemical attributes, however these properties usually overlap (Milletti, 2012). Having at least 5 positively charged aa, like lysine or arginine, renders the cationic net charge of the majority of CPPs at physiological pH. The quantity and location of positively charged aa in their structure can influence their activity (J. Xu et al., 2019). It has been stated in several studies that peptides with many arginines allows the most effective cellular internalization (Alhakamy & Berkland, 2013; Liu et al., 2012; Melikov & Chernomordik, 2005; Tung & Weissleder, 2003). Nuclear localization sequences (NLS) embody a set of tiny cationic CPPs that contain either poly-lysine or poly-arginine or poly-proline sequences, which are recognized for translocating to the

nucleus via the nuclear pore complex (Ragin et al., 2002). However, NLS present a moderate cationic charge, restraining biological membrane penetration. To balance this disadvantage, NLS are usually joined to other hydrophobic sequences, creating new amphipathic CPP with higher transfection efficiency, e.g. vectors such as Pep-1 and MPG (Lee et al., 2014; Yang et al., 2005). This brings us to the second class of CPPs, the amphipathic peptides, that can be either alpha-helical or beta-sheet configurations, due to their hydrophobic and hydrophilic regions. Depending how the amphipathicity is achieved, they can be divided into primary or secondary. The peptides that are amphipathic because of their sole sequence or due to their stable arrangement of alpha-helical structure are considered as primary, while the peptides that become amphipathic after interaction with the negatively charged plasma membrane are classified as secondary (El-Andaloussi et al., 2007; Pooga & Langel, 2015; Ziegler, 2008). Peptides like C105Y and K-FGF, are examples of hydrophobic CPP, which are characterized by having mostly non-polar residues with scarce polar aa (Carnevale et al., 2018; Rhee & Davis, 2006).

Another classification is based in their conformation, that splits CPP into linear or cyclic forms. The latter revealed better capacity to cross the cellular membrane, enhanced linking affinity to receptors, and greater resistance to enzyme breakdown, whereas linear peptides are more prone to proteolytic cleavage (Dougherty et al., 2019; Qian et al., 2016).

CPPs can also be categorized in two groups, depending their cellular affinity: cell-specific peptides, such as tumour penetrating peptides, and non-cell-specific peptides, where they are internalized by many cells types (Langel, 2015; Zahid & Robbins, 2015). Cancer penetrating peptides are selected to be either tailored to the tumour microenvironment, the cancer cells, the stroma or the blood vessels within the tumour, and are normally used for drug administration or as a tool for diagnosis (Ruoslahti, 2017; Teesalu et al., 2013). Also, peptides that have the competence to selectively detect overexpressed membrane receptors in cancer cells are typically known as tumour-targeting peptides (Ma et al., 2017b; Reubi, 2003; Vhora et al., 2014).

3.1.2 Internalization mechanisms of CPPs

Many internalization mechanisms have been proposed for CPPs, but still have not been completely elucidated. Several reviews discussing this field have been published, and the current consensus has reported that CPPs use one or both of the following routes for cellular internalization: direct penetration and/or endocytosis (Gestin et al., 2017; Madani et al., 2011; Ruseska & Zimmer, 2020; Tashima, 2017; Trabulo et al., 2010; Yang et al., 2019). Figure 9, illustrates a representation of both energy-based and energy-independent internalization mechanisms for CPPs.

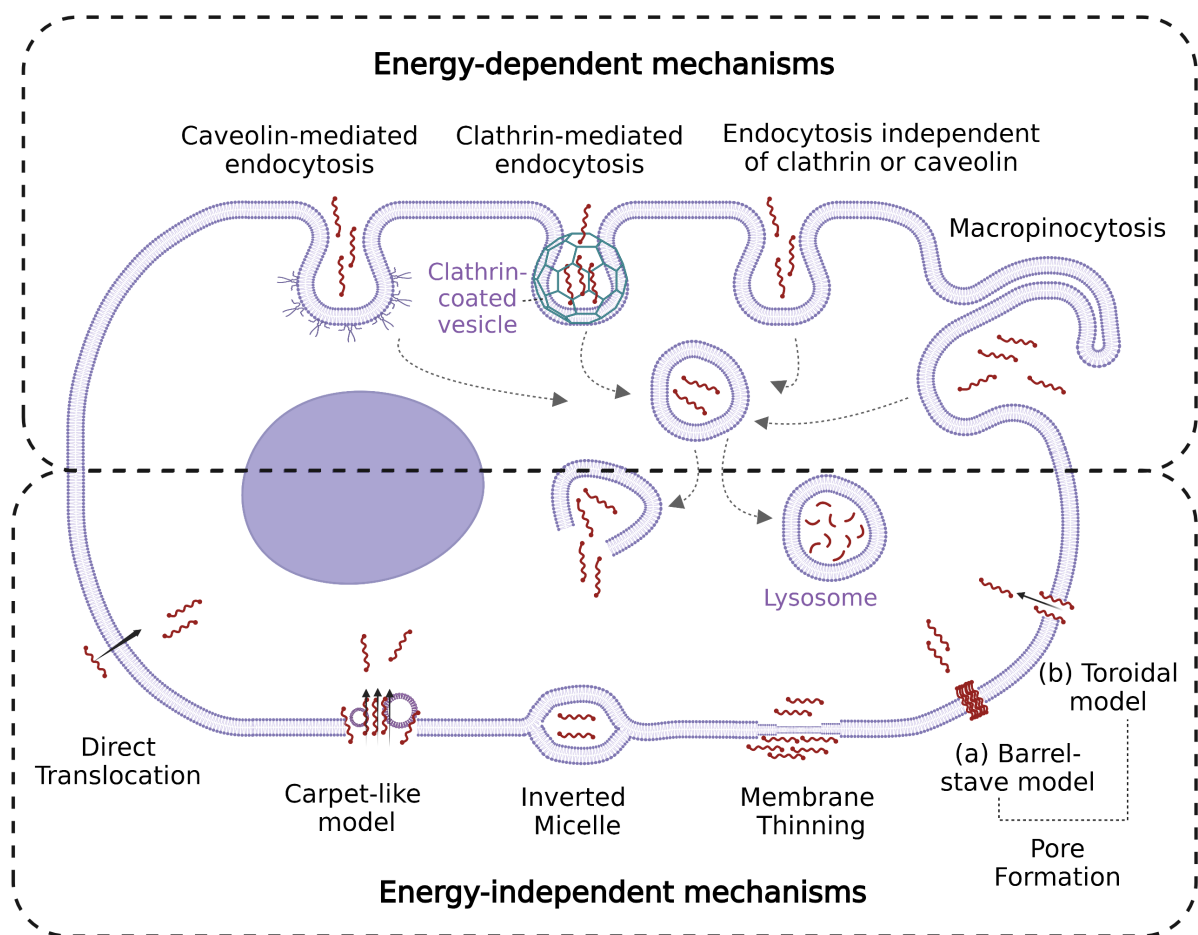


Fig. 9. CPP internalization mechanisms. Upper section includes endocytic-based uptake mechanisms and lower panel indicates direct mechanisms. CPP are represented as red helical peptides, that are internalized in endosomal vesicles after energy-dependant mechanisms. Some CPP are hypothesized to escape from lysosomal route, however other might undergo proteolytic disintegration in lysosomes. Created with BioRender.com

The direct translocation hypothesis, which is an energy-free mechanism, that was proposed after some CPPs were absorbed by cells at 4 °C, and later tested using drugs that block endocytosis (Derossi et al., 1996; Kosuge et al., 2008; Pooga et al., 1998; Vivès et al., 1997). In this mechanism, the interaction between the CPPs and the bilayer of phospholipids implies electrostatic contact and hydrogen bonding, that ends up in temporary membrane distortions or pore induction. Diverse strategies have been proposed to explain the membrane destabilization, prior to peptide translocation into the cytoplasm, including transmembrane pores and inverted micelle formation, and the carpet-like and membrane thinning models (G. Grasso et al., 2018; Hirose et al., 2012; Islam et al., 2018).

The generation of pores comprises the toroidal and barrel-stave models. In the barrel-stave model, the transmembrane opening is created by the incorporation of the amphipathic peptides into the lipid bilayer in an arrangement comparable to staves in a barrel, where their polar regions face the inward part of the pore (Baumann & Mueller, 1974; Pieta et al., 2012). While in toroidal model, a hole forms from peptides and the lipid headgroups (Matsuzaki et al., 1996; Yang et al., 2001). The binding between cationic aa, such as lysine or arginines with the phosphate groups of the phospholipids, within the membrane, leads to the pore seeding (Herce et al., 2009; Herce & Garcia, 2007).

Entrance to the cell via micelle inversion was originally described for penetratin, and then confirmed for several poly-arginine peptides (Derossi et al., 1998; Kawamoto et al., 2011). The penetration of peptides through the generation of inverted micelles happens when the lipid heads of the bilayer and the non-polar residues of the peptides display a strong interaction that induces an infolding of phospholipids. The CPPs enter the cell restrained in the micelles and then are liberated into the cytoplasm.

The carpet-like model consists in the parallel accumulation of cationic peptides along the exterior of the membrane, similar to a carpet, which triggers provisional fluidity of the lipid bilayer (Pouny et al., 1992; Thennarasu et al., 2010). The thinning membrane model arises in a comparable way to the carpet-like model, where the connections among the phospholipids and cationic peptides also produce the reduction of the thickness of the membrane that permits their translocation (M.-T. Lee et al., 2005).

This tactic was initially reported for magainin, an amphipathic peptide (Ludtke et al., 1995). The thinning and carpeting of the cellular membrane can only take place when the concentration of the peptides gets to a specific threshold.

Endocytosis can be defined as an energy supported mechanism in which diverse and complex modular molecules are moved in vesicles or invaginations from the plasma membrane into endosomes inside the cell (F. Zhao et al., 2011). In 2003, endocytosis was first proposed as an uptake mechanism for CPPs (Richard et al., 2003). Currently, four endocytic pathways have been identified for drug delivery peptides: clathrin-mediated endocytosis (CME), caveolae-mediated endocytosis (CvME), macropinocytosis and endocytosis independent from clathrin and caveolin (Ruseska & Zimmer, 2020).

Briefly, CME is engaged after ligand-receptor interactions on the cell surface, involving membrane tension and forces, inducing the membrane into a vesicle. Adaptor proteins such as adaptor protein complex 2 (AP-2) interact with phospholipids, enabling the recruitment and association of clathrins into a polyhedral coating structure that prompts an invagination, termed the “clathrin-coated vesicle” as illustrated in Figure 9 (Kaksonen & Roux, 2018). The GTPase, dynamin 1 (DNM1), is responsible for the separation of the clathrin-coated vesicle from the membrane through guanosine-5'-triphosphate (GTP) hydrolysis (Antonny et al., 2016). Then clathrin and dynamin are depolymerized, the vesicles are uncoated, followed by their transfer to intracellular trafficking endosomes. The cargoes are involved in a myriad of physiological processes, including nutrient uptake, which are continuously internalised into the cells through this process, e.g. transferrin and cholesterol etc.

A variety of peptides have been reported to enter the cells via CME. The TAT peptide without any cargo employs CME to gain access to HeLa cells (Richard et al., 2005). The peptide known as MPG, was originally employed by Morris and collaborators. The structure of MPG is composed of a hydrophilic region obtained from the nuclear localization sequence of SV40 T-antigen, merged with the N-terminal fusion sequence of the HIV-1 glycoprotein 41, which has hydrophobic nature (Morris, 1997). However, MPG α is an analogue of MPG, that has helical configuration due to the addition of 6 aa in its hydrophobic region. The MPG α /siRNA complex has been confirmed to use

CME to transport siRNAs, however in a previous study, it was reported that MPG enter the cells in an energy-free mechanism in the absence of cargo (Laufer et al., 2010; Veldhoen et al., 2006). Although the uptake mechanism of MPG and its derivative is controversial, they hypothesized that the type of cargo could have had an impact on their internalization route, as they had confirmed that the amount of MPGα/siRNA conjugates was decreased by CME inhibitors. Octa-arginine R8 peptide has been validated to target syndecan-4, which then prompts the internalization by CME (Kawaguchi et al., 2016a). And it has been suggested that syndecan transmembrane receptors are implicated in multiple uptake mechanisms as contradictory results have identified R8 peptide using macropinocytosis (Futaki & Nakase, 2017). Another example that uses CME is NickFect1 peptide conjugated with plasmid DNA (Arukuusk et al., 2013).

CvME represents another strategy employed by some CPP. This process starts after receptor recognition on the lipid rafts, which are hydrophobic areas rich in sphingomyelin and cholesterol, encouraging the interaction of caveolin and cavin-1, that will eventually generate a caveolin-coated vesicle (Yang et al., 2019). Caveolae, first characterized in numerous cell types in the 1950s, contain invaginations with a size of 50 to 100 nm in diameter (Palade, 1953; Pelkmans & Helenius, 2002). Caveolae not only participates in the endocytosis of a set of molecules, but also in lipid regulation and cell signalling (Branza-Nichita et al., 2012).

TAT conjugated proteins were the first CPPs confirmed to be internalized via CvME, where the coupled proteins seem to define the uptake mechanism (Fittipaldi et al., 2003). The internalization of transportan and transportan 10 were reduced after Cav1 knockdown and cholesterol depletion, as well as their colocalization in caveosomes (Säälik et al., 2009). In both cases, TAT and transportan conjugates, the larger size due to conjugation of cargo might benefit their engulfment through CvME (Rejman et al., 2004). Proline-rich amphipathic peptides are internalised through CvME, in a glycosaminoglycans dependent manner (Pujals & Giralt, 2008). The scavenger receptor, SCARA, has also been proven to mediate the internalization via CvME of PepFect14 DNA conjugates (Veiman et al., 2013). CvME has been pointed out in the uptake of azurin-derived alpha helical peptides, namely p18 and p19 (Mehta et al.,

2011; B. Taylor et al., 2009); and in the case of CVP1, an alpha helical peptide derived from chicken anemia virus, consisting of the N-terminal of VP1 (Hu et al., 2018).

A few CPPs use alternative routes to entering cells other than caveolin or clathrin. For instance, p18 and p19 azurin originated fragments and transportan conjugates have been identified as using alternative entry methods (Mehta et al., 2011; Säälik et al., 2009; B. Taylor et al., 2009). The peptide, low molecular weight protamine (LMWP), conjugated to siRNAs has shown to be not reliant on clathrins, caveolae, nor dynamin, as treatment with inhibitors of the recognised endocytic mechanisms and GTPase blockers did not affect its endocytic uptake significantly (Ye et al., 2018).

Macropinocytosis is a quick endocytic process which relies upon lipid-rafts. This mechanism initiates after the binding of the CPP to the proteoglycans in the lipid bilayer. The activation of the ras-related C3 botulinum toxin substrate 1 (RAC) protein in turn stimulates F-actin configurations in combination with growth factors, which facilitates the deformation of the membrane into large vesicles (Lim & Gleeson, 2011). These vesicles are termed macropinosomes which are distinguish by the absence of protein-coating and heterogenous dimensions with diameters between 0.2 to 5µm (Swanson & Watts, 1995). The reconstruction of the cytoskeleton prior to the development of macropinosomes is regulated by a series of molecules: GTPases, including the Ras, Rho and Rab families, kinases such as PI3K, and growth factors like the epidermal growth factor (Haigler et al., 1979; Lim & Gleeson, 2011).

Bulky peptides with huge cargos are more commonly internalised through macropinocytosis, for instance TAT peptide fused to conjugates (Kaplan et al., 2005; Wadia et al., 2004). This uptake mechanism has also been identified for poly-arginine peptides, such as octa-arginine R8, nona-arginine R9, dodeca-arginine R12 and the Flock-House-Virus-derived peptide (Duchardt et al., 2007; Nakase et al., 2004; Nakase et al., 2007; Tanaka et al., 2012). The C-X-C Motif Chemokine Receptor 4 (CXCR4) has been suggested as a receptor target of R12 peptides that could lead to macropinocytosis (Tanaka et al., 2012). The anionic peptide called NickFect51 has been confirmed to use macropinocytosis to enter the cells through the interaction of two SR, specifically SR class A3 (SR-A3) and SR class A5 (SR-A5) (Arukuusk et al., 2013).

3.1.3 Key factors in the cellular uptake of drug delivery peptides

The preference of drug delivery peptides to different ways of entry to the cells can be delimited by several key aspects. One of the most influential factors is the concentration of the peptides, which can directly affect the mechanism of entry into cells; e.g. direct penetration is often presented with elevated concentrations, while endocytosis is more usual to be associated with reduced concentrations (Fretz et al., 2007; Jones & Sayers, 2012; Kosuge et al., 2008). At elevated concentrations, some amphipathic and cationic CPPs have been demonstrated to provoke pores in the plasma membrane (Saar et al., 2005). Penetratin is an exception to this argument, as it is internalized via endocytosis at high concentrations but turns to direct translocation at low concentration (Alves et al., 2010).

The structure of CPPs is important in their uptake because the arrangement, number, and composition of aa define their precise physicochemical traits, necessary for interactions with the membrane and its components (Ruseska & Zimmer, 2020). Among the physicochemical characteristics, amphipathicity is known to have an impact on the route of entry, being common for amphipathic peptides to use direct penetration (Milletti, 2012). The cationic property of CPPs has been exposed to be another aspect to determine direct translocation, for example arginines are more successful than lysines (Futaki et al., 2001; Mitchell et al., 2000).

The conjugated molecule to the peptide has also been confirmed as an important parameter, due to the difference in size from the original molecule (Rejman et al., 2004; Tünnemann et al., 2006). For instance, the naked TAT peptide is internalized via clathrin-mediated endocytosis, however TAT conjugates shift to caveolin-mediated endocytosis (Ferrari et al., 2003; Fittipaldi et al., 2003; Richard et al., 2005).

The dependency on the cell type is another key aspect that contributes to the internalization mechanism for peptides. This is probably linked to the interaction with the components in the negatively charged plasma membrane. The peptide-to-cell ratio was found to impact the internalization efficiency of CPPs in CHO cells, which could have been a result of the membrane constituents per se or the cellular behaviour (Hällbrink et al., 2004). In another study, the internalization of 22 known peptides was

analysed in the following cell lines: HEK293, Cos-7, MDCK and HeLa; and what they demonstrated was that some peptides display cell dependency, such as penetratin having preference for HeLa cells (Mueller et al., 2008). Cell selectivity towards tumorigenic cells is another recognized characteristic of some CPP. For instance, the CPP, sC18 that is derived from an antimicrobial peptide, has been shown to display cancer cell selectivity, since it is only internalised by several cancer cell lines but not by non-cancer cell lines (Gronewold et al., 2017). In Table 7, several examples of peptides with cancer cell specificity are presented.

The composition of the biological membrane has been suggested as another valuable factor. Usually, the direct penetration of CPPs is promoted by membrane components such as fatty acids and lipids but obstructed by the presence of cholesterol (Herce et al., 2014; Lorents et al., 2018; Sharmin et al., 2016; Swiecicki et al., 2014; Terrone et al., 2003; Via et al., 2018). For instance, in one study, they used membranes with different constituents to assess the uptake of a peptide rich in arginines, and they discovered that only membranes containing cholesterol prevented the peptide uptake (Crosio et al., 2019). Other external elements that can also impact in the internalization dynamics are the temperature, pH gradient and presence of ions (Fretz et al., 2007; Herce et al., 2014; Kauffman et al., 2015).

Table 7. Cancer cell specific peptides

Peptide	Targeted Receptor	Cancer expression	References
RGD-based peptides, e.g. c(RGDfK) and iRGD	Integrins ($\alpha\beta3$, $\alpha\beta5$, $\alpha\beta6$, $\alpha\beta8$, and $\alpha5\beta1$)	PCa, glioblastoma, breast cancer, and melanoma	(Chen & Chen, 2011; Desgrosellier & Cheresch, 2010; Sugahara et al., 2009)
GE11 peptide (YHWYGYTPQNVV)	EGFR	Glioblastoma, PCa, colorectal, breast, lung, bladder, ovarian, head and neck cancer	(Ai et al., 2013; Li et al., 2005; Salomon et al., 1995; Yarden & Pines, 2012)
Bombesin peptide analogs	Bombesin receptors (NMBR, GRPR and BRS-3)	Neuroblastoma, glioblastoma, PCa, pancreatic, lung, breast, colon, ovarian, uterine, head/neck, renal cell, intestinal, and bronchial cancer	(Hoppenz et al., 2019; Jensen et al., 2008; Mantey et al., 1997; Reubi et al., 2002; Sancho et al., 2011; Schroeder, et al., 2009)
SST peptide analogs, e.g. octreotide and lanreotide	Somatostatin receptors (SSTR2 and SSTR5)	PCa, neuroendocrine tumor, small cell lung, breast, gastric, colorectal, and hepatocellular cancer	(Sun & Coy, 2011; Volante et al., 2008)
NAPamide	Melanocortin receptor 1 (MC1R)	Melanoma	(Froidevaux et al., 2005; Froidevaux & Eberle, 2002; Miao & Quinn, 2008)
G-202	Prostate-specific membrane antigen (PSMA)	PCa, hepatocellular, renal, ovarian, bladder, breast cancers, melanoma samples	(Chang et al., 1999; Denmeade et al., 2012; Liu et al., 1997; Mahalingam et al., 2016; Silver et al., 1997)
BT5528	Hepatocyte receptor A2 (EphA2)	PCa, glioblastoma ovarian, pancreas esophagus cancer	(Bennett et al., 2020; Gan et al., 2022; Lindberg & Hunter, 1990; Mudd et al., 2020; Walker-Daniels et al., 2003)
BT1718	Membrane type-1 matrix metalloproteinase (MT1-MMP)	Melanoma, ovarian, breast, colon, pancreatic and lung cancers	(Gifford & Itoh, 2019; Gowland et al., 2021; Knapinska & Fields, 2019)

3.2 Results

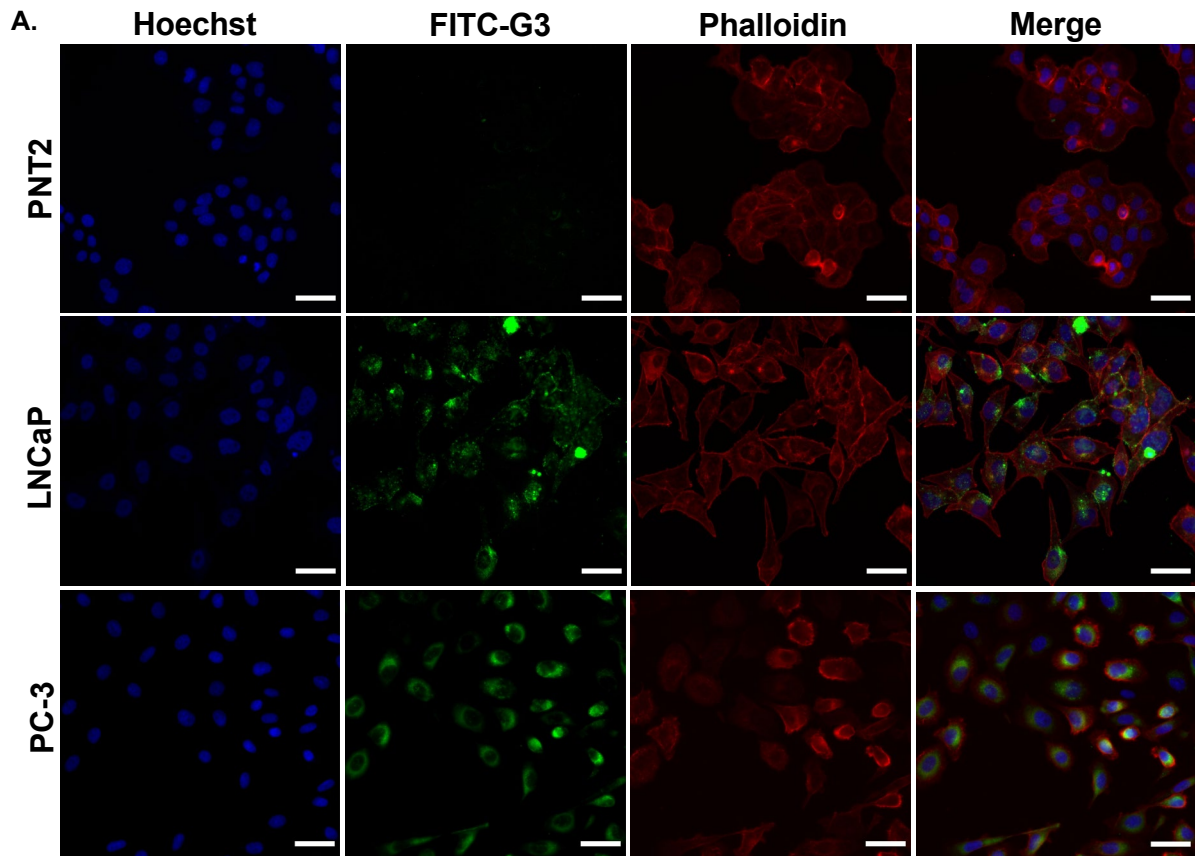
3.2.1 G3 uptake in prostate cancer vs non-cancer prostate cells

As mentioned in chapter 1, studies have confirmed that G(IKK)₃I-NH₂ or G3 peptide has internalization preference towards cancer cells, including HCT-116, HeLa and HL60, while there is minimal uptake in healthy cells, such as HDF (Chen et al., 2012; Chen, et al., 2014; Cirillo et al., 2021). However, the internalization pathway and cell specificity of G3 has never been investigated in prostate cancer cells before.

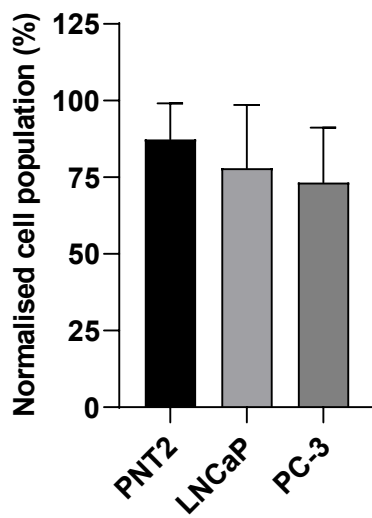
LNCaP and PC-3 are some of the most employed cell lines in PCa research. PC-3 is a highly differentiated cell line that was formerly obtained from a biopsy of a 62 year-old man with aggressive metastasis in the bones, that is characterized by atypical nuclei and nucleoli, frequent microvilli, irregular mitochondria and being not responsive to AR, nor express PSA (Kaighn et al., 1979; van Bokhoven et al., 2003). Conversely, LNCaP constitutes a more indolent adenocarcinoma cell line that was originated from a 50-year-old man's lymph nodes and has high expression of AR and PSA (Horoszewicz et al., 1983; van Bokhoven et al., 2003).

PC-3 and LNCaP were used to examine whether prostate cancer cell lines, representatives of different stages of the disease, could internalize the FITC-labelled version of the peptide at the same or different extent than the prostate cell line, PNT2. Phalloidin (594 nm) was used to stain F-actin filaments that facilitate the imaging of the structure and dimensions of the cell. FITC-G3 uptake was analysed using High Content Microscopy (Figure 10A). After 24 hours treatment with the peptide, PCa cell lines presented significantly higher uptake when compared with PNT2 cells, shown in Figure 6C. The internalization of FITC-G3 was measured as FITC integrated intensity values and a one-way ANOVA test was calculated (**p < 0.001).

The total number of cells in each condition was counted and normalised to the negative control. The cellular populations of the 3 cell lines were not affected after the treatment with FITC-G3 at 4 µM for 24 hrs (Fig. 10B), demonstrating that FITC-G3 over 24 hours of treatment had no effect on cell viability.



B.



C.

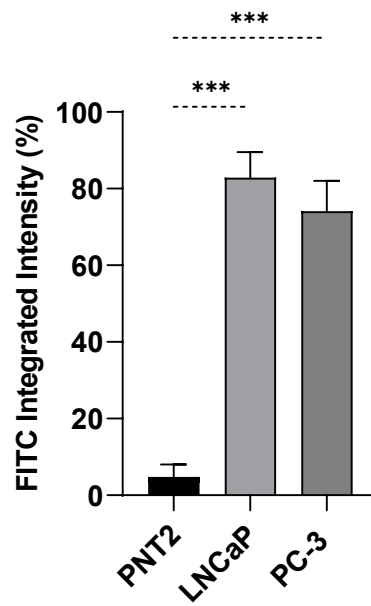


Fig. 10. FITC-G3 uptake in prostate cancer vs non-cancer prostate cells. (A) High content images of prostate cancer cell lines, LNCaP and PC-3, and prostate normal cells, PNT2, exposed to FITC-G3 at 4 μ M for 24 hrs. The Nuclei was stained with Hoechst 33342 and the cytoplasm was delimited with Flash Red Phalloidin. Scale bar 50 μ m, 20X magnification. (B) Data was normalised against the PNT2 control, and the cell populations were analysed after 24 hrs of FITC-G3 exposure. (C) FITC integrated intensity values are representative of 3 different experiments with 3 replicates each. All data is displayed as means and \pm SD and the statistical significance was calculated using one way ANOVA test (** $p < 0.001$).

Although red phalloidin was used to determine the cellular morphology, that in turn can help in the estimation of FITC puncta inside the cells, it is not possible to assess the internalization of the peptide, due to the resolution of the microscope. Thus, the same experimental conditions were repeated and analysed using confocal microscopy to validate the cell specificity of FITC-G3 in PCa cell lines.

Samples were exposed to FITC-G3 at 4 μ M for 24 hrs. Consecutive sections of the cells were taken and saved as a compilation in z-stacks. The z-stacks were transformed to maximum projection images to measure the FITC signal inside the cells. Weak internalization of FITC-G3 was observed in PNT2 cells, in contrast to the high green fluorescence puncta inside of LNCaP and PC-3 cells (Fig. 11A). Hoechst was used as nuclear staining and red phalloidin for the cytoplasm. In the merging images of the 3 channels, it is possible to observe which green fluorescence from FITC-G3 is inside the cells and which is not. ROI (Regions of Interest) were delimited based on the phalloidin localising with the cell's actin. FITC integrated intensity values were plotted as the mean of each z-stack (Fig. 11B). Statistically significant differences between FITC integrative intensity values were obtained for PCa cells when compared to PNT2 cells after analysed by ANOVA (** $p < 0.001$), confirming previous data obtained by HCS.

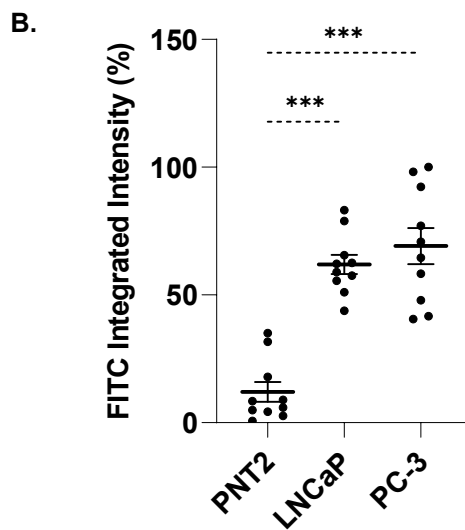
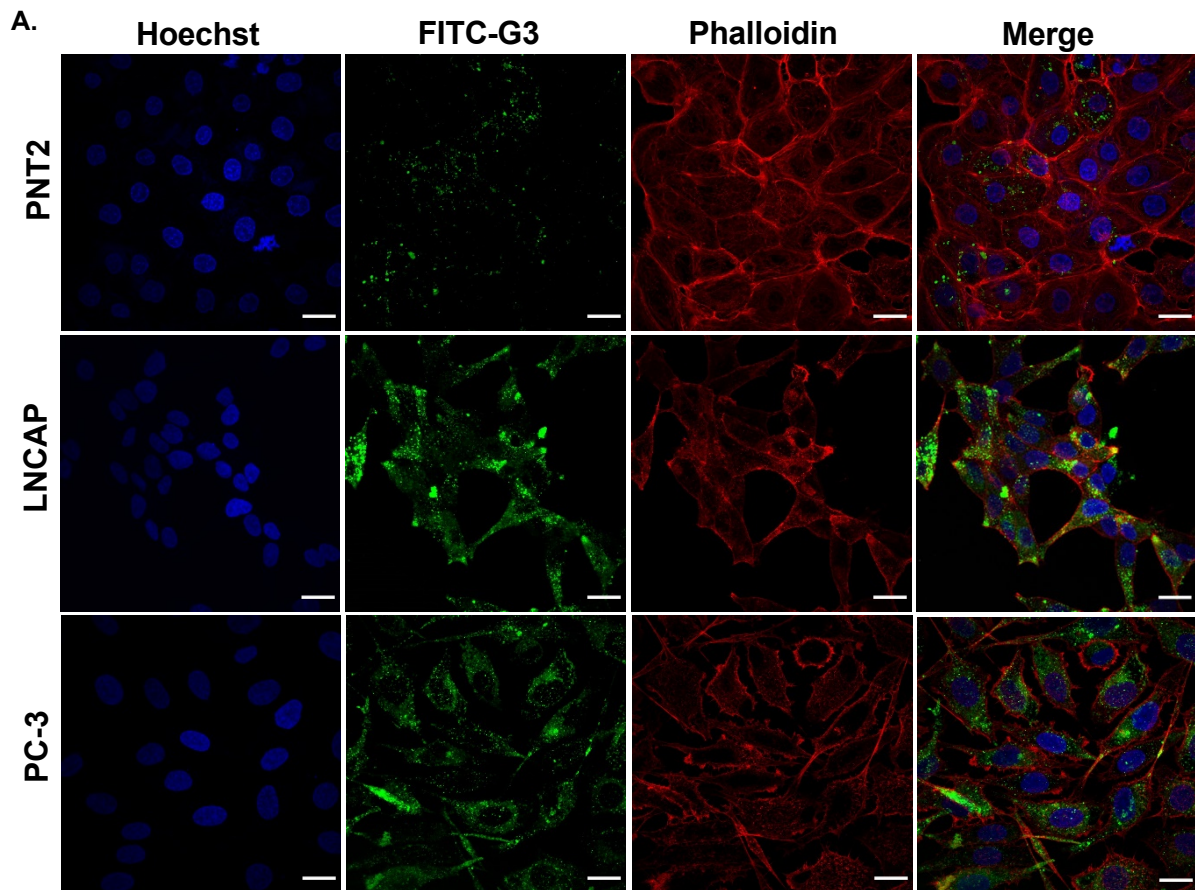


Fig. 11. Z-stacks of prostate cancer cells after FITC-G3 treatment. (A) Superimposed Z-stack images of prostate cancer cells and healthy prostate cells treated with FITC-G3 at 4 μ M for 24 hrs. Hoechst and Flash Red Phalloidin were used to stain the nuclei and cytoplasm respectively. Scale bar 25 μ m, 60X objective. (B) FITC integrated intensity values were measured in 10 FOV. Data is shown as means with \pm standard error mean (\pm SEM) of one biological experiment. The statistical significance was determined using one way ANOVA test (** $p < 0.001$).

3.2.2 Cytotoxic analysis

Elevated concentrations of G3 have demonstrated the concentration-dependant cytotoxic effect of the peptide in several cancer cell lines including, HCT-116, HeLa, HL60 and HepG2 cells (Chen et al., 2014a; Chen et al., 2014b; Chen et al., 2015; Cirillo et al., 2021; Hu et al., 2011). To test if each cell type can take up FITC-G3, at each concentration tested, cells were incubated with peptides and images were acquired by HCS. Figure 12 depicts the plot of integrated intensity of FITC-G3 for each concentration tested over the three cell lines. Both, PC-3 and LNCaP cells followed the same rising tendency of the FITC integrated intensity values, while there was a clear difference with PNT2 cells, even more than a 2-fold difference at high concentrations. These data confirmed that PCa cells internalized the G3 peptide at a much higher degree than PNT2 cells.

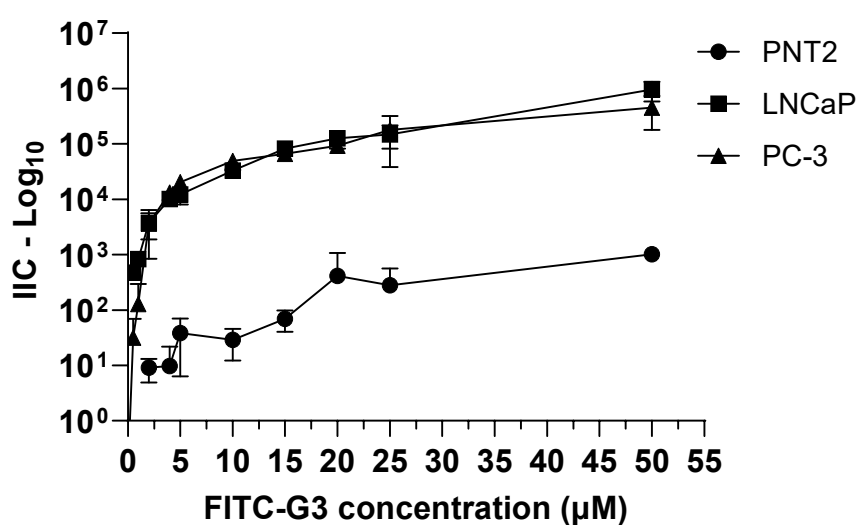
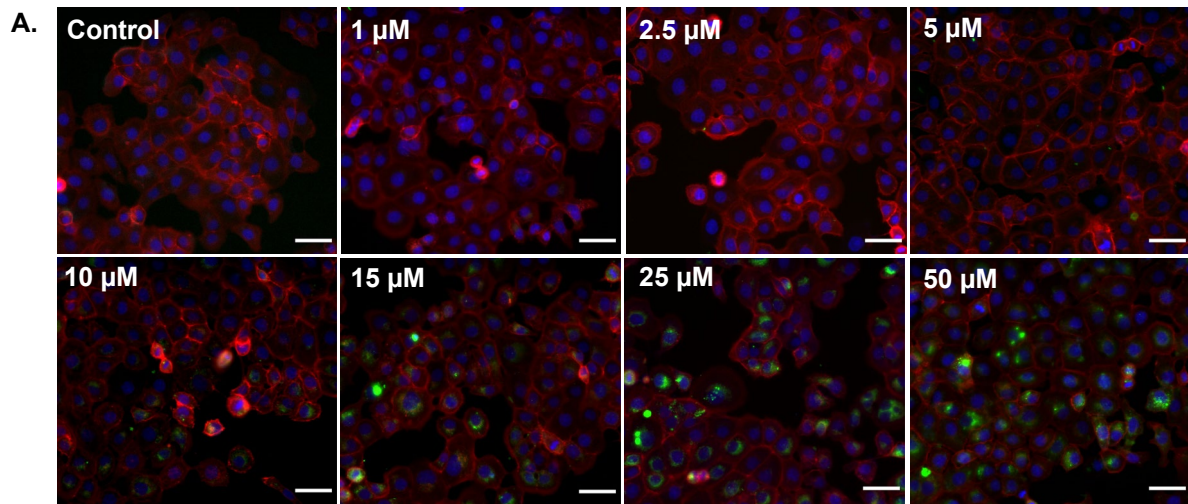


Fig. 12. FITC-G3 uptake at increasing concentrations. Normalised FITC integrated intensity log 10 values at increasing concentrations of FITC-G3 in either prostate cancer cells (LNCaP and PC-3) or non-cancer cells (PNT2), after 24 hrs exposure. One biological experiment was done in 3 replicates. Data is displayed as means and \pm SD .

Either declines in cell counts or increased cell death are direct indicators of cell viability. Thus, the cytotoxic activity was analysed by acquiring nuclei images with High Content Microscopy and by counting nuclei automatically using the Multi Wavelength Cell Scoring (MWCS) algorithm. The MWCS algorithm functions by detecting the Hoechst nuclear staining in the cells. To investigate whether FITC-G3 peptide could affect the cell populations of LNCaP, PC-3 or PNT2 cells, a set of serial dilutions were analysed from 1 to 50 μM concentrations.

The data revealed that even though PNT2 prostatic epithelial cells positively internalised G3 at high concentrations, from 10 to 50 μM , the cell viability was not particularly affected at any point of the treatments, as observed in Figure 13A, and the data from the image analysis in 13B. PNT2 cells at reduced concentrations did not uptake FITC-G3 as shown in the images up to 5 μM . The normalization of the data was done to the non-treated control and represented as percentages.

Surprisingly, LNCaP and PC-3 cell populations were reduced significantly after 25 and 50 μM concentrations of the peptide, as measured in Figure 14B and Figure 15B respectively. The statistical significance was calculated using one way ANOVA (** $p < 0.001$) for both LNCaP and PC-3 IIC values. The internalization of FITC-G3 was observed in the high content images of LNCaP and PC-3 increasing exponentially from the lowest concentration to the highest concentration (Figure 14A & Figure 15A). At the highest concentration, FITC images represent high levels in PCa cells and a drastic reduction in the number of cells at 50 μM was also showed in their representative images. From 25 to 50 μM concentrations of FITC-G3, the actin staining revealed morphological alterations in LNCaP and PC-3 cells, characterized by reduced size, a round shape, and membrane blebbing. These observed changes in LNCaP and PC-3 cells may suggest apoptosis. In contrast, PNT2 cells maintained their structure under these concentrations.



B.

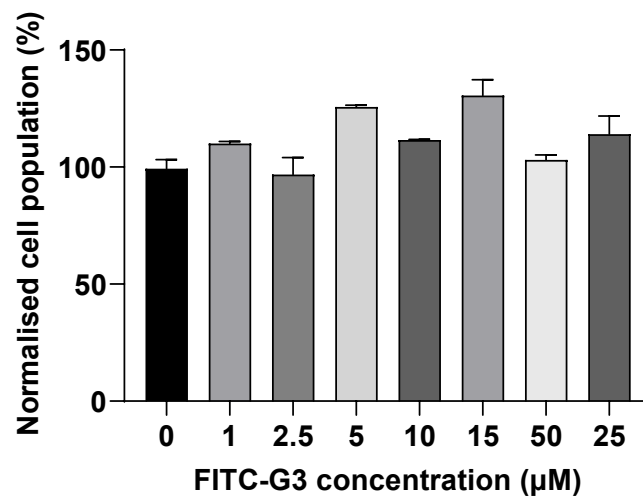


Fig. 13. FITC-G3 cell viability analysis in PNT2. (A) High content images of PNT2 cells after addition of FITC-G3 at increasing concentrations for 24 hrs. Scale bar 50 μm , 20X magnification. Hoechst and red Phalloidin were used for staining of nuclei and cytoplasm, respectively. (B) Normalised cell population after 24 hrs of FITC-G3 treatments. Data is represented as means and $\pm\text{SD}$ of one biological experiments with 3 replicates.

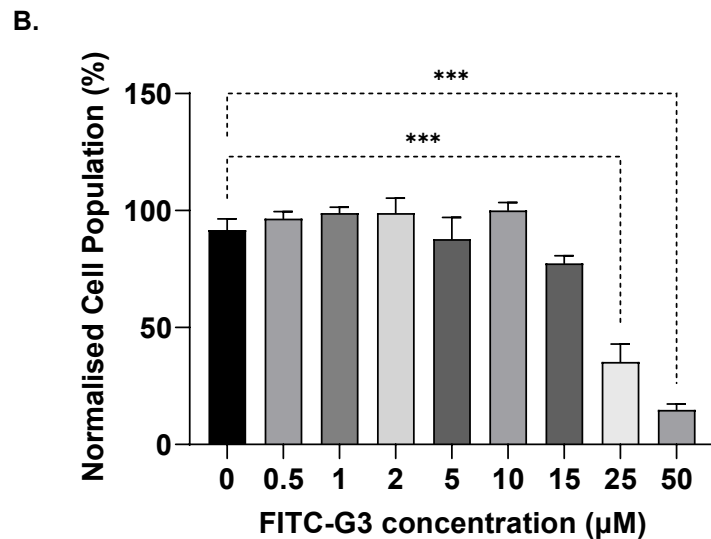
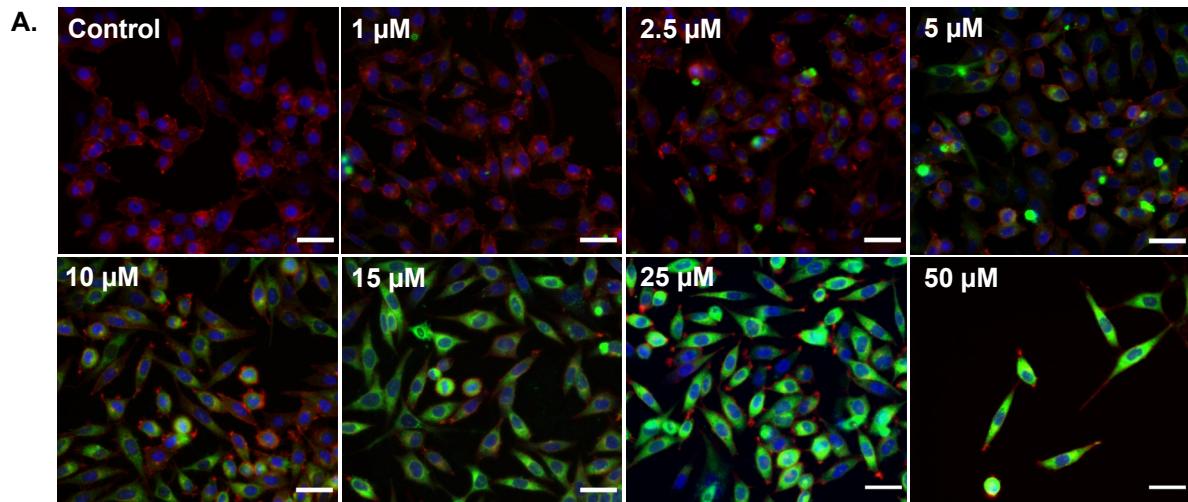


Fig. 14. FITC-G3 cytotoxic analysis in LNCaP. (A) High content images of LNCaP cells treated with FITC-G3 increasing concentrations for 24 hrs. Scale bar 50 μm , 20X magnification. Hoechst and red Phalloidin were used for staining of nuclei and cytoplasm respectively. (B) Cell population normalised to the untreated control after 24 hrs of FITC-G3 treatments. Data is represented as means and $\pm\text{SD}$ of one biological experiment with 3 replicates. One way ANOVA analysis was calculated (** $p < 0.001$).

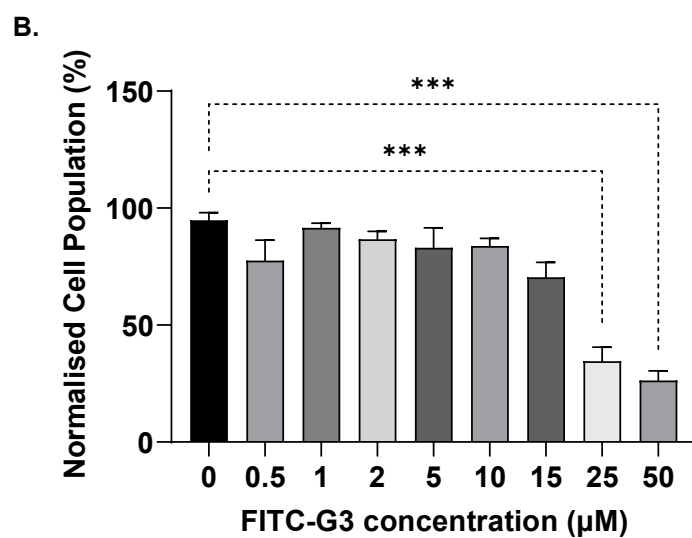
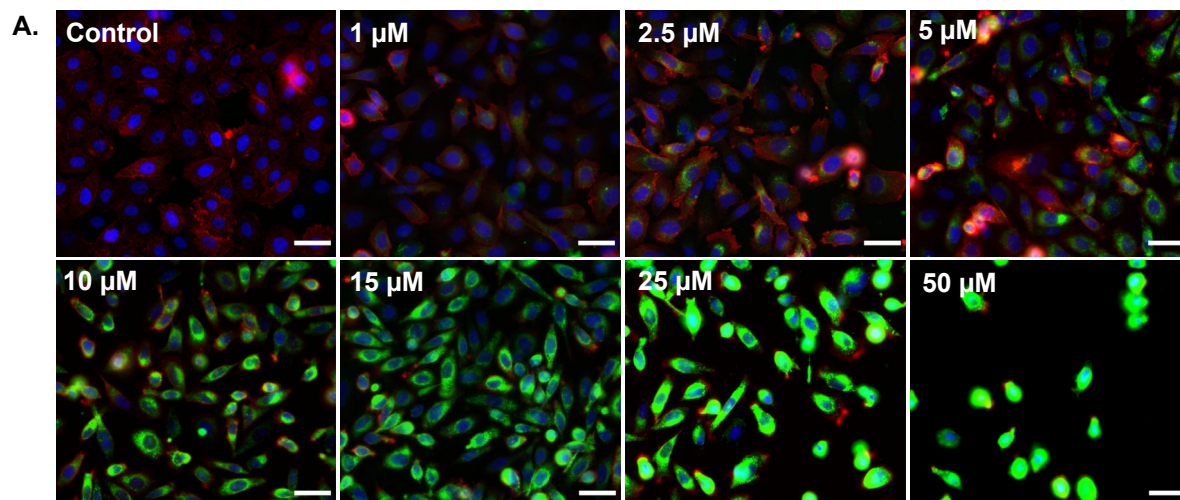


Fig. 15. FITC-G3 cytotoxic analysis in PC-3. (A) High content images of FITC-G3 increasing concentrations. Scale bar 50 μm, 20X magnification. Hoechst and red Phalloidin were used for staining of nuclei and cytoplasm respectively. (B) Normalised cell population after 24 hrs of FITC-G3 treatments. Data is exemplified as means and \pm SD of one biological experiment with 3 replicates. One way ANOVA analysis was calculated for normalised cell populations (** $p < 0.001$).

Previously, our laboratory has investigated the ability of FITC-G3 peptide to penetrate and deliver siRNA molecules in colon cancer spheroids (Cirillo et al., 2021). To complement the FITC-G3 uptake assays, and to establish whether G3 could be suitable for potential tumour treatment, the penetration of the peptide was tested in a 3D model using prostate cancer spheroids. In Figure 16, the uptake of FITC-G3 peptide treatment is visualised in both cell line models, using PCa spheroids. From the images taken of the spheroids, it can be seen that the morphology of PC-3 spheroids was not as homogenous as LNCaP spheroids, which has been reported before in the literature (Hedlund et al., 1999; Ivascu & Kubbies, 2006; Mittler et al., 2017). However, both spheroid models show that FITC-G3 can be visualised throughout the spheroids.

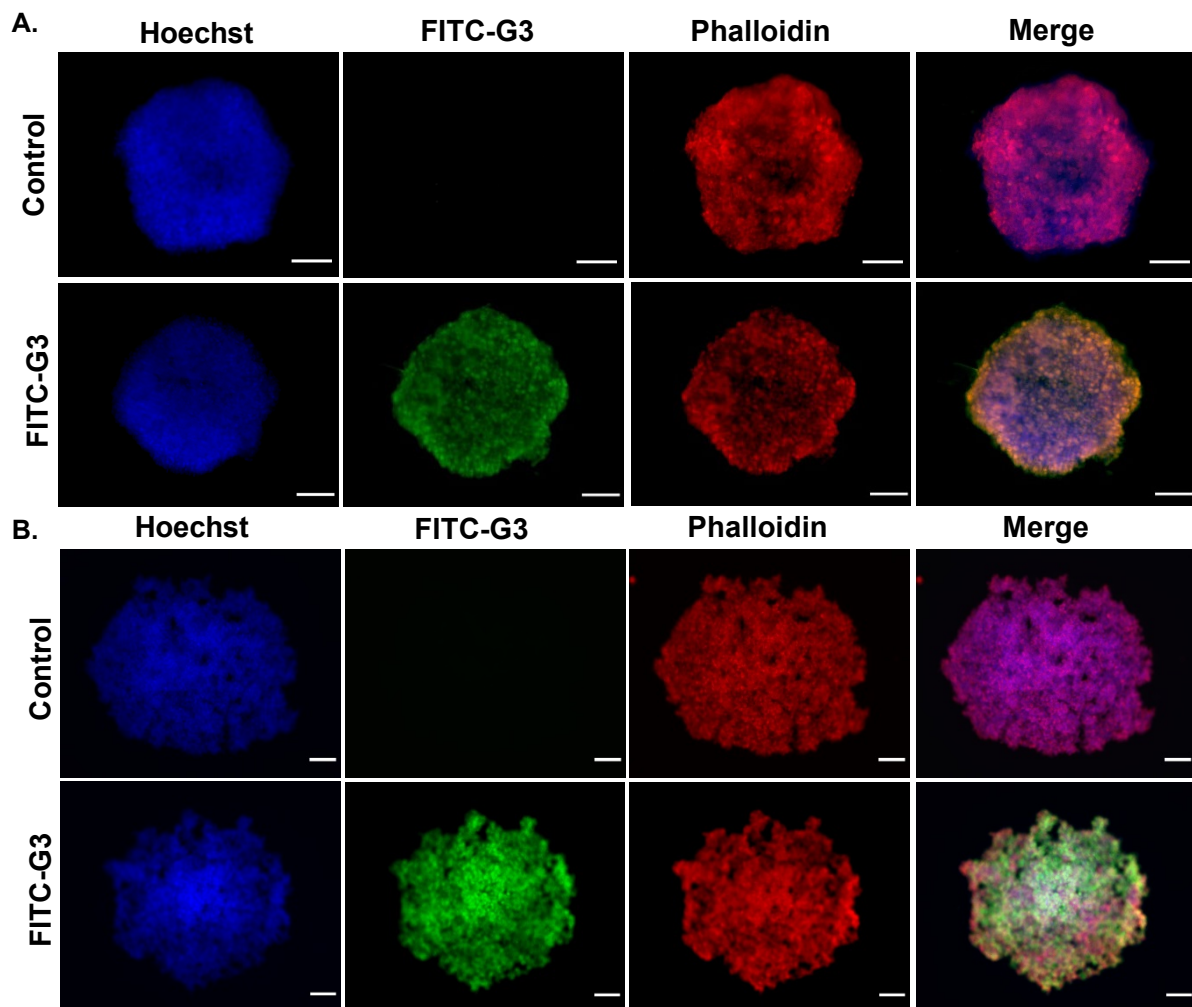


Fig. 16. FITC-G3 internalization in PCa spheroids. (A) LNCaP and (B) PC-3 spheroids treated with FITC-G3 at 4 μ M or 0.1% of DMSO for 24 hours. Cells were stained with Hoechst and Red Phalloidin. Scale bar 100 μ M. Image represents data from a single biological experiment.

3.2.3 Co-culture assay

CD44 is considered a prostate cancer stem cell marker (Hiraga et al., 2013; Hurt et al., 2008; Tang et al., 2007). CD44 is highly expressed in PC-3 cells, while there is a lack of expression in LNCaP cells (Desai et al., 2009; Dhir et al., 1997; Gupta et al., 2012; Liu, 1994; Stevens et al., 1996; Tai et al., 2011). PNT2 cells have been reported as a normal prostatic epithelial cell line, that have a luminal phenotype, and low levels of CD44 expression (Cussenot et al., 1991; Jung et al., 2020; S. H. Lang et al., 2001). To get a deeper understanding of the cell selectivity to prostate cancer cells, a co-culture experiment was designed using PNT2 and PC-3 cells in a 1:1 ratio. The rationale behind this experiment was to use CD44 antibody to discriminate PC-3 from PNT2 populations in the co-culture environment to quantify the number of cells that internalized FITC-G3.

First, the antibody labelling of CD44 was tested independently in both cell lines, using HCS, resulting in PC-3 cells being the only ones that exhibit the positive signal (Fig. 17). Integrated intensity values, corresponding to the CD44 antibody, were measured and normalised individually. PNT2 and PC-3 negative controls were treated only with the secondary antibody in absence of the primary antibody. A student t-test (**p<0.001) was executed to compare integrated intensity values between the two cell lines.

Both cells were simultaneously exposed to 4 μ M of FITC-G3 for 24 hrs and acquired using confocal microscopy in the co-culture experiment. The nuclei staining of both populations was done with Hoechst. Total cell populations were calculated and divided into two clusters, namely CD44+ and CD44-, followed by the calculation of the total number of FITC+ cells in each cluster and presented as percentages. Statistical significance was calculated using student t test (**p<0.001). Figure 18 shows images from the co-culture analysis and it can be seen that FITC-G3 was mainly internalized by CD44+ cells showing a preferential uptake by the CD44+ cell line, which represent the PC-3 populations in the co-culture assay.

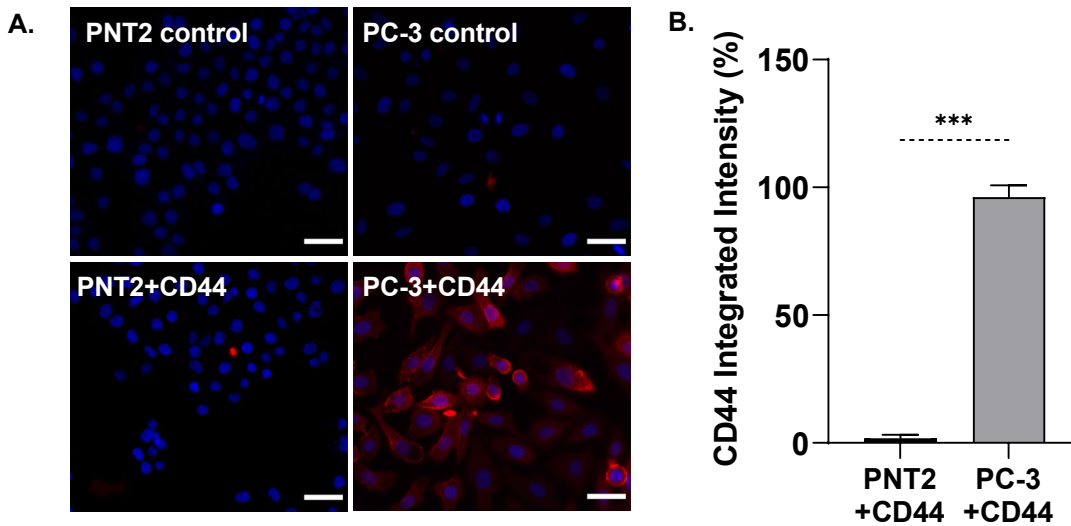


Fig. 17. CD44 antibody specificity test. (A) High content images of CD44 antibody labelling of PNT2 and PC-3 cells. The controls were treated with Alexa Red secondary ab. Scale bar 50 μ m, 20X magnification. (B) Normalised integrated intensity percentages of CD44 staining between PNT2 and PC-3 cells. Data is presented as mean and \pm SD, representative of one experiment with 3 replicates. Statistical significance was calculated using student t test (** $p < 0.001$).

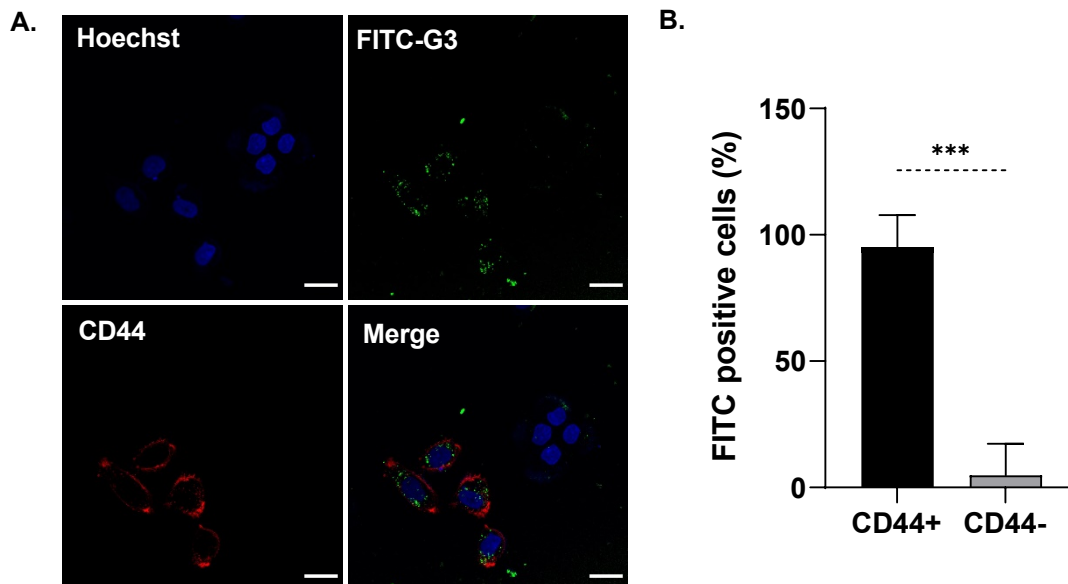


Fig. 18. Cell selectivity analysis in co-culture system. (A) Confocal images of PNT2 normal cells and PC3 cancer cells co-cultured in a 1:1 ratio. The CD44 ab with Alexa Red 595 secondary ab was used to define CD44+ populations. All cells without red fluorescence were counted as CD44- populations. Scale bar 25 μ m, 60X objective. (B) FITC positive cells were calculated for both CD44+ and CD44- groups in 6 FOV. Data is presented as means of 1 experiment with 7 replicates and \pm SD. Statistical significance was calculated using a student-t test (** $p < 0.001$).

3.2.4 Colocalization analysis and endosomal distribution

A colocalization analysis was executed to investigate the distribution of peptides or molecules that gain access to the cell by hijacking endocytic machinery. Previously, the first evidence of G3 using endocytic pathways was identified in colon cancer cells. Specifically, the peptide was observed inside vesicular compartments in colon cancer cells using transmission electron microscopy (TEM), and later on, using RNAi screenings of the endocytic machinery, which resulted in poor uptake of the peptide (Cirillo et al., 2021). However, no subcellular colocalization imaging has been done. To identify if FITC-G3 was present in early and/or late endosomes in LNCaP and PC-3 cells, antibodies that label endocytic proteins were used. The colocalization analysis was done using the Colocalization Colormap plugin and superimposed images were obtained by confocal microscopy.

Transferrin (TF) is an iron-complexing protein that uses CME after engaging with the TF receptor, enabling the absorption of iron into cells. (Pearse & Robinson, 1990). Conversely, one of the most representative markers for macropinocytosis is Dextran (DXT) (Falcone et al., 2006; Nakase et al., 2009). Based on this, an analysis was done to determine the extent of colocalization of TF and DXT with FITC-G3. TF was selected as a positive control for endocytosis, and DXT as a negative control of CME.

In Figure 19A and Figure 20A, the representative images of the colocalization analysis are displayed for LNCaP and PC3, respectively. FITC-G3 is shown in the green channel and TF or DXT in the red channel. By contrast, FITC-G3 and TF both localise together as defined by yellow puncta, indicating colocalization, whereas in FITC-G3 and DXT images there is almost none. The index of correlation (Icorr), that is based on the nMDP values, meaning above 0 to 1 for positive colocalization and below 0 to -1 for no colocalization. High Icorr values from 0.5 to 0.6, were obtained for TF and FITC-G3, while low Icorr values, around 0.2 to 0.3, were calculated for DXT and FITC-G3 in both cell lines, as presented in Figure 19B and Figure 20B. Student t test were performed to compare the statistical differences between Icorr means. In both cell lines, p values <0.001 were obtained between TF and DXT groups. These data indicate that the peptide, at 4 μ M, might enter the cell via CME rather than using macropinocytosis.

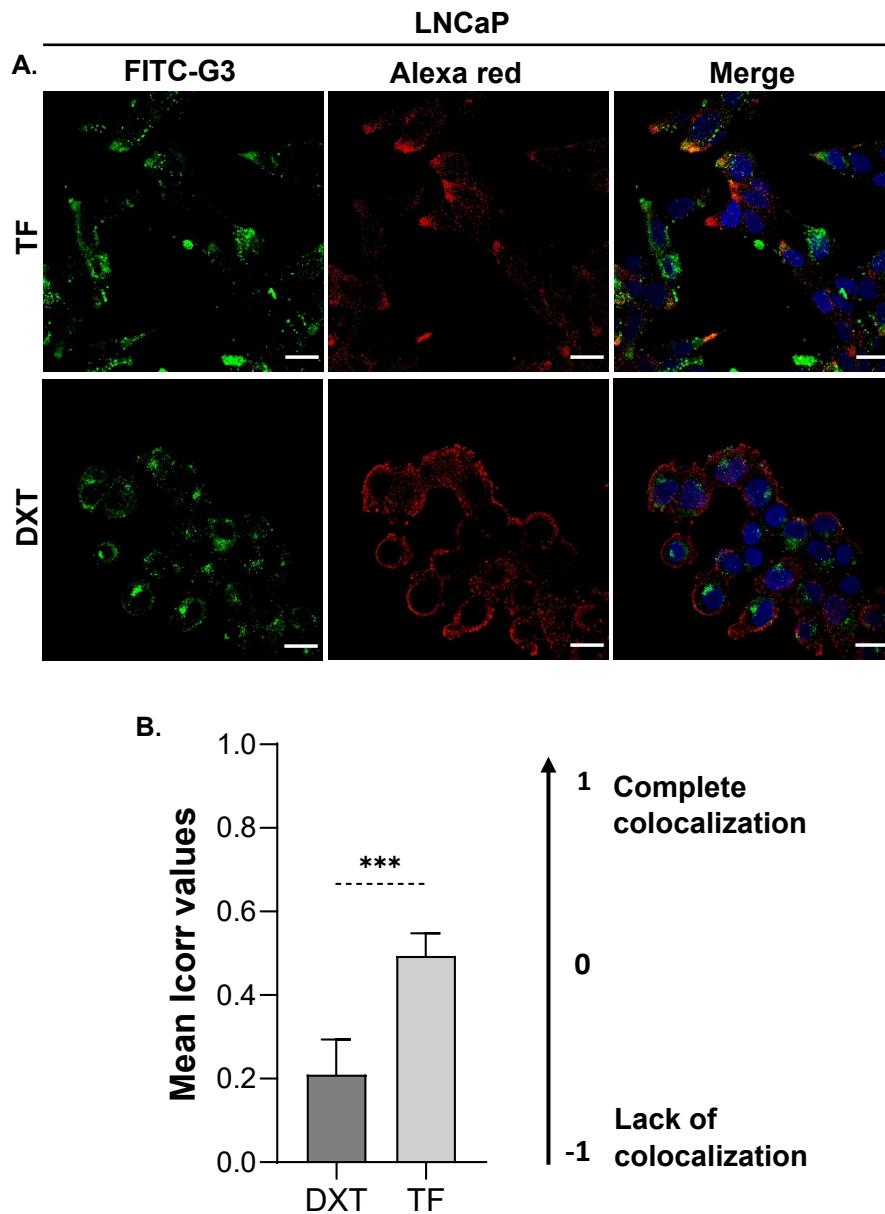


Fig. 19. Colocalization analysis of FITC-G3 and key markers of endocytosis in LNCaP. (A) Confocal images of LNCaP cells treated with FITC-G3 for 1 hr followed by 25 min exposure to Transferrin (TF) or 45 min with Dextran (DXT). Hoechst was used as a nuclear staining. Scale bar 25 μ m, 60X objective. (B) Mean Icorr values were calculated where negative values represent no colocalization and positive values complete colocalization. Statistical significance was calculated using a T test (** $p < 0.001$). Data is presented as means and \pm SD of one biological experiment with 6 FOV.

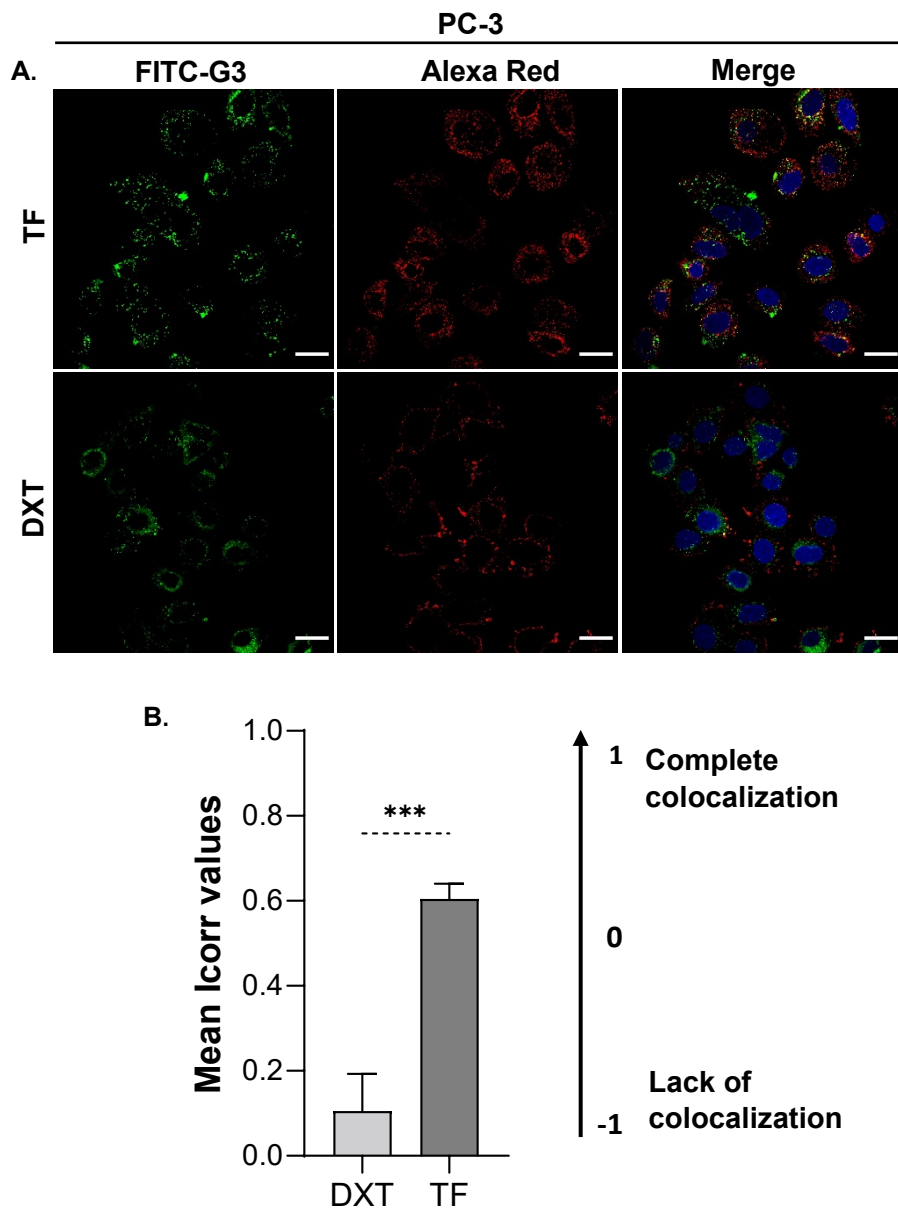


Fig. 20. Colocalization analysis of FITC-G3 and key markers of endocytosis in PC-3. (A) Confocal images of PC-3 cells treated with FITC-G3 for 1 hr followed by 25 min exposure to Transferrin (TF) or 45 min with Dextran (DXT). Hoechst was used as a nuclear staining. Scale bar 25 μ m, 60X objective. (B) Mean Icorr values were calculated where negative values represent no colocalization and positive values complete colocalization. Statistical significance was calculated using a T test (** $p < 0.001$). Data is presented as means and \pm SD of one biological experiment with 6 FOV.

The important function of the Rab-GTPase protein family in intracellular vesicular trafficking is well established (Pfeffer, 2013; Stenmark & Olkkonen, 2001). Among them, Ras-related protein Rab-5 (RAB5) is widely used as an early endosomal marker, due to its interaction with varied effectors to mediate vesicle fusion, biogenesis and maturation (Bucci et al., 1992; Gorvel et al., 1991; Hutagalung & Novick, 2011; Rink et al., 2005). Early-endosomal autoantigen 1 (EEA1) is another well-known marker for early endosomes, which is a RAB5 effector that participates in the endosome fusion (Christoforidis et al., 1999; Mishra et al., 2010; Mu et al., 1995). To establish whether endosomal markers could colocalize with FITC-G3 in PCa cells, we examined in the context of these two early endosomal markers, RAB5 and EEA1.

Figure 21 and Figure 22 present the colocalization analysis between early endosomal markers and FITC-G3 peptide in LNCaP and PC-3, respectively. Images of FITC-G3 in the green channel, RAB5 or EEA1 in the red channel and the merging of both channels are depicted (Fig. 21A and Fig. 22A). In some images the yellow puncta is evident, and even though in others is not as clear, the colocalization algorithm is capable of detecting colocalised values that are not as visible by naked eye. Similar mean Icorr values were obtained for EEA1 and RAB5 in both cell lines (Fig. 21B and 22B). Statistical significance was obtained with p values of less than 0.001, between mean Icorr values of early endosomes against DXT, using one way ANOVA analysis with multiple comparisons in both PCa cell lines. Overall, these data indicates that FITC-G3 initiates an endosomal pathway, since it is localized in early endosomes of LNCaP and PC-3 cells.

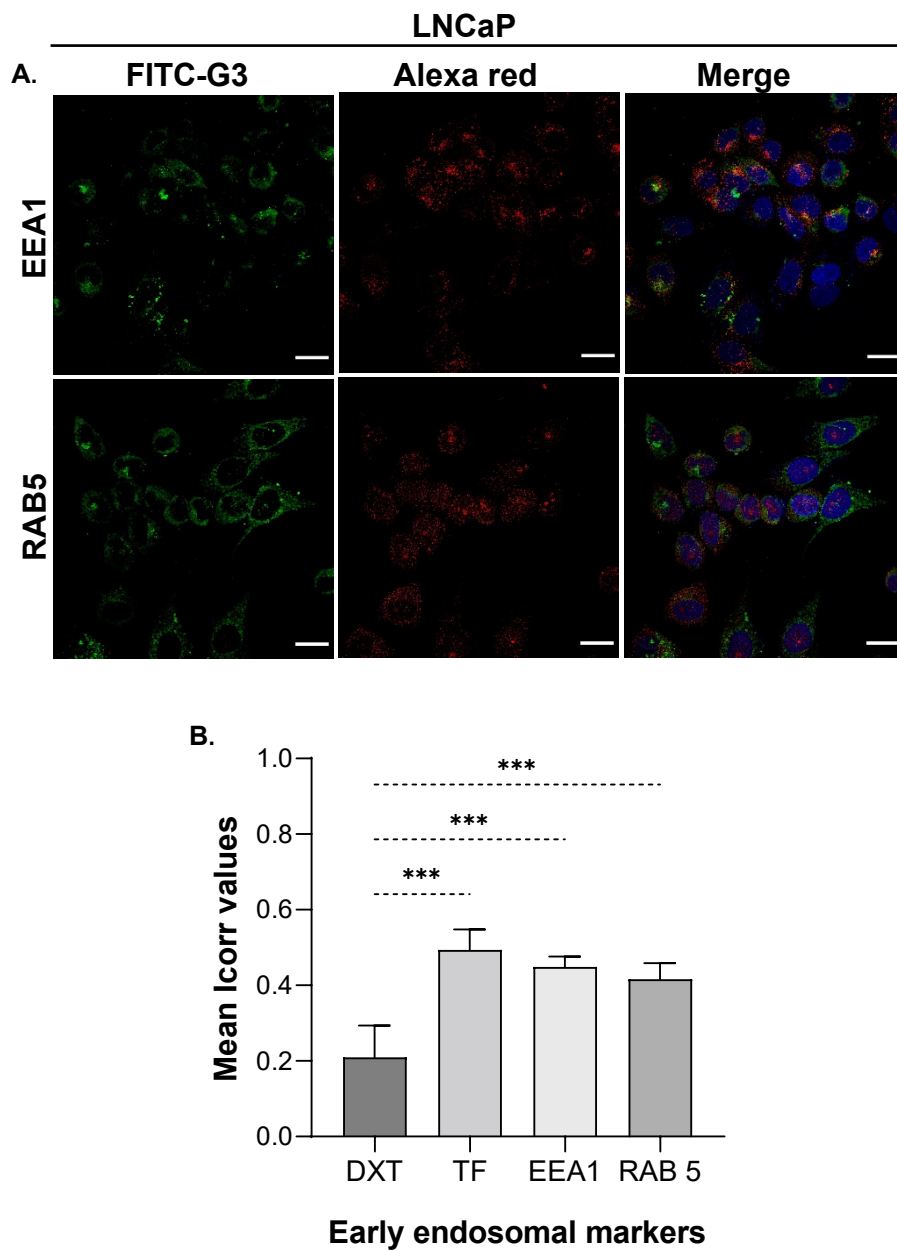


Fig. 21. Colocalization analysis of FITC-G3 and early markers of endocytosis in LNCaP. (A) Confocal images of LNCaP cells treated with FITC-G3 and EEA1 or RAB5 abs. TF and DXT were used as positive and negative controls of clathrin-mediated endocytosis. Hoechst was used as a nuclear staining. Scale bar 25 μ m, 60X objective. (B) Mean Icorr values of early endosomal markers and FITC-G3. The statistical significance was calculated using one way ANOVA analysis (** $p < 0.001$). Data is presented as means and \pm SD of one biological experiment with 6 FOV.

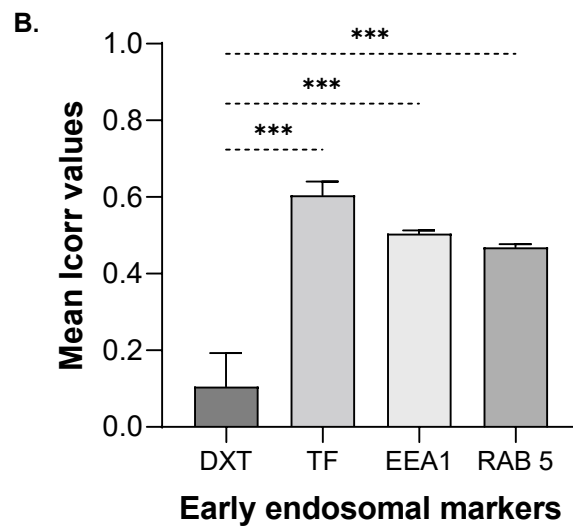
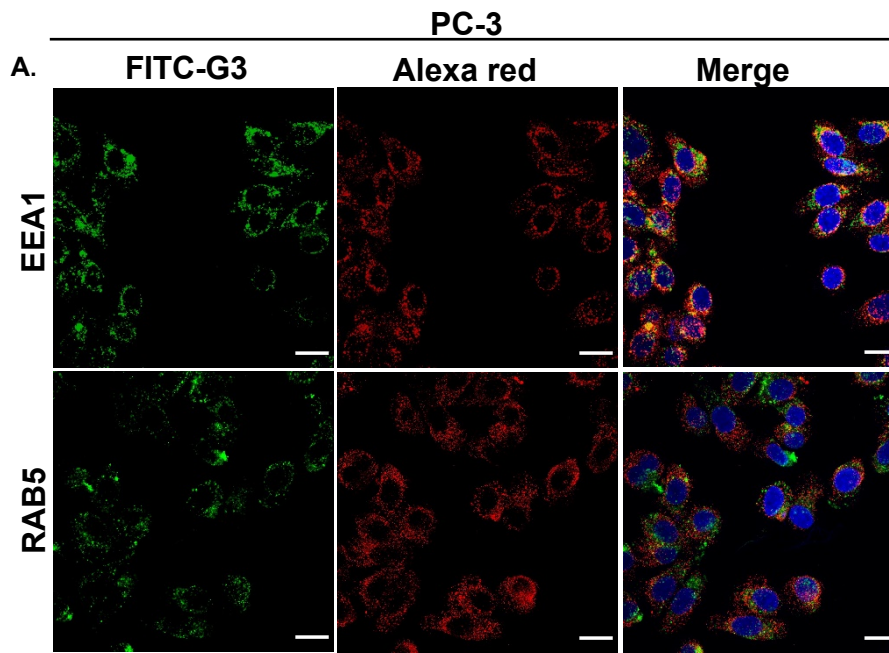


Fig. 22. Colocalization analysis of FITC-G3 and early markers of endocytosis PC-3. (A) Confocal images of PC-3 cells treated with FITC-G3 and EEA1 or RAB5 abs. TF and DXT were used as positive and negative controls of clathrin-mediated endocytosis. Hoechst was used as a nuclear staining. Scale bar 25 μ m, 60X objective. (B) Mean Icorr values of early endosomal markers and FITC-G3. The statistical significance was calculated using one way ANOVA analysis (** $p < 0.001$). Data is presented as means and \pm SD of one biological experiment with 6 FOV.

The recognition of late endosomes often utilizes Ras-related protein Rab-7 (RAB7), another Rab GTPase family member, which is implicated in the formation of lysosomes and mostly in late endosome trafficking (Guerra & Bucci, 2016; T. Wang et al., 2011). It has been reported in the literature that during the maturation process of endosomes, RAB5 gets replaced by RAB7 in late endosomes (Poteryaev et al., 2010; Rink et al., 2005). Another recognized indicator of late endosomes and multi-vesicular bodies, is cluster of differentiation 63 (CD63) (Kobayashi et al., 2000).

To test for late endosomal localization, RAB7 and CD63 antibodies were analysed in the colocalization analysis with FITC-G3 (Fig. 23A, for LNCaP, and 24A for PC-3). Positive colocalization was obtained between Rab7 and FITC-G3, and between CD63 and FITC-G3 in LNCaP and PC-3 cells. There was a statistical significance between Icorr mean values of the late endosomal markers when compared with DXT control in both prostate cancer cell lines (Fig. 23B and 24B). The high colocalization of FITC-G3 and late endosomal markers in both PCa cell lines, is consistent with the positive colocalization in early endosomal compartments.

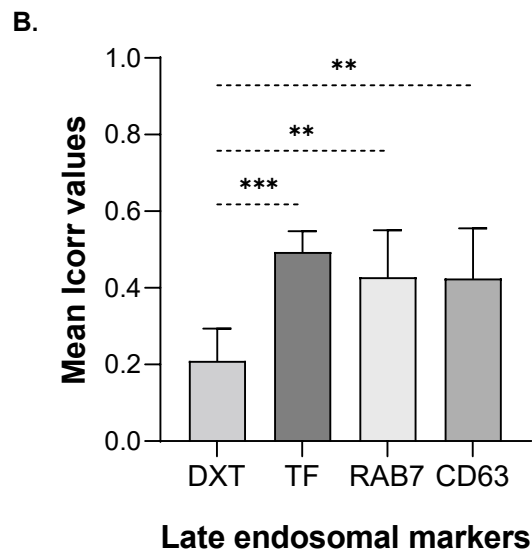
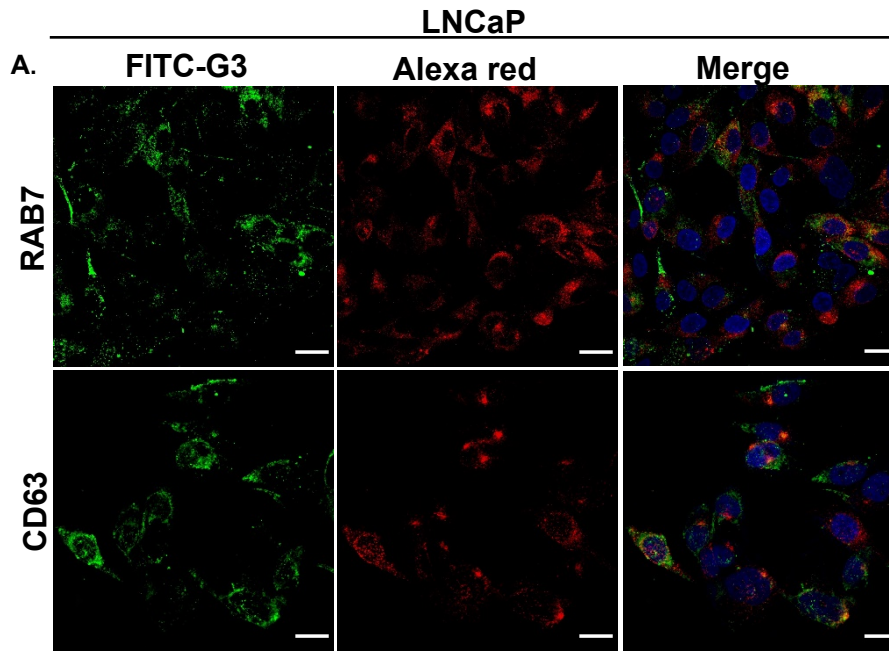


Fig. 23. Colocalization analysis of FITC-G3 and late markers of endocytosis LNCaP. (A) Confocal images of LNCaP cells treated with FITC-G3 and RAB7 or CD63 abs. TF and DXT were used as positive and negative controls of clathrin-mediated endocytosis. Hoechst was used as a nuclear staining. Scale bar 25 μ m, 60X objective. (B) Mean Icorr values were calculated and the statistical significance was calculated using one way ANOVA analysis (** $p < 0.01$; *** $p < 0.001$). Data is presented as means and \pm SD of one biological experiment with 6 FOV.

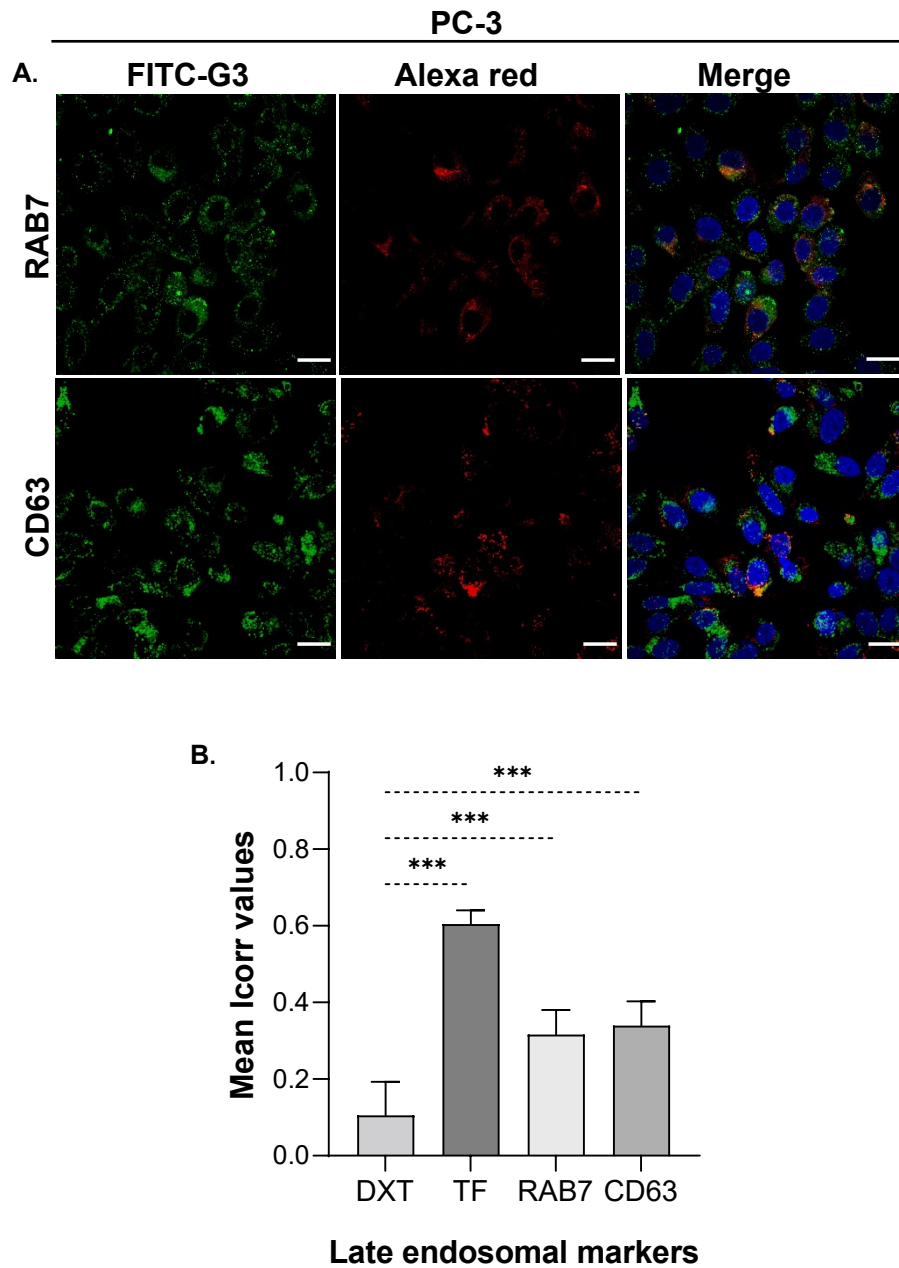


Fig. 24. Colocalization analysis of FITC-G3 and late markers of endocytosis in PC-3. (A) Confocal images of PC-3 cells treated with FITC-G3 and RAB7 or CD63 abs. TF and DXT were used as positive and negative controls of clathrin-mediated endocytosis. Hoechst was used as a nuclear staining. Scale bar 25 μ m, 60X objective. (B) Mean Icorr values of late endosomal markers and FITC-G3. The statistical significance was calculated using one way ANOVA analysis (** $p < 0.001$). Data is presented as means and \pm SD of one biological experiment with 6 FOV.

Lysosomal-associated membrane protein 1 (LAMP1) represents a well-recognized marker of lysosomes (Eskelinen, 2006; Kornfeld & Mellman, 1989; Wartosch et al., 2015). Finally, in the analysis of endosomal pathways, the analysis of LAMP-1 was done. The representative images of the colocalization analysis between LAMP1 and FITC-G3 is presented in Figure 25A for LNCaP and Figure 26A for PC-3 cells. LAMP1 fluorescent marker displayed positive colocalization with FITC-G3, in LNCaP and PC-3 cells. In Figure 25B and Figure 26B, mean Icorr values are presented and the statistical significance was calculated using ANOVA analysis in both prostate cancer cell lines. The p values for LNCaP were less than 0.01 and less than 0.001 for PC-3.

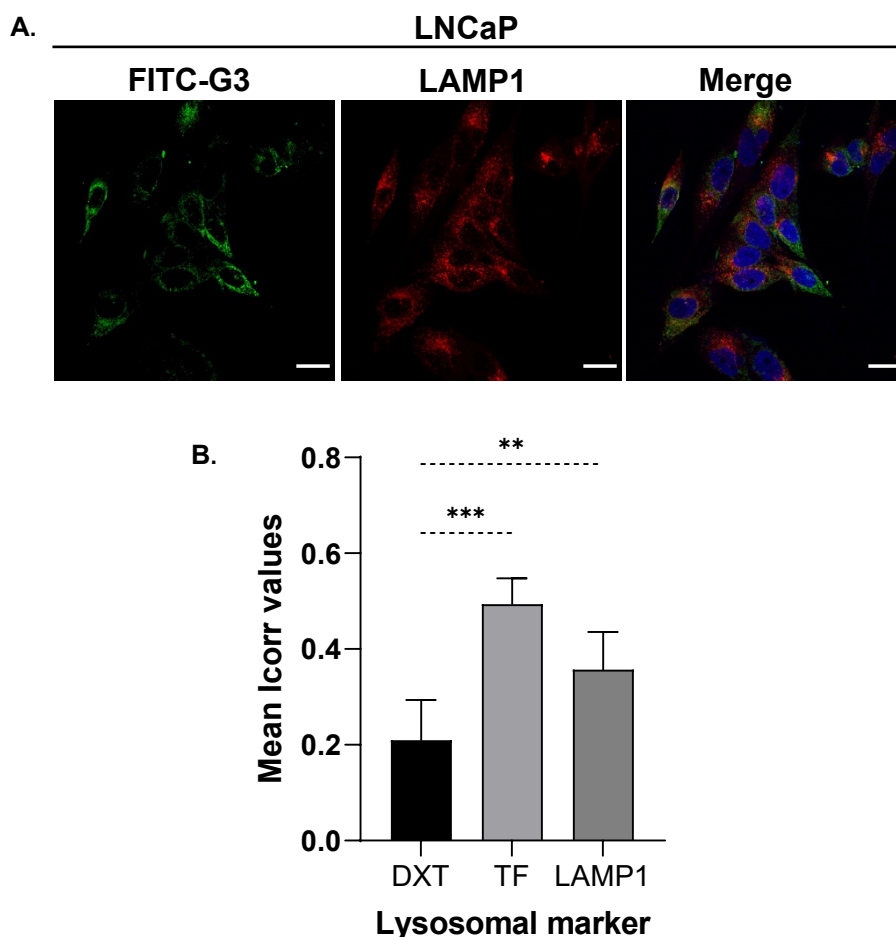


Fig. 25. Colocalization analysis of FITC-G3 and LAMP1 in LNCaP. (A) Confocal images of LNCaP cells treated with FITC-G3 and LAMP1 ab. TF and DXT were used as positive and negative controls of clathrin-mediated endocytosis. Hoechst was used as a nuclear staining. Scale bar 25 μ m, 60X objective. (B) Mean Icorr values of LAMP1 and FITC-G3. The statistical significance was calculated using one way ANOVA analysis (** $p < 0.01$; *** $p < 0.001$). Data is presented as means and \pm SD of one biological experiment with 6 FOV.

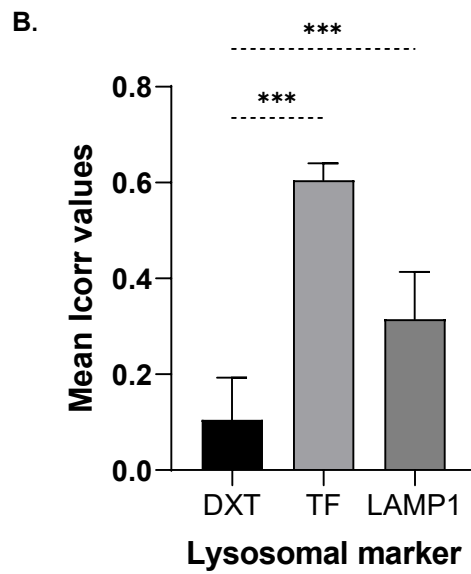
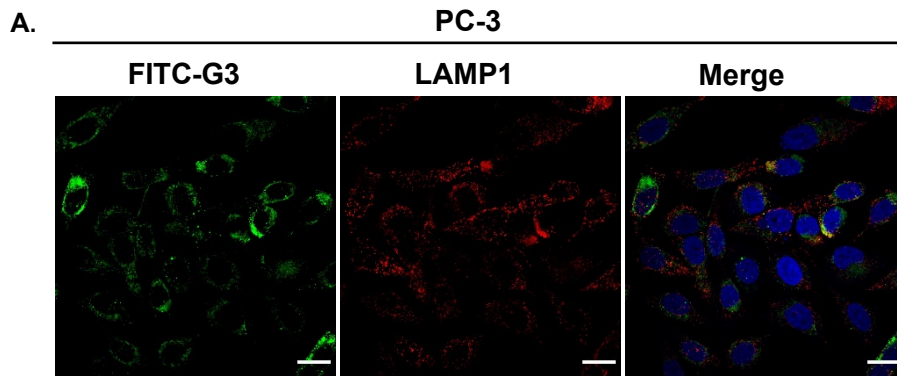


Fig. 26. Colocalization analysis of FITC-G3 and LAMP1 in PC-3. (A) Confocal images of PC-3 cells treated with FITC-G3 labelled with LAMP1 ab. TF and DXT were used as positive and negative controls of clathrin-mediated endocytosis. Hoechst was used as a nuclear staining. Scale bar 25 μ m, 60X objective. (B) Mean Icorr values were calculated and statistical significance was analysed using ANOVA analysis (** $p < 0.001$). Data is presented as means and \pm SD of one biological experiment with 6 FOV.

3.2.5 Macropinocytosis Inhibition

Diverse CPP employ macropinocytosis as an internalization mechanism, which is characterized by using macropinosomes to swallow substantial volumes of solute and non-selective molecules (Lim & Gleeson, 2011). To provide more evidence about the uptake mechanism of G3, an experiment was designed to measure whether the FITC-G3 peptide is capable of entry inside cells after inducing the chemical inhibition of macropinocytosis in prostate cancer cells. Control and treated cells were exposed to equal amounts of FITC-G3 (4 μ M) and DXT, and EIPA inhibitor, used to block macropinocytosis only in treated dishes.

In Figure 27A for LNCaP and Figure 28A for PC-3, images of the inhibition of macropinocytosis are presented. In the red channel images, the reduction of DXT marker is visualized in the cells that were treated with EIPA inhibitor. FITC-G3 internalization is observed in both, controls and treated images. Red integrated intensity values were acquired for the two cell lines and as expected, DXT signal was drastically decreased in treated dishes (Fig. 27B and Fig. 28B). A student t test was executed to compare mean differences against the control. The FITC integrated intensity was plotted in Figure 27C for LNCaP and Figure 28C for PC-3, however no difference was obtained for FITC-G3 values between the ones with EIPA inhibitor and the control. These data support the conclusion that FITC-G3 internalization is not affected after macropinocytosis inhibition in PCa cells and thus FITC-G3 is not internalised through macropinocytosis, at least at 4 μ M.

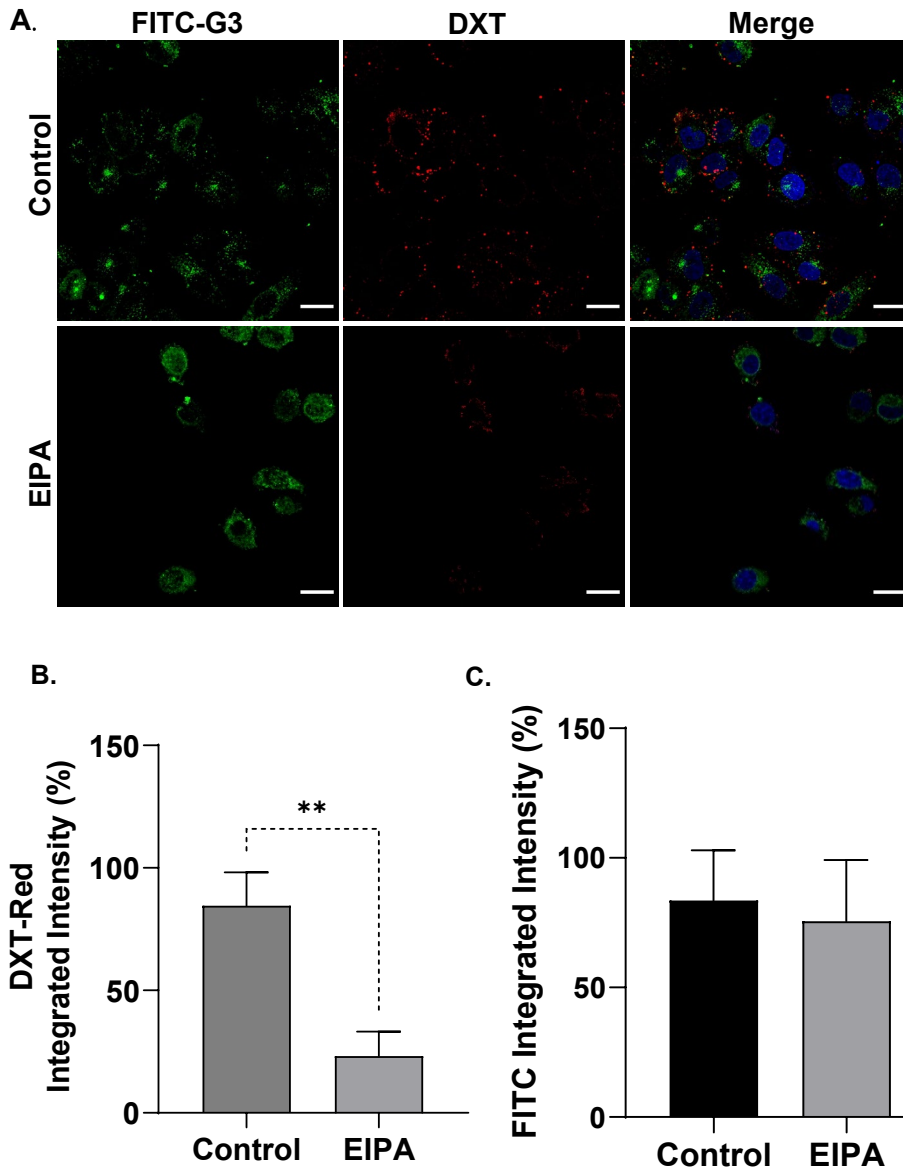


Fig. 27. Macropinocytosis inhibition analysis in LNCaP. (A) Confocal images of LNCaP cells, either only exposed with FITC-G3 and Dextran (DXT) as control or cells treated with EIPA inhibitor as well. Nuclei were labelled using Hoechst. Scale bar 25 μ m, 60X objective. (B) DXT-red integrated intensity values presented as percentages. A T-test was done to analyse significant differences between means (** $p < 0.01$). (C) FITC integrated intensity values were graphed. Data is presented as means and \pm SD of one biological experiment with 6 FOV.

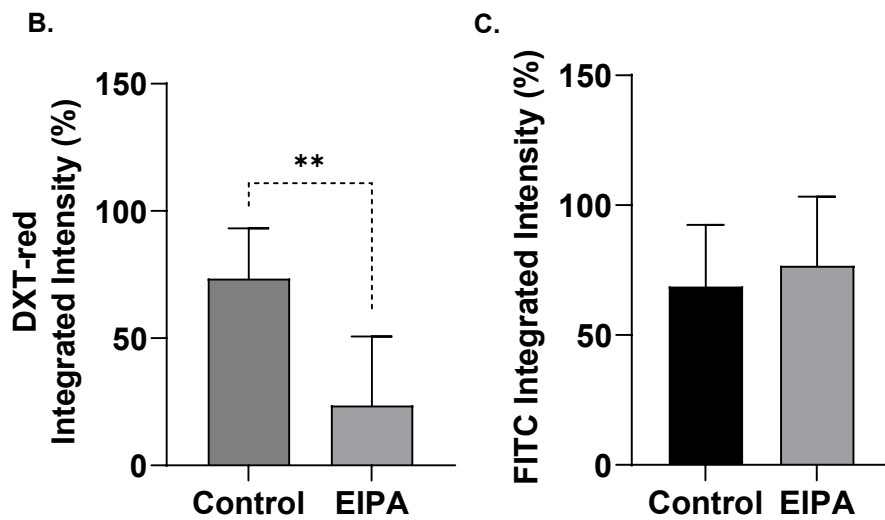
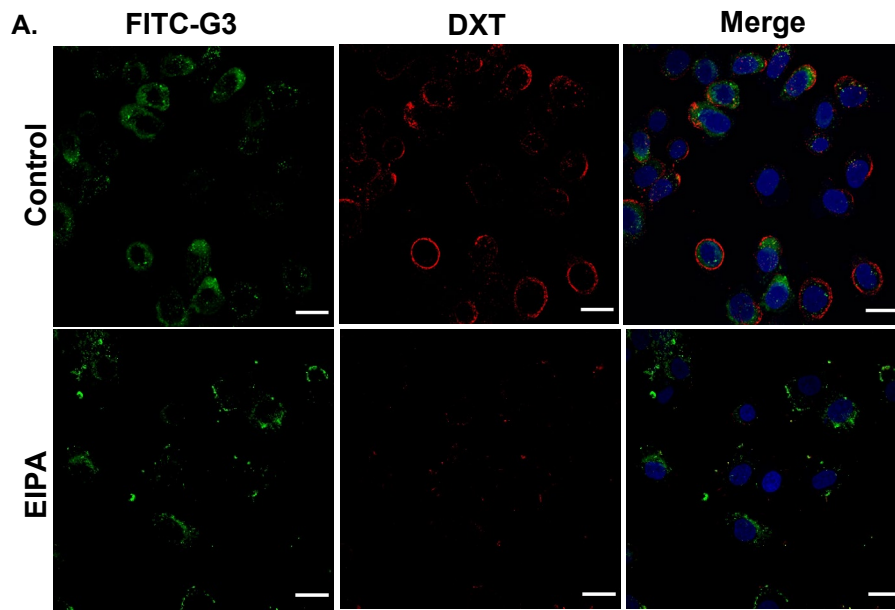


Fig. 28. Macropinocytosis inhibition analysis in PC-3. (A) Confocal images of PC-3 cells, either only exposed to FITC-G3 and Dextran (DXT) as control or cells treated with EIPA inhibitor as well. Nuclei was labelled using Hoechst. Scale bar 25 μ m, 60X objective. (B) DXT-red integrated intensity values are presented as percentages. A T-test was done to analyse significant differences between means (** $p < 0.01$). (C) FITC integrated intensity values were graphed. Data is shown as means and \pm SD of one biological experiment with 6 FOV.

3.3 Discussion

In summary of Chapter 3, the prostate cancer cell selectivity of FITC-G3 peptide was demonstrated, as well as its cytotoxic effect at high dosages. On the contrary, normal prostate cells displayed poor internalization of the peptide and they did not show a cytotoxic effect in response to any of the given concentrations. These findings are in alignment with prior studies in the literature that have confirmed the cancer cell selectivity and cytotoxic activity at high concentrations of G3 (Chen et al., 2014a; Chen et al., 2014b; Cirillo et al., 2021; Hu et al., 2011). Furthermore, the chemical inhibition of macropinocytosis did not affect the internalization of the peptide, and all endosomal markers tested, together with the lysosomal marker, indicate that FITC-G3 colocalizes with them, agreeing with previous siRNA screen data and provide further evidence of G3 being internalized via the canonical CME (Cirillo et al., 2021).

3.3.1 Does G3 have prostate cancer cell selectivity?

For tumour targeting peptides, it is vital to initially demonstrate their discrimination of normal cells and selective preference to malignant cells. Due to the lack of prior research on G3 uptake in PCa, two cell lines were chosen based on their disease phenotypes. LNCaP represents a prostate adenocarcinoma cell line that is AR responsive, while PC-3 characterizes a more aggressive metastatic cell line that is non-responsive to AR (Horoszewicz et al., 1983; Kaighn et al., 1979; van Bokhoven et al., 2003). FITC-labelled G3 was used to quantify and compare their cellular uptake with PNT2, a cell line that was derived from a 33-year-old man's non-cancerous prostate tissue (Cussenot et al., 1991).

The results of the G3 internalization assays show that FITC-G3 enters PCa cells, and displays enhanced cell affinity against PC-3 and LNCaP cells, compared with marginal uptake in PNT2 cells, which was further validated by high resolution imaging. These results are in alignment with previous studies that have reported G3 being internalized preferentially by HCT-116 colon cancer cells, Hep-G2 liver cancer cell, HeLa cervical cancer cells and HL60 leukemia cells, in comparison with their negligible internalization in benign cells, such as HDF and NIH 3T3 cells (Chen et al., 2014a; Chen et al., 2014b; Cirillo et al., 2021; Hu et al., 2011). The exposure of the peptide in the internalization assays was determined as 24 hrs based on the mentioned study in

colon cancer cells, and the dose used was 4 μ M. PNT2 cells were tested at early passages as differences in morphology were observed at late passages, that could hint to accumulation of mutations and changes in gene expression (Chang-Liu & Woloschak, 1997; Kim et al., 2017). According to the findings of the cell counts by HCS, neither the PCa cells nor the control cell's viability were impacted by FITC-G3 exposure at the specified dose. Due to the low spatial resolution of the HCS microscope, Z-stacks compilations using confocal microscopy helped to confirm the uptake discrepancies between PCa and normal cells. Given phalloidin stains F-actin filaments in cells, it was utilized to outline cells by ROI, to facilitate the FITC-G3 puncta measurements. In agreement with prior experiments, in which FITC-G3 was demonstrated to access and unload siRNA into colon cancer spheroids, in this work it was shown the positive penetration of FITC-G3 in PCa spheroids (Cirillo et al., 2021). These observations highlight a consistency in the behaviour of FITC-G3 in colon and prostate cancerous tissues, which raises the possibility of a wider applicability across various cancer types. Images of the spheroids depicted that, according to previous reports in the literature, the morphology of PC-3 spheroids was not as uniform as that of LNCaP spheroids (Hedlund et al., 1999; Ivascu & Kubbies, 2006; Mittler et al., 2017).

A co-culture experiment was designed based on the fact that CD44 has been found highly upregulated in PC-3 cells, while poor or lack of expression has been reported in PNT2 cells (B. Desai et al., 2009; Dhir et al., 1997; Draffin et al., 2004; A. Gupta et al., 2012; Jung et al., 2020; S. H. Lang et al., 2001; Liu, 1994; S. Tai et al., 2011). The goal of this experiment was to count the number of cells that internalised FITC-G3 by using CD44 antibodies to distinguish PC-3 from PNT2 populations in a 1:1 co-culture environment. The important function of CD44 in metastasis, invasion, and progression in cancer has been documented (Senbanjo & Chellaiah, 2017). In particular, high expression levels of CD44+ cells have been associated with metastatic features and PCa stem cell potential (Patrawala et al., 2006). Also, CD44 has been proposed as a PCa stem cell marker (Collins et al., 2005; Hiraga et al., 2013; Hurt et al., 2008; Tang et al., 2007). The CD44 antibody specificity was tested in PNT2 and PC-3 cells independently by HCS, which confirmed the CD44+ fluorescence intensity exclusively in PC-3 cells. Thus, the results of the co-culture test revealed that the PC-3 populations, which were represented by CD44+ cells, demonstrated the majority of

the FITC-G3 uptake. These results align with the stated studies that have demonstrated high expression of CD44, specifically in PC-3 cells and with low or absence of CD44 in PNT2 cells. In a similar way, the specificity of G3 has been evaluated in other co-culture experiments with different settings that are consistent with our findings. For instance, in a co-culture of HCT-116 and HDF it was possible to observe the G3-mediated internalization of siGLO mostly in colon cancer cells (Cirillo et al., 2021), or in another dual culture the uptake of FITC-G3 was clearly observed in HL60 but not in NIH-3T3 fibroblasts (Hu et al., 2011). The co-culture experiment's findings in this work added to the body of data supporting G3 uptake preference for metastatic PC-3 cells over normal prostate PNT2 cells.

3.3.2 Does G3 exhibit a cytotoxic effect in prostate cancer cells?

Cytotoxicity to non-cancer cells is an undesired effect for drug delivery systems. LNCaP, PC-3, and PNT2 cells were treated with various doses ranging from 1 to 50 μM of FITC-G3 with the intention to assess if it has cytotoxic action against PCa. In these assays, the internalization of FITC-G3 by LNCaP and PC-3 cells was substantial, without impairing their viability at low concentrations (4 μM), but at high concentrations (20 to 50 μM), the peptide exerted a drastic cytotoxic effect, as evidenced by significant cell death. Conversely, the normal PNT2 cell viability remained largely unaffected throughout the treatment process. Even though PNT2 cells, did internalize the peptide at high concentrations (10 to 50 μM), the internalization of G3 was more markedly pronounced in PCa cells, since the difference between them was more than two-fold. The elevated cytotoxicity obtained in PCa cells at 25 to 50 μM dosages of FITC-G3 is in accordance with earlier reports, as at 25 μM there was a decrease of around half of the cellular populations. Accordingly, using MTT assays it was shown that HL60 and HpeG2 cells presented an IC_{50} of ~ 25 μM of G3 and an IC_{50} of ~ 15 μM for Hela cells. In agreement with our research, these analyses also showed little toxicity to the fibroblasts, a non-malignant control (Chen et al., 2014a; Chen et al., 2014b; Hu et al., 2011). In line with our experiments, the IC_{50} reported for HCT-116 cells is ~ 50 μM for non-conjugated G3 and ~ 60 μM for FITC-G3, while they calculated an IC_{50} of 86 μM for FITC-G3 being more sensitive towards fibroblasts than naked G3 which no cytotoxicity was detected (Cirillo et al., 2021).

While we did not evaluate the cytotoxic effect of naked G3 on PCa cells, based on observed trends in the cited cancer cell lines and our results with FITC-G3, it's tentatively speculated that a similar IC50 difference might be seen in PCa cells. Nonetheless, it would be necessary to evaluate the cytotoxicity of non-conjugated G3 in PCa cells to corroborate this.

3.3.3 Is the subcellular localization of G3 in clathrin-associated compartments?

CPP can gain access to the interior of the cells by two different mechanisms: direct penetration without energy input or by an energy-mediated endocytic pathway (Gestin et al., 2017; Madani et al., 2011; Ruseska & Zimmer, 2020; Tashima, 2017; Trabulo et al., 2010; Yang et al., 2019). In our laboratory, several pieces of evidence have indicated that the uptake of G3 occurs through endocytosis. Using TEM, Cirillo and collaborators treated HCT-116 cells with FITC-G3, that was linked to an antibody anti-FITC and gold nanoparticles, which allowed the visualization of the internalization of the peptide in vesicles. Following this experiment, they exposed the peptide to cold temperature (4 °C) to impede energy-dependent cellular functions, including endocytosis; the internalisation of G3 was entirely inhibited and it could only resume when the temperature was raised to 37 °C. Moreover, impairment of the internalization of G3 resulted after knocking down the endocytic machinery using RNAi (Cirillo et al., 2021).

In this work, a colocalization study using the Colormap Colocalization Image J plugin was done to provide a more comprehensive understanding of the intracellular localization of the peptide. The results demonstrated high degree of colocalization of FITC-G3 with the markers of the endo-lysosomal system in PCa cells, which enriches the previous body of evidence reported by Cirillo and colleagues, that supports G3's uptake via clathrin-mediated endocytosis. There was an overlap of puncta of both FITC-G3 and TF, which is used typically as a standard indicator of CME (Pearse & Robinson, 1990). The colocalization assessment resulted in high Icorr values for LNCaP and PC-3, clearly suggesting that the peptide enters the cells using CME. In both cell lines, DXT a widely recognized macropinocytosis marker (Falcone et al., 2006; Nakase et al., 2009), demonstrated poor colocalization with FITC-G3 and the

internalisation of the peptide was unaffected by the chemical suppression of macropinocytosis using EIPA, indicating that the peptide is not internalized through this mechanism, where EIPA is considered the most potent and specific pharmaceutical agent to prevent macropinocytosis (Commisso et al., 2013; Ivanov, 2008). EIPA activity was verified by the reduction of DXT puncta observed in PCa cells and its integrated intensity estimations.

Furthermore, the analysis applied to Z-sections of the confocal images, revealed that FITC-G3 highly colocalizes with the biomarkers EEA1, RAB5, RAB7, and CD63 at a similar degree, which indicates the accumulation of the peptide in early and late endosomes. Fusion and fission processes are commonly experienced by endosomes during endocytosis (Gautreau et al., 2014). In early endosomes, RAB5 is stimulated by Rabex-5, facilitating the synthesis of phosphatidylinositol 3-phosphate (PI(3)P) through the recruitment of phosphatidylinositol 3-kinase catalytic subunit type 3 (PIK3C3) (Murray et al., 2016). EEA1 takes part in endosome fusion through its interaction with Rab5 and PI(3)P (Christoforidis et al., 1999; Mishra et al., 2010; Mu et al., 1995). As endosomes mature, Rab5 is eventually substituted by Rab7 in late endosomes (Poteryaev et al., 2010; Rink et al., 2005). Rab7 encompasses pivotal functions including, modulation of lysosome creation and transport and maturation from late endosomes to lysosomal organelles (Guerra & Bucci, 2016; Wang et al., 2011). Thus, following an energy-dependant endocytic route, it was logical to find G3 colocalized with EEA1 and the two Rab GTPase family members, Rab5 and Rab7.

Although CD63 is not implicated in endosomal trafficking regulation per se, it is an established component of both late endosomes and lysosomal membranes (Kobayashi et al., 2000). Due to the location of CD63 in late endosomes, multivesicular bodies, and lysosomes, the positive colocalization that resulted with G3 peptide supports the premise of being routed to these organelles. In addition, CD63, as other tetraspanins, is also typically utilized as a marker for exosomes, which may suggest that the peptide is associated with or packaged within exosomes into multivesicular bodies (Escola et al., 1998; Logozzi et al., 2009; Yoshioka et al., 2013). This might have implications of the extracellular release of the peptide, which would be interesting to investigate in future experiments. However, the fact that it was found in our analysis that FITC-G3 positively colocalizes with LAMP1, a standard lysosomal marker

(Eskelinen, 2006; Kornfeld & Mellman, 1989; Wartosch et al., 2015), suggests that at least some of the peptide goes directly to the lysosomes and potentially be exposed to proteolytic degradation in both PCa cell lines. The maturation of Lamp1-positive lysosomes requires Rab7, which G3 was discovered to colocalized as well (Lee et al., 2011; Yap et al., 2018). However, latest research shows that LAMP1-labelled pits aren't always degradative as some of them lack acid hydrolases, such as cathepsin B and D; or even if they contain acid enzymes, they might not display the correct pH for their activity (Cheng et al., 2018; Trofimenko et al., 2021a; Yap et al., 2018). Also, the presence of LAMP1 has been detected in late endosomes, LAMP transient vesicles and at the cellular membrane (Baba et al., 2020; Pols et al., 2013). Thus, the positive colocalization of G3 with LAMP1 doesn't necessarily mean it undergoes lysosomal degradation.

The subcellular localization of several CPP or cell targeting peptides has been investigated using colocalization analysis with varied endosomal markers. In a comparable way to our study, a cancer targeting peptide called Pep42 was revealed to localize in CME compartments, testing transferrin in combination with endocytic inhibitors, a marker for lipid rafts and organelle-focused fluorescent tracers through a colocalization analysis (Liu et al., 2007). Lack of colocalization with clathrin-related endosomal markers such as transferrin and EEA1 have been reported for the HIV-1 TAT peptide, while increased colocalization with cholera toxin B, indicating a caveolae-mediated mechanism (Fittipaldi et al., 2003). Differing from our observations, one research identified a distinct endocytic mechanism for certain cationic CPPs, including Transportan, TAT, Penetratin, R9, and MAP, using live colocalization with pulse-chase experiments. Their data supports a Ras-related protein Rab-14 (RAB14)-dependent mechanism for endosomal progression, bypassing the usual RAB5/RAB7 GTPases. Remarkably, they reported the engagement of EEA1 to early endosomes even without the presence of RAB5 (Trofimenko et al., 2021a). Their study is the first one that has reported such endocytic process for cationic CPP and for other positively charged molecules. Considering that these CPP are cationic but have diverse physicochemical properties, it leads to the question of whether a cationic CPP, such as G3, might also utilize a RAB14-based endocytic mechanism in cells where RAB14 is inactive. Nevertheless, our colocalization findings are in agreement with a RAB5/RAB7-associated pathway which is the leading endosomal route for CPPs that are up taken

via CME (Bechara & Sagan, 2013; Madani et al., 2011; Ruseska & Zimmer, 2020; Trabulo et al., 2010).

In addition, potential upcoming experiments to expand our knowledge on the subject could involve testing G3's colocalization with markers of the recycling machinery such as RAB11 (Ullrich et al., 1996; Wandinger-Ness & Zerial, 2014), or tracers of intracellular organelles. Currently there are commercial probes designed for specific organelles, for example the use of ER-tracker for endoplasmic reticulum identification, MitoTracker for mitochondria, and Golgi-targeted ceramides with fluorescent labels. Although LAMP1 localizes mostly in lysosomes, it can also be present in lysosomal-associated compartments that do not have enrichment of proteolytic enzymes (Cheng et al., 2018; Trofimenko, et al., 2021a; Yap et al., 2018), therefore future experiments could be done to corroborate whether G3 locates precisely in lysosomes, and hence is susceptible to lysosomal degradation. For instance, an approach that could be tested to verify G3's location in lysosomes is determining the pH of the lysosomal-related compartments where G3 was colocalized using a LysoSensor Dye, which fluorescence rises in acidic settings (Diwu et al., 1999; L. Ma et al., 2017a).

CHAPTER 4

4. ROLE OF SCAVENGER RECEPTORS IN THE UPTAKE MECHANISM OF G3

4.1 Introduction

4.2 Scavenger receptors diversity and classification

Scavenger receptors (SR) embody a supergroup of cell surface receptors, diverse in both structure and functionality, that are classified into 12 classes, from A to L (Alquraini & El Khoury, 2020; PrabhuDas et al., 2017). Their protein structure and aa sequences set the parameters for their classification (PrabhuDas et al., 2017; Zani et al., 2015). They were identified for the first time on the surface of macrophages in the 70s (J. Goldstein et al., 1979). Goldstein and collaborators discovered that the altered, acetylated or oxidized, low-density lipoprotein (LDL) undergoes internalization and degradation after binding to SR, while the native LDL stays unaffected. SR are particularly flexible in their responses due to their capacity to bind with various co-receptors. Their functions are quite heterogeneous including, lipid transportation, and metabolism, cell adhesion, cargo delivery, pathogen removal, host defense, immunological reaction, inflammation and presentation of antigens (Canton et al., 2013; Taban et al., 2022).

Damage-associated molecular patterns (DAMPs) are defined as a cluster of molecules with unintended alterations, which can be lipids, proteins or even DNA, that jeopardize an organism's ability to function adequately (Hartvigsen et al., 2009; Matzinger, 2002). DAMPs can be modified self-molecules, like oxidized or acetylated LDL. SR are capable of interacting, not only with DAMPs, but also with a huge repertoire of ligands, such as apoptotic cells, endogenous proteins, and polyionic ligands; including

lipoproteins, phospholipids, proteoglycans, ferritin, carbohydrates, and cholesterol ester (Taban et al., 2022). In addition, they are classified as pattern recognition receptors (PRRs) owing to their capacity to detect specific components present in bacteria and other pathogens. SR play a vital role in the innate immune response by identifying pathogen-associated molecular patterns (PAMPs). PAMPs are molecular motifs of tiny size that are conserved in diverse microorganisms, such as lipopolysaccharide (LPS), lipoteichoic acid (LTA), and beta-glucan (Areschoug & Gordon, 2008; Areschoug & Gordon 2009; Mukhopadhyay & Gordon, 2004; Plüddemann et al., 2007).

For the scope and context of this chapter, brief introductory sections of SR class B and class F are covered, since SR from these classes are relevant to the experimental results.

4.2.1 SR Class B

The structure of SR class B is distinguished by having an extracellular loop, with 2 transmembrane domains and the N- and C- terminals in the cytoplasm (Figure 29) (Asch et al., 1987). Class B has 3 members, SR class B1 (SR-B1) also called SCARB1, SR class B2 (SR-B2) also known as CD63, and SR class B3 (SR-B3). Factors that help SR-B1 and SR-B2 in their tasks in cell signaling and lipid exchange, are their location in caveolae-like areas of biological membranes and their sequence homology (Patel et al., 2008).

SR-B1 was identified to bind modified LDL and native LDL with high affinity (Acton et al., 1994). Later, SR-B1 and SR-B2 were shown to bind to anionic phospholipids and high-density lipoprotein (HDL) (Acton et al., 1996; Rigotti et al., 1995); which opened the doors to several studies that revealed its function in lipid trafficking and uptake. SR-B1 can carry cholesteryl esters from HDL or various lipoproteins and deliver them inside the cells through a process known as selective uptake (Azhar et al., 2003; Brundert et al., 2005; Connelly & Williams, 2004; X. Gu et al., 1998; Krieger, 1999; Rigotti et al., 2003; W.-J. Shen et al., 2018). The selective uptake differs from the typical endocytic route; where

the lipoprotein stays outside the membrane avoiding lysosomal degradation, while the cholesterol ester is internalized in a non-endocytic manner (Glass et al., 1983; Pittman et al., 1987). The function of SR-B1 is bidirectional since it is required for influx or efflux of cholesterol from the cells to HDL (De la Llera-Moya et al., 1999; X. Gu et al., 2000; Ji et al., 1997; Jian et al., 1998). Additionally, SR-B1 is involved in reverse cholesterol transport, which entails the removal of free cholesterol from peripheral cells, e.g., epithelial cells or macrophages, to ship it to the liver for disposal or redistribution (Ji et al., 1999; Out et al., 2004). In cultured endothelial cells, it has been demonstrated that SR-B1 controls the activation of endothelial nitric oxide synthase (eNOS) through HDL (Mineo et al., 2003; Yuhanna et al., 2001).

Although SR-B1 is expressed at modest levels throughout the body in multiple tissues, it is concentrated mainly in the liver, adrenal glands, and gonads, which are involved in the metabolism of cholesterol (Landschulz et al., 1996; Nakagawa-Toyama et al., 2005). Infertility, atherosclerosis, and compromised innate immune response, have been associated to allelic variants or mutations in the SR-B1 gene (Yates et al., 2011).

SR-B1 is among the most versatile SR since it cooperates with a wide spectrum of ligands, comprising maleylated BSA, carotenoids, vitamin E, silica, unesterified cholesterol or reconstructed phospholipid elements that include apolipoproteins, e.g. apoA-I/II, apoC-III, or apoE (During et al., 2005; Li et al., 2002; Reboul et al., 2006; Rigotti et al., 2003; Tsugita et al., 2017; Xu et al., 1997). SR-B1 has also been proven to participate in the recognition and phagocytosis of cells that undergo apoptosis (Fukasawa et al., 1996; Imachi et al., 2000; Murao et al., 1997; Shiratsuchi et al., 1999). Furthermore, binding to bacterial constituents, such as LPS, LTA, and amphipathic helix, has been reported (Bocharov et al., 2004; Vishnyakova et al., 2003). SR-B1 associates to viruses as well, easing their access into the cells. For instance, it is a key participant in the entry of the hepatitis C virus (HCV) via recognition of viral envelope units (Barth et al., 2008; Catanese et al., 2007; Catanese et al., 2010; Scarselli et al., 2002); as well as, its novel role in the internalization of SARS-CoV-2 virus in cells expressing angiotensin converting enzyme-2 (ACE2)

receptor, in which SRB1 increases the virus attachment because the virus binds to its ligands such as cholesterol and probably to HDL (C. Wei et al., 2020).

Another B SR family member is SR-B2 identified as a receptor for thrombospondin and to have a function as a down regulator of angiogenesis (Asch et al., 1987). However, now it is well documented that it can also bind to a variety of molecules including, altered lipid particles, fatty acids, oxidized phospholipids or lipoproteins, apoptotic cells, and pathogens (Silverstein & Febbraio, 2009). Diverse cell types express SR-B2, including macrophages, microglia, dendritic cells, monocytes, and endothelial cells from various tissues, such as kidney, adipose tissue, gut, breast, adrenal glands and testis (Febbraio et al., 2001). Several co-receptors have been credited to interact with this receptor, including integrins, toll-like receptors (TLRs) and tetraspanins (W.-M. Miao et al., 2001). Specifically, it triggers a proinflammatory cascade as a reaction to modified LDL, that happens when SR-B2 collaborates with TLR4 or TLR6 (Stewart et al., 2010).

SR-B2 is a dynamic player in processes such as lipid buildup, inflammatory damage, oxidative stress and programmed cell death (X. Yang et al., 2017). Consequently, it has also been implicated in the development of numerous diseases, principally atherosclerosis, non-alcoholic fatty liver disease and diabetes (Miquilena-Colina et al., 2011; Moon et al., 2020; Nicholson et al., 2000).

The final family member, SR-B3 is a surface receptor not only present in macrophages and smooth muscle cells, but in other tissues, e.g. heart, liver and brain (Ishikawa et al., 2009). SR-B3 contributes in the restructuring of endosomes and lysosomes, and in membrane trafficking, since it is one of the most prevalent proteins in the membrane of lysosomes (Kuronita et al., 2002). Furthermore, its involvement in the exportation of cholesterol from the lysosomal compartments has been postulated (Heybrock et al., 2019). Together with another protein known as P-selectin glycoprotein ligand-1, they serve as receptors for the enterovirus 71 and some Coxsackievirus family members, contributing in binding and internalization, however only SR-B3

participates in the uncoating of the virus (Yamayoshi et al., 2009; Yamayoshi et al., 2013).

4.2.2 SR Class F

Three are the members of SR class F, namely SR class F1 (SR-F1) or SCARF1/SRECI, SR class F2 (SR-F2) or SCARF2/SRECI and SR class F3 (SR-F3). SR class F are denoted by the presence of epidermal growth factor–like (EGF-like) domains followed by a transmembrane region, and ending in an elongated tail in the cytoplasm (Fig. 29).

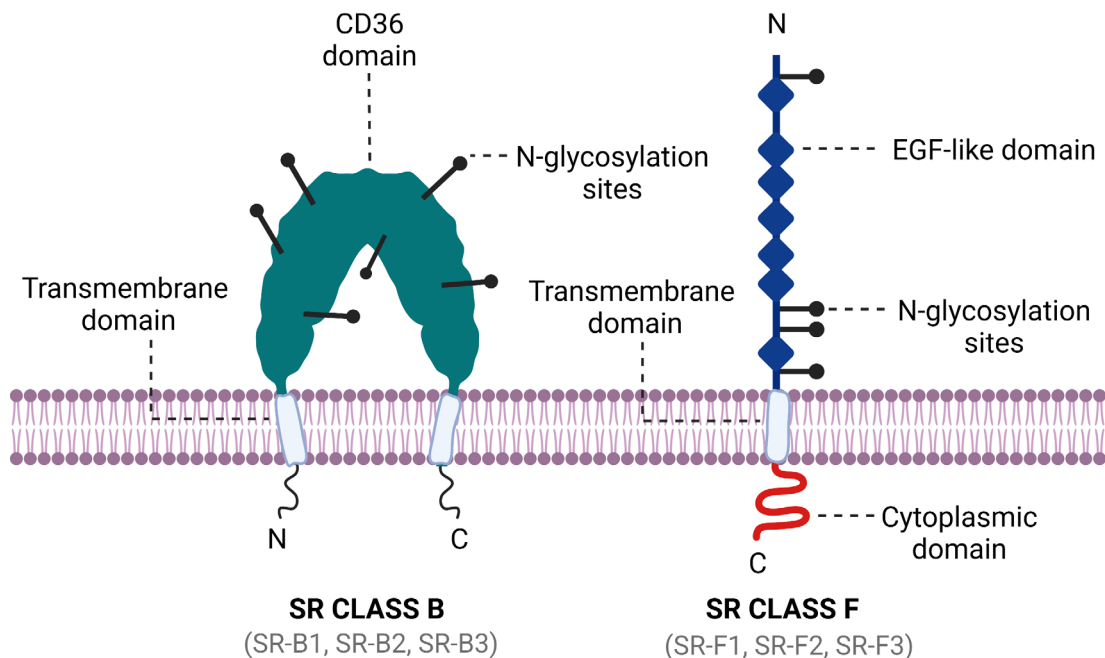


Fig. 29. Representation of SR class B and F structure. A loop-shaped CD36 domain with two transmembrane domains and the N- and C-terminal ends in the cytoplasm are characteristics of SR class B. The architecture of SR class F is composed of varying numbers of EGF-like domains, followed by a transmembrane domain and their cytoplasmic domain is abundant in serine, proline, glycine, and/or arginine and lysine residues. The extracellular N-glycosylation sites are illustrated for both classes. Created with BioRender.com.

The initial identification of SR-F1 was as a receptor that could recognize altered LDL specifically in endothelial cells (Adachi et al., 1997). While SR-F1 contains regions in its cytoplasmic tail that are enriched with serine and proline followed by a poly-glycine region, SR-F2 possess positively charged arginine

and lysine residues as well (J. Ishii et al., 2002). SR-F1 and SR-F2 share structural similarities, to a degree of roughly 50% in their extracellular domain, but only to a lesser level (20%) in their cytoplasmic domains. A soluble, shortened form of SR-F1 (~60 kDa) has been identified in serum from human samples (Patten et al., 2017). The trans-interaction between both receptors is possible via their ectodomains blocking their binding sites and any scavenger functionality (J. Ishii et al., 2002). Even though the distribution of expression of SR-F1 and SR-F2 is widely expressed in different tissues, the two receptors are located principally in lung, spleen, placenta, heart, ovary and small intestine (J. Ishii et al., 2002).

The ligand diversity of SR-F1 is abundant, involving molecules from endogenous and exogenous sources. SR-F1 can bind and transport glycoprotein 96 (Gp96) and calreticulin (CRT), chaperones of the major histocompatibility complex (MHC) class 1 antigen presentation system (Berwin et al., 2004). SR-F1 can associate with proteins from *Klebsiella pneumoniae*, in a TLR2-dependent mechanism, triggering proinflammatory signals (Jeannin et al., 2005). Furthermore, SR-F1 has roles in pathogen infection, through binding of yeast β -glucans, and bacteria, such as *Staphylococcus aureus* and *Neisseria gonorrhoeae*, and viral antigens, such as the non-structural Protein 3 (NS3) from the hepatitis C virus and viral double stranded RNA (Baur et al., 2014; Beauvillain et al., 2010; Means et al., 2009; Rechner et al., 2007). The attachment of SR-F1 to two endogenous molecules, namely granule protein 2 (GP2) and the Tamm–Horsfall protein, has been reported in which the receptor may indirectly contribute in the capture and absorption of bacteria (Hölzl et al., 2011; Pfistershammer et al., 2008).

Several heat shock proteins (HSP), such as HSP70, HSP90, HSP110 and glucose-regulated protein 170 (GRP170) have been identified as ligands of SR-F1 (Facciponte et al., 2007; Murshid et al., 2010; Thériault et al., 2006). In the work of Murshid and collaborators, it was identified that SR-F1 facilitated a dynamin and clathrin-independent mechanism to internalize HSP90 complexes. In this pathway the GTPase, cell division cycle 42 (Cdc42), controlled internalization via GPI-enriched endosomal compartment (GEEC) to

recycling compartments. The removal of dying cells through complement factor C1q interaction has been reported as another function of SR-F1 in macrophages, dendritic cells and epithelial cells (Ramirez-Ortiz et al., 2013).

There is a lack of studies regarding the functionality, ligands-interaction, protein expression and signalling pathways of SR-F2. Currently its precise functions have not been determined yet, however mutations in the *SCARF2* gene are directly connected to fatal conditions such as Van den Ende–Gupta Syndrome and the 22q11.2 deletion syndrome (Anastasio et al., 2010; McDonald-McGinn et al., 2015). Apart from the tissues previously mentioned for SR-F1, SR-F2 is also predominantly present in the prostate, endometrium, gall bladder, fat and kidney (Ishii et al., 2002).

In contrast to SR-F1, SR-F2 exhibits limited scavenging activity as its binding capacity to modified LDL is absent, and it has only been detected to adhere to maleylated BSA (MaIBSA) and acetylated BSA (AcBSA) (Wicker-Planquart et al., 2021). In addition, it could be possible that SR-F2 has different binding domains because when tested in soluble form it can associate with CRT and C1q, both ligands of SR-F1 (Wicker-Planquart et al., 2021).

SR-F3, also known as multiple EGF like domains 10 (MEGF10), is mainly expressed in astrocytes and myosatellite cells in the brain (Cahoy et al., 2008; Nagase, 2001). It has been proposed that SR-F3 is internalized through CME after binding to AP50 subunit and cooperating with the AP-2 complex. This receptor has also been related to Alzheimer's disease as it is capable of associating to amyloid- β peptide and facilitating its internalization (Singh et al., 2010). In the mouse cerebellum, MEGF10 is a receptor for the C1q similar to SR-F1, and thus involved in efferocytosis (Iram et al., 2016). Its purpose is to be a phagocytic receptor for astrocytes, both in development or ischemic damage (Chung et al., 2013; Morizawa et al., 2017).

4.3 Scavenger receptors in prostate cancer

It is not surprising that SR are active contributors to cancer biology due to their multifunctional involvement in normal physiological processes and its vast interactome network. The role of SR in the development and malignancy of PCa is still not entirely clear, however the impact and overexpression of several SR in disease has been examined (Figure 30).

SR class A1 (SR-A1) is an essential receptor for the management of tissue homeostasis and it has been implicated in disease pathogenesis, such as neurodegeneration, atherosclerosis and cancer (Frenkel et al., 2013; Khoury et al., 1996; Kuchibhotla et al., 2008; Kzhyshkowska et al., 2012; Suzuki et al., 1997; Yu et al., 2015). Similar to several cancers, poor prognosis has been correlated to expression of SR-A1 in tumour associated macrophages (TAMs) in PCa (Yang et al., 2004).

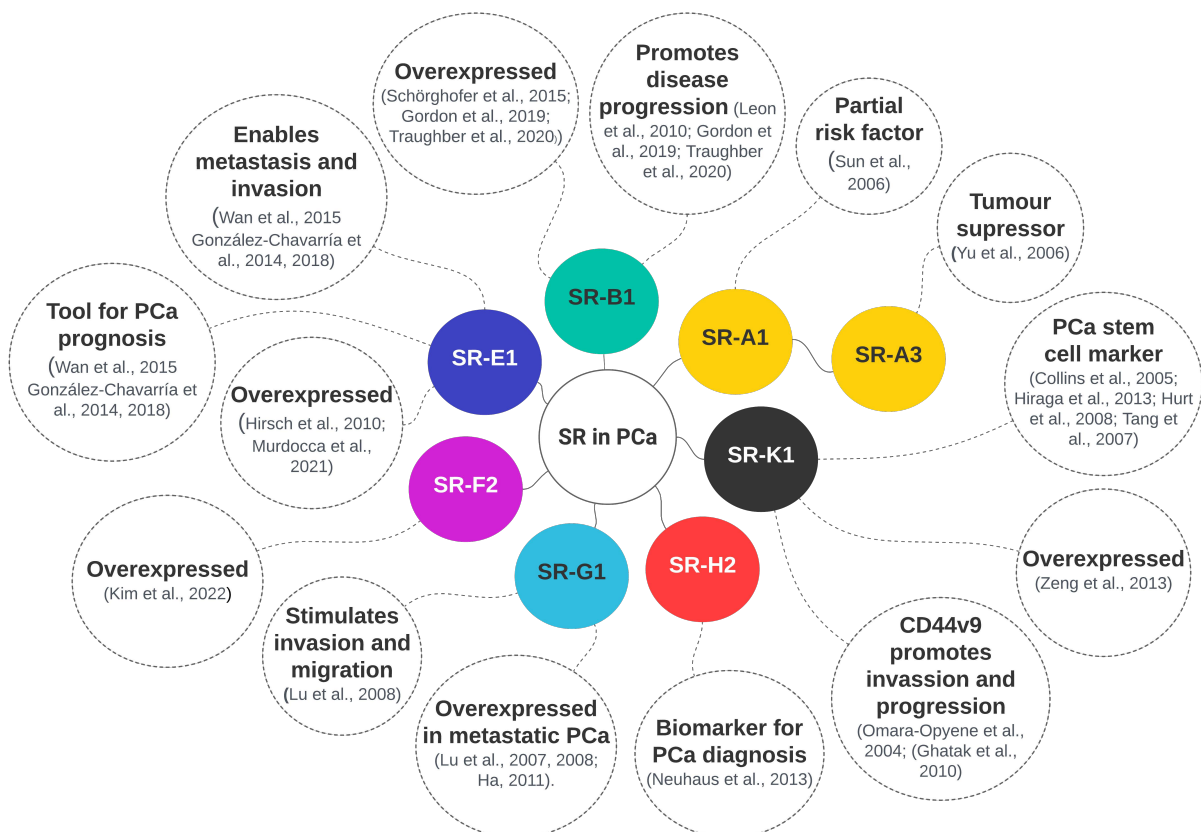


Fig. 30. Scavenger receptors involved in prostate cancer. Colour circles represent SRs and dotted circles their main features in the disease.

Inherited PCa has been associated with chromosome 8p22, the location of SR-A1 (Bova et al., 1996; Suzuki et al., 1995). Other cancers have been connected with the deletion of this region as well (Low et al., 2011). In addition, high risk of PCa has been linked to specific genetic variations or mutations of SR-A1 (Miller et al., 2003; Xu et al., 2002; Xu et al., 2003). However, contradictory studies suggest that there is no causal association between them, because their data suggest that SR-A1 alone is not enough to determine PCa risk and there could be other unknown genes or factors involved (Hope et al., 2005; Rennert et al., 2005, 2008; Seppälä et al., 2003; Wang et al., 2003). In a meta-analysis study, they examined published articles on SR-A1 up to 2005, and they concluded that even though some variants like D174Y in African-American people and R293X in Caucasian people, had significant correlation with PCa risk, the overall panorama implied a modest risk to PCa, with more susceptibility in African-American men, rather than the SR-A1 gene representing a core risk by itself (J. Sun et al., 2006).

SR class A3 (SR-A3) is an important player in PCa, where metastasis has been linked to the methylation of its gene promoter and to the downregulation of protein expression. It has been proposed as a tumour suppressor in PCa as well, since its forced upregulation impacts upon tumour development and expansion (Yu et al., 2006).

Androgens are derived from cholesterol and they are necessary for both normal function of the prostate and PCa survival. SR-B1, one of the principal facilitators of cholesterol trafficking within the cells and tissues, has been recently verified to be implicated in the progression of PCa. High expression levels of SR-B1 were observed in a LNCaP xenograft model that exhibited a castration-resistance prostate cancer stage, but not in the prostate cancer cell line itself, denoting the key function of this receptor in the modulation of cholesterol internalization in PCa aggressiveness and advancement (Leon et al., 2010). In another study, they contrasted two diets in TRAMP (transgenic adenocarcinoma of mouse prostate) mice, in which a transgene governs the expression of the Simian Virus 40 (SV40) large T antigen through a prostate-specific promoter, leading to spontaneous multistage PCa that progresses from PIN to adenocarcinoma. The TRAMP mice that were fed with a western-based diet, presented increased levels of SR-B1 expression and HDL-cholesterol, resulting

in an increment in the incidence of tumour size (Llaverias et al., 2010). In a different research, the siRNA-mediated KD of SR-B1 in the PCa cell lines, C4-2 and LNCaP, reduced PSA levels and adversely affected cancer cell survival. (Twiddy et al., 2012). Additionally, SR-B1 is upregulated in metastatic and high Gleason grade PCa patient samples, in comparison with primary PCa or low-grade tumour biopsies (Schörghofer et al., 2015). Similarly, SR-B1 expression is highly regulated in primary PCa and metastatic CRPC biopsies in comparison with healthy prostate samples (Gordon et al., 2019; Traugber et al., 2020). Both studies, demonstrated by different routes that PCa proliferation and progression are stimulated via SR-B1 uptake of HDL-cholesterol.

SR class E1 (SR-E1) is upregulated in diverse cancers, and PCa is not the exemption (Hirsch et al., 2010; Murdocca et al., 2021). Lymph node metastasis and aggressive late stages of PCa have been related to abundant serum levels of SR-E1 and high oxidized low density lipoprotein receptor 1 (OLR1) gene expression (Wan et al., 2015). In the same study, they identified that one of the ligands of SR-E1, oxidized LDL (oxLDL), endorses the migration, proliferation, and invasion of LNCaP and PC-3 cells. The stimulation of SR-E1 upon oxLDL interaction in PCa cells boosted tumour angiogenesis as well (González-Chavarría et al., 2014). Moreover, the augmentation of invasion and metastasis in PCa cells was detected after oxLDL-dependent activation of SR-E1 through alterations in the epithelial to mesenchymal transition (González-Chavarría et al., 2018). The study showed that the oxLDL-driven stimulation of SR-E1 resulted in a diminished expression of epithelial markers, including plakoglobin and E-cadherin, alongside an increase in mesenchymal markers such as matrix metalloproteinase 2 (MMP-2) and matrix metalloproteinase 9 (MMP-9). This transition lead to cytoskeleton rearrangement, thereby amplifying cellular migration potential. These studies support SR-E1 as a tool for PCa prognosis and diagnosis.

SR-F2 has been recently proposed as a diagnostic indicator and therapy target in glioblastoma, due to its high levels in patient samples and cell lines (C. Kim et al., 2022). In the same study, they used data from The Cancer Genome Atlas, where they identified the upregulation of SR-F2 in numerous cancer tissues, including prostate

cancer. Also, SR-F2 has been recognized as a key biomarker in urothelial and renal cancer, that could impact the survival rate after diagnosis (Vo et al., 2023). However, there is a lack of research about the molecular mechanisms where SR-F2 overexpression could be contributing to PCa.

Enhanced protein and RNA levels of SR class G1 (SR-G1) have been reported in metastatic PCa cells and tissues in comparison to LNCaP or normal prostate cells or healthy tissues (Lu et al., 2007; Lu et al., 2008). In vitro studies have revealed that SR-G1 stimulates PCa cell invasion and migration (Lu et al., 2008). In another large analysis they identified that SR-G1 was elevated in late stages and metastatic PCa patient samples (Ha, 2011). Also, the promotion of PCa progression after SR-G1 and C-X-C Motif Chemokine Receptor 6 (CXCR6) activation was linked to high regulation of proangiogenic proteins via the AKT/mTOR cascade, however the article has been recently retracted and further confirmation its required (Wang et al., 2008). SR-G1 overexpression has been recognized in other types of cancers and further investigation is needed to understand its further therapeutic implications in PCa (Yu et al., 2015).

Interestingly, SR class H2 (SR-H2) has been proposed as a seminal plasma biomarker for diagnosis of PCa, based on its contrasting expression levels in PCa patient samples compared with controls (Neuhaus et al., 2013).

As mentioned in Chapter 3, CD44 or SR class K1 (SR-K1) is not only considered a cancer stem cell marker in PCa (Collins et al., 2005; Hiraga et al., 2013; Hurt et al., 2008; Tang et al., 2007), but also its overexpression is acknowledged in various cancers, including prostate, breast, bladder, colon, lymphoma, lung, gall bladder, and endometrial cancer (Fujita et al., 1994; Guo et al., 2017; He et al., 2018; Zeng et al., 2013; S. Zhao et al., 2016). However, results obtained in a recent study, in which they analysed expression levels of SR-K1 in tissues with either high-grade prostatic intraepithelial neoplasia or PCa or benign prostate hyperplasia, indicated that there were no correlation towards PCa (Kalantari et al., 2017). In other work, it was found that in localized PCa, variants of SR-K1 were mis-expressed, with some variants associated with better survival outcome and phenotypic behaviour (Hernandez et al., 2015; Kalantari et al., 2017). Actually, the silencing of CD44 splice form variant 6

(CD44v6) caused the downregulation of Wnt/ β -catenin and PI3K/Akt/mTOR signalling pathways, as well as a decline in tumorigenic capacities, increased chemo-/radiosensitivity and loss of epithelial mesenchymal transition markers (Ni et al., 2014). This study proposed CD44v6 as a cancer stem cell marker. The malignant behaviour of PCa cells is associated by increased expression of CD44 splice form variant 9 (CD44v9) (Omara-Opyene et al., 2004). It has been proposed that the androgen receptor's ability to collaborate with CD44v9 is crucial for controlling prostate cancer's hyaluronan-mediated invasiveness (Ghatak et al., 2010).

4.4 Targeted receptors for peptides uptake

Peptides and PDCs, with their diversity of form and function, is also paralleled by their varied routes to passively or actively cross biological membranes. In Chapter 3, the multiple uptake mechanisms exerted by peptides were explained in detail. In contrast to peptides that directly penetrate membranes or use receptor-independent endocytosis, peptides that enter biological membranes through receptor-mediated endocytosis could potentially be used for targeted cancer therapy (Reubi, 2003; Vhora et al., 2014). The increased targeting of diseased cells relies upon the binding of peptides or PDCs to surface receptors and one would expect these to be overexpressed, when compared to healthy cells, to guarantee that the drug is delivered for the intended therapeutic effect (Reubi, 2003; Vrettos et al., 2018). For these receptor-mediated peptides, several cell surface receptors have been proposed as active collaborators in their uptake, comprising SR, integrins, membrane type-1 matrix metalloproteinase, EGFR, bombesin receptors, somatostatin receptors, syndecans, neuropilins, melanocortin receptor 1, PSMA, aminopeptidase N, hepatocyte receptor A2, chemokine receptor 4, vasoactive intestinal peptide receptors, transferrin receptors, melanocortin receptor 1, GnRH-R, and neuropeptide Y receptors (Vrettos et al., 2018; Worm et al., 2020; Zhu et al., 2021a).

Multiple SRs are highly upregulated in several cancers, including PCa, which positions them as potential targeted receptors that can be used for cancer therapy (Table 8) (Yu et al., 2015). It has been proved that oligonucleotide-functionalized gold nanoparticles, double-stranded RNA (dsRNA), and nucleic acids are all taken up by SR-As (DeWitte-

Orr et al., 2010; Limmon et al., 2008; Patel et al., 2010; Pearson et al., 1993; Saleh et al., 2006). Using RNAi knockdown, overexpression assays and pharmacological drugs, it has been revealed that specifically SR-A3 and SR-A5 are at some extent responsible for the internalization of peptides-based complexes (Arukuusk, et al., 2013; Ezzat et al., 2012; Helmfors et al., 2015; Lindberg et al., 2013; Veiman et al., 2013). Interestingly, it was discovered that both SRs help internalise different peptide conjugates through diverse internalization routes; for instance PepFect14 (PF14) complexes with plasmid DNA (pDNA) enter the cells via CvME, NickFect51-pDNA (NF51-pDNA) and NickFect1-pDNA (NF1-pDNA) through macropinocytosis, but NF1-pDNA can also use CME or CvME (Arukuusk et al., 2013; Ezzat et al., 2012; Veiman et al., 2013).

Table 8. Peptide-binding Scavenger receptors

Scavenger receptor	Peptide or PDC	Cancer expression	References
SR-A3 & SR-A5	NF51-pDNA, NF1-pDNA, PF14, PF32-pDNA	HeLa cells, brain endothelial cells	(Arukuusk, et al., 2013; Ezzat et al., 2012; Helmfors et al., 2015; Lindberg et al., 2013; Srimanee et al., 2016; Veiman et al., 2013)
SR-B1	PF32-pDNA	Brain endothelial cells	(Srimanee et al., 2016)
SR-L1	Angiopep-2 peptide, ANG1005, PF32-pDNA	Neurovascular endothelial cells, brain and breast cancer	(Deane et al., 2008; Kumthekar et al., 2020; Ruzali et al., 2012; K. Sakamoto et al., 2017)

Furthermore, the overexpression of SR class L1 (SR-L1) or most commonly known low density lipoprotein receptor-related protein 1 (LRP1), was found in epithelial cells lining the capillaries of the blood-brain barrier and in the meninges and choroid plexus vasculature (Deane et al., 2008; Ruzali et al., 2012; K. Sakamoto et al., 2017). The angiopep-2 peptide was identified to interact with SR-L1 followed by its internalization

in blood brain barrier associated cells (Demeule, Currie, et al., 2008; Demeule, Régina, et al., 2008). Recently an effective PDC referred to as ANG1005, was produced through covalent conjugation between the angiopep-2 peptide and paclitaxel molecules, which was created to undergo SR-L1-mediated transcytosis to overcome the central nervous system (CNS) barrier (Kumthekar et al., 2020). Intriguingly, SR-As and SR-B1 are also overexpressed in brain capillary endothelial cells and it was demonstrated that the transcytosis and delivery of PepFect32-pDNA (PF32-pDNA) nanocomplexes was not only mediated by SR-L1, but also via SR-A3, SR-A5 and SR-B1 in those cells (Srimanee et al., 2016).

4.5 Targeting SR with peptides in PCa

In drug delivery systems, it is essential to determine and understand the internalization mechanism to target cells, so as to improve future therapies. G3 peptide revealed high binding strength and precision for targeting malignant cells, however its route of entrance to cancer cells is not entirely understood. Previous research by Cirillo and collaborators provided the first evidence of G3 being internalized by energy dependant endocytosis (Cirillo et al., 2021). In images acquired by TEM, they demonstrated that the peptide was internalized by colon cancer cells through vesicular compartments. Additionally, using siRNA silencing they revealed that G3 enters colon cancer cells by means of the endocytic machinery.

As previously described, SR embody a miscellaneous supergroup of promiscuous receptors that are involved in multiple biological and tumorigenic events (PrabhuDas et al., 2017; Taban et al., 2022; Yu et al., 2015). Given their diverse and vast interactome; their involvement in the internalization of PDC, CPP, polyanionic molecules and peptide-related nanocomplexes; and their overexpression in carcinogenic tissues, SR could potentially be implicated in the uptake of unknown peptides and hence PDCs for cancer therapeutics. Following this rationale and based in published studies regarding SR as binding receptors of PDC/peptides and in their implications and upregulation of some SR in PCa, the role of SR in the internalization mechanism of FITC-G3 peptide in PCa cells was explored in this chapter.

4.6 Results

4.6.1 Endocytic proteins siRNA knockdown

To analyse if SR are implicated in the internalization mechanism of G3 peptide in PCa cells, a series of KD experiments using RNAi were performed and their validation was evaluated using HCS and WB. The optimization of the siRNA silencing assays was executed using DF1 as a transfection reagent and siGLO red as a fluorescent indicator of positive transfection (Appendix B). Cells without any treatment and a pool of non-target siRNAs were used as negative control, and UBB was selected as positive control.

During the optimization process, varying concentrations of DF1 were initially tested to determine the optimal conditions for siRNA delivery. Depending on the DF1 concentration, the transfection efficiency changed, showing minimal siGLO red fluorescence at lower levels and increased fluorescence at higher concentrations, indicating improved siRNA delivery. However, the balance between cellular viability and transfection efficiency became an important factor to consider. Increased DF1 concentrations improved siRNA transfection, but also generated cytotoxic side effects, including morphological changes in cells and impaired cell survival. To address this issue, the cellular seeding population was increased to provide a higher cell density, which helped mitigate the cytotoxic effects observed at higher DF1 concentrations. This adjustment aimed to enhance the overall resilience of the cells to the transfection process, thereby allowing for effective siRNA delivery while minimizing cellular stress and maintaining overall cell health. Furthermore, because of possible edge effects and environmental fluctuations that can compromise the validity of the data, the wells located at the edges of the screening plates were deliberately avoided in the transfection experiments. Utilizing UBB siRNA as a functional positive control was effective, as indicated by gene silencing patterns that were in agreement with siGLO red fluorescence. Therefore, the optimal condition for LNCaP and PC-3 cells was selected based on both, siGLO and UBB siRNA. This condition was characterized by an approximate 50% decrease in cell number and elevated siGLO red fluorescence, as presented in Appendix B in Figure B1 for LNCaP and Figure B2 for PC-3 cells.

Based on the premise that G3 enters the cells via endocytic vesicles, the following genes were selected and silenced using siRNAs: MYO5B, MYO5C, MYO5A and CAV1. To assess the uptake of G3, a FITC-labelled peptide was used to measure the integrated intensity values after 24 hrs of exposure in PCa cells. The high-content images of the KD of the endocytic-related genes in LNCaP and in PC-3 cells are presented in Figure 31A and Figure 32A, respectively. The integrated intensity values of FITC-G3 uptake were measured and normalized to the scrambled non-targeted controls. After the KD of MYO5B and MYO5C in LNCaP cells, a significant decrease was obtained in their FITC integrated intensity values, when compared to the non-targeting siRNA control; while the KD of MYO5A and CAV1 did not exhibit significant difference in their uptake of FITC-G3 (Fig. 31B). In PC-3 cells, the KD of MYO5C was the only one to exhibit a significant reduction in the internalization of FITC-G3 (Fig. 32B). Statistical differences were assessed using ANOVA analysis with multiple comparisons.

The cell number per condition was calculated after 72 hours of transfection and no significant difference resulted between the treated and control samples (Fig. 31C and 32C). UBB was used as a control of the transfection and presented a significant decrease in cell viability in both cell lines. Based on these results, MYO5C was selected as positive control for LNCaP and PC-3 in the following SR knockdowns due to the reduction in FITC-G3 uptake after it's silencing.

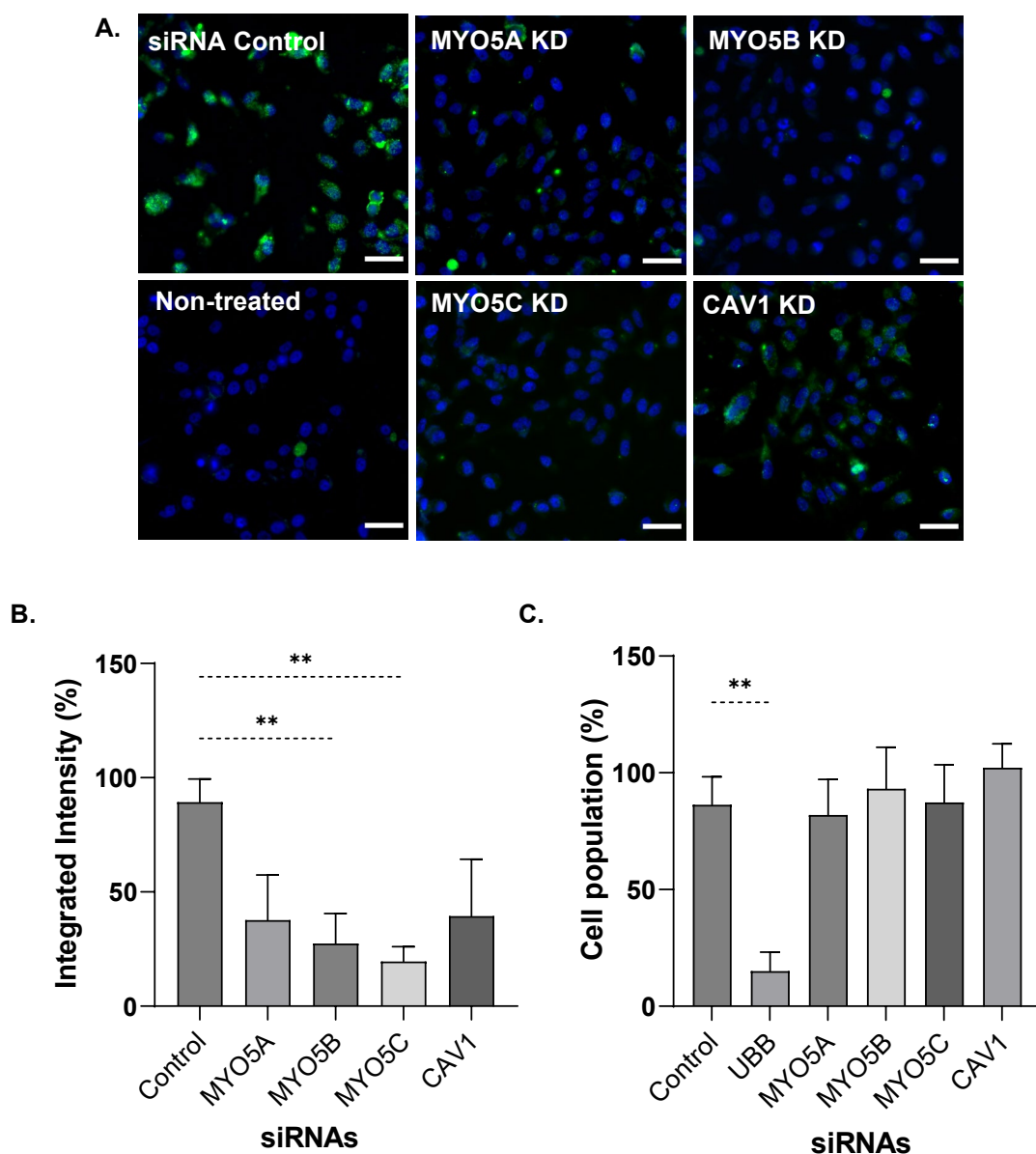


Fig. 31. Endocytic genes knockdown in LNCaP. (A) High content images of LNCaP cells after 72 hrs RNAi KD and 24 hrs of FITC-G3 exposure. Scale bar 50 μ m and 20X magnification. (B) FITC integrated intensity values normalised to the non-targeted siRNA control. The statistical significance was calculated using one way ANOVA test (** $p < 0.01$). (C) Normalized cell population after 72 hrs transfection. Data is expressed as mean and \pm SD of 3 different experiments with 3 replicates each. A student's t-test was calculated between UBB and the control (** $p < 0.01$).

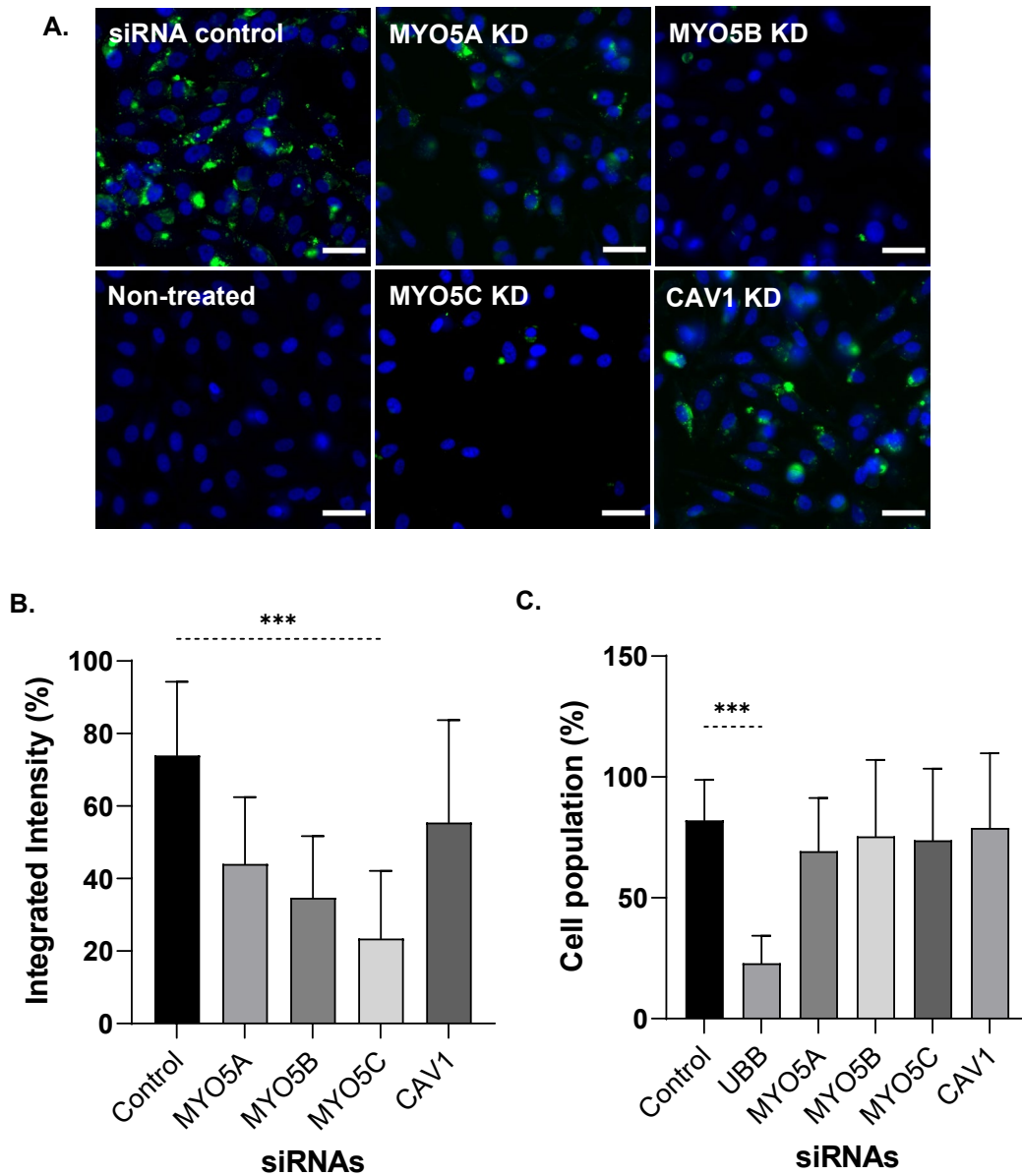


Fig. 32. Endocytic genes knockdown in PC-3. (A) High content images of PC-3 cells after 72 hrs RNAi KD and 24 hrs of FITC-G3 exposure. Scale bar 50 μ m and 20X magnification. (B) FITC integrated intensity values normalised to the non-targeted siRNA control. The statistical significance was calculated using one way ANOVA test ($***p < 0.001$). (C) Normalized cell population after 72 hrs transfection. Data is expressed as mean and \pm SD of 3 different experiments with 3 replicates each. A student's t-test was calculated between UBB and the control ($***p < 0.001$).

4.6.2 Scavenger receptor siRNA screen

A few types of SR have been reported to be overexpressed in PCa, however there is a lack of information about the degree of expression of additional SR in the disease. Based on that premise, LNCaP and PC-3 cells were transfected with a siRNA library of 19 SRs was KD from the SiGenome and ON-target collections, to indirectly evaluate whether changes in the uptake of FITC-G3 could be reliant on SR silencing. The reduction in the integrated intensity values of FITC-G3 could represent the active involvement in the internalization mechanism of the peptide.

FITC-G3 integrated intensity values were calculated and normalized to the siRNA non-targeted control in both cell lines, and presented as percentages in Figure 33, for LNCaP cells, and Figure 34 for PC-3 cells. Both data sets were analysed using a non-parametric test because the Q-Q plots, histogram distributions, and the Shapiro-Wilk normality tests, revealed that the values did not follow a normal distribution. A Kruskal-Wallis test with corrected multiple comparisons was applied to determine statistical differences between medians. The correction of multiple comparisons was done to avoid False Discovery Rate, using the Benjamini, Krieger and Yekutieli test. A significant decrease of FITC-G3 values was obtained for MYO5C in LNCaP and PC-3 cells, which was used as a positive control of the assays.

For both cell lines, the internalization of G3 peptide was statistically reduced after the KD of the following SRs: SR-B1, SR-F1, and SR-F2, as displayed in Figure 33 and Figure 34. Based on the degree of significance of their q values being less than 0.05, these SR (SR-B1, SR-F1, and SR-F2) were selected as significant hits for validation in the subsequent secondary screens for both PCa cell lines.

These results suggest that 3 SR hits could be participants in the uptake of G3 peptide in prostate cancer cell lines, thus further RNAi mini screenings were conducted.

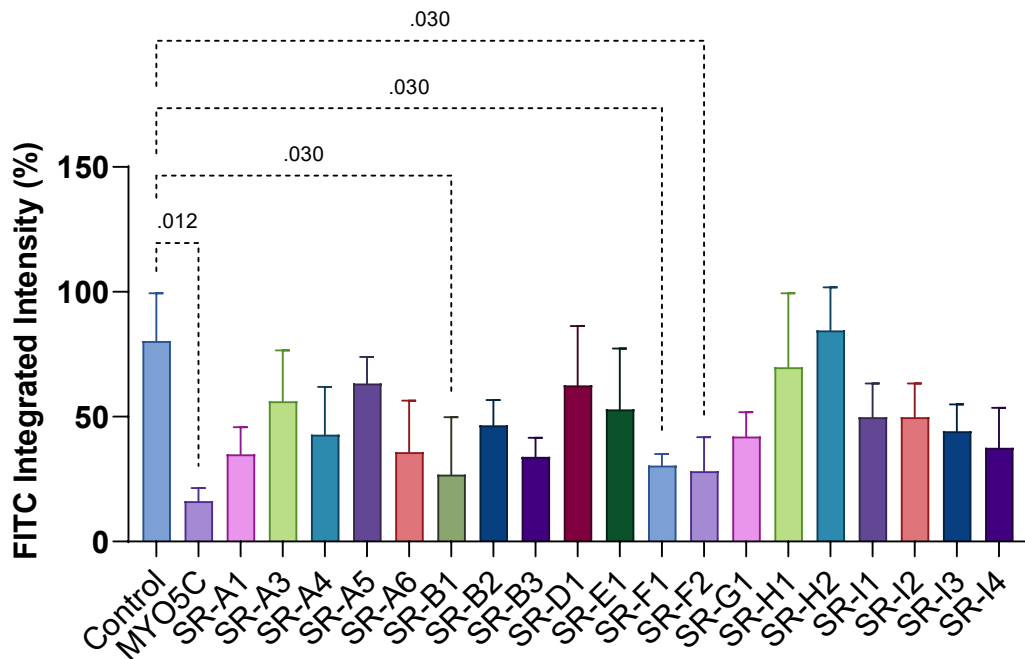


Fig. 33. Scavenger receptors pool knockdown in LNCaP. FITC integrated intensity normalised values. Data is expressed as medians with ranges of one biological repeat with 3 replicates. A mix of non-targeting siRNAs were used as negative control and MYO5C siRNA as positive control. Statistical significance was calculated using Kruskal-Wallis test with multiple comparisons, along with False Discovery Rate correction by Benjamini, Krieger and Yekutieli test. Significant q values are displayed in the graph.

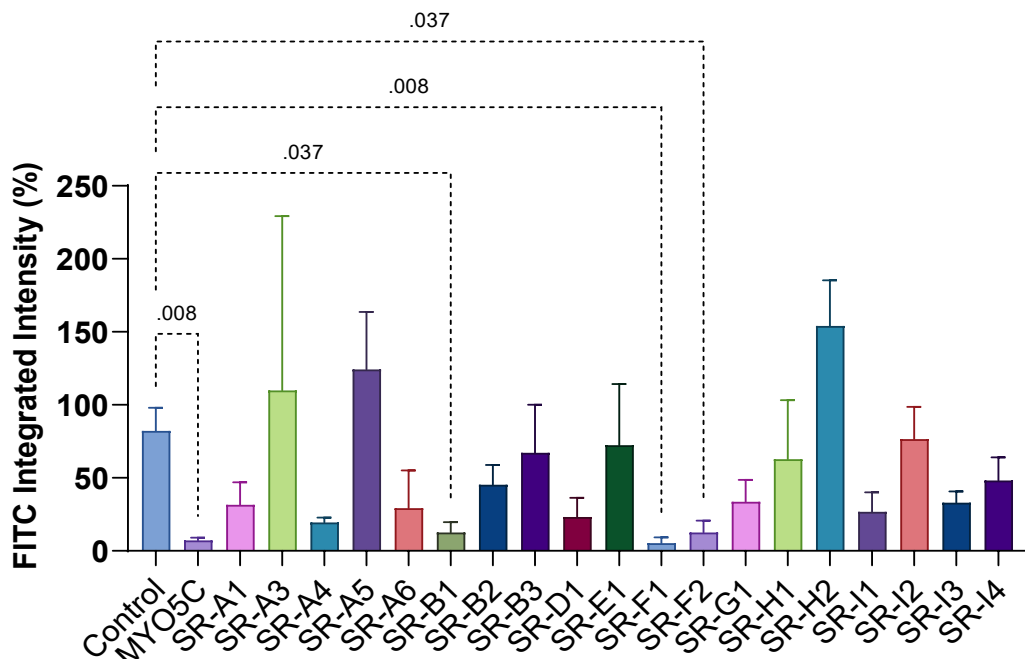


Fig. 34. Scavenger receptors pool knockdown in PC-3. FITC integrated intensity normalised values. Data is expressed as medians with ranges of one biological repeat with 3 replicates. A mix of non-targeting siRNAs were used as negative control and MYO5C siRNA as positive control. Statistical significance was calculated using Kruskal-Wallis test with multiple comparisons, along with False Discovery Rate correction by Benjamini, Krieger and Yekutieli test. Significant q values are displayed in the graph.

4.6.3 Validation of scavenger receptors

Validation of the 3 selected SR hits: SR-B1, SR-F1, and SR-F2 were done following the same principle of determining differences in the internalization of FITC-G3 after siRNA silencing. Experiments were done in LNCaP and PC-3 cells, in triplicate with 3 independent biological repeats. MYO5C was used as positive control and the non-targeted siRNAs as negative control. The exact same siRNAs from siGenome and ON-target sets were employed.

High-content images of the non-targeted control and the KD of SR-B1, SR-F1, and SR-F2 are shown in Figure 35A, for LNCaP cells. Higher degree of FITC integrated intensity puncta is visualized in the non-targeted control image than in the representative images corresponding to the KD of SR-B1, SR-F1, and SR-F2. FITC integrated intensity data for LNCaP cells was normalized to the negative control and graphed as percentages (Figure 35B). Integrated intensity data was analysed using one-way ANOVA test with multiple comparisons test. For LNCaP cells, the uptake of FITC-G3 was significantly decreased in MYO5C ($***p<0.001$), SR-F1 ($***p<0.001$), and SR-F2 ($***p<0.001$), while in a lesser extent in SR-B1 ($*p=0.027$). The cell viability of LNCaP values was assessed and normalized to the negative control. Cellular impairment was obtained for SR-B1 when compared to the control using Student-t test analysis, displaying a p value of less than 0.01 (Figure 35C). The cell number of MYO5C, SR-F1 and SR-F2 were not affected when compared with control cell population.

In Figure 36A, the high-content images of the secondary screening of PC-3 cells are illustrated. Similar to LNCaP images, in the PC-3 cells the non-targeted control presented more internalization of the FITC-G3 than in the SR KD images. One-way ANOVA test with multiple comparisons was applied to evaluate the integrated intensity values. The internalization of FITC-G3 in PC-3 cells was significantly lower, as calculated in Figure 36B, for the positive control MYO5C ($***p<0.001$) and the 3 SR: SR-B1 ($***p<0.001$), SR-F1 ($***p<0.001$), and SR-F2 ($***p<0.001$). PC-3 cell populations were normalized to the negative control and displayed in percentages. PC-3 cell populations were not reduced after SR knockdown in any of the treated samples as presented in Figure 36C.

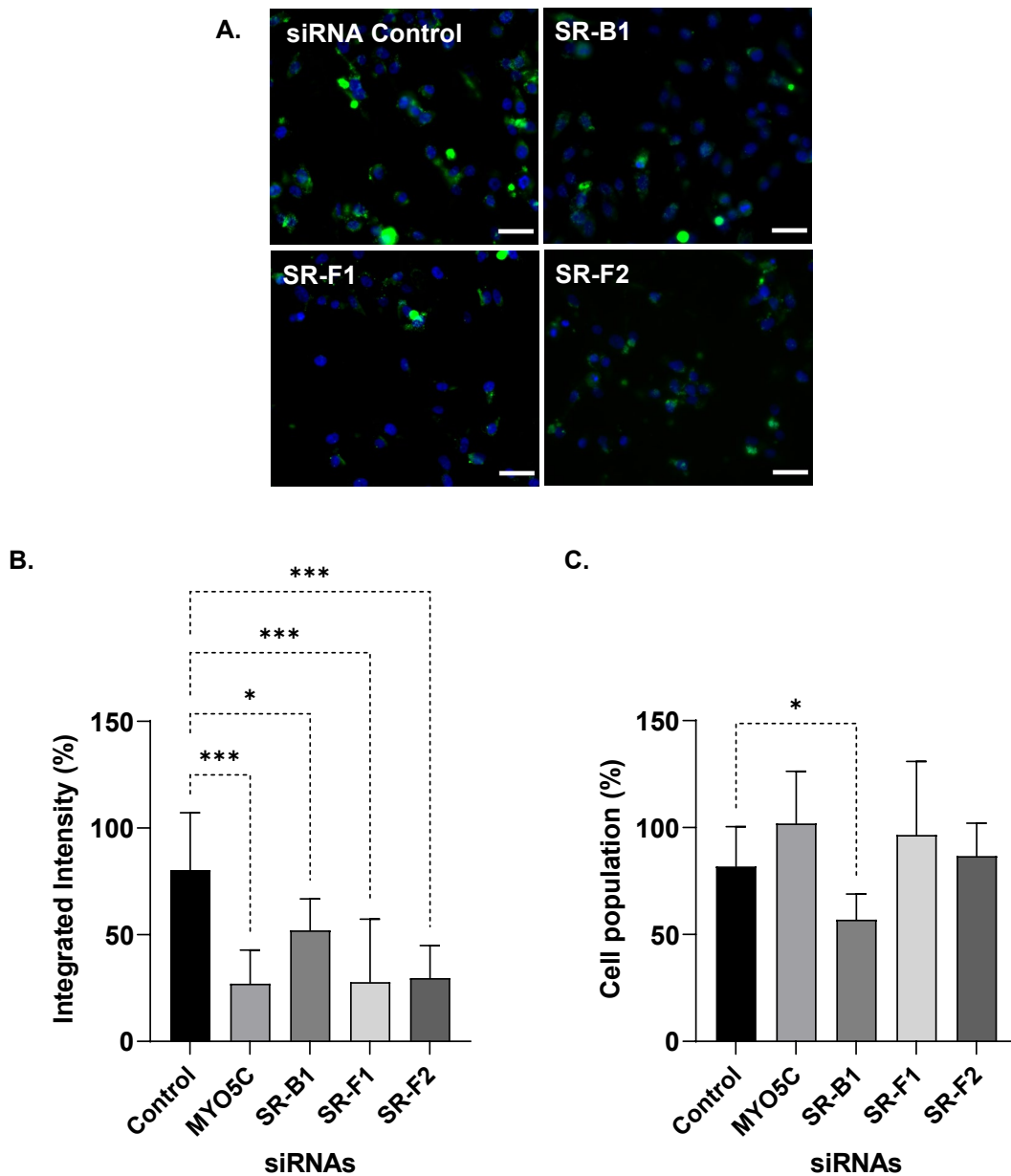


Fig. 35. SR hits knockdown in LNCaP. (A) High content images of LNCaP cells after 72 hrs KD and 24 hrs of FITC-G3 exposure. Scale bar 50 μ m and 20X magnification. (B) FITC integrated intensity normalised values of 3 independent experiments. Data is expressed as means \pm SD. Non-targeting siRNAs were used as negative control. The statistical significance was determined using one way ANOVA test (* p <0.05,** p <0.01,*** p <0.001). (C) Normalized cell population after 72 hrs transfection. Significant difference between SR-B1 cell population and the control were calculated using student's t-test (* p <0.05).

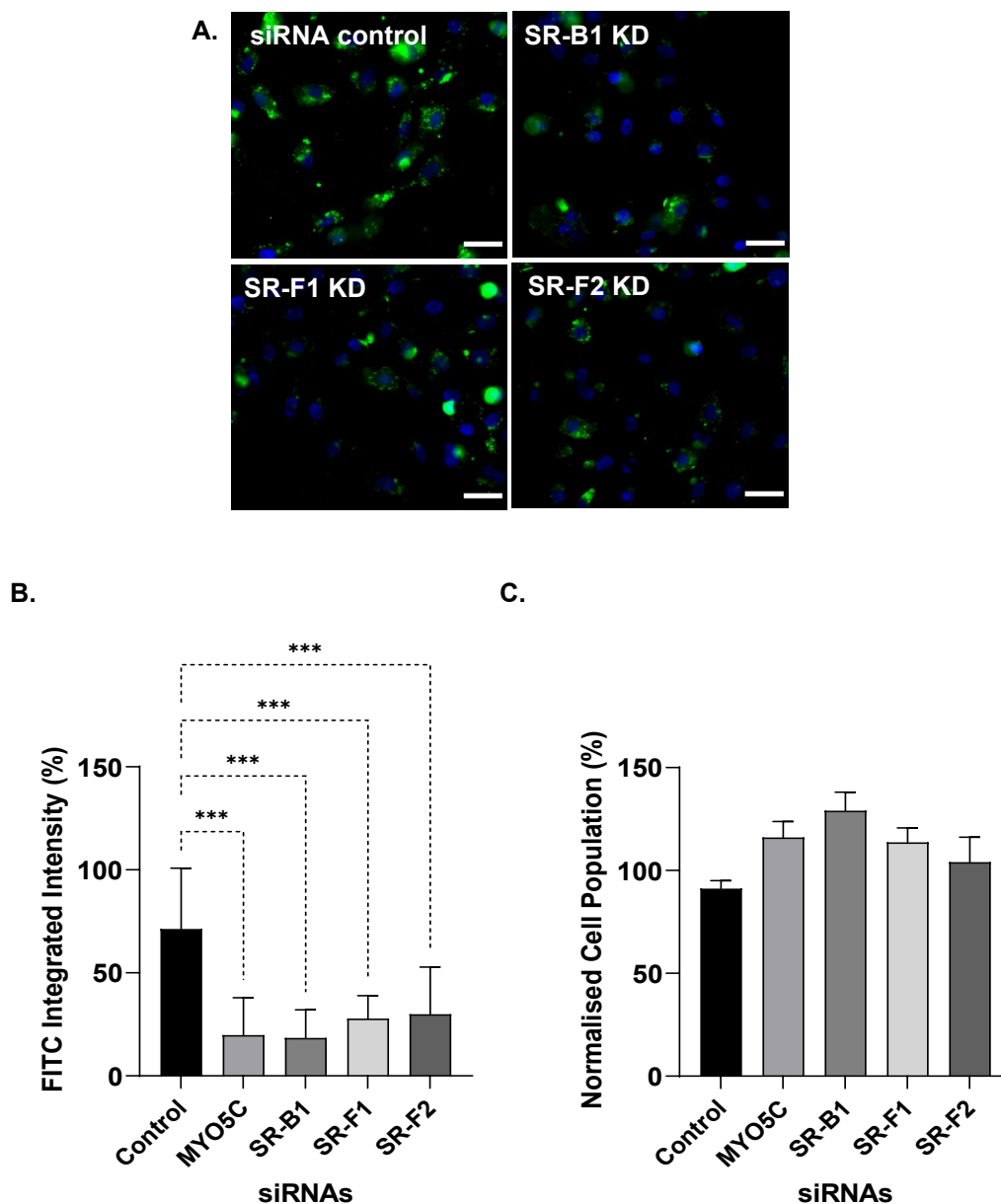


Fig. 36. SR hits knockdown in PC-3. (A) High content images of PC-3 cells after 72 hrs KD and 24 hrs of FITC-G3 exposure. Scale bar 50 μ m and 20X magnification. (B) FITC integrated intensity normalised values of 3 independent experiments. Data is expressed as means \pm SD. Non-targeted siRNAs was used as negative control. The statistical significance was determined using one way ANOVA test (** $p < 0.001$). (C) Normalized cell population after 72 hrs transfection.

The data from the SR hits screen in LNCaP and PC-3, corroborated the results from the previous SR library screens, indicating that SR-B1, SR-F1, SR-F2 might be responsible at some degree of the internalization of FITC-G3, since their silencing was reflected in a reduction of fluorescence intensity. None of the cell populations were

altered after transfection, however the KD of SR-B1 in LNCaP cells had a negative influence on cell survival.

4.6.4 Protein expression RNAi knockdown validation

The RNAi silencing of the SR hits was further validated by two techniques that measure protein levels in LNCaP and PC-3 cells: 1) antibody labelling using HCS and 2) Western blot (WB).

4.6.5 SR antibody labelling using HCS

To test if we could detect MYO5C, SR-B1, SR-F1, and SR-F protein and establish whether the siRNAs were specific for our target genes a series of experiments were done. HCS was used to image and quantitate antibodies to MYO5C, SR-B1, SR-F1, and SR-F2 and integrated intensity values of the images were analysed to assess protein level and location. The antibodies against SR-F1 and SR-B1 employed in this research have been reported in other publications, for immunofluorescence analysis (Ramirez-Ortiz et al., 2013; Tsuzuki et al., 2018a ; Tsuzuki et al., 2018b). However, to our knowledge, there are no publications for the MYO5C and SR-F2 antibodies that were used here.

The MYO5C was KD using siRNA and presented in Figure 37 for LNCaP cells and Figure 38 for PC-3 cells. Images of the non-targeted siRNA control and MYO5C KD are exhibited in Figure 37A and Figure 38A, for LNCaP and PC-3 cells in that order. In Figure 37B for LNCaP and Figure 38B for PC-3, the integrated intensity values corresponding to Alexa red antibody labelling of MYO5C were graphed and analysed using student-t test. The integrated intensity graph demonstrated at least a 2-fold decrease in MYO5C KD for both cell lines.

Similar to MYO5C, SR-B1 expression was KD in LNCaP and PC-3 cells using siRNA (Fig. 39 and Fig. 40). Images of the SR-B1 KD assay are represented in Figure 39A for LNCaP and Figure 40A for PC-3. In Figure 39B for LNCaP and Figure 40B for PC-3, the integrated intensity percentages of the SR-B1 KDs were calculated and

analysed using student-t test, comparing the treated samples to the siRNA controls. The KD of SR-B1 in both cell lines showed a significant decrease in antibody labelling values, displaying p values <0.001.

To test the effect of the SR-F1 antibody and siRNA KD, Figure 41 and Figure 42 present the SR-F1 data. The KD images of SR-F1 in LNCaP and PC-3 cells indicated low levels of immunolabelling marks when compared to the higher degree of fluorescence in the siRNA controls (Fig. 41A and Fig. 42A). Integrated intensities were acquired and statistical comparisons between groups were calculated through student-t test. A significant reduction of SR-F1 protein staining levels were obtained in the SR-F1 KD in LNCaP and PC-3 cells, when compared to the control (Fig. 41B and Fig. 42B).

Again, to test the KD of SR-F2 with the siRNA and to test the specificity of the antibody, the SR-F2 experiments were performed on LNCaP and PC-3 cells (Figure 43 and Figure 44). The SR-F2 KD images revealed a reduction in antibody staining in contrast to the high degree of antibody labelling of the controls (Figure 43A and Figure 44A). In Figure 43B for LNCaP and Figure 44B for PC-3, the antibody labelling for controls and KD of SR-F2 were represented on a graph as integrated intensity percentages and student-t test were performed to determine the statistical difference between the groups. At least a 2-fold decline in integrated intensity values were obtained for the KD groups for both cell lines.

According to the results of the antibody labelling of the 3 SR (SR-B1, SR-F1, SR-F2) and MYO5C following 3 days post transfection, the protein staining levels were lowered in both PCa cell lines. These results mean that the target genes were indeed downregulated via siRNA silencing.

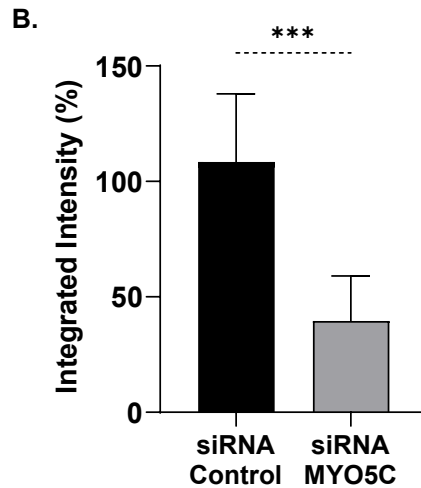
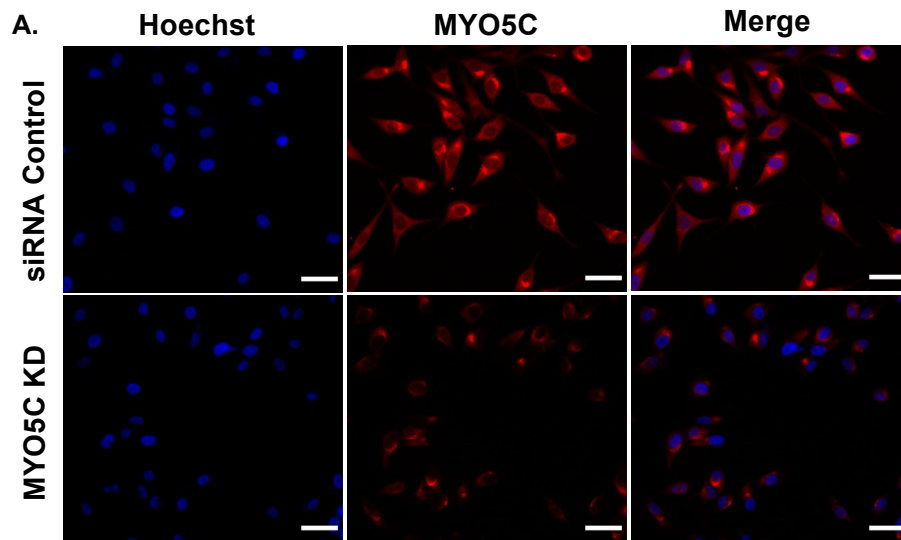


Fig. 37. MYO5C antibody labelling after siRNA knockdown in LNCaP. (A) High content images of LNCaP cells labelled with MYO5C ab after 72 hrs KD. The following channels are shown: Hoechst (nuclei staining), Alexa Red (MYO5C ab) and merged. Scale bar 50 μ m and 20X magnification. (B) Alexa red integrated intensity normalised values to the siRNA control. Data is expressed as means and \pm SD of 3 different experiments with 3 replicates each. A mix of non-targeting siRNAs were used as negative control. The statistical significance was calculated using student's t-test (** $p < 0.001$).

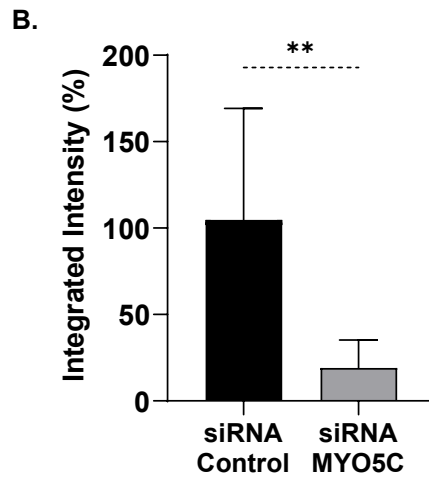
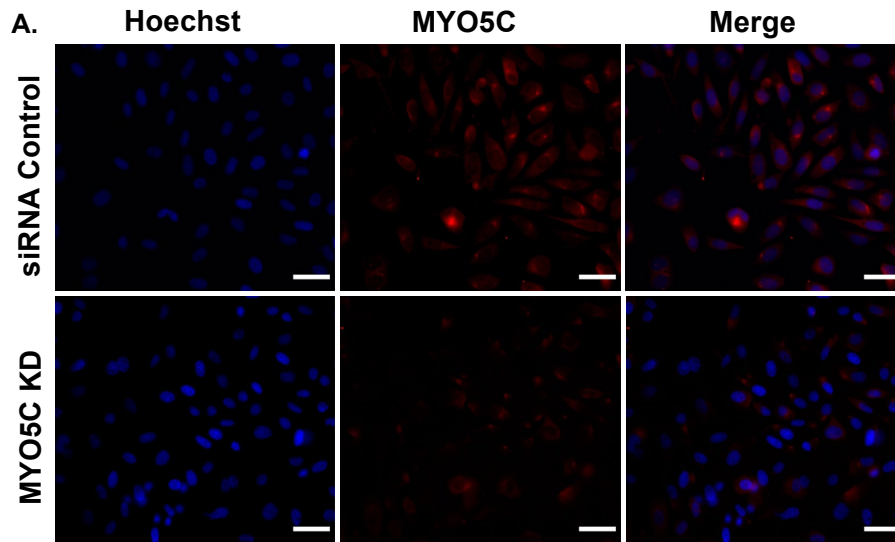


Fig. 38. MYO5C antibody labelling after siRNA knockdown in PC-3. (A) High content images of PC-3 cells labelled with MYO5C ab after 72 hrs KD. The following channels are shown: Hoechst (nuclear staining), Alexa Red (MYO5C ab) and merged. Scale bar 50 μ m and 20X magnification. (B) Alexa red integrated intensity normalised values to the siRNA control. Data is expressed as means and \pm SD of 3 different experiments with 3 replicates each. A mix of non-targeting siRNAs were used as negative control. The statistical significance was calculated using student's t-test (** $p < 0.01$).

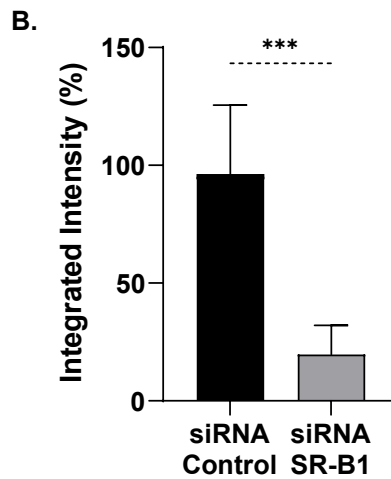
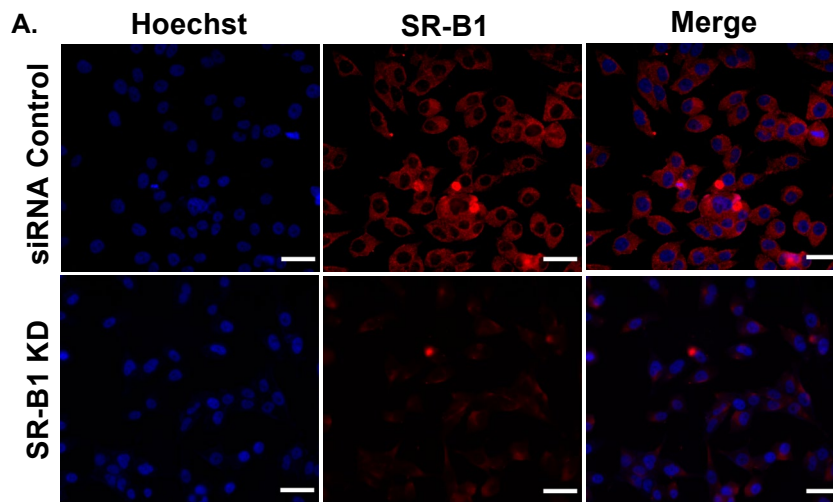


Fig. 39. SR-B1 antibody labelling after siRNA knockdown in LNCaP. (A) High content images of LNCaP cells labelled with SR-B1 ab after 72 hrs KD. The following channels are shown: Hoechst (nuclei staining), Alexa Red (SR-B1 ab) and merged. Scale bar 50 μ m and 20X magnification. (B) Alexa red integrated intensity normalised values to the siRNA control. Data is expressed as means and \pm SD of 3 different experiments with 3 replicates each. A mix of non-targeting siRNAs were used as negative control. The statistical significance was calculated using student's t-test (** $p < 0.001$).

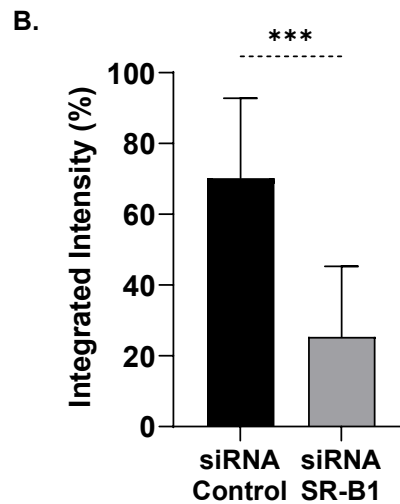
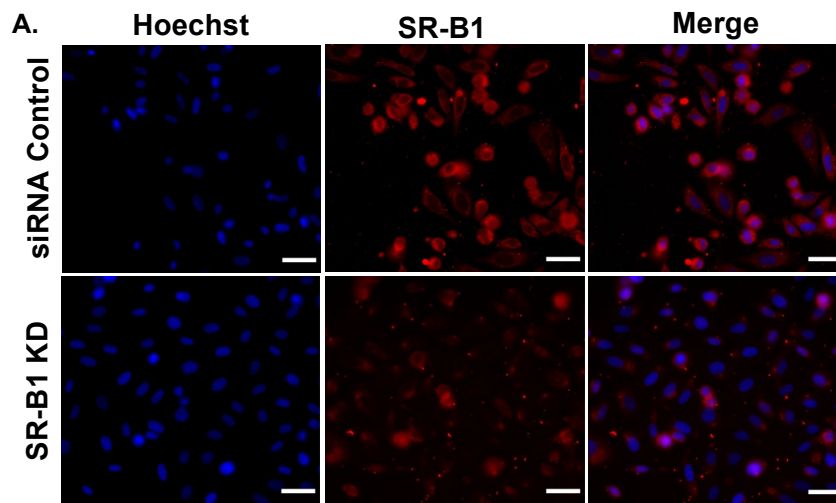


Fig. 40. SR-B1 antibody labelling after siRNA knockdown in PC-3. (A) High content images of PC-3 cells labelled with SR-B1 ab after 72 hrs KD. The following channels are shown: Hoechst (nuclear staining), Alexa Red (SR-B1 ab) and merged. Scale bar 50 μ m and 20X magnification. (B) Alexa red integrated intensity normalised values to the siRNA control. Data is expressed as means and \pm SD of 3 different experiments with 3 replicates each. A mix of non-targeting siRNAs were used as negative control. The statistical significance was calculated using student's t-test (** $p < 0.001$).

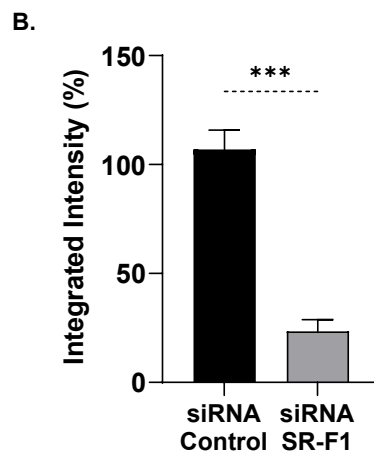
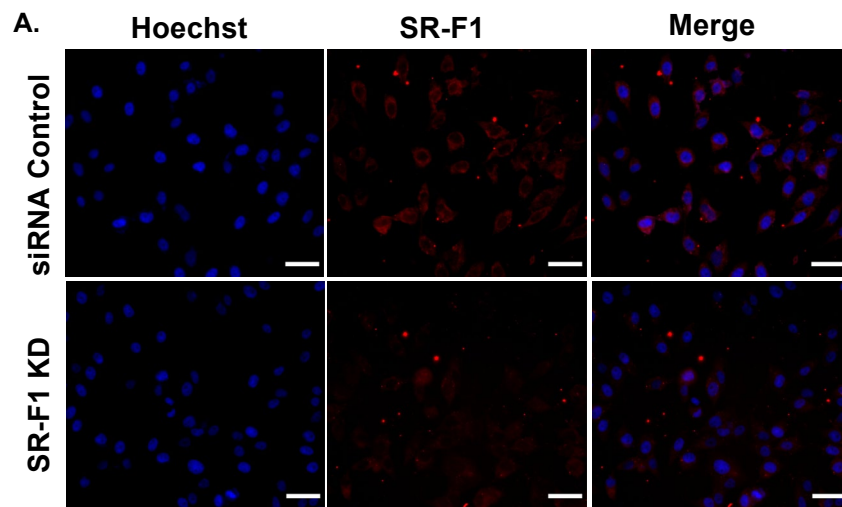


Fig. 41. SR-F1 antibody labelling after siRNA knockdown in LNCaP. (A) High content images of LNCaP cells labelled with SR-F1 ab after 72 hrs KD. The following channels are shown: Hoechst (nuclei staining), Alexa Red (SR-F1 ab) and merged. Scale bar 50 μ m and 20X magnification. (B) Alexa red integrated intensity normalised values to the siRNA control. Data is expressed as means and \pm SD of 3 different experiments with 3 replicates each. A mix of non-targeting siRNAs were used as negative control. The statistical significance was calculated using student's t-test (** $p < 0.001$).

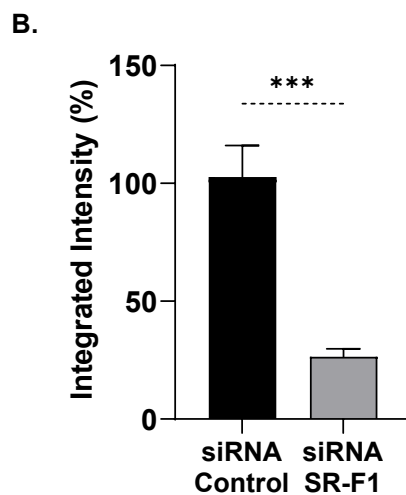
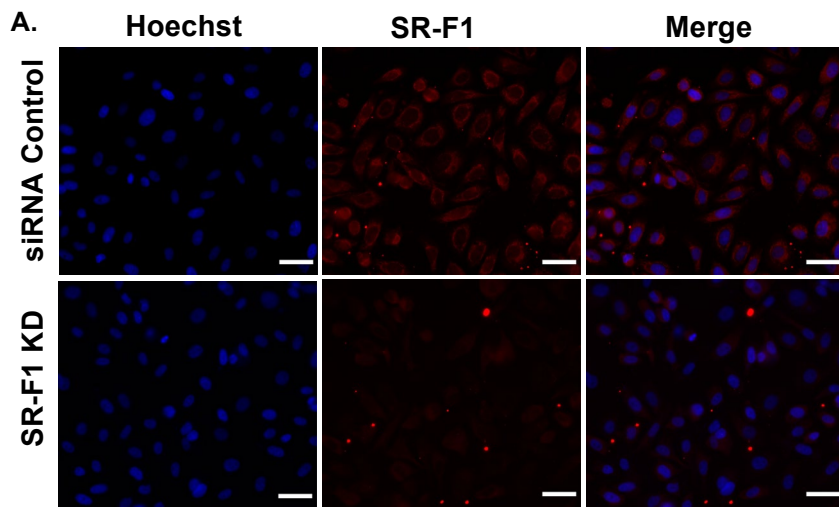


Fig. 42. SR-F1 antibody labelling after siRNA knockdown in PC-3. (A) High content images of PC-3 cells labelled with SR-F1 ab after 72 hrs KD. The following channels are presented: Hoechst (nuclei staining), Alexa Red (SR-F1 ab) and merged. Scale bar 50 μ m and 20X magnification. (B) Alexa red integrated intensity normalised values to the siRNA control. Data is expressed as means and \pm SD of 3 different experiments with 3 replicates each. A mix of non-targeting siRNAs were used as negative control. The statistical significance was calculated using student's t-test (** $p < 0.001$).

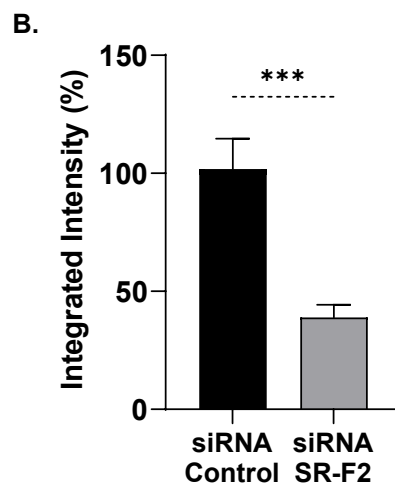
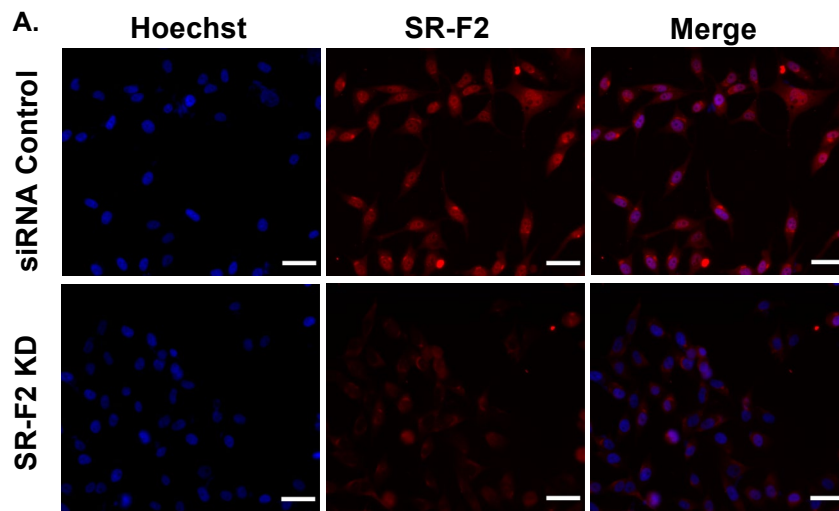


Fig. 43. SR-F2 antibody labelling after siRNA knockdown in LNCaP. (A) High content images of LNCaP cells labelled with SR-F2 ab after 72 hrs KD. The following channels are illustrated: Hoechst (nuclear staining), Alexa Red (SR-F2 ab) and merged. Scale bar 50 μ m and 20X magnification. (B) Alexa red integrated intensity normalised values to the siRNA control. Data is expressed as means and \pm SD of 3 different experiments with 3 replicates each. A mix of non-targeting siRNAs were used as negative control. The statistical significance was calculated using student's t-test (** $p < 0.001$).

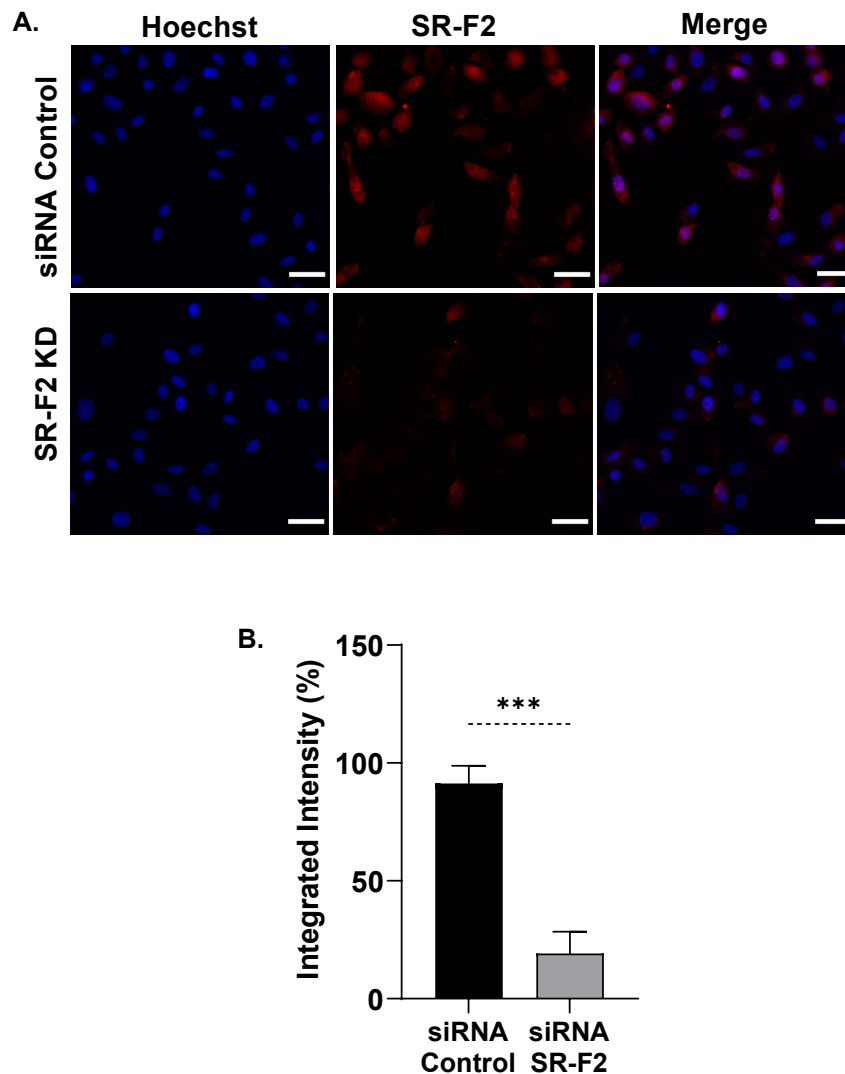


Fig. 44. SR-F2 antibody labelling after siRNA knockdown in PC-3.

(A) High content images of PC-3 cells labelled with SR-F2 ab after 72 hrs KD. The following channels are shown: Hoechst (nuclei staining), Alexa Red (SR-F2 ab) and merged. Scale bar 50 μ m and 20X magnification. (B) Alexa red integrated intensity normalised values to the siRNA control. Data is expressed as means and \pm SD of 3 different experiments with 3 replicates each. A mix of non-targeting siRNAs were used as negative control. The statistical significance was calculated using student's t-test (** $p < 0.001$).

4.6.6 SR antibody labelling using WB

Furthermore, the siRNA knockdowns of the SR hits, SR-B1, SR-F1 and SR-F2 in PC-3 and LNCaP cells were validated by analysing the protein expression levels using western blots. The house keeping protein (HKP) selected for all immunoblots was glyceraldehyde 3-phosphate dehydrogenase (GAPDH), which has been used in other studies as HKP for the normalization of SR protein expression, precisely in PCa cells (Gordon et al., 2019; Tousignant et al., 2019; Traugber et al., 2020). Graphs depicting the linear range of the target SR proteins and the HKP are provided in Appendix C. The corresponding blots of the increased amounts of lysates of SR-B1, SR-F1, and SR-F2 can be viewed in Figures C1A, C3A, and C5A for LNCaP and Figures C2A, C4A, and C6A for PC-3, respectively. The region of linear association between relative protein levels for every targeted protein and HKP were created to select optimal lysate concentration for LNCaP and PC-3 (Fig. C1B, C2B, C3B, C4B, C5B, and C6B). The antibody probing of MYO5C was not possible to accomplish using WB due to the lack of specificity from the primary ab (Data not provided).

Confluent LNCaP and PC-3 cells cultivated in T-75 flasks were transfected with the corresponding siRNAs for 72 hrs, before protein extraction and WB evaluation. Cells treated with the same mixture of non-targeted siRNAs as the ones used in the RNAi screens, were used as negative controls. The WB validation analysis of the RNAi KD of SR-B1 is depicted in Figure 45, for the two PCa cell lines. Representative blots of the SR-B1 control and SR-B1 KD bands (~82 kDa) are displayed in Figure 45A for LNCaP and Figure 45B for PC-3. At around 37 kDa, specific bands of the GAPDH were detected. Relative levels of SR-B1 expression were semi-quantified using Image Studio software and normalized using the HKP following LICOR protocol. Same method of normalization was applied for all the WBs. A significant 2-fold decline resulted for SR-B1 protein expression after KD when compared to the total protein levels in the control, for LNCaP (Fig. 45C) and for PC-3 lysates (Fig. 45D).

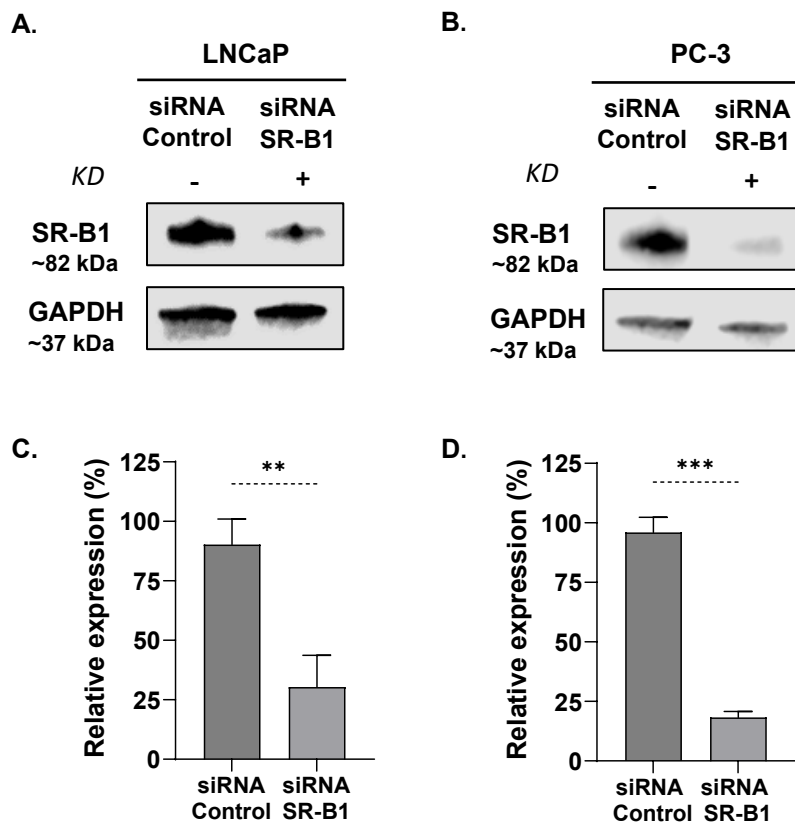


Fig. 45. Analysis of SR-B1 protein levels and knockdown using siRNA in PCa cells. Representative western blots of 3 different experiments for (A) LNCaP and (B) PC-3. Proteins were extracted after 3 days siRNA transfection with a mix of non-targeting siRNAs or SR-B1. GAPDH (~37 kDa) was used as housekeeping protein (HKP) and SR-B1 bands (~82 kDa) are shown. Relative protein levels were expressed as percentages after normalization against the HKP in (C) LNCaP and (D) PC-3. Data was used as means and \pm SD, 3 biological repeats. The statistical significance were determined using student's t-test (** $p < 0.01$, *** $p < 0.001$).

SR-F1 protein levels were determined using WB in LNCaP and PC-3 cells after siRNA transfection (Fig 46). In Figure 46A for LNCaP and Figure 46B for PC-3, the western blots indicating the differences amid SR-F1 KD and non-targeted control protein bands (~87 kDa) are provided. The HKP bands were detected at approximately 37 kDa. Figure 46C for LNCaP and Figure 46D for PC-3, evidenced a significant decrease in the relative SR-F1 protein levels after silencing. Student's t-test was applied between siRNA controls and SR-F1 KD groups to assess the significance.

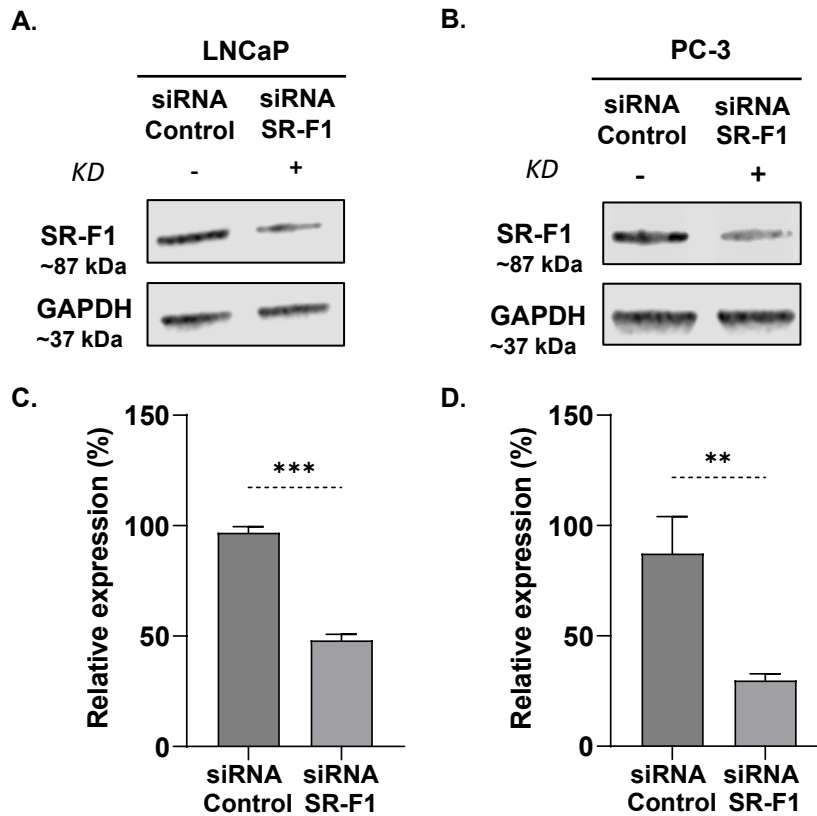


Fig. 46. Analysis of SR-F1 protein levels and knockdown using siRNA in PCa cells. Representative western blots of 3 different experiments for (A) LNCaP and (B) PC-3. Proteins were extracted after 3 days siRNA transfection with a mix of non-targeting siRNAs or SR-F1. GAPDH (~37 kDa) was used as housekeeping protein (HKP) and SR-F1 bands (~87 kDa) are depicted. Relative protein levels were expressed as percentages after normalization against the HKP in (C) LNCaP and (D) PC-3. Data was used as means and \pm SD, 3 biological repeats. The statistical significance were determined using student's t-test (** $p < 0.01$, *** $p < 0.001$).

Figure 47 confirms the KD of SR-F2 in LNCaP and PC-3 cells. Representative images of SR-F2 KD immunoblots are depicted in Figure 47A for LNCaP and Figure 47B for PC-3. The SR-F2 bands at approximately 90 kDa and GAPDH bands at 37 kDa are shown, indicating the correct protein sizes. SR-F2 protein expression was measured for both cell lines and normalized using the HKP, in Figure 47C and Figure 47D. To ascertain statistical significance, a student's t-test was implemented, and the results revealed that diminished transcript levels due to the KD, indeed resulted in lowered protein levels of SR-F2 than those of the control groups.

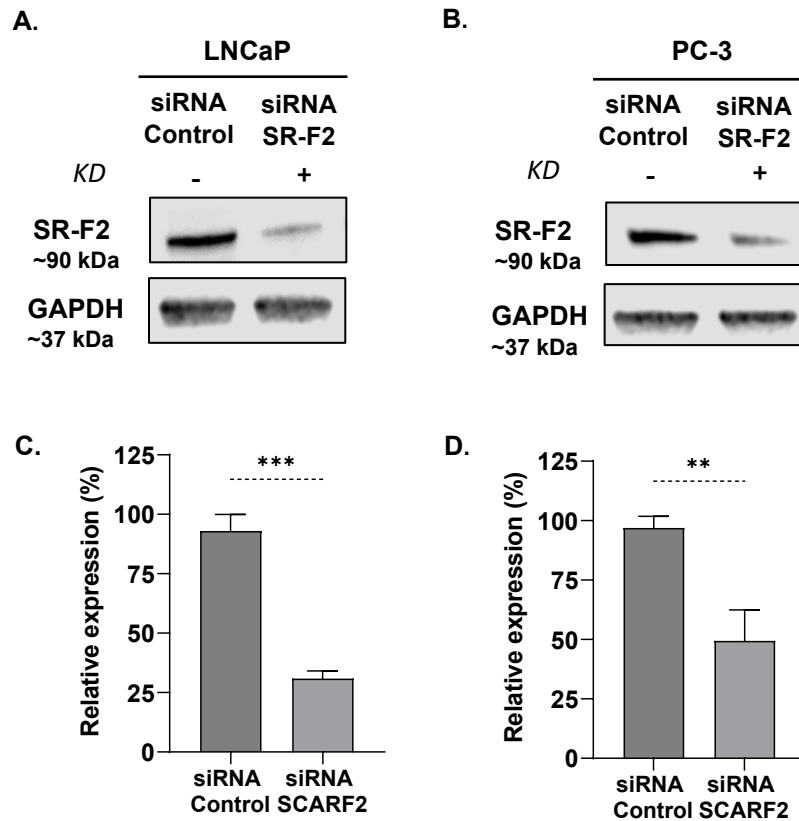


Fig. 47. Analysis of SR-F2 protein levels and knockdown using siRNA in PCa cells. Representative western blots of 3 different experiments for (A) LNCaP and (B) PC-3. Proteins were extracted after 3 days siRNA transfection with a mix of non-targeting siRNAs or SR-F2. GAPDH (~37 kDa) was used as housekeeping protein (HKP) and SR-F2 bands (~90 kDa) are shown. Relative protein levels were expressed as percentages after normalization against the HKP in (C) LNCaP and (D) PC-3. Data was used as means and \pm SD, 3 biological repeats. The statistical significance were determined using student's t-test (** $p < 0.01$, *** $p < 0.001$).

All western blotting experiments demonstrated successful SR-F1, SR-F2 and SR-B1 KD in both, LNCaP and PC-3 cells, after 3 days transfection. These data in combination with the immunolabelling analysis, further validated the RNAi screen findings.

4.6.7 Colocalization analysis of scavenger receptors and FITC-G3

To expand upon SRs possible involvement in the internalization process of G3 peptide, a colocalization study was performed between FITC-labelled peptide and either SR-B1 or SR-F1 or SR-F2 antibody stains. Transferrin (TF) and dextran (DXT) were used as positive and negative colocalization controls, respectively. LNCaP and PC-3 cells were grown in μ -Dishes and exposed to FITC-G3 at 4 μ M for 1 hr and 25 min (same time as TF control). Meanwhile, DXT samples were subjected to FITC-G3 for an initial 60 minutes period, followed by an incubation of 40 minutes with DXT. After treatment, samples were labelled with the appropriate SR antibodies, following previously established procedures. Confocal microscopy was used to image all samples and for each control and treated μ -Dishes, 6 to 12 z-stacks (0.15 μ m each) were generated.

The Colocalization Colormap ImageJ plugin was used to determine the Icorr, that is based on the normalized mean deviation product (nMDP) (Gorlewicz et al., 2020; Jaskolski et al., 2005). The confocal images displaying Hoechst, Alexa Red and merged channels of the colocalization analysis are illustrated in Figure 48 for LNCaP and in Figure 49 for PC-3. Mean Icorr values were calculated and presented in Figure 50A for LNCaP and in Figure 50B for PC-3 cells. The Icorr values of the SRs and FITC-G3 were contrasted with the negative control using one-way ANOVA analysis. These results indicated that FITC-G3 has strong colocalization with SR-F1 and SR-F2 for both cell lines, while at a lesser extent with SR-B1 for LNCaP cells (Fig. 50A and Fig. 50B). No significant colocalization resulted between FITC-G3 and SR-B1 in PC-3 cells, when contrasted to DXT.

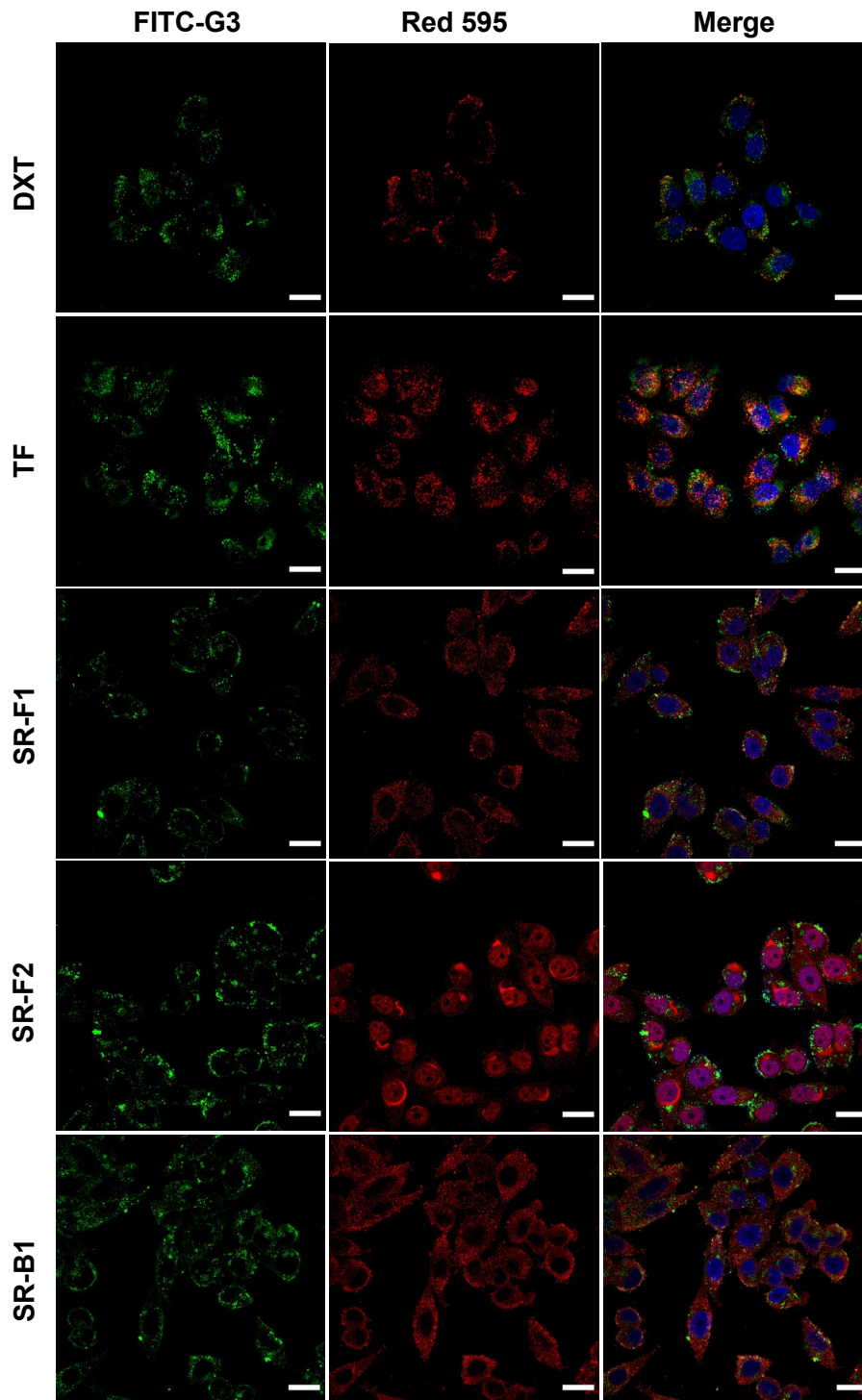


Fig. 48. Colocalization of scavenger receptors and FITC-G3 in LNCaP. This figure represents a single biological experiment with 6 FOV. Maximum projection images of z-stacks were used for the colocalization analysis. Control cells were treated with FITC-G3 at 4 μ M followed by addition of Transferrin (TF) or Dextran (DXT). Treated cells were fixed after FITC-G3 exposure and labelled with anti-SCARF1, anti-SCARF2 and anti-SRB1 using Alexa red 595 as secondary antibody. Scale bar 25 μ m.

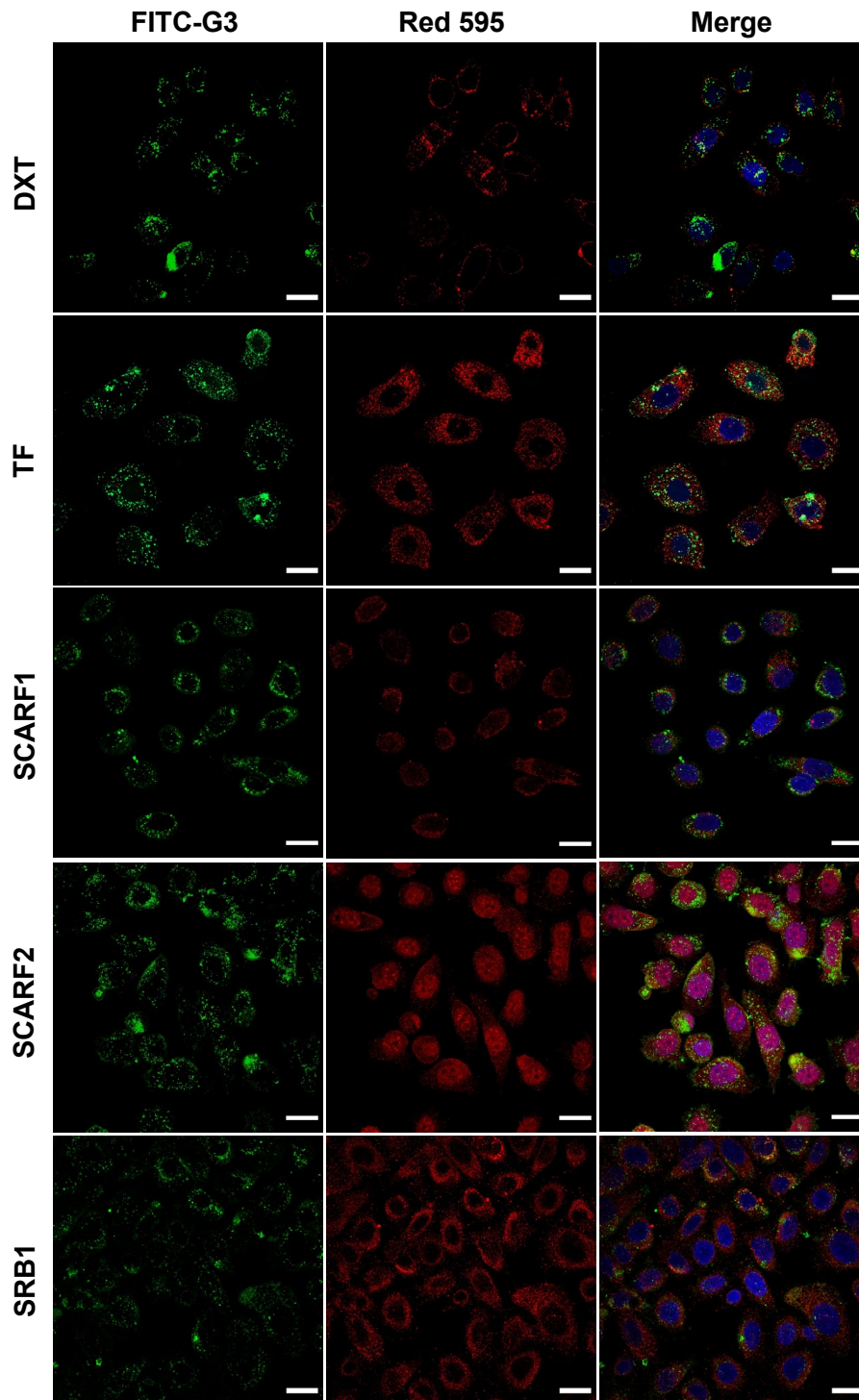


Fig. 49. Colocalization of scavenger receptors and FITC-G3 in PC-3. This figure represents a single biological experiment with 6 FOV. Maximum projection images of z-stacks were used for the colocalization analysis. Control cells were treated with FITC-G3 at 4 μ M followed by addition of Transferrin (TF) or Dextran (DXT). Treated cells were fixed after FITC-G3 exposure and labelled with anti-SCARF1, anti-SCARF2 and anti-SRB1 using Alexa red 595 as secondary antibody. Scale bar 25 μ m.

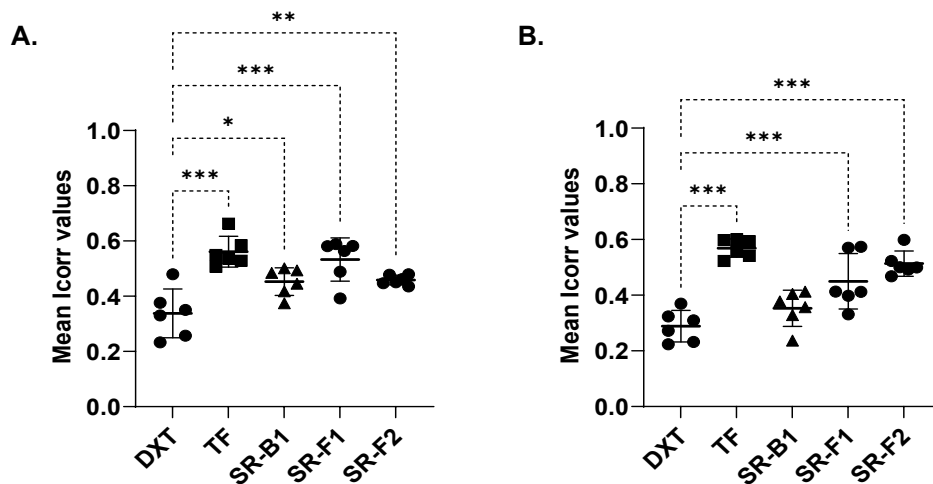


Fig. 50. Colormap colocalization analysis of scavenger receptors and FITC-G3. Mean Icorr values of (A) LNCaP and (B) PC-3 cells. Data is exhibited as means \pm SD of one biological experiment with 6 FOV. One way ANOVA analysis was used to compare SR clusters to dextran (DXT) negative ctrl (* p = .014, ** p < 0.01, *** p < 0.001).

4.7 Discussion

In summary, the data collected in this chapter revealed the potential contribution of 3 SR, namely SR-B1, SR-F1, and SR-F2, to the internalization of FITC-G3 in LNCaP and PC-3 cells. All these findings formed a coherent narrative that supports the role of these SR as participants in the receptor-mediated endocytosis of the peptide. From the initial RNAi knockdown assays evaluating endocytic genes, resulting in the selection of MYO5C as a positive control, to the small screen of the library of SR, in which the SR hits were identified by their significant impact in reducing the amount of peptide internalized in the two cell lines. Secondary RNAi KD of SR-B1, SR-F1, and SR-F2 were repeated 3 times in both PCa cells to corroborate their effect in impairing FITC-G3 uptake. Moreover, the validation of the siRNA silencing was executed by two techniques, WB and immunofluorescence analysis, which verified the reduction of SR protein expression and effectivity of transfections. Lastly, the results of the colocalization analysis between FITC-G3 and SR-B1 or SR-F1, or SR-F2, provided further insights of their subcellular localization in PCa cells, since SR-F1 and SR-F2 were found to positively colocalized with the peptide, however SR-B1 did not significantly colocalized in PC-3 cells. In the case of LNCaP cells, the degree of colocalization was less significant than SR-F1 and SR-F2. These results indicate that

at least SR-F1 and SR-F2 in both cell lines, are located in the same compartments as FITC-G3, contributing to the argument of them being key players in its endocytic pathway.

4.7.1 Could scavenger receptors be involved in the uptake of G3? Scavenger receptor and G3 internalization: A Possible Connection?

In order to explore the possible role of SR, a series of RNAi screens were conducted using FITC-labelled G3 in LNCaP and PC-3 cells. The FITC integrated intensity values were quantified and interpreted as indicative of the level of FITC-G3 uptake. Based on the premise that G3 is internalized by endocytosis, the initial siRNA KDs were performed with the purpose of detecting genes associated to endocytosis that could disrupt the internalization of the peptide. The following endocytic-related genes were knocked down, MYO5A, MYO5B, MYO5C and CAV1. Among them, the KD of MYO5C and MYO5B showed a significant decrease in the internalization levels of FITC-G3 in LNCaP cells, but only MYO5C had a similar significant effect in PC-3 cells. Since CAV1 is a key player in CvME (Li et al., 2001; Liu et al., 2002), the absence of a substantial decrease in FITC-G3 fluorescence intensity following KD experiments, suggests that G3 is not internalized via CvME in either LNCaP or PC-3 cells.

Organelle trafficking through actins is facilitated by the family of molecular motor proteins encompassed by myosins class V (Berg et al., 2001; Jacobs et al., 2009; Trybus, 2008). Although Myo5A is expressed in endocrine cells, where it engages in the transport of secretory granules, it is predominately expressed in neurons and melanocytes (Desnos et al., 2007; Rosé et al., 2002; Rudolf et al., 2003; Varadi et al., 2005). MYO5B and MYO5C, the other two members of the family of myosins class V, have a broader distribution. MYO5C is highly expressed in exocrine tissues, including the prostate, pancreas, colon, breast, and stomach; whereas MYO5B is fairly abundant in tissues such as the liver, kidney, and placenta, with lesser expression in the prostate (Rodriguez & Cheney, 2002; Uhlen et al., 2010). The RNA expression of both, MYO5B and MYO5C has been detected in PC-3 and LNCaP cells, while a lack of MYO5A expression in both cell lines was reported, which may account for its non-significant effect on the uptake of G3 after KD (Makowska et al., 2015). Given that the

silencing of MYO5C was the only endocytic-associated gene inducing a clear and substantial decline in the fluorescence intensity of FITC-G3 in both PCa cell lines, effect that was reported in HCT-116 cells as well, and due to its role in secretory pathways, comprising transferrin receptor transport and polarization of epithelial cells (Cirillo et al., 2021; Farquhar et al., 2017; Jacobs et al., 2009; Marchelletta et al., 2008; Rodriguez & Cheney, 2002), MYO5C served as a valuable positive control to evaluate SR possible involvement using RNAi, and evidently supports an energy-dependant endocytic pathway for the peptide internalization in prostate cancer cells.

The cell viability after the endocytic-related siRNA transfections was not affected as the cell numbers in both populations of LNCaP and PC-3 were not diminished, except for the UBB functional control. This observation aligns with the known effects, as the silencing of UBB has been reported to stimulate apoptosis and cause significant reduction in the proliferation of several cancer cells, including PCa (Oh et al., 2013).

A library of SR was KD using siRNAs from the SiGenome and ON-target collections, to evaluate the FITC-G3 uptake in LNCaP and PC-3 cells. The SR RNAi screens resulted in the identification of 3 hits, SR-B1, SR-F1 and SR-F2, since their KD induced a significant reduction of FITC-G3 internalization, similar to the positive control MYO5C. The SR hits were further evaluated in secondary mini screenings using the same rationale. The data of the secondary RNAi screens reiterated their impact on the internalization of FITC-G3, as in the 3 biological repeats their silencing was correlated to a significant reduction of fluorescence intensity. At the same time, cell viability was assessed. In LNCaP cells, the silencing of SR-B1 caused a significant reduction in cell numbers, impairing their cell viability. This result is consistent with a study that demonstrated that the siRNA KD of SR-B1 specifically in PCa cell lines, including LNCaP, produces a 2- fold decrease of cell viability (Twiddy et al., 2012). The KD of SR-B1 did not impact the cell viability of PC-3, which in our knowledge that effect has not been reported in the literature.

The RNAi screening was employed as an indirect method to assess variations in FITC-G3 uptake, under the assumption that the genes were effectively knocked down, as evidenced by the UBB functional control. However, to directly evaluate the effectiveness of the siRNAs in inducing post-transcriptional gene silencing, the

expression of SR proteins was confirmed through antibody labelling and Western blotting. The basic mechanism of RNAi gene silencing entails Dicer's cleavage of dsRNA into siRNAs, followed by their association with the nuclease RISC complex and subsequent recognition of the target mRNA sequence. Finally, the degradation of the target mRNA is induced by argonaute RISC catalytic component 2 (AGO2), which is part of the RNA-induced silencing complex (RISC) (Dana et al., 2017). This, in turn results in a significant reduction of the target protein levels (Elbashir et al., 2001). Thus, both techniques were employed to evaluate protein levels succeeding the 72-hrs siRNA transfections and consolidated previous transfections. The protein expression levels of SR-B1, SR-F1, and SR-F2 were found to be significantly diminished, thereby corroborating the RNAi results. Although the protein expression of the positive control MYO5C after siRNA transfections was not possible to assess by WB, because the antibody anti-MYO5C lacked specificity, its reduction of fluorescence intensity was verified by antibody labelling using HCS.

As a complementary assessment, the colocalization of FITC-G3 and SR-B1, SR-F1 and SR-F2 were conducted independently. TF and DXT were used as positive and negative control based on the previous colocalization analysis. FITC-G3 positively colocalized with SR-F1 and SR-F2 in LNCaP and PC-3 cells. In PC-3 cells, the results show that FITC-G3 and SR-B1 did not colocalize in a meaningful way, as it was not statistically different from the control (DXT). This indicates that SR-B1 and FITC-G3 do not share the same endosomal compartments at the time of analysis, which was 85 min in total. If SR-B1 is involved in the uptake of the peptide, the interaction could be transient. There was SR-B1 positive colocalization with FITC-G3 in LNCaP cells, but not as statistically significant as SR-F1 and SR-F2 when contrasted to the control. These findings support the notion that FITC-G3's endocytic pathway includes SR-F1 and SR-F2, at the very least, because they are found in the same subcellular regions than FITC-G3.

Collectively, the RNAi screenings and their gene-silencing validation by protein expression assessments, along with the colocalization analysis of FITC-G3 with SR, suggest that SR-F1, SF2-F2 and SR-B1 might be involved in the internalization of the peptide. These findings are in alignment with other studies that have reported SR as mediators of the internalization of peptides. It has been established that SR-A3 and

SR-A5 are to some degree accountable for the internalization of peptide-based complexes (Arukuusk, et al., 2013; Ezzat et al., 2012; Helmfors et al., 2015; Lindberg et al., 2013; Veiman et al., 2013). However, to our knowledge this is the first time that SR from class F are proposed as mediators of a CPP. In PCa, SR-F2 and SR-B1 are overexpressed, and the latter has been implicated in a human disease (C. Kim et al., 2022; Leon et al., 2010). There are no published studies regarding the function of SR-F1 in PCa.

According to the rationale of the assay, these findings could mean in the most probable scenario, that either SR-B1, or SR-F1, or SR-F2 are mediating at some extent the endocytic internalization of G3, or that the 3 SR are actively participating in the process to some level, as illustrated in Figure 51A. This hypothetical model is based on the data obtained in this research, in which the downregulation of the SR reflected on the receptors levels on the plasma membrane, and hence disrupted the amount of peptide uptake. However, there might be other possible explanations underlying these results.

SR have been recognized to behave as co-receptors for other proteins such as TLR, integrins, tetraspanins, and other molecules, to form intricate structures that influence the internalization of various antigens or act as signal transduction mediators depending the context (Taban et al., 2022). SR-B1 is one of the most notable example of a SR functioning as a co-receptor. In cooperation with the main receptor cluster of differentiation 81 (CD81), it was discovered that SR-B1 facilitates the internalization of the hepatitis C virus via the recognition of the E2 envelop glycoprotein (Scarselli et al., 2002; Zeisel et al., 2007). Similarly, SR-F1 is also known to partner with TLR receptors (Beauvillain et al., 2010; Jeannin et al., 2005; Means et al., 2009b; Murshid et al., 2016).

Moreover, it has been reported on the literature, that SR-F1 and SR-F2, have around 50% structural similarity in their ectodomain, and precisely through that domain they can trans-interact with each other (Ishii et al., 2002). Although it has been postulated that their ligand recognition properties are blocked through the heterodimerization of SR-F1 with SR-F2 (Ishii et al., 2002). Homophilic and heterophilic protein-protein interactions have been associated with the EGF-like regions of SR-F in their extracellular domains. In particular, SR-F1's EGF-like domains have been claimed to

contribute to protein oligomerization or to operate as the ligand binding domain (Adachi et al., 1997; Ishii et al., 2002). Also, in a study, they show that SR-F2 doesn't bind to C1q and CRT on the cell surface, but its soluble version can do so extracellularly. Thus, they hypothesized that SR-F2 may act as mediator of SR-F1 by influencing its access to certain proteins, due to its higher association to those ligands, combined with its capacity to interact with SR-F1 (Wicker-Planquart et al., 2021).

All these observations lead to considerate a hypothetical model, in which either SR-F1, or SR-B1, or even SR-F2 could be possibly acting as co-receptors to intermediate G3 internalization. The hypothetical primary receptor could be SR-F1, given it has a greater interactome than SR-F2, and SR-F2 could be acting as a co-receptor, facilitating ligand recognition or receptor activation, thus its presence would be necessary (Figure 51B). Likewise, the 3 SRs could be functioning as co-receptors of another unknown main receptor that is in control of the peptide uptake (Figure 51C).

SR-B1 has been recognized as an important target in PCa and previous research has discovered that the inhibition of SR-B1 causes cell death in PCa cells (Twiddy et al., 2012). The role of SR-B1 in G3's internalization may indicate that the observed reduction in fluorescence intensity following SR-B1 downregulation could be an outcome of cellular impairment and induction of apoptosis, rather than a direct indication of the receptor's role in endocytosis (Figure 51D). This hypothetical model could apply to LNCaP cells, as a significant reduction in cell viability resulted after SR-B1 KD. Although it would not apply to PC-3 cells, because the cell viability was not affected after SR-B1 silencing. The latter three theoretical assumptions go beyond the available evidence, but their relevance resides in reframing our knowledge of the subject matter.

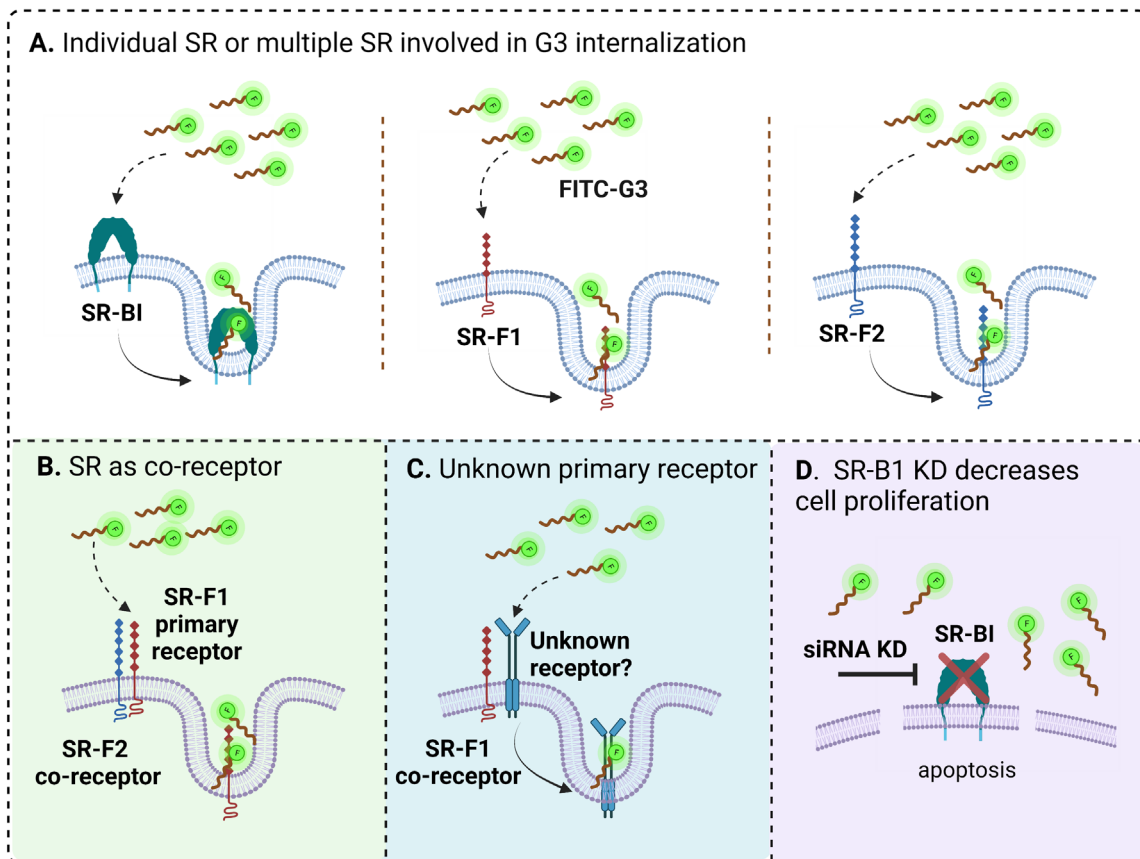


Fig. 51. Hypothetical models of SR phenotypes. (A) Our data supports a SR-mediated endocytic uptake, that could be partially regulated by either SR-B1 or SR-F1 or SR-F2. Another possibility is that the 3 SR are active participants in the endocytic process. (B) Another scenario implicates the SR functioning as co-receptors of each other or (C) as co-receptors of an unknown main receptor, taking part in the facilitation of ligand recognition or receptor activation. (D) The last model explains the reduction in FITC-G3 internalization as a consequence of cell death. The knockdown of SR-B1 induces prostate cancer cell impairment and thus could be the reason why the peptide uptake was diminished. Created with BioRender.com.

CHAPTER 5

5. PEPTIDE DRUG CONJUGATES USING G3 AND LSD1 INHIBITORS

5.1 Introduction

5.2 Peptide drug conjugates against prostate cancer

The field of PDC for the targeted administration of chemotherapeutic medications is evolving rapidly. As discussed on Chapter 1, multiple PDC are currently on clinical trials and some have been FDA approved. The status of ongoing clinical trials can be searched at <https://beta.clinicaltrials.gov/> (McCray & Ide, 2000). Several radioligand conjugates targeting PSMA and gastrin-releasing peptide receptor (GRPR) are either on clinical assessment or have been already FDA validated for PCa diagnostic and molecular imaging (Liolios et al., 2019; Ristau et al., 2014; Roberts et al., 2023). Specifically for PCa therapy, no PDC has been authorized by the FDA at this time, nevertheless peptide-based conjugates have been subjected to clinical investigations and several are in preclinical development.

Based on the recognition of the RGD motif (Arg-Gly-Asp), a series of cyclic peptides with high binding affinity to α_v integrins were conjugated to camptothecin derivatives, to create tumour specific PDC (Dal Pozzo et al., 2010). Even though the RGD peptides-CPT displayed high uptake in the following cancer cell lines: PC-3, ovarian carcinoma A2780 and renal carcinoma A498; their activity was restricted due to poor solubility when tested in a mouse xenograft with ovarian carcinoma.

One study investigated a PDC, named KCC-TGX, that consisted of a phosphoinositide 3-kinase β (PI3K β) inhibitor conjugated to a peptide specific to human epidermal

growth factor receptor 2 (HER2) and a PSA cleavable linkage unit (W. Tai et al., 2011). KCC-TGX displayed increased internalization in PCa cells and similar inhibition activity to the parent drug, that was reliant on PSA to free the active molecule. The same research lab identified a peptide, designated as KYLAYPDSVHIW (KYL) that binds exclusively to LNCaP cells (Qin et al., 2011). They demonstrated that the KYL peptide facilitated the uptake of fluorescein-labelled siRNA and proapoptotic peptides. Additionally, they generated a PDC known as KYL-TGX, combining the LNCaP-targeting KYL peptide, a PSA detachable peptide-based linker and TGX-D1, a PI3K inhibitor as payload (Barve et al., 2016). Their biodistribution analysis using mouse tumour xenografts exposed that KYL-TGX gathered in high concentrations specifically in the tumour area and that the cellular internalization in PCa cells increased considerably.

Another example of a PDC that targets PSMA in PCa cells is mipsagargin (G-202), that upon receptor binding it induces detachment of the peptide, allowing the inhibition of the sarcoplasmic or endoplasmic reticulum calcium adenosine triphosphatase (SERCA) protein via a thapsigargin analogue (Denmeade et al., 2003; Denmeade et al., 2012). The SERCA pump is vital for cell survival and due to its function of Ca^{2+} exchange from the cytosol to the lumen of the endoplasmic and sarcoplasmic reticulum, it represents a molecular target for PCa (Denmeade & Isaacs, 2005; Furuya et al., 1994). Thus, the cytotoxic effect of G-202, consequence of prolonged SERCA blockage, is directed to tumour cells expressing PSMA, and it is being tested in clinical trials (Mahalingam et al., 2016).

A GnRH-R peptide (EHWSYKLRPG) was conjugated with a derivative of gemcitabine to treat androgen independent prostate cancer (Karampelas et al., 2014). The delivery of the cytotoxic compounds was achieved by the PDC in vivo and in vitro.

Other unconventional PDC have been developed using superparamagnetic iron oxide nanoparticles or liposomal agents coupled to a PCa-targeting peptide named SP204, which was discovered after a phage screening (Yeh et al., 2016). These PDC revealed possible synergetic applications as diagnostic and biodistribution cancer tools, as well as directed drug delivery against PCa. Also, other study reported the application of multi-drug PDC using the peptide P12 (Bashari et al., 2017). They identified that PDC

conjugated to both, Combretastatin, an inhibitor of tubulin polymerization and Chlorambucil, a DNA alkylator, presented the highest cytotoxic profile in PCa cells, including PC-3 and LNCaP cells.

Furthermore, PDC were produced using peptides that recognize the extra-domain B fibronectin (EDB-FN) and coupled with docetaxel or doxorubicin to target PCa cell lines (Park et al., 2019). The cytotoxic effect caused by the PDC, conjugate 13, was minimal in the control RWPE-1 cells, when compared to the enhanced cell death induced in PCa cells.

In 2018, the FDA granted their approval of the PDC referred to as 177Lu-DOTA-TATE, which effectively targets the somatostatin receptor and has been tested in patients with gastroenteropancreatic neuroendocrine tumours (Das et al., 2019). For PCa and castration resistant prostate cancer therapy, numerous PDC based on Lu-177 peptide technology have been developed to recognize PSMA receptor, which are currently in different phases of clinical trials (Heh et al., 2023).

5.3 Understanding LSD1 demethylation of histones and non-histone proteins

DNA is enclosed as chromatin into nucleosomes, that are basic structural units formed by an octamer core of four recurring histones, H2A, H2B, H3 and H4 (Onufriev & Schiessel, 2019). Gene expression and chromatin organization can be controlled in an environment-specific manner by histone post-translational modifications, such as methylation, acetylation, ubiquitination, phosphorylation, butyrylation, sumoylation, propionylation, glycosylation, crotonylation, malonylation, lactylation, among others; that together form the histone code (Jenuwein & Allis, 2001; R. Liu et al., 2023).

Demethylation targets the removal of methyl groups from arginine or lysine in the amino-terminal tails of histones. Lysine-specific demethylase 1 (LSD1) is capable of demethylating, histone 3 lysine 4 (H3K4) via an oxidative reaction using the cofactor flavin (Shi et al., 2004). It was established that in collaboration with the complex co-repressor for element-1-silencing transcription factor (CoREST), LSD1 could induce transcriptional repression through the demethylation of either H3K4me1 or H3K4me2

(Forneris et al., 2006; M. G. Lee et al., 2005; Shi et al., 2004). In a similar way, LSD1 works as a transcriptional co-repressor with other complexes, such as the nucleosome remodelling and deacetylase (NuRD) and C-terminal-binding protein 1 (CtBP) (Shi et al., 2003; Wang et al., 2009).

Further studies discovered that LSD1 could also enable gene activation by binding to AR and demethylating histone 3 mono lysine 9 (H3K9me1) and/or histone 3 dimethyl lysine 9 (H3K9me2) (Laurent et al., 2015; Metzger et al., 2005; Wang et al., 2007). Additionally, LSD1 acts as a context-specific transcriptional activator by demethylating mono- or dimethyl H3K9 marks in association with estrogen receptor (Garcia-Bassets et al., 2007; Perillo et al., 2008). In 2015, histone 4 dimethyl lysine 20 (H4K20me2) was identified as a histone substrate for demethylation via a neuronal isoform of LSD1 (LSD1n), in cooperation with transcription factors such as myocyte enhancer factor 2 (MEF2) or cAMP-response element-binding protein (CREB), LSD1n functions as a co-activator of neuronal-linked gene expression (Wang et al., 2015). Thus, LSD1 represents a crucial transcriptional regulator that modifies gene expression through histone demethylation, depending upon the contextual setting (Fig. 52) (Højfeldt et al., 2013).

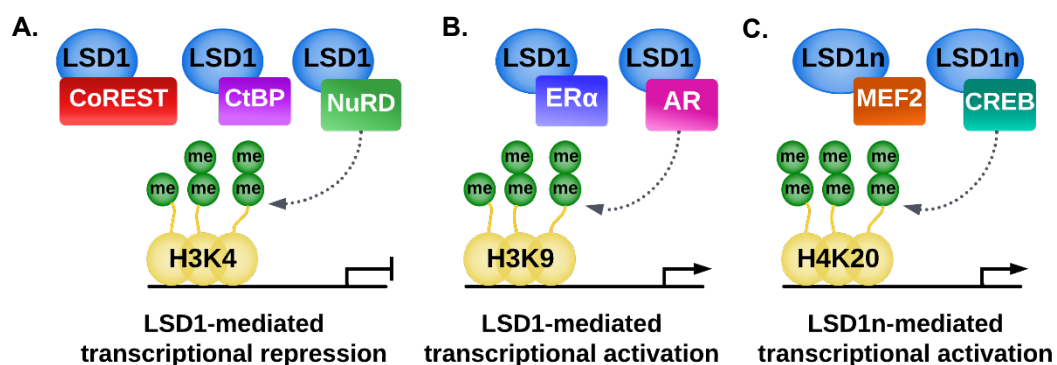


Fig. 52. LSD1 serves as an epigenetic regulator. (A) LSD1 promotes gene suppression through interaction with NuRD, CtBP or CoREST complex leading to the removal of methyl groups from H3K4me1/2. (B) By binding to AR or ER α , LSD1 demethylates H3K9me2 and induces gene activation. (C) By association with CREB or MEF2, the neuronal-specific isoform, LSD1n catalyses the demethylation reaction of H4K20me2 enabling the activation of neuronal gene network. Adapted from Gu et al., 2020.

LSD1 interacts with a vast number of non-histone proteins, exposing its functional plasticity. Some of the most important LSD1 substrate partners that are not categorized as histones, are listed in Table 9. It is understood that LSD1 coordinates a variety of biological and malignant processes via altering methylation shifting patterns not only of histones, but of approximately 60 protein targets, some within protein complexes, as well as of long coding RNAs (lncRNAs) (F. Gu et al., 2020; Majello et al., 2019; Martinez-Gamero et al., 2021). The identification of LSD1 interacting with multiple lncRNAs is relatively new. Among them, some of the most common are HOX antisense intergenic RNA (HOTAIR), steroid receptor RNA activator (SRA) and telomeric repeat-containing RNA (TERRA), which in collaboration with LSD1 provoke distinct oncogenic phenotypes (Majello et al., 2019). The regulatory function of LSD1 has been detected in a plethora of biological and pathological events, including cancer progression, neurodegenerative conditions, epithelial-mesenchymal transition, autophagy, stem cell pluripotency, senescence, metabolism, development, chromosome allocation, cell growth and differentiation (Ambrosio et al., 2017; Ambrosio et al., 2019; Ambrosio & Majello, 2018; Amente et al., 2013; Castex et al., 2017; Lan et al., 2008; Sakamoto et al., 2015; Whyte et al., 2012).

Initially it was discovered that LSD1 could associate with p53 in cancer cells and demethylate its K370 residue, triggering the suppression of p53 gene expression (J. Huang et al., 2007). In p53-negative cancer cells, LSD1 is involved in cell death in response to DNA damage by demethylation K185 of the transcription factor E2 promoter binding factor 1 (E2F1) (Kontaki & Talianidis, 2010). The stabilization of proteins through LSD1 mediation has been exposed not only for E2F1, but also for hypoxia-inducible factor 1-alpha (HIF-1 α), AGO2, ubiquitin like with PHD and ring finger domains 1 (UHRF1) and DNA methyltransferase 1 (DNMT1); whilst LSD1 regulates the opposite effect for myosin phosphatase targeting subunit1 (MYPT1) causing its instability after K442 demethylation, which in turn contributes to cell cycle dynamics in cancer cells by enhancing the phosphorylation of RB1 (Baek & Kim, 2016; Cho et al., 2011; Hahm et al., 2019; Sheng et al., 2018; Wang et al., 2009; Zhang et al., 2019). In the case of AGO2, protein stability and T cell tumour reactivity are achieved after LSD1 demethylation of K726 by building up dsRNA (Sheng et al., 2018). Also, the demethylation of K270 from FOXA1 mediated by LSD1 has been recently demonstrated in PCa (Gao et al., 2020).

Three different routes have been proposed for the improvement of HIF-1 α stability under hypoxia exerted by LSD1. First, LSD1 counteracts the methylation of K32 or K391 by SET domain containing 7, histone lysine methyltransferase (SETD7) and consequent protein breakdown, by direct demethylation sustaining HIF-1 α stability and hypoxia-related genes transcription (Baek & Kim, 2016; Kim et al., 2016; Lee et al., 2017). The second involves the stabilization by an indirect mechanism in which LSD1 blocks hydroxylation of prolyl hydroxylase domain (PHD) enzymes and further degradation, enabling deacetylation of K532 residues of HIF-1 α (Lee et al., 2017). Third, the K271 of the receptor for activated C kinase 1 (RACK1) is demethylated by LSD1, which inhibits the association with HIF-1 α and hence its posterior proteolytic degradation (Yang et al., 2017). LSD1 interaction with HIF-1 α and its regulatory effects have been linked to the metabolic reprogramming favouring glycolysis, as well as to angiogenesis and cancer (A. Sakamoto et al., 2015).

LSD1 is also implicated in the transcriptional control of several protein targets. For instance, the gene expression of myocyte enhancer factor 2D (MEFD2) and the differentiation of skeletal muscle cells is facilitated by LSD1 demethylation of its K267 (Choi et al., 2014). LSD1 also associates with signal transducers and activators of transcription 3 (STAT3), altering the expression of STAT3-related subset genes, by the removal of methyl groups from its K140 (Yang et al., 2010). Also, following estrogen stimulation, LSD1 demethylates estrogen receptor alpha (ER α) at K266 site in order to allow the p300 and cAMP response element-binding protein-binding protein (CBP) to acetylate ER α at the same location (X. Zhang et al., 2013). The stimulation of ER α genes of interest is caused by this acetylation, which encourages ER α transactivation. Even though it was identified that LSD1 demethylates HSP90 in its K615 site, the effect is not entirely understood as it was hypothesized that it might be inducing protein degradation (Abu-Farha et al., 2011). Additionally, LSD1 demethylates the metastatic tumor antigen 1 (MTA1) at residue K532, which causes the destabilization of the NuRD repressor complex, that in turn favours the acetylation via p300/CBP H3K9me2 (Nair et al., 2013). Due to the cycle of methylated and demethylated MTA1, the NuRD or nucleosome remodelling factor (NURF) complexes are created inducing contrary effects.

Table 9. LSD1 non-histone substrate partners

Protein	Lysine site	General effect/Outcome	References
p53	370	Impairs p53 function in apoptosis by suppressing its transcriptional activity	(Huang et al., 2007)
E2F1	185	Enables protein stability, leading to the stimulation of proapoptotic genes	(Kontaki & Talianidis, 2010)
HIF1 α and RACK1	32 and 391 in HIF1 α /271 in RACK1	Induces HIF1 α stability, which enhances hypoxia-induced tumor angiogenesis and cancer progression	(Baek & Kim, 2016; Kim et al., 2016; Lee et al., 2017; Yang et al., 2017)
MYPT1	442	Sustains protein instability, improving rates of cell cycle phosphorylation via RB1	(Cho et al., 2011)
AGO2	726	Causes protein stability and T cell response to cancer cells	(Sheng et al., 2018)
DNMT1	1096 (mouse), 1094 (human), and 142	Strengthens stability to preserve DNA methylation patterns	(Leng et al., 2018; Wang et al., 2009)
FOXA1	270	Increases optimal chromatin binding promoting PCa advancement	(Gao et al., 2020)
MEF2D	267	Boosts its gene expression and regulates skeletal muscle differentiation	(Choi et al., 2014)
STAT3	140	Modulates its transcriptional activity, which influences subsets of STAT3-related genes	(Yang et al., 2010)
ER α	266	Stimulates ER α -associated genes, however the general outcome is unclear	(X. Zhang et al., 2013)
UHRF1	385	Induces protein stability regulating its activity in DNA damage repair	(Hahm et al., 2019; Zhang et al., 2019)
HSP90	615	It might have a regulatory mechanism via HSP90 degradation	(Abu-Farha et al., 2011)
MTA1	532	Disrupts the creation of the NuRD complex and unmethylated MTA1 supports acetylation of demethylated H3K9 contributing to transcriptional dynamics	(Nair et al., 2013)
OCT4	222	Facilitates PORE-motif gene expression maintaining pluripotency	(Dan et al., 2021)

In stem cells, the stabilization of octamer-binding transcription factor 4 (OCT4) and the preservation of their pluripotency capacity is triggered by LSD1 demethylation of K222 (Dan et al., 2021). This can be accomplished by limiting OCT4 homodimer binding in a 'locked-in' status and thus enabling the transcription of a set of PORE-motif-containing genes. Further actions in stem cells endorsed by LSD1 demethylation of these non-histones targets have been identified, however for purposes of this chapter they are not covered in the section.

5.4 LSD1 structural components

LSD1 has the synonyms, flavin-containing amine oxidase domain-containing protein 2 (AOF2) and lysine-specific demethylase 1A (KDM1A). Lysine-specific demethylase 2 (LSD2) is a homolog of LSD1 belonging to the same FAD-dependant demethylase family and having around 30% of sequence resemblance (Yang et al., 2010). As characterized by crystallography studies, LSD1 comprises 3 main domains and a total length of 852 aa (Fig. 53).

The FAD-binding subdomain (aa 271-416), which has a high affinity to the cofactor flavin adenine dinucleotide (FAD), and the substrate-binding subdomain (aa 522-852), which is responsible for the efficient association and detection of LSD1 substrates, are both located within the amine oxidase-like (AOL) domains, which are distinguished for their catalytic properties (Chen et al., 2006; Yang et al., 2007b). The Tower domain placed in the middle of the AOL, is elongated into 2 alpha helical structures that supplies a binding region for key protein interactions, including CoREST (M. G. Lee et al., 2005; Stavropoulos et al., 2006). The third domain, SWIRM, is situated in the N-terminal and it is known for providing structural stability and for its dynamic interactions with several proteins (Aravind & Iyer, 2002).

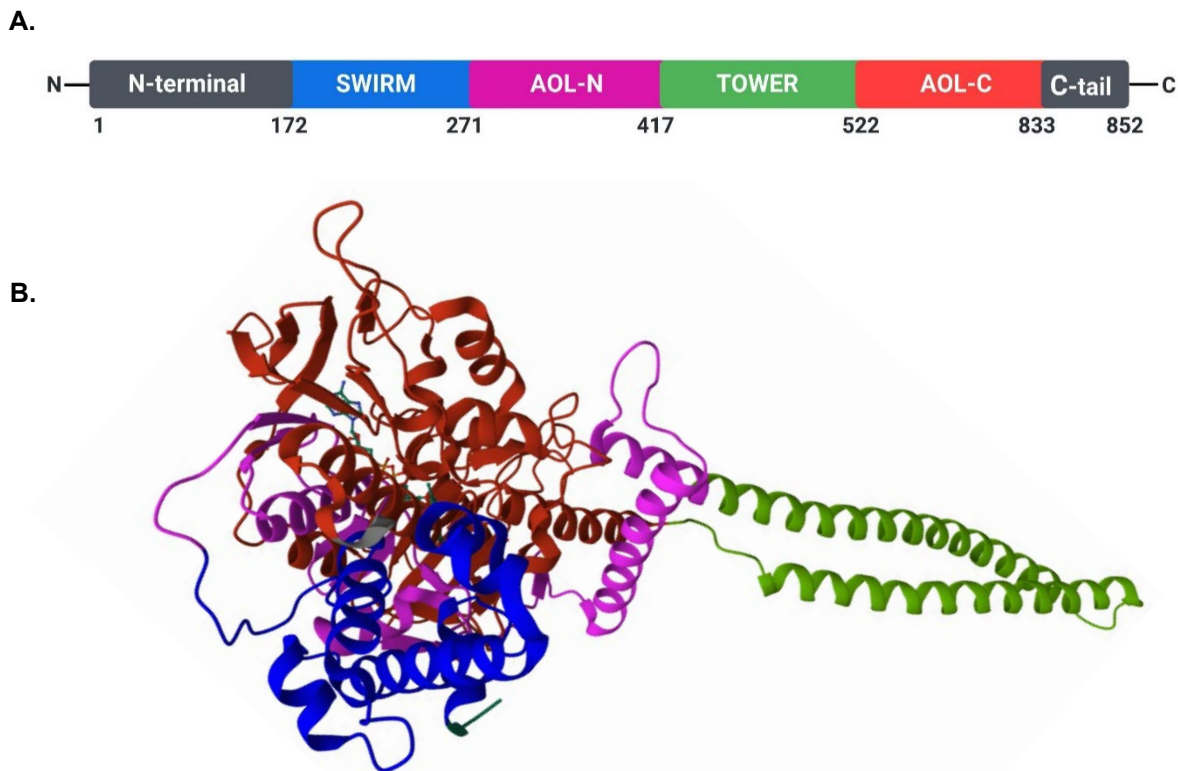


Fig. 53. LSD1 structure. (A) LSD1 3 structural domains: the catalytic amine oxidase-like (AOL) domains are depicted in red and pink, the N-terminal SWIRM domain in blue and the central TOWER domain in green. (B) LSD1 crystal structure was obtained from the RCSB Protein Data Bank (PDB code 5L3D, <https://www.rcsb.org/>, accessed on 03/10/ 2023). It maintains the same colour scheme for the domains as presented in (A).

5.5 LSD1 demethylation reaction

Histone N-terminal extensions in H3K4, H3K9 or H4K20 are exposed to mono- and dimethyl groups subtraction by means of the enzymatic activity of LSD1. The demethylation process starts by the oxidation of the amino residue of the mono or dimethylated lysine by FAD, producing an imine intermediate that in turn, is hydrolysed to yield the histone tail free of methyl groups and formaldehyde (Fig. 54) (Forneris et al., 2008; Forneris et al., 2005). Molecular oxygen is employed as an electron acceptor throughout the re-oxidation of the reduced FADH₂, regaining the native FAD molecule and causing hydrogen peroxide (H₂O₂) release.

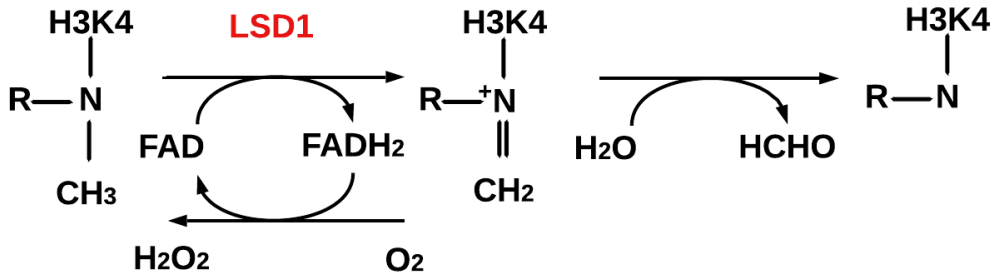


Fig. 54. LSD1 demethylation reaction. By transferring 2 hydrogen atoms from the methylated H3K4 to FAD, LSD1 catalyses an oxidation reaction that originates an imine intermediate. Formaldehyde and an amine are produced after the hydrolyzation of the intermediate molecule, while hydrogen peroxide is produced after FADH₂ is re-oxidised.

5.6 LSD1 demethylase-independent activity

LSD1 is categorized as a transcriptional switch via its demethylation capacity of histones and non-histone targets. However, beyond its demethylation functionality it has been identified that LSD1 also exhibits demethylase-free activity (F. Gu et al., 2020). A few studies have reported the interaction of LSD1 with other proteins through a non-canonical route leading to varied biological impacts. Among them, the couple of proteins that have been determined so far for PCa will be covered in the following relevant section.

One of them is the tumour suppressor called F-box and WD repeat domain-containing 7 (FBXW7), which works through the induction of ubiquitylation and oncoprotein destruction after substrate detection (R. Davis et al., 2014; Welcker & Clurman, 2008). FBXW7 is recognized by LSD1 through the same C-terminal binding sites as its oncogenic substrates, prompting FBXW7 destabilization by self-ubiquitylation following proteasomal and/or lysosomal degradation and cancer cell outgrowth (Lan et al., 2019).

Another non-canonical binding partner of LSD1 is the estrogen-related receptor α (ERR α), which is a nuclear receptor that functions as a gene expression modulator (Horard & Vanacker, 2003). In 2017, it was identified that cell invasion was influenced

by LSD1-mediated transcriptional repression of various genes, though the demethylation of H3K9 after interaction with ERR α (Carnesecchi et al., 2017a). The same research group uncovered that LSD1 supported the protein steadiness and further defence against proteasomal breakdown by interacting with ERR α in a demethylase free manner (Carnesecchi et al 2017b). Both non-canonical and canonical interactions of LSD1 with ERR α create a reinforcing cycle whose underlying mechanisms and interferences still need to be addressed (F. Gu et al., 2020).

A promoter, autophagy receptor p62 (p62), is also destabilized via LSD1 demethylation-independent interaction, inducing suppression of autophagy in ovarian and endometrial cancers (Chao et al., 2017). Despite it was recognized that LSD1 association with p62 also encouraged its ubiquitylation and protein digestion, the molecular mechanism implicated behind it is not clear.

5.7 Role of LSD1 in prostate cancer

Elevated expression of LSD1 has not only been documented in numerous types of solid and hematologic cancers, including primary PCa, but also it has been linked to its development and progression through adjustments of chromatin architecture (Kahl et al., 2006; Majello et al., 2019). PCa must have AR signalling in order to survive and progress, and if androgens are suppressed by ADT, patients often recover for a brief interval of time ultimately developing lethal CRPC (Nuhn et al., 2019). In PCa, the central function of LSD1 is to coactivate AR key genes (e.g. including kallikrein 2 or PSA) via H3K9me_{1/2} demethylation (Cai et al., 2014; Metzger et al., 2005; Wissmann et al., 2007). It was postulated that the exchange from H3K4me_{1/2} to H3K9me_{1/2} substrate was generated through androgen-promoted phosphorylation of H3T6 and H3T11 (Metzger et al., 2010; Metzger et al., 2008). However, genome-wide studies verified that LSD1 can still preserve its H3K4me_{1/2} demethylase activity at AR enhancers (Cai et al., 2014). According to their data, LSD1 works as a corepressor of AR target genes, as well as a coactivator in prostate cancer cells; and they postulated that the co-stimulation could potentially be encouraged not only by H3K9me_{1/2} demethylation, but also by other non-histone partners (Cai et al., 2011; Cai et al., 2014).

In 2014, Cai and collaborators also revealed a crucial interaction of LSD1 with the transcription factor, FOX1A. This transcription factor is known for enabling chromatin access to AR and other steroid-responsive receptors (Gao et al., 2003; Jozwik & Carroll, 2012; Yang & Yu, 2015). And in a recent study, it was discovered that in order to achieve effective association to the chromatin, the removal of methyl groups from K270 residue of FOXA1 by LSD1 is vital (Gao et al., 2020). FOX1A global binding capacity was confirmed to be severely disturbed after the suppression of LSD1, specifically because FOX1A maintained its methylated status, which in turn reduced access to enhancers and altered AR association and signalling.

Furthermore, it has been proven that LSD1 can form a complex with the JMJD2C demethylase of tri-methyl lysines, and together control the transcriptional expression of AR-driven genes (Wissmann et al., 2007). The LSD1-mediated demethylation of p53 has been proven to alter the cell cycle and decrease the cell viability in CRPC (J. Huang et al., 2007; Metzger et al., 2005). Also, it was exposed that LSD1 controls the expression of vascular endothelial growth factor A (VEGF-A), which is a proangiogenic factor that is necessary for tumour development, in AR-dependent and AR-independent PCa, as well as of other related genes such as, PSA and TMPRSS2 (Kashyap et al., 2013). By controlling the transcription of focal adhesion protein paxillin (PXN) and the lysophosphatidic acid receptor 6 (LPAR6), it has been demonstrated that LSD1 is also involved in the induction of PCa cells' ability to metastasize in the absence of AR (Ketscher et al., 2014). The cell-cycle gene centrosome-associated protein E (CENPE) has been found in CRPC cells, upon LSD1 and AR association with its promoter, enhanced expression of CENPE was activated leading to malignancy evolution (Y. Liang et al., 2017). LSD1 has also been hypothesized to promote the PI3K/AKT signalling pathway, by activating the transcription of the PI3-kinase controlling component, p85 α in both AR-related PCa and CRPC (Wang et al., 2019).

An interesting study revealed that LSD1 in conjunction with zinc finger protein 217 (ZNF217), is capable of triggering a fatal gene network supporting CRPC cell survival, while exhibiting a demethylase-free activity and no apparent interaction with AR (Sehrawat et al., 2018) In the same study, they also validated that LSD1 is overexpressed not only in initial stages of the disease but in metastatic PCa. Sehrawat

and collaborators also tested an allosteric inactivator of LSD1, called SP-2509, which successfully inhibited LSD1 demethylation-independent activity, decreasing the cell survival rate of CRPC cells.

Another recent investigation about LSD1 demethylation-independent functions in PCa, followed the previous report of LSD1-mediated stability impairment of the tumour suppressor, FBXW7 (Lan et al., 2019). The research established that LSD1 increased PCa cell endurance by preventing FBXW7 from being expressed at a protein level (Qin et al., 2021). Additionally, they discovered that the interaction between LSD1 and FBXW7 was inhibited by SP-2509 inhibitor, following the suppression of cancer cell survival.

In a RNA-seq study using LSD1 inhibitors that was published this year, they identified that LSD1 can target a variety of tumour-promoting pathways including transcriptional networks of MYC, FOXA1, and E2F, via super enhancers activation (M. Li et al., 2023). The study concluded that patients that suffer from CRPC could potentially benefit from dual therapy, by providing reduced doses of LSD1 and bromodomain-containing protein 4 (BRD4) inhibitors, to avoid adverse side effects and target the oncogenic super enhancers that force CRPC viability and development.

5.8 Diversity of LSD1 inhibitors

As covered in prior sections, LSD1 is implicated in many oncogenic signalling pathways and its overexpression has been connected to its direct involvement in the promotion and spread of multiple cancers. In fact, numerous inhibitors of LSD1 demethylase activity have been identified and some of them are already being tested in clinical trials for cancer treatment or other malignancies (Dong et al., 2022; Fang et al., 2019; Hosseini & Minucci, 2017).

The traditional LSD1 inhibitors are monoamine oxidases (MAO) inactivators due to their structural homology between the catalytic domains of LSD1 and MAO; comprising tranylcypromine, phenelzine, and pargyline (Y. Zheng et al., 2016). Among them, tranylcypromine (TCP), or trans-2-phenylcyclopropylamine, also referred to as

2-PCP, is the most characterized. In the 1960's, TCP was used in the clinic as an antidepressant drug to treat anxiety and depression (Shih et al., 1999). The irreversible inactivation of LSD1 by TCP is achieved by the creation of a covalent adduct within the flavin ring, specifically between TCP and LSD1's FAD cofactor, succeeding the aperture of the cyclopropyl loop and one-electron oxidation (Binda et al., 2010; Yang et al., 2007a). TCP displays an inhibitory constant (K_i) of $243\mu\text{M}$ and limited selectivity towards LSD1 (Schmidt & McCafferty, 2007). TCP has been analysed for synergistic therapy, with other active molecules such as all-trans retinoic acid (ATRA) or Azacitidine, which are currently at different clinical phases for treatment of diverse oncogenic conditions (ClinicalTrials.gov, Identifier: NCT02717884, NCT02273102, NCT02261779).

Several TCP derivatives have been designed based on its scaffold for potency enhancement. TCP analogs inactivate LSD1 by employing a single electron reduction process that induces varied TCP-FAD bonds through homolytic cleavage routes of the cyclopropyl ring (Mohammad et al., 2015; Yang et al., 2007a). In contrast, TCP generates the TCP-FAD adduct by weak van der Waals bonds in association with two aa, T335 and T810. For instance, the phenyl ring of TCP has been tailored by attaching hydrophilic and hydrophobic groups to produce a variety of irreversible LSD1 inhibitors (Binda et al., 2010). The same research team produced TCP variants in 2020, by adjoining benzamide residues to the phenyl ring's para-position (Fioravanti et al., 2020). Their results revealed that their compound 3 had an IC_{50} of 90 nM and effective anticancer activity.

The majority of LSD1 inhibitors now undergoing clinical development are TCP N-alkylated analogs, which are distinguished by the presence of a peptide scaffold on the TCP's amino group (Dong et al., 2022). In clinical assessments (ClinicalTrials.gov Identifier: NCT02913443; EudraCT 2013-002447-29, 2018-000469-35, 2018-000482-36), the LSD1 inhibitor ORY-1001 is a N-alkylated TCP derivative with an IC_{50} of 18 nM against LSD1 that was designed by Oryzon Genomics (Maes et al., 2018). Because the health risks did not outweigh the efficacy of another TCP N-alkylated derivative, known as GSK2879552, the clinical trials were stopped after testing on patients suffering from acute myeloid leukemia or small cell lung carcinoma (Bauer et al., 2019; Roboz et al., 2022). Currently undertaking four clinical investigations for the

treatment of various cancers (ClinicalTrials.gov Identifier: INCB059872, NCT02712905, NCT03514407, NCT02959437), INCB059872 another N-alkylated TCP-based LSD1 blocker, demonstrated notable efficacy in preclinical analysis by diminishing the proliferation of small cell lung cancer cells and hindering the survival and self-renewal of prostate cancer stem cells (Civenni et al., 2018; Lee et al., 2016). Dual inhibitors have been developed using N-alkylated TCP variants and histone deacetylases (HDAC) suppressors, that demonstrated favourable LSD1 inhibition and cell growth reduction (Duan et al., 2017).

Reversible inactivators are considered safer and more effective than irreversible blockers, due to the creation of a non-covalent adduct to inhibit LSD1 (Stazi et al., 2016). The first of them, designated as CC-90011, demonstrated high inhibition of LSD1 demethylation with an IC₅₀ of 0.30 nM (Kanouni et al., 2020). Either alone or in synergy with other compounds, CC-90011 is under three clinical studies for different conditions and cancer (ClinicalTrials.gov, Identifier: NCT02875223, NCT03850067, NCT04350463). SP2577, another reversible LSD1 inhibitor, is also in clinical testing against relapsed Erwin Sarcoma (NCT03600649) and late-stage solid tumours (NCT03895684) (Reed et al., 2021).

Peptides that are structurally similar to histones have been discovered to suppress LSD1 demethylation activity. As part of co-repressor complexes such as CoREST, HDAC1/2, and CtBP, snail family transcriptional repressor 1 (SNAIL1) is a transcription factor that has been confirmed to associate with LSD1 via its SNAG domain (Y. Lin et al., 2010; Shi, 2007). Lin and collaborators exposed that specifically the SNAG domain presents high level of similarity to the N-terminal of histone 3, and that it can work as a pseudo-substrate for LSD1. Several SNAIL1-derived or histone-based peptides have been synthesized and analysed for LSD1 inactivation (Itoh et al., 2016; Kakizawa et al., 2015; Kumarasinghe & Woster, 2014; Kumarasinghe & Woster, 2018; Tortorici et al., 2013).

Other antagonists have been discovered that consist of naturally occurring compounds that have been found to block LSD1 functionality. Natural LSD1 inhibitors including flavonoids, isoquinoline alkaloids, capsaicin, isoquercitrin, derivatives from *Salvia miltiorrhiza* and stilbene byproducts, display diverse mechanisms of anticancer

properties (Dong et al., 2022). In addition, various metal-derived LSD1 inhibitors have been proposed, such as rhodium (III) complex 1, which was the first LSD1 inhibitor of this type to be identified in PCa (Yang et al., 2017). Due to their ability to prevent LSD1 from attaching to the lysine groups in histones, rhodium (III) complex 1 has a stronger selectivity towards LSD1 than other synthetic and natural inactivators.

5.9 PDC using G3 and TCP-based LSD1 inhibitors

Peptide drug conjugates unveil specialized molecular machinery in which each component has a sole purpose, that together elevates the broad therapeutic outcome. Therefore, the selection and thorough evaluation of the delivery unit and the active molecule, is rather essential. In previous studies, G3 has revealed high degree of cancer cell selectivity and tumour infiltration, as well as modification of gene transcription in cancer cells by targeting and delivering siRNAs (Chen et al., 2014a; Chen et al., 2014b; Cirillo et al., 2021; Hu et al., 2011). Its small size allows simplicity for conjugation and represents lower risk of inducing immune responses in the body. Based on this, G3 peptide embodies the necessary qualities to be a strong candidate for the production of PDCs.

Under the guidance of Dr. Simon Turega from Sheffield Hallam University, Dr. Philip Lane created a series of PDC utilising click chemistry to conjugate their modified LSD1 inhibitors to G3. Previous reports in the literature have proven that by modifying the phenyl ring of TCP derivatives, the selectivity and efficacy towards LSD1 may be enhanced (Binda et al., 2010; Fioravanti et al., 2020; Yang et al., 2007a). They designed new LSD1 inhibitors by inserting azide tags into the TCP scaffold's para or meta motifs, followed by the attachment of the G3 peptide in the C-terminal, via Cu(I) catalyzed click reaction. Five of the PDC designated as PDC-1 to 5 were supplied as part of a collaboration with Turega's research group, to test whether G3 could improve their effectivity and cell permeabilization through smart delivery into PCa cells.

Despite other PDC have been developed for the treatment of PCa, it is a multifactorial disease that could benefit from different targeting strategies. Also, the field of LSD1 inhibitors in cancer and other malignancies is emerging as a novel class of epigenetic

regulators, which modulate gene expression through modification of methylation patterns of histone tails and from a huge range of proteins, and multi-protein assemblies. Based on the aberrant elevated expression of LSD1 in earlier and late stages of PCa, and due to its key functions in the disease, including the demethylation of either H3K4/H3K9 or other important substrates, and the non-canonical pathway that is not related to AR, LSD1 represents a promising biomolecular target. Hence, Chapter 5 is focused on investigating if the novel PDC with adjusted LSD1 inhibitors and G3 as targeting peptide, could display higher potency than the LSD1 commercial inactivator in PCa cells; and to expand upon G3 therapeutic potential, to analyse whether G3 is capable of transporting siRNAs into PCa.

5.10 Results

5.10.1 Cell viability assays using G3 conjugates

To determine whether the modified LSD1 inhibitors coupled to the G3 peptide, as a novel PDC, could have an impact on cell viability in prostate cancer cells a pilot analysis was executed using TCP inactivator. As mentioned previously, TCP is a standard LSD1 inhibitor that prevents LSD1 action by covalently associating with its FAD cofactor (Binda et al., 2010; Yang et al., 2007a) Increasing concentrations of TCP from 100 μ M to 1 mM were assessed in LNCaP and PC-3 cells, to generate a dose-response curve (Fig. 55A and 55B). The TCP optimal concentration was selected as 250 μ M for both cell lines, where at least 50% of the population was reduced. TCP at 250 μ M was used as a positive control in the following PDC cell viability assay. The degree of statistical significance was assessed through ANOVA analysis with multiple comparisons. The fraction of LNCaP and PC-3 viable cells was drastically declined as the TCP concentration was increased, demonstrating a dose-dependency cytotoxicity.

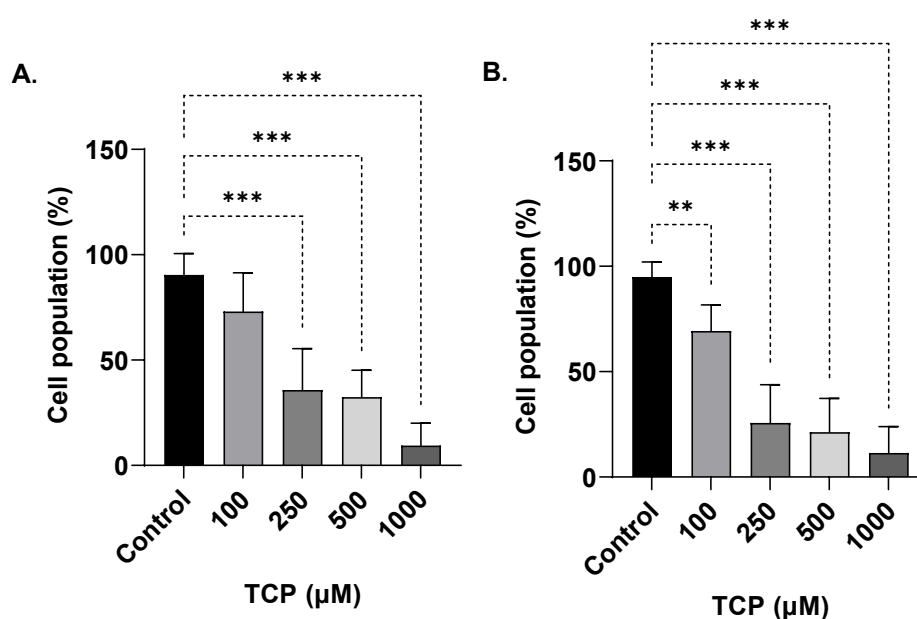


Fig. 55. Cell viability impairment after TCP treatment. Normalized cell population to the non-treated control in (A) LNCaP and (B) PC-3. Cells were treated with increasing concentrations of tranilcypromine (TCP) for 24 hrs. Data is presented as means of 3 different experiments with 3 replicates each, and \pm SD. One way ANOVA analysis was determined for normalised cell populations (** p <0.01; *** p <0.001).

In Chapter 2, the chemical structure and type of modification of the five G3 PDC are presented on page 80, in Figure 8 and Table 6, respectively. PC-3 and LNCaP cells were exposed to PDC-1, PDC-2, PDC-3, PDC-4, and PDC-5 from 0.25-5 μM concentrations, to evaluate the cell viability after 24 hrs treatment. Cells treated with unconjugated G3 were used as negative control and for data normalization. For LNCaP cells, PDC-2 and PDC-4 exhibited a significant decrease in cell populations at 1 and 5 μM (Figure 56). Similarly in PC-3 cells, PDC-2 exhibited reduced cell numbers at 2.5 and 5 μM , while PDC-4 presented substantial decline of cell numbers at 2.5 μM only (Figure 57). Statistical significance in both cell viability assays was determined from $p < 0.01$ (**) and $p < 0.001$ (***) using two-way ANOVA with multiple comparisons, applying Dunnett's correction.

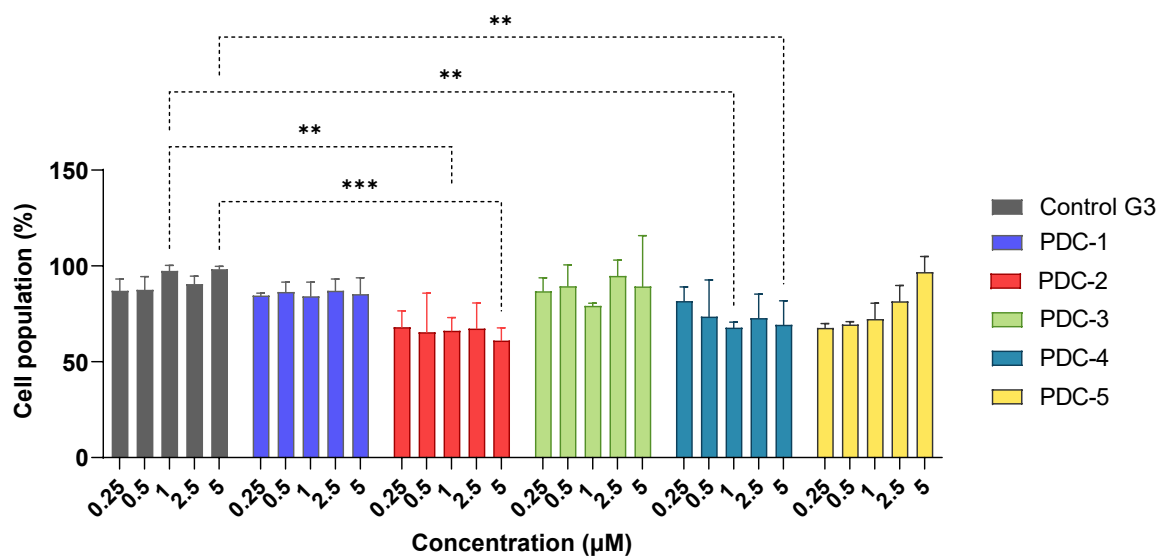


Fig. 56. LNCaP cell viability analysis using PDC. Data was normalized to the negative control that corresponded to cells exposed to naked G3 peptide. PDC2 to 5 were added to the cells from 0.25 up to 5 μM . Data is presented as means and $\pm\text{SD}$ of one biological experiment with 3 replicates. Two-way ANOVA analysis was calculated using multiple comparisons and Dunnett's correction (** $p < 0.01$; *** $p < 0.001$).

Overall, the cellular impairment induced via PDC-2 and PDC-4 in PCa cells, ranging from 2.5 to 5 μM dosage, indicate high potency of the linked LSD1 inhibitors, probe 5 and probe 7, respectively, and hint to a plausible scenario of LSD1 inactivation.

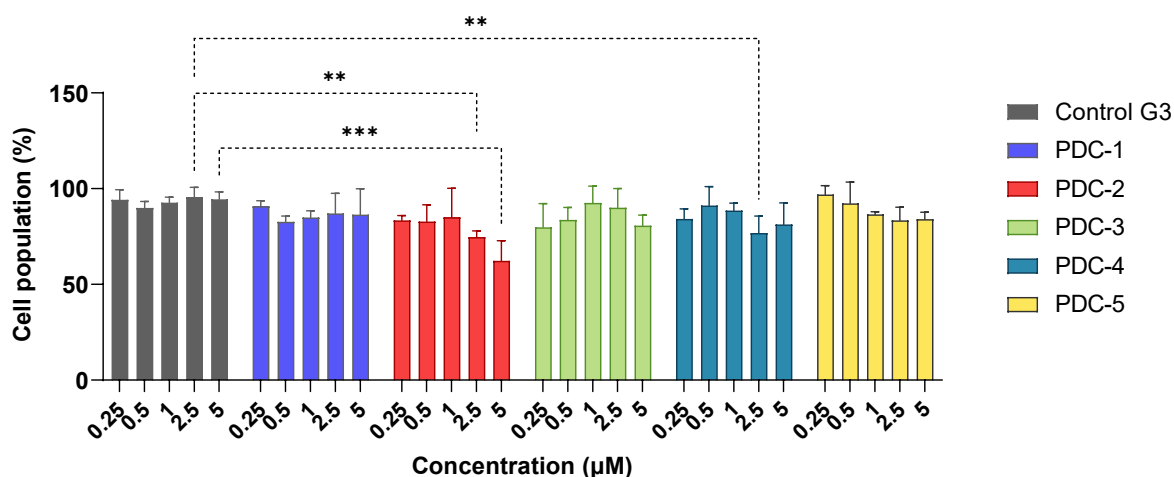


Fig. 57. PC-3 cell viability analysis using PDC. Data was normalized to the negative control that corresponded to cells exposed to naked G3 peptide. PDC-1 to 5 were added to the cells from 0.25 up to 5 µM for 24 hrs. Data is presented as means and ±SD of one biological experiment with 3 replicates. Two-way ANOVA analysis was calculated using multiple comparisons and Dunnett's correction (**p<0.01; ***p<0.001).

5.10.2 Hydrogen peroxide assay

A common and straightforward technique to investigate LSD1 functioning is through an indirect method that measures hydrogen peroxide (H₂O₂). The rationale behind this assay is that LSD1 enzymatic activity could be evaluated by detecting the H₂O₂ side-product of the demethylation reaction. When H₂O₂ is available, it associates with the Amplex Red reagent (10-acetyl-3,7-dihydroxyphenoxazine) in a 1:1 ratio, and the HRP catalyses an oxidation reaction to produce a red fluorescent molecule, called resorufin. Due to its excitation wavelength of 571 nm and emission wavelength of 585 nm, resorufin can be fluorescently detected and quantified.

In a few studies, hydrogen peroxide activity has been measured and correlated to LSD1 activity using the Amplex Red assay in various cell types (Mohanty et al., 1997; Song et al., 2001; Votyakova & Reynolds, 2008; Wagner et al., 2005). Based on these studies, the manufacturer protocol of the Amplex Red Assay was adjusted on an attempt to evaluate H₂O₂ from either LNCaP or PC-3 cells after PDC treatment.

H₂O₂ and TCP were employed as positive controls, while non-treated cells and cells supplied with unconjugated G3 were used as negative controls of the assays. Cells

were exposed to PDC-2 at doses ranging from 100 nM to 2.5 μ M, and H₂O₂ levels were measured at 60, 120 and 180 minutes. The data in both cell lines indicated that it was not possible to evaluate LSD1 activity in PCa cells. There were no significant differences between the levels of H₂O₂ of the non-treated cells or cells with naked G3, and TCP or PDC-2 at any of the given concentrations in both PCa cell lines (Figure 58 and Figure 59).

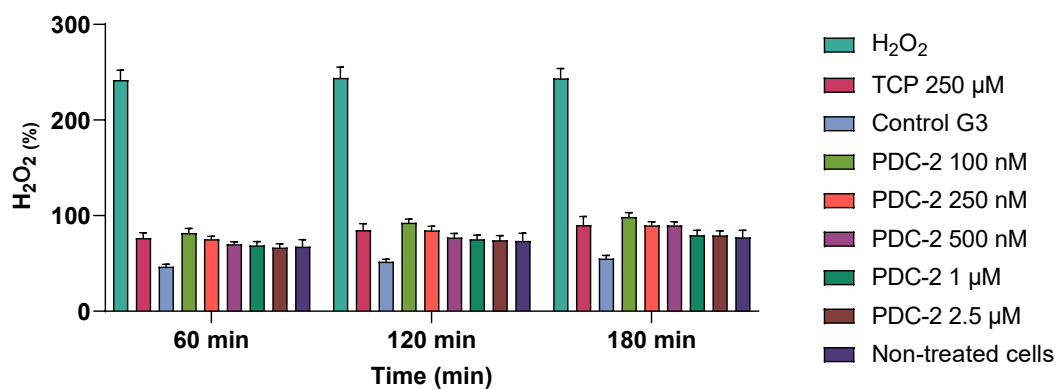


Fig. 58. HRP-coupled assay in LNCaP. Hydrogen peroxide levels were assessed after 60, 120 and 180 min treatment with increasing concentrations of PDC-2 or TCP. Unconjugated G3 and non-treated cells were employed as negative controls. Data was normalized and displayed as means and \pm SD of one experiment with 3 replicates.

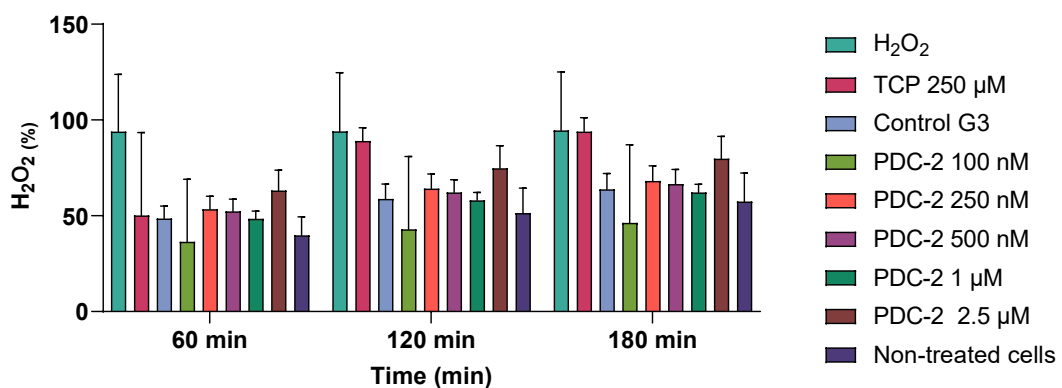


Fig. 59. HRP-coupled assay in PC-3. Hydrogen peroxide levels were assessed after 60, 120 and 180 min treatment with increasing concentrations of PDC-5 or TCP. As negative controls, cells were exposed to naked G3 or cells without treatment were used. Data was normalized and graphed as means and \pm SD of one experiment with 3 replicates.

These results strongly implicate that the Amplex Red assay is ineffective in identifying increases in hydrogen peroxide as a byproduct of LSD1 demethylation activity, in PCa cells. Additionally, the multiple sources of hydrogen peroxide in living cells cannot be distinguished using this method, representing another layer of limitation to the assay.

5.10.3 Histone demethylation analysis by HCS

The demethylation of mono and dimethyl groups from H3K4 and H3K9 is promoted by LSD1 for the epigenetic regulation of gene expression (Cai et al., 2014; Forneris et al., 2006; Metzger et al., 2005; Yujiang Shi et al., 2004; Wissmann et al., 2007). Inactivators of LSD1 demethylation activity operate by preventing both its catalytic activity and its attachment to chromatin. Thus, substantial increases in H3K4 or H3K9 methylation levels are reliable indicators of LSD1 inhibition.

To determine the histone demethylation signature changes by TCP, immunofluorescence of H3K4me and H3K4me2 were assessed in LNCaP and PC-3 cells. In Figure 60A and Figure 61A for LNCaP, and Figure 62A and Figure 63A for PC-3, the representative high content images of the H3K4me and H3K4me2 antibody labelling of the non-treated controls and the highest concentration of TCP are illustrated, respectively. There is a distinct immunofluorescence difference between the treated and TCP samples, at 250 μ M, being evident in the high content images corresponding to H3K4me2 than H3K4me, in both cell lines.

Quantitative data of the immunofluorescence experiment of both histone marks revealed similar results for LNCaP and PC-3 cells. In LNCaP cells, TCP treatments from 50 to 150 μ M, pointed to a minor rise in integrated intensity data in comparison to the control. However, after 250 μ M TCP exposure there was a dramatic increase of both histone marks integrated intensity percentages. Even though the H3K4me integrated intensity levels significantly increased at 250 μ M in LNCaP cells ($p = 0.0185$), the H3K4me2 integrated intensity values were more significantly enhanced at 250 μ M, displaying a p value of 0.005, after ANOVA test with Dunnett's multiple comparisons (Figure 60B and Figure 61B).

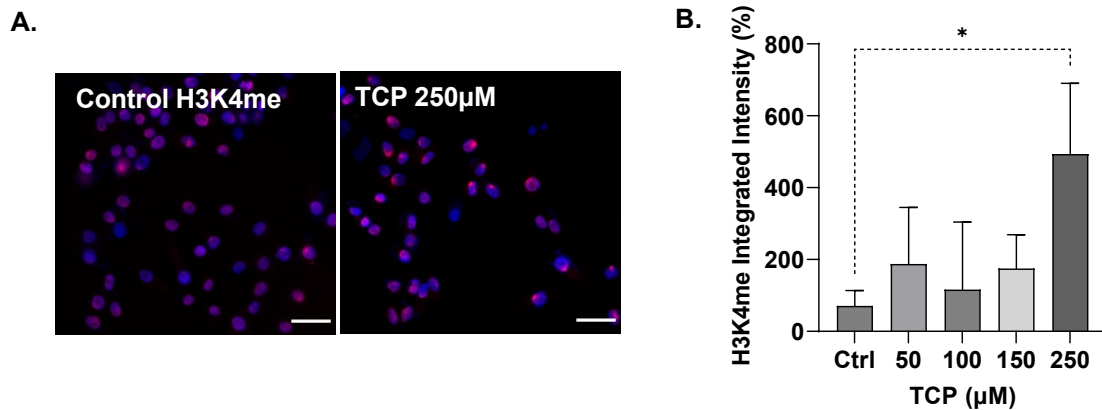


Fig. 60. H3K4me antibody labelling after TCP treatment in LNCaP. (A) High content images of H3K4me red immunofluorescence of the non-treated control cells vs treated cells with TCP at 250 µM. Hoechst was used to stain the nuclei. Scale bar 50 µm and 20X magnification. (B) H3K4me integrated intensity quantification normalized to the control. Cells were treated with different concentrations of TCP inhibitor for 24 hrs. Values are expressed as means and ± SD of one experiment with 3 replicates. The statistical significance was calculated using one way ANOVA with multiple comparisons (* $p < 0.05$).

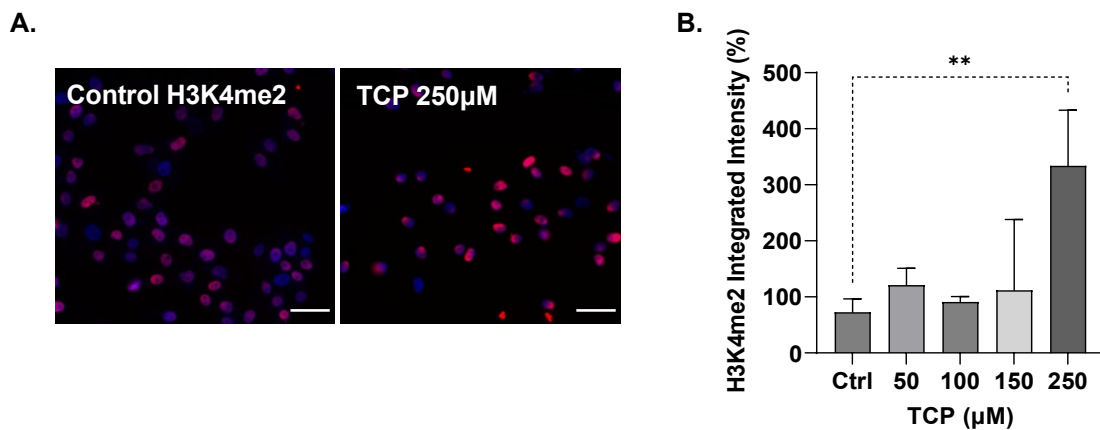


Fig. 61. H3K4me2 antibody labelling after TCP treatment in LNCaP. (A) High content images of H3K4me2 red immunofluorescence of the non-treated control cells vs treated cells with TCP at 250 µM. Hoechst was used to stain the nuclei. Scale bar 50 µm and 20X magnification. (B) H3K4me2 integrated intensity quantification normalized to the control. Cells were treated with different concentrations of TCP inhibitor for 24 hrs. Values are expressed as means and ± SD of one experiment with 3 replicates. The statistical significance was calculated using one way ANOVA with multiple comparisons (** $p < 0.01$).

For PC-3 cells, the H3K4me integrated intensity data exhibited a trend proportional to the higher doses of TCP, however there was no significant difference between the treated cells and the control, when examined using ANOVA analysis (Fig. 62B). Also, the considerable length of the SD error bars exposed a high degree of variability of the H3K4me integrated intensity data. In contrast, the H3K4me2 integrated intensity data in PC-3 cells presented a clear and significant enrichment in cells exposed to TCP at 250 μ M, after estimating statistical significance using ANOVA analysis with multiple comparisons and Dunnett's correction method (Fig. 63B).

Taken together, these findings demonstrate that TCP at 250 μ M inhibits LSD1 demethylation activity, as determined by a buildup of dimethyl residues in H3K4 in PCa cells.

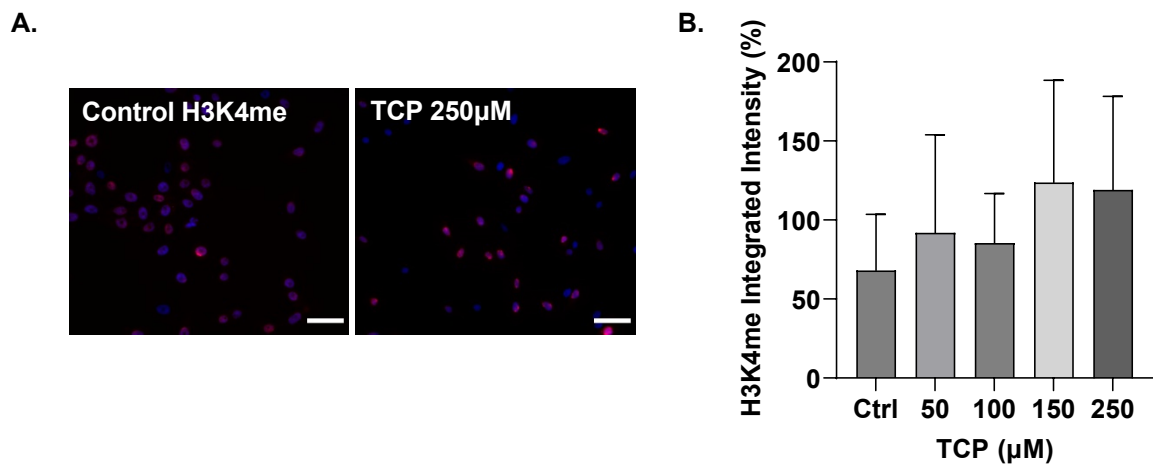


Fig. 62. H3K4me antibody labelling after TCP treatment in PC-3. (A) High content images of H3K4me red immunofluorescence of the non-treated control cells vs treated cells with TCP at 250 μ M. Hoechst was used as nuclear staining. Scale bar 50 μ m and 20X magnification. (B) Quantification of H3K4me integrated intensity normalized to the control. For 24 hours, cells were exposed to various TCP inhibitor doses. Values are expressed as means and \pm SD of one experiment with 3 replicates. No substantial differences were identified after ANOVA analysis with multiple comparisons.

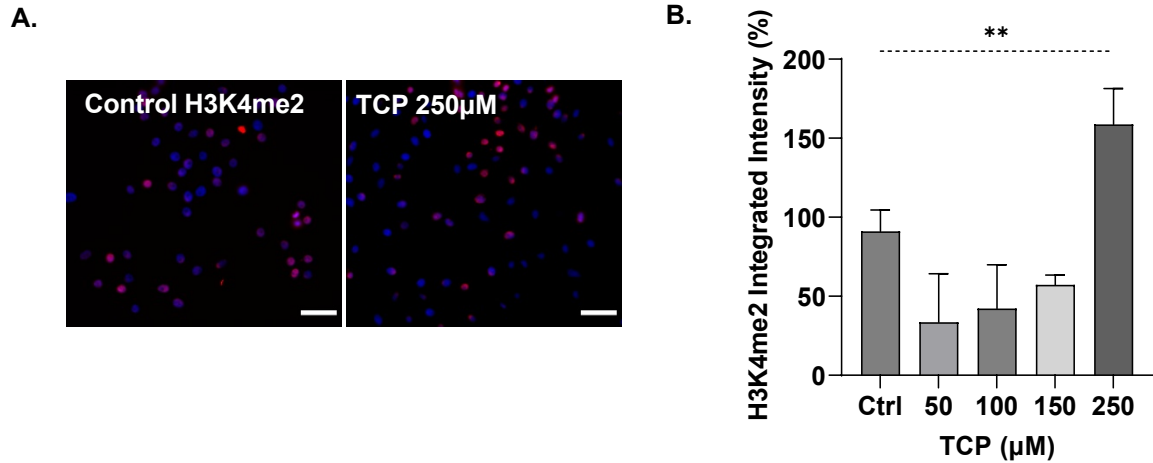


Fig. 63. H3K4me2 antibody labelling after TCP treatment in PC-3. (A) High content images of H3K4me2 red immunofluorescence of the non-treated control cells vs treated cells with TCP at 250 µM. The nuclei was labelled with Hoechst. Scale bar 50 µm and 20X magnification. (B) Normalized H3K4me2 integrated intensity percentages. For 24 hours, PC-3 cells were exposed to various TCP inhibitor concentrations. Data is displayed as means and \pm SD of one experiment with 3 replicates. The statistical significance was calculated using one way ANOVA with multiple comparisons (** $p < 0.01$).

Based on the previous results, the histone mark H3K4me2 was selected to investigate the efficacy of the LSD1 inhibitors that formed part of PDC in PCa cells; and TCP at a dose of 250 µM was used as a positive control of the assay. Due to the impact on cell viability produced by PDC-2 and PDC-4 in both cell lines, further LSD1 inhibition assessments were done just with these 2 PDC. Baseline cells and cells supplemented with unlinked G3 at 5 µM were employed as negative controls.

The potency of PDC-2 and PDC-4 was examined by immunofluorescence of H3K4me2 mark in LNCaP cells and PC-3 cells after one day exposure. H3K4me2 antibody labelling of LNCaP cells treated with both, PDC-2 and PDC-4 at 5 µM and the controls are presented in Figure 64A. The quantification of H3K4me2 integrated intensity was normalized to the control with G3 alone and presented as percentages. Although PDC-2 and PDC-4 exhibited higher H3K4me2 intensity values than the controls, only PDC-2 revealed statistical significance when analysed by ANOVA test with multiple comparisons (Figure 64B).

Cell number of 3 different experiments was calculated and normalized to the control. And in accordance with previous cell viability analysis in LNCaP cells, a meaningful decrease of the cell population was obtained using ANOVA analysis for PDC-2 (Fig. 64C). However, PDC-4 did not exhibit considerable reduction in the cell number in comparison to the control.

The antibody labelling of H3K4me2 after PDC-2 and PDC-4 treatment in PC-3 cells is depicted in Figure 65A. Normalized integrated intensity values in PC-3 cells were calculated and analysed by one-way ANOVA with multiple comparisons (Fig. 65B). The IIC data in PC-3 cells revealed that H3K4me2 levels were significantly higher after both, PDC-2 (** $p < 0.01$) and PDC-4 (** $p < 0.001$) treatment, as well as obtained for TCP (** $p < 0.001$).

In addition, the total cell count was calculated for PC-3 cells after 24 hrs PDC treatment. The data reflected 3 different experiments, each with 3 replicates. PDC-2 and PDC-4 provoked cellular impairment in PC-3 cells at 5 μM , as revealed when compared with the control and analysed by ANOVA test (Fig. 65C). The cell viability was more affected in cells that received TCP treatment than PDC, displaying a higher statistical difference.

The results of the immunofluorescence of the histone signature in PCa cell lines, provided initial evidence of the effectivity of using PDC (5 μM) in contrast to standard TCP inhibitor (250 μM), considering that there was a 50 times difference between the doses. PDC-2 and PDC-4 demonstrated a discernible increasing effect on the H3K4me2 mark, even at far lesser concentrations, that in synergy with their considerable impact in cell survival, imply the suppression of LSD1-mediated demethylation.

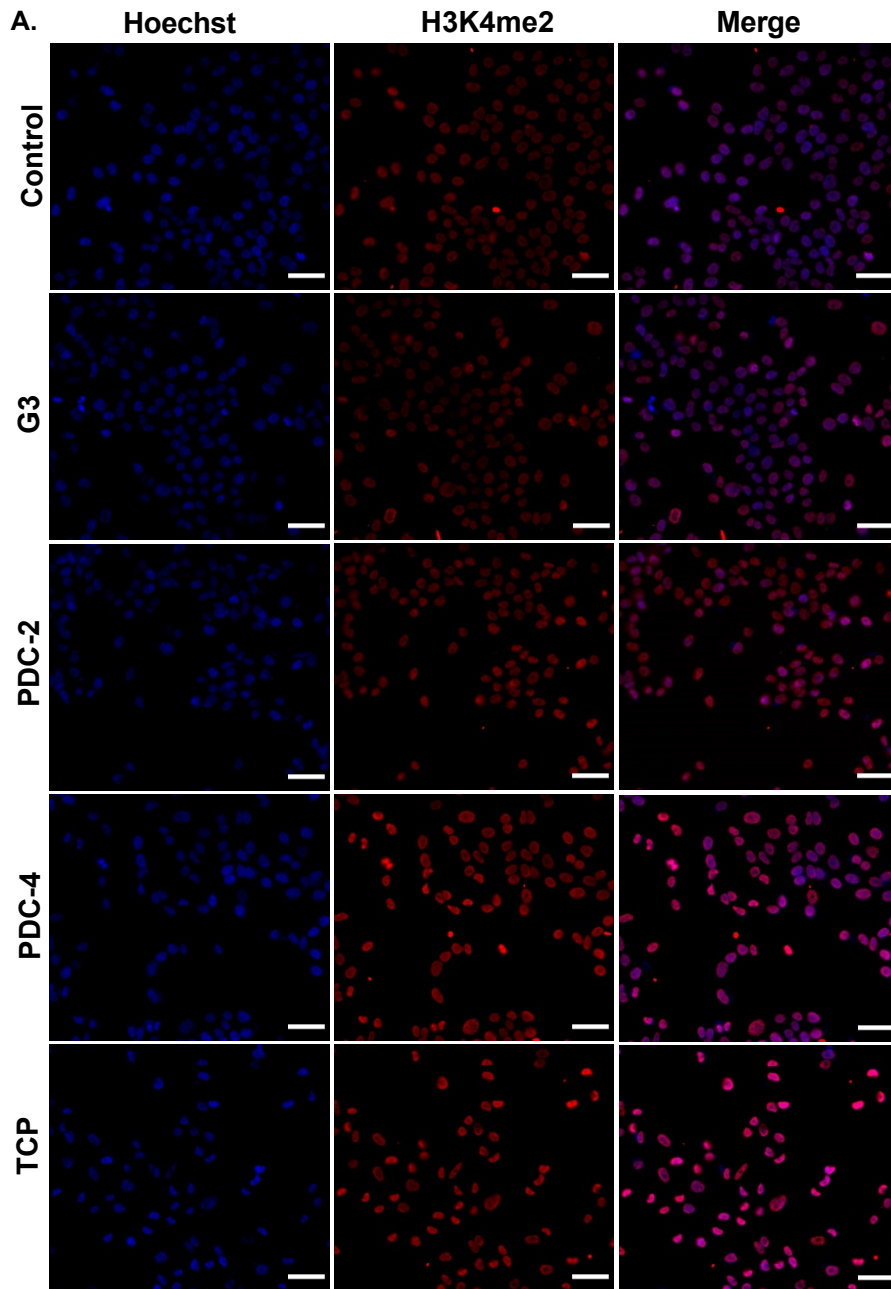
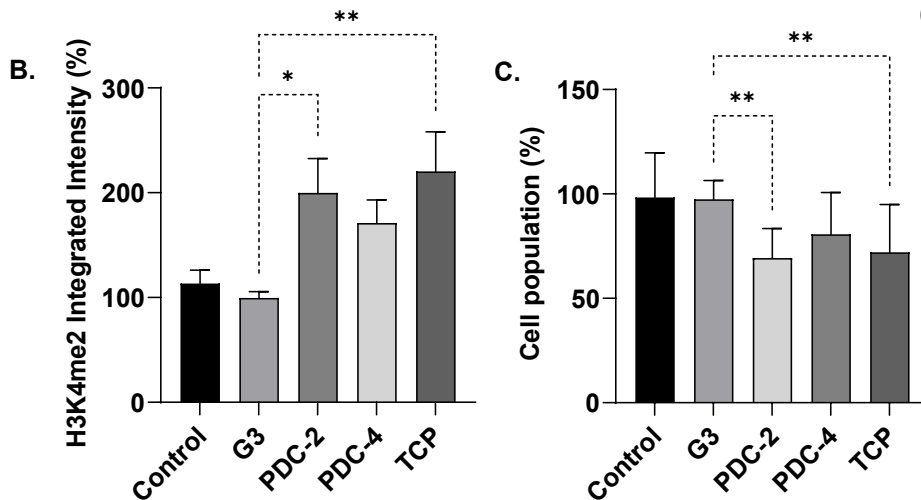


Fig. 64. H3K4me2 labelling after PDC treatment in LNCaP. (A) Representative images of LNCaP cells after 24 hours exposure with naked G3 peptide (5 μ M), or PDC-2/PDC-4 (5 μ M), or TCP (250 μ M). Cells without any treatment were used as negative control as well. The nuclei was stained with Hoechst. Scale bar 50 μ m and 20X magnification. (B) Normalized H3K4me2 integrated intensity values. Means and \pm SD of 3 biological experiments with 3 replicates each are presented. The differences between treated groups was calculated using one-way ANOVA with multiple comparisons (* p <0.05, ** p <0.01). (C) Normalized cell populations of 3 different experiments with 3 replicates each. One way ANOVA with multiple comparisons was calculated to determine statistical differences between control and PDC (** p <0.01).



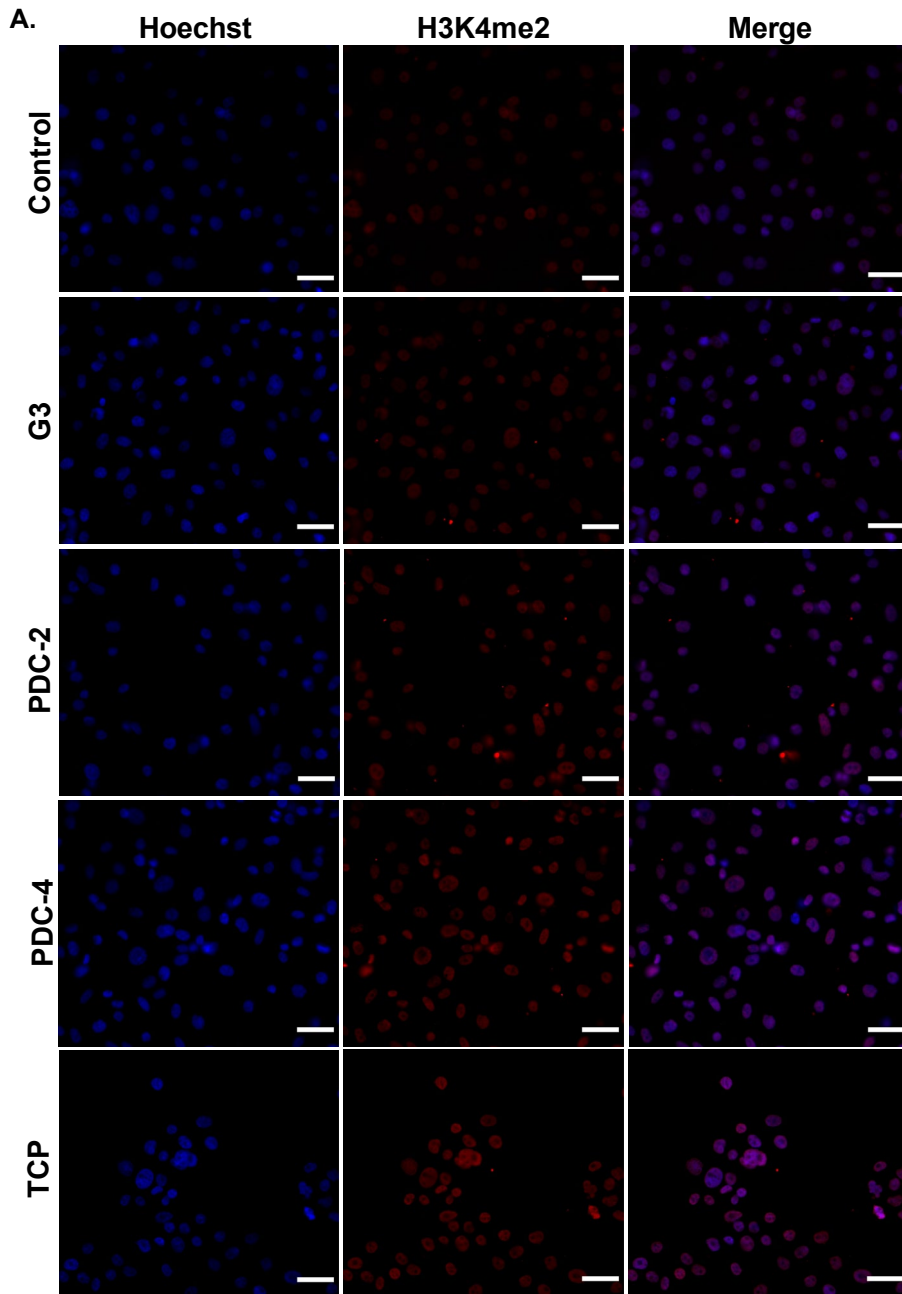
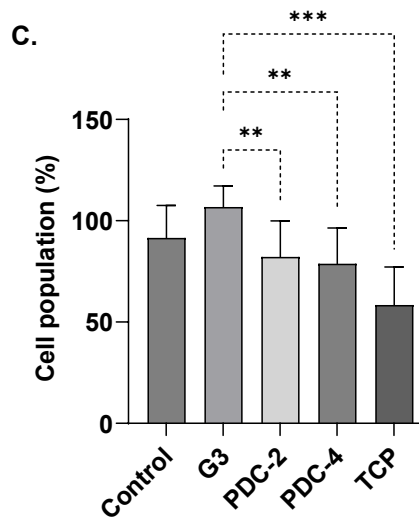
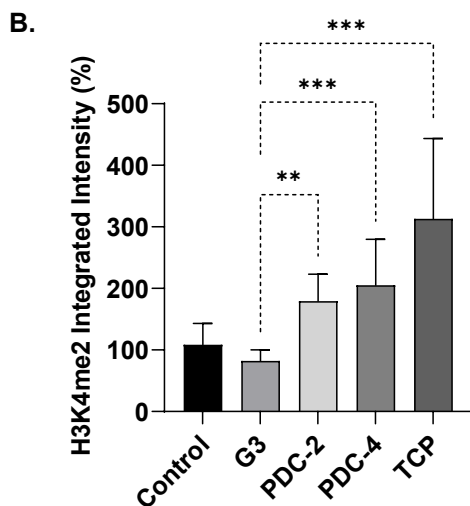


Fig. 65. H3K4me2 labelling after PDC treatment in PC-3. (A) Representative images of PC-3 cells after 24 hours exposure with unconjugated G3 peptide (5 μ M), or PDC-2/PDC-4 (5 μ M), or TCP (250 μ M). Non-treated cells were used as negative control. The nuclei was stained with Hoechst. Scale bar 50 μ m and 20X magnification. (B) Normalized H3K4me2 integrated intensity values. Means and \pm SD of 3 biological experiments with 3 replicates each, are presented. The differences between treated groups was calculated using one way ANOVA with multiple comparisons (** $p < 0.01$; *** $p < 0.001$). (C) Normalized cell populations of 3 different experiments with 3 replicates each. One way ANOVA with multiple comparisons was calculated to determine statistical differences between control and PDC (** $p < 0.01$; *** $p < 0.001$).



5.10.4 Histone demethylation analysis by WB

To corroborate the findings obtained by H3K4me2 immunofluorescence, protein levels of the histone mark were evaluated by western blot in LNCaP and PC-3. The technique of western blotting is very useful for semi-quantitative analysis of protein levels in samples. The optimal load concentration for H3K4me2 was selected as 4 μg per lane, as determined by the linear range of relative protein levels for H3 and H3K4me2 for LNCaP (Figure 66), and for PC-3 (Figure 67).

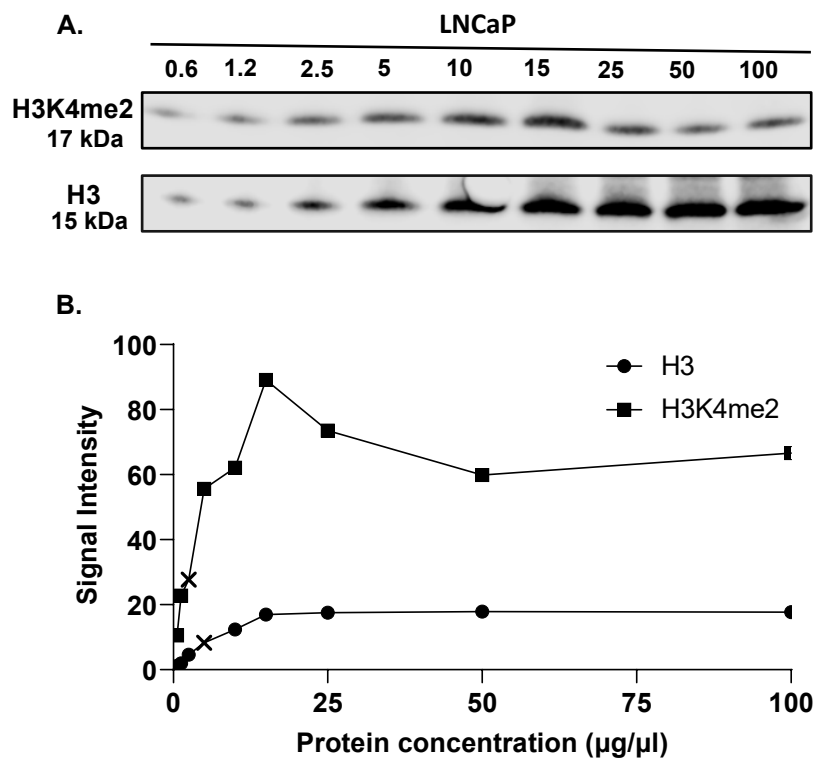


Fig. 66. H3K4me2 and H3K linear range detection in LNCaP lysates. (A) Western blots of lysate dilutions of H3K4me2 and Histone 3 (H3) from one biological experiment. The total protein load (μg) is indicated in lane labels. (B) Semi-quantification of protein relative levels. Cross symbols define the interval of linear association between H3K4me2 and H3K.

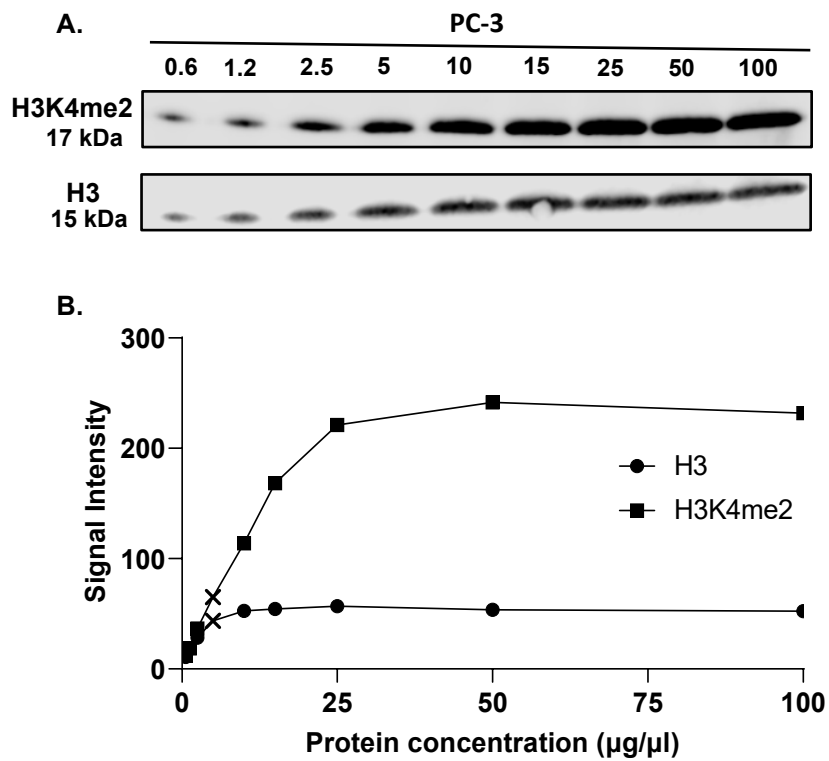


Fig. 67. H3K4me2 and HKP linear range detection in PC-3 lysates. (A) Western blots of lysate dilutions of H3K4me2 and Histone 3 (H3) from one biological experiment. The total protein load (μg) is indicated in lane labels. (B) Semi-quantification of protein relative levels. Cross symbols define the interval of linear association between H3K4me2 and HKP.

PCa cells were treated with the same experimental procedure of PDC-2 and PDC-4, as well as the same positive and negative controls as employed for the immunofluorescence assays. After one day treatment with either PDC-2 or PDC-5, proteins were extracted from LNCaP and PC-3 cells. The representative Western blots of H3K4me2 expression of 2 biological analyses are illustrated in Figure 68A for LNCaP cells, and in Figure 69A for PC-3 cells. PDC-4 exhibited the strongest bands as visualized in the LNCaP and PC-3 blots, similarly to the TCP bands.

In accordance with the bands in the blots, H3K4me2 relative levels were semi-quantified for each cell line. One-way ANOVA test was applied to compare the controls to the treated groups, and the protein abundance of the histone mark were revealed to be significantly increased for PDC-4 for both LNCaP and PC-3 cells (Figure 68B and Figure 69B). The augmentation of H3K4me2 levels after one day treatment of PDC-4 at 5 μ M indicates that this LSD1 inhibitor probe had a blocking effect in LSD1 demethylation activity. In contrast to the rise in H3K4me2 integrated intensity obtained in the antibody labelling results, PDC-2 did not present significant increase in H3K4me2 protein expression in LNCaP cells. Likewise, in PC-3 cells, the protein levels of H3K4me2 after PDC-2 exposure were no different from the controls.

Dual protein data analysis in PCa cells, using immunofluorescence and WB, showed that at least PDC-4 was effective in delivering the probe 7 inhibitor, as well as, inducing cellular phenotypes in PC-3 cells. In both assays, PDC-4 activity induced accumulation of H3K4me2 levels, which implicate an impairment in LSD1 and its role of removing methyl groups from histones. Even though, the H3K4me2 levels after PDC-2 treatment were contradictory, immunofluorescence assays and the reduction in cell viability of both LNCaP and PC-3 cells caused by PDC-2, suggest that PDC-2 might have an effect in blocking LSD1 activity that would benefit of further assessment.

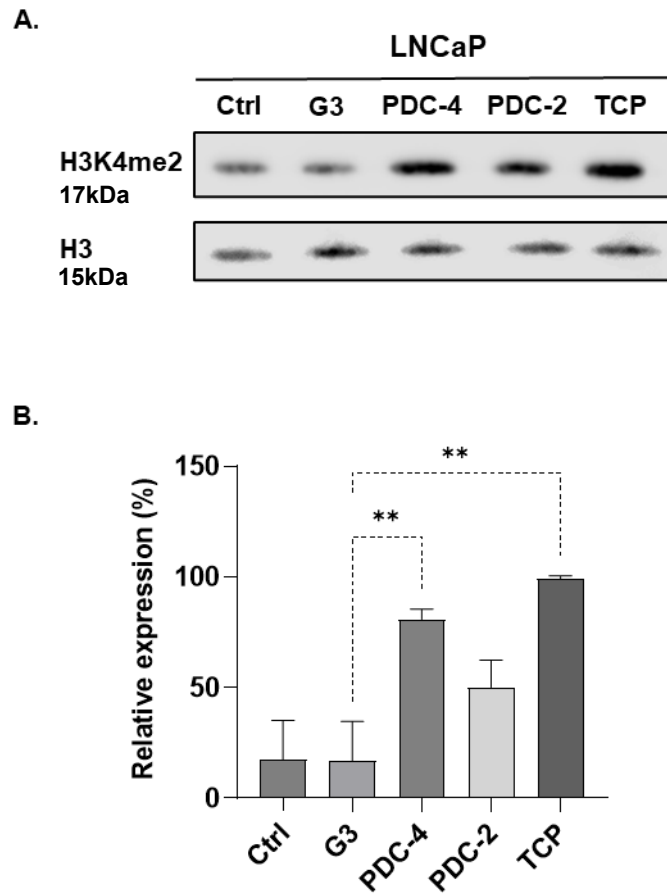


Fig. 68. H3K4me2 protein levels after PDC treatment in LNCaP. (A) Representative western blots of H3K4me2 levels, using H3 as HKP control. Proteins were extracted after 24 hours treatment with PDC-2 and PDC-4 at 5 μ M, or TCP at 250 μ M. Cells with no treatment and cells with unconjugated G3 were utilized as negative controls. (B) Semi-quantification of relative protein levels from 2 biological experiments. Data were normalized presented as means and \pm SD. The statistical significance was determined using one way ANOVA with multiple comparisons (** $p < 0.01$).

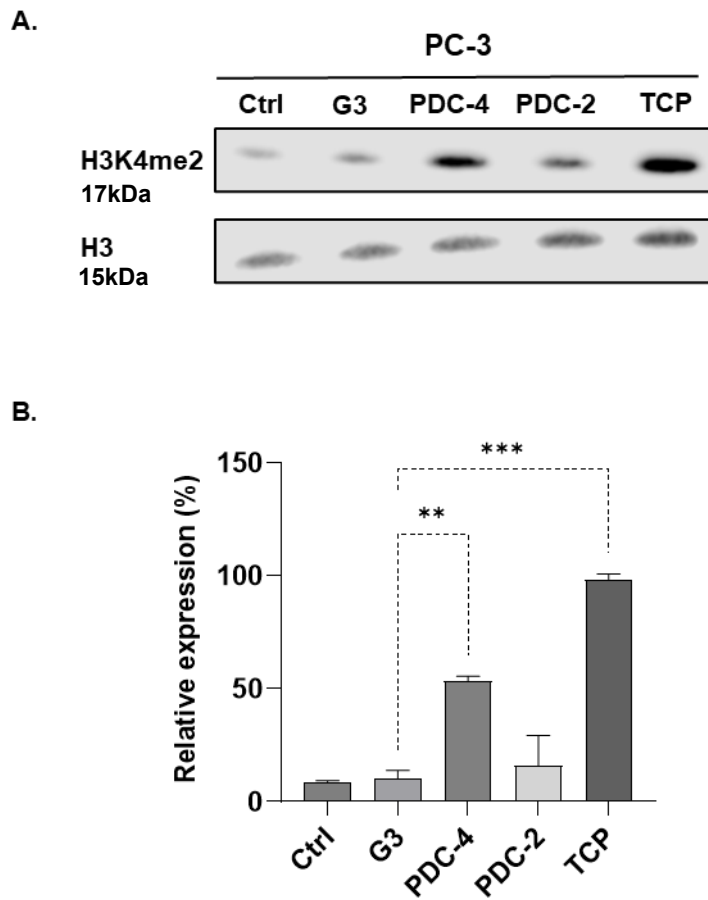


Fig. 69. H3K4me2 protein levels after PDC treatment in PC-3. (A) Representative western blots of H3K4me2 levels, using H3 as HKP control. Proteins were extracted after 24 hours treatment with PDC-2 and PDC-4 at 5 μ M, or TCP at 250 μ M. Cells with no treatment and cells with unconjugated G3 were utilized as negative controls (B) Semi-quantification of relative protein levels from 2 biological experiments. Data were normalized presented as means and \pm SD. The statistical significance was determined using one way ANOVA with multiple comparisons (** $p < 0.01$, *** $p < 0.001$).

5.10.5 Targeted delivery of siRNAs into prostate cancer cells using G3

Following the assessment of PDC using G3 peptide as drug delivery agent of LSD1 inhibitors, the targeted delivery potential of G3 was investigated from another perspective using RNAi. RNAi silencing is an excellent tool to modulate the transcription of specific genes. In one previous study, it has been reported that G3 can associate to anionic siRNAs due to G3's cationic nature, and successfully delivered them into colon cancer cells (Cirillo et al., 2021). Thus, to analyse if G3 peptide is capable of transporting siRNAs and to regulate gene expression in PCa cells, which has not been evaluated before, siGLO red transfection reagent and UBB siRNA were tested using DF1 transfection agent as positive control. The KD of UBB has been shown to strongly reduce cell growth and increase cell death.

In Figure 70A for LNCaP and Figure 71A PC-3, images of the effective siGLO delivery by G3 are exhibited. Images of the negative and positive controls are shown as well. The siGLO integrated intensity values were calculated and normalized to the negative control as previously stated. In both cell lines, the IIC of siGLO (100 nM) was higher when using DF1 as transfection reagent (1:1), than when using G3 (100 nM) as a nanocarrier of siGLO at 200 nM (Figure 70B and Figure 71B). Previous assessments of complexed G3 and siGLO at a 1:1 (100 nM) presented minimal integrated intensity values (Data not provided). The cell number was determined to assess the knockdown of UBB in both PCa cell lines. Using one-way ANOVA with multiple comparisons, the silencing of UBB using either DF1 or G3, was proven as both conditions exhibited a significant decrease in LNCaP and PC-3 cell populations, suggesting UBB-related apoptosis (Fig. 70C and 71C, respectively). Together, siGLO and UBB results proved that siRNAs were successfully delivered into PCa cells by the G3 peptide.

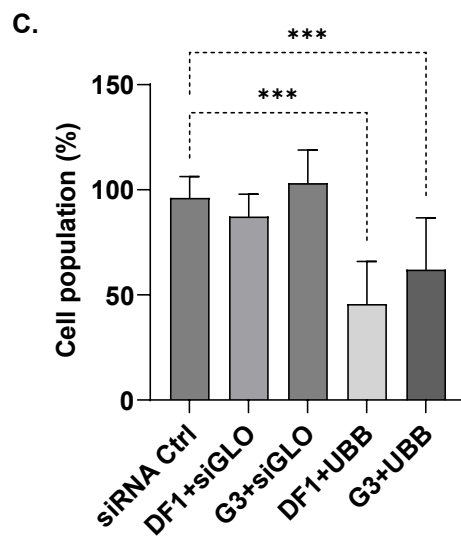
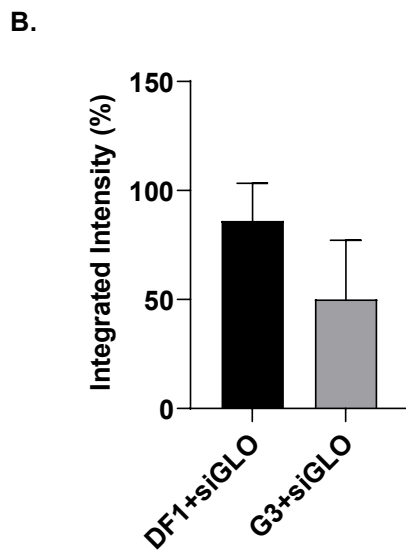
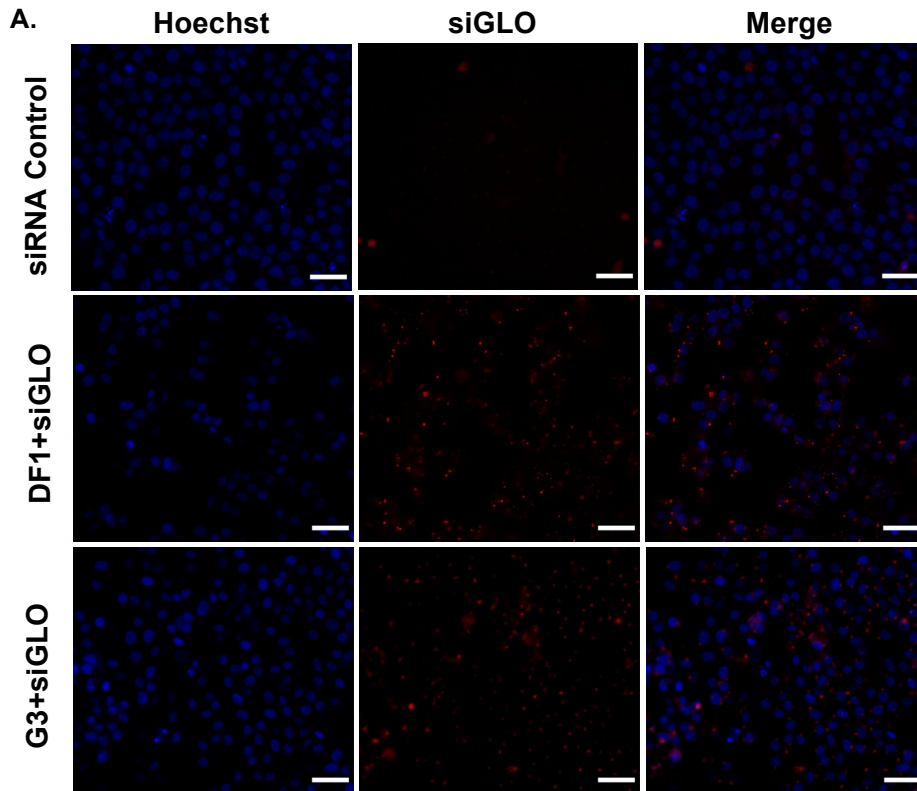


Fig. 70. G3 siGLO targeted delivery in LNCaP. (A) High content images of control cells treated with non-targeting siRNAs and cells with siGLO (100 nM) marker transfected with DF1, and cells with siGLO (200 nM) delivery by G3 peptide. The nuclei were labelled with Hoechst and are represented in blue. Scale bar 50 μ m and 20X magnification. (B) Normalized siGLO integrated intensity. For 24 hours, LNCaP cells were treated with non-targeting siRNAs, siGLO or UBB siRNA. Data is displayed as means and \pm SD of 3 different experiments with 3 replicates. (C) Cell number normalized to the non-targeted siRNA control. The statistical significance was estimated using one way ANOVA with multiple comparisons (** $p < 0.001$).

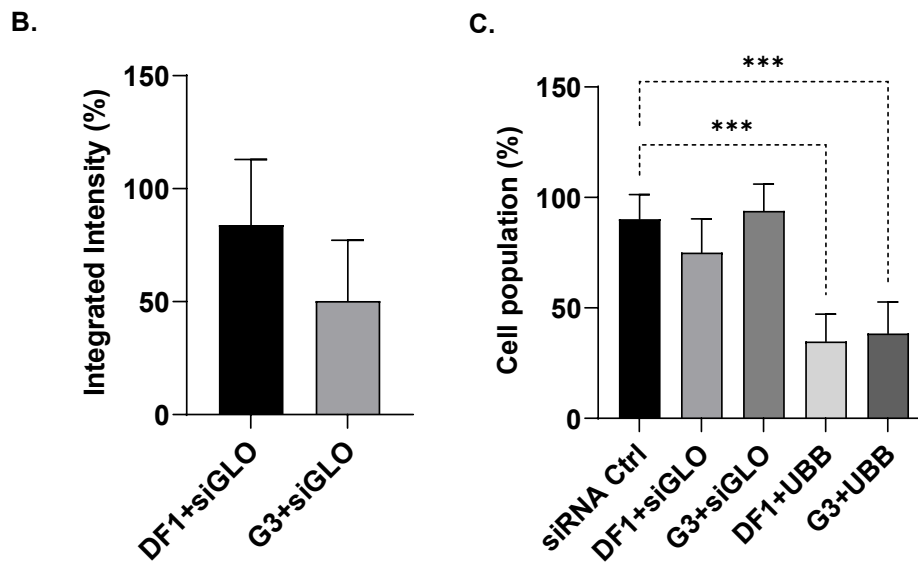
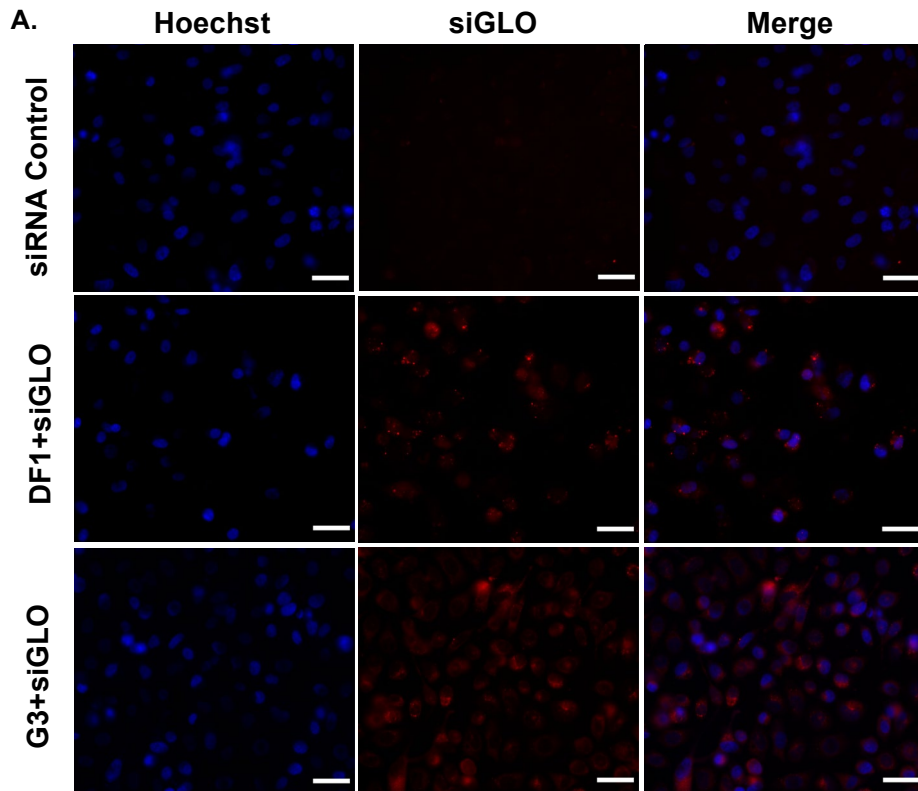


Fig. 71. G3 siRNAs targeted delivery in PC-3. (A) High content images of cells with a mix of non-targeting siRNAs as control and cells with siGLO (100 nM) marker transfected with DF1, and cells with siGLO (200 nM) delivery by G3 peptide. Hoechst was applied to label the nuclei represented in blue. Scale bar 50 μ m and 20X magnification. (B) Normalized siGLO integrated intensity. For 24 hours, LNCaP cells were treated with non-targeting siRNAs, siGLO or UBB siRNA. Data is displayed as means and \pm SD of 3 different experiments with 3 replicates. (C) Cell number was normalized to the non-targeted siRNA control. The statistical significance was estimated using one way ANOVA with multiple comparisons (** $p < 0.001$).

Furthermore, the targeted siRNA LSD1 delivery by G3 was analysed in LNCaP and PC-3 cells, following the same conditions. G3 at 100 nM was complexed to siRNAs at 200 nM for an hour and 2 biological experimental repeats were done. In Figure 72A and Figure 73A, the images of LSD1 antibody labelling of LNCaP cells and PC-3 cells, respectively, are presented after siRNA KD using either DF1 or G3 as delivery agent. LSD1 antibody labelling of the nuclei is indicated in magenta. The graphs indicate the mean integrated intensity values of LSD1 antibody labelling are shown in Figure 72B for LNCaP, and in Figure 73B for PC-3. When contrast to the control groups using ANOVA analysis, both DF1 and G3 demonstrated significant decrease in LSD1 immunofluorescence, with slightly more reduction in DF1 samples, in LNCaP and PC-3 cells. G3 transfection efficiency of siRNA LSD1 in both PCa cell lines, was comparable to that of the commercial DF1 transfection agent.

The quantification of cell number after LSD1 KDs was calculated using High Content data analysis. Nonetheless, when cell numbers were examined after LSD1 KD using DF1 or G3, only DF1 revealed a significant reduction in cell numbers for both cell lines, suggesting that the knockdown was successful only using DF1 or that the LSD1 silencing induced by G3 delivery was not as effective, or retarded (Figure 72C and Figure 73C). The cell number could have been impacted after the LSD1 KD using G3 in PCa cells, but as the assays were analysed after 72 hrs, the proportion of non-transfected cells might have proliferated to a degree it was not possible to determine an impact in cell viability.

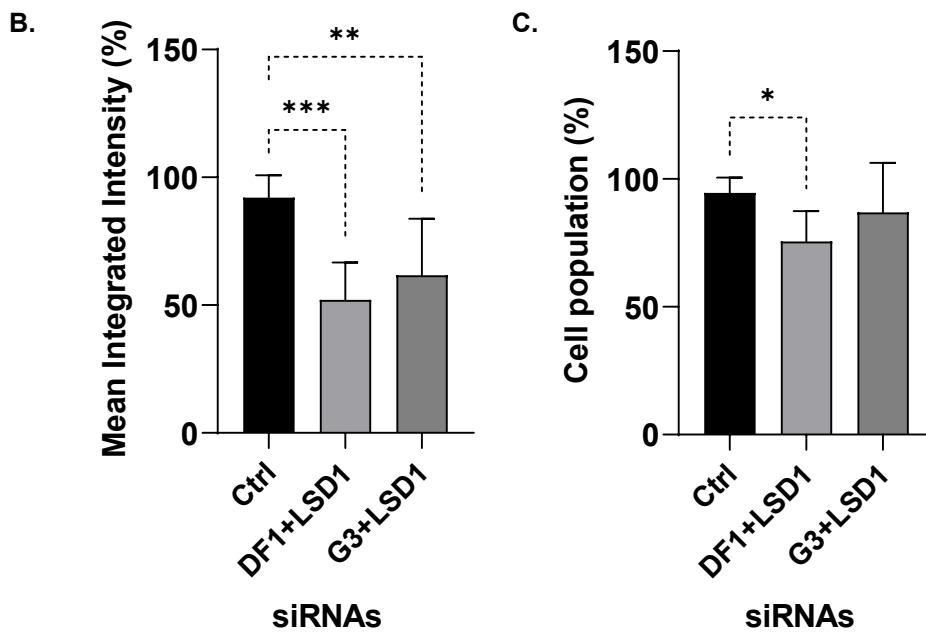
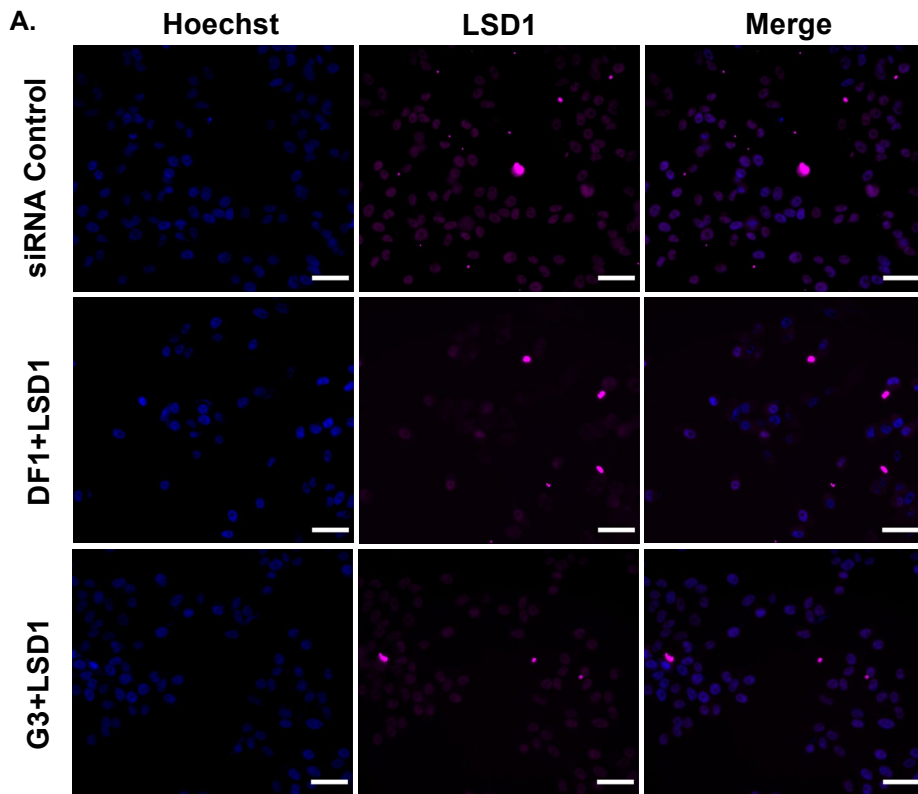


Fig. 72. LSD1 siRNA targeted delivery by G3 in LNCaP. (A) High content images of control cells treated with a combination of non-targeting siRNAs. Transfected cells with DF1 and LSD1 siRNAs at 100 nM or cells treated with G3 peptide at 100 nM and LSD1 siRNAs at 200 nM, for 72 hrs. Nuclei were stained with Hoechst and LSD1 nuclei labelling is represented in magenta. Scale bar 50 μ m and 20X magnification. (B) Normalized LSD1 integrated intensity. Data is displayed as means and \pm SD of 2 different experiments with 3 replicates. Statistical significance was assessed by ANOVA with multiple comparisons (** $p < 0.01$, *** $p < 0.001$). (C) Cell number was calculated and normalized to the non-targeted siRNA control. The statistical significance was estimated using one way ANOVA with multiple comparisons (* $p < 0.05$).

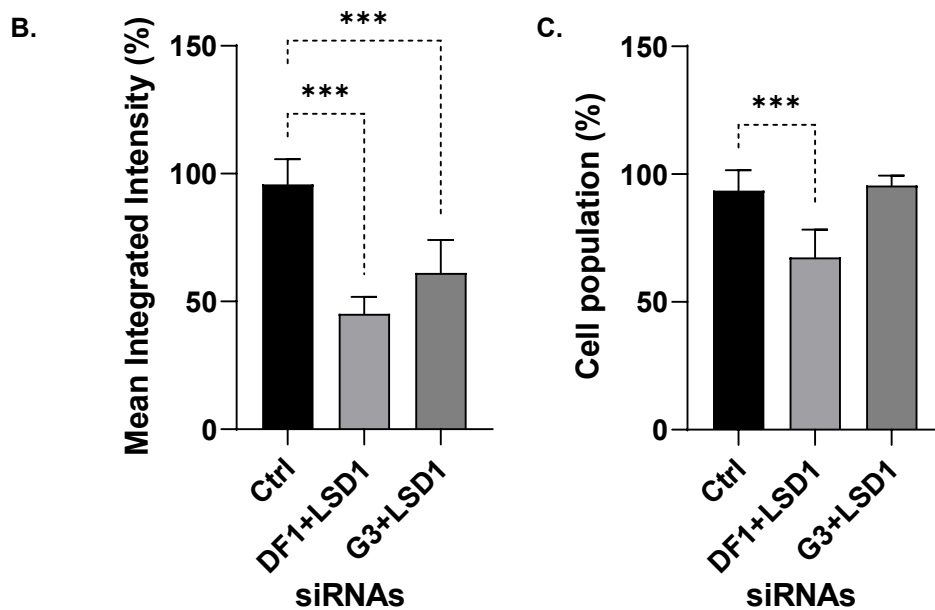
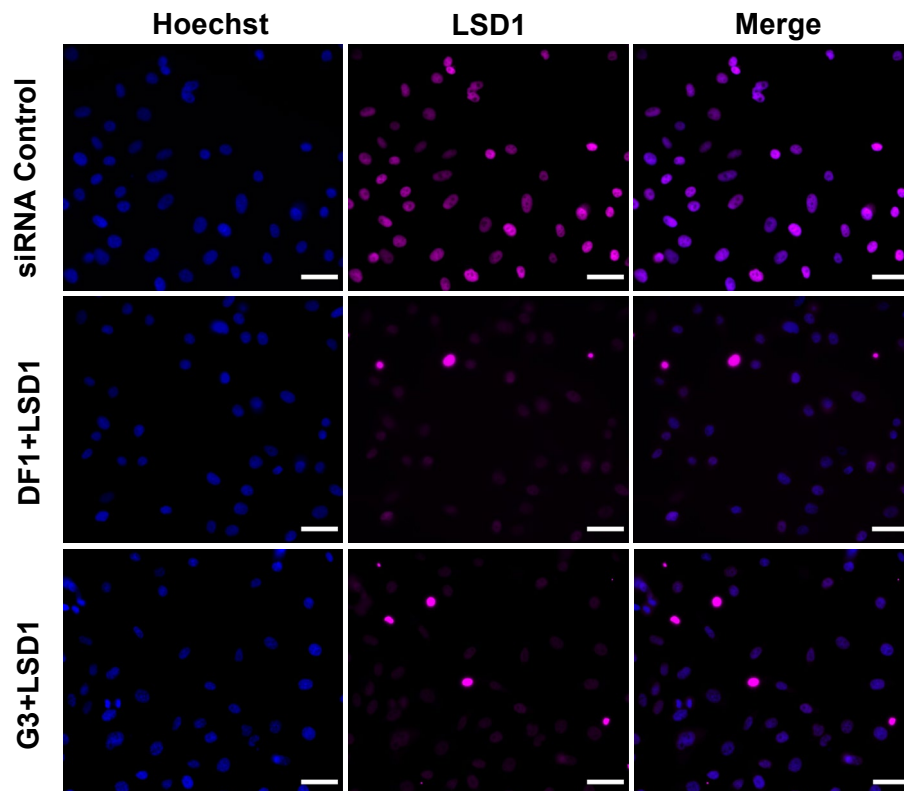


Fig. 73. LSD1 siRNA targeted delivery by G3 in PC-3. (A) High content images of control cells exposed with a mixture of non-targeting siRNAs, and cells transfected for 72 hrs with DF1 and siRNA LSD1 at 100 nM, and cells with G3 peptide complexed with siRNA LSD1 at 200 nM. The nuclei were labelled with Hoechst. Scale bar 50 μ m and 20X magnification. (B) Normalized LSD1 mean integrated intensity. Data is showed as means and \pm SD of 2 different experiments with 3 replicates. (C) Cell number was normalized to the non-targeted siRNA control. The statistical significance of IIC and cell number was estimated using one way ANOVA with multiple comparisons (***) $p < 0.001$.

5.11 Discussion

To summarize, Chapter 5 confirmed that G3 PDC with LSD1 inhibitors holds strong potential in comparison to the commercial TCP inhibitor in LNCaP and PC-3 cells. At reduced doses (5 μ M), the data of the cell viability analysis exposed that PDC-2 and PDC-4 prompted cytotoxic activity towards PCa cells, since the cell populations were statistically declined. Nonetheless, the immunofluorescence and WB data disclosed that PDC-4 exhibited higher effectivity of LSD1 demethylation inhibition than PDC-2. The data in PCa cells show enhancement of the histone signature in both analysis which is evidence that LSD1 demethylation suppression has occurred.

The capacity of carrying nucleic acids by G3 into prostate cancer cells was verified, as siGLO red puncta was localized in the cytoplasmic area and the G3-UBB complexes disrupted the cell viability in a comparable way to the DF1 control. The LSD1 siRNA targeting was not as efficient as DF1 targeting, based on the results of the G3-LSD1 siRNA complexes, which indicate a decline in LSD1 antibody labelling values but no impact upon cell survival.

5.11.1 Cellular impairment after LSD1 inhibition

The abnormal enhanced expression of LSD1 has been detected in PCa (Kashyap et al., 2013; Ketscher et al., 2014; Willmann et al., 2012). LSD1 is an epigenetic modulator that has been identified as a key target in cancer, including PCa (Kahl et al., 2006; Majello et al., 2019). The well-known LSD1 inhibitor, TCP was employed as a control at 250 μ M, dose at which in our analysis it induced at least a 2-fold reduction in cell viability in agreement with its anti-proliferative capacities (Dai et al., 2020). The way this inactivator works is through an irreversible mechanism, in which it covalently binds to the FAD cofactor to restrain LSD1 from operating (Binda et al., 2010; Yang et al., 2007a). TCP has non-selectivity towards LSD1, displaying a K_i of 243 μ M (Schmidt & McCafferty, 2007), which is consistent with the LSD1-associated cell death obtained at 250 μ M. The cell viability was assessed in all five G3 PDC, resulting in a significant reduction of the PCa cell numbers only for PDC-2 and PDC-4, at concentrations of 2.5 to 5 μ M. Their reduction of cell viability at low doses suggests that the LSD1 inhibitors linked to the G3 peptide, displayed strong potency against LSD1. These outcomes are

in agreement with earlier studies, which showed that blocking LSD1 using RNAi or pharmacological inhibitors induces suppression of PCa cell proliferation (Willmann et al., 2012). The LSD1 inhibitors, components of PDC-2 and PDC-4 correspond to probe 5 and probe 7 in Lane's unpublished research work, which have the following IC50 values of 14 ± 2 and 8 ± 3 μM , respectively. Both, IC50 values of the LSD1 inhibitors alone and the IC50 of the PDC obtained in Lane's thesis research are displayed on Table 10 (Lane, 2021). The IC50 were calculated using histone methylated H3K4me2 peptide substrates with an enzymatic assay, not living cells. Even though their enzymatic data showed that the insertion of G3 to the LSD1 inactivators resulted in a reduction in the selectivity towards LSD1, our findings of those PDC in PCa cells exhibited cell growth inhibition at low concentrations. This indicates that the enzymatic results may not directly translate to how the inhibitors behave within living organisms.

Table 10. G3 PDC-2 and PDC-4 (Lane, 2021)

Assigned name	LSD1 inhibitor	Modification	*IC50 Probes (μM)	**IC50 PDC (μM)
PDC-2	Probe 5	Alkyl-azide	14 ± 2	72 ± 16
PDC-4	Probe 7	Alkyl-azide	8 ± 3	145 ± 44

* LSD1 inhibitory values (IC50) refer to the LSD1 inhibitors without conjugation of the peptide.

** LSD1 inhibitory values (IC50) refer to the PDC.

5.11.2 The limitations of using hydrogen peroxide assay in PCa cells

As an initial effort to measure LSD1 inhibition by G3 PDC, an Amplex Red Assay was done in PCa cells. Extracellular hydrogen peroxide levels have been correlated to LSD1 activity using this assay in various cell types (Mohanty et al., 1997; Song et al., 2001; Votyakova & Reynolds, 2008; Wagner et al., 2005). This assay's underlying concept is that the enzymatic activity of LSD1 can be indirectly assessed through monitoring of the H_2O_2 byproduct of the demethylation reaction. Upon its formation, hydrogen peroxide combines with the Amplex Red reagent in a 1:1 proportion, leading to an HRP-mediated oxidation into the resorufin. Cells without any treatment and cells

exposed to naked G3 were used as negative controls. TCP and hydrogen peroxide (2.5 μM) were employed as positive controls. The PDC-2 was selected for the assay and cells were treated with different concentrations (100 nM to 2.5 μM) and resorufin values were measured at 3 time points (60, 120 and 180 min). The results conclusively showed that the LSD1 activity in PCa cells could not be measured using the Amplex Red assay. There were no noticeable differences in hydrogen peroxide levels in the media of the controls in comparison with the PDC-2 at any concentration. Hydrogen peroxide production occurs during biological processes in the cytosol and other organelles (Chance et al., 1979). The method does not allow to differentiate between various sources of hydrogen peroxide in PCa living cells and hence is ineffective in discriminating hydrogen peroxide as a byproduct of LSD1 demethylation reaction.

5.11.3 Does the G3 PDC deliver LSD1 inhibitors in prostate cancer cells?

LSD1 controls gene expression via epigenetics, specifically through the demethylation of mono and dimethyl groups from H3K4 and H3K9 (H3K4me1/2 and H3K9me1/2) (Cai et al., 2014; Forneris et al., 2006; Metzger et al., 2005; Shi et al., 2004; Wissmann et al., 2007). Therefore, the inhibition of LSD1 activity was investigated by assessing the protein expression of histone marks using immunofluorescence and WB. In LNCaP and PC-3, it was shown that TCP at 250 μM significantly increased H3K4me2 fluorescence intensity when compared to the non-treated control cells. Thus, TCP was set as a positive control at 250 μM to evaluate the potential of the G3 PDC to block LSD1, and non-treated cells and cells with naked G3 were employed as negative controls.

Due to their anti-proliferative effects, PDC-2 and PDC-4 were selected to test LSD1 inhibition. Increased H3K4me2 integrated intensity levels were achieved in PC-3 and LNCaP cells with PDC-2 and PDC-4 when compared to the G3 naked control. However, statistical differences in H3K4me2 in LNCaP were not achieved for PDC-4. The H3K4me2 results were consistent with the reduction in cell viability showed for PDC-2 and PDC-4 in PC-3 cells, and only for PDC-2 in LNCaP. Further LSD1 suppression was confirmed by WBs. To our surprise, the only conjugate that increased the expression of the H3K4me2 in the LNCaP and PC-3 blots was PDC-4 inhibitor.

This findings in combination with the antibody labelling and cell proliferation assays indicate that PDC-4 has an increasing capacity of transporting LSD1 inhibitors and releasing them into prostate cancer cells, as illustrated in Figure 74. Once internalised, the endocytic payload may be transported to other parts of the cell, including lysosomes or returned to the cell surface. The data suggests that the inhibitors must undergo endosomal escape at some point, or that they are active in conjugation with the peptide. Immunofluorescence experiments and the decrease in cell survival produced by PDC-2 in both LNCaP and PC-3 cells imply that PDC-2 may have an impact in suppressing LSD1 activity, which would profit from further investigation even if the H3K4me2 levels after PDC-2 treatment were inconsistent with the WBs. The potent delivery capability of PDC-4, could be extrapolated to other cancer cell lines where LSD1 has been found to have a role in disease progression, such as breast cancer, ovarian cancer and colon cancer, among others (Dong et al., 2022).

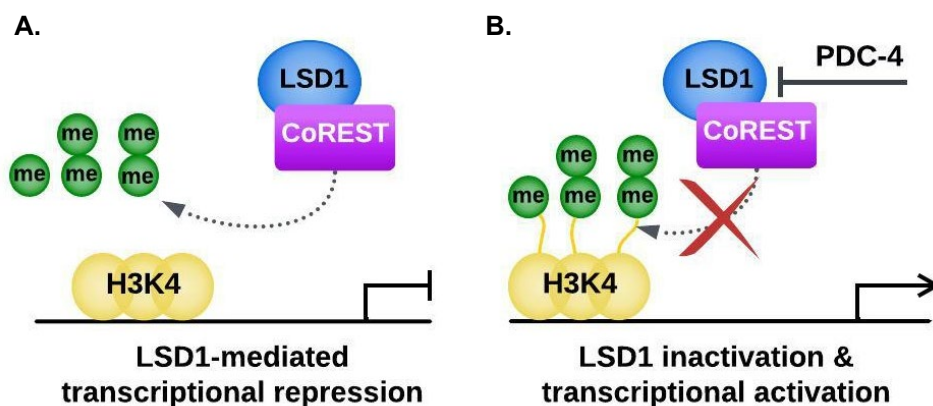


Fig. 74. G3 PDC inhibition of LSD1 in PCa. (A) LSD1 is upregulated in PCa, and it regulates transcriptional repression of genes by demethylating H3K4 in combination with complexes, such as CoREST. (B) G3 is the targeting peptide of PDC-4 that has a LSD1 inhibitor as payload. Our data show that PDC-4 induced the inhibition of LSD1 presenting a significant increase of dimethyl residues in H3K4. Adapted from Gu et al., 2020.

Our findings are in line with similar studies that evaluate the differences between histone signatures of modified LSD1 inhibitors in cancer cells. Fioravanti and colleagues tested different analogs of LSD1 inactivators, that were modified by moving the 4-phenyl ring to a 3-position and substituting with heterocyclic units (furan, pyridine

or thiophene), resulting in cell death and elevated levels of H3K4me2 and/or H3K9me2 as corroborating their inhibition of LSD1 in LNCaP and U937 AML cells (Fioravanti et al., 2022). In another research project, they modified the phenyl ring of TCP-based inhibitors by adding trifluoromethyl group (CF₃) and methoxyl group (OCH₃), and in particular their compound 29b, trigger H3K4me_{1/2} accumulation and prevented metastasis in MGC-803 cells (Huang et al., 2021).

5.11.4 G3 facilitates the delivery of siRNAs into prostate cancer cells

The capacity for molecular and gene therapy of siRNA, which specifically repress their target genes, is considerable. In the literature multiple CPP have been proven to transport siRNA with successful delivery. The ability of G3 peptide to carry and release siRNAs that modulate the transcription of genes in PCa cells was studied in Chapter 5. It has been postulated that the cationic property of G3 can be exploited to complex anionic molecules, such as nucleic acids. Thus, the peptide was complexed to siGLO and UBB siRNAs by 60-minutes incubation and DF1 transfection agent was employed as positive control. High Content Screening was used to assess the RNAi G3 delivery. Following optimisation, the 2:1 ratio of 200 nM siRNA to 100 nM G3 was determined to be the most effective setting. DF1 was employed at 1:1 as usual, but with higher concentration 100 nM of siGLO/UBB. The images exposed fluorescent puncta of the siGLO precisely internalised in the cytoplasm for the G3-siGLO complexes. These results indicate that G3 was indeed capable of complexing siRNAs and transporting them into LNCaP and PC-3 cells. However, G3 was not as effective as transfection using DF1, because there was a two-fold difference of the integrated intensity values. DF1 is a commercial experimental cell reagent and is not in use for clinical testing. Results of the G3-UBB complexes show a significant decrease of cell numbers, similar to UBB transfected with DF1. Taken together the siGLO and UBB siRNAs G3-mediated targeted delivery, was in accordance with prior studies from Cirillo and colleagues that demonstrated G3 carrying and loading siRNA into colon cancer cells and spheroids (Cirillo et al., 2021). Following the pronounced uptake of G3 peptide in LNCaP spheroids, our next steps could be to test G3-siRNA complexes in these 3-D models as well.

Furthermore, the evaluation of LSD1 siRNA delivery by G3 resulted in a comparable drop in integrated intensity values to DF1 delivery in LNCaP and PC-3 cells. However, while G3-LSD1 siRNA targeting did not affect cell viability, LSD1 silencing with DF1 demonstrated a decline in both cellular populations. Cellular impairment in cancer cells has been reported as a common outcome of LSD1 inhibition, whether by RNAi or chemical drugs (Willmann et al., 2012). This suggests that the knockdown of LSD1 siRNAs utilising G3 as a delivery vehicle was less successful than DF1, possibly due to a slower release of the siRNA. Thus, additional time-points may provide further insights in future investigations. The cell viability may have been affected by the G3-LSD1 siRNA complexes in PCa cells, but because the experiments were performed after 72 hours, the fraction of non-transfected cells might have proliferated to the point where an influence on cell viability could not be determined. Considering that two biological repeats were conducted of the G3-LSD1 siRNA assay, three experimental repeats would have been ideal to increase the reliability and statistical confidence.

Other experimental approaches could have provided more insights into the siRNA-delivering capacity of G3 peptide. LSD1 protein expression could have been evaluated through WBs to verify successful delivery by G3. In addition, the use of live cell imaging in future experiments could be beneficial to elucidate the differences in cell numbers attributable to the delivery of LSD1 siRNA by G3 compared to DF1.

CHAPTER 6

6. GENERAL DISCUSSION

Peptides are extremely useful in cancer therapeutics, given their biological potency and exceptional capacity for tailored transport (Chatzisideri et al., 2018; Gronewold et al., 2018). The α -helix synthetic peptide, known as G3, was designed based on the following sequence: G(IKK)₃-NH₂ (Hu et al. 2011). Due to its antibacterial, antitumour and cancer affinity properties, G3 peptide has been the scope of previous studies (Chen et al., 2015; Chen et al., 2014a; Chen et al., 2014b; Cirillo et al., 2021; Gong et al., 2019; Gong et al., 2020; Hu et al., 2011). To broaden the horizons of what is known of G3's therapeutic potential, the major aims in Chapter 3 were to analyse whether the peptide could be internalized by prostate cancer cells and/or normal prostate cells, which could provide evidence of cancer cell selectivity towards the disease; and secondly to get a deeper understanding of its intracellular localization in PCa cells.

Chapter 3 presents several key findings related to G3 peptide and its behaviour in PCa cells. First, the G3 peptide exhibited elevated selectivity towards prostate cancer cells, along with increased uptake. Subcellular localization studies revealed that G3 is predominantly situated within endosomal compartments, including lysosomes. Additionally, the peptide demonstrated a high dose-dependent cytotoxic effect in PCa cell lines, while remaining non-toxic to PNT2 cells. The existing evidence supporting clathrin-mediated endocytosis as the primary internalization pathway for G3 was further strengthened by colocalization with endosomal and lysosomal markers, a minimal colocalization with a macropinocytosis biomarker, and sustained high uptake even after the chemical inhibition of macropinocytosis. These findings reinforce the idea that G3 is internalized through clathrin-mediated endocytosis (CME), at least within the concentration range used in this study.

The main findings in Chapter 3 guided the transition into Chapter 4, where the focus shifted to explore the role of scavenger receptors (SR) in G3 internalization. The massive interactome of SR is indicative of their complex function as membrane-bound receptors (Taban et al., 2022). In drug delivery systems, SR have been recognized to uptake vectors and cargos, such as oligonucleotide-complexed, nanoparticles, nucleic acids, and double-stranded RNA (DeWitte-Orr et al., 2010; Limmon et al., 2008; Patel et al., 2010; Pearson et al., 1993; Saleh et al., 2006). Various studies have reported that drug delivery CPP uptake is in part controlled by SR (Arukuusk, et al., 2013; Ezzat et al., 2012; Helmfors et al., 2015; Lindberg et al., 2013; Veiman et al., 2013). Interestingly, PDC have also been discovered to enter the cells through SR (Kumthekar et al., 2020a; Srimanee et al., 2016). In addition, the potential of SR as targeted receptors of CPP/PDC is highlighted by their substantial upregulation in various cancers, such as PCa (X. Yu et al., 2015). Therefore, the main goal of Chapter 4 was to determine whether SR could have an input in the CME of the G3 peptide in PCa cells.

Briefly, the key results from Chapter 4, suggest that 3 SR, namely SR-B1, SR-F1 and SR-F2 might contribute towards FITC-G3 internalization in PCa cells. Taken together, the data from the RNAi screens, their complementary validation using two independent methods (WB and immunofluorescence assays), and their colocalization analysis of FITC-G3 with the SR, provided more evidence to support a scavenger receptor-mediated endocytosis for G3 peptide, precisely in prostate malignant cells.

The use of peptides as molecular drug transporters within the context of PDC offers a therapeutic approach that could be beneficial for patients with PCa (Wang et al., 2017; Zhu et al., 2021). Given G3's therapeutic properties that have been established in the literature and the findings in this work, including its PCa cell selectivity, the last experimental chapter was focused on investigating its delivering capacity as part of PDC. Five PDC were obtained as part of a collaboration with Turega's research team from Sheffield Hallam University. By incorporating azide tags to the TCP scaffold's para or meta motifs and then coupling our G3 peptide to the C-terminal using a Cu(I)-catalyzed azide–alkyne 1,3-dipolar cycloaddition (CuAAC) or the “click reaction”, they were able to synthesize distinctive LSD1 inhibitors. Therefore, the core aim in Chapter 5 was to explore the therapeutic potential of these PDC by employing G3 as a targeting

unit and customized LSD1 inhibitors as payload. In order to test the effectiveness of these PDC against PCa, the impact upon cell viability and differences of histone marks were analysed through HCS and WBs. Additionally, another purpose was to examine if the G3 peptide had the capacity to carry and deliver siRNA molecules into PCa cells.

In Chapter 5, the most notable findings demonstrated robust treatment potential of the G3 PDC in combination with LSD1 inhibitors against both LNCaP and PC-3 cells. The results of the cell viability assay revealed that PDC-2 and PDC-4 have a cytotoxic effect at reasonably low doses in PCa cells. However, PDC-4 displayed higher effectivity than PDC-2, as validated by antibody labelling and WB. PDC-4 caused a noticeable increase in dimethyl groups of H3K4 in comparison to the cells exposed to the naked G3 peptide, which is clear indication of LSD1 demethylation inactivation in PCa cells. The major findings regarding G3 peptide siRNA targeted delivery were partially successful. Although, G3 was capable of delivering siGLO and UBB siRNAs into PCa, the data exposed that it was not as effective as the commercial transfection reagent DF1. Despite the mean integrated intensity values showed a decreased in LSD1 labelling, it was not possible to confirmed if G3 peptide successfully delivered siRNA LSD1 into PCa, because there was no decrease in the total cell number.

6.1 Factors contributing to prostate cancer cell selectivity and uptake

Together, the findings of FITC-G3 uptake using HCS and high-resolution imaging and the co-culture assays in PCa cells vs non-cancer prostate cells, support the high affinity of the peptide to these cancer cell lines. Multiple factors could explain why PCa cells exhibit such selectivity, like the peptide physicochemical properties (e.g. cationicity and amphipathicity), experimental settings (e.g. concentration or peptide-cell ratio), or membrane interactions specific to the cell types. According to the literature, it is well recognized that to aid cellular entry, amphipathic peptides can use hydrophobic/hydrophilic interactions with the plasma membrane, as well as peptides with a cationic nature, due to their lysine or arginine residues, have a tendency to greater interactions with membranes that are negatively charged (Madani et al., 2011; Ruseska & Zimmer, 2020). The architecture of G3 consists of only 14 aa displayed in a 1:1 ratio of cationic lysine (K) and hydrophobic isoleucine (I) residues, organized in

three IKK repeated series (Hu et al. 2011). Prior studies have identified that G3 embraces an α -helical arrangement when associating with synthetic membranes, like small unilamellar vesicles (SUVs), that imitate cancer or bacterial surfaces (Gong et al 2019; Gong et al., 2020; Hu et al., 2011). In addition, it was suggested that this mechanism could be contributing to its favoured uptake, penetrating cells as a result of its α -helical configuration and contact between its cationic net charges with the anionic charges and high unsaturated lipid content in the membranes of cancer cells (Chen, et al., 2014a, 2014b; Hu et al., 2011). In contrast, the findings presented herein, combined with findings from Cirillo's previous work, highlight an energy-based internalization mechanism evident at lower concentrations of G3 (Cirillo et al., 2021). Therefore, the concentration of G3 may have a major role in its internalization mechanism. In the analysis done in this research, G3 was generally employed at the relatively low dose of 4 μ M, close to the concentration reported by Cirillo (6.25 μ M) in their internalization experiments, which supports a CME pathway (Cirillo et al., 2021). In the literature, it has been reported a concentration-based tendency for numerous peptides, in which endocytosis is employed at reduced doses, while at elevated concentrations there is a shift to direct translocation (Fretz et al., 2007; Jones & Sayers, 2012; Kosuge et al., 2008). Thus, it could be possible that this is the case for the G3 peptide. This could explain its energy-dependant process at low doses and the cytotoxic effect that displays at high concentrations.

A notable study showed the crucial function of the transmembrane potential in the direct penetration mechanism of CPP. They engineered a KCNN4 potassium channel knockout HeLa cell line that induced membrane polarization decreased that demonstrated the complete disruption of CPP uptake (Trofimenko et al., 2021b). Furthermore, the same research team use the KCNN4 knockout cell line to verify that endocytosis was not affected in the internalization of several endocytic CPP (Trofimenko et al., 2021a). This genetic strategy could be applied to verify the internalization of G3 by direct penetration at high concentrations.

The cell type with its specific membranal components, such as transmembrane receptors, represents another contributing factor to the uptake of CPP reported in the literature. For example, in a study they demonstrated the cell-dependent behaviour using HeLa, HEK293, Cos-7, and MDCK cells, by testing the uptake efficiencies of 22

recognized CPP, including TAT, Pep-1, transportan, MAP, MPG and penetratin (Mueller et al., 2008). They divided the peptides into groups according to how well they internalised into the cells, with transportan having a similar efficiency in all cell types and penetratin presenting a cell-specific affinity to HeLa cells. In addition, the overexpression of several receptors has been reported in different cancers. In the existing literature, cancer-targeting peptides are a group of small-sized peptides, and their internalization relies on the recognition and connection with transmembrane receptors that have a 3:1 prevalence on oncogenic cells versus non-cancerous cells (Reubi, 2003; Vrettos et al., 2018). Thus, it could be plausible that the selective uptake of G3 into cancer cells at reduced concentrations (4 μ M), including PCa cells, could have been driven by an underlying mechanism mediated by their interaction with overexpressed surface-bound receptors in PCa cells.

6.2 Future investigations: Beyond scavenger receptor knockdown in G3 uptake

The promise of G3 peptide as a drug delivery agent is rooted in its ability to specifically target cancer cells. Its remarkable ability to discriminate between prostate normal cells and PCa cells, sets the stage for its potential role in PCa therapeutics. For a comprehensive understanding of its applicability, further examination of G3 is essential to ascertain whether it exhibits selective entry into more cancer cell lines, focusing in those that exhibit upregulation of SR. It's also important to evaluate its specificity and drug delivery capacity in diverse oncogenic animal models, which could provide a more accurate cytotoxic profile. This will not only broaden our understanding of its potential applications but will also provide insights into any unforeseen challenges or limitations that might arise in more complex biological systems. The first insight into G3's cytotoxic properties in an in vivo setting came from Cirillo's work model, specifically observing zebrafish embryos over a period of 72 hours. In their evaluations involving FITC-G3 and G3-siRNA complexes, they noted an escalating toxicity pattern for the peptide in correlation with its concentration, while they revealed toxicity attenuation for the G3-siRNA complexes and minimal toxicity for the scope of dosages that were used for drug delivery (Cirillo et al., 2021).

HCS is an innovative tool that has a wide range of applications, from drug discovery and toxicology to functional genomics (Fraietta & Gasparri, 2016; Li & Xia, 2019). Furthermore, the speed and broad screening potential of HCS are of particular advantage in scenarios where time is of the essence or where there is a need to navigate through extensive libraries of compounds. In this research, the use of HCS to analyse RNAi screenings provided an effective and useful method to generate a substantial amount of data within a limited time frame. The RNAi-based HCS offered an initial unbiased approach to investigating the active players in the uptake of G3 peptide, and thus represents a suitable technique for application in future experiments to identify potential hits.

RNAi silencing is a prevalent approach for understanding the internalization mechanism of CPP. Based on the results, SR-B1, SR-F1, or SR-F2 might play significant roles in G3 internalization. While our findings are compelling, deeper investigations are necessary to strengthen and confirm SR-mediated endocytosis. For instance, evaluating the internalization efficiencies of the peptide after stimulating overexpression of these SR in cells, that if SR are key players in the uptake of G3, one would expect that peptide internalization would be more pronounced. Testing the internalization of the peptide in combination with known ligands of the SR could be another tentative approach. For instance, SR-F2 displays high affinity towards maleylated BSA (Wicker-Planquart et al., 2021), an experiment could be design by treating prostate cancer cells with this ligand and FITC-G3 simultaneously to determine if the uptake of the peptide is affected. Likewise, acetylated low-density lipoprotein (AcLDL), a ligand with increased affinity to SR-F1 and to a lesser extent to SR-B1, could be tested in the same way for both receptors (S. Acton et al., 1994; Adachi et al., 1997). This can be paired with a SR-B1 inhibitor like block lipid transport-1 (BLT-1), which blocks HDL, a ligand known for its non-endocytic route, from being transferred (Nieland et al., 2008; Nieland et al., 2002). Prior research utilized BLT-1 to validate PF/32pDNA peptide complex uptake via SR-B1, revealing that the internalization remained unchanged and distinct from SR-B1-mediated HDL uptake (Srimanee et al., 2016). A more robust experimental approach could involve using genetically engineered stable cells, lacking functional SR-B1/SR-F1/SR-2 to evaluate FITC-G3 uptake.

Another reliable approach is through peptide-membrane interaction analysis. The SR as potential partners of G3 could be verified by synthesizing a biotinylated version of G3 peptide and performing a streptavidin pull-down assay after treatment in PCa cells, followed protein identification by mass spectrometry. An alternative strategy to verify peptide-protein interaction could be by using proximity ligation assay (PLA), by employing a primary ab specific to each of the SR and another one targeted to FITC in G3 peptide. Consequently, if the SR and the FITC-G3 peptide are within a proximity of 40 nm, the PLA would generate a detectable fluorescence signal, indicating interaction (Hegazy et al., 2020). Other techniques have been used to assess CPP-membrane interactions, including X-ray scattering, differential scanning calorimetry, circular dichroism, nuclear magnetic resonance, among others (Liu & Afshar, 2020).

6.3 2D Maximum Intensity Projection: A Reliable Approach for Colocalization?

Fluorescence-based methods, such as colocalization analysis are widely used to understand the internalization and intracellular placement of CPP. In this research, MIPs were employed in all of the colocalization assessments, which involves the condensation of a 3D z-stack into a 2D projection image. Although advanced fluorescence microscopy generates in-depth 3D data, MIPs are still typically employed for 2D colocalization analyses and ROI selection (Dunn et al., 2011; Zinchuk & Grossenbacher-Zinchuk, 2009). This technique holds some advantages, including the simplicity of ROI identification in 2D images, a faster analysis of the data and the enhancement of the visibility of signals; however, MIP possesses restricted applicability for accurate colocalization, because it can lead to omission of key data points, as well as to addition of extraneous data (Pike et al., 2017; Theart et al., 2018). In addition, the MIP-based colocalization assays were performed at fixed time points, 2 hrs for early endosomal markers, 6 hrs for late endosomal markers, and 18 hrs for lysosomal markers, which limits the time-frame of the results. Even though colocalization static analysis is still a valuable strategy that is routinely used, it can be prone to fixation artifacts (Comeau et al., 2006; Pawley, 2006).

In hindsight, the 2D MIP colocalization studies did offer additional data to support our hypothesis. However, this could have been improved by using 3D live cell high-

resolution microscopy in time-course experiments. This could have guaranteed a more robust assessment and a dynamic view into the progression of G3 through the endocytic pathway or in the trafficking with SR, potentially revealing intermediary steps that might have been missed in the fixed-time point assays or in the MIP analysis (Koyama-Honda et al., 2005; Watson, 2009; Wombacher & Cornish, 2011). The employment of MIP for colocalization analysis could be convenient mostly in situations where the budget or the time are constrained.

6.4 Avoiding lysosomal degradation and embracing endosomal escape in peptide therapeutics

Endocytosis of peptides and their cargo entails their trafficking into endosomal vesicles, which will need to undergo endosomal escape to avoid fusion into the lysosome (Bareford & Swaan, 2007; Huotari & Helenius, 2011). Endosomal escape is a crucial step in the intracellular delivery of peptides, safeguarding them from lysosomal degradation and enabling payload release into the cytoplasm for its intended biological action (Lee et al., 2013; Pei & Buyanova, 2019; Voltà-Durán et al., 2023). The results from the colocalization analysis with endocytic markers support the idea of G3 following an endocytic mechanism to enter PCa cells, which progresses from early to late endosomes, and its subsequent internalization into lamp1-positive compartments that might be lysosomes. Lysosomes owe their acidic surroundings to the v-ATPase enzymes that pump protons, using ATP as an energy source (Forgac, 2007). While the exposure of the G3 peptide to lysosomal enzymes entails proteolytic disintegration, this could also be used as an advantage for cargo unloading. As mentioned in Chapter 1, multiple PDC, utilize specialized linkers to conjugate the peptide vehicle to the cytotoxic agent, that are cleaved specifically by esterase, amidases, or proteases in the lysosome or that its detachment relies on acidic conditions (Alas et al., 2021; Bargh et al., 2019). G3 PDC could be engineered with enzyme-sensitive or pH-sensitive linker technology to deliver their cargo within the cell's cytoplasm.

Peptides that are directed to lysosomes have been applied to target genetic deficiencies of lysosomal components, such as lysosomal storage disorders (Bonam,

Wang, & Muller, 2019; Ferreira & Gahl, 2017; Urandur & Sullivan, 2023). For example, the K10H16 peptide has been successfully employed to deliver and restore a recombinant enzyme to lysosomes for the treatment of Fabry disease, a lysosomal condition characterized by a defect in the enzyme alpha-galactosidase A (Iwasaki et al., 2020). Therefore, if G3 is transported to lysosomes, it might have the capacity to be utilized for delivering enzyme replacement therapeutics for lysosomal storage disorders.

For endocytic CPP, endosomal escape is key for intracellular drug release. Cargo confined inside endosomes remains biologically inactive, which is the principal reason for the poor efficacy of some CPP (LeCher et al., 2017; Shete et al., 2014). The notable rise in H3K4me2 levels in our study suggests that G3 PDC successfully delivered the LSD1 inhibitor that was used as the payload. Likewise, G3 siRNA targeted delivery was effectively achieved for siGLO and UBB siRNAs. This implies that, during endosomal trafficking, the LSD1 inhibitor and the siRNAs, either on their own or in a conjugated state with G3, managed to overcome endosomal confinement. Various endosomal escape strategies have been proposed, however it is not fully understood how CPPs exit the endocytic organelles and access the cytosolic space. It has been suggested that certain CPPs are more adept at compromising the membrane integrity of organelles than that on the cytoplasmic membrane. For example, the mechanisms of energy-independent internalization into cells of CPP, covered in the introduction of Chapter 3 in section 3.1.2, namely barrel-stave, carpet, and toroidal models, have been hypothesized to be employed as endosomal escape tactics of cationic endocytic peptides (LeCher et al., 2017).

Another strategy and perhaps the most commonly accepted, involves peptides with high content of alanine, glycine, and hydrophobic residues, that upon fluctuations of pH during endosomal transportation, they undergo conformational changes exposing their hydrophobic residues to interact with the organelle membrane (Pei & Buyanova, 2019; Varkouhi, et al., 2011). This interaction will result in the fusion and destabilization of the bilayer membrane and subsequent release of endosomal content (Salomone et al., 2012; Yang et al., 2010), which is a technique typically utilized by viral-associated proteins (Pal, 2021; Somiya & Kuroda, 2020).

The proton-sponge effect is another mechanism that has been postulated to explain the endosomal escape of peptides. This applies to histidine-rich peptides that at acidic pH they become protonated, which causes protons to reach the interior of the endosome, along with the balance of charges by chloride ions. Finally, an increase in the osmotic pressure results in endosome lysis and liberation of the content into the cytosol (J. He et al., 2020; Váňová et al., 2022).

While G3 peptide could have employed one of the known endosomal escape strategies, our findings open new questions about the complexities of understanding peptide intracellular behaviours. Specifically, the precise mechanisms G3 employs within the context of LSD1-based PDC or siRNA complexes remain a compelling area for further research.

6.5 G3 PDC wider implications & G3 therapeutic applications

In multiple cancers, LSD1 has been well-established as a key player in epigenetic control (Kahl et al., 2006; Majello et al., 2019). LSD1's abnormally enhanced expression contributes significantly to the early development and spread of PCa (Kahl et al., 2006; H. Lan et al., 2019; Metzger et al., 2005; Metzger et al., 2010; Sehrawat et al., 2018). In this research, G3 PDC-4 and to a lesser extent, PDC-2 show evidence of suppression of LSD1 demethylation activity and cell viability impairment in two PCa cell lines with diverse disease phenotypes. These results emphasize the application of G3 PDC as targeted therapies, that in comparison to LSD1 inhibitors alone, their biological activity is exerted exclusively in malignant cells. This entails maintaining the inhibitor potency at the same time as reducing potential side effects due to unwanted cytotoxicity. Thus the therapeutic use of G3 PDCs combined with LSD1 inhibitors could extend to a variety of cancers, such as breast, bladder, hepatocellular and small cell lung cancer, where LSD1 is implicated in disease advancement.

At present, a lineup of LSD1 inhibitors, which includes TCP, SP2577, IMG-7289, CC-90011, INCB059872, ORY-1001, and GSK2879552, is under clinical examination for the treatment of multiple cancer types, including leukaemias (Dong et al., 2022; Fang et al., 2019; Hosseini & Minucci, 2017). G3 PDC might be a potential drug carrier for

LSD1 inhibitors that have been previously ruled out from clinical trials because their benefits did not justify their health risks. A case in point is GSK2879552, whose clinical examinations on patients with acute myeloid leukemia and small cell lung carcinoma were discontinued (Bauer et al., 2019; Roboz et al., 2022). Also, PDC using G3 as a targeting vehicle could be used for LSD1 inhibitors that have a limited potency towards LSD1. For example, TCP is in clinical trials because is not used alone, but in dual treatment with all-trans retinoic acid or Azacitidine for cancer therapy. Equally, the reintroduction of other drugs that have been previously discarded from clinical investigations due to unacceptable results, could be retested in conjugation with G3 peptide.

Delivering siRNAs into cells efficiently has always been a challenge. The exact process by which G3 forms complexes with siRNAs remains elusive, but it has been documented that CPPs, due to their elevated positive charge density, can bind to negatively charged nucleic acids (Deshayes et al., 2008; Huang et al., 2015; Lehto et al., 2016). In cancer therapy, some cationic and amphipathic peptides have been reported to efficiently deliver siRNAs in both, in vivo and in vitro models, including G3 in colon cancer cells, 3D spheroids, and zebrafish embryos (Cirillo et al., 2021; Crombez et al., 2009; S. W. Kim et al., 2010; Lundberg et al., 2007). Even though G3 peptide was not as effective in transporting siRNAs (siGLO and UBB) than DF1 transfection reagent, its definitive capability to release them into the cytoplasm positions it with significant potential for wider applications in PCa therapeutics that should be the subject of further evaluations in 3D models and animal xenografts models.

The versatility of G3 PDC lies in its capability for precise delivery of personalized medicine. PCa is a heterogeneous disease with multiple genetic components, as several molecular pathways are disrupted including AR, PI3K–AKT, WNT, and DDR (Abeshouse et al., 2015; Robinson et al., 2015). Conjugation of heterogeneous drugs to combat prostate cancer cells on several fronts and target key dysregulated pathways may be possible as a result of G3's capacity to transport both siRNAs and LSD1 inhibitors.

Furthermore, G3 PDC with LSD1 inhibitors as cargo could be used in combinatorial therapeutics, which might be promising for overcoming resistance mechanisms in CRPC through multiple mechanisms. For instance, targeting LSD1 with G3-based PDC could potentially suppress EMT dynamics and possibly delay the onset of CRPC (Wang et al., 2015). The use of LSD1 inhibitors in docetaxel-resistant CRPC has also been proposed. It has been demonstrated that c-MYC can be downregulated using the LSD1 inhibitor called HCI-2509, which in turn enhances the sensitivity of resistant cancer cells to docetaxel and reduces their proliferation (Gupta et al., 2016). In another study, promising evidence was shown for the use of LSD1 inhibitors in co-therapy with ADT. Since the therapeutic impact of ADT in hormone-sensitive PCa cells was amplified by suppressing LSD1 activity (Wang et al., 2020). Lastly, AR-V7 expression contributes to CRPC progression and resistance to therapies, such as abiraterone or enzalutamide, however AR-V7 activation can be reduced by approximately 50% with the use of LSD1 inhibitors (Antonarakis et al., 2014; Regufe da Mota et al., 2018).

CHAPTER 7

7. CONCLUSION & FUTURE PERSPECTIVES

In conclusion, the research presented in this thesis highlights and contributes to the biomedical and treatment potential of the cationic α -helical G3 peptide in PCa, specifically as a pivotal component of PDC. Initially, it was hypothesized that the peptide would act as part of a targeted delivery system, that could transport and release drugs precisely to prostate cancer cells. This assertion was backed by the peptide's distinct attributes, including its affinity to cancer cells and high internalization rates in other oncogenic cell types, reduced costs of manufacture, and simplicity of manipulation and conjugation. Given that overall survival continues to pose a major concern in PCa treatments, the incorporation of PDC using G3 stands out as a promising addition to emerging tailored therapies. Such advancements could potentially mitigate adverse events and enhance treatment efficacy.

The series of High Content Screenings coupled with the confocal microscopy experiments confirmed that the G3 peptide exhibits cell preference towards prostate cancer cells. This is in contrast to the limited internalization shown in benevolent prostate epithelial cells. The factors impacting the cell selectivity of the peptide are not entirely clear, however based on our outcomes and previous work, the concentration appears to have a key role. The findings also demonstrated that FITC-G3 displayed cytotoxicity towards PCa cells in a high-dose dependant fashion, while marginal uptake in non-cancer prostate cells. This aligns with prior studies in the literature and implies that FITC-G3 might have a favourable safety profile in more extensive clinical evaluations and diverse therapeutic settings. Therefore, to broaden its applications in prostate cancer research, subsequent experiments should explore whether G3 exhibits the same cell selectivity pattern in various animal cancer models and in other cancer cell types.

This work also provided a further understanding of the subcellular localization of G3 within prostate cancer cells. The presence of G3 was detected in both early and late endosomes, and in lysosomal compartments of PCa. This aligns with the RAB5/RAB7-associated pathway in the presence of EEA1, a predominant endosomal route for CPPs. Therefore, these results reinforced its uptake via clathrin-mediated endocytosis. Since G3 was located in LAMP1-labelled lysosomal compartments which might lack acidic conditions and proteolytic enzymes, future experiments to verify whether the peptide goes into the lysosome would be beneficial.

The subsequent RNAi screens and the SR colocalization tests provided promising evidence that supports 3 SR: SR-F1, SR-F2 and SRB1, as potentially responsible at some degree for the internalization mechanism of G3 peptide in PCa cells. To the best of our understanding, SR-F1 and SR-F2 have never previously been acknowledged as CPP endocytosis facilitators. Although the siRNA-mediated suppression of target SR genes was successfully validated through two protein detection techniques, more investigation, such as peptide-membrane interaction studies, is necessary to confirm the role of these SR in the uptake of G3 peptide.

Furthermore, the evaluation of G3 PDC with customised LSD1 inhibitors yielded encouraging results. In PCa cells, PDC-2 and PDC-4 demonstrated a reduction in cellular survival at low concentrations, which is a typical effect of LSD1 restriction in cancer cells. According to the protein expression analysis, PDC-4 demonstrated LSD1 inactivation through an increase in H3K4me2 levels, while PDC-2 presented only the accumulation of the H3K4me2 mark by antibody labelling and not by WBs. At the very least, the overall results show an excellent delivery capacity for PDC-4. Prospective experiments could involve evaluating its activity in other cancer cell lines that have LSD1 overexpressed and where LSD1 has been reported as an epigenetic target. Wider implications of G3 as a delivering agent of PDC is for its conjugation with LSD1 inhibitors that have been withdrawn from patient's trials as a result of an unfavourable risk-benefit ratio. On a similar note, it was revealed that G3 is capable of delivering siRNAs to prostate cancer cells. Despite the transfection efficiency of the commercial transfection reagent was higher than G3, DF1 is not in use for clinical testing.

The cellular trafficking of peptides and their associated cargo, from endocytosis to lysosomal degradation or cytosolic release, is a dynamic and intricate process. The prominent surge in H3K4me2 levels is a clear indication of the effective delivery of LSD1 inhibitor, as well as the G3-tailored release of siGLO and UBB siRNA in PCa cells. Both results support the notion that the peptide or the cargo must have successfully avoided endosomal entrapment, which is an unknown mechanism that could be explored in upcoming research.

The field of peptide therapeutics continues to develop, and so does the imperative to deepen our understanding of these processes. Together all these findings established the groundwork for a novel alternative to treating PCa in which G3, may be employed as a carrier for siRNA-based medications or epigenetic personalized medicine, such as LSD1 inhibitors. At the core of the therapeutic applications of G3 PDC is the smart transport of personalized medicine. Such molecular-based drugs could benefit patients in PCa that have a particular genetic profile, targeting dysregulated signalling pathways, such as PI3K–AKT, DDR, WNT, or the imbalanced epigenetic landscape.

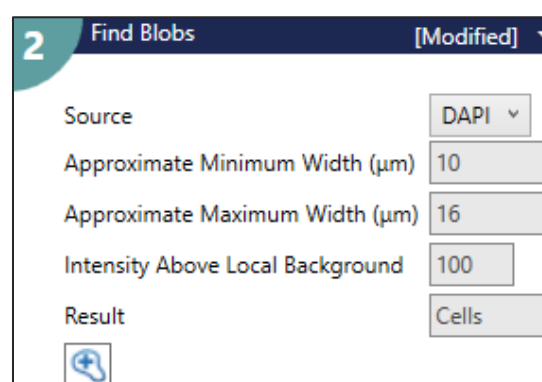
8. APPENDICES

Appendix A. Analysis of non-specific staining removal in High Content Screening.

In some of the HCS analysis, a custom module editor (CuME) was designed using MetaXpress software, to identify cells and eliminate spurious staining, particularly focusing on issues like clumps and non-specific staining. This section provides a detailed description of the parameters used in the CuME and the representation of each step is illustrated in Figure A1.

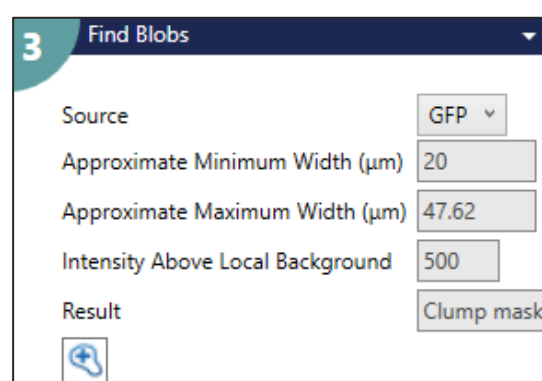
- 1. Image selection:** Random images from different wells were visually inspected to detect the presence of clumps or non-specific staining in the green channel. One image that exemplifies these features was selected for the generation of the CuME. This step is critical for ensuring that the CuME is designed against typical anomalies encountered in the dataset.

- 2. Cells Mask:** Nuclei were identified by setting the approximate minimum and maximum width in μM , using the “Find Blobs” tool in the blue channel. The detected nuclei are delineated by the “Cells” mask produced by this process. The value of intensity above local background refers to the background fluorescence that was subtracted.



2 Find Blobs [Modified]	
Source	DAPI
Approximate Minimum Width (μm)	10
Approximate Maximum Width (μm)	16
Intensity Above Local Background	100
Result	Cells

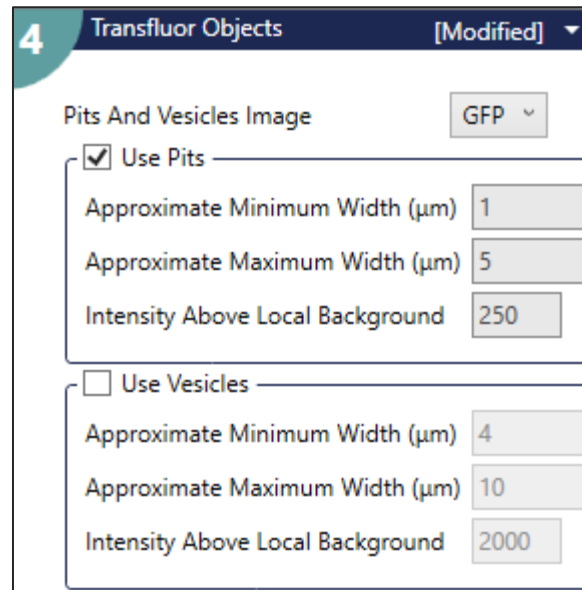
- 3. Clump Mask:** FITC clumps were identified using the “Find Blobs” tool in the green channel. Similar to the nuclei detection, the minimum and maximum widths of these clumps were specified by setting the approximate minimum and maximum



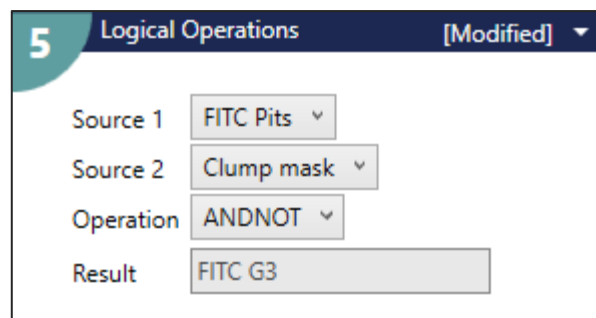
3 Find Blobs	
Source	GFP
Approximate Minimum Width (μm)	20
Approximate Maximum Width (μm)	47.62
Intensity Above Local Background	500
Result	Clump mask

width in μM . The outcome of this step is a “clump mask” that isolates these larger and irregular formations.

4. **Transflour Objects:** This step entails the identification of FITC pits or/and vesicles that is executed in the green channel. In this CuME, only the pits were chosen, which were defined by setting the minimum and maximum width parameters. The value of intensity above local background was subtracted to emphasize these fluorescent features. The result is a “FITC mask” that highlights the positively identified pits/puncta.

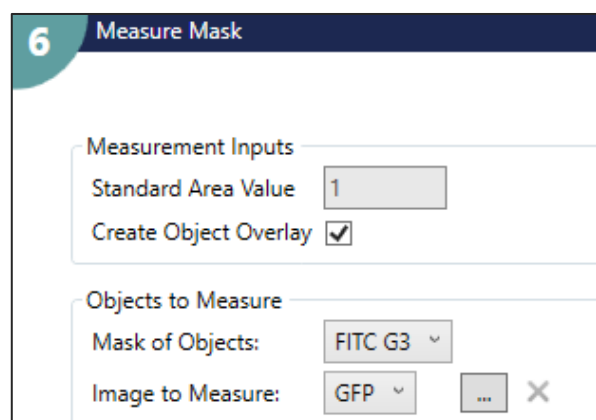


5. **Logical Operations:** The “clump mask” was removed from the “FITC mask” with the “Logical operations” tool using the “ANDNOT” operation. This step effectively removes any



overlapping areas between the two masks, resulting in a new mask termed “FITC G3” mask. This mask represents the specific areas of interest, excluding clumps and focusing on individual FITC-positive objects.

6. **Cellular Integrated Intensity (IIC):** In this final step, the IIC of the FITC fluorescence within the cellular boundaries is quantified employing the “FITC G3” mask. The quantification is performed in the green channel, providing a measure of the positive pits associated with each cell that correspond to the FITC G3 peptide.



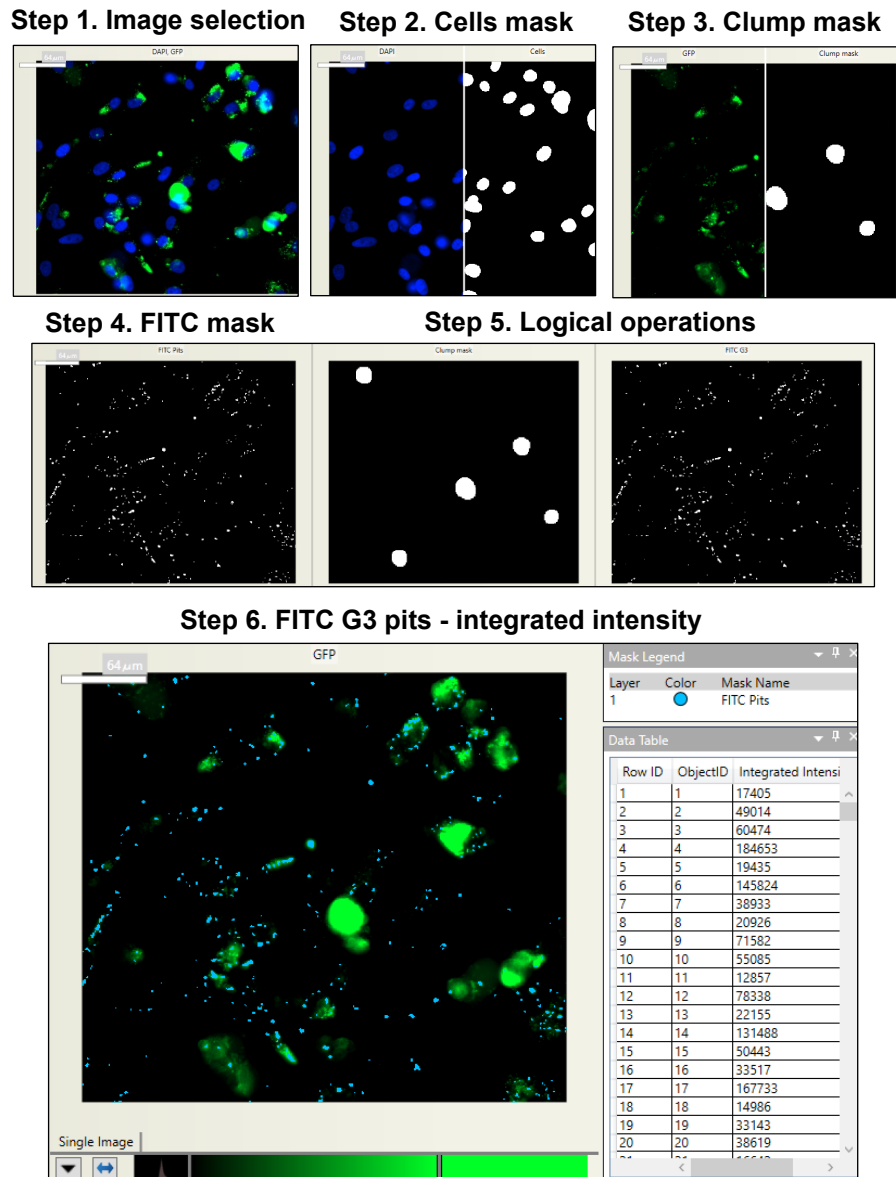


Fig. A1. Visual representation of CuME steps for non-specific staining removal. (Step 1) An image that shows the presence of FITC large clumps for the generation of the custom module editor (CuME). (Step 2) A representation of the "Cells" mask presenting the detected nuclei in white colour on the blue channel. (Step 3) The "Clump Mask" is represented in white, isolating large FITC clumps within the green channel. (Step 4) The identification of FITC Pits is depicted in white puncta in the "FITC" mask, highlighting these features after the subtraction of intensity values above local background levels. (Step 5) The "Logical Operations" tool utilizing the "ANDNOT" option, demonstrates the exclusion of the "Clump Mask" from the "FITC mask", resulting in the "FITC G3" mask that isolates individual FITC-positive objects. (Step 6) The quantification of the cellular integrated intensity (IIC) within the positive pits of the "FITC G3" mask is represented in blue over the green channel. A data table is automatically generated, listing individual IIC values.

Appendix B. Optimization of siRNA transfections.

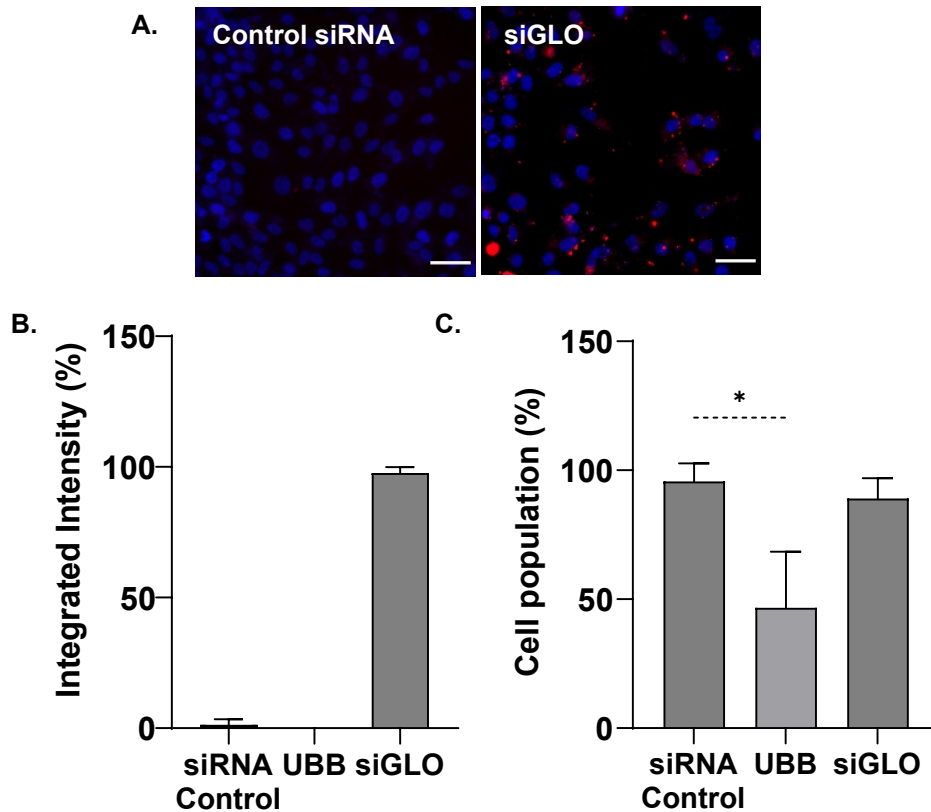


Fig. B1. Red-siGLO transfection optimization in LNCaP. (A) High content images of red siGLO transfection indicator inside LNCaP cells. Scale bar 50 μ m, 20X magnification. Nuclei is stained with Hoechst. (B) Integrated intensity values of red fluorescence expressed in percentages. Data is presented as means and \pm SD of one biological experiment with 3 replicates. Non-targeting siRNAs were used as a negative control. (C) Normalized cell population after UBB siRNA transfection. The statistical significance was established using student's t-test (*p=0.0204).

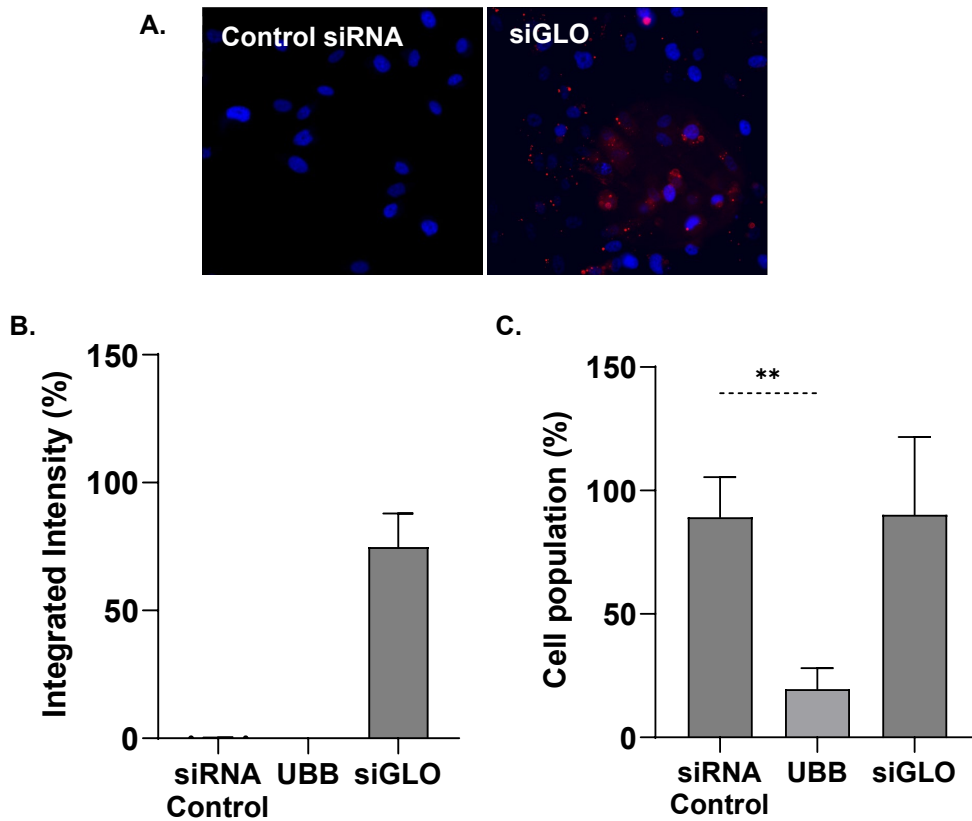


Fig. B2. Red-siGLO transfection optimization in PC-3. (A) High content images of red siGLO transfection indicator inside PC-3 cells. Scale bar 50 μm , 20X magnification. Nuclei is stained with Hoechst. (B) Integrated intensity values of red fluorescence expressed in percentages. Data is presented as means and \pm SD of one biological experiment with 3 replicates. Non-targeting siRNAs were used as a negative control. (C) Normalized cell population after UBB siRNA transfection. The statistical significance was established using student's t-test (** $p=0.0027$).

Appendix C. Optimization of Western Blots.

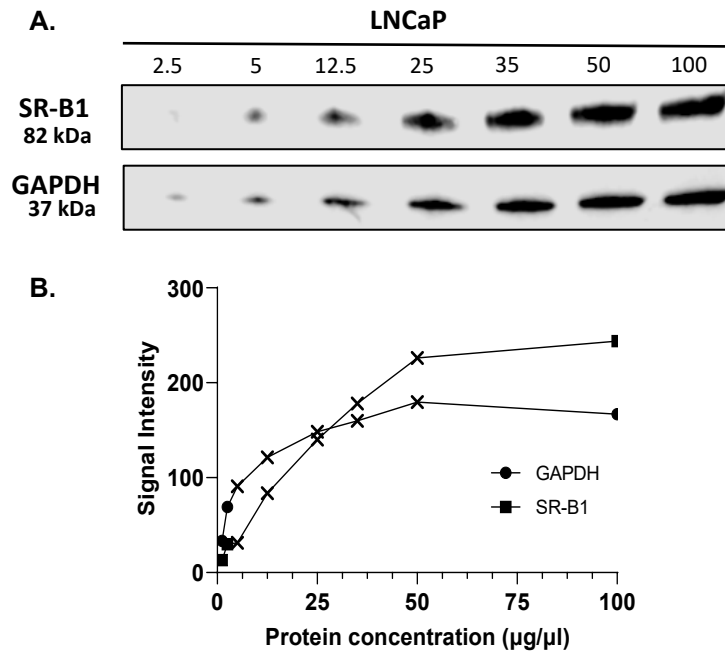


Fig. C1. SR-B1 and HKP linear range detection in LNCaP lysates. (A) Western blots of lysate dilutions of SR-B1 and GAPDH. Total protein load (μg) is indicated in lane labels. (B) Semi-quantification of protein relative levels. Cross symbols confines the interval of linear association between SR-B1 and HKP.

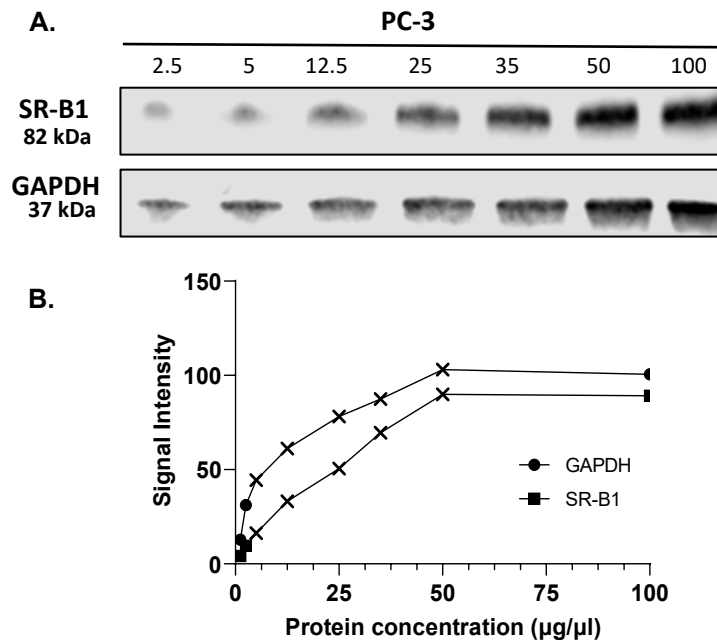


Fig. C2. SR-B1 and HKP linear range detection in PC-3 lysates. (A) Western blots of lysate dilutions of SR-B1 and GAPDH. Total protein load (μg) is indicated in lane labels. (B) Semi-quantification of protein relative levels. Cross symbols confines the interval of linear association between SR-B1 and HKP.

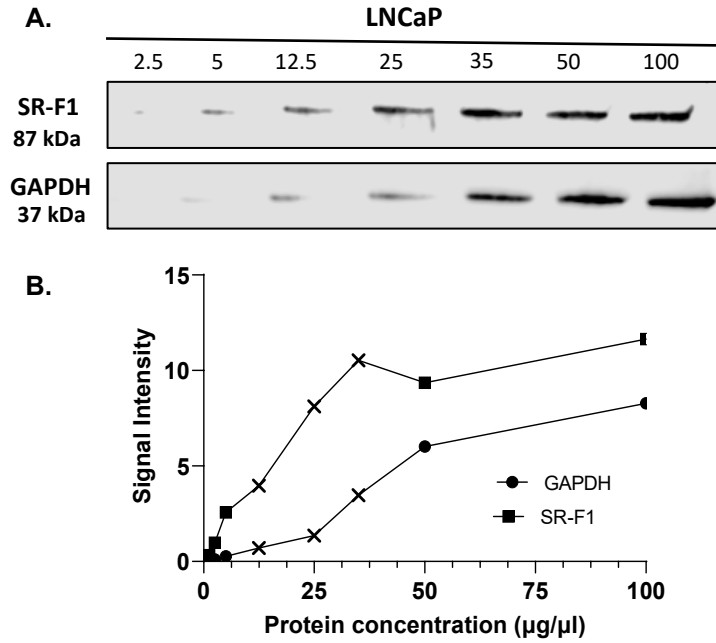


Fig. C3. SR-F1 and HKP linear range detection in LNCaP lysates. (A) Western blots of lysate dilutions of SR-F1 and GAPDH. Total protein load (μg) is indicated in lane labels. (B) Semi-quantification of protein relative levels. Cross symbols confines the interval of linear association between SR-F1 and HKP.

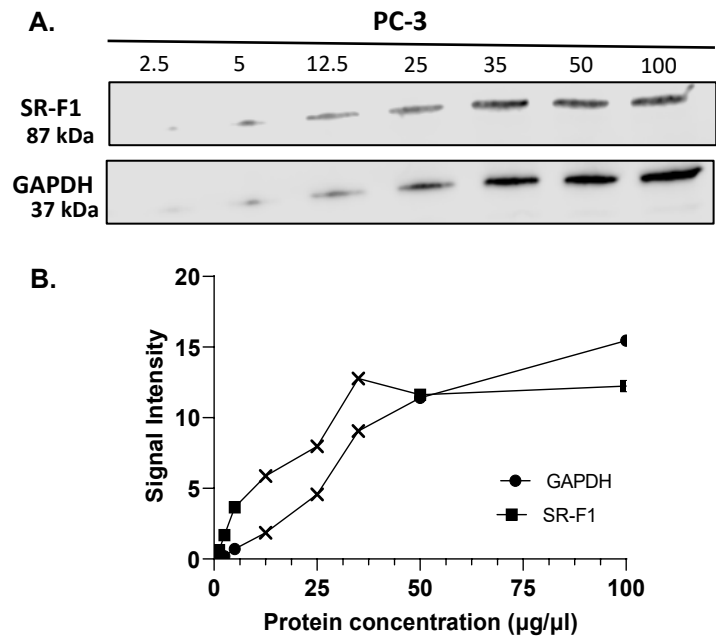


Fig. C4. SR-F1 and HKP linear range detection in PC-3 lysates. (A) Western blots of lysate dilutions of SR-F1 and GAPDH. Total protein load (μg) is indicated in lane labels. (B) Semi-quantification of protein relative levels. Cross symbols confines the interval of linear association between SR-F1 and HKP.

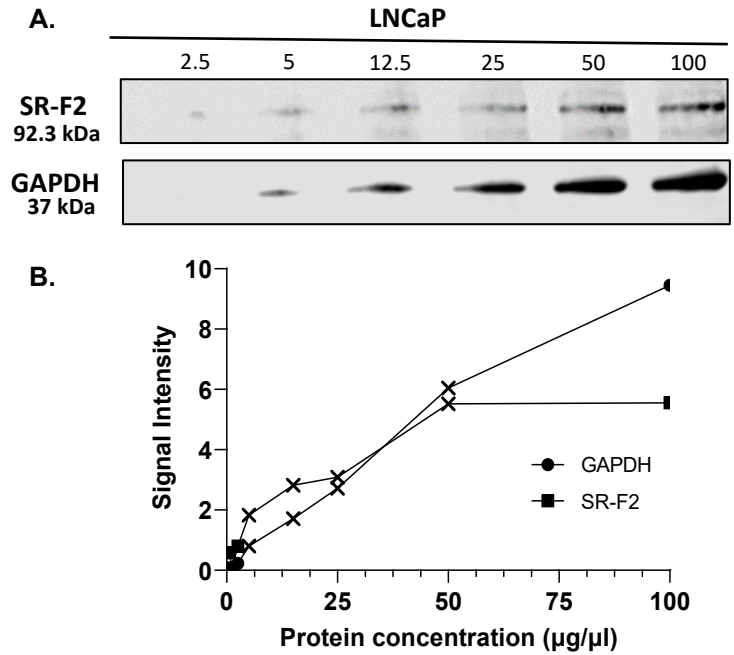


Fig. C5. SR-F2 and HKP linear range detection in LNCaP lysates. (A) Western blots of lysate dilutions of SR-F2 and GAPDH. Total protein load (μg) is indicated in lane labels. (B) Semi-quantification of protein relative levels. Cross symbols confines the interval of linear association between SR-F2 and HKP.

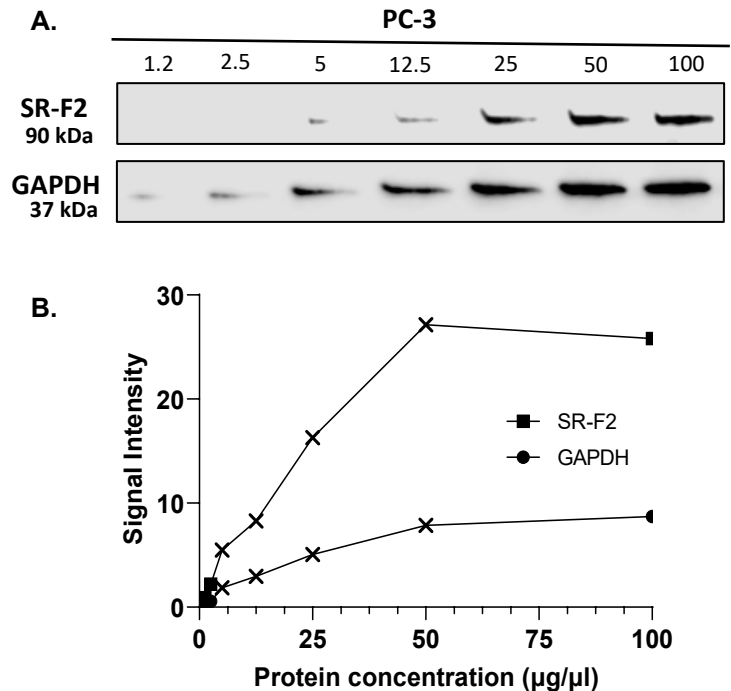


Fig. C6. SR-F2 and HKP linear range detection in PC-3 lysates. (A) Western blots of lysate dilutions of SR-F2 and GAPDH. Total protein load (μg) is indicated in lane labels. (B) Semi-quantification of protein relative levels. Cross symbols confines the interval of linear association between SR-F2 and HKP.

9. REFERENCES

- Abdul, M., Anezinis, P. E., Logothetis, C. J., & Hoosein, N. M. (1994). Growth inhibition of human prostatic carcinoma cell lines by serotonin antagonists. *Anticancer Research*, 14(3A), 1215–1220.
- Abeshouse, A., Ahn, J., Akbani, R., Ally, A., Amin, S., Andry, C. D., Annala, M., Aprikian, A., Armenia, J., Arora, A., Auman, J. T., Balasundaram, M., Balu, S., Barbieri, C. E., Bauer, T., Benz, C. C., Bergeron, A., Beroukhim, R., Berrios, M., ... Zmuda, E. (2015). The Molecular Taxonomy of Primary Prostate Cancer. *Cell*, 163(4), 1011–1025. <https://doi.org/10.1016/j.cell.2015.10.025>
- Abida, W., Armenia, J., Gopalan, A., Brennan, R., Walsh, M., Barron, D., Danila, D., Rathkopf, D., Morris, M., Slovin, S., McLaughlin, B., Curtis, K., Hyman, D. M., Durack, J. C., Solomon, S. B., Arcila, M. E., Zehir, A., Syed, A., Gao, J., ... Scher, H. I. (2017). Prospective Genomic Profiling of Prostate Cancer Across Disease States Reveals Germline and Somatic Alterations That May Affect Clinical Decision Making. *JCO Precision Oncology*, 1, 1–16. <https://doi.org/10.1200/PO.17.00029>
- Abida, W., Cheng, M. L., Armenia, J., Middha, S., Autio, K. A., Vargas, H. A., Rathkopf, D., Morris, M. J., Danila, D. C., Slovin, S. F., Carbone, E., Barnett, E. S., Hullings, M., Hechtman, J. F., Zehir, A., Shia, J., Jonsson, P., Stadler, Z. K., Srinivasan, P., ... Scher, H. I. (2019). Analysis of the Prevalence of Microsatellite Instability in Prostate Cancer and Response to Immune Checkpoint Blockade. *JAMA Oncology*, 5(4), 471. <https://doi.org/10.1001/jamaoncol.2018.5801>
- Abida, W., Cyrta, J., Heller, G., Prandi, D., Armenia, J., Coleman, I., Cieslik, M., Benelli, M., Robinson, D., Van Allen, E. M., Sboner, A., Fedrizzi, T., Mosquera, J. M., Robinson, B. D., De Sarkar, N., Kunju, L. P., Tomlins, S., Wu, Y. M., Nava Rodrigues, D., ... Sawyers, C. L. (2019). Genomic correlates of clinical outcome in advanced prostate cancer. *Proceedings of the National Academy of Sciences*, 116(23), 11428–11436. <https://doi.org/10.1073/pnas.1902651116>
- Abida, W., Patnaik, A., Campbell, D., Shapiro, J., Bryce, A. H., McDermott, R., Sautois, B., Vogelzang, N. J., Bambury, R. M., Voog, E., Zhang, J., Piulats, J. M., Ryan, C. J., Merseburger, A. S., Daugaard, G., Heidenreich, A., Fizazi, K., Higano, C. S., Krieger, L. E., ... Chowdhury, S. (2020). Rucaparib in Men With Metastatic Castration-Resistant Prostate Cancer Harboring a BRCA1 or BRCA2 Gene Alteration. *Journal of Clinical Oncology*, 38(32), 3763–3772. <https://doi.org/10.1200/JCO.20.01035>
- Abrahamsson, P.-A., Wadström, L. B., Alumets, J., Falkmer, S., & Grimelius, L. (1987). Peptide-Hormone- And Serotonin-Immunoreactive Tumour Cells in Carcinoma of the Prostate. *Pathology - Research and Practice*, 182(3), 298–307. [https://doi.org/10.1016/S0344-0338\(87\)80065-1](https://doi.org/10.1016/S0344-0338(87)80065-1)

- Abu-Farha, M., Lanouette, S., Elisma, F., Tremblay, V., Butson, J., Figeys, D., & Couture, J.-F. (2011). Proteomic analyses of the SMYD family interactomes identify HSP90 as a novel target for SMYD2. *Journal of Molecular Cell Biology*, 3(5), 301–308. <https://doi.org/10.1093/jmcb/mjr025>
- Acton, S., Rigotti, A., Landschulz, K. T., Xu, S., Hobbs, H. H., & Krieger, M. (1996). Identification of Scavenger Receptor SR-BI as a High Density Lipoprotein Receptor. *Science*, 271(5248), 518–520. <https://doi.org/10.1126/science.271.5248.518>
- Acton, S., Scherer, P., Lodish, H., & Krieger, M. (1994). Expression cloning of SR-BI, a CD36-related class B scavenger receptor. *The Journal of Biological Chemistry*, 269(33), 21003–21009.
- Adachi, H., Tsujimoto, M., Arai, H., & Inoue, K. (1997). Expression Cloning of a Novel Scavenger Receptor from Human Endothelial Cells. *Journal of Biological Chemistry*, 272(50), 31217–31220. <https://doi.org/10.1074/jbc.272.50.31217>
- Agrawal, P., Bhalla, S., Usmani, S. S., Singh, S., Chaudhary, K., Raghava, G. P. S., & Gautam, A. (2016). CPPsite 2.0: a repository of experimentally validated cell-penetrating peptides. *Nucleic Acids Research*, 44. <https://doi.org/10.1093/nar/gkv1266>
- Aguiar, L., Biosca, A., Lantero, E., Gut, J., Vale, N., Rosenthal, P. J., Nogueira, F., Andreu, D., Fernández-Busquets, X., & Gomes, P. (2019). Coupling the Antimalarial Cell Penetrating Peptide TP10 to Classical Antimalarial Drugs Primaquine and Chloroquine Produces Strongly Hemolytic Conjugates. *Molecules*, 24(24), 4559. <https://doi.org/10.3390/molecules24244559>
- Ahn, S., Lee, I.-H., Lee, E., Kim, H., Kim, Y.-C., & Jon, S. (2013). Oral delivery of an anti-diabetic peptide drug via conjugation and complexation with low molecular weight chitosan. *Journal of Controlled Release*, 170(2), 226–232. <https://doi.org/10.1016/j.jconrel.2013.05.031>
- Ahrens, V. M., Bellmann-Sickert, K., & Beck-Sickinger, A. G. (2012). Peptides and peptide conjugates: therapeutics on the upward path. *Future Medicinal Chemistry*, 4(12), 1567–1586. <https://doi.org/10.4155/fmc.12.76>
- Ai, S., Jia, T., Ai, W., Duan, J., Liu, Y., Chen, J., Liu, X., Yang, F., Tian, Y., & Huang, Z. (2013). Targeted delivery of doxorubicin through conjugation with EGF receptor-binding peptide overcomes drug resistance in human colon cancer cells. *British Journal of Pharmacology*, 168(7), 1719–1735. <https://doi.org/10.1111/bph.12055>
- Airhart, R. A., Barnett, T. F., Sullivan, J. W., Levine, R. L., & Schlegel, J. U. (1978). Flutamide therapy for carcinoma of the prostate. *Southern Medical Journal*, 71(7), 798–801. <https://doi.org/10.1097/00007611-197807000-00018>
- Alas, M., Saghaidehkordi, A., & Kaur, K. (2021). Peptide–Drug Conjugates with Different Linkers for Cancer Therapy. *Journal of Medicinal Chemistry*, 64(1), 216–232. <https://doi.org/10.1021/acs.jmedchem.0c01530>

- Al-Fayez, S., & El-Metwally, A. (2023). Cigarette smoking and prostate cancer: A systematic review and meta-analysis of prospective cohort studies. *Tobacco Induced Diseases*, 21(February), 1–12. <https://doi.org/10.18332/tid/157231>
- Alhakamy, N. A., & Berkland, C. J. (2013). Polyarginine Molecular Weight Determines Transfection Efficiency of Calcium Condensed Complexes. <https://doi.org/10.1021/mp3007117>
- Alquraini, A., & El Khoury, J. (2020). Scavenger receptors. *Current Biology*, 30(14), R790–R795. <https://doi.org/10.1016/J.CUB.2020.05.051>
- Alves, I. D., Jiao, C.-Y., Aubry, S., Aussedat, B., Burlina, F., Chassaing, G., & Sagan, S. (2010). Cell biology meets biophysics to unveil the different mechanisms of penetratin internalization in cells. *Biochimica et Biophysica Acta (BBA) - Biomembranes*, 1798(12), 2231–2239. <https://doi.org/10.1016/j.bbamem.2010.02.009>
- Ambrosio, S., Ballabio, A., & Majello, B. (2019). Histone methyl-transferases and demethylases in the autophagy regulatory network: the emerging role of KDM1A/LSD1 demethylase. *Autophagy*, 15(2), 187–196. <https://doi.org/10.1080/15548627.2018.1520546>
- Ambrosio, S., & Majello, B. (2018). Targeting Histone Demethylase LSD1/KDM1a in Neurodegenerative Diseases. *Journal of Experimental Neuroscience*, 12, 117906951876574. <https://doi.org/10.1177/1179069518765743>
- Ambrosio, S., Saccà, C. D., & Majello, B. (2017). Epigenetic regulation of epithelial to mesenchymal transition by the Lysine-specific demethylase LSD1/KDM1A. *Biochimica et Biophysica Acta (BBA) - Gene Regulatory Mechanisms*, 1860(9), 905–910. <https://doi.org/10.1016/j.bbagrm.2017.07.001>
- Amente, S., Lania, L., & Majello, B. (2013). The histone LSD1 demethylase in stemness and cancer transcription programs. *Biochimica et Biophysica Acta (BBA) - Gene Regulatory Mechanisms*, 1829(10), 981–986. <https://doi.org/10.1016/j.bbagrm.2013.05.002>
- Anastasio, N., Ben-Omran, T., Teebi, A., Ha, K. C. H., Lalonde, E., Ali, R., Almureikhi, M., Der Kaloustian, V. M., Liu, J., Rosenblatt, D. S., Majewski, J., & Jerome-Majewska, L. A. (2010). Mutations in SCARF2 Are Responsible for Van Den Ende-Gupta Syndrome. *The American Journal of Human Genetics*, 87(4), 553–559. <https://doi.org/10.1016/j.ajhg.2010.09.005>
- Antonarakis, E. S., Lu, C., Wang, H., Luber, B., Nakazawa, M., Roeser, J. C., Chen, Y., Mohammad, T. A., Chen, Y., Fedor, H. L., Lotan, T. L., Zheng, Q., De Marzo, A. M., Isaacs, J. T., Isaacs, W. B., Nadal, R., Paller, C. J., Denmeade, S. R., Carducci, M. A., ... Luo, J. (2014). AR-V7 and Resistance to Enzalutamide and Abiraterone in Prostate Cancer. *New England Journal of Medicine*, 371(11), 1028–1038. <https://doi.org/10.1056/NEJMoa1315815>
- Antonarakis, E. S., Shaikat, F., Isaacsson Velho, P., Kaur, H., Shenderov, E., Pardoll, D. M., & Lotan, T. L. (2019). Clinical Features and Therapeutic Outcomes in Men with Advanced Prostate Cancer and DNA Mismatch Repair Gene Mutations. *European Urology*, 75(3), 378–382. <https://doi.org/10.1016/j.eururo.2018.10.009>

- Antonny, B., Burd, C., De Camilli, P., Chen, E., Daumke, O., Faelber, K., Ford, M., Frolov, V. A., Frost, A., Hinshaw, J. E., Kirchhausen, T., Kozlov, M. M., Lenz, M., Low, H. H., McMahon, H., Merrifield, C., Pollard, T. D., Robinson, P. J., Roux, A., & Schmid, S. (2016). Membrane fission by dynamin: what we know and what we need to know. *The EMBO Journal*, 35(21), 2270–2284. <https://doi.org/10.15252/emj.201694613>
- Aparicio, A. M., Harzstark, A. L., Corn, P. G., Wen, S., Araujo, J. C., Tu, S.-M., Pagliaro, L. C., Kim, J., Millikan, R. E., Ryan, C., Tannir, N. M., Zurita, A. J., Mathew, P., Arap, W., Troncoso, P., Thall, P. F., & Logothetis, C. J. (2013). Platinum-Based Chemotherapy for Variant Castrate-Resistant Prostate Cancer. *Clinical Cancer Research*, 19(13), 3621–3630. <https://doi.org/10.1158/1078-0432.CCR-12-3791>
- Aprikian, A. G., Tremblay, L., Han, K., & Chevalier, S. (1997). Bombesin stimulates the motility of human prostate-carcinoma cells through tyrosine phosphorylation of focal adhesion kinase and of integrin-associated proteins. *J. Cancer*, 72, 498–504. [https://doi.org/10.1002/\(SICI\)1097-0215\(19970729\)72:3](https://doi.org/10.1002/(SICI)1097-0215(19970729)72:3)
- Arap, W., Pasqualini, R., & Ruoslahti, E. (1998). Cancer Treatment by Targeted Drug Delivery to Tumor Vasculature in a Mouse Model. *Science*, 279(5349), 377–380. <https://doi.org/10.1126/science.279.5349.377>
- Aravind, L., & Iyer, L. M. (2002). The SWIRM domain: a conserved module found in chromosomal proteins points to novel chromatin-modifying activities. *Genome Biology*, 3(8), RESEARCH0039. <https://doi.org/10.1186/gb-2002-3-8-research0039>
- Areschoug, T., & Gordon, S. (2008). Pattern Recognition Receptors and Their Role in Innate Immunity: Focus on Microbial Protein Ligands. In *Trends in Innate Immunity* (pp. 45–60). KARGER. <https://doi.org/10.1159/000135685>
- Areschoug, T., & Gordon, S. (2009). Scavenger receptors: role in innate immunity and microbial pathogenesis. *Cellular Microbiology*, 11(8), 1160–1169. <https://doi.org/10.1111/j.1462-5822.2009.01326.x>
- Armenia, J., Wankowicz, S. A. M., Liu, D., Gao, J., Kundra, R., Reznik, E., Chatila, W. K., Chakravarty, D., Han, G. C., Coleman, I., Montgomery, B., Pritchard, C., Morrissey, C., Barbieri, C. E., Beltran, H., Sboner, A., Zafeiriou, Z., Miranda, S., Bielski, C. M., ... Van Allen, E. M. (2018). The long tail of oncogenic drivers in prostate cancer. *Nature Genetics*, 50(5), 645–651. <https://doi.org/10.1038/s41588-018-0078-z>
- Armstrong, A. J., Szmulewitz, R. Z., Petrylak, D. P., Holzbeierlein, J., Villers, A., Azad, A., Alcaraz, A., Alekseev, B., Iguchi, T., Shore, N. D., Rosbrook, B., Sugg, J., Baron, B., Chen, L., & Stenzl, A. (2019). ARCHES: A Randomized, Phase III Study of Androgen Deprivation Therapy With Enzalutamide or Placebo in Men With Metastatic Hormone-Sensitive Prostate Cancer. *Journal of Clinical Oncology*, 37(32), 2974–2986. <https://doi.org/10.1200/JCO.19.00799>
- Arukuusk, P., Pärnaste, L., Margus, H., Eriksson, N. K. J., Vasconcelos, L., Padari, K., Pooga, M., & Langel, Ü. (2013). Differential Endosomal Pathways for

- Radically Modified Peptide Vectors. *Bioconjugate Chemistry*, 24(10), 1721–1732. <https://doi.org/10.1021/bc4002757>
- Asch, A. S., Barnwell, J., Silverstein, R. L., & Nachman, R. L. (1987). Isolation of the thrombospondin membrane receptor. *Journal of Clinical Investigation*, 79(4), 1054–1061. <https://doi.org/10.1172/JCI112918>
- Attard, G., Parker, C., Eeles, R. A., Schröder, F., Tomlins, S. A., Tannock, I., Drake, C. G., & de Bono, J. S. (2016). Prostate cancer. *The Lancet*, 387(10013), 70–82. [https://doi.org/10.1016/S0140-6736\(14\)61947-4](https://doi.org/10.1016/S0140-6736(14)61947-4)
- Augello, M. A., Liu, D., Deonaraine, L. D., Robinson, B. D., Huang, D., Stelloo, S., Blattner, M., Doane, A. S., Wong, E. W. P., Chen, Y., Rubin, M. A., Beltran, H., Elemento, O., Bergman, A. M., Zwart, W., Sboner, A., Dephoure, N., & Barbieri, C. E. (2019). CHD1 Loss Alters AR Binding at Lineage-Specific Enhancers and Modulates Distinct Transcriptional Programs to Drive Prostate Tumorigenesis. *Cancer Cell*, 35(4), 603-617.e8. <https://doi.org/10.1016/j.ccell.2019.03.001>
- Azhar, S., Leers-Sucheta, S., & Reaven, E. (2003). Cholesterol uptake in adrenal and gonadal tissues: the SR-BI and 'selective' pathway connection. *Frontiers in Bioscience : A Journal and Virtual Library*, 8, s998-1029. <https://doi.org/10.2741/1165>
- Baba, K., Kuwada, S., Nakao, A., Li, X., Okuda, N., Nishida, A., Mitsuda, S., Fukuoka, N., Takeya, H., & Kataoka, T. (2020). Different localization of lysosomal-associated membrane protein 1 (LAMP1) in mammalian cultured cell lines. *Histochemistry and Cell Biology*, 153(4), 199–213. <https://doi.org/10.1007/s00418-019-01842-z>
- Baca, S. C., Prandi, D., Lawrence, M. S., Mosquera, J. M., Romanel, A., Drier, Y., Park, K., Kitabayashi, N., MacDonald, T. Y., Ghandi, M., Van Allen, E., Kryukov, G. V., Sboner, A., Theurillat, J.-P., Soong, T. D., Nickerson, E., Auclair, D., Tewari, A., Beltran, H., ... Garraway, L. A. (2013). Punctuated Evolution of Prostate Cancer Genomes. *Cell*, 153(3), 666–677. <https://doi.org/10.1016/j.cell.2013.03.021>
- Baek, S. H., & Kim, K. II. (2016). Regulation of HIF-1 α stability by lysine methylation. *BMB Reports*, 49(5), 245–246. <https://doi.org/10.5483/BMBRep.2016.49.5.053>
- Bansal, A., & Simon, M. C. (2018). Glutathione metabolism in cancer progression and treatment resistance. *Journal of Cell Biology*, 217(7), 2291–2298. <https://doi.org/10.1083/jcb.201804161>
- Barber, L., Gerke, T., Markt, S. C., Peisch, S. F., Wilson, K. M., Ahearn, T., Giovannucci, E., Parmigiani, G., & Mucci, L. A. (2018). Family History of Breast or Prostate Cancer and Prostate Cancer Risk. *Clinical Cancer Research*, 24(23), 5910–5917. <https://doi.org/10.1158/1078-0432.CCR-18-0370>
- Bareford, L. M., & Swaan, P. W. (2007). Endocytic mechanisms for targeted drug delivery. *Advanced Drug Delivery Reviews*, 59(8), 748–758. <https://doi.org/10.1016/j.addr.2007.06.008>

- Bargh, J. D., Isidro-Llobet, A., Parker, J. S., & Spring, D. R. (2019). Cleavable linkers in antibody–drug conjugates. *Chemical Society Reviews*, 48(16), 4361–4374. <https://doi.org/10.1039/C8CS00676H>
- Barth, H., Schnober, E. K., Neumann-Haefelin, C., Thumann, C., Zeisel, M. B., Diepolder, H. M., Hu, Z., Liang, T. J., Blum, H. E., Thimme, R., Lambotin, M., & Baumert, T. F. (2008). Scavenger Receptor Class B Is Required for Hepatitis C Virus Uptake and Cross-Presentation by Human Dendritic Cells. *Journal of Virology*, 82(7), 3466–3479. <https://doi.org/10.1128/JVI.02478-07>
- Bartl, R., Bartl, C., & Gradingner, R. (2008). Einsatz der Bisphosphonate in der Orthopädie und Unfallchirurgie. *Der Orthopäde*, 37(6), 595–614. <https://doi.org/10.1007/s00132-008-1280-y>
- Barve, A., Jain, A., Liu, H., Jin, W., & Cheng, K. (2016). An enzyme-responsive conjugate improves the delivery of a PI3K inhibitor to prostate cancer. *Nanomedicine: Nanotechnology, Biology and Medicine*, 12(8), 2373–2381. <https://doi.org/10.1016/j.nano.2016.07.007>
- Bashari, O., Redko, B., Cohen, A., Luboshits, G., Gellerman, G., & Firer, M. A. (2017). Discovery of peptide drug carrier candidates for targeted multi-drug delivery into prostate cancer cells. *Cancer Letters*, 408, 164–173. <https://doi.org/10.1016/j.canlet.2017.08.040>
- Baskar, R., Lee, K. A., Yeo, R., & Yeoh, K.-W. (2012). Cancer and Radiation Therapy: Current Advances and Future Directions. *International Journal of Medical Sciences*, 9(3), 193–199. <https://doi.org/10.7150/ijms.3635>
- Basourakos, S. P., Tzeng, M., Lewicki, P. J., Patel, K., Al Hussein Al Awamlh, B., Venkat, S., Shoag, J. E., Gorin, M. A., Barbieri, C. E., & Hu, J. C. (2021). Tissue-Based Biomarkers for the Risk Stratification of Men With Clinically Localized Prostate Cancer. *Frontiers in Oncology*, 11. <https://doi.org/10.3389/fonc.2021.676716>
- Batra, A., & Winquist, E. (2018). Emerging cell cycle inhibitors for treating metastatic castration-resistant prostate cancer. *Expert Opinion on Emerging Drugs*, 23(4), 271–282. <https://doi.org/10.1080/14728214.2018.1547707>
- Bauer, T. M., Besse, B., Martinez-Marti, A., Trigo, J. M., Moreno, V., Garrido, P., Ferron-Brady, G., Wu, Y., Park, J., Collingwood, T., Kruger, R. G., Mohammad, H. P., Ballas, M. S., Dhar, A., & Govindan, R. (2019). Phase I, Open-Label, Dose-Escalation Study of the Safety, Pharmacokinetics, Pharmacodynamics, and Efficacy of GSK2879552 in Relapsed/Refractory SCLC. *Journal of Thoracic Oncology*, 14(10), 1828–1838. <https://doi.org/10.1016/j.jtho.2019.06.021>
- Baumann, G., & Mueller, P. (1974). A molecular model of membrane excitability. *Journal of Supramolecular Structure*, 2(5–6), 538–557. <https://doi.org/10.1002/jss.400020504>
- Baur, S., Rautenberg, M., Faulstich, M., Grau, T., Severin, Y., Unger, C., Hoffmann, W. H., Rudel, T., Autenrieth, I. B., & Weidenmaier, C. (2014). A Nasal Epithelial Receptor for *Staphylococcus aureus* WTA Governs Adhesion to Epithelial Cells and Modulates Nasal Colonization. *PLoS Pathogens*, 10(5), e1004089. <https://doi.org/10.1371/journal.ppat.1004089>

- Beauvillain, C., Meloni, F., Sirard, J.-C., Blanchard, S., Jarry, U., Scotet, M., Magistrelli, G., Delneste, Y., Barnaba, V., & Jeannin, P. (2010). The scavenger receptors SRA-1 and SREC-I cooperate with TLR2 in the recognition of the hepatitis C virus non-structural protein 3 by dendritic cells. *Journal of Hepatology*, 52(5), 644–651. <https://doi.org/10.1016/j.jhep.2009.11.031>
- Bechara, C., & Sagan, S. (2013). Cell-penetrating peptides: 20 years later, where do we stand? *FEBS Letters*, 587(12), 1693–1702. <https://doi.org/10.1016/j.febslet.2013.04.031>
- Beltran, H. (2013). DNA Mismatch Repair in Prostate Cancer. *Journal of Clinical Oncology*, 31(14), 1782–1784. <https://doi.org/10.1200/JCO.2012.48.4667>
- Beltran, H., Tomlins, S., Aparicio, A., Arora, V., Rickman, D., Ayala, G., Huang, J., True, L., Gleave, M. E., Soule, H., Logothetis, C., & Rubin, M. A. (2014). Aggressive Variants of Castration-Resistant Prostate Cancer. *Clinical Cancer Research*, 20(11), 2846–2850. <https://doi.org/10.1158/1078-0432.CCR-13-3309>
- Bennett, G., Brown, A., Mudd, G., Huxley, P., Van Rietschoten, K., Pavan, S., Chen, L., Watcham, S., Lahdenranta, J., & Keen, N. (2020). MMAE Delivery Using the Bicycle Toxin Conjugate BT5528. *Molecular Cancer Therapeutics*, 19(7), 1385–1394. <https://doi.org/10.1158/1535-7163.MCT-19-1092>
- Berg, J. S., Powell, B. C., & Cheney, R. E. (2001). A Millennial Myosin Census. *Molecular Biology of the Cell*, 12(4), 780–794. <https://doi.org/10.1091/mbc.12.4.780>
- Berwin, B., Delneste, Y., Lovingood, R. V., Post, S. R., & Pizzo, S. V. (2004). SREC-I, a Type F Scavenger Receptor, Is an Endocytic Receptor for Calreticulin. *Journal of Biological Chemistry*, 279(49), 51250–51257. <https://doi.org/10.1074/jbc.M406202200>
- Bhanji, Y., Isaacs, W. B., Xu, J., & Cooney, K. A. (2021). Prostate Cancer Predisposition. *Urologic Clinics of North America*, 48(3), 283–296. <https://doi.org/10.1016/j.ucl.2021.03.001>
- Bhat, M., Robichaud, N., Hulea, L., Sonenberg, N., Pelletier, J., & Topisirovic, I. (2015). Targeting the translation machinery in cancer. *Nature Reviews Drug Discovery*, 14(4), 261–278. <https://doi.org/10.1038/nrd4505>
- Bildstein, L., Dubernet, C., & Couvreur, P. (2011). Prodrug-based intracellular delivery of anticancer agents. *Advanced Drug Delivery Reviews*, 63(1–2), 3–23. <https://doi.org/10.1016/j.addr.2010.12.005>
- Binda, C., Valente, S., Romanenghi, M., Pilotto, S., Cirilli, R., Karytinis, A., Ciossani, G., Botrugno, O. A., Forneris, F., Tardugno, M., Edmondson, D. E., Minucci, S., Mattevi, A., & Mai, A. (2010). Biochemical, Structural, and Biological Evaluation of Tranylcyproamine Derivatives as Inhibitors of Histone Demethylases LSD1 and LSD2. *Journal of the American Chemical Society*, 132(19), 6827–6833. <https://doi.org/10.1021/ja101557k>
- Bocharov, A. V., Baranova, I. N., Vishnyakova, T. G., Remaley, A. T., Csako, G., Thomas, F., Patterson, A. P., & Eggerman, T. L. (2004). Targeting of

- Scavenger Receptor Class B Type I by Synthetic Amphipathic α -Helical-containing Peptides Blocks Lipopolysaccharide (LPS) Uptake and LPS-induced Pro-inflammatory Cytokine Responses in THP-1 Monocyte Cells. *Journal of Biological Chemistry*, 279(34), 36072–36082. <https://doi.org/10.1074/jbc.M314264200>
- Böhme, D., & Beck-Sickinger, A. G. (2015a). Controlling Toxicity of Peptide-Drug Conjugates by Different Chemical Linker Structures. *ChemMedChem*, 10(5), 804–814. <https://doi.org/10.1002/cmdc.201402514>
- Böhme, D., & Beck-Sickinger, A. G. (2015b). Controlling Toxicity of Peptide-Drug Conjugates by Different Chemical Linker Structures. *ChemMedChem*, 10(5), 804–814. <https://doi.org/10.1002/cmdc.201402514>
- Böhme, D., Krieghoff, J., & Beck-Sickinger, A. G. (2016). Double Methotrexate-Modified Neuropeptide Y Analogues Express Increased Toxicity and Overcome Drug Resistance in Breast Cancer Cells. *Journal of Medicinal Chemistry*, 59(7), 3409–3417. <https://doi.org/10.1021/acs.jmedchem.6b00043>
- Bonam, S. R., Wang, F., & Muller, S. (2019). Lysosomes as a therapeutic target. *Nature Reviews Drug Discovery*, 18(12), 923–948. <https://doi.org/10.1038/s41573-019-0036-1>
- Bonkhoff, H., Stein, U., & Remberger, K. (1994a). Multidirectional differentiation in the normal, hyperplastic, and neoplastic human prostate: Simultaneous demonstration of cell-specific epithelial markers. *Human Pathology*, 25(1), 42–46. [https://doi.org/10.1016/0046-8177\(94\)90169-4](https://doi.org/10.1016/0046-8177(94)90169-4)
- Bonkhoff, H., Stein, U., & Remberger, K. (1994b). The proliferative function of basal cells in the normal and hyperplastic human prostate. *The Prostate*, 24(3), 114–118. <https://doi.org/10.1002/PROS.2990240303>
- Borsi, L., Balza, E., Bestagno, M., Castellani, P., Carnemolla, B., Biro, A., Leprini, A., Sepulveda, J., Burrone, O., Neri, D., & Zardi, L. (2002). Selective targeting of tumoral vasculature: Comparison of different formats of an antibody (L19) to the ED-B domain of fibronectin. *International Journal of Cancer*, 102(1), 75–85. <https://doi.org/10.1002/ijc.10662>
- Bova, G. S., MacGrogan, D., Levy, A., Pin, S. S., Bookstein, R., & Isaacs, W. B. (1996). Physical Mapping of Chromosome 8p22 Markers and Their Homozygous Deletion in a Metastatic Prostate Cancer. *Genomics*, 35(1), 46–54. <https://doi.org/10.1006/geno.1996.0321>
- Bowen, C., Bubendorf, L., Voeller, H. J., Slack, R., Willi, N., Sauter, G., Gasser, T. C., Koivisto, P., Lack, E. E., Kononen, J., Kallioniemi, O. P., & Gelmann, E. P. (2000). Loss of NKX3.1 expression in human prostate cancers correlates with tumor progression. *Cancer Research*, 60(21), 6111–6115.
- Brankiewicz, W., Okońska, J., Serbakowska, K., Lica, J., Drab, M., Ptaszyńska, N., Łęgowska, A., Rolka, K., & Szweda, P. (2022). New Peptide Based Fluconazole Conjugates with Expanded Molecular Targets. *Pharmaceutics*, 14(4), 693. <https://doi.org/10.3390/pharmaceutics14040693>

- Branza-Nichita, N., Macovei, A., & Lazar, C. (2012). Caveolae-Dependent Endocytosis in Viral Infection. In *Molecular Regulation of Endocytosis*. InTech. <https://doi.org/10.5772/48538>
- Bray, F., Ferlay, J., Soerjomataram, I., Siegel, R. L., Torre, L. A., & Jemal, A. (2018). Global cancer statistics 2018: GLOBOCAN estimates of incidence and mortality worldwide for 36 cancers in 185 countries. *CA: A Cancer Journal for Clinicians*, 68(6), 394–424. <https://doi.org/10.3322/CAAC.21492>
- Brooke, G., & Bevan, C. (2009). The Role of Androgen Receptor Mutations in Prostate Cancer Progression. *Current Genomics*, 10(1), 18–25. <https://doi.org/10.2174/138920209787581307>
- Brundert, M., Ewert, A., Heeren, J., Behrendt, B., Ramakrishnan, R., Greten, H., Merkel, M., & Rinninger, F. (2005). Scavenger Receptor Class B Type I Mediates the Selective Uptake of High-Density Lipoprotein-Associated Cholesteryl Ester by the Liver in Mice. *Arteriosclerosis, Thrombosis, and Vascular Biology*, 25(1), 143–148. <https://doi.org/10.1161/01.ATV.0000149381.16166.c6>
- Bryant, H. E., Schultz, N., Thomas, H. D., Parker, K. M., Flower, D., Lopez, E., Kyle, S., Meuth, M., Curtin, N. J., & Helleday, T. (2005). Specific killing of BRCA2-deficient tumours with inhibitors of poly(ADP-ribose) polymerase. *Nature*, 434(7035), 913–917. <https://doi.org/10.1038/nature03443>
- Bubendorf, L., Kononen, J., Koivisto, P., Schraml, P., Moch, H., Gasser, T. C., Willi, N., Mihatsch, M. J., Sauter, G., & Kallioniemi, O. P. (1999). Survey of gene amplifications during prostate cancer progression by high-throughout fluorescence in situ hybridization on tissue microarrays. *Cancer Research*, 59(4), 803–806.
- Bucci, C., Parton, R. G., Mather, I. H., Stunnenberg, H., Simons, K., Hoflack, B., & Zerial, M. (1992). The small GTPase rab5 functions as a regulatory factor in the early endocytic pathway. *Cell*, 70(5), 715–728. [https://doi.org/10.1016/0092-8674\(92\)90306-W](https://doi.org/10.1016/0092-8674(92)90306-W)
- Burkhardt, L., Fuchs, S., Krohn, A., Masser, S., Mader, M., Kluth, M., Bachmann, F., Huland, H., Steuber, T., Graefen, M., Schlomm, T., Minner, S., Sauter, G., Sirma, H., & Simon, R. (2013). CHD1 Is a 5q21 Tumor Suppressor Required for ERG Rearrangement in Prostate Cancer. *Cancer Research*, 73(9), 2795–2805. <https://doi.org/10.1158/0008-5472.CAN-12-1342>
- Caffo, O., Veccia, A., Kinspergher, S., & Maines, F. (2018). Abiraterone acetate and its use in the treatment of metastatic prostate cancer: a review. *Future Oncology*, 14(5), 431–442. <https://doi.org/10.2217/fo-2017-0430>
- Cahoy, J. D., Emery, B., Kaushal, A., Foo, L. C., Zamanian, J. L., Christopherson, K. S., Xing, Y., Lubischer, J. L., Krieg, P. A., Krupenko, S. A., Thompson, W. J., & Barres, B. A. (2008). A Transcriptome Database for Astrocytes, Neurons, and Oligodendrocytes: A New Resource for Understanding Brain Development and Function. *The Journal of Neuroscience*, 28(1), 264–278. <https://doi.org/10.1523/JNEUROSCI.4178-07.2008>
- Cai, C., He, H. H., Chen, S., Coleman, I., Wang, H., Fang, Z., Chen, S., Nelson, P. S., Liu, X. S., Brown, M., & Balk, S. P. (2011). Androgen Receptor Gene

- Expression in Prostate Cancer Is Directly Suppressed by the Androgen Receptor Through Recruitment of Lysine-Specific Demethylase 1. *Cancer Cell*, 20(4), 457–471. <https://doi.org/10.1016/j.ccr.2011.09.001>
- Cai, C., He, H. H., Gao, S., Chen, S., Yu, Z., Gao, Y., Chen, S., Chen, M. W., Zhang, J., Ahmed, M., Wang, Y., Metzger, E., Schüle, R., Liu, X. S., Brown, M., & Balk, S. P. (2014). Lysine-Specific Demethylase 1 Has Dual Functions as a Major Regulator of Androgen Receptor Transcriptional Activity. *Cell Reports*, 9(5), 1618–1627. <https://doi.org/10.1016/j.celrep.2014.11.008>
- Canton, J., Neculai, D., & Grinstein, S. (2013). Scavenger receptors in homeostasis and immunity. *Nature Publishing Group*, 13. <https://doi.org/10.1038/nri3515>
- Carnesecchi, J., Cerutti, C., Vanacker, J.-M., & Forcet, C. (2017). ERR α protein is stabilized by LSD1 in a demethylation-independent manner. *PLOS ONE*, 12(11), e0188871. <https://doi.org/10.1371/journal.pone.0188871>
- Carnesecchi, J., Forcet, C., Zhang, L., Tribollet, V., Barenton, B., Boudra, R., Cerutti, C., Billas, I. M. L., Sérandour, A. A., Carroll, J. S., Beaudoin, C., & Vanacker, J.-M. (2017). ERR α induces H3K9 demethylation by LSD1 to promote cell invasion. *Proceedings of the National Academy of Sciences*, 114(15), 3909–3914. <https://doi.org/10.1073/pnas.1614664114>
- Carnevale, K. J. F., Muroski, M. E., Vakil, P. N., Foley, M. E., Laufersky, G., Kenworthy, R., Zorio, D. A. R., Morgan, T. J., Levenson, C. W., & Strouse, G. F. (2018). Selective Uptake into Drug Resistant Mammalian Cancer by Cell Penetrating Peptide-Mediated Delivery. *Bioconjugate Chemistry*, 29(10), 3273–3284. https://doi.org/10.1021/ACS.BIOCONJCHEM.8B00429/SUPPL_FILE/BC8B00429_SI_001.PDF
- Carrasco-Triguero, M., Yi, J.-H., Dere, R., Qiu, Z. J., Lei, C., Li, Y., Mahood, C., Wang, B., Leipold, D., Poon, K. A., & Kaur, S. (2013). Immunogenicity assays for antibody–drug conjugates: case study with ado-trastuzumab emtansine. *Bioanalysis*, 5(9), 1007–1023. <https://doi.org/10.4155/bio.13.64>
- Carver, B. S., Tran, J., Chen, Z., Carracedo-Perez, A., Alimonti, A., Nardella, C., Gopalan, A., Scardino, P. T., Cordon-Cardo, C., Gerald, W., & Pandolfi, P. P. (2009). ETS rearrangements and prostate cancer initiation. *Nature*, 457(7231), E1–E1. <https://doi.org/10.1038/nature07738>
- Castex, J., Willmann, D., Kanouni, T., Arrigoni, L., Li, Y., Friedrich, M., Schleicher, M., Wöhrle, S., Pearson, M., Kraut, N., Méret, M., Manke, T., Metzger, E., Schüle, R., & Günther, T. (2017). Inactivation of Lsd1 triggers senescence in trophoblast stem cells by induction of Sirt4. *Cell Death & Disease*, 8(2), e2631–e2631. <https://doi.org/10.1038/cddis.2017.48>
- Catalona, W. J., Smith, D. S., Ratliff, T. L., Dodds, K. M., Coplen, D. E., Yuan, J. J. J., Petros, J. A., & Andriole, G. L. (1991). Measurement of Prostate-Specific Antigen in Serum as a Screening Test for Prostate Cancer. *New England Journal of Medicine*, 324(17), 1156–1161. <https://doi.org/10.1056/NEJM199104253241702>

- Catanese, M. T., Ansuini, H., Graziani, R., Huby, T., Moreau, M., Ball, J. K., Paonessa, G., Rice, C. M., Cortese, R., Vitelli, A., & Nicosia, A. (2010). Role of Scavenger Receptor Class B Type I in Hepatitis C Virus Entry: Kinetics and Molecular Determinants. *Journal of Virology*, 84(1), 34–43. <https://doi.org/10.1128/JVI.02199-08>
- Catanese, M. T., Graziani, R., von Hahn, T., Moreau, M., Huby, T., Paonessa, G., Santini, C., Luzzago, A., Rice, C. M., Cortese, R., Vitelli, A., & Nicosia, A. (2007). High-Avidity Monoclonal Antibodies against the Human Scavenger Class B Type I Receptor Efficiently Block Hepatitis C Virus Infection in the Presence of High-Density Lipoprotein. *Journal of Virology*, 81(15), 8063–8071. <https://doi.org/10.1128/JVI.00193-07>
- Cato, L., de Tribolet-Hardy, J., Lee, I., Rottenberg, J. T., Coleman, I., Melchers, D., Houtman, R., Xiao, T., Li, W., Uo, T., Sun, S., Kuznik, N. C., Göppert, B., Ozgun, F., van Royen, M. E., Houtsmuller, A. B., Vadhi, R., Rao, P. K., Li, L., ... Brown, M. (2019). ARv7 Represses Tumor-Suppressor Genes in Castration-Resistant Prostate Cancer. *Cancer Cell*, 35(3), 401-413.e6. <https://doi.org/10.1016/j.ccell.2019.01.008>
- Chabner, B. A., & Roberts, T. G. (2005). Chemotherapy and the war on cancer. *Nature Reviews Cancer*, 5(1), 65–72. <https://doi.org/10.1038/nrc1529>
- Chance, B., Sies, H., & Boveris, A. (1979). Hydroperoxide metabolism in mammalian organs. *Physiological Reviews*, 59(3), 527–605. <https://doi.org/10.1152/physrev.1979.59.3.527>
- Chang, S. S., O'Keefe, D. S., Bacich, D. J., Reuter, V. E., Heston, W. D., & Gaudin, P. B. (1999). Prostate-specific membrane antigen is produced in tumor-associated neovasculature. *Clinical Cancer Research : An Official Journal of the American Association for Cancer Research*, 5(10), 2674–2681.
- Chang-Liu, C.-M., & Woloschak, G. E. (1997). Effect of passage number on cellular response to DNA-damaging agents: cell survival and gene expression. *Cancer Letters*, 113(1–2), 77–86. [https://doi.org/10.1016/S0304-3835\(97\)04599-0](https://doi.org/10.1016/S0304-3835(97)04599-0)
- Chao, A., Lin, C.-Y., Chao, A.-N., Tsai, C.-L., Chen, M.-Y., Lee, L.-Y., Chang, T.-C., Wang, T.-H., Lai, C.-H., & Wang, H.-S. (2017). Lysine-specific demethylase 1 (LSD1) destabilizes p62 and inhibits autophagy in gynecologic malignancies. *Oncotarget*, 8(43), 74434–74450. <https://doi.org/10.18632/oncotarget.20158>
- Chatzisideri, T., Leonidis, G., & Sarli, V. (2018). Cancer-targeted delivery systems based on peptides. *Future Medicinal Chemistry*, 10(18), 2201–2226. <https://doi.org/10.4155/fmc-2018-0174>
- Chen, C., Chen, Y., Yang, C., Zeng, P., Xu, H., Pan, F., & Lu, J. R. (2015). High Selective Performance of Designed Antibacterial and Anticancer Peptide Amphiphiles. *ACS Applied Materials and Interfaces*. <https://doi.org/10.1021/acsami.5b04547>
- Chen, C., Hu, J., Yang, C., Zhang, Y., Wang, F., Mu, Q., Pan, F., Xu, H., & Lu, J. R. (2016a). Amino acid side chains affect the bioactivity of designed short

- peptide amphiphiles. *Journal of Materials Chemistry B*, 4(13), 2359–2368. <https://doi.org/10.1039/C6TB00155F>
- Chen, C., Hu, J., Zeng, P., Chen, Y., Xu, H., & Lu, J. R. (2014). High Cell Selectivity and Low-Level Antibacterial Resistance of Designed Amphiphilic Peptide G(IKK) 3 I-NH 2. *ACS Applied Materials & Interfaces*, 6(19), 16529–16536. <https://doi.org/10.1021/am504973d>
- Chen, C., Hu, J., Zeng, P., Pan, F., Yaseen, M., Xu, H., & Lu, J. R. (2014a). Molecular mechanisms of anticancer action and cell selectivity of short α -helical peptides. *Biomaterials*, 35(5), 1552–1561. <https://doi.org/10.1016/j.biomaterials.2013.10.082>
- Chen, C., Hu, J., Zeng, P., Pan, F., Yaseen, M., Xu, H., & Lu, J. R. (2014b). Molecular mechanisms of anticancer action and cell selectivity of short α -helical peptides. *Biomaterials*, 35(5), 1552–1561. <https://doi.org/10.1016/j.biomaterials.2013.10.082>
- Chen, C., Hu, J., Zhang, S., Zhou, P., Zhao, X., Xu, H., Zhao, X., Yaseen, M., & Lu, J. R. (2012). Molecular mechanisms of antibacterial and antitumor actions of designed surfactant-like peptides. *Biomaterials*, 33(2), 592–603. <https://doi.org/10.1016/j.biomaterials.2011.09.059>
- Chen, C., Yang, C., Chen, Y., Wang, F., Mu, Q., Zhang, J., Li, Z., Pan, F., Xu, H., & Lu, J. R. (2016b). Surface Physical Activity and Hydrophobicity of Designed Helical Peptide Amphiphiles Control Their Bioactivity and Cell Selectivity. *ACS Applied Materials & Interfaces*, 8(40), 26501–26510. <https://doi.org/10.1021/acsami.6b08297>
- Chen, K., & Chen, X. (2011). Integrin Targeted Delivery of Chemotherapeutics. *Theranostics*, 1, 189–200. <https://doi.org/10.7150/thno/v01p0189>
- Chen, Y., Yang, Y., Wang, F., Wan, K., Yamane, K., Zhang, Y., & Lei, M. (2006). Crystal structure of human histone lysine-specific demethylase 1 (LSD1). *Proceedings of the National Academy of Sciences*, 103(38), 13956–13961. <https://doi.org/10.1073/pnas.0606381103>
- Chen, Y., Zhou, Q., Hankey, W., Fang, X., & Yuan, F. (2022). Second generation androgen receptor antagonists and challenges in prostate cancer treatment. *Cell Death & Disease*, 13(7), 632. <https://doi.org/10.1038/s41419-022-05084-1>
- Chen, Z., Wu, D., Thomas-Ahner, J. M., Lu, C., Zhao, P., Zhang, Q., Geraghty, C., Yan, P. S., Hankey, W., Sunkel, B., Cheng, X., Antonarakis, E. S., Wang, Q.-E., Liu, Z., Huang, T. H.-M., Jin, V. X., Clinton, S. K., Luo, J., Huang, J., & Wang, Q. (2018). Diverse AR-V7 cistromes in castration-resistant prostate cancer are governed by HoxB13. *Proceedings of the National Academy of Sciences*, 115(26), 6810–6815. <https://doi.org/10.1073/pnas.1718811115>
- Chen, Z., Zhang, P., Cheetham, A. G., Moon, J. H., Moxley, J. W., Lin, Y., & Cui, H. (2014). Controlled release of free doxorubicin from peptide–drug conjugates by drug loading. *Journal of Controlled Release*, 191, 123–130. <https://doi.org/10.1016/j.jconrel.2014.05.051>

- Cheng, X., Li, F., & Liang, L. (2022). Boron Neutron Capture Therapy: Clinical Application and Research Progress. *Current Oncology*, 29(10), 7868–7886. <https://doi.org/10.3390/currenconcol29100622>
- Cheng, X.-T., Xie, Y.-X., Zhou, B., Huang, N., Farfel-Becker, T., & Sheng, Z.-H. (2018). Characterization of LAMP1-labeled nondegradative lysosomal and endocytic compartments in neurons. *The Journal of Cell Biology*, 217(9), 3127–3139. <https://doi.org/10.1083/jcb.201711083>
- Chi, K. N., Agarwal, N., Bjartell, A., Chung, B. H., Pereira de Santana Gomes, A. J., Given, R., Juárez Soto, Á., Merseburger, A. S., Özgüroğlu, M., Uemura, H., Ye, D., Deprince, K., Naini, V., Li, J., Cheng, S., Yu, M. K., Zhang, K., Larsen, J. S., McCarthy, S., & Chowdhury, S. (2019). Apalutamide for Metastatic, Castration-Sensitive Prostate Cancer. *New England Journal of Medicine*, 381(1), 13–24. <https://doi.org/10.1056/NEJMoa1903307>
- Chiang, Y. T., Wang, K., Fazli, L., Qi, R. Z., Gleave, M. E., Collins, C. C., Gout, P. W., & Wang, Y. (2014). GATA2 as a potential metastasis-driving gene in prostate cancer. *Oncotarget*, 5(2), 451–461. <https://doi.org/10.18632/oncotarget.1296>
- Cho, H.-S., Suzuki, T., Dohmae, N., Hayami, S., Unoki, M., Yoshimatsu, M., Toyokawa, G., Takawa, M., Chen, T., Kurash, J. K., Field, H. I., Ponder, B. A. J., Nakamura, Y., & Hamamoto, R. (2011). Demethylation of RB Regulator MYPT1 by Histone Demethylase LSD1 Promotes Cell Cycle Progression in Cancer Cells. *Cancer Research*, 71(3), 655–660. <https://doi.org/10.1158/0008-5472.CAN-10-2446>
- Choi, J., Jang, H., Kim, H., Lee, J.-H., Kim, S.-T., Cho, E.-J., & Youn, H.-D. (2014). Modulation of lysine methylation in myocyte enhancer factor 2 during skeletal muscle cell differentiation. *Nucleic Acids Research*, 42(1), 224–234. <https://doi.org/10.1093/nar/gkt873>
- Choo, R., Klotz, L., Danjoux, C., Morton, G. C., DeBoer, G., Szumacher, E., Fleshner, N., Bunting, P., & Hruby, G. (2002). Feasibility study: watchful waiting for localized low to intermediate grade prostate carcinoma with selective delayed intervention based on prostate specific antigen, histological and/or clinical progression. *The Journal of Urology*, 167(4), 1664–1669.
- Christoforidis, S., McBride, H. M., Burgoyne, R. D., & Zerial, M. (1999). The Rab5 effector EEA1 is a core component of endosome docking. *Nature*, 397(6720), 621–625. <https://doi.org/10.1038/17618>
- Chua, C. W., Shibata, M., Lei, M., Toivanen, R., Barlow, L. J., Bergren, S. K., Badani, K. K., McKiernan, J. M., Benson, M. C., Hibshoosh, H., & Shen, M. M. (2014). Single luminal epithelial progenitors can generate prostate organoids in culture. *Nature Cell Biology*, 16(10), 951–961. <https://doi.org/10.1038/ncb3047>
- Chua, M. L. K., Lo, W., Pintilie, M., Murgic, J., Lalonde, E., Bhandari, V., Mahamud, O., Gopalan, A., Kweldam, C. F., van Leenders, G. J. L. H., Verhoef, E. I., Hoogland, A. M., Livingstone, J., Berlin, A., Dal Pra, A., Meng, A., Zhang, J., Orain, M., Picard, V., ... Bristow, R. G. (2017). A Prostate Cancer “Nimbusus”: Genomic Instability and SChLAP1 Dysregulation

- Underpin Aggression of Intraductal and Cribriform Subpathologies. *European Urology*, 72(5), 665–674. <https://doi.org/10.1016/j.eururo.2017.04.034>
- Chung, W.-S., Clarke, L. E., Wang, G. X., Stafford, B. K., Sher, A., Chakraborty, C., Joung, J., Foo, L. C., Thompson, A., Chen, C., Smith, S. J., & Barres, B. A. (2013). Astrocytes mediate synapse elimination through MEGF10 and MERTK pathways. *Nature*, 504(7480), 394–400. <https://doi.org/10.1038/nature12776>
- Ciriello, G., Miller, M. L., Aksoy, B. A., Senbabaoglu, Y., Schultz, N., & Sander, C. (2013). Emerging landscape of oncogenic signatures across human cancers. *Nature Genetics*, 45(10), 1127–1133. <https://doi.org/10.1038/ng.2762>
- Cirillo, S., Tomeh, M. A., Wilkinson, R. N., Hill, C., Brown, S., & Zhao, X. (2021). Designed Antitumor Peptide for Targeted siRNA Delivery into Cancer Spheroids. *ACS Applied Materials & Interfaces*, 13(42), 49713–49728. <https://doi.org/10.1021/acscami.1c14761>
- Civenni, G., Zoppi, G., Vazquez, R., Shinde, D., Paganoni, A., Kokanovic, A., Lee, S. H., Ruggeri, B., Carbone, G. M., & Catapano, C. V. (2018). INCB059872, a novel FAD-directed LSD1 Inhibitor, is active in prostate cancer models and impacts prostate cancer stem-like cells. *Cancer Research*, 78(13_Supplement), 1379–1379. <https://doi.org/10.1158/1538-7445.AM2018-1379>
- Claps, M., Mennitto, A., Guadalupi, V., Sepe, P., Stellato, M., Zattarin, E., Gillissen, S. S., Sternberg, C. N., Berruti, A., De Braud, F. G. M., Verzoni, E., & Procopio, G. (2020). Immune-checkpoint inhibitors and metastatic prostate cancer therapy: Learning by making mistakes. *Cancer Treatment Reviews*, 88, 102057. <https://doi.org/10.1016/j.ctrv.2020.102057>
- Clegg, N. J., Wongvipat, J., Joseph, J. D., Tran, C., Ouk, S., Dilhas, A., Chen, Y., Grillot, K., Bischoff, E. D., Cai, L., Aparicio, A., Dorow, S., Arora, V., Shao, G., Qian, J., Zhao, H., Yang, G., Cao, C., Sensintaffar, J., ... Hager, J. H. (2012). ARN-509: A Novel Antiandrogen for Prostate Cancer Treatment. *Cancer Research*, 72(6), 1494–1503. <https://doi.org/10.1158/0008-5472.CAN-11-3948>
- Cockshott, I. D., Cooper, K. J., Sweetmore, D. S., Blacklock, N. J., & Denis, L. (1990). The Pharmacokinetics of Casodex in Prostate Cancer Patients after Single and during Multiple Dosing. *European Urology*, 18(3), 10–17. <https://doi.org/10.1159/000463972>
- Collin, S. M., Metcalfe, C., Donovan, J., Lane, J. A., Davis, M., Neal, D., Hamdy, F., & Martin, R. M. (2008). Associations of lower urinary tract symptoms with prostate-specific antigen levels, and screen-detected localized and advanced prostate cancer: a case-control study nested within the UK population-based ProtecT (Prostate testing for cancer and Treatment) study. *BJU International*, 0(0), 080606123516618- <https://doi.org/10.1111/j.1464-410X.2008.07817.x>
- Collins, A. T., Berry, P. A., Hyde, C., Stower, M. J., & Maitland, N. J. (2005). Prospective Identification of Tumorigenic Prostate Cancer Stem Cells. *Cancer Research*, 65(23), 10946–10951. <https://doi.org/10.1158/0008-5472.CAN-05-2018>

- Comeau, J. W. D., Costantino, S., & Wiseman, P. W. (2006). A guide to accurate fluorescence microscopy colocalization measurements. *Biophysical Journal*, 91(12), 4611–4622. <https://doi.org/10.1529/biophysj.106.089441>
- Commisso, C., Davidson, S. M., Soydaner-Azeloglu, R. G., Parker, S. J., Kamphorst, J. J., Hackett, S., Grabocka, E., Nofal, M., Drebin, J. A., Thompson, C. B., Rabinowitz, J. D., Metallo, C. M., Vander Heiden, M. G., & Bar-Sagi, D. (2013). Macropinocytosis of protein is an amino acid supply route in Ras-transformed cells. *Nature*, 497(7451), 633–637. <https://doi.org/10.1038/nature12138>
- Connelly, M. A., & Williams, D. L. (2004). Scavenger receptor BI: A scavenger receptor with a mission to transport high density lipoprotein lipids. *Current Opinion in Lipidology*, 15(3), 287–295. <https://doi.org/10.1097/00041433-200406000-00008>
- Cooper, B. M., Iegre, J., O' Donovan, D. H., Ölwegård Halvarsson, M., & Spring, D. R. (2021). Peptides as a platform for targeted therapeutics for cancer: peptide–drug conjugates (PDCs). *Chemical Society Reviews*, 50(3), 1480–1494. <https://doi.org/10.1039/D0CS00556H>
- Cornford, P., van den Bergh, R. C. N., Briers, E., Van den Broeck, T., Cumberbatch, M. G., De Santis, M., Fanti, S., Fossati, N., Gandaglia, G., Gillissen, S., Grivas, N., Grummet, J., Henry, A. M., der Kwast, T. H. van, Lam, T. B., Laldas, M., Liew, M., Mason, M. D., Moris, L., ... Mottet, N. (2021). EAU-EANM-ESTRO-ESUR-SIOG Guidelines on Prostate Cancer. Part II—2020 Update: Treatment of Relapsing and Metastatic Prostate Cancer. *European Urology*, 79(2), 263–282. <https://doi.org/10.1016/j.eururo.2020.09.046>
- Cozzi, S., Bardoscia, L., Najafi, M., Igdem, S., Triggiani, L., Magrini, S. M., Botti, A., Guedea, F., Melocchi, L., Ciammella, P., Iotti, C., & Gutierrez, C. (2022). Ductal prostate cancer: Clinical features and outcomes from a multicenter retrospective analysis and overview of the current literature. *Current Urology*, 16(4), 218–226. <https://doi.org/10.1097/CU9.000000000000118>
- Crawford, E. D., Higano, C. S., Shore, N. D., Hussain, M., & Petrylak, D. P. (2015). Treating Patients with Metastatic Castration Resistant Prostate Cancer: A Comprehensive Review of Available Therapies. *Journal of Urology*, 194(6), 1537–1547. <https://doi.org/10.1016/j.juro.2015.06.106>
- Crawford, E. D., Schellhammer, P. F., McLeod, D. G., Moul, J. W., Higano, C. S., Shore, N., Denis, L., Iversen, P., Eisenberger, M. A., & Labrie, F. (2018). Androgen Receptor Targeted Treatments of Prostate Cancer: 35 Years of Progress with Antiandrogens. *Journal of Urology*, 200(5), 956–966. <https://doi.org/10.1016/j.juro.2018.04.083>
- Crombez, L., Morris, M. C., Dufort, S., Aldrian-Herrada, G., Nguyen, Q., Mc Master, G., Coll, J.-L., Heitz, F., & Divita, G. (2009). Targeting cyclin B1 through peptide-based delivery of siRNA prevents tumour growth. *Nucleic Acids Research*, 37(14), 4559–4569. <https://doi.org/10.1093/nar/gkp451>
- Crosio, M. A., Via, M. A., Cámara, C. I., Mangiarotti, A., Del Pópolo, M. G., & Wilke, N. (2019). Interaction of a Polyarginine Peptide with Membranes of

Different Mechanical Properties. *Biomolecules*, 9(10), 625.
<https://doi.org/10.3390/biom9100625>

- Culp, M. B., Soerjomataram, I., Efstathiou, J. A., Bray, F., & Jemal, A. (2020). Recent Global Patterns in Prostate Cancer Incidence and Mortality Rates. *European Urology*, 77(1), 38–52. <https://doi.org/10.1016/j.eururo.2019.08.005>
- Curnis, F., Sacchi, A., Borgna, L., Magni, F., Gasparri, A., & Corti, A. (2000). Enhancement of tumor necrosis factor α antitumor immunotherapeutic properties by targeted delivery to aminopeptidase N (CD13). *Nature Biotechnology*, 18(11), 1185–1190. <https://doi.org/10.1038/81183>
- Cussenot, O., Berthon, Ph., Berger, R., Mowszowicz, I., Faille, A., Hojman, F., Teillac, P., Le Duc, A., & Calvo, F. (1991). Immortalization of Human Adult Normal Prostatic Epithelial Cells by Liposomes Containing Large T-SV40 Gene. *Journal of Urology*, 146(3), 881–886. [https://doi.org/10.1016/S0022-5347\(17\)37953-3](https://doi.org/10.1016/S0022-5347(17)37953-3)
- Dai, X.-J., Liu, Y., Xiong, X.-P., Xue, L.-P., Zheng, Y.-C., & Liu, H.-M. (2020). Tranylcypromine Based Lysine-Specific Demethylase 1 Inhibitor: Summary and Perspective. *Journal of Medicinal Chemistry*, 63(23), 14197–14215. <https://doi.org/10.1021/acs.jmedchem.0c00919>
- Dal Pozzo, A., Ni, M.-H., Esposito, E., Dallavalle, S., Musso, L., Bargiotti, A., Pisano, C., Vesci, L., Bucci, F., Castorina, M., Foderà, R., Giannini, G., Aulicino, C., & Penco, S. (2010). Novel tumor-targeted RGD peptide–camptothecin conjugates: Synthesis and biological evaluation. *Bioorganic & Medicinal Chemistry*, 18(1), 64–72. <https://doi.org/10.1016/j.bmc.2009.11.019>
- Daly, M. B., Pal, T., Berry, M. P., Buys, S. S., Dickson, P., Domchek, S. M., Elkhanany, A., Friedman, S., Goggins, M., Hutton, M. L., Karlan, B. Y., Khan, S., Klein, C., Kohlmann, W., Kurian, A. W., Laronga, C., Litton, J. K., Mak, J. S., Menendez, C. S., ... Dwyer, M. A. (2021). Genetic/Familial High-Risk Assessment: Breast, Ovarian, and Pancreatic, Version 2.2021, NCCN Clinical Practice Guidelines in Oncology. *Journal of the National Comprehensive Cancer Network*, 19(1), 77–102. <https://doi.org/10.6004/jnccn.2021.0001>
- Dan, S., Song, Y., Duan, X., Pan, X., Chen, C., She, S., Su, T., Li, J., Chen, X., Zhou, Y., Chen, W., Zhang, X., Pan, X., Wang, Y.-J., & Kang, B. (2021). LSD1-mediated demethylation of OCT4 safeguards pluripotent stem cells by maintaining the transcription of PORE-motif-containing genes. *Scientific Reports*, 11(1), 10285. <https://doi.org/10.1038/s41598-021-89734-y>
- Dana, H., Chalbatani, G. M., Mahmoodzadeh, H., Karimloo, R., Rezaiean, O., Moradzadeh, A., Mehmandoust, N., Moazzen, F., Mazraeh, A., Marmari, V., Ebrahimi, M., Rashno, M. M., Abadi, S. J., & Gharagouzlo, E. (2017). Molecular Mechanisms and Biological Functions of siRNA. *International Journal of Biomedical Science : IJBS*, 13(2), 48–57.
- Darcey, E., & Boyle, T. (2018). Tobacco smoking and survival after a prostate cancer diagnosis: A systematic review and meta-analysis. *Cancer Treatment Reviews*, 70, 30–40. <https://doi.org/10.1016/j.ctrv.2018.07.001>
- Das, S., Al-Toubah, T., El-Haddad, G., & Strosberg, J. (2019). 177 Lu-DOTATATE for the treatment of gastroenteropancreatic neuroendocrine tumors. *Expert*

Review of Gastroenterology & Hepatology, 13(11), 1023–1031.
<https://doi.org/10.1080/17474124.2019.1685381>

- Davis, I. D., Martin, A. J., Stockler, M. R., Begbie, S., Chi, K. N., Chowdhury, S., Coskinas, X., Frydenberg, M., Hague, W. E., Horvath, L. G., Joshua, A. M., Lawrence, N. J., Marx, G., McCaffrey, J., McDermott, R., McJannett, M., North, S. A., Parnis, F., Parulekar, W., ... Sweeney, C. J. (2019). Enzalutamide with Standard First-Line Therapy in Metastatic Prostate Cancer. *New England Journal of Medicine*, 381(2), 121–131.
<https://doi.org/10.1056/NEJMoa1903835>
- Davis, R., Welcker, M., & Clurman, B. E. (2014). Tumor Suppression by the Fbw7 Ubiquitin Ligase: Mechanisms and Opportunities. *Cancer Cell*, 26(4), 455–464. <https://doi.org/10.1016/j.ccell.2014.09.013>
- De Bono, J., Mateo, J., Fizazi, K., Saad, F., Shore, N., Sandhu, S., Chi, K. N., Sartor, O., Agarwal, N., Olmos, D., Thiery-Vuillemin, A., Twardowski, P., Mehra, N., Goessl, C., Kang, J., Burgents, J., Wu, W., Kohlmann, A., Adelman, C. A., & Hussain, M. (2020). Olaparib for Metastatic Castration-Resistant Prostate Cancer. *New England Journal of Medicine*, 382(22), 2091–2102. <https://doi.org/10.1056/NEJMoa1911440>
- De la Llera-Moya, M., Rothblat, G. H., Connelly, M. A., Kellner-Weibel, G., Sakr, S. W., Phillips, M. C., & Williams, D. L. (1999). Scavenger receptor BI (SR-BI) mediates free cholesterol flux independently of HDL tethering to the cell surface. *Journal of Lipid Research*, 40(3), 575–580.
- Deane, R., Sagare, A., & Zlokovic, B. (2008). The Role of the Cell Surface LRP and Soluble LRP in Blood-Brain Barrier Aβ Clearance in Alzheimers Disease. *Current Pharmaceutical Design*, 14(16), 1601–1605.
<https://doi.org/10.2174/138161208784705487>
- DeBerardinis, R. J., & Chandel, N. S. (2016). Fundamentals of cancer metabolism. *Science Advances*, 2(5). <https://doi.org/10.1126/sciadv.1600200>
- Demeule, M., Currie, J.-C., Bertrand, Y., Ché, C., Nguyen, T., Régina, A., Gabathuler, R., Castaigne, J.-P., & Béliveau, R. (2008). Involvement of the low-density lipoprotein receptor-related protein in the transcytosis of the brain delivery vector Angiopep-2. *Journal of Neurochemistry*, 106(4), 1534–1544.
<https://doi.org/10.1111/j.1471-4159.2008.05492.x>
- Demeule, M., Régina, A., Ché, C., Poirier, J., Nguyen, T., Gabathuler, R., Castaigne, J.-P., & Béliveau, R. (2008). Identification and Design of Peptides as a New Drug Delivery System for the Brain. *Journal of Pharmacology and Experimental Therapeutics*, 324(3), 1064–1072.
<https://doi.org/10.1124/jpet.107.131318>
- Denmeade, S. R., & Isaacs, J. T. (2005). The SERCA pump as a therapeutic target: Making a “smart bomb” for prostate cancer. *Cancer Biology & Therapy*, 4(1), 21–29. <https://doi.org/10.4161/cbt.4.1.1505>
- Denmeade, S. R., Jakobsen, C. M., Janssen, S., Khan, S. R., Garrett, E. S., Lilja, H., Christensen, S. B., & Isaacs, J. T. (2003). Prostate-Specific Antigen-Activated Thapsigargin Prodrug as Targeted Therapy for Prostate Cancer.

JNCI Journal of the National Cancer Institute, 95(13), 990–1000.
<https://doi.org/10.1093/jnci/95.13.990>

- Denmeade, S. R., Mhaka, A. M., Rosen, D. M., Brennen, W. N., Dalrymple, S., Dach, I., Olesen, C., Gurel, B., DeMarzo, A. M., Wilding, G., Carducci, M. A., Dionne, C. A., Møller, J. V., Nissen, P., Christensen, S. B., & Isaacs, J. T. (2012). Engineering a Prostate-Specific Membrane Antigen–Activated Tumor Endothelial Cell Prodrug for Cancer Therapy. *Science Translational Medicine*, 4(140). <https://doi.org/10.1126/scitranslmed.3003886>
- Derakhshankhah, H., & Jafari, S. (2018). Cell penetrating peptides: A concise review with emphasis on biomedical applications. *Biomedicine & Pharmacotherapy*, 108, 1090–1096.
<https://doi.org/10.1016/J.BIOPHA.2018.09.097>
- Derossi, D., Calvet, S., Trembleau, A., Brunissen, A., Chassaing, G., & Prochiantz, A. (1996). Cell Internalization of the Third Helix of the Antennapedia Homeodomain Is Receptor-independent. *Journal of Biological Chemistry*, 271(30), 18188–18193. <https://doi.org/10.1074/jbc.271.30.18188>
- Derossi, D., Chassaing, G., & Prochiantz, A. (1998). Trojan peptides: the penetratin system for intracellular delivery. *Trends in Cell Biology*, 8(2), 84–87. [https://doi.org/10.1016/S0962-8924\(98\)80017-2](https://doi.org/10.1016/S0962-8924(98)80017-2)
- Desai, B., Ma, T., Zhu, J., & Chellaiah, M. A. (2009). Characterization of the expression of variant and standard CD44 in prostate cancer cells: Identification of the possible molecular mechanism of CD44/MMP9 complex formation on the cell surface. *Journal of Cellular Biochemistry*, 108(1), 272–284. <https://doi.org/10.1002/jcb.22248>
- Desai, K., McManus, J. M., & Sharifi, N. (2021). Hormonal Therapy for Prostate Cancer. *Endocrine Reviews*, 42(3), 354–373.
<https://doi.org/10.1210/endrev/bnab002>
- Desgrosellier, J. S., & Cheresh, D. A. (2010). Integrins in cancer: biological implications and therapeutic opportunities. *Nature Reviews Cancer*, 10(1), 9–22. <https://doi.org/10.1038/nrc2748>
- Deshayes, S., Morris, M., Heitz, F., & Divita, G. (2008). Delivery of proteins and nucleic acids using a non-covalent peptide-based strategy. *Advanced Drug Delivery Reviews*, 60(4–5), 537–547.
<https://doi.org/10.1016/j.addr.2007.09.005>
- Desnos, C., Huet, S., & Darchen, F. (2007). ‘Should I stay or should I go?’: myosin V function in organelle trafficking. *Biology of the Cell*, 99(8), 411–423.
<https://doi.org/10.1042/BC20070021>
- Dess, R. T., Hartman, H. E., Mahal, B. A., Soni, P. D., Jackson, W. C., Cooperberg, M. R., Amling, C. L., Aronson, W. J., Kane, C. J., Terris, M. K., Zumsteg, Z. S., Butler, S., Osborne, J. R., Morgan, T. M., Mehra, R., Salami, S. S., Kishan, A. U., Wang, C., Schaeffer, E. M., ... Spratt, D. E. (2019). Association of Black Race With Prostate Cancer–Specific and Other-Cause Mortality. *JAMA Oncology*, 5(7), 975.
<https://doi.org/10.1001/jamaoncol.2019.0826>

- DeVita, V. T., & Chu, E. (2008). A History of Cancer Chemotherapy. *Cancer Research*, 68(21), 8643–8653. <https://doi.org/10.1158/0008-5472.CAN-07-6611>
- DeWitte-Orr, S. J., Collins, S. E., Bauer, C. M. T., Bowdish, D. M., & Mossman, K. L. (2010). An Accessory to the 'Trinity': SR-As Are Essential Pathogen Sensors of Extracellular dsRNA, Mediating Entry and Leading to Subsequent Type I IFN Responses. *PLoS Pathogens*, 6(3), e1000829. <https://doi.org/10.1371/journal.ppat.1000829>
- Dhir, R., Gau, J., Krill, D., Bastacky, S., Bahnson, R., Cooper, D., & Becich, M. (1997). CD44 Expression in Benign and Neoplastic Human Prostates. *Molecular Diagnosis : A Journal Devoted to the Understanding of Human Disease through the Clinical Application of Molecular Biology*, 2(3), 197–204. <https://doi.org/10.1054/MODI00200197>
- Di Sant'Agnese, P. A., & De Mesy Jensen, K. L. (1984). Somatostatin and/or somatostatinlike immunoreactive endocrine-paracrine cells in the human prostate gland. *Archives of Pathology and Laboratory Medicine*, 108(9), 693–696.
- Di Sant'Agnese, P. A., De Mesy Jensen, K. L., & Ackroyd, R. K. (1989). Calcitonin, katalcalcin, and calcitonin gene-related peptide in the human prostate. An immunocytochemical and immunoelectron microscopic study. *Archives of Pathology and Laboratory Medicine*, 113(7), 790–796.
- Diwu, Z., Chen, C. S., Zhang, C., Klaubert, D. H., & Haugland, R. P. (1999). A novel acidotropic pH indicator and its potential application in labeling acidic organelles of live cells. *Chemistry & Biology*, 6(7), 411–418. [https://doi.org/10.1016/s1074-5521\(99\)80059-3](https://doi.org/10.1016/s1074-5521(99)80059-3)
- Dominguez-Valentin, M., Sampson, J. R., Seppälä, T. T., ten Broeke, S. W., Plazzer, J.-P., Nakken, S., Engel, C., Aretz, S., Jenkins, M. A., Sunde, L., Bernstein, I., Capella, G., Balaguer, F., Thomas, H., Evans, D. G., Burn, J., Greenblatt, M., Hovig, E., de Vos tot Nederveen Cappel, W. H., ... Møller, P. (2020). Cancer risks by gene, age, and gender in 6350 carriers of pathogenic mismatch repair variants: findings from the Prospective Lynch Syndrome Database. *Genetics in Medicine*, 22(1), 15–25. <https://doi.org/10.1038/s41436-019-0596-9>
- Dong, J., Pervaiz, W., Tayyab, B., Li, D., Kang, L., Zhang, H., Gong, H., Ma, X., Li, J., Agboyibor, C., Bi, Y., & Liu, H. (2022). A comprehensive comparative study on LSD1 in different cancers and tumor specific LSD1 inhibitors. *European Journal of Medicinal Chemistry*, 240, 114564. <https://doi.org/10.1016/j.ejmech.2022.114564>
- Dougherty, P. G., Sahni, A., & Pei, D. (2019). Understanding Cell Penetration of Cyclic Peptides. *Chemical Reviews*, 119(17), 10241–10287. https://doi.org/10.1021/ACS.CHEMREV.9B00008/ASSET/IMAGES/MEDIUM/CR-2019-000087_0023.GIF
- Draffin, J. E., McFarlane, S., Hill, A., Johnston, P. G., & Waugh, D. J. J. (2004). CD44 Potentiates the Adherence of Metastatic Prostate and Breast Cancer

- Cells to Bone Marrow Endothelial Cells. *Cancer Research*, 64(16), 5702–5711. <https://doi.org/10.1158/0008-5472.CAN-04-0389>
- Dreher, M. R., Liu, W., Michelich, C. R., Dewhirst, M. W., Yuan, F., & Chilkoti, A. (2006). Tumor Vascular Permeability, Accumulation, and Penetration of Macromolecular Drug Carriers. *JNCI: Journal of the National Cancer Institute*, 98(5), 335–344. <https://doi.org/10.1093/jnci/djj070>
- Duan, Y.-C., Ma, Y.-C., Qin, W.-P., Ding, L.-N., Zheng, Y.-C., Zhu, Y.-L., Zhai, X.-Y., Yang, J., Ma, C.-Y., & Guan, Y.-Y. (2017). Design and synthesis of tranylcypramine derivatives as novel LSD1/HDACs dual inhibitors for cancer treatment. *European Journal of Medicinal Chemistry*, 140, 392–402. <https://doi.org/10.1016/j.ejmech.2017.09.038>
- Duchardt, F., Fotin-Mleczek, M., Schwarz, H., Fischer, R., & Brock, R. (2007). A Comprehensive Model for the Cellular Uptake of Cationic Cell-penetrating Peptides. *Traffic*, 8(7), 848–866. <https://doi.org/10.1111/j.1600-0854.2007.00572.x>
- Duncan, M. W., & Thompson, H. S. (2007). Proteomics of semen and its constituents. *Proteomics Clin. Appl*, 1, 861–875. <https://doi.org/10.1002/prca.200700228>
- Dunn, K. W., Kamocka, M. M., & McDonald, J. H. (2011). A practical guide to evaluating colocalization in biological microscopy. *American Journal of Physiology-Cell Physiology*, 300(4), C723–C742. <https://doi.org/10.1152/ajpcell.00462.2010>
- During, A., Dawson, H. D., & Harrison, E. H. (2005). Carotenoid Transport Is Decreased and Expression of the Lipid Transporters SR-BI, NPC1L1, and ABCA1 Is Downregulated in Caco-2 Cells Treated with Ezetimibe. *The Journal of Nutrition*, 135(10), 2305–2312. <https://doi.org/10.1093/jn/135.10.2305>
- Eberle, R. J., Gering, I., Tusche, M., Ostermann, P. N., Müller, L., Adams, O., Schaal, H., Olivier, D. S., Amaral, M. S., Arni, R. K., Willbold, D., & Coronado, M. A. (2022). Design of D-Amino Acids SARS-CoV-2 Main Protease Inhibitors Using the Cationic Peptide from Rattlesnake Venom as a Scaffold. *Pharmaceuticals*, 15(5), 540. <https://doi.org/10.3390/ph15050540>
- Edwards, S., Campbell, C., Flohr, P., Shipley, J., Giddings, I., te-Poele, R., Dodson, A., Foster, C., Clark, J., Jhavar, S., Kovacs, G., & Cooper, C. S. (2005). Expression analysis onto microarrays of randomly selected cDNA clones highlights HOXB13 as a marker of human prostate cancer. *British Journal of Cancer*, 92(2), 376–381. <https://doi.org/10.1038/sj.bjc.6602261>
- Eggerer, S. E., Rumble, R. B., Armstrong, A. J., Morgan, T. M., Crispino, T., Cornford, P., van der Kwast, T., Grignon, D. J., Rai, A. J., Agarwal, N., Klein, E. A., Den, R. B., & Beltran, H. (2020). Molecular Biomarkers in Localized Prostate Cancer: ASCO Guideline. *Journal of Clinical Oncology*, 38(13), 1474–1494. <https://doi.org/10.1200/JCO.19.02768>
- Ehrlich, P. (1901). Die seitenkettentheorie und ihre gegner. *Münchner Med Wochenschr* 52: 2123-2124.

- Eiselt, É., Otis, V., Belleville, K., Yang, G., Larocque, A., Régina, A., Demeule, M., Sarret, P., & Gendron, L. (2020). Use of a Noninvasive Brain-Penetrating Peptide-Drug Conjugate Strategy to Improve the Delivery of Opioid Pain Relief Medications to the Brain. *Journal of Pharmacology and Experimental Therapeutics*, 374(1), 52–61. <https://doi.org/10.1124/jpet.119.263566>
- El-Andaloussi, S., Johansson, H. J., Holm, T., & Langel, Ü. (2007). A Novel Cell-penetrating Peptide, M918, for Efficient Delivery of Proteins and Peptide Nucleic Acids. *Molecular Therapy*, 15(10), 1820–1826. <https://doi.org/10.1038/SJ.MT.6300255>
- Elbashir, S. M., Harborth, J., Lendeckel, W., Yalcin, A., Weber, K., & Tuschl, T. (2001). Duplexes of 21-nucleotide RNAs mediate RNA interference in cultured mammalian cells. *Nature*, 411(6836), 494–498. <https://doi.org/10.1038/35078107>
- Elia, A. R., Caputo, S., & Bellone, M. (2018). Immune Checkpoint-Mediated Interactions Between Cancer and Immune Cells in Prostate Adenocarcinoma and Melanoma. *Frontiers in Immunology*, 9. <https://doi.org/10.3389/fimmu.2018.01786>
- Engel, J. C., Palsdottir, T., Aly, M., Egevad, L., Grönberg, H., Eklund, M., & Nordström, T. (2020). Lower urinary tract symptoms (LUTS) are not associated with an increased risk of prostate cancer in men 50–69 years with PSA \geq 3 ng/ml. *Scandinavian Journal of Urology*, 54(1), 1–6. <https://doi.org/10.1080/21681805.2019.1703806>
- Epstein, J. I., Amin, M. B., Fine, S. W., Algaba, F., Aron, M., Baydar, D. E., Beltran, A. L., Brimo, F., Cheville, J. C., Coicchia, M., Comperat, E., da Cunha, I. W., Delprado, W., DeMarzo, A. M., Giannico, G. A., Gordetsky, J. B., Guo, C. C., Hansel, D. E., Hirsch, M. S., ... Trpkov, K. (2021). The 2019 Genitourinary Pathology Society (GUPS) White Paper on Contemporary Grading of Prostate Cancer. *Archives of Pathology & Laboratory Medicine*, 145(4), 461–493. <https://doi.org/10.5858/arpa.2020-0015-RA>
- Epstein, J. I., Zelefsky, M. J., Sjoberg, D. D., Nelson, J. B., Egevad, L., Magi-Galluzzi, C., Vickers, A. J., Parwani, A. V., Reuter, V. E., Fine, S. W., Eastham, J. A., Wiklund, P., Han, M., Reddy, C. A., Ciezki, J. P., Nyberg, T., & Klein, E. A. (2016). A Contemporary Prostate Cancer Grading System: A Validated Alternative to the Gleason Score. *European Urology*, 69(3), 428–435. <https://doi.org/10.1016/j.eururo.2015.06.046>
- Eri, L. M., & Tveter, K. J. (1993). A Prospective, Placebo-Controlled Study of the Antiandrogen Casodex as Treatment for Patients with Benign Prostatic Hyperplasia. *Journal of Urology*, 150(1), 90–94. [https://doi.org/10.1016/S0022-5347\(17\)35406-X](https://doi.org/10.1016/S0022-5347(17)35406-X)
- Escola, J.-M., Kleijmeer, M. J., Stoorvogel, W., Griffith, J. M., Yoshie, O., & Geuze, H. J. (1998). Selective Enrichment of Tetraspan Proteins on the Internal Vesicles of Multivesicular Endosomes and on Exosomes Secreted by Human B-lymphocytes. *Journal of Biological Chemistry*, 273(32), 20121–20127. <https://doi.org/10.1074/jbc.273.32.20121>

- Eskelinen, E.-L. (2006). Roles of LAMP-1 and LAMP-2 in lysosome biogenesis and autophagy. *Molecular Aspects of Medicine*, 27(5–6), 495–502. <https://doi.org/10.1016/j.mam.2006.08.005>
- Ewing, C. M., Ray, A. M., Lange, E. M., Zuhlke, K. A., Robbins, C. M., Tembe, W. D., Wiley, K. E., Isaacs, S. D., Johng, D., Wang, Y., Bizon, C., Yan, G., Gielzak, M., Partin, A. W., Shanmugam, V., Izatt, T., Sinari, S., Craig, D. W., Zheng, S. L., ... Cooney, K. A. (2012). Germline Mutations in HOXB13 and Prostate-Cancer Risk. *New England Journal of Medicine*, 366(2), 141–149. <https://doi.org/10.1056/NEJMoa1110000>
- Ezzat, K., Helmfors, H., Tudoran, O., Juks, C., Lindberg, S., Padari, K., El-Andaloussi, S., Pooga, M., & Langel, Ü. (2012). Scavenger receptor-mediated uptake of cell-penetrating peptide nanocomplexes with oligonucleotides. *The FASEB Journal*, 26(3), 1172–1180. <https://doi.org/10.1096/fj.11-191536>
- Facciponte, J. G., Wang, X.-Y., & Subject, J. R. (2007). Hsp110 and Grp170, members of the Hsp70 superfamily, bind to scavenger receptor-A and scavenger receptor expressed by endothelial cells-I. *European Journal of Immunology*, 37(8), 2268–2279. <https://doi.org/10.1002/eji.200737127>
- Falcone, S., Cocucci, E., Podini, P., Kirchhausen, T., Clementi, E., & Meldolesi, J. (2006). Macropinocytosis: regulated coordination of endocytic and exocytic membrane traffic events. *Journal of Cell Science*, 119(22), 4758–4769. <https://doi.org/10.1242/jcs.03238>
- Fang, Y., Liao, G., & Yu, B. (2019). LSD1/KDM1A inhibitors in clinical trials: advances and prospects. *Journal of Hematology & Oncology*, 12(1), 129. <https://doi.org/10.1186/s13045-019-0811-9>
- Farmer, H., McCabe, N., Lord, C. J., Tutt, A. N. J., Johnson, D. A., Richardson, T. B., Santarosa, M., Dillon, K. J., Hickson, I., Knights, C., Martin, N. M. B., Jackson, S. P., Smith, G. C. M., & Ashworth, A. (2005). Targeting the DNA repair defect in BRCA mutant cells as a therapeutic strategy. *Nature*, 434(7035), 917–921. <https://doi.org/10.1038/nature03445>
- Farnsworth, W. E. (1999). Prostate Stroma: Physiology. *The Prostate*, 38(1), 60–72. [https://doi.org/10.1002/\(SICI\)1097-0045\(19990101\)38:1<60::AID-PROS8>3.0.CO;2-3](https://doi.org/10.1002/(SICI)1097-0045(19990101)38:1<60::AID-PROS8>3.0.CO;2-3)
- Farnung, L., Vos, S. M., Wigge, C., & Cramer, P. (2017). Nucleosome–Chd1 structure and implications for chromatin remodelling. *Nature*, 550(7677), 539–542. <https://doi.org/10.1038/nature24046>
- Farquhar, R. E., Rodrigues, E., & Hamilton, K. L. (2017). The Role of the Cytoskeleton and Myosin-Vc in the Targeting of KCa3.1 to the Basolateral Membrane of Polarized Epithelial Cells. *Frontiers in Physiology*, 7. <https://doi.org/10.3389/fphys.2016.00639>
- Febbraio, M., Hajjar, D. P., & Silverstein, R. L. (2001). CD36: a class B scavenger receptor involved in angiogenesis, atherosclerosis, inflammation, and lipid metabolism. *Journal of Clinical Investigation*, 108(6), 785–791. <https://doi.org/10.1172/JCI14006>

- Feldman, B. J., & Feldman, D. (2001). The development of androgen-independent prostate cancer. *Nature Reviews Cancer*, 1(1), 34–45.
<https://doi.org/10.1038/35094009>
- Feni, L., & Neundorff, I. (2017). The current role of cell-penetrating peptides in cancer therapy. *Advances in Experimental Medicine and Biology*, 1030, 279–295. https://doi.org/10.1007/978-3-319-66095-0_13/COVER
- Ferlay, J., Soerjomataram, I., Dikshit, R., Eser, S., Mathers, C., Rebelo, M., Parkin, D. M., Forman, D., & Bray, F. (2015). Cancer incidence and mortality worldwide: Sources, methods and major patterns in GLOBOCAN 2012. *International Journal of Cancer*, 136(5), E359–E386.
<https://doi.org/10.1002/ijc.29210>
- Ferrari, A., Pellegrini, V., Arcangeli, C., Fittipaldi, A., Giacca, M., & Beltram, F. (2003). Caveolae-Mediated internalization of extracellular HIV-1 tat fusion proteins visualized in real time. *Molecular Therapy*, 8(2), 284–294.
[https://doi.org/10.1016/S1525-0016\(03\)00122-9](https://doi.org/10.1016/S1525-0016(03)00122-9)
- Ferreira, C. R., & Gahl, W. A. (2017). Lysosomal storage diseases. *Translational Science of Rare Diseases*, 2(1–2), 1–71. <https://doi.org/10.3233/TRD-160005>
- Fioravanti, R., Rodriguez, V., Caroli, J., Chianese, U., Benedetti, R., Di Bello, E., Noce, B., Zwergel, C., Corinti, D., Viña, D., Altucci, L., Mattevi, A., Valente, S., & Mai, A. (2022). Heterocycle-containing tranylcypromine derivatives endowed with high anti-LSD1 activity. *Journal of Enzyme Inhibition and Medicinal Chemistry*, 37(1), 973–985.
<https://doi.org/10.1080/14756366.2022.2052869>
- Fioravanti, R., Romanelli, A., Mautone, N., Di Bello, E., Rovere, A., Corinti, D., Zwergel, C., Valente, S., Rotili, D., Botrugno, O. A., Dessanti, P., Vultaggio, S., Vianello, P., Cappa, A., Binda, C., Mattevi, A., Minucci, S., Mercurio, C., Varasi, M., & Mai, A. (2020). Tranylcypromine-Based LSD1 Inhibitors: Structure-Activity Relationships, Antiproliferative Effects in Leukemia, and Gene Target Modulation. *ChemMedChem*, 15(7), 643–658.
<https://doi.org/10.1002/cmdc.201900730>
- Firer, M. A., & Gellerman, G. (2012). Targeted drug delivery for cancer therapy: the other side of antibodies. *Journal of Hematology & Oncology*, 5(1), 70.
<https://doi.org/10.1186/1756-8722-5-70>
- Fittipaldi, A., Ferrari, A., Zoppé, M., Arcangeli, C., Pellegrini, V., Beltram, F., & Giacca, M. (2003). Cell Membrane Lipid Rafts Mediate Caveolar Endocytosis of HIV-1 Tat Fusion Proteins. *Journal of Biological Chemistry*, 278(36), 34141–34149. <https://doi.org/10.1074/jbc.M303045200>
- Fizazi, K., Carducci, M., Smith, M., Damião, R., Brown, J., Karsh, L., Milecki, P., Shore, N., Rader, M., Wang, H., Jiang, Q., Tadros, S., Dansey, R., & Goessl, C. (2011). Denosumab versus zoledronic acid for treatment of bone metastases in men with castration-resistant prostate cancer: a randomised, double-blind study. *The Lancet*, 377(9768), 813–822.
[https://doi.org/10.1016/S0140-6736\(10\)62344-6](https://doi.org/10.1016/S0140-6736(10)62344-6)
- Fizazi, K., Tran, N., Fein, L., Matsubara, N., Rodriguez-Antolin, A., Alekseev, B. Y., Özgüroğlu, M., Ye, D., Feyerabend, S., Protheroe, A., De Porre, P., Kheoh,

- T., Park, Y. C., Todd, M. B., & Chi, K. N. (2017). Abiraterone plus Prednisone in Metastatic, Castration-Sensitive Prostate Cancer. *New England Journal of Medicine*, 377(4), 352–360. <https://doi.org/10.1056/NEJMoa1704174>
- Flanagan, K., Kumari, R., Miettinen, J. J., Haney, S. L., Varney, M. L., Williams, J. T., Majumder, M. M., Suvela, M., Slipicevic, A., Lehmann, F., Nupponen, N. N., Holstein, S. A., & Heckman, C. A. (2022). The Peptide–Drug Conjugate Melflufen Modulates the Unfolded Protein Response of Multiple Myeloma and Amyloidogenic Plasma Cells and Induces Cell Death. *HemaSphere*, 6(3), e687. <https://doi.org/10.1097/HS9.0000000000000687>
- Fong, L., Brockstedt, D., Benike, C., Breen, J. K., Strang, G., Ruegg, C. L., & Engleman, E. G. (2001). Dendritic Cell-Based Xenoantigen Vaccination for Prostate Cancer Immunotherapy. *The Journal of Immunology*, 167(12), 7150–7156. <https://doi.org/10.4049/jimmunol.167.12.7150>
- Fong, L., Morris, M. J., Sartor, O., Higano, C. S., Pagliaro, L., Alva, A., Appleman, L. J., Tan, W., Vaishampayan, U., Porcu, R., Tayama, D., Kadel, E. E., Yuen, K. C., Datye, A., Armstrong, A. J., & Petrylak, D. P. (2021). A Phase Ib Study of Atezolizumab with Radium-223 Dichloride in Men with Metastatic Castration-Resistant Prostate Cancer. *Clinical Cancer Research*, 27(17), 4746–4756. <https://doi.org/10.1158/1078-0432.CCR-21-0063>
- Forgac, M. (2007). Vacuolar ATPases: rotary proton pumps in physiology and pathophysiology. *Nature Reviews. Molecular Cell Biology*, 8(11), 917–929. <https://doi.org/10.1038/nrm2272>
- Forneris, F., Binda, C., Battaglioli, E., & Mattevi, A. (2008). LSD1: oxidative chemistry for multifaceted functions in chromatin regulation. *Trends in Biochemical Sciences*, 33(4), 181–189. <https://doi.org/10.1016/j.tibs.2008.01.003>
- Forneris, F., Binda, C., Dall’Aglia, A., Fraaije, M. W., Battaglioli, E., & Mattevi, A. (2006). A Highly Specific Mechanism of Histone H3-K4 Recognition by Histone Demethylase LSD1. *Journal of Biological Chemistry*, 281(46), 35289–35295. <https://doi.org/10.1074/jbc.M607411200>
- Forneris, F., Binda, C., Vanoni, M. A., Battaglioli, E., & Mattevi, A. (2005). Human Histone Demethylase LSD1 Reads the Histone Code. *Journal of Biological Chemistry*, 280(50), 41360–41365. <https://doi.org/10.1074/jbc.M509549200>
- Fraietta, I., & Gasparri, F. (2016). The development of high-content screening (HCS) technology and its importance to drug discovery. *Expert Opinion on Drug Discovery*, 11(5), 501–514. <https://doi.org/10.1517/17460441.2016.1165203>
- Frankel, A. D., & Pabo, C. O. (1988). Cellular uptake of the tat protein from human immunodeficiency virus. *Cell*, 55(6), 1189–1193. [https://doi.org/10.1016/0092-8674\(88\)90263-2](https://doi.org/10.1016/0092-8674(88)90263-2)
- Frånlund, M., Carlsson, S., Stranne, J., Aus, G., & Hugosson, J. (2012). The absence of voiding symptoms in men with a prostate-specific antigen (PSA) concentration of ≥ 3.0 ng/mL is an independent risk factor for prostate cancer: results from the Gothenburg Randomized Screening Trial. *BJU*

International, 110(5), 638–643. <https://doi.org/10.1111/j.1464-410X.2012.10962.x>

- Fraser, M., Sabelnykova, V. Y., Yamaguchi, T. N., Heisler, L. E., Livingstone, J., Huang, V., Shiah, Y.-J., Yousif, F., Lin, X., Masella, A. P., Fox, N. S., Xie, M., Prokopec, S. D., Berlin, A., Lalonde, E., Ahmed, M., Trudel, D., Luo, X., Beck, T. A., ... Boutros, P. C. (2017). Genomic hallmarks of localized, non-indolent prostate cancer. *Nature*, 541(7637), 359–364. <https://doi.org/10.1038/nature20788>
- Freer, R. J., & Stewart, J. M. (1972). Alkylating analogs of peptide hormones. 1. Synthesis and properties of p-[N,N-bis(2-chloroethyl)amino]phenylbutyryl derivatives of bradykinin and bradykinin potentiating factor. *Journal of Medicinal Chemistry*, 15(1), 1–5. <https://doi.org/10.1021/jm00271a001>
- Frenkel, D., Wilkinson, K., Zhao, L., Hickman, S. E., Means, T. K., Puckett, L., Farfara, D., Kingery, N. D., Weiner, H. L., & El Khoury, J. (2013). Scara1 deficiency impairs clearance of soluble Amyloid- β by mononuclear phagocytes and accelerates Alzheimer's-like disease progression. *Nature Communications*, 4, 2030. <https://doi.org/10.1038/NCOMMS3030>
- Fretz, M. M., Penning, N. A., Al-Taei, S., Futaki, S., Takeuchi, T., Nakase, I., Storm, G., & Jones, A. T. (2007). Temperature-, concentration- and cholesterol-dependent translocation of <sc>L</sc> - and <sc>D</sc> - octa-arginine across the plasma and nuclear membrane of CD34+ leukaemia cells. *Biochemical Journal*, 403(2), 335–342. <https://doi.org/10.1042/BJ20061808>
- Froidevaux, S., Calame-Christe, M., Tanner, H., & Eberle, A. N. (2005). Melanoma targeting with DOTA-alpha-melanocyte-stimulating hormone analogs: structural parameters affecting tumor uptake and kidney uptake. *Journal of Nuclear Medicine : Official Publication, Society of Nuclear Medicine*, 46(5), 887–895.
- Froidevaux, S., & Eberle, A. N. (2002). Homologous regulation of melanocortin-1 receptor (MC1R) expression in melanoma tumor cells in vivo. *Journal of Receptors and Signal Transduction*, 22(1–4), 111–121. <https://doi.org/10.1081/RRS-120014590>
- Fu, C., Yu, L., Miao, Y., Liu, X., Yu, Z., & Wei, M. (2023). Peptide-drug conjugates (PDCs): a novel trend of research and development on targeted therapy, hype or hope? *Acta Pharmaceutica Sinica. B*, 13(2), 498–516. <https://doi.org/10.1016/j.apsb.2022.07.020>
- Fujita, K., & Nonomura, N. (2019). Role of Androgen Receptor in Prostate Cancer: A Review. *The World Journal of Men's Health*, 37(3), 288–295.
- Fujita, N., Yaegashi, N., Ide, Y., Sato, S., Nakamura, M., Ishiwata, I., & Yajima, A. (1994). Expression of CD44 in normal human versus tumor endometrial tissues: possible implication of reduced expression of CD44 in lymph-vascular space involvement of cancer cells. *Cancer Research*, 54(14), 3922–3928.
- Fukasawa, M., Adachi, H., Hirota, K., Tsujimoto, M., Arai, H., & Inoue, K. (1996). SRB1, a Class B Scavenger Receptor, Recognizes both Negatively Charged

- Liposomes and Apoptotic Cells. *Experimental Cell Research*, 222(1), 246–250. <https://doi.org/10.1006/excr.1996.0030>
- Furuya, Y., Lundmo, P., Short, A. D., Gill, D. L., & Isaacs, J. T. (1994). The role of calcium, pH, and cell proliferation in the programmed (apoptotic) death of androgen-independent prostatic cancer cells induced by thapsigargin. *Cancer Research*, 54(23), 6167–6175.
- Futaki, S., & Nakase, I. (2017). Cell-Surface Interactions on Arginine-Rich Cell-Penetrating Peptides Allow for Multiplex Modes of Internalization. *Accounts of Chemical Research*, 50(10), 2449–2456. <https://doi.org/10.1021/acs.accounts.7b00221>
- Futaki, S., Suzuki, T., Ohashi, W., Yagami, T., Tanaka, S., Ueda, K., & Sugiura, Y. (2001). Arginine-rich Peptides. *Journal of Biological Chemistry*, 276(8), 5836–5840. <https://doi.org/10.1074/jbc.M007540200>
- Galletti, G., Leach, B. I., Lam, L., & Tagawa, S. T. (2017). Mechanisms of resistance to systemic therapy in metastatic castration-resistant prostate cancer. *Cancer Treatment Reviews*, 57, 16–27. <https://doi.org/10.1016/j.ctrv.2017.04.008>
- Galmarini, C. M., Mackey, J. R., & Dumontet, C. (2002). Nucleoside analogues and nucleobases in cancer treatment. *The Lancet Oncology*, 3(7), 415–424. [https://doi.org/10.1016/S1470-2045\(02\)00788-X](https://doi.org/10.1016/S1470-2045(02)00788-X)
- Gan, H. K., Parakh, S., Lee, F. T., Tebbutt, N. C., Ameratunga, M., Lee, S. T., O'Keefe, G. J., Gong, S. J., Vanrenen, C., Caine, J., Giovannetti, M., Murone, C., Scott, F. E., Guo, N., Burvenich, I. J. G., Paine, C., Macri, M. J., Kotsuma, M., Senaldi, G., ... Scott, A. M. (2022). A phase 1 safety and bioimaging trial of antibody DS-8895a against EphA2 in patients with advanced or metastatic EphA2 positive cancers. *Investigational New Drugs*, 40(4), 747–755. <https://doi.org/10.1007/s10637-022-01237-3>
- Gao, N., Zhang, J., Rao, M. A., Case, T. C., Mirosevich, J., Wang, Y., Jin, R., Gupta, A., Rennie, P. S., & Matusik, R. J. (2003). The Role of Hepatocyte Nuclear Factor-3 α (Forkhead Box A1) and Androgen Receptor in Transcriptional Regulation of Prostatic Genes. *Molecular Endocrinology*, 17(8), 1484–1507. <https://doi.org/10.1210/me.2003-0020>
- Gao, S., Chen, S., Han, D., Wang, Z., Li, M., Han, W., Besschetnova, A., Liu, M., Zhou, F., Barrett, D., Luong, M. P., Owiredu, J., Liang, Y., Ahmed, M., Petricca, J., Patalano, S., Macoska, J. A., Corey, E., Chen, S., ... Cai, C. (2020). Chromatin binding of FOXA1 is promoted by LSD1-mediated demethylation in prostate cancer. *Nature Genetics*, 52(10), 1011–1017. <https://doi.org/10.1038/s41588-020-0681-7>
- Garcia-Bassets, I., Kwon, Y.-S., Telese, F., Prefontaine, G. G., Hutt, K. R., Cheng, C. S., Ju, B.-G., Ohgi, K. A., Wang, J., Escoubet-Lozach, L., Rose, D. W., Glass, C. K., Fu, X.-D., & Rosenfeld, M. G. (2007). Histone Methylation-Dependent Mechanisms Impose Ligand Dependency for Gene Activation by Nuclear Receptors. *Cell*, 128(3), 505–518. <https://doi.org/10.1016/j.cell.2006.12.038>

- Gartrell, B. A., Coleman, R. E., Fizazi, K., Miller, K., Saad, F., Sternberg, C. N., & Galsky, M. D. (2014). Toxicities Following Treatment with Bisphosphonates and Receptor Activator of Nuclear Factor- κ B Ligand Inhibitors in Patients with Advanced Prostate Cancer. *European Urology*, 65(2), 278–286. <https://doi.org/10.1016/j.eururo.2013.05.015>
- Gautreau, A., Oguievetskaia, K., & Ungermann, C. (2014). Function and regulation of the endosomal fusion and fission machineries. *Cold Spring Harbor Perspectives in Biology*, 6(3). <https://doi.org/10.1101/cshperspect.a016832>
- Gayraud, F., Klußmann, M., & Neundorff, I. (2021). Recent Advances and Trends in Chemical CPP–Drug Conjugation Techniques. *Molecules*, 26(6), 1591. <https://doi.org/10.3390/molecules26061591>
- Gelmann, E. P. (2002). Molecular Biology of the Androgen Receptor. *Journal of Clinical Oncology*, 20(13), 3001–3015. <https://doi.org/10.1200/JCO.2002.10.018>
- Gestin, M., Dowaidar, M., & Langel, Ü. (2017). Uptake Mechanism of Cell-Penetrating Peptides. *Advances in Experimental Medicine and Biology*, 1030, 255–264. https://doi.org/10.1007/978-3-319-66095-0_11
- Ghatak, S., Hascall, V. C., Markwald, R. R., & Misra, S. (2010). Stromal Hyaluronan Interaction with Epithelial CD44 Variants Promotes Prostate Cancer Invasiveness by Augmenting Expression and Function of Hepatocyte Growth Factor and Androgen Receptor. *Journal of Biological Chemistry*, 285(26), 19821–19832. <https://doi.org/10.1074/jbc.M110.104273>
- Gifford, V., & Itoh, Y. (2019). MT1-MMP-dependent cell migration: proteolytic and non-proteolytic mechanisms. *Biochemical Society Transactions*, 47(3), 811–826. <https://doi.org/10.1042/BST20180363>
- Giri, V. N., & Beebe-Dimmer, J. L. (2016). Familial prostate cancer. *Seminars in Oncology*, 43(5), 560–565. <https://doi.org/10.1053/j.seminoncol.2016.08.001>
- Gkonos, P. J., Ashby, M. H., & Andrade, A. A. (1996). Vasoactive intestinal peptide stimulates prostate-specific antigen secretion by LNCaP prostate cancer cells. *Regulatory Peptides*, 65(2), 153–157. [https://doi.org/10.1016/0167-0115\(96\)00086-9](https://doi.org/10.1016/0167-0115(96)00086-9)
- Glass, C., Pittman, R. C., Weinstein, D. B., & Steinberg, D. (1983). Dissociation of tissue uptake of cholesterol ester from that of apoprotein A-I of rat plasma high density lipoprotein: selective delivery of cholesterol ester to liver, adrenal, and gonad. *Proceedings of the National Academy of Sciences*, 80(17), 5435–5439. <https://doi.org/10.1073/pnas.80.17.5435>
- Gleason, D. F. (1966). Classification of prostatic carcinomas. *Cancer Chemotherapy Reports*, 50(3), 125–128.
- Gnanapragasam, V. J., Greenberg, D., & Burnet, N. (2022). Urinary symptoms and prostate cancer-the misconception that may be preventing earlier presentation and better survival outcomes. *BMC Medicine*, 20(1), 264. <https://doi.org/10.1186/s12916-022-02453-7>

- Goldstein, A. S., Huang, J., Guo, C., Garraway, I. P., & Witte, O. N. (2010). Identification of a Cell of Origin for Human Prostate Cancer. *Science*, 329(5991), 568–571. <https://doi.org/10.1126/science.1189992>
- Goldstein, J. L., Ho, Y. K., Basu, S. K., & Brown, M. S. (1979). Binding site on macrophages that mediates uptake and degradation of acetylated low density lipoprotein, producing massive cholesterol deposition. *Proceedings of the National Academy of Sciences*, 76(1), 333–337. <https://doi.org/10.1073/pnas.76.1.333>
- Gong, H., Liao, M., Hu, X., Fa, K., Phanphak, S., Ciunac, D., Hollowell, P., Shen, K., Clifton, L. A., Campana, M., Webster, J. R. P., Fragneto, G., Waigh, T. A., McBain, A. J., & Lu, J. R. (2020). Aggregated Amphiphilic Antimicrobial Peptides Embedded in Bacterial Membranes. *ACS Applied Materials & Interfaces*, 12(40), 44420–44432. <https://doi.org/10.1021/acsami.0c09931>
- Gong, H., Zhang, J., Hu, X., Li, Z., Fa, K., Liu, H., Waigh, T. A., McBain, A., & Lu, J. R. (2019). Hydrophobic Control of the Bioactivity and Cytotoxicity of de Novo-Designed Antimicrobial Peptides. *ACS Applied Materials & Interfaces*, 11(38), 34609–34620. <https://doi.org/10.1021/acsami.9b10028>
- Gong, J., Hu, X., Zhang, J., Du, Y., Huang, R., Teng, Y., Tan, W., & Shen, L. (2021). Phase Ia study of CBP-1008, a bi-specific ligand drug conjugate targeting FR α and TRPV6, in patients with advanced solid tumors. *Journal of Clinical Oncology*, 39(15_suppl), 3077–3077. https://doi.org/10.1200/JCO.2021.39.15_suppl.3077
- Gong, L., Zhao, H., Liu, Y., Wu, H., Liu, C., Chang, S., Chen, L., Jin, M., Wang, Q., Gao, Z., & Huang, W. (2023). Research advances in peptide–drug conjugates. *Acta Pharmaceutica Sinica B*. <https://doi.org/10.1016/j.apsb.2023.02.013>
- González-Chavarría, I., Cerro, R. P., Parra, N. P., Sandoval, F. A., Zuñiga, F. A., Omazábal, V. A., Lamperti, L. I., Jiménez, S. P., Fernandez, E. A., Gutiérrez, N. A., Rodriguez, F. S., Onate, S. A., Sánchez, O., Vera, J. C., & Toledo, J. R. (2014). Lectin-Like Oxidized LDL Receptor-1 Is an Enhancer of Tumor Angiogenesis in Human Prostate Cancer Cells. *PLoS ONE*, 9(8), e106219. <https://doi.org/10.1371/journal.pone.0106219>
- González-Chavarría, I., Fernandez, E., Gutierrez, N., González-Horta, E. E., Sandoval, F., Cifuentes, P., Castillo, C., Cerro, R., Sanchez, O., & Toledo, J. R. (2018). LOX-1 activation by oxLDL triggers an epithelial mesenchymal transition and promotes tumorigenic potential in prostate cancer cells. *Cancer Letters*, 414, 34–43. <https://doi.org/10.1016/j.canlet.2017.10.035>
- Gordon, J. A., Noble, J. W., Midha, A., Derakhshan, F., Wang, G., Adomat, H. H., Tomlinson Guns, E. S., Lin, Y.-Y., Ren, S., Collins, C. C., Nelson, P. S., Morrissey, C., Wasan, K. M., & Cox, M. E. (2019). Upregulation of Scavenger Receptor B1 Is Required for Steroidogenic and Nonsteroidogenic Cholesterol Metabolism in Prostate Cancer. *Cancer Research*, 79(13), 3320–3331. <https://doi.org/10.1158/0008-5472.CAN-18-2529>
- Gorlewicz, A., Krawczyk, K., Szczepankiewicz, A. A., Trzaskoma, P., Mülle, C., & Wilczynski, G. M. (2020). Colocalization Colormap –an ImageJ Plugin for the

- Quantification and Visualization of Colocalized Signals. *Neuroinformatics*, 18(4), 661–664. <https://doi.org/10.1007/s12021-020-09465-9>
- Corvel, J.-P., Chavrier, P., Zerial, M., & Gruenberg, J. (1991). rab5 controls early endosome fusion in vitro. *Cell*, 64(5), 915–925. [https://doi.org/10.1016/0092-8674\(91\)90316-Q](https://doi.org/10.1016/0092-8674(91)90316-Q)
- Gowland, C., Berry, P., Errington, J., Jeffrey, P., Bennett, G., Godfrey, L., Pittman, M., Niewiarowski, A., Symeonides, S. N., & Veal, G. J. (2021). Development of a LC–MS/MS method for the quantification of toxic payload DM1 cleaved from BT1718 in a Phase I study. *Bioanalysis*, 13(2), 101–113. <https://doi.org/10.4155/bio-2020-0256>
- Graff, J. N., Gordon, M. J., & Beer, T. M. (2015). Safety and effectiveness of enzalutamide in men with metastatic, castration-resistant prostate cancer. *Expert Opinion on Pharmacotherapy*, 16(5), 749–754. <https://doi.org/10.1517/14656566.2015.1016911>
- Graff, J. N., Liang, L. W., Kim, J., & Stenzl, A. (2021). KEYNOTE-641: a Phase III study of pembrolizumab plus enzalutamide for metastatic castration-resistant prostate cancer. *Future Oncology*, 17(23), 3017–3026. <https://doi.org/10.2217/fon-2020-1008>
- Grasso, C. S., Wu, Y.-M., Robinson, D. R., Cao, X., Dhanasekaran, S. M., Khan, A. P., Quist, M. J., Jing, X., Lonigro, R. J., Brenner, J. C., Asangani, I. A., Ateeq, B., Chun, S. Y., Siddiqui, J., Sam, L., Anstett, M., Mehra, R., Prensner, J. R., Palanisamy, N., ... Tomlins, S. A. (2012). The mutational landscape of lethal castration-resistant prostate cancer. *Nature*, 487(7406), 239–243. <https://doi.org/10.1038/nature11125>
- Grasso, G., Muscat, S., Rebella, M., Morbiducci, U., Audenino, A., Danani, A., & Deriu, M. A. (2018). Cell penetrating peptide modulation of membrane biomechanics by Molecular dynamics. *Journal of Biomechanics*, 73, 137–144. <https://doi.org/10.1016/j.jbiomech.2018.03.036>
- Green, M., & Loewenstein, P. M. (1988). Autonomous functional domains of chemically synthesized human immunodeficiency virus tat trans-activator protein. *Cell*, 55(6), 1179–1188. [https://doi.org/10.1016/0092-8674\(88\)90262-0](https://doi.org/10.1016/0092-8674(88)90262-0)
- Gregorc, V., Cavina, R., Novello, S., Grossi, F., Lazzari, C., Capelletto, E., Genova, C., Salini, G., Lambiase, A., & Santoro, A. (2018). NGR-hTNF and Doxorubicin as Second-Line Treatment of Patients with Small Cell Lung Cancer. *The Oncologist*, 23(10), 1133-e112. <https://doi.org/10.1634/theoncologist.2018-0292>
- Gronewold, A., Horn, M., & Neundorff, I. (2018). Design and biological characterization of novel cell-penetrating peptides preferentially targeting cell nuclei and subnuclear regions. *Beilstein Journal of Organic Chemistry*, 14, 1378–1388. <https://doi.org/10.3762/bjoc.14.116>
- Gronewold, A., Horn, M., Randelović, I., Tóvári, J., Muñoz Vázquez, S., Schomäcker, K., & Neundorff, I. (2017). Characterization of a Cell-Penetrating Peptide with Potential Anticancer Activity. *ChemMedChem*, 12(1), 42–49. <https://doi.org/10.1002/cmdc.201600498>

- Grossmann, M., & Zajac, J. D. (2011). Management of Side Effects of Androgen Deprivation Therapy. *Endocrinology and Metabolism Clinics of North America*, 40(3), 655–671. <https://doi.org/10.1016/j.ecl.2011.05.004>
- Gu, F., Lin, Y., Wang, Z., Wu, X., Ye, Z., Wang, Y., & Lan, H. (2020). Biological roles of LSD1 beyond its demethylase activity. *Cellular and Molecular Life Sciences*, 77(17), 3341–3350. <https://doi.org/10.1007/s00018-020-03489-9>
- Gu, X., Kozarsky, K., & Krieger, M. (2000). Scavenger Receptor Class B, Type I-mediated [3H]Cholesterol Efflux to High and Low Density Lipoproteins Is Dependent on Lipoprotein Binding to the Receptor. *Journal of Biological Chemistry*, 275(39), 29993–30001. <https://doi.org/10.1074/jbc.275.39.29993>
- Gu, X., Trigatti, B., Xu, S., Acton, S., Babitt, J., & Krieger, M. (1998). The Efficient Cellular Uptake of High Density Lipoprotein Lipids via Scavenger Receptor Class B Type I Requires Not Only Receptor-mediated Surface Binding but Also Receptor-specific Lipid Transfer Mediated by Its Extracellular Domain. *Journal of Biological Chemistry*, 273(41), 26338–26348. <https://doi.org/10.1074/jbc.273.41.26338>
- Guedes, L. B., Antonarakis, E. S., Schweizer, M. T., Mirkheshti, N., Almutairi, F., Park, J. C., Glavaris, S., Hicks, J., Eisenberger, M. A., De Marzo, A. M., Epstein, J. I., Isaacs, W. B., Eshleman, J. R., Pritchard, C. C., & Lotan, T. L. (2017). MSH2 Loss in Primary Prostate Cancer. *Clinical Cancer Research*, 23(22), 6863–6874. <https://doi.org/10.1158/1078-0432.CCR-17-0955>
- Guerra, F., & Bucci, C. (2016). Multiple Roles of the Small GTPase Rab7. *Cells*, 5(3), 34. <https://doi.org/10.3390/cells5030034>
- Guo, J.-Y., Hsu, H.-S., Tyan, S.-W., Li, F.-Y., Shew, J.-Y., Lee, W.-H., & Chen, J.-Y. (2017). Serglycin in tumor microenvironment promotes non-small cell lung cancer aggressiveness in a CD44-dependent manner. *Oncogene*, 36(17), 2457–2471. <https://doi.org/10.1038/onc.2016.404>
- Gupta, A., Cao, W., & Chellaiah, M. A. (2012). Integrin $\alpha\beta3$ and CD44 pathways in metastatic prostate cancer cells support osteoclastogenesis via a Runx2/Smad 5/receptor activator of NF- κ B ligand signaling axis. *Molecular Cancer*, 11, 66. <https://doi.org/10.1186/1476-4598-11-66>
- Gupta, S., Li, J., Kemeny, G., Bitting, R. L., Beaver, J., Somarelli, J. A., Ware, K. E., Gregory, S., & Armstrong, A. J. (2017). Whole Genomic Copy Number Alterations in Circulating Tumor Cells from Men with Abiraterone or Enzalutamide-Resistant Metastatic Castration-Resistant Prostate Cancer. *Clinical Cancer Research*, 23(5), 1346–1357. <https://doi.org/10.1158/1078-0432.CCR-16-1211>
- Gupta, S., Weston, A., Bearrs, J., Thode, T., Neiss, A., Soldi, R., & Sharma, S. (2016). Reversible lysine-specific demethylase 1 antagonist HCl-2509 inhibits growth and decreases c-MYC in castration- and docetaxel-resistant prostate cancer cells. *Prostate Cancer and Prostatic Diseases*, 19(4), 349–357. <https://doi.org/10.1038/pcan.2016.21>
- Gurel, B., Iwata, T., M Koh, C., Jenkins, R. B., Lan, F., Van Dang, C., Hicks, J. L., Morgan, J., Cornish, T. C., Sutcliffe, S., Isaacs, W. B., Luo, J., & De Marzo, A. M. (2008). Nuclear MYC protein overexpression is an early alteration in

- human prostate carcinogenesis. *Modern Pathology*, 21(9), 1156–1167.
<https://doi.org/10.1038/modpathol.2008.111>
- Ha, H. (2011). Clinical significance of CXCL16/CXCR6 $\frac{1}{2}$ expression in patients with prostate cancer. *Molecular Medicine Reports*.
<https://doi.org/10.3892/mmr.2011.446>
- Haffner, J., Potiron, E., Bouyé, S., Puech, P., Leroy, X., Lemaitre, L., & Villers, A. (2009). Peripheral zone prostate cancers: Location and intraprostatic patterns of spread at histopathology. *The Prostate*, 69(3), 276–282.
<https://doi.org/10.1002/pros.20881>
- Hahm, J. Y., Kim, J.-Y., Park, J. W., Kang, J.-Y., Kim, K.-B., Kim, S.-R., Cho, H., & Seo, S.-B. (2019). Methylation of UHRF1 by SET7 is essential for DNA double-strand break repair. *Nucleic Acids Research*, 47(1), 184–196.
<https://doi.org/10.1093/nar/gky975>
- Hahn, A. W., Higano, C. S., Taplin, M.-E., Ryan, C. J., & Agarwal, N. (2018). Metastatic Castration-Sensitive Prostate Cancer: Optimizing Patient Selection and Treatment. *American Society of Clinical Oncology Educational Book*, 38, 363–371. https://doi.org/10.1200/EDBK_200967
- Haigler, H. T., McKanna, J. A., & Cohen, S. (1979). Rapid stimulation of pinocytosis in human carcinoma cells A-431 by epidermal growth factor. *Journal of Cell Biology*, 83(1), 82–90. <https://doi.org/10.1083/jcb.83.1.82>
- Hällbrink, M., Oehlke, J., Papsdorf, G., & Bienert, M. (2004). Uptake of cell-penetrating peptides is dependent on peptide-to-cell ratio rather than on peptide concentration. *Biochimica et Biophysica Acta (BBA) - Biomembranes*, 1667(2), 222–228. <https://doi.org/10.1016/j.bbamem.2004.10.009>
- Hameed, O., & Humphrey, P. A. (2005a). Immunohistochemistry in diagnostic surgical pathology of the prostate. *Seminars in Diagnostic Pathology*, 22(1), 88–104. <https://doi.org/10.1053/j.semmp.2005.11.001>
- Hameed, O., & Humphrey, P. A. (2005b). p63/AMACR Antibody Cocktail Restaining of Prostate Needle Biopsy Tissues After Transfer to Charged Slides. *American Journal of Clinical Pathology*, 124(5), 708–715.
<https://doi.org/10.1309/JXK1-BVAT-GBVN-Q9J9>
- Hameed, O., & Humphrey, P. A. (2006). Stratified epithelium in prostatic adenocarcinoma: a mimic of high-grade prostatic intraepithelial neoplasia. *Modern Pathology*, 19(7), 899–906.
<https://doi.org/10.1038/modpathol.3800601>
- Han, J., Fu, J., Yang, Q., Zhou, F., Chen, X., Li, C., & Yin, J. (2020). Rational design and biological evaluation of gemfibrozil modified Xenopus GLP-1 derivatives as long-acting hypoglycemic agents. *European Journal of Medicinal Chemistry*, 198, 112389.
<https://doi.org/10.1016/j.ejmech.2020.112389>
- Hanahan, D., & Weinberg, R. A. (2011). Hallmarks of Cancer: The Next Generation. *Cell*, 144(5), 646–674. <https://doi.org/10.1016/j.cell.2011.02.013>
- Harris, W. P., Mostaghel, E. A., Nelson, P. S., & Montgomery, B. (2009). Androgen deprivation therapy: progress in understanding mechanisms of resistance and

- optimizing androgen depletion. *Nature Clinical Practice Urology*, 6(2), 76–85.
<https://doi.org/10.1038/ncpuro1296>
- Hartvigsen, K., Chou, M.-Y., Hansen, L. F., Shaw, P. X., Tsimikas, S., Binder, C. J., & Witztum, J. L. (2009). The role of innate immunity in atherogenesis. *Journal of Lipid Research*, 50, S388–S393.
<https://doi.org/10.1194/jlr.R800100-JLR200>
- Hayward, S. W., & Cunha, G. R. (2000). THE PROSTATE: DEVELOPMENT AND PHYSIOLOGY. *Radiologic Clinics of North America*, 38(1), 1–14.
[https://doi.org/10.1016/S0033-8389\(05\)70146-9](https://doi.org/10.1016/S0033-8389(05)70146-9)
- He, B., Lanz, R. B., Fiskus, W., Geng, C., Yi, P., Hartig, S. M., Rajapakshe, K., Shou, J., Wei, L., Shah, S. S., Foley, C., Chew, S. A., Eedunuri, V. K., Bedoya, D. J., Feng, Q., Minami, T., Mitsiades, C. S., Frolov, A., Weigel, N. L., ... Mitsiades, N. (2014). GATA2 facilitates steroid receptor coactivator recruitment to the androgen receptor complex. *Proceedings of the National Academy of Sciences of the United States of America*, 111(51), 18261–18266. <https://doi.org/10.1073/pnas.1421415111>
- He, J., Xu, S., & Mixson, A. J. (2020). The Multifaceted Histidine-Based Carriers for Nucleic Acid Delivery: Advances and Challenges. *Pharmaceutics*, 12(8), 774. <https://doi.org/10.3390/pharmaceutics12080774>
- He, L., Wang, L., Wang, Z., Li, T., Chen, H., Zhang, Y., Hu, Z., Dimitrov, D. S., Du, J., & Liao, X. (2021). Immune Modulating Antibody–Drug Conjugate (IM-ADC) for Cancer Immunotherapy. *Journal of Medicinal Chemistry*, 64(21), 15716–15726. <https://doi.org/10.1021/acs.jmedchem.1c00961>
- He, S., Cen, B., Liao, L., Wang, Z., Qin, Y., Wu, Z., Liao, W., Zhang, Z., & Ji, A. (2017). A tumor-targeting cRGD-EGFR siRNA conjugate and its anti-tumor effect on glioblastoma in vitro and in vivo. *Drug Delivery*, 24(1), 471–481. <https://doi.org/10.1080/10717544.2016.1267821>
- He, Y., Xu, W., Xiao, Y.-T., Huang, H., Gu, D., & Ren, S. (2022). Targeting signaling pathways in prostate cancer: mechanisms and clinical trials. *Signal Transduction and Targeted Therapy*, 7(1), 198. <https://doi.org/10.1038/s41392-022-01042-7>
- He, Y., Xue, C., Yu, Y., Chen, J., Chen, X., Ren, F., Ren, Z., Cui, G., & Sun, R. (2018). CD44 is overexpressed and correlated with tumor progression in gallbladder cancer. *Cancer Management and Research*, Volume 10, 3857–3865. <https://doi.org/10.2147/CMAR.S175681>
- Hedlund, T. E., Duke, R. C., & Miller, G. J. (1999). Three-dimensional spheroid cultures of human prostate cancer cell lines. *The Prostate*, 41(3), 154–165. [https://doi.org/10.1002/\(SICI\)1097-0045\(19991101\)41:3<154::AID-PROS2>3.0.CO;2-M](https://doi.org/10.1002/(SICI)1097-0045(19991101)41:3<154::AID-PROS2>3.0.CO;2-M)
- Hegazy, M., Cohen-Barak, E., Koetsier, J. L., Najor, N. A., Arvanitis, C., Sprecher, E., Green, K. J., & Godsel, L. M. (2020). Proximity Ligation Assay for Detecting Protein-Protein Interactions and Protein Modifications in Cells and Tissues in Situ. *Current Protocols in Cell Biology*, 89(1). <https://doi.org/10.1002/cpcb.115>

- Heh, E., Allen, J., Ramirez, F., Lovasz, D., Fernandez, L., Hogg, T., Riva, H., Holland, N., & Chacon, J. (2023). Peptide Drug Conjugates and Their Role in Cancer Therapy. *International Journal of Molecular Sciences*, 24(1). <https://doi.org/10.3390/ijms24010829>
- Helmfors, H., Lindberg, S., & Langel, Ü. (2015). SCARA Involvement in the Uptake of Nanoparticles Formed by Cell-Penetrating Peptides (pp. 163–174). https://doi.org/10.1007/978-1-4939-2806-4_11
- Herce, H. D., & Garcia, A. E. (2007). Molecular dynamics simulations suggest a mechanism for translocation of the HIV-1 TAT peptide across lipid membranes. *Proceedings of the National Academy of Sciences*, 104(52), 20805–20810. <https://doi.org/10.1073/pnas.0706574105>
- Herce, H. D., Garcia, A. E., & Cardoso, M. C. (2014). Fundamental Molecular Mechanism for the Cellular Uptake of Guanidinium-Rich Molecules. *Journal of the American Chemical Society*, 136(50), 17459–17467. <https://doi.org/10.1021/ja507790z>
- Herce, H. D., Garcia, A. E., Litt, J., Kane, R. S., Martin, P., Enrique, N., Rebolledo, A., & Milesi, V. (2009). Arginine-Rich Peptides Destabilize the Plasma Membrane, Consistent with a Pore Formation Translocation Mechanism of Cell-Penetrating Peptides. *Biophysical Journal*, 97(7), 1917–1925. <https://doi.org/10.1016/j.bpj.2009.05.066>
- Hernandez, J. R., Kim, J. J., Verdone, J. E., Liu, X., Torga, G., Pienta, K. J., & Mooney, S. M. (2015). Alternative CD44 splicing identifies epithelial prostate cancer cells from the mesenchymal counterparts. *Medical Oncology*, 32(5), 159. <https://doi.org/10.1007/s12032-015-0593-z>
- Heybrock, S., Kanerva, K., Meng, Y., Ing, C., Liang, A., Xiong, Z.-J., Weng, X., Kim, Y. A., Collins, R., Trimble, W., Pomès, R., Privé, G. G., Annaert, W., Schwake, M., Heeren, J., Lüllmann-Rauch, R., Grinstein, S., Ikonen, E., Saftig, P., & Neculai, D. (2019). Lysosomal integral membrane protein-2 (LIMP-2/ SCARB2) is involved in lysosomal cholesterol export. <https://doi.org/10.1038/s41467-019-11425-0>
- Hieronimus, H., Schultz, N., Gopalan, A., Carver, B. S., Chang, M. T., Xiao, Y., Heguy, A., Huberman, K., Bernstein, M., Assel, M., Murali, R., Vickers, A., Scardino, P. T., Sander, C., Reuter, V., Taylor, B. S., & Sawyers, C. L. (2014). Copy number alteration burden predicts prostate cancer relapse. *Proceedings of the National Academy of Sciences*, 111(30), 11139–11144. <https://doi.org/10.1073/pnas.1411446111>
- Hiraga, T., Ito, S., & Nakamura, H. (2013). Cancer Stem-like Cell Marker CD44 Promotes Bone Metastases by Enhancing Tumorigenicity, Cell Motility, and Hyaluronan Production. *Cancer Research*, 73(13), 4112–4122. <https://doi.org/10.1158/0008-5472.CAN-12-3801>
- Hirose, H., Takeuchi, T., Osakada, H., Pujals, S., Katayama, S., Nakase, I., Kobayashi, S., Haraguchi, T., & Futaki, S. (2012). Transient Focal Membrane Deformation Induced by Arginine-rich Peptides Leads to Their Direct Penetration into Cells. *Molecular Therapy*, 20(5), 984–993. <https://doi.org/10.1038/mt.2011.313>

- Hirsch, H. A., Iliopoulos, D., Joshi, A., Zhang, Y., Jaeger, S. A., Bulyk, M., Tschlis, P. N., Shirley Liu, X., & Struhl, K. (2010). A Transcriptional Signature and Common Gene Networks Link Cancer with Lipid Metabolism and Diverse Human Diseases. *Cancer Cell*, 17(4), 348–361. <https://doi.org/10.1016/j.ccr.2010.01.022>
- Hofmann, M. R., Hussain, M., Dehm, S. M., Beltran, H., Wyatt, A. W., Halabi, S., Sweeney, C., Scher, H. I., Ryan, C. J., Feng, F. Y., Attard, G., Klein, E., Miyahira, A. K., Soule, H. R., & Sharifi, N. (2021). Prostate Cancer Foundation Hormone-Sensitive Prostate Cancer Biomarker Working Group Meeting Summary. *Urology*, 155, 165–171. <https://doi.org/10.1016/j.urology.2020.12.021>
- Højfeldt, J. W., Agger, K., & Helin, K. (2013). Histone lysine demethylases as targets for anticancer therapy. *Nature Reviews Drug Discovery*, 12(12), 917–930. <https://doi.org/10.1038/nrd4154>
- Hölzl, M. A., Hofer, J., Kovarik, J. J., Roggenbuck, D., Reinhold, D., Goihl, A., Gärtner, M., Steinberger, P., & Zlabinger, G. J. (2011). The zymogen granule protein 2 (GP2) binds to scavenger receptor expressed on endothelial cells I (SREC-I). *Cellular Immunology*, 267(2), 88–93. <https://doi.org/10.1016/j.cellimm.2010.12.001>
- Hope, Q., Bullock, S., Evans, C., Meitz, J., Hamel, N., Edwards, S. M., Severi, G., Dearnaley, D., Jhavar, S., Southgate, C., Falconer, A., Dowe, A., Muir, K., Houlston, R. S., Engert, J. C., Roquis, D., Sinnett, D., Simard, J., Heimdal, K., ... Giles, G. G. (2005). Macrophage Scavenger Receptor 1 999C>T (R293X) Mutation and Risk of Prostate Cancer. *Cancer Epidemiology, Biomarkers & Prevention*, 14(2), 397–402. <https://doi.org/10.1158/1055-9965.EPI-04-0202>
- Hoppenz, P., Els-Heindl, S., & Beck-Sickingler, A. G. (2019). Identification and stabilization of a highly selective gastrin-releasing peptide receptor agonist. *Journal of Peptide Science*, 25(12). <https://doi.org/10.1002/psc.3224>
- Hoppenz, P., Els-Heindl, S., & Beck-Sickingler, A. G. (2020). Peptide-Drug Conjugates and Their Targets in Advanced Cancer Therapies. *Frontiers in Chemistry*, 8. <https://doi.org/10.3389/fchem.2020.00571>
- Horard, B., & Vanacker, J. (2003). Estrogen receptor-related receptors: orphan receptors desperately seeking a ligand. *Journal of Molecular Endocrinology*, 31(3), 349–357. <https://doi.org/10.1677/jme.0.0310349>
- Hörnberg, E., Ylitalo, E. B., Crnalic, S., Antti, H., Stattin, P., Widmark, A., Bergh, A., & Wikström, P. (2011). Expression of Androgen Receptor Splice Variants in Prostate Cancer Bone Metastases is Associated with Castration-Resistance and Short Survival. *PLoS ONE*, 6(4), e19059. <https://doi.org/10.1371/journal.pone.0019059>
- Horoszewicz, J. S., Leong, S. S., Kawinski, E., Karr, J. P., Rosenthal, H., Chu, T. M., Mirand, E. A., & Murphy, G. P. (1983). LNCaP model of human prostatic carcinoma. *Cancer Research*, 43(4), 1809–1818.
- Hoskin, P., Sartor, O., O'Sullivan, J. M., Johannessen, D. C., Helle, S. I., Logue, J., Bottomley, D., Nilsson, S., Vogelzang, N. J., Fang, F., Wahba, M., Aksnes,

- A.-K., & Parker, C. (2014). Efficacy and safety of radium-223 dichloride in patients with castration-resistant prostate cancer and symptomatic bone metastases, with or without previous docetaxel use: a prespecified subgroup analysis from the randomised, double-blind, phase 3 ALSYMPCA trial. *The Lancet Oncology*, 15(12), 1397–1406. [https://doi.org/10.1016/S1470-2045\(14\)70474-7](https://doi.org/10.1016/S1470-2045(14)70474-7)
- Hosseini, A., & Minucci, S. (2017). A comprehensive review of lysine-specific demethylase 1 and its roles in cancer. *Epigenomics*, 9(8), 1123–1142. <https://doi.org/10.2217/epi-2017-0022>
- Hu, G., Zheng, W., Li, A., Mu, Y., Shi, M., Li, T., Zou, H., Shao, H., Qin, A., & Ye, J. (2018). A novel CAV derived cell-penetrating peptide efficiently delivers exogenous molecules through caveolae-mediated endocytosis. *Veterinary Research*, 49(1), 16. <https://doi.org/10.1186/s13567-018-0513-2>
- Hu, J., Chen, C., Zhang, S., Zhao, X., Xu, H., Zhao, X., & Lu, J. R. (2011). Designed Antimicrobial and Antitumor Peptides with High Selectivity. *Biomacromolecules*, 12(11), 3839–3843. <https://doi.org/10.1021/bm201098j>
- Hu, J.-R., Duncan, M. S., Morgans, A. K., Brown, J. D., Meijers, W. C., Freiberg, M. S., Salem, J.-E., Beckman, J. A., & Moslehi, J. J. (2020). Cardiovascular Effects of Androgen Deprivation Therapy in Prostate Cancer: Contemporary Meta-Analyses. *Arteriosclerosis, Thrombosis, and Vascular Biology*, 40(3). <https://doi.org/10.1161/ATVBAHA.119.313046>
- Hu, R., Dunn, T. A., Wei, S., Isharwal, S., Veltri, R. W., Humphreys, E., Han, M., Partin, A. W., Vessella, R. L., Isaacs, W. B., Bova, G. S., & Luo, J. (2009). Ligand-Independent Androgen Receptor Variants Derived from Splicing of Cryptic Exons Signify Hormone-Refractory Prostate Cancer. *Cancer Research*, 69(1), 16–22. <https://doi.org/10.1158/0008-5472.CAN-08-2764>
- Hu, R., Lu, C., Mostaghel, E. A., Yegnasubramanian, S., Gurel, M., Tannahill, C., Edwards, J., Isaacs, W. B., Nelson, P. S., Bluemn, E., Plymate, S. R., & Luo, J. (2012). Distinct Transcriptional Programs Mediated by the Ligand-Dependent Full-Length Androgen Receptor and Its Splice Variants in Castration-Resistant Prostate Cancer. *Cancer Research*, 72(14), 3457–3462. <https://doi.org/10.1158/0008-5472.CAN-11-3892>
- Huang, J., Sengupta, R., Espejo, A. B., Lee, M. G., Dorsey, J. A., Richter, M., Opravil, S., Shiekhhattar, R., Bedford, M. T., Jenuwein, T., & Berger, S. L. (2007). p53 is regulated by the lysine demethylase LSD1. *Nature*, 449(7158), 105–108. <https://doi.org/10.1038/nature06092>
- Huang, J., Yao, J. L., Di Sant’Agnese, P. A., Yang, Q., Bourne, P. A., & Na, Y. (2006). Immunohistochemical characterization of neuroendocrine cells in prostate cancer. *The Prostate*, 66(13), 1399–1406. <https://doi.org/10.1002/PROS.20434>
- Huang, M.-J., Guo, J.-W., Fu, Y.-D., You, Y.-Z., Xu, W.-Y., Song, T.-Y., Li, R., Chen, Z.-T., Huang, L.-H., & Liu, H.-M. (2021). Discovery of new tranylcypromine derivatives as highly potent LSD1 inhibitors. *Bioorganic & Medicinal Chemistry Letters*, 41, 127993. <https://doi.org/10.1016/j.bmcl.2021.127993>

- Huang, S., Gulzar, Z. G., Salari, K., Lapointe, J., Brooks, J. D., & Pollack, J. R. (2012). Recurrent deletion of CHD1 in prostate cancer with relevance to cell invasiveness. *Oncogene*, 31(37), 4164–4170. <https://doi.org/10.1038/onc.2011.590>
- Huang, Y.-W., Lee, H.-J., Tolliver, L. M., & Aronstam, R. S. (2015). Delivery of Nucleic Acids and Nanomaterials by Cell-Penetrating Peptides: Opportunities and Challenges. *BioMed Research International*, 2015, 1–16. <https://doi.org/10.1155/2015/834079>
- Huggins, C., & Hodges, C. V. (1941). The effect of castration, of estrogen, and of androgen injection on serum phosphatases in metastatic carcinoma of the prostate. *Cancer Research*, 7, 1–293.
- Huotari, J., & Helenius, A. (2011). Endosome maturation. *The EMBO Journal*, 30(17), 3481–3500. <https://doi.org/10.1038/emboj.2011.286>
- Hurt, E. M., Kawasaki, B. T., Klarmann, G. J., Thomas, S. B., & Farrar, W. L. (2008). CD44+CD24– prostate cells are early cancer progenitor/stem cells that provide a model for patients with poor prognosis. *British Journal of Cancer*, 98(4), 756–765. <https://doi.org/10.1038/sj.bjc.6604242>
- Hutagalung, A. H., & Novick, P. J. (2011). Role of Rab GTPases in Membrane Traffic and Cell Physiology. *Physiological Reviews*, 91(1), 119–149. <https://doi.org/10.1152/physrev.00059.2009>
- Huttner, W. B., Gerdes, H. H., & Rosa, P. (1991). The granin-(chromogranin/secretogranin) family. *Trends in Biochemical Sciences*, 16, 27–30. [https://doi.org/10.1016/0968-0004\(91\)90012-K](https://doi.org/10.1016/0968-0004(91)90012-K)
- Imachi, H., Murao, K., Hiramane, C., Sayo, Y., Sato, M., Hosokawa, H., Ishida, T., Kodama, T., Quehenberger, O., Steinberg, D., & Takahara, J. (2000). Human Scavenger Receptor B1 Is Involved in Recognition of Apoptotic Thymocytes by Thymic Nurse Cells. *Laboratory Investigation*, 80(2), 263–270. <https://doi.org/10.1038/labinvest.3780029>
- Iram, T., Ramirez-Ortiz, Z., Byrne, M. H., Coleman, U. A., Kingery, N. D., Means, T. K., Frenkel, D., & El Khoury, J. (2016). Megf10 Is a Receptor for C1Q That Mediates Clearance of Apoptotic Cells by Astrocytes. *The Journal of Neuroscience*, 36(19), 5185–5192. <https://doi.org/10.1523/JNEUROSCI.3850-15.2016>
- Ishii, J., Adachi, H., Aoki, J., Koizumi, H., Tomita, S., Suzuki, T., Tsujimoto, M., Inoue, K., & Arai, H. (2002). SREC-II, a New Member of the Scavenger Receptor Type F Family, Trans-interacts with SREC-I through Its Extracellular Domain. *Journal of Biological Chemistry*, 277(42), 39696–39702. <https://doi.org/10.1074/jbc.M206140200>
- Ishikawa, Y., Kimura-Matsumoto, M., Murakami, M., Murakami, M., Yamamoto, K., Akasaka, Y., Uzuki, M., Yuri, Y., Inomata, N., Yokoo, T., & Ishii, T. (2009). Distribution of Smooth Muscle Cells and Macrophages Expressing Scavenger Receptor BI/II in Atherosclerosis. *Journal of Atherosclerosis and Thrombosis*, 16(6), 829–839. <https://doi.org/10.5551/jat.1941>

- Islam, Md. Z., Sharmin, S., Moniruzzaman, Md., & Yamazaki, M. (2018). Elementary processes for the entry of cell-penetrating peptides into lipid bilayer vesicles and bacterial cells. *Applied Microbiology and Biotechnology*, 102(9), 3879–3892. <https://doi.org/10.1007/s00253-018-8889-5>
- Itoh, Y., Aihara, K., Mellini, P., Tojo, T., Ota, Y., Tsumoto, H., Solomon, V. R., Zhan, P., Suzuki, M., Ogasawara, D., Shigenaga, A., Inokuma, T., Nakagawa, H., Miyata, N., Mizukami, T., Otaka, A., & Suzuki, T. (2016). Identification of SNAI1 Peptide-Based Irreversible Lysine-Specific Demethylase 1-Selective Inactivators. *Journal of Medicinal Chemistry*, 59(4), 1531–1544. <https://doi.org/10.1021/acs.jmedchem.5b01323>
- Ivanov, A. I. (2008). Pharmacological inhibition of endocytic pathways: is it specific enough to be useful? *Methods in Molecular Biology (Clifton, N.J.)*, 440, 15–33. https://doi.org/10.1007/978-1-59745-178-9_2
- Ivascu, A., & Kubbies, M. (2006). Rapid Generation of Single-Tumor Spheroids for High-Throughput Cell Function and Toxicity Analysis. *SLAS Discovery*, 11(8), 922–932. <https://doi.org/10.1177/1087057106292763>
- Iwasaki, T., Murakami, N., & Kawano, T. (2020). A polylysine–polyhistidine fusion peptide for lysosome-targeted protein delivery. *Biochemical and Biophysical Research Communications*, 533(4), 905–912. <https://doi.org/10.1016/j.bbrc.2020.09.087>
- Jacobo, E., Schmidt, J. D., Weinstein, S. H., & Flocks, R. H. (1976). Comparison of flutamide (SCH-13521) and diethylstilbestrol in untreated advanced prostatic cancer. *Urology*, 8(3), 231–233. [https://doi.org/10.1016/0090-4295\(76\)90373-3](https://doi.org/10.1016/0090-4295(76)90373-3)
- Jacobs, D. T., Weigert, R., Grode, K. D., Donaldson, J. G., & Cheney, R. E. (2009). Myosin Vc Is a Molecular Motor That Functions in Secretory Granule Trafficking. *Molecular Biology of the Cell*, 20(21), 4471–4488. <https://doi.org/10.1091/mbc.e08-08-0865>
- Jain, R. K., & Stylianopoulos, T. (2010). Delivering nanomedicine to solid tumors. *Nature Reviews. Clinical Oncology*, 7(11), 653–664. <https://doi.org/10.1038/nrclinonc.2010.139>
- James, N. D., Sydes, M. R., Clarke, N. W., Mason, M. D., Dearnaley, D. P., Spears, M. R., Ritchie, A. W. S., Parker, C. C., Russell, J. M., Attard, G., de Bono, J., Cross, W., Jones, R. J., Thalmann, G., Amos, C., Matheson, D., Millman, R., Alzouebi, M., Beesley, S., ... Parmar, M. K. B. (2016). Addition of docetaxel, zoledronic acid, or both to first-line long-term hormone therapy in prostate cancer (STAMPEDE): survival results from an adaptive, multiarm, multistage, platform randomised controlled trial. *The Lancet*, 387(10024), 1163–1177. [https://doi.org/10.1016/S0140-6736\(15\)01037-5](https://doi.org/10.1016/S0140-6736(15)01037-5)
- Jaskolski, F., Mülle, C., & Manzoni, O. J. (2005). An automated method to quantify and visualize colocalized fluorescent signals. *Journal of Neuroscience Methods*, 146(1), 42–49. <https://doi.org/10.1016/j.jneumeth.2005.01.012>
- Jeannin, P., Bottazzi, B., Sironi, M., Doni, A., Rusnati, M., Presta, M., Maina, V., Magistrelli, G., Haeuw, J. F., Hoeffel, G., Thieblemont, N., Corvaia, N., Garlanda, C., Delneste, Y., & Mantovani, A. (2005). Complexity and

Complementarity of Outer Membrane Protein A Recognition by Cellular and Humoral Innate Immunity Receptors. *Immunity*, 22(5), 551–560.
<https://doi.org/10.1016/j.immuni.2005.03.008>

Jensen, R. T., Battey, J. F., Spindel, E. R., & Benya, R. V. (2008). International Union of Pharmacology. LXVIII. Mammalian Bombesin Receptors: Nomenclature, Distribution, Pharmacology, Signaling, and Functions in Normal and Disease States. *Pharmacological Reviews*, 60(1), 1–42.
<https://doi.org/10.1124/pr.107.07108>

Jenuwein, T., & Allis, C. D. (2001). Translating the Histone Code. *Science*, 293(5532), 1074–1080. <https://doi.org/10.1126/science.1063127>

Ji, Y., Jian, B., Wang, N., Sun, Y., Moya, M. de la L., Phillips, M. C., Rothblat, G. H., Swaney, J. B., & Tall, A. R. (1997). Scavenger Receptor BI Promotes High Density Lipoprotein-mediated Cellular Cholesterol Efflux. *Journal of Biological Chemistry*, 272(34), 20982–20985.
<https://doi.org/10.1074/jbc.272.34.20982>

Ji, Y., Wang, N., Ramakrishnan, R., Sehayek, E., Huszar, D., Breslow, J. L., & Tall, A. R. (1999). Hepatic Scavenger Receptor BI Promotes Rapid Clearance of High Density Lipoprotein Free Cholesterol and Its Transport into Bile. *Journal of Biological Chemistry*, 274(47), 33398–33402.
<https://doi.org/10.1074/jbc.274.47.33398>

Jian, B., de la Llera-Moya, M., Ji, Y., Wang, N., Phillips, M. C., Swaney, J. B., Tall, A. R., & Rothblat, G. H. (1998). Scavenger Receptor Class B Type I as a Mediator of Cellular Cholesterol Efflux to Lipoproteins and Phospholipid Acceptors. *Journal of Biological Chemistry*, 273(10), 5599–5606.
<https://doi.org/10.1074/jbc.273.10.5599>

Jiao, S., Subudhi, S. K., Aparicio, A., Ge, Z., Guan, B., Miura, Y., & Sharma, P. (2019). Differences in Tumor Microenvironment Dictate T Helper Lineage Polarization and Response to Immune Checkpoint Therapy. *Cell*, 179(5), 1177–1190.e13. <https://doi.org/10.1016/j.cell.2019.10.029>

Jonasch, E., & Haluska, F. G. (2001). Interferon in Oncological Practice: Review of Interferon Biology, Clinical Applications, and Toxicities. *The Oncologist*, 6(1), 34–55. <https://doi.org/10.1634/theoncologist.6-1-34>

Jones, A. T., & Sayers, E. J. (2012). Cell entry of cell penetrating peptides: tales of tails wagging dogs. *Journal of Controlled Release*, 161(2), 582–591.
<https://doi.org/10.1016/j.jconrel.2012.04.003>

Joubert, N., Denevault-Sabourin, C., Bryden, F., & Viaud-Massuard, M.-C. (2017). Towards antibody-drug conjugates and prodrug strategies with extracellular stimuli-responsive drug delivery in the tumor microenvironment for cancer therapy. *European Journal of Medicinal Chemistry*, 142, 393–415.
<https://doi.org/10.1016/j.ejmech.2017.08.049>

Jozwik, K. M., & Carroll, J. S. (2012). Pioneer factors in hormone-dependent cancers. *Nature Reviews Cancer*, 12(6), 381–385.
<https://doi.org/10.1038/nrc3263>

- Jung, Y., Kim, J. K., Lee, E., Cackowski, F. C., Decker, A. M., Krebsbach, P. H., & Taichman, R. S. (2020). CXCL12 γ induces human prostate and mammary gland development. *The Prostate*, 80(13), 1145–1156. <https://doi.org/10.1002/pros.24043>
- Kaelin, W. G. (2005). The Concept of Synthetic Lethality in the Context of Anticancer Therapy. *Nature Reviews Cancer*, 5(9), 689–698. <https://doi.org/10.1038/nrc1691>
- Kahl, P., Gullotti, L., Heukamp, L. C., Wolf, S., Friedrichs, N., Vorreuther, R., Solleder, G., Bastian, P. J., Ellinger, J., Metzger, E., Schüle, R., & Buettner, R. (2006). Androgen Receptor Coactivators Lysine-Specific Histone Demethylase 1 and Four and a Half LIM Domain Protein 2 Predict Risk of Prostate Cancer Recurrence. *Cancer Research*, 66(23), 11341–11347. <https://doi.org/10.1158/0008-5472.CAN-06-1570>
- Kaighn, M. E., Narayan, K. S., Ohnuki, Y., Lechner, J. F., & Jones, L. W. (1979). Establishment and characterization of a human prostatic carcinoma cell line (PC-3). *Investigative Urology*, 17(1), 16–23.
- Kakizawa, T., Ota, Y., Itoh, Y., Tsumoto, H., & Suzuki, T. (2015). Histone H3 peptide based LSD1-selective inhibitors. *Bioorganic & Medicinal Chemistry Letters*, 25(9), 1925–1928. <https://doi.org/10.1016/j.bmcl.2015.03.030>
- Kaksonen, M., & Roux, A. (2018). Mechanisms of clathrin-mediated endocytosis. *Nature Reviews. Molecular Cell Biology*, 19(5), 313–326. <https://doi.org/10.1038/nrm.2017.132>
- Kalantari, E., Asgari, M., Nikpanah, S., Salarieh, N., Asadi Lari, M. H., & Madjd, Z. (2017). Co-Expression of Putative Cancer Stem Cell Markers CD44 and CD133 in Prostate Carcinomas. *Pathology & Oncology Research*, 23(4), 793–802. <https://doi.org/10.1007/s12253-016-0169-z>
- Kanouni, T., Severin, C., Cho, R. W., Yuen, N. Y.-Y., Xu, J., Shi, L., Lai, C., Del Rosario, J. R., Stansfield, R. K., Lawton, L. N., Hosfield, D., O'Connell, S., Kreilein, M. M., Tavares-Greco, P., Nie, Z., Kaldor, S. W., Veal, J. M., Stafford, J. A., & Chen, Y. K. (2020). Discovery of CC-90011: A Potent and Selective Reversible Inhibitor of Lysine Specific Demethylase 1 (LSD1). *Journal of Medicinal Chemistry*, 63(23), 14522–14529. <https://doi.org/10.1021/acs.jmedchem.0c00978>
- Kantoff, P. W., Higano, C. S., Shore, N. D., Berger, E. R., Small, E. J., Penson, D. F., Redfern, C. H., Ferrari, A. C., Dreicer, R., Sims, R. B., Xu, Y., Frohlich, M. W., & Schellhammer, P. F. (2010). Sipuleucel-T Immunotherapy for Castration-Resistant Prostate Cancer. *New England Journal of Medicine*, 363(5), 411–422. <https://doi.org/10.1056/NEJMoa1001294>
- Kaplan, I. M., Wadia, J. S., & Dowdy, S. F. (2005). Cationic TAT peptide transduction domain enters cells by macropinocytosis. *Journal of Controlled Release*, 102(1), 247–253. <https://doi.org/10.1016/j.jconrel.2004.10.018>
- Karampelas, T., Argyros, O., Sayyad, N., Spyridaki, K., Pappas, C., Morgan, K., Kolios, G., Millar, R. P., Liapakis, G., Tzakos, A. G., Fokas, D., & Tamvakopoulos, C. (2014). GnRH-Gemcitabine Conjugates for the Treatment of Androgen-Independent Prostate Cancer: Pharmacokinetic Enhancements

- Combined with Targeted Drug Delivery. *Bioconjugate Chemistry*, 25(4), 813–823. <https://doi.org/10.1021/bc500081g>
- Kari, V., Mansour, W. Y., Raul, S. K., Baumgart, S. J., Mund, A., Grade, M., Sirma, H., Simon, R., Will, H., Dobbelstein, M., Dikomey, E., & Johnsen, S. A. (2016). Loss of CHD1 causes DNA repair defects and enhances prostate cancer therapeutic responsiveness. *EMBO Reports*, 17(11), 1609–1623. <https://doi.org/10.15252/embr.201642352>
- Kashyap, V., Ahmad, S., Nilsson, E. M., Helczynski, L., Kenna, S., Persson, J. L., Gudas, L. J., & Mongan, N. P. (2013). The lysine specific demethylase-1 (LSD1/KDM1A) regulates VEGF-A expression in prostate cancer. *Molecular Oncology*, 7(3), 555–566. <https://doi.org/10.1016/j.molonc.2013.01.003>
- Kasisvisvanathan, V., Rannikko, A. S., Borghi, M., Panebianco, V., Mynderse, L. A., Vaarala, M. H., Briganti, A., Budäus, L., Hellawell, G., Hindley, R. G., Roobol, M. J., Eggener, S., Ghei, M., Villers, A., Bladou, F., Villeirs, G. M., Viridi, J., Boxler, S., Robert, G., ... Moore, C. M. (2018). MRI-Targeted or Standard Biopsy for Prostate-Cancer Diagnosis. *New England Journal of Medicine*, 378(19), 1767–1777. <https://doi.org/10.1056/NEJMoa1801993>
- Kauffman, W. B., Fuselier, T., He, J., & Wimley, W. C. (2015). Mechanism Matters: A Taxonomy of Cell Penetrating Peptides. *Trends in Biochemical Sciences*, 40(12), 749–764. <https://doi.org/10.1016/j.tibs.2015.10.004>
- Kawaguchi, Y., Takeuchi, T., Kuwata, K., Chiba, J., Hatanaka, Y., Nakase, I., & Futaki, S. (2016). Syndecan-4 Is a Receptor for Clathrin-Mediated Endocytosis of Arginine-Rich Cell-Penetrating Peptides. *Bioconjugate Chemistry*, 27(4), 1119–1130. <https://doi.org/10.1021/acs.bioconjchem.6b00082>
- Kawamoto, S., Takasu, M., Miyakawa, T., Morikawa, R., Oda, T., Futaki, S., & Nagao, H. (2011). Inverted micelle formation of cell-penetrating peptide studied by coarse-grained simulation: Importance of attractive force between cell-penetrating peptides and lipid head group. *The Journal of Chemical Physics*, 134(9), 095103. <https://doi.org/10.1063/1.3555531>
- Kellokumpu-Lehtinen, P., & Pelliniemi, L. J. (1988). Hormonal regulation of differentiation of human fetal prostate and Leydig cells in vitro. *Folia Histochemica et Cytobiologica*, 26(3), 113–117.
- Kellokumpu-Lehtinen, P., Santti, R. S., & Pelliniemi, L. J. (1981). Development of human fetal prostate in culture. *Urological Research*, 9(2), 89–98. <https://doi.org/10.1007/BF00256682/METRICS>
- Kenrick, N., Smith, S., & Shamash, J. (2020). Metastatic Hormone-Sensitive Prostate Cancer (mHSPC): Advances and Treatment Strategies in the First-Line Setting. *Oncology and Therapy*, 8(2), 209–230. <https://doi.org/10.1007/s40487-020-00119-z>
- Kesch, C., Heidegger, I., Kasisvisvanathan, V., Kretschmer, A., Marra, G., Preisser, F., Tilki, D., Tsaur, I., Valerio, M., van den Bergh, R. C. N., Fankhauser, C. D., Zattoni, F., & Gandaglia, G. (2021). Radical Prostatectomy: Sequelae in the Course of Time. *Frontiers in Surgery*, 8. <https://doi.org/10.3389/fsurg.2021.684088>

- Ketscher, A., Jilg, C. A., Willmann, D., Hummel, B., Imhof, A., Rüsseler, V., Hölz, S., Metzger, E., Müller, J. M., & Schüle, R. (2014). LSD1 controls metastasis of androgen-independent prostate cancer cells through PXN and LPAR6. *Oncogenesis*, 3(10), e120–e120. <https://doi.org/10.1038/oncsis.2014.34>
- Khoury, J. El, Hickman, S. E., Thomas, C. A., Cao, L., Silverstein, S. C., & Loike, J. D. (1996). Scavenger receptor-mediated adhesion of microglia to β -amyloid fibrils. *Nature*, 382(6593), 716–719. <https://doi.org/10.1038/382716a0>
- Kim, C., Kong, G., Lee, H., Tran, Q., Vo, T.-T. T., Kwon, S. H., Park, J., Kim, S.-H., & Park, J. (2022). Scavenger receptor class F member 2 (SCARF2) as a novel therapeutic target in glioblastoma. *Toxicological Research*, 38(2), 249–256. <https://doi.org/10.1007/s43188-022-00125-5>
- Kim, M., Rhee, J.-K., Choi, H., Kwon, A., Kim, J., Lee, G. D., Jekarl, D. W., Lee, S., Kim, Y., & Kim, T.-M. (2017). Passage-dependent accumulation of somatic mutations in mesenchymal stromal cells during in vitro culture revealed by whole genome sequencing. *Scientific Reports*, 7(1), 14508. <https://doi.org/10.1038/s41598-017-15155-5>
- Kim, S. W., Kim, N. Y., Choi, Y. Bin, Park, S. H., Yang, J. M., & Shin, S. (2010). RNA interference in vitro and in vivo using an arginine peptide/siRNA complex system. *Journal of Controlled Release*, 143(3), 335–343. <https://doi.org/10.1016/j.jconrel.2010.01.009>
- Kim, Y., Nam, H. J., Lee, J., Park, D. Y., Kim, C., Yu, Y. S., Kim, D., Park, S. W., Bhin, J., Hwang, D., Lee, H., Koh, G. Y., & Baek, S. H. (2016). Methylation-dependent regulation of HIF-1 α stability restricts retinal and tumour angiogenesis. *Nature Communications*, 7(1), 10347. <https://doi.org/10.1038/ncomms10347>
- Kim, Y.-R., Oh, K.-J., Park, R.-Y., Xuan, N. T., Kang, T.-W., Kwon, D.-D., Choi, C., Kim, M. S., Nam, K. Il, Ahn, K. Y., & Jung, C. (2010). HOXB13 promotes androgen independent growth of LNCaP prostate cancer cells by the activation of E2F signaling. *Molecular Cancer*, 9(1), 124. <https://doi.org/10.1186/1476-4598-9-124>
- Kind, F., Michalski, K., Yousefzadeh-Nowshahr, E., Meyer, P. T., Mix, M., & Ruf, J. (2022). Bone marrow impairment during early [177Lu]PSMA-617 radioligand therapy: Haematotoxicity or tumour progression? *EJNMMI Research*, 12(1), 20. <https://doi.org/10.1186/s13550-022-00891-1>
- Kiviharju-af Hällström, T. M., Jäämaa, S., Mönkkönen, M., Peltonen, K., Andersson, L. C., Medema, R. H., Peehl, D. M., & Laiho, M. (2007). Human prostate epithelium lacks Wee1A-mediated DNA damage-induced checkpoint enforcement. *Proceedings of the National Academy of Sciences*, 104(17), 7211–7216. <https://doi.org/10.1073/pnas.0609299104>
- Klimpel, A., Lützenburg, T., & Neundorf, I. (2019). Recent advances of anti-cancer therapies including the use of cell-penetrating peptides. *Current Opinion in Pharmacology*, 47, 8–13. <https://doi.org/10.1016/J.COPH.2019.01.003>
- Klotz, L., O'Callaghan, C., Ding, K., Toren, P., Dearnaley, D., Higano, C. S., Horwitz, E., Malone, S., Goldenberg, L., Gospodarowicz, M., & Crook, J. M. (2015). Nadir Testosterone Within First Year of Androgen-Deprivation

- Therapy (ADT) Predicts for Time to Castration-Resistant Progression: A Secondary Analysis of the PR-7 Trial of Intermittent Versus Continuous ADT. *Journal of Clinical Oncology*, 33(10), 1151–1156.
<https://doi.org/10.1200/JCO.2014.58.2973>
- Knapinska, A. M., & Fields, G. B. (2019). The Expanding Role of MT1-MMP in Cancer Progression. *Pharmaceuticals*, 12(2), 77.
<https://doi.org/10.3390/ph12020077>
- Kobayashi, T., Vischer, U. M., Rosnoblet, C., Lebrand, C., Lindsay, M., Parton, R. G., Kruithof, E. K. O., & Gruenberg, J. (2000). The Tetraspanin CD63/lamp3 Cycles between Endocytic and Secretory Compartments in Human Endothelial Cells. *Molecular Biology of the Cell*, 11(5), 1829–1843.
<https://doi.org/10.1091/mbc.11.5.1829>
- Kohaar, I., Petrovics, G., & Srivastava, S. (2019). A Rich Array of Prostate Cancer Molecular Biomarkers: Opportunities and Challenges. *International Journal of Molecular Sciences*, 20(8), 1813. <https://doi.org/10.3390/ijms20081813>
- Kontaki, H., & Talianidis, I. (2010). Lysine Methylation Regulates E2F1-Induced Cell Death. *Molecular Cell*, 39(1), 152–160.
<https://doi.org/10.1016/j.molcel.2010.06.006>
- Kornfeld, S., & Mellman, I. (1989). The Biogenesis of Lysosomes. *Annual Review of Cell Biology*, 5(1), 483–525.
<https://doi.org/10.1146/annurev.cb.05.110189.002411>
- Kosuge, M., Takeuchi, T., Nakase, I., Jones, A. T., & Futaki, S. (2008). Cellular Internalization and Distribution of Arginine-Rich Peptides as a Function of Extracellular Peptide Concentration, Serum, and Plasma Membrane Associated Proteoglycans. *Bioconjugate Chemistry*, 19(3), 656–664.
<https://doi.org/10.1021/bc700289w>
- Kotamarti, S., & Polascik, T. J. (2023). Focal cryotherapy for prostate cancer: a contemporary literature review. *Annals of Translational Medicine*, 11(1), 26–26. <https://doi.org/10.21037/atm-21-5033>
- Koyama-Honda, I., Ritchie, K., Fujiwara, T., Iino, R., Murakoshi, H., Kasai, R. S., & Kusumi, A. (2005). Fluorescence Imaging for Monitoring the Colocalization of Two Single Molecules in Living Cells. *Biophysical Journal*, 88(3), 2126–2136.
<https://doi.org/10.1529/biophysj.104.048967>
- Kraus, L. A., Samuel, S. K., Schmid, S. M., Dykes, D. J., Waud, W. R., & Bissery, M. C. (2003). The mechanism of action of docetaxel (Taxotere®) in xenograft models is not limited to bcl-2 phosphorylation. *Investigational New Drugs*, 21(3), 259–268. <https://doi.org/10.1023/A:1025436307913>
- Krieger, M. (1999). Charting the Fate of the “Good Cholesterol”: Identification and Characterization of the High-Density Lipoprotein Receptor SR-BI. *Annual Review of Biochemistry*, 68(1), 523–558.
<https://doi.org/10.1146/annurev.biochem.68.1.523>
- Krijnen, J. L., Janssen, P. J., Ruizeveld de Winter, J. A., van Krimpen, H., Schröder, F. H., & van der Kwast, T. H. (1993). Do neuroendocrine cells in

- human prostate cancer express androgen receptor? *Histochemistry*, 100(5), 393–398. <https://doi.org/10.1007/BF00268938>
- Kroon, J., Kooijman, S., Cho, N.-J., Storm, G., & van der Pluijm, G. (2016). Improving Taxane-Based Chemotherapy in Castration-Resistant Prostate Cancer. *Trends in Pharmacological Sciences*, 37(6), 451–462. <https://doi.org/10.1016/j.tips.2016.03.003>
- Kuchibhotla, S., Vanegas, D., Kennedy, D. J., Guy, E., Nimako, G., Morton, R. E., & Febbraio, M. (2008). Absence of CD36 protects against atherosclerosis in ApoE knock-out mice with no additional protection provided by absence of scavenger receptor A I/II. *Cardiovascular Research*, 78(1), 185–196. <https://doi.org/10.1093/cvr/cvm093>
- Kumarasinghe, I. R., & Woster, P. M. (2014). Synthesis and Evaluation of Novel Cyclic Peptide Inhibitors of Lysine-Specific Demethylase 1. *ACS Medicinal Chemistry Letters*, 5(1), 29–33. <https://doi.org/10.1021/ml4002997>
- Kumarasinghe, I. R., & Woster, P. M. (2018). Cyclic peptide inhibitors of lysine-specific demethylase 1 with improved potency identified by alanine scanning mutagenesis. *European Journal of Medicinal Chemistry*, 148, 210–220. <https://doi.org/10.1016/j.ejmech.2018.01.098>
- Kumthekar, P., Tang, S.-C., Brenner, A. J., Kesari, S., Piccioni, D. E., Anders, C., Carrillo, J., Chalasani, P., Kabos, P., Puhalla, S., Tkaczuk, K., Garcia, A. A., Ahluwalia, M. S., Wefel, J. S., Lakhani, N., & Ibrahim, N. (2020). ANG1005, a Brain-Penetrating Peptide-Drug Conjugate, Shows Activity in Patients with Breast Cancer with Leptomeningeal Carcinomatosis and Recurrent Brain Metastases. *Clinical Cancer Research : An Official Journal of the American Association for Cancer Research*, 26(12), 2789–2799. <https://doi.org/10.1158/1078-0432.CCR-19-3258>
- Kuronita, T., Eskelinen, E.-L., Fujita, H., Saftig, P., Himeno, M., & Tanaka, Y. (2002). A role for the lysosomal membrane protein LGP85 in the biogenesis and maintenance of endosomal and lysosomal morphology. *Journal of Cell Science*, 115(21), 4117–4131. <https://doi.org/10.1242/jcs.00075>
- Kwekkeboom, D. J., Kam, B. L., van Essen, M., Teunissen, J. J. M., van Eijck, C. H. J., Valkema, R., de Jong, M., de Herder, W. W., & Krenning, E. P. (2010). Somatostatin receptor-based imaging and therapy of gastroenteropancreatic neuroendocrine tumors. *Endocrine-Related Cancer*, 17(1), R53–R73. <https://doi.org/10.1677/ERC-09-0078>
- Kweldam, C. F., van Leenders, G. J., & van der Kwast, T. (2019). Grading of prostate cancer: a work in progress. *Histopathology*, 74(1), 146–160. <https://doi.org/10.1111/his.13767>
- Kzhyshkowska, J., Neyen, C., & Gordon, S. (2012). Role of macrophage scavenger receptors in atherosclerosis. *Immunobiology*, 217(5), 492–502. <https://doi.org/10.1016/j.imbio.2012.02.015>
- Lalonde, E., Ishkanian, A. S., Sykes, J., Fraser, M., Ross-Adams, H., Erho, N., Dunning, M. J., Halim, S., Lamb, A. D., Moon, N. C., Zafarana, G., Warren, A. Y., Meng, X., Thoms, J., Grzadkowski, M. R., Berlin, A., Have, C. L., Ramnarine, V. R., Yao, C. Q., ... Bristow, R. G. (2014). Tumour genomic and

- microenvironmental heterogeneity for integrated prediction of 5-year biochemical recurrence of prostate cancer: a retrospective cohort study. *The Lancet Oncology*, 15(13), 1521–1532. [https://doi.org/10.1016/S1470-2045\(14\)71021-6](https://doi.org/10.1016/S1470-2045(14)71021-6)
- Lan, F., Nottke, A. C., & Shi, Y. (2008). Mechanisms involved in the regulation of histone lysine demethylases. *Current Opinion in Cell Biology*, 20(3), 316–325. <https://doi.org/10.1016/j.ceb.2008.03.004>
- Lan, H., Tan, M., Zhang, Q., Yang, F., Wang, S., Li, H., Xiong, X., & Sun, Y. (2019). LSD1 destabilizes FBXW7 and abrogates FBXW7 functions independent of its demethylase activity. *Proceedings of the National Academy of Sciences*, 116(25), 12311–12320. <https://doi.org/10.1073/pnas.1902012116>
- Landschulz, K. T., Pathak, R. K., Rigotti, A., Krieger, M., & Hobbs, H. H. (1996). Regulation of scavenger receptor, class B, type I, a high density lipoprotein receptor, in liver and steroidogenic tissues of the rat. *Journal of Clinical Investigation*, 98(4), 984–995. <https://doi.org/10.1172/JCI118883>
- Lane, P. E. (2021). A Mechanism Based Probe for Visualising Chromatin-modifying Enzyme Lysine-Specific Histone Demethylase 1. Doctoral, Sheffield Hallam University. <https://doi.org/10.7190/shu-thesis-00391>
- Lang, S. H., Sharrard, R. M., Stark, M., Villette, J. M., & Maitland, N. J. (2001). Prostate epithelial cell lines form spheroids with evidence of glandular differentiation in three-dimensional Matrigel cultures. *British Journal of Cancer*, 85(4), 590–599. <https://doi.org/10.1054/bjoc.2001.1967>
- Lang, S., Swift, S., White, H., Misso, K., Kleijnen, J., & Quek, R. (2019). A systematic review of the prevalence of DNA damage response gene mutations in prostate cancer. *International Journal of Oncology*. <https://doi.org/10.3892/ijo.2019.4842>
- Langel, Ü. (2015). *Cell-Penetrating Peptides* (Ü. Langel, Ed.; Third, Vol. 683). Humana Press. <https://doi.org/10.1007/978-1-60761-919-2>
- Langel, Ü. (2019). *CPP, Cell-Penetrating Peptides*. Springer Singapore. <https://doi.org/10.1007/978-981-13-8747-0>
- Langer, M., Kratz, F., Rothen-Rutishauser, B., Wunderli-Allenspach, H., & Beck-Sickinger, A. G. (2001). Novel Peptide Conjugates for Tumor-Specific Chemotherapy. *Journal of Medicinal Chemistry*, 44(9), 1341–1348. <https://doi.org/10.1021/jm001065f>
- Lau, J. L., & Dunn, M. K. (2018). Therapeutic peptides: Historical perspectives, current development trends, and future directions. *Bioorganic & Medicinal Chemistry*, 26(10), 2700–2707. <https://doi.org/10.1016/j.bmc.2017.06.052>
- Laufer, S. D., Detzer, A., Sczakiel, G., & Restle, T. (2010). Selected Strategies for the Delivery of siRNA In Vitro and In Vivo. In *RNA Technologies and Their Applications* (pp. 29–58). Springer Berlin Heidelberg. https://doi.org/10.1007/978-3-642-12168-5_2
- Laurent, B., Ruitu, L., Murn, J., Hempel, K., Ferrao, R., Xiang, Y., Liu, S., Garcia, B. A., Wu, H., Wu, F., Steen, H., & Shi, Y. (2015). A Specific LSD1/KDM1A

- Isoform Regulates Neuronal Differentiation through H3K9 Demethylation. *Molecular Cell*, 57(6), 957–970. <https://doi.org/10.1016/j.molcel.2015.01.010>
- Le, D. T., Durham, J. N., Smith, K. N., Wang, H., Bartlett, B. R., Aulakh, L. K., Lu, S., Kemberling, H., Wilt, C., Lubber, B. S., Wong, F., Azad, N. S., Rucki, A. A., Laheru, D., Donehower, R., Zaheer, A., Fisher, G. A., Crocenzi, T. S., Lee, J. J., ... Diaz, L. A. (2017). Mismatch repair deficiency predicts response of solid tumors to PD-1 blockade. *Science*, 357(6349), 409–413. <https://doi.org/10.1126/science.aan6733>
- LeCher, J. C., Nowak, S. J., & McMurry, J. L. (2017). Breaking in and busting out: cell-penetrating peptides and the endosomal escape problem. *Biomolecular Concepts*, 8(3–4), 131–141. <https://doi.org/10.1515/bmc-2017-0023>
- Ledet, E. M., Lilly, M. B., Sonpavde, G., Lin, E., Nussenzveig, R. H., Barata, P. C., Yandell, M., Nagy, R. J., Kiedrowski, L., Agarwal, N., & Sartor, O. (2020). Comprehensive Analysis of AR Alterations in Circulating Tumor DNA from Patients with Advanced Prostate Cancer. *The Oncologist*, 25(4), 327–333. <https://doi.org/10.1634/theoncologist.2019-0115>
- Lee, J.-Y., Park, J.-H., Choi, H.-J., Won, H.-Y., Joo, H., Shin, D.-H., Park, M. K., Han, B., Kim, K. P., Lee, T. J., Croce, C. M., & Kong, G. (2017). LSD1 demethylates HIF1 α to inhibit hydroxylation and ubiquitin-mediated degradation in tumor angiogenesis. *Oncogene*, 36(39), 5512–5521. <https://doi.org/10.1038/onc.2017.158>
- Lee, M. G., Wynder, C., Cooch, N., & Shiekhhattar, R. (2005). An essential role for CoREST in nucleosomal histone 3 lysine 4 demethylation. *Nature*, 437(7057), 432–435. <https://doi.org/10.1038/nature04021>
- Lee, M.-T., Hung, W.-C., Chen, F.-Y., & Huang, H. W. (2005). Many-Body Effect of Antimicrobial Peptides: On the Correlation Between Lipid's Spontaneous Curvature and Pore Formation. *Biophysical Journal*, 89(6), 4006–4016. <https://doi.org/10.1529/biophysj.105.068080>
- Lee, S. H., Castagner, B., & Leroux, J.-C. (2013). Is there a future for cell-penetrating peptides in oligonucleotide delivery? *European Journal of Pharmaceutics and Biopharmaceutics*, 85(1), 5–11. <https://doi.org/10.1016/j.ejpb.2013.03.021>
- Lee, S. H., Liu, X. M., Diamond, M., Dostalík, V., Favata, M., He, C., Wu, L., Wynn, R., Yao, W., Hollis, G., Huber, R., Scherle, P., & Ruggeri, B. (2016). Abstract 4704: The evaluation of INCB059872, an FAD-directed inhibitor of LSD1, in preclinical models of human small cell lung cancer. *Cancer Research*, 76(14_Supplement), 4704–4704. <https://doi.org/10.1158/1538-7445.AM2016-4704>
- Lee, S. H., Moroz, E., Castagner, B., & Leroux, J.-C. (2014). Activatable Cell Penetrating Peptide–Peptide Nucleic Acid Conjugate via Reduction of Azobenzene PEG Chains. *Journal of the American Chemical Society*, 136(37), 12868–12871. <https://doi.org/10.1021/ja507547w>
- Lee, S. H., & Shen, M. M. (2015). Cell types of origin for prostate cancer. *Current Opinion in Cell Biology*, 37, 35–41. <https://doi.org/10.1016/j.ceb.2015.10.002>

- Lee, S., Sato, Y., & Nixon, R. A. (2011). Lysosomal proteolysis inhibition selectively disrupts axonal transport of degradative organelles and causes an Alzheimer's-like axonal dystrophy. *The Journal of Neuroscience : The Official Journal of the Society for Neuroscience*, 31(21), 7817–7830. <https://doi.org/10.1523/JNEUROSCI.6412-10.2011>
- Lee, Y. T., Tan, Y. J., & Oon, C. E. (2018). Molecular targeted therapy: Treating cancer with specificity. *European Journal of Pharmacology*, 834, 188–196. <https://doi.org/10.1016/j.ejphar.2018.07.034>
- Lehto, T., Ezzat, K., Wood, M. J. A., & EL Andaloussi, S. (2016). Peptides for nucleic acid delivery. *Advanced Drug Delivery Reviews*, 106, 172–182. <https://doi.org/10.1016/j.addr.2016.06.008>
- Leng, F., Yu, J., Zhang, C., Alejo, S., Hoang, N., Sun, H., Lu, F., & Zhang, H. (2018). Methylated DNMT1 and E2F1 are targeted for proteolysis by L3MBTL3 and CRL4DCAF5 ubiquitin ligase. *Nature Communications*, 9(1), 1641. <https://doi.org/10.1038/s41467-018-04019-9>
- Leon, C. G., Locke, J. A., Adomat, H. H., Etinger, S. L., Twiddy, A. L., Neumann, R. D., Nelson, C. C., Guns, E. S., & Wasan, K. M. (2010). Alterations in cholesterol regulation contribute to the production of intratumoral androgens during progression to castration-resistant prostate cancer in a mouse xenograft model. *The Prostate*, 70(4), 390–400. <https://doi.org/10.1002/pros.21072>
- Li, H., Wang, Y., Lin, K., Venkadakrishnan, V. B., Bakht, M., Shi, W., Meng, C., Zhang, J., Tremble, K., Liang, X., Song, J. H., Feng, X., Van, V., Deng, P., Burks, J. K., Aparicio, A., Keyomarsi, K., Chen, J., Lu, Y., ... Zhao, D. (2022). CHD1 Promotes Sensitivity to Aurora Kinase Inhibitors by Suppressing Interaction of AURKA with Its Coactivator TPX2. *Cancer Research*, 82(17), 3088–3101. <https://doi.org/10.1158/0008-5472.CAN-22-0631>
- Li, M., Liu, M., Han, W., Wang, Z., Han, D., Patalano, S., Macoska, J. A., Balk, S. P., He, H. H., Corey, E., Gao, S., & Cai, C. (2023). LSD1 Inhibition Disrupts Super-Enhancer–Driven Oncogenic Transcriptional Programs in Castration-Resistant Prostate Cancer. *Cancer Research*, 83(10), 1684–1698. <https://doi.org/10.1158/0008-5472.CAN-22-2433>
- Li, S., & Roberts, R. W. (2003). A Novel Strategy for In Vitro Selection of Peptide-Drug Conjugates. *Chemistry & Biology*, 10(3), 233–239. [https://doi.org/10.1016/S1074-5521\(03\)00047-4](https://doi.org/10.1016/S1074-5521(03)00047-4)
- Li, S., & Xia, M. (2019). Review of high-content screening applications in toxicology. *Archives of Toxicology*, 93(12), 3387–3396. <https://doi.org/10.1007/s00204-019-02593-5>
- Li, W., Hao, Q., He, L., Meng, J., Li, M., Xue, X., Zhang, C., Li, H., Zhang, W., & Zhang, Y. (2015). Recombinant IFN- α 2a-NGR exhibits higher inhibitory function on tumor neovessels formation compared with IFN- α 2a in vivo and in vitro. *Cytotechnology*, 67(6), 1039–1050. <https://doi.org/10.1007/s10616-014-9743-y>
- Li, W.-P., Liu, P., Pilcher, B. K., & Anderson, R. G. W. (2001). Cell-specific targeting of caveolin-1 to caveolae, secretory vesicles, cytoplasm or

- mitochondria. *Journal of Cell Science*, 114(7), 1397–1408.
<https://doi.org/10.1242/jcs.114.7.1397>
- Li, X., Kan, H.-Y., Lavrentiadou, S., Krieger, M., & Zannis, V. (2002). Reconstituted Discoidal ApoE-Phospholipid Particles Are Ligands for the Scavenger Receptor BI. *Journal of Biological Chemistry*, 277(24), 21149–21157.
<https://doi.org/10.1074/jbc.M200658200>
- Li, Z., Zhao, R., Wu, X., Sun, Y., Yao, M., Li, J., Xu, Y., & Gu, J. (2005). Identification and characterization of a novel peptide ligand of epidermal growth factor receptor for targeted delivery of therapeutics. *The FASEB Journal*, 19(14), 1978–1985. <https://doi.org/10.1096/fj.05-4058com>
- Liang, H., Liu, Y., Guo, J., Dou, M., Zhang, X., Hu, L., & Chen, J. (2023). Progression in immunotherapy for advanced prostate cancer. *Frontiers in Oncology*, 13. <https://doi.org/10.3389/fonc.2023.1126752>
- Liang, Y., Ahmed, M., Guo, H., Soares, F., Hua, J. T., Gao, S., Lu, C., Poon, C., Han, W., Langstein, J., Ekram, M. B., Li, B., Davicioni, E., Takhar, M., Erho, N., Karnes, R. J., Chadwick, D., van der Kwast, T., Boutros, P. C., ... He, H. H. (2017). LSD1-Mediated Epigenetic Reprogramming Drives CENPE Expression and Prostate Cancer Progression. *Cancer Research*, 77(20), 5479–5490. <https://doi.org/10.1158/0008-5472.CAN-17-0496>
- Lim, J. P., & Gleeson, P. A. (2011). Macropinocytosis: an endocytic pathway for internalising large gulps. *Immunology & Cell Biology*, 89(8), 836–843.
<https://doi.org/10.1038/icb.2011.20>
- Limmon, G. V., Arredouani, M., McCann, K. L., Minor, R. A. C., Kobzik, L., & Imani, F. (2008). Scavenger receptor class-A is a novel cell surface receptor for double-stranded RNA. *The FASEB Journal*, 22(1), 159–167.
<https://doi.org/10.1096/fj.07-8348com>
- Lin, P., Aronson, W., & Freedland, S. (2015). Nutrition, dietary interventions and prostate cancer: the latest evidence. *BMC Medicine*, 13(1), 3.
<https://doi.org/10.1186/s12916-014-0234-y>
- Lin, Y., Wu, Y., Li, J., Dong, C., Ye, X., Chi, Y.-I., Evers, B. M., & Zhou, B. P. (2010). The SNAG domain of Snail1 functions as a molecular hook for recruiting lysine-specific demethylase 1. *The EMBO Journal*, 29(11), 1803–1816. <https://doi.org/10.1038/emboj.2010.63>
- Lindberg, R. A., & Hunter, T. (1990). cDNA Cloning and Characterization of eck , an Epithelial Cell Receptor Protein-Tyrosine Kinase in the eph/elk Family of Protein Kinases. *Molecular and Cellular Biology*, 10(12), 6316–6324.
<https://doi.org/10.1128/mcb.10.12.6316-6324.1990>
- Lindberg, S., Muñoz-Alarcón, A., Helmfors, H., Mosqueira, D., Gyllborg, D., Tudoran, O., & Langel, Ü. (2013). PepFect15, a novel endosomolytic cell-penetrating peptide for oligonucleotide delivery via scavenger receptors. *International Journal of Pharmaceutics*, 441(1–2), 242–247.
<https://doi.org/10.1016/j.ijpharm.2012.11.037>

- Lindgren, M., Hällbrink, M., Prochiantz, A., & Langel, Ü. (2000). Cell-penetrating peptides. *Trends in Pharmacological Sciences*, 21(3), 99–103.
[https://doi.org/10.1016/S0165-6147\(00\)01447-4](https://doi.org/10.1016/S0165-6147(00)01447-4)
- Liolios, C., Sachpekidis, C., Schäfer, M., & Kopka, K. (2019). Bispecific radioligands targeting prostate-specific membrane antigen and gastrin-releasing peptide receptors on the surface of prostate cancer cells. *Journal of Labelled Compounds and Radiopharmaceuticals*, 62(8), 510–522.
<https://doi.org/10.1002/jlcr.3749>
- Liu, A. Y. (1994). Expression of CD44 in prostate cancer cells. *Cancer Letters*, 76(1), 63–69. [https://doi.org/10.1016/0304-3835\(94\)90135-X](https://doi.org/10.1016/0304-3835(94)90135-X)
- Liu, A. Y., True, L. D., Latray, L., Nelson, P. S., Ellis, W. J., Vessella, R. L., Lange, P. H., Hood, L., & Van Engh, G. Den. (1997). Cell–cell interaction in prostate gene regulation and cytodifferentiation. *Proceedings of the National Academy of Sciences of the United States of America*, 94(20), 10705.
<https://doi.org/10.1073/PNAS.94.20.10705>
- Liu, B. R., Lin, M. Der, Chiang, H. J., & Lee, H. J. (2012). Arginine-rich cell-penetrating peptides deliver gene into living human cells. *Gene*, 505(1), 37–45. <https://doi.org/10.1016/J.GENE.2012.05.053>
- Liu, H., Moy, P., Kim, S., Xia, Y., Rajasekaran, A., Navarro, V., Knudsen, B., & Bander, N. H. (1997). Monoclonal antibodies to the extracellular domain of prostate-specific membrane antigen also react with tumor vascular endothelium. *Cancer Research*, 57(17), 3629–3634.
- Liu, J., & Afshar, S. (2020). In Vitro Assays: Friends or Foes of Cell-Penetrating Peptides. *International Journal of Molecular Sciences*, 21(13), 4719.
<https://doi.org/10.3390/ijms21134719>
- Liu, P., Rudick, M., & Anderson, R. G. W. (2002). Multiple Functions of Caveolin-1. *Journal of Biological Chemistry*, 277(44), 41295–41298.
<https://doi.org/10.1074/jbc.R200020200>
- Liu, R., Wu, J., Guo, H., Yao, W., Li, S., Lu, Y., Jia, Y., Liang, X., Tang, J., & Zhang, H. (2023). Post-translational modifications of histones: Mechanisms, biological functions, and therapeutic targets. *MedComm*, 4(3).
<https://doi.org/10.1002/mco2.292>
- Liu, W., Lindberg, J., Sui, G., Luo, J., Egevad, L., Li, T., Xie, C., Wan, M., Kim, S.-T., Wang, Z., Turner, A. R., Zhang, Z., Feng, J., Yan, Y., Sun, J., Bova, G. S., Ewing, C. M., Yan, G., Gielzak, M., ... Xu, J. (2012). Identification of novel CHD1-associated collaborative alterations of genomic structure and functional assessment of CHD1 in prostate cancer. *Oncogene*, 31(35), 3939–3948.
<https://doi.org/10.1038/onc.2011.554>
- Liu, Y., Steiniger, S. C. J., Kim, Y., Kaufmann, G. F., Felding-Habermann, B., & Janda, K. D. (2007). Mechanistic Studies of a Peptidic GRP78 Ligand for Cancer Cell-Specific Drug Delivery. *Molecular Pharmaceutics*, 4(3), 435–447.
<https://doi.org/10.1021/mp060122j>
- Llaverias, G., Danilo, C., Wang, Y., Witkiewicz, A. K., Daumer, K., Lisanti, M. P., & Frank, P. G. (2010). A Western-Type Diet Accelerates Tumor Progression in

- an Autochthonous Mouse Model of Prostate Cancer. *The American Journal of Pathology*, 177(6), 3180–3191. <https://doi.org/10.2353/ajpath.2010.100568>
- Lloyd, T., Hounsome, L., Mehay, A., Mee, S., Verne, J., & Cooper, A. (2015). Lifetime risk of being diagnosed with, or dying from, prostate cancer by major ethnic group in England 2008–2010. *BMC Medicine*, 13(1), 171. <https://doi.org/10.1186/s12916-015-0405-5>
- Logozzi, M., De Milito, A., Lugini, L., Borghi, M., Calabrò, L., Spada, M., Perdicchio, M., Marino, M. L., Federici, C., Iessi, E., Brambilla, D., Venturi, G., Lozupone, F., Santinami, M., Huber, V., Maio, M., Rivoltini, L., & Fais, S. (2009). High Levels of Exosomes Expressing CD63 and Caveolin-1 in Plasma of Melanoma Patients. *PLoS ONE*, 4(4), e5219. <https://doi.org/10.1371/journal.pone.0005219>
- Lord, C. J., & Ashworth, A. (2017). PARP inhibitors: Synthetic lethality in the clinic. *Science*, 355(6330), 1152–1158. <https://doi.org/10.1126/science.aam7344>
- Lorents, A., Säälk, P., Langel, Ü., & Pooga, M. (2018). Arginine-Rich Cell-Penetrating Peptides Require Nucleolin and Cholesterol-Poor Subdomains for Translocation across Membranes. *Bioconjugate Chemistry*, 29(4), 1168–1177. <https://doi.org/10.1021/acs.bioconjchem.7b00805>
- Low, J. S. W., Tao, Q., Ng, K. M., Goh, H. K., Shu, X.-S., Woo, W. L., Ambinder, R. F., Srivastava, G., Shamay, M., Chan, A. T. C., Popescu, N. C., & Hsieh, W.-S. (2011). A novel isoform of the 8p22 tumor suppressor gene DLC1 suppresses tumor growth and is frequently silenced in multiple common tumors. *Oncogene*, 30(16), 1923–1935. <https://doi.org/10.1038/onc.2010.576>
- Lu, Y., Cai, Z., Xiao, G., Keller, E. T., Mizokami, A., Yao, Z., Roodman, G. D., & Zhang, J. (2007). Monocyte Chemotactic Protein-1 Mediates Prostate Cancer-Induced Bone Resorption. *Cancer Research*, 67(8), 3646–3653. <https://doi.org/10.1158/0008-5472.CAN-06-1210>
- Lu, Y., Wang, J., Xu, Y., Koch, A. E., Cai, Z., Chen, X., Galson, D. L., Taichman, R. S., & Zhang, J. (2008). CXCL16 Functions as a Novel Chemotactic Factor for Prostate Cancer Cells In vitro. *Molecular Cancer Research*, 6(4), 546–554. <https://doi.org/10.1158/1541-7786.MCR-07-0277>
- Ludtke, S., He, K., & Huang, H. (1995). Membrane thinning caused by magainin 2. *Biochemistry*, 34(51), 16764–16769. <https://doi.org/10.1021/bi00051a026>
- Lundberg, P., El-Andaloussi, S., Sütllü, T., Johansson, H., & Langel, Ü. (2007). Delivery of short interfering RNA using endosomolytic cell-penetrating peptides. *The FASEB Journal*, 21(11), 2664–2671. <https://doi.org/10.1096/fj.06-6502com>
- Ma, J., Li, L., Liao, T., Gong, W., & Zhang, C. (2022). Efficacy and Safety of 225Ac-PSMA-617-Targeted Alpha Therapy in Metastatic Castration-Resistant Prostate Cancer: A Systematic Review and Meta-Analysis. *Frontiers in Oncology*, 12. <https://doi.org/10.3389/fonc.2022.796657>
- Ma, L., Ouyang, Q., Werthmann, G. C., Thompson, H. M., & Morrow, E. M. (2017a). Live-cell Microscopy and Fluorescence-based Measurement of

- Luminal pH in Intracellular Organelles. *Frontiers in Cell and Developmental Biology*, 5, 71. <https://doi.org/10.3389/fcell.2017.00071>
- Ma, L., Wang, C., He, Z., Cheng, B., Zheng, L., & Huang, K. (2017b). Peptide-Drug Conjugate: A Novel Drug Design Approach. *Current Medicinal Chemistry*, 24(31). <https://doi.org/10.2174/0929867324666170404142840>
- Madani, F., Lindberg, S., Langel, Ü., Futaki, S., & Gräslund, A. (2011). Mechanisms of Cellular Uptake of Cell-Penetrating Peptides. *Journal of Biophysics*, 2011, 1–10. <https://doi.org/10.1155/2011/414729>
- Mäde, V., Els-Heindl, S., & Beck-Sickinger, A. G. (2014). Automated solid-phase peptide synthesis to obtain therapeutic peptides. *Beilstein Journal of Organic Chemistry*, 10, 1197–1212. <https://doi.org/10.3762/bjoc.10.118>
- Maes, T., Mascaró, C., Tirapu, I., Estiarte, A., Ciceri, F., Lunardi, S., Guibourt, N., Perdonés, A., Lufino, M. M. P., Somervaille, T. C. P., Wiseman, D. H., Duy, C., Melnick, A., Willekens, C., Ortega, A., Martinell, M., Valls, N., Kurz, G., Fyfe, M., ... Buesa, C. (2018). ORY-1001, a Potent and Selective Covalent KDM1A Inhibitor, for the Treatment of Acute Leukemia. *Cancer Cell*, 33(3), 495-511.e12. <https://doi.org/10.1016/j.ccell.2018.02.002>
- Mahalingam, D., Wilding, G., Denmeade, S., Sarantopoulos, J., Cosgrove, D., Cetnar, J., Azad, N., Bruce, J., Kurman, M., Allgood, V. E., & Carducci, M. (2016). Mipsagargin, a novel thapsigargin-based PSMA-activated prodrug: results of a first-in-man phase I clinical trial in patients with refractory, advanced or metastatic solid tumours. *British Journal of Cancer*, 114(9), 986–994. <https://doi.org/10.1038/bjc.2016.72>
- Majello, B., Gorini, F., Saccà, C., & Amente, S. (2019). Expanding the Role of the Histone Lysine-Specific Demethylase LSD1 in Cancer. *Cancers*, 11(3), 324. <https://doi.org/10.3390/cancers11030324>
- Makowska, K. A., Hughes, R. E., White, K. J., Wells, C. M., & Peckham, M. (2015). Specific Myosins Control Actin Organization, Cell Morphology, and Migration in Prostate Cancer Cells. *Cell Reports*, 13(10), 2118–2125. <https://doi.org/10.1016/j.celrep.2015.11.012>
- Malhotra, V., & Perry, M. C. (2003). Classical Chemotherapy: Mechanisms, Toxicities and the Therapeutic Window. *Cancer Biology & Therapy*, 2(sup1), 1–3. <https://doi.org/10.4161/cbt.199>
- Mantey, S. A., Weber, H. C., Sainz, E., Akesson, M., Ryan, R. R., Pradhan, T. K., Searles, R. P., Spindel, E. R., Battey, J. F., Coy, D. H., & Jensen, R. T. (1997). Discovery of a High Affinity Radioligand for the Human Orphan Receptor, Bombesin Receptor Subtype 3, Which Demonstrates That It Has a Unique Pharmacology Compared with Other Mammalian Bombesin Receptors. *Journal of Biological Chemistry*, 272(41), 26062–26071. <https://doi.org/10.1074/jbc.272.41.26062>
- Marchelletta, R. R., Jacobs, D. T., Schechter, J. E., Cheney, R. E., & Hamm-Alvarez, S. F. (2008). The class V myosin motor, myosin 5c, localizes to mature secretory vesicles and facilitates exocytosis in lacrimal acini. *American Journal of Physiology. Cell Physiology*, 295(1), C13-28. <https://doi.org/10.1152/ajpcell.00330.2007>

- Marcus, L., Lemery, S. J., Keegan, P., & Pazdur, R. (2019). FDA Approval Summary: Pembrolizumab for the Treatment of Microsatellite Instability-High Solid Tumors. *Clinical Cancer Research*, 25(13), 3753–3758. <https://doi.org/10.1158/1078-0432.CCR-18-4070>
- Martinez-Gamero, C., Malla, S., & Aguilo, F. (2021). LSD1: Expanding Functions in Stem Cells and Differentiation. *Cells*, 10(11), 3252. <https://doi.org/10.3390/cells10113252>
- Maselli, F. M., Giuliani, F., Laface, C., Perrone, M., Melaccio, A., De Santis, P., Santoro, A. N., Guarini, C., Iaia, M. L., & Fedele, P. (2023). Immunotherapy in Prostate Cancer: State of Art and New Therapeutic Perspectives. *Current Oncology*, 30(6), 5769–5794. <https://doi.org/10.3390/curroncol30060432>
- Mateos, M.-V., Bladé, J., Bringhen, S., Ocio, E. M., Efebera, Y., Pour, L., Gay, F., Sonneveld, P., Gullbo, J., & Richardson, P. G. (2020). Melflufen: A Peptide–Drug Conjugate for the Treatment of Multiple Myeloma. *Journal of Clinical Medicine*, 9(10), 3120. <https://doi.org/10.3390/jcm9103120>
- Matsuzaki, K., Yoneyama, S., Murase, O., & Miyajima, K. (1996). Transbilayer Transport of Ions and Lipids Coupled with Mastoparan X Translocation. *Biochemistry*, 35(25), 8450–8456. <https://doi.org/10.1021/bi960342a>
- Matzinger, P. (2002). The Danger Model: A Renewed Sense of Self. *Science*, 296(5566), 301–305. <https://doi.org/10.1126/science.1071059>
- McCray, A. T., & Ide, N. C. (2000). Design and Implementation of a National Clinical Trials Registry. *Journal of the American Medical Informatics Association*, 7(3), 313–323. <https://doi.org/10.1136/jamia.2000.0070313>
- McDonald-McGinn, D. M., Sullivan, K. E., Marino, B., Philip, N., Swillen, A., Vorstman, J. A. S., Zackai, E. H., Emanuel, B. S., Vermeesch, J. R., Morrow, B. E., Scambler, P. J., & Bassett, A. S. (2015). 22q11.2 deletion syndrome. *Nature Reviews Disease Primers*, 1(1), 15071. <https://doi.org/10.1038/nrdp.2015.71>
- McKay, R. R., Werner, L., Jacobus, S. J., Jones, A., Mostaghel, E. A., Marck, B. T., Choudhury, A. D., Pomerantz, M. M., Sweeney, C. J., Slovin, S. F., Morris, M. J., Kantoff, P. W., & Taplin, M. (2019). A phase 2 trial of abiraterone acetate without glucocorticoids for men with metastatic castration-resistant prostate cancer. *Cancer*, 125(4), 524–532. <https://doi.org/10.1002/cncr.31836>
- McNeal, J. E. (1981). The zonal anatomy of the prostate. *The Prostate*, 2(1), 35–49. <https://doi.org/10.1002/pros.2990020105>
- McNeal, J. E. (1988). Normal Histology of the Prostate. *The American Journal of Surgical Pathology*, 12(8), 619–633. <https://doi.org/10.1097/00000478-198808000-00003>
- Means, T. K., Mylonakis, E., Tampakakis, E., Colvin, R. A., Seung, E., Puckett, L., Tai, M. F., Stewart, C. R., Pukkila-Worley, R., Hickman, S. E., Moore, K. J., Calderwood, S. B., Hacohen, N., Luster, A. D., & El Khoury, J. (2009). Evolutionarily conserved recognition and innate immunity to fungal pathogens by the scavenger receptors SCARF1 and CD36. *Journal of Experimental Medicine*, 206(3), 637–653. <https://doi.org/10.1084/jem.20082109>

- Mehta, R. R., Yamada, T., Taylor, B. N., Christov, K., King, M. L., Majumdar, D., Lekmine, F., Tirupathi, C., Shilkaitis, A., Bratescu, L., Green, A., Beattie, C. W., & Das Gupta, T. K. (2011). A cell penetrating peptide derived from azurin inhibits angiogenesis and tumor growth by inhibiting phosphorylation of VEGFR-2, FAK and Akt. *Angiogenesis*, 14(3), 355–369. <https://doi.org/10.1007/s10456-011-9220-6>
- Melikov, K., & Chernomordik, L. V. (2005). Review Arginine-rich cell penetrating peptides: from endosomal uptake to nuclear delivery. *Cell. Mol. Life Sci*, 62, 2739–2749. <https://doi.org/10.1007/s00018-005-5293-y>
- Metzger, E., Imhof, A., Patel, D., Kahl, P., Hoffmeyer, K., Friedrichs, N., Müller, J. M., Greschik, H., Kirfel, J., Ji, S., Kunowska, N., Beisenherz-Huss, C., Günther, T., Buettner, R., & Schüle, R. (2010). Phosphorylation of histone H3T6 by PKC β controls demethylation at histone H3K4. *Nature*, 464(7289), 792–796. <https://doi.org/10.1038/nature08839>
- Metzger, E., Wissmann, M., Yin, N., Müller, J. M., Schneider, R., Peters, A. H. F. M., Günther, T., Buettner, R., & Schüle, R. (2005). LSD1 demethylates repressive histone marks to promote androgen-receptor-dependent transcription. *Nature*, 437(7057), 436–439. <https://doi.org/10.1038/nature04020>
- Metzger, E., Yin, N., Wissmann, M., Kunowska, N., Fischer, K., Friedrichs, N., Patnaik, D., Higgins, J. M. G., Potier, N., Scheidtmann, K.-H., Buettner, R., & Schüle, R. (2008). Phosphorylation of histone H3 at threonine 11 establishes a novel chromatin mark for transcriptional regulation. *Nature Cell Biology*, 10(1), 53–60. <https://doi.org/10.1038/ncb1668>
- Miao, W.-M., Vasile, E., Lane, W. S., & Lawler, J. (2001). CD36 associates with CD9 and integrins on human blood platelets. *Blood*, 97(6), 1689–1696. <https://doi.org/10.1182/blood.V97.6.1689>
- Miao, Y., & Quinn, T. P. (2008). Peptide-targeted radionuclide therapy for melanoma. *Critical Reviews in Oncology/Hematology*, 67(3), 213–228. <https://doi.org/10.1016/j.critrevonc.2008.02.006>
- Mijuskovic, M., Saunders, E. J., Leongamornlert, D. A., Wakerell, S., Whitmore, I., Dadaev, T., Cieza-Borrella, C., Govindasami, K., Brook, M. N., Haiman, C. A., Conti, D. V., Eeles, R. A., & Kote-Jarai, Z. (2018). Rare germline variants in DNA repair genes and the angiogenesis pathway predispose prostate cancer patients to develop metastatic disease. *British Journal of Cancer*, 119(1), 96–104. <https://doi.org/10.1038/s41416-018-0141-7>
- Miller, D. C., Zheng, S. L., Dunn, R. L., Sarma, A. V, Montie, J. E., Lange, E. M., Meyers, D. A., Xu, J., & Cooney, K. A. (2003). Germ-line mutations of the macrophage scavenger receptor 1 gene: association with prostate cancer risk in African-American men. *Cancer Research*, 63(13), 3486–3489.
- Milletti, F. (2012). Cell-penetrating peptides: classes, origin, and current landscape. *Drug Discovery Today*, 17(15–16), 850–860. <https://doi.org/10.1016/J.DRUDIS.2012.03.002>
- Mineo, C., Yuhanna, I. S., Quon, M. J., & Shaul, P. W. (2003). High Density Lipoprotein-induced Endothelial Nitric-oxide Synthase Activation Is Mediated

by Akt and MAP Kinases. *Journal of Biological Chemistry*, 278(11), 9142–9149. <https://doi.org/10.1074/jbc.M211394200>

- Miquilena-Colina, M. E., Lima-Cabello, E., Sanchez-Campos, S., Garcia-Mediavilla, M. V., Fernandez-Bermejo, M., Lozano-Rodriguez, T., Vargas-Castrillon, J., Buque, X., Ochoa, B., Aspichueta, P., Gonzalez-Gallego, J., & Garcia-Monzon, C. (2011). Hepatic fatty acid translocase CD36 upregulation is associated with insulin resistance, hyperinsulinaemia and increased steatosis in non-alcoholic steatohepatitis and chronic hepatitis C. *Gut*, 60(10), 1394–1402. <https://doi.org/10.1136/gut.2010.222844>
- Mishra, A., Eathiraj, S., Corvera, S., & Lambright, D. G. (2010). Structural basis for Rab GTPase recognition and endosome tethering by the C2H2 zinc finger of Early Endosomal Autoantigen 1 (EEA1). *Proceedings of the National Academy of Sciences*, 107(24), 10866–10871. <https://doi.org/10.1073/pnas.1000843107>
- Mitchell, D. J., Kim, D. T., Steinman, L., Fathman, C. G., & Rothbard, J. B. (2000). Polyarginine enters cells more efficiently than other polycationic homopolymers. *The Journal of Peptide Research : Official Journal of the American Peptide Society*, 56(5), 318–325. <https://doi.org/10.1034/j.1399-3011.2000.00723.x>
- Mittler, F., Obeid, P., Rulina, A. V., Haguet, V., Gidrol, X., & Balakirev, M. Y. (2017). High-Content Monitoring of Drug Effects in a 3D Spheroid Model. *Frontiers in Oncology*, 7. <https://doi.org/10.3389/fonc.2017.00293>
- Mohammad, H. P., Smitheman, K. N., Kamat, C. D., Soong, D., Federowicz, K. E., Van Aller, G. S., Schneck, J. L., Carson, J. D., Liu, Y., Butticello, M., Bonnette, W. G., Gorman, S. A., Degenhardt, Y., Bai, Y., McCabe, M. T., Pappalardi, M. B., Kaspavec, J., Tian, X., McNulty, K. C., ... Kruger, R. G. (2015). A DNA Hypomethylation Signature Predicts Antitumor Activity of LSD1 Inhibitors in SCLC. *Cancer Cell*, 28(1), 57–69. <https://doi.org/10.1016/j.ccell.2015.06.002>
- Mohanty, J. G., Jaffe, J. S., Schulman, E. S., & Raible, D. G. (1997). A highly sensitive fluorescent micro-assay of H₂O₂ release from activated human leukocytes using a dihydroxyphenoxazine derivative. *Journal of Immunological Methods*, 202(2), 133–141. [https://doi.org/10.1016/S0022-1759\(96\)00244-X](https://doi.org/10.1016/S0022-1759(96)00244-X)
- Mohler, J., Bahnson, R. R., Boston, B., Busby, J. E., D'Amico, A., Eastham, J. A., Enke, C. A., George, D., Horwitz, E. M., Huben, R. P., Kantoff, P., Kawachi, M., Kuettel, M., Lange, P. H., MacVicar, G., Plimack, E. R., Pow-Sang, J. M., Roach, M., Rohren, E., ... Walsh, P. C. (2010). Prostate Cancer. *Journal of the National Comprehensive Cancer Network*, 8(2), 162–200. <https://doi.org/10.6004/jnccn.2010.0012>
- Moilanen, A.-M., Riikonen, R., Oksala, R., Ravanti, L., Aho, E., Wohlfahrt, G., Nykänen, P. S., Törmäkangas, O. P., Palvimo, J. J., & Kallio, P. J. (2015). Discovery of ODM-201, a new-generation androgen receptor inhibitor targeting resistance mechanisms to androgen signaling-directed prostate cancer therapies. *Scientific Reports*, 5(1), 12007. <https://doi.org/10.1038/srep12007>

- Moon, J. S., Karunakaran, U., Suma, E., Chung, S. M., & Won, K. C. (2020). The Role of CD36 in Type 2 Diabetes Mellitus: β -Cell Dysfunction and Beyond. *Diabetes & Metabolism Journal*, 44(2), 222. <https://doi.org/10.4093/dmj.2020.0053>
- Moreira, R., Jervis, P. J., Carvalho, A., Ferreira, P. M. T., Martins, J. A., Valentão, P., Andrade, P. B., & Pereira, D. M. (2020). Biological Evaluation of Naproxen–Dehydrodipeptide Conjugates with Self-Hydrogelation Capacity as Dual LOX/COX Inhibitors. *Pharmaceutics*, 12(2), 122. <https://doi.org/10.3390/pharmaceutics12020122>
- Morizawa, Y. M., Hirayama, Y., Ohno, N., Shibata, S., Shigetomi, E., Sui, Y., Nabekura, J., Sato, K., Okajima, F., Takebayashi, H., Okano, H., & Koizumi, S. (2017). Author Correction: Reactive astrocytes function as phagocytes after brain ischemia via ABCA1-mediated pathway. *Nature Communications*, 8(1), 1598. <https://doi.org/10.1038/s41467-017-01594-1>
- Morris, M. (1997). A new peptide vector for efficient delivery of oligonucleotides into mammalian cells. *Nucleic Acids Research*, 25(14), 2730–2736. <https://doi.org/10.1093/nar/25.14.2730>
- Mottet, N., Bellmunt, J., Bolla, M., Briers, E., Cumberbatch, M. G., De Santis, M., Fossati, N., Gross, T., Henry, A. M., Joniau, S., Lam, T. B., Mason, M. D., Matveev, V. B., Moldovan, P. C., van den Bergh, R. C. N., Van den Broeck, T., van der Poel, H. G., van der Kwast, T. H., Rouvière, O., ... Cornford, P. (2017). EAU-ESTRO-SIOG Guidelines on Prostate Cancer. Part 1: Screening, Diagnosis, and Local Treatment with Curative Intent. *European Urology*, 71(4), 618–629. <https://doi.org/10.1016/j.eururo.2016.08.003>
- Mottet, N., van den Bergh, R. C. N., Briers, E., Van den Broeck, T., Cumberbatch, M. G., De Santis, M., Fanti, S., Fossati, N., Gandaglia, G., Gillissen, S., Grivas, N., Grummet, J., Henry, A. M., van der Kwast, T. H., Lam, T. B., Lardas, M., Liew, M., Mason, M. D., Moris, L., ... Cornford, P. (2021). EAU-EANM-ESTRO-ESUR-SIOG Guidelines on Prostate Cancer—2020 Update. Part 1: Screening, Diagnosis, and Local Treatment with Curative Intent. *European Urology*, 79(2), 243–262. <https://doi.org/10.1016/j.eururo.2020.09.042>
- Mu, F.-T., Callaghan, J. M., Steele-Mortimer, O., Stenmark, H., Parton, R. G., Campbell, P. L., McCluskey, J., Yeo, J.-P., Tock, E. P. C., & Toh, B.-H. (1995). EEA1, an Early Endosome-Associated Protein. *Journal of Biological Chemistry*, 270(22), 13503–13511. <https://doi.org/10.1074/jbc.270.22.13503>
- Mucci, L. A., Hjelmborg, J. B., Harris, J. R., Czene, K., Havelick, D. J., Scheike, T., Graff, R. E., Holst, K., Möller, S., Unger, R. H., McIntosh, C., Nuttall, E., Brandt, I., Penney, K. L., Hartman, M., Kraft, P., Parmigiani, G., Christensen, K., Koskenvuo, M., ... Kaprio, J. (2016). Familial Risk and Heritability of Cancer Among Twins in Nordic Countries. *JAMA*, 315(1), 68. <https://doi.org/10.1001/jama.2015.17703>
- Mudd, G. E., Brown, A., Chen, L., van Rietschoten, K., Watcham, S., Teufel, D. P., Pavan, S., Lani, R., Huxley, P., & Bennett, G. S. (2020). Identification and Optimization of EphA2-Selective Bicycles for the Delivery of Cytotoxic

- Payloads. *Journal of Medicinal Chemistry*, 63(8), 4107–4116.
<https://doi.org/10.1021/acs.jmedchem.9b02129>
- Mueller, J., Kretzschmar, I., Volkmer, R., & Boisguerin, P. (2008). Comparison of Cellular Uptake Using 22 CPPs in 4 Different Cell Lines. *Bioconjugate Chemistry*, 19(12), 2363–2374. <https://doi.org/10.1021/bc800194e>
- Mukhopadhyay, S., & Gordon, S. (2004). The role of scavenger receptors in pathogen recognition and innate immunity. *Immunobiology*, 209(1–2), 39–49. <https://doi.org/10.1016/J.IMBIO.2004.02.004>
- Mulholland, D. J., Kobayashi, N., Ruscetti, M., Zhi, A., Tran, L. M., Huang, J., Gleave, M., & Wu, H. (2012). Pten loss and RAS/MAPK activation cooperate to promote EMT and metastasis initiated from prostate cancer stem/progenitor cells. *Cancer Research*, 72(7), 1878–1889. <https://doi.org/10.1158/0008-5472.CAN-11-3132>
- Munjal, A., & Leslie, S. W. (2023). Gleason Score. In *StatPearls*. StatPearls Publishing.
- Muralidhar, A., Potluri, H. K., Jaiswal, T., & McNeel, D. G. (2023). Targeted Radiation and Immune Therapies—Advances and Opportunities for the Treatment of Prostate Cancer. *Pharmaceutics*, 15(1), 252. <https://doi.org/10.3390/pharmaceutics15010252>
- Murao, K., Terpstra, V., Green, S. R., Kondratenko, N., Steinberg, D., & Quehenberger, O. (1997). Characterization of CLA-1, a Human Homologue of Rodent Scavenger Receptor BI, as a Receptor for High Density Lipoprotein and Apoptotic Thymocytes. *Journal of Biological Chemistry*, 272(28), 17551–17557. <https://doi.org/10.1074/jbc.272.28.17551>
- Murdocca, M., De Masi, C., Pucci, S., Mango, R., Novelli, G., Di Natale, C., & Sangiuolo, F. (2021). LOX-1 and cancer: an indissoluble liaison. *Cancer Gene Therapy*, 28(10–11), 1088–1098. <https://doi.org/10.1038/s41417-020-00279-0>
- Murray, D. H., Jahnel, M., Lauer, J., Avellaneda, M. J., Brouilly, N., Cezanne, A., Morales-Navarrete, H., Perini, E. D., Ferguson, C., Lupas, A. N., Kalaidzidis, Y., Parton, R. G., Grill, S. W., & Zerial, M. (2016). An endosomal tether undergoes an entropic collapse to bring vesicles together. *Nature*, 537(7618), 107–111. <https://doi.org/10.1038/nature19326>
- Murshid, A., Borges, T. J., Lang, B. J., & Calderwood, S. K. (2016). The Scavenger Receptor SREC-I Cooperates with Toll-Like Receptors to Trigger Inflammatory Innate Immune Responses. *Frontiers in Immunology*, 7. <https://doi.org/10.3389/fimmu.2016.00226>
- Murshid, A., Gong, J., & Calderwood, S. K. (2010). Heat Shock Protein 90 Mediates Efficient Antigen Cross Presentation through the Scavenger Receptor Expressed by Endothelial Cells-I. *The Journal of Immunology*, 185(5), 2903–2917. <https://doi.org/10.4049/jimmunol.0903635>
- Na, R., Zheng, S. L., Han, M., Yu, H., Jiang, D., Shah, S., Ewing, C. M., Zhang, L., Novakovic, K., Petkewicz, J., Gulukota, K., Helseth Jr, D. L., Quinn, M., Humphries, E., Wiley, K. E., Isaacs, S. D., Wu, Y., Liu, X., Zhang, N., ...

- Isaacs, W. B. (2017). Germline Mutations in ATM and BRCA1/2 Distinguish Risk for Lethal and Indolent Prostate Cancer and are Associated with Early Age at Death. *European Urology*, 71(5), 740–747. <https://doi.org/10.1016/j.eururo.2016.11.033>
- Nagase, T. (2001). Prediction of the Coding Sequences of Unidentified Human Genes. XX. The Complete Sequences of 100 New cDNA Clones from Brain Which Code for Large Proteins in vitro. *DNA Research*, 8(2), 85–95. <https://doi.org/10.1093/dnares/8.2.85>
- Nair, S. S., Li, D.-Q., & Kumar, R. (2013). A Core Chromatin Remodeling Factor Instructs Global Chromatin Signaling through Multivalent Reading of Nucleosome Codes. *Molecular Cell*, 49(4), 704–718. <https://doi.org/10.1016/j.molcel.2012.12.016>
- Nakagawa-Toyama, Y., Hirano, K., Tsujii, K., Nishida, M., Miyagawa, J., Sakai, N., & Yamashita, S. (2005). Human scavenger receptor class B type I is expressed with cell-specific fashion in both initial and terminal site of reverse cholesterol transport. *Atherosclerosis*, 183(1), 75–83. <https://doi.org/10.1016/j.atherosclerosis.2005.02.035>
- Nakase, I., Hirose, H., Tanaka, G., Tadokoro, A., Kobayashi, S., Takeuchi, T., & Futaki, S. (2009). Cell-surface Accumulation of Flock House Virus-derived Peptide Leads to Efficient Internalization via Macropinocytosis. *Molecular Therapy*, 17(11), 1868–1876. <https://doi.org/10.1038/mt.2009.192>
- Nakase, I., Katayama, M., Hattori, Y., Ishimura, M., Inaura, S., Fujiwara, D., Takatani-Nakase, T., Fujii, I., Futaki, S., & Kirihata, M. (2019). Intracellular target delivery of cell-penetrating peptide-conjugated dodecaborate for boron neutron capture therapy (BNCT). *Chemical Communications*, 55(93), 13955–13958. <https://doi.org/10.1039/C9CC03924D>
- Nakase, I., Niwa, M., Takeuchi, T., Sonomura, K., Kawabata, N., Koike, Y., Takehashi, M., Tanaka, S., Ueda, K., Simpson, J. C., Jones, A. T., Sugiura, Y., & Futaki, S. (2004). Cellular Uptake of Arginine-Rich Peptides: Roles for Macropinocytosis and Actin Rearrangement. *Molecular Therapy*, 10(6), 1011–1022. <https://doi.org/10.1016/j.ymthe.2004.08.010>
- Nakase, I., Tadokoro, A., Kawabata, N., Takeuchi, T., Katoh, H., Hiramoto, K., Negishi, M., Nomizu, M., Sugiura, Y., & Futaki, S. (2007). Interaction of Arginine-Rich Peptides with Membrane-Associated Proteoglycans Is Crucial for Induction of Actin Organization and Macropinocytosis. *Biochemistry*, 46(2), 492–501. <https://doi.org/10.1021/bi0612824>
- Nakazawa, M., Paller, C., & Kyprianou, N. (2017). Mechanisms of Therapeutic Resistance in Prostate Cancer. *Current Oncology Reports*, 19(2), 13. <https://doi.org/10.1007/s11912-017-0568-7>
- Namer, M., Amiel, J., & Toubol, J. (1988). Anandron (RU 23908) Associated with Orchiectomy in Stage D Prostate Cancer Preliminary Results of a Randomized, Double-Blind Study. *American Journal of Clinical Oncology*, 11, S191. <https://doi.org/10.1097/00000421-198801102-00044>
- Navratil, H. (1987). Double-blind study of Anandron versus placebo in stage D2 prostate cancer patients receiving buserelin. Results on 49 cases from a

- multicentre study. *Progress in Clinical and Biological Research*, 243A, 401–410.
- Nejadmoghaddam, M.-R., Minai-Tehrani, A., Ghahremanzadeh, R., Mahmoudi, M., Dinarvand, R., & Zarnani, A.-H. (2019). Antibody-Drug Conjugates: Possibilities and Challenges. *Avicenna Journal of Medical Biotechnology*, 11(1), 3–23.
- Nelson, Q., Agarwal, N., Stephenson, R., & Cannon-Albright, L. A. (2013). A population-based analysis of clustering identifies a strong genetic contribution to lethal prostate cancer. *Frontiers in Genetics*, 4. <https://doi.org/10.3389/fgene.2013.00152>
- Neuhaus, J., Schiffer, E., von Wilcke, P., Bauer, H. W., Leung, H., Siwy, J., Ulrici, W., Paasch, U., Horn, L.-C., & Stolzenburg, J.-U. (2013). Seminal Plasma as a Source of Prostate Cancer Peptide Biomarker Candidates for Detection of Indolent and Advanced Disease. *PLoS ONE*, 8(6), e67514. <https://doi.org/10.1371/journal.pone.0067514>
- Ni, J., Cozzi, P. J., Hao, J. L., Beretov, J., Chang, L., Duan, W., Shigdar, S., Delprado, W. J., Graham, P. H., Bucci, J., Kearsley, J. H., & Li, Y. (2014). CD44 variant 6 is associated with prostate cancer metastasis and chemo-/radioresistance. *The Prostate*, 74(6), 602–617. <https://doi.org/10.1002/pros.22775>
- Nicholson, A. C., Febbraio, M., Han, J., Silverstein, R. L., & Hajjar, D. P. (2000). CD36 in atherosclerosis. The role of a class B macrophage scavenger receptor. *Annals of the New York Academy of Sciences*, 902, 128–131; discussion 131-3.
- Nieland, T. J. F., Penman, M., Dori, L., Krieger, M., & Kirchhausen, T. (2002). Discovery of chemical inhibitors of the selective transfer of lipids mediated by the HDL receptor SR-BI. *Proceedings of the National Academy of Sciences*, 99(24), 15422–15427. <https://doi.org/10.1073/pnas.222421399>
- Nieland, T. J. F., Shaw, J. T., Jaipuri, F. A., Duffner, J. L., Koehler, A. N., Banakos, S., Zannis, V. I., Kirchhausen, T., & Krieger, M. (2008). Identification of the Molecular Target of Small Molecule Inhibitors of HDL Receptor SR-BI Activity. *Biochemistry*, 47(1), 460–472. <https://doi.org/10.1021/bi701277x>
- Nuhn, P., De Bono, J. S., Fizazi, K., Freedland, S. J., Grilli, M., Kantoff, P. W., Sonpavde, G., Sternberg, C. N., Yegnasubramanian, S., & Antonarakis, E. S. (2019). Update on Systemic Prostate Cancer Therapies: Management of Metastatic Castration-resistant Prostate Cancer in the Era of Precision Oncology. *European Urology*, 75(1), 88–99. <https://doi.org/10.1016/j.eururo.2018.03.028>
- Oehlke, J., Scheller, A., Wiesner, B., Krause, E., Beyermann, M., Klauschenz, E., Melzig, M., & Bienert, M. (1998). Cellular uptake of an α -helical amphipathic model peptide with the potential to deliver polar compounds into the cell interior non-endocytically. *Biochimica et Biophysica Acta (BBA) - Biomembranes*, 1414(1–2), 127–139. [https://doi.org/10.1016/S0005-2736\(98\)00161-8](https://doi.org/10.1016/S0005-2736(98)00161-8)

- Oh, C., Park, S., Lee, E. K., & Yoo, Y. J. (2013). Downregulation of ubiquitin level via knockdown of polyubiquitin gene Ubb as potential cancer therapeutic intervention. *Scientific Reports*, 3(1), 2623. <https://doi.org/10.1038/srep02623>
- Okada, H., Tsubura, A., Okamura, A., Senzaki, H., Naka, Y., Komatz, Y., & Morii, S. (1992). Keratin profiles in normal/hyperplastic prostates and prostate carcinoma. *Virchows Archiv. A, Pathological Anatomy and Histopathology*, 421(2), 157–161. <https://doi.org/10.1007/BF01607049>
- Omara-Opyene, A. L., Qiu, J., Shah, G. V., & Iczkowski, K. A. (2004). Prostate cancer invasion is influenced more by expression of a CD44 isoform including variant 9 than by Muc18. *Laboratory Investigation*, 84(7), 894–907. <https://doi.org/10.1038/labinvest.3700112>
- Onufriev, A. V., & Schiessel, H. (2019). The nucleosome: from structure to function through physics. *Current Opinion in Structural Biology*, 56, 119–130. <https://doi.org/10.1016/j.sbi.2018.11.003>
- O'Sullivan, C. C., Lindenberg, M., Bryla, C., Patronas, N., Peer, C. J., Amiri-Kordestani, L., Davarpanah, N., Gonzalez, E. M., Burotto, M., Choyke, P., Steinberg, S. M., Liewehr, D. J., Figg, W. D., Fojo, T., Balasubramaniam, S., & Bates, S. E. (2016). ANG1005 for breast cancer brain metastases: correlation between 18F-FLT-PET after first cycle and MRI in response assessment. *Breast Cancer Research and Treatment*, 160(1), 51–59. <https://doi.org/10.1007/s10549-016-3972-z>
- Oudard, S., Fizazi, K., Sengeløv, L., Daugaard, G., Saad, F., Hansen, S., Hjälm-Eriksson, M., Jassem, J., Thiery-Vuillemin, A., Caffo, O., Castellano, D., Mainwaring, P. N., Bernard, J., Shen, L., Chadjaa, M., & Sartor, O. (2017). Cabazitaxel Versus Docetaxel As First-Line Therapy for Patients With Metastatic Castration-Resistant Prostate Cancer: A Randomized Phase III Trial—FIRSTANA. *Journal of Clinical Oncology*, 35(28), 3189–3197. <https://doi.org/10.1200/JCO.2016.72.1068>
- Out, R., Hoekstra, M., Spijkers, J. A. A., Kruijt, J. K., van Eck, M., Bos, I. S. T., Twisk, J., & Van Berkel, T. J. C. (2004). Scavenger receptor class B type I is solely responsible for the selective uptake of cholesteryl esters from HDL by the liver and the adrenals in mice. *Journal of Lipid Research*, 45(11), 2088–2095. <https://doi.org/10.1194/jlr.M400191-JLR200>
- Pal, D. (2021). Spike protein fusion loop controls SARS-CoV-2 fusogenicity and infectivity. *Journal of Structural Biology*, 213(2), 107713. <https://doi.org/10.1016/j.jsb.2021.107713>
- Palade G. (1953). Fine structure of blood capillaries. *J Appl Physics*, 24, 1424–1448.
- Parimi, V., Goyal, R., Poropatich, K., & Yang, X. J. (2014). Neuroendocrine differentiation of prostate cancer: a review. *American Journal of Clinical and Experimental Urology*, 2(4), 273–285.
- Park, S. E., Shamloo, K., Kristedja, T. A., Darwish, S., Bisoffi, M., Parang, K., & Tiwari, R. K. (2019). EDB-FN Targeted Peptide–Drug Conjugates for Use against Prostate Cancer. *International Journal of Molecular Sciences*, 20(13), 3291. <https://doi.org/10.3390/ijms20133291>

- Parker, C., Nilsson, S., Heinrich, D., Helle, S. I., O'Sullivan, J. M., Fosså, S. D., Chodacki, A., Wiechno, P., Logue, J., Seke, M., Widmark, A., Johannessen, D. C., Hoskin, P., Bottomley, D., James, N. D., Solberg, A., Syndikus, I., Kliment, J., Wedel, S., ... Sartor, O. (2013). Alpha Emitter Radium-223 and Survival in Metastatic Prostate Cancer. *New England Journal of Medicine*, 369(3), 213–223. <https://doi.org/10.1056/NEJMoa1213755>
- Parolia, A., Cieslik, M., Chu, S.-C., Xiao, L., Ouchi, T., Zhang, Y., Wang, X., Vats, P., Cao, X., Pitchiaya, S., Su, F., Wang, R., Feng, F. Y., Wu, Y.-M., Lonigro, R. J., Robinson, D. R., & Chinnaiyan, A. M. (2019). Distinct structural classes of activating FOXA1 alterations in advanced prostate cancer. *Nature*, 571(7765), 413–418. <https://doi.org/10.1038/s41586-019-1347-4>
- Patel, H. H., Murray, F., & Insel, P. A. (2008). Caveolae as Organizers of Pharmacologically Relevant Signal Transduction Molecules. *Annual Review of Pharmacology and Toxicology*, 48(1), 359–391. <https://doi.org/10.1146/annurev.pharmtox.48.121506.124841>
- Patel, P. C., Giljohann, D. A., Daniel, W. L., Zheng, D., Prigodich, A. E., & Mirkin, C. A. (2010). Scavenger Receptors Mediate Cellular Uptake of Polyvalent Oligonucleotide-Functionalized Gold Nanoparticles. *Bioconjugate Chemistry*, 21(12), 2250–2256. <https://doi.org/10.1021/bc1002423>
- Patrawala, L., Calhoun, T., Schneider-Broussard, R., Li, H., Bhatia, B., Tang, S., Reilly, J. G., Chandra, D., Zhou, J., Claypool, K., Coghlan, L., & Tang, D. G. (2006). Highly purified CD44+ prostate cancer cells from xenograft human tumors are enriched in tumorigenic and metastatic progenitor cells. *Oncogene*, 25(12), 1696–1708. <https://doi.org/10.1038/sj.onc.1209327>
- Patten, D. A., Kamarajah, S. K., Rose, J. M., Tickle, J., Shepherd, E. L., Adams, D. H., Weston, C. J., & Shetty, S. (2017). SCARF-1 promotes adhesion of CD4 + T cells to human hepatic sinusoidal endothelium under conditions of shear stress. <https://doi.org/10.1038/s41598-017-17928-4>
- Pauwels, E., Cleeren, F., Bormans, G., & Deroose, C. M. (2018). Somatostatin receptor PET ligands - the next generation for clinical practice. *American Journal of Nuclear Medicine and Molecular Imaging*, 8(5), 311–331.
- Pawley, J. (2006). *Handbook of Biological Confocal Microscopy*. https://books.google.co.uk/books?hl=en&lr=&id=E2maxdEXFNoC&oi=fnd&pg=PR7&ots=bki8oMzeEW&sig=YIW6RARb803WqZu_PYX97iShosY&redir_esc=y#v=onepage&q&f=false
- Pearse, B. M. F., & Robinson, M. S. (1990). Clathrin, Adaptors, and Sorting. *Annual Review of Cell Biology*, 6(1), 151–171. <https://doi.org/10.1146/annurev.cb.06.110190.001055>
- Pearson, A. M., Rich, A., & Krieger, M. (1993). Polynucleotide binding to macrophage scavenger receptors depends on the formation of base-quartet-stabilized four-stranded helices. *The Journal of Biological Chemistry*, 268(5), 3546–3554.
- Pei, D., & Buyanova, M. (2019). Overcoming Endosomal Entrapment in Drug Delivery. *Bioconjugate Chemistry*, 30(2), 273–283. <https://doi.org/10.1021/acs.bioconjchem.8b00778>

- Pelkmans, L., & Helenius, A. (2002). Endocytosis Via Caveolae. *Traffic*, 3(5), 311–320. <https://doi.org/10.1034/j.1600-0854.2002.30501.x>
- Perillo, B., Ombra, M. N., Bertoni, A., Cuzzo, C., Sacchetti, S., Sasso, A., Chiariotti, L., Malorni, A., Abbondanza, C., & Avvedimento, E. V. (2008). DNA Oxidation as Triggered by H3K9me2 Demethylation Drives Estrogen-Induced Gene Expression. *Science*, 319(5860), 202–206. <https://doi.org/10.1126/science.1147674>
- Pernar, C. H., Ebot, E. M., Wilson, K. M., & Mucci, L. A. (2018). The Epidemiology of Prostate Cancer. *Cold Spring Harbor Perspectives in Medicine*, 8(12), a030361. <https://doi.org/10.1101/cshperspect.a030361>
- Petrylak, D. P., Ratta, R., Gafanov, R., Facchini, G., Piulats, J. M., Kramer, G., Flaig, T. W., Chandana, S. R., Li, B., Burgents, J., & Fizazi, K. (2021). KEYNOTE-921: Phase III study of pembrolizumab plus docetaxel for metastatic castration-resistant prostate cancer. *Future Oncology*, 17(25), 3291–3299. <https://doi.org/10.2217/fon-2020-1133>
- Pettinato, M. C. (2021). Introduction to Antibody-Drug Conjugates. *Antibodies*, 10(4), 42. <https://doi.org/10.3390/antib10040042>
- Pfeffer, S. R. (2013). Rab GTPase regulation of membrane identity. *Current Opinion in Cell Biology*, 25(4), 414–419. <https://doi.org/10.1016/j.ceb.2013.04.002>
- Pfister, S. X., & Ashworth, A. (2017). Marked for death: targeting epigenetic changes in cancer. *Nature Reviews Drug Discovery*, 16(4), 241–263. <https://doi.org/10.1038/nrd.2016.256>
- Pfistershammer, K., Klauser, C., Leitner, J., Stöckl, J., Majdic, O., Weichhart, T., Sobanov, Y., Bochkov, V., Säemann, M., Zlabinger, G., & Steinberger, P. (2008). Identification of the scavenger receptors SREC-I, Cla-1 (SR-BI), and SR-AI as cellular receptors for Tamm-Horsfall protein. *Journal of Leukocyte Biology*, 83(1), 131–138. <https://doi.org/10.1189/jlb.0407231>
- Pieta, P., Mirza, J., & Lipkowski, J. (2012). Direct visualization of the alamethicin pore formed in a planar phospholipid matrix. *Proceedings of the National Academy of Sciences*, 109(52), 21223–21227. <https://doi.org/10.1073/pnas.1201559110>
- Pittman, R. C., Knecht, T. P., Rosenbaum, M. S., & Taylor, C. A. (1987). A nonendocytotic mechanism for the selective uptake of high density lipoprotein-associated cholesterol esters. *The Journal of Biological Chemistry*, 262(6), 2443–2450.
- Plüddemann, A., Neyen, C., & Gordon, S. (2007). Macrophage scavenger receptors and host-derived ligands. *Methods*, 43(3), 207–217. <https://doi.org/10.1016/j.ymeth.2007.06.004>
- Pols, M. S., van Meel, E., Oorschot, V., ten Brink, C., Fukuda, M., Swetha, M. G., Mayor, S., & Klumperman, J. (2013). hVps41 and VAMP7 function in direct TGN to late endosome transport of lysosomal membrane proteins. *Nature Communications*, 4(1), 1361. <https://doi.org/10.1038/ncomms2360>

- Pomerantz, M. M., Li, F., Takeda, D. Y., Lenci, R., Chonkar, A., Chabot, M., Cejas, P., Vazquez, F., Cook, J., Shivdasani, R. A., Bowden, M., Lis, R., Hahn, W. C., Kantoff, P. W., Brown, M., Loda, M., Long, H. W., & Freedman, M. L. (2015). The androgen receptor cistrome is extensively reprogrammed in human prostate tumorigenesis. *Nature Genetics*, 47(11), 1346–1351. <https://doi.org/10.1038/ng.3419>
- Pooga, M., Hällbrink, M., Zorko, M., & Langel, U. (1998). Cell penetration by transportan. *The FASEB Journal*, 12(1), 67–77. <https://doi.org/10.1096/fasebj.12.1.67>
- Pooga, M., & Langel, Ü. (2015). *Classes of Cell-Penetrating Peptides* (pp. 3–28). https://doi.org/10.1007/978-1-4939-2806-4_1
- Porzycki, P., & Ciszkowicz, E. (2020). Modern biomarkers in prostate cancer diagnosis. *Central European Journal of Urology*, 73(3), 300–306. <https://doi.org/10.5173/cej.2020.0067R>
- Poteryaev, D., Datta, S., Ackema, K., Zerial, M., & Spang, A. (2010). Identification of the Switch in Early-to-Late Endosome Transition. *Cell*, 141(3), 497–508. <https://doi.org/10.1016/j.cell.2010.03.011>
- Pouny, Y., Rapaport, D., Mor, A., Nicolas, P., & Shai, Y. (1992). Interaction of antimicrobial dermaseptin and its fluorescently labeled analogs with phospholipid membranes. *Biochemistry*, 31(49), 12416–12423. <https://doi.org/10.1021/bi00164a017>
- PrabhuDas, M. R., Baldwin, C. L., Bollyky, P. L., Bowdish, D. M. E., Drickamer, K., Febbraio, M., Herz, J., Kobzik, L., Krieger, M., Loike, J., McVicker, B., Means, T. K., Moestrup, S. K., Post, S. R., Sawamura, T., Silverstein, S., Speth, R. C., Telfer, J. C., Thiele, G. M., ... El Khoury, J. (2017). A Consensus Definitive Classification of Scavenger Receptors and Their Roles in Health and Disease. *The Journal of Immunology*, 198(10), 3775–3789. <https://doi.org/10.4049/jimmunol.1700373>
- Prins, G. S., & Putz, O. (2008). Molecular signaling pathways that regulate prostate gland development. *Differentiation*, 76(6), 641–659. <https://doi.org/10.1111/j.1432-0436.2008.00277.x>
- Pritchard, C. C., Morrissey, C., Kumar, A., Zhang, X., Smith, C., Coleman, I., Salipante, S. J., Milbank, J., Yu, M., Grady, W. M., Tait, J. F., Corey, E., Vessella, R. L., Walsh, T., Shendure, J., & Nelson, P. S. (2014). Complex MSH2 and MSH6 mutations in hypermutated microsatellite unstable advanced prostate cancer. *Nature Communications*, 5(1), 4988. <https://doi.org/10.1038/ncomms5988>
- Pujals, S., & Giral, E. (2008). Proline-rich, amphipathic cell-penetrating peptides. *Advanced Drug Delivery Reviews*, 60(4–5), 473–484. <https://doi.org/10.1016/j.addr.2007.09.012>
- Qian, Z., Martyna, A., Hard, R. L., Wang, J., Appiah-Kubi, G., Coss, C., Phelps, M. A., Rossman, J. S., & Pei, D. (2016). Discovery and Mechanism of Highly Efficient Cyclic Cell-Penetrating Peptides. *Biochemistry*, 55(18), 2601–2612. <https://doi.org/10.1021/acs.biochem.6b00226>

- Qin, B., Tai, W., Shukla, R. S., & Cheng, K. (2011). Identification of a LNCaP-Specific Binding Peptide Using Phage Display. *Pharmaceutical Research*, 28(10), 2422–2434. <https://doi.org/10.1007/s11095-011-0469-7>
- Qin, X., Du, Y., Liu, X., & Wang, L. (2021). LSD1 Promotes Prostate Cancer Cell Survival by Destabilizing FBXW7 at Post-Translational Level. *Frontiers in Oncology*, 10. <https://doi.org/10.3389/fonc.2020.616185>
- Qiu, M., Wang, X., Sun, H., Zhang, J., Deng, C., & Zhong, Z. (2018). Cyclic RGD-Peptide-Functionalized Poly(lipopeptide) Micelles for Enhanced Loading and Targeted Delivery of Monomethyl Auristatin E. *Molecular Pharmaceutics*, 15(11), 4854–4861. <https://doi.org/10.1021/acs.molpharmaceut.8b00498>
- Qu, Y., Dai, B., Ye, D., Kong, Y., Chang, K., Jia, Z., Yang, X., Zhang, H., Zhu, Y., & Shi, G. (2015). Constitutively Active AR-V7 Plays an Essential Role in the Development and Progression of Castration-Resistant Prostate Cancer. *Scientific Reports*, 5(1), 7654. <https://doi.org/10.1038/srep07654>
- Quigley, D. A., Dang, H. X., Zhao, S. G., Lloyd, P., Aggarwal, R., Alumkal, J. J., Foye, A., Kothari, V., Perry, M. D., Bailey, A. M., Playdle, D., Barnard, T. J., Zhang, L., Zhang, J., Youngren, J. F., Cieslik, M. P., Parolia, A., Beer, T. M., Thomas, G., ... Feng, F. Y. (2018). Genomic Hallmarks and Structural Variation in Metastatic Prostate Cancer. *Cell*, 175(3), 889. <https://doi.org/10.1016/j.cell.2018.10.019>
- Ragin, A. D., Morgan, R. A., & Chmielewski, J. (2002). Cellular import mediated by nuclear localization signal peptide sequences. *Chemistry and Biology*, 9(8), 943–948. [https://doi.org/10.1016/S1074-5521\(02\)00189-8](https://doi.org/10.1016/S1074-5521(02)00189-8)
- Ramirez-Ortiz, Z. G., Pendergraft, W. F., Prasad, A., Byrne, M. H., Iram, T., Blanchette, C. J., Luster, A. D., Hacohen, N., Khoury, J. El, & Means, T. K. (2013). The scavenger receptor SCARF1 mediates the clearance of apoptotic cells and prevents autoimmunity. *Nature Immunology*, 14(9), 917–926. <https://doi.org/10.1038/ni.2670>
- Rao, V., Garudadri, G., Shilpa, A., Fonseca, D., Sudha, Sm., Sharma, R., Subramanyeshwar, Tr., & Challa, S. (2018). Validation of the WHO 2016 new Gleason score of prostatic carcinoma. *Urology Annals*, 10(3), 324. https://doi.org/10.4103/UA.UA_185_17
- Rebbeck, T. R. (2017). Prostate Cancer Genetics: Variation by Race, Ethnicity, and Geography. *Seminars in Radiation Oncology*, 27(1), 3–10. <https://doi.org/10.1016/j.semradonc.2016.08.002>
- Rebello, R. J., Oing, C., Knudsen, K. E., Loeb, S., Johnson, D. C., Reiter, R. E., Gillissen, S., Van der Kwast, T., & Bristow, R. G. (2021). Prostate cancer. *Nature Reviews Disease Primers*, 7(1), 9. <https://doi.org/10.1038/s41572-020-00243-0>
- Reboul, E., Klein, A., Bietrix, F., Gleize, B., Malezet-Desmoulins, C., Schneider, M., Margotat, A., Lagrost, L., Collet, X., & Borel, P. (2006). Scavenger Receptor Class B Type I (SR-BI) Is Involved in Vitamin E Transport across the Enterocyte. *Journal of Biological Chemistry*, 281(8), 4739–4745. <https://doi.org/10.1074/jbc.M509042200>

- Rechner, C., Kühlewein, C., Müller, A., Schild, H., & Rudel, T. (2007). Host Glycoprotein Gp96 and Scavenger Receptor SREC Interact with PorB of Disseminating *Neisseria gonorrhoeae* in an Epithelial Invasion Pathway. *Cell Host & Microbe*, 2(6), 393–403. <https://doi.org/10.1016/j.chom.2007.11.002>
- Reddy, E. K., Robinson, R. G., & Mansfield, C. M. (1986). Strontium 89 for palliation of bone metastases. *Journal of the National Medical Association*, 78(1), 27–32.
- Reed, D. R., Chawla, S. P., Setty, B., Mascarenhas, L., Meyers, P. A., Metts, J., Harrison, D. J., Loeb, D., Crompton, B. D., Wages, D. S., Stenehjem, D. D., Santiesteban, D. Y., Mirza, N. Q., & DuBois, S. G. (2021). Phase 1 trial of seclidemstat (SP-2577) in patients with relapsed/refractory Ewing sarcoma. *Journal of Clinical Oncology*, 39(15_suppl), 11514–11514. https://doi.org/10.1200/JCO.2021.39.15_suppl.11514
- Régina, A., Demeule, M., Ché, C., Lavallée, I., Poirier, J., Gabathuler, R., Béliveau, R., & Castaigne, J.-P. (2008). Antitumour activity of ANG1005, a conjugate between paclitaxel and the new brain delivery vector Angiopep-2. *British Journal of Pharmacology*, 155(2), 185–197. <https://doi.org/10.1038/bjp.2008.260>
- Regufe da Mota, S., Bailey, S., Strivens, R. A., Hayden, A. L., Douglas, L. R., Duriez, P. J., Borrello, M. T., Benelkebir, H., Ganesan, A., Packham, G., & Crabb, S. J. (2018). LSD1 inhibition attenuates androgen receptor V7 splice variant activation in castration resistant prostate cancer models. *Cancer Cell International*, 18(1), 71. <https://doi.org/10.1186/s12935-018-0568-1>
- Rehman, Y., & Rehman, Y. (2012). Abiraterone acetate: oral androgen biosynthesis inhibitor for treatment of castration-resistant prostate cancer. *Drug Design, Development and Therapy*, 13. <https://doi.org/10.2147/DDDT.S15850>
- Rejman, J., Oberle, V., Zuhorn, I. S., & Hoekstra, D. (2004). Size-dependent internalization of particles via the pathways of clathrin- and caveolae-mediated endocytosis. *Biochemical Journal*, 377(1), 159–169. <https://doi.org/10.1042/bj20031253>
- Ren, Z.-J., Cao, D.-H., Zhang, Q., Ren, P.-W., Liu, L.-R., Wei, Q., Wei, W.-R., & Dong, Q. (2019). First-degree family history of breast cancer is associated with prostate cancer risk: a systematic review and meta-analysis. *BMC Cancer*, 19(1), 871. <https://doi.org/10.1186/s12885-019-6055-9>
- Rennert, H., Zeigler-Johnson, C. M., Addya, K., Finley, M. J., Walker, A. H., Spangler, E., Leonard, D. G. B., Wein, A., Malkowicz, S. B., & Rebbeck, T. R. (2005). Association of Susceptibility Alleles in ELAC2/HPC2, RNASEL/HPC1, and MSR1 with Prostate Cancer Severity in European American and African American Men. *Cancer Epidemiology, Biomarkers & Prevention*, 14(4), 949–957. <https://doi.org/10.1158/1055-9965.EPI-04-0637>
- Rennert, H., Zeigler-Johnson, C., Mittal, R. D., Tan, Y., Sadowl, C. M., Edwards, J., Finley, M. J., Mandhani, A., Mital, B., & Rebbeck, T. R. (2008). Analysis of the RNASEL/HPC1, and Macrophage Scavenger Receptor 1 in Asian-Indian

- Advanced Prostate Cancer. *Urology*, 72(2), 456–460.
<https://doi.org/10.1016/j.urology.2007.11.139>
- Reubi, J. C. (2003). Peptide Receptors as Molecular Targets for Cancer Diagnosis and Therapy. *Endocrine Reviews*, 24(4), 389–427.
<https://doi.org/10.1210/er.2002-0007>
- Reubi, J. C., Wenger, S., Schmuckli-Maurer, J., Schaer, J.-C., & Gugger, M. (2002). Bombesin receptor subtypes in human cancers: detection with the universal radioligand (125)I-[D-TYR(6), beta-ALA(11), PHE(13), NLE(14)] bombesin(6-14). *Clinical Cancer Research : An Official Journal of the American Association for Cancer Research*, 8(4), 1139–1146.
- Rhee, M., & Davis, P. (2006). Mechanism of uptake of C105Y, a novel cell-penetrating peptide. *Journal of Biological Chemistry*, 281(2), 1233–1240.
<https://doi.org/10.1074/JBC.M509813200>
- Richard, J. P., Melikov, K., Brooks, H., Prevot, P., Lebleu, B., & Chernomordik, L. V. (2005). Cellular Uptake of Unconjugated TAT Peptide Involves Clathrin-dependent Endocytosis and Heparan Sulfate Receptors. *Journal of Biological Chemistry*, 280(15), 15300–15306. <https://doi.org/10.1074/jbc.M401604200>
- Richard, J. P., Melikov, K., Vives, E., Ramos, C., Verbeure, B., Gait, M. J., Chernomordik, L. V., & Lebleu, B. (2003). Cell-penetrating Peptides. *Journal of Biological Chemistry*, 278(1), 585–590.
<https://doi.org/10.1074/jbc.M209548200>
- Rigotti, A., Acton, S. L., & Krieger, M. (1995). The Class B Scavenger Receptors SR-BI and CD36 Are Receptors for Anionic Phospholipids. *Journal of Biological Chemistry*, 270(27), 16221–16224.
<https://doi.org/10.1074/jbc.270.27.16221>
- Rigotti, A., Miettinen, H. E., & Krieger, M. (2003). The Role of the High-Density Lipoprotein Receptor SR-BI in the Lipid Metabolism of Endocrine and Other Tissues. *Endocrine Reviews*, 24(3), 357–387. <https://doi.org/10.1210/er.2001-0037>
- Rink, J., Ghigo, E., Kalaidzidis, Y., & Zerial, M. (2005). Rab Conversion as a Mechanism of Progression from Early to Late Endosomes. *Cell*, 122(5), 735–749. <https://doi.org/10.1016/j.cell.2005.06.043>
- Ristau, B. T., O'Keefe, D. S., & Bacich, D. J. (2014). The prostate-specific membrane antigen: Lessons and current clinical implications from 20 years of research. *Urologic Oncology: Seminars and Original Investigations*, 32(3), 272–279. <https://doi.org/10.1016/j.urolonc.2013.09.003>
- Roberts, M. J., Maurer, T., Perera, M., Eiber, M., Hope, T. A., Ost, P., Siva, S., Hofman, M. S., Murphy, D. G., Emmett, L., & Fendler, W. P. (2023). Using PSMA imaging for prognostication in localized and advanced prostate cancer. *Nature Reviews Urology*, 20(1), 23–47. <https://doi.org/10.1038/s41585-022-00670-6>
- Robinson, D., Van Allen, E. M., Wu, Y.-M., Schultz, N., Lonigro, R. J., Mosquera, J.-M., Montgomery, B., Taplin, M.-E., Pritchard, C. C., Attard, G., Beltran, H., Abida, W., Bradley, R. K., Vinson, J., Cao, X., Vats, P., Kunju, L. P., Hussain,

- M., Feng, F. Y., ... Chinnaiyan, A. M. (2015). Integrative Clinical Genomics of Advanced Prostate Cancer. *Cell*, 162(2), 454.
<https://doi.org/10.1016/j.cell.2015.06.053>
- Roboz, G. J., Yee, K., Verma, A., Borthakur, G., de la Fuente Burguera, A., Sanz, G., Mohammad, H. P., Kruger, R. G., Karpinich, N. O., Ferron-Brady, G., Acosta, A., Del Buono, H., Collingwood, T., Ballas, M., Dhar, A., & Wei, A. H. (2022). Phase I trials of the lysine-specific demethylase 1 inhibitor, GSK2879552, as mono- and combination-therapy in relapsed/refractory acute myeloid leukemia or high-risk myelodysplastic syndromes. *Leukemia & Lymphoma*, 63(2), 463–467. <https://doi.org/10.1080/10428194.2021.2012667>
- Rodriguez, O. C., & Cheney, R. E. (2002). Human myosin-Vc is a novel class V myosin expressed in epithelial cells. *Journal of Cell Science*, 115(5), 991–1004. <https://doi.org/10.1242/jcs.115.5.991>
- Rodriguez-Bravo, V., Carceles-Cordon, M., Hoshida, Y., Cordon-Cardo, C., Galsky, M. D., & Domingo-Domenech, J. (2017). The role of GATA2 in lethal prostate cancer aggressiveness. *Nature Reviews Urology*, 14(1), 38–48.
<https://doi.org/10.1038/nrurol.2016.225>
- Rohrmann, S., Linseisen, J., Allen, N., Bueno-de-Mesquita, H. B., Johnsen, N. F., Tjønneland, A., Overvad, K., Kaaks, R., Teucher, B., Boeing, H., Pischon, T., Lagiou, P., Trichopoulou, A., Trichopoulos, D., Palli, D., Krogh, V., Tumino, R., Ricceri, F., Argüelles Suárez, M. V., ... Key, T. J. (2013). Smoking and the risk of prostate cancer in the European Prospective Investigation into Cancer and Nutrition. *British Journal of Cancer*, 108(3), 708–714.
<https://doi.org/10.1038/bjc.2012.520>
- Rosé, S. D., Lejen, T., Casaletti, L., Larson, R. E., Pene, T. D., & Trifaró, J.-M. (2002). Molecular motors involved in chromaffin cell secretion. *Annals of the New York Academy of Sciences*, 971, 222–231.
<https://doi.org/10.1111/j.1749-6632.2002.tb04466.x>
- Ross, A. E., Hurley, P. J., Tran, P. T., Rowe, S. P., Benzon, B., Neal, T. O., Chapman, C., Harb, R., Milman, Y., Trock, B. J., Drake, C. G., & Antonarakis, E. S. (2020). A pilot trial of pembrolizumab plus prostatic cryotherapy for men with newly diagnosed oligometastatic hormone-sensitive prostate cancer. *Prostate Cancer and Prostatic Diseases*, 23(1), 184–193.
<https://doi.org/10.1038/s41391-019-0176-8>
- Rubin, M. A., & Demichelis, F. (2018). The Genomics of Prostate Cancer: emerging understanding with technologic advances. *Modern Pathology*, 31, 1–11. <https://doi.org/10.1038/modpathol.2017.166>
- Rudolf, R., Kögel, T., Kuznetsov, S. A., Salm, T., Schlicker, O., Hellwig, A., Hammer, J. A., & Gerdes, H.-H. (2003). Myosin Va facilitates the distribution of secretory granules in the F-actin rich cortex of PC12 cells. *Journal of Cell Science*, 116(7), 1339–1348. <https://doi.org/10.1242/jcs.00317>
- Ruoslahti, E. (2017). Tumor penetrating peptides for improved drug delivery. *Advanced Drug Delivery Reviews*, 110–111, 3–12.
<https://doi.org/10.1016/J.ADDR.2016.03.008>

- Ruseska, I., & Zimmer, A. (2020). Internalization mechanisms of cell-penetrating peptides. *Beilstein Journal of Nanotechnology*, 11, 101–123. <https://doi.org/10.3762/bjnano.11.10>
- Ruzali, W. A. W., Kehoe, P. G., & Love, S. (2012). LRP1 expression in cerebral cortex, choroid plexus and meningeal blood vessels: relationship to cerebral amyloid angiopathy and APOE status. *Neuroscience Letters*, 525(2), 123–128. <https://doi.org/10.1016/j.neulet.2012.07.065>
- Saad, F., Gleason, D. M., Murray, R., Tchekmedyan, S., Venner, P., Lacombe, L., Chin, J. L., Vinholes, J. J., Goas, J. A., & Chen, B. (2002). A Randomized, Placebo-Controlled Trial of Zoledronic Acid in Patients With Hormone-Refractory Metastatic Prostate Carcinoma. *JNCI Journal of the National Cancer Institute*, 94(19), 1458–1468. <https://doi.org/10.1093/jnci/94.19.1458>
- Säälik, P., Padari, K., Niinep, A., Lorents, A., Hansen, M., Jokitalo, E., Langel, Ü., & Pooga, M. (2009). Protein Delivery with Transportans Is Mediated by Caveolae Rather Than Flotillin-Dependent Pathways. *Bioconjugate Chemistry*, 20(5), 877–887. <https://doi.org/10.1021/bc800416f>
- Saar, K., Lindgren, M., Hansen, M., Eiríksdóttir, E., Jiang, Y., Rosenthal-Aizman, K., Sassian, M., & Langel, Ü. (2005). Cell-penetrating peptides: A comparative membrane toxicity study. *Analytical Biochemistry*, 345(1), 55–65. <https://doi.org/10.1016/j.ab.2005.07.033>
- Sakamoto, A., Hino, S., Nagaoka, K., Anan, K., Takase, R., Matsumori, H., Ojima, H., Kanai, Y., Arita, K., & Nakao, M. (2015). Lysine Demethylase LSD1 Coordinates Glycolytic and Mitochondrial Metabolism in Hepatocellular Carcinoma Cells. *Cancer Research*, 75(7), 1445–1456. <https://doi.org/10.1158/0008-5472.CAN-14-1560>
- Sakamoto, K., Shinohara, T., Adachi, Y., Asami, T., & Ohtaki, T. (2017). A novel LRP1-binding peptide L57 that crosses the blood brain barrier. *Biochemistry and Biophysics Reports*, 12, 135–139. <https://doi.org/10.1016/j.bbrep.2017.07.003>
- Saleh, M.-C., van Rij, R. P., Hekele, A., Gillis, A., Foley, E., O'Farrell, P. H., & Andino, R. (2006). The endocytic pathway mediates cell entry of dsRNA to induce RNAi silencing. *Nature Cell Biology*, 8(8), 793–802. <https://doi.org/10.1038/ncb1439>
- Salomon, D. S., Brandt, R., Ciardiello, F., & Normanno, N. (1995). Epidermal growth factor-related peptides and their receptors in human malignancies. *Critical Reviews in Oncology/Hematology*, 19(3), 183–232. [https://doi.org/10.1016/1040-8428\(94\)00144-I](https://doi.org/10.1016/1040-8428(94)00144-I)
- Salomone, F., Cardarelli, F., Di Luca, M., Boccardi, C., Nifosi, R., Bardi, G., Di Bari, L., Serresi, M., & Beltram, F. (2012). A novel chimeric cell-penetrating peptide with membrane-disruptive properties for efficient endosomal escape. *Journal of Controlled Release : Official Journal of the Controlled Release Society*, 163(3), 293–303. <https://doi.org/10.1016/j.jconrel.2012.09.019>
- Sancho, V., Di Florio, A., W. Moody, T., & T. Jensen, R. (2011). Bombesin Receptor-Mediated Imaging and Cytotoxicity: Review and Current Status.

- Current Drug Delivery, 8(1), 79–134.
<https://doi.org/10.2174/156720111793663624>
- Sandhu, S., Moore, C. M., Chiong, E., Beltran, H., Bristow, R. G., & Williams, S. G. (2021). Prostate cancer. *The Lancet*, 398(10305), 1075–1090.
[https://doi.org/10.1016/S0140-6736\(21\)00950-8](https://doi.org/10.1016/S0140-6736(21)00950-8)
- Santamaría, L., Martín, R., Martín, J. J., & Alonso, L. (2002). Stereologic estimation of the number of neuroendocrine cells in normal human prostate detected by immunohistochemistry. *Applied Immunohistochemistry & Molecular Morphology : AIMM*, 10(3), 275–281.
<https://doi.org/10.1097/00129039-200209000-00016>
- Sartor, O., de Bono, J., Chi, K. N., Fizazi, K., Herrmann, K., Rahbar, K., Tagawa, S. T., Nordquist, L. T., Vaishampayan, N., El-Haddad, G., Park, C. H., Beer, T. M., Armour, A., Pérez-Contreras, W. J., DeSilvio, M., Kpamegan, E., Gericke, G., Messmann, R. A., Morris, M. J., & Krause, B. J. (2021). Lutetium-177–PSMA-617 for Metastatic Castration-Resistant Prostate Cancer. *New England Journal of Medicine*, 385(12), 1091–1103.
<https://doi.org/10.1056/NEJMoa2107322>
- Sartor, O., Reid, R. H., Hoskin, P. J., Quick, D. P., Ell, P. J., Coleman, R. E., Kotler, J. A., Freeman, L. M., & Olivier, P. (2004). Samarium-153-Lexidronam complex for treatment of painful bone metastases in hormone-refractory prostate cancer. *Urology*, 63(5), 940–945.
<https://doi.org/10.1016/j.urology.2004.01.034>
- Scarselli, E., Ansuini, H., Cerino, R., Roccasecca, R. M., Acali, S., Filocamo, G., Traboni, C., Nicosia, A., Cortese, R., & Vitelli, A. (2002). The human scavenger receptor class B type I is a novel candidate receptor for the hepatitis C virus. *The EMBO Journal*, 21(19), 5017–5025.
<https://doi.org/10.1093/emboj/cdf529>
- Scher, H. I., & Sawyers, C. L. (2005). Biology of Progressive, Castration-Resistant Prostate Cancer: Directed Therapies Targeting the Androgen-Receptor Signaling Axis. *Journal of Clinical Oncology*, 23(32), 8253–8261.
<https://doi.org/10.1200/JCO.2005.03.4777>
- Schmidt, D. M. Z., & McCafferty, D. G. (2007). trans -2-Phenylcyclopropylamine Is a Mechanism-Based Inactivator of the Histone Demethylase LSD1. *Biochemistry*, 46(14), 4408–4416. <https://doi.org/10.1021/bi0618621>
- Schörghofer, D., Kinslechner, K., Preitschopf, A., Schütz, B., Röhr, C., Hengstschläger, M., Stangl, H., & Mikula, M. (2015). The HDL receptor SR-BI is associated with human prostate cancer progression and plays a possible role in establishing androgen independence. *Reproductive Biology and Endocrinology*, 13(1), 88. <https://doi.org/10.1186/s12958-015-0087-z>
- Schroeder, R. P. J., Weerden, W. M. van, Bangma, C., Krenning, E. P., & Jong, M. de. (2009). Peptide receptor imaging of prostate cancer with radiolabelled bombesin analogues. *Methods*, 48(2), 200–204.
<https://doi.org/10.1016/j.ymeth.2009.04.002>
- Schweizer, M. T., Antonarakis, E. S., Bismar, T. A., Guedes, L. B., Cheng, H. H., Tretiakova, M. S., Vakar-Lopez, F., Klemfuss, N., Konnick, E. Q., Mostaghel,

- E. A., Hsieh, A. C., Nelson, P. S., Yu, E. Y., Montgomery, R. B., True, L. D., Epstein, J. I., Lotan, T. L., & Pritchard, C. C. (2019). Genomic Characterization of Prostatic Ductal Adenocarcinoma Identifies a High Prevalence of DNA Repair Gene Mutations. *JCO Precision Oncology*, 3, 1–9. <https://doi.org/10.1200/PO.18.00327>
- Sedhom, R., & Antonarakis, E. S. (2019). Clinical implications of mismatch repair deficiency in prostate cancer. *Future Oncology*, 15(20), 2395–2411. <https://doi.org/10.2217/fon-2019-0068>
- Sehrawat, A., Gao, L., Wang, Y., Bankhead, A., McWeeney, S. K., King, C. J., Schwartzman, J., Urrutia, J., Bisson, W. H., Coleman, D. J., Joshi, S. K., Kim, D.-H., Sampson, D. A., Weinmann, S., Kallakury, B. V. S., Berry, D. L., Haque, R., Van Den Eeden, S. K., Sharma, S., ... Alumkal, J. J. (2018). LSD1 activates a lethal prostate cancer gene network independently of its demethylase function. *Proceedings of the National Academy of Sciences of the United States of America*, 115(18), E4179–E4188. <https://doi.org/10.1073/pnas.1719168115>
- Sekhoacha, M., Riet, K., Motloung, P., Gumenku, L., Adegoke, A., & Mashele, S. (2022). Prostate Cancer Review: Genetics, Diagnosis, Treatment Options, and Alternative Approaches. *Molecules*, 27(17), 5730. <https://doi.org/10.3390/molecules27175730>
- Senbanjo, L. T., & Chellaiah, M. A. (2017). CD44: A Multifunctional Cell Surface Adhesion Receptor Is a Regulator of Progression and Metastasis of Cancer Cells. *Frontiers in Cell and Developmental Biology*, 5, 18. <https://doi.org/10.3389/fcell.2017.00018>
- Seppälä, E. H., Ikonen, T., Autio, V., Rökman, A., Mononen, N., Matikainen, M. P., Tammela, T. L. J., & Schleutker, J. (2003). Germ-line alterations in MSR1 gene and prostate cancer risk. *Clinical Cancer Research : An Official Journal of the American Association for Cancer Research*, 9(14), 5252–5256.
- Sexton, W. J., Lance, R. E., Reyes, A. O., Pisters, P. W., Tu, S. M., & Pisters, L. L. (2001). Adult prostate sarcoma: the M. D. Anderson Cancer Center Experience. *The Journal of Urology*, 166(2), 521–525. [https://doi.org/10.1016/s0022-5347\(05\)65974-5](https://doi.org/10.1016/s0022-5347(05)65974-5)
- Sfanos, K. S., Yegnasubramanian, S., Nelson, W. G., & De Marzo, A. M. (2018). The inflammatory microenvironment and microbiome in prostate cancer development. *Nature Reviews Urology*, 15(1), 11–24. <https://doi.org/10.1038/nrurol.2017.167>
- Shah, G. V., Rayford, W., Noble, M. J., Austenfeld, M., Weigel, J., Vamos, S., & Mebust, W. K. (1994). Calcitonin stimulates growth of human prostate cancer cells through receptor-mediated increase in cyclic adenosine 3',5'-monophosphates and cytoplasmic Ca²⁺ transients. *Endocrinology*, 134(2), 596–602. <https://doi.org/10.1210/endo.134.2.8299557>
- Sharmin, S., Islam, Md. Z., Karal, M. A. S., Alam Shibly, S. U., Dohra, H., & Yamazaki, M. (2016). Effects of Lipid Composition on the Entry of Cell-Penetrating Peptide Oligoarginine into Single Vesicles. *Biochemistry*, 55(30), 4154–4165. <https://doi.org/10.1021/acs.biochem.6b00189>

- Sharp, A., Coleman, I., Yuan, W., Sprenger, C., Dolling, D., Rodrigues, D. N., Russo, J. W., Figueiredo, I., Bertan, C., Seed, G., Riisnaes, R., Uo, T., Neeb, A., Welti, J., Morrissey, C., Carreira, S., Luo, J., Nelson, P. S., Balk, S. P., ... Plymate, S. R. (2018). Androgen receptor splice variant-7 expression emerges with castration resistance in prostate cancer. *Journal of Clinical Investigation*, 129(1), 192–208. <https://doi.org/10.1172/JCI122819>
- Shen, M. M., & Abate-Shen, C. (2010). Molecular genetics of prostate cancer: new prospects for old challenges. *Genes & Development*, 24(18), 1967–2000. <https://doi.org/10.1101/GAD.1965810>
- Shen, W.-J., Azhar, S., & Kraemer, F. B. (2018). SR-B1: A Unique Multifunctional Receptor for Cholesterol Influx and Efflux. *Annual Review of Physiology*, 80, 95–116. <https://doi.org/10.1146/annurev-physiol-021317-121550>
- Sheng, W., LaFleur, M. W., Nguyen, T. H., Chen, S., Chakravarthy, A., Conway, J. R., Li, Y., Chen, H., Yang, H., Hsu, P.-H., Van Allen, E. M., Freeman, G. J., De Carvalho, D. D., He, H. H., Sharpe, A. H., & Shi, Y. (2018). LSD1 Ablation Stimulates Anti-tumor Immunity and Enables Checkpoint Blockade. *Cell*, 174(3), 549–563.e19. <https://doi.org/10.1016/j.cell.2018.05.052>
- Shenoy, T. R., Boysen, G., Wang, M. Y., Xu, Q. Z., Guo, W., Koh, F. M., Wang, C., Zhang, L. Z., Wang, Y., Gil, V., Aziz, S., Christova, R., Rodrigues, D. N., Crespo, M., Rescigno, P., Tunariu, N., Riisnaes, R., Zafeiriou, Z., Flohr, P., ... Wu, H. (2017). CHD1 loss sensitizes prostate cancer to DNA damaging therapy by promoting error-prone double-strand break repair. *Annals of Oncology*, 28(7), 1495–1507. <https://doi.org/10.1093/annonc/mdx165>
- Shete, H. K., Prabhu, R. H., & Patravale, V. B. (2014). Endosomal Escape: A Bottleneck in Intracellular Delivery. *Journal of Nanoscience and Nanotechnology*, 14(1), 460–474. <https://doi.org/10.1166/jnn.2014.9082>
- Shi, Y. (2007). Histone lysine demethylases: emerging roles in development, physiology and disease. *Nature Reviews. Genetics*, 8(11), 829–833. <https://doi.org/10.1038/nrg2218>
- Shi, Y., Lan, F., Matson, C., Mulligan, P., Whetstine, J. R., Cole, P. A., Casero, R. A., & Shi, Y. (2004). Histone Demethylation Mediated by the Nuclear Amine Oxidase Homolog LSD1. *Cell*, 119(7), 941–953. <https://doi.org/10.1016/j.cell.2004.12.012>
- Shi, Y., Sawada, J., Sui, G., Affar, E. B., Whetstine, J. R., Lan, F., Ogawa, H., Po-Shan Luke, M., Nakatani, Y., & Shi, Y. (2003). Coordinated histone modifications mediated by a CtBP co-repressor complex. *Nature*, 422(6933), 735–738. <https://doi.org/10.1038/nature01550>
- Shih, J. C., Chen, K., & Ridd, M. J. (1999). Monoamine oxidase: From Genes to Behavior. *Annual Review of Neuroscience*, 22(1), 197–217. <https://doi.org/10.1146/annurev.neuro.22.1.197>
- Shiratsuchi, A., Kawasaki, Y., Ikemoto, M., Arai, H., & Nakanishi, Y. (1999). Role of Class B Scavenger Receptor Type I in Phagocytosis of Apoptotic Rat Spermatogenic Cells by Sertoli Cells. *Journal of Biological Chemistry*, 274(9), 5901–5908. <https://doi.org/10.1074/jbc.274.9.5901>

- Siegel, D. A., O'Neil, M. E., Richards, T. B., Dowling, N. F., & Weir, H. K. (2020). Prostate Cancer Incidence and Survival, by Stage and Race/Ethnicity — United States, 2001–2017. *MMWR. Morbidity and Mortality Weekly Report*, 69(41), 1473–1480. <https://doi.org/10.15585/mmwr.mm6941a1>
- Siegel, R. L., Miller, K. D., Wagle, N. S., & Jemal, A. (2023). Cancer statistics, 2023. *CA: A Cancer Journal for Clinicians*, 73(1), 17–48. <https://doi.org/10.3322/caac.21763>
- Signoretti, S., Waltregny, D., Dilks, J., Isaac, B., Lin, D., Garraway, L., Yang, A., Montironi, R., McKeon, F., & Loda, M. (2000). p63 Is a Prostate Basal Cell Marker and Is Required for Prostate Development. *The American Journal of Pathology*, 157(6), 1769. [https://doi.org/10.1016/S0002-9440\(10\)64814-6](https://doi.org/10.1016/S0002-9440(10)64814-6)
- Silver, D. A., Pellicer, I., Fair, W. R., Heston, W. D., & Cordon-Cardo, C. (1997). Prostate-specific membrane antigen expression in normal and malignant human tissues. *Clinical Cancer Research: An Official Journal of the American Association for Cancer Research*, 3(1), 81–85.
- Silverstein, R. L., & Febbraio, M. (2009). CD36, a Scavenger Receptor Involved in Immunity, Metabolism, Angiogenesis, and Behavior. *Science Signaling*, 2(72). <https://doi.org/10.1126/scisignal.272re3>
- Singh, T. D., Park, S.-Y., Bae, J., Yun, Y., Bae, Y.-C., Park, R.-W., & Kim, I.-S. (2010). MEGF10 functions as a receptor for the uptake of amyloid- β . *FEBS Letters*, 584(18), 3936–3942. <https://doi.org/10.1016/j.febslet.2010.08.050>
- Smith, M., Parker, C., Saad, F., Miller, K., Tombal, B., Ng, Q. S., Boegemann, M., Matveev, V., Piulats, J. M., Zucca, L. E., Karyakin, O., Kimura, G., Matsubara, N., Nahas, W. C., Nolè, F., Rosenbaum, E., Heidenreich, A., Kakehi, Y., Zhang, A., ... Higano, C. (2019). Addition of radium-223 to abiraterone acetate and prednisone or prednisolone in patients with castration-resistant prostate cancer and bone metastases (ERA 223): a randomised, double-blind, placebo-controlled, phase 3 trial. *The Lancet Oncology*, 20(3), 408–419. [https://doi.org/10.1016/S1470-2045\(18\)30860-X](https://doi.org/10.1016/S1470-2045(18)30860-X)
- Smith, M. R., Hussain, M., Saad, F., Fizazi, K., Sternberg, C. N., Crawford, E. D., Kopyltsov, E., Park, C. H., Alekseev, B., Montesa-Pino, Á., Ye, D., Parnis, F., Cruz, F., Tammela, T. L. J., Suzuki, H., Utriainen, T., Fu, C., Uemura, M., Méndez-Vidal, M. J., ... Tombal, B. (2022). Darolutamide and Survival in Metastatic, Hormone-Sensitive Prostate Cancer. *New England Journal of Medicine*, 386(12), 1132–1142. <https://doi.org/10.1056/NEJMoa2119115>
- Sohn, M., Kwon, T., Jeong, I. G., Hong, S., You, D., Hong, J. H., Ahn, H., & Kim, C.-S. (2014). Histologic Variability and Diverse Oncologic Outcomes of Prostate Sarcomas. *Korean Journal of Urology*, 55(12), 797. <https://doi.org/10.4111/kju.2014.55.12.797>
- Solano, R. M., Carmena, M. J., Carrero, I., Cavallaro, S., Roman, F., Hueso, C., Travali, S., Lopez-Fraile, N., Guijarro, L. G., & Prieto, J. C. (1996). Characterization of vasoactive intestinal peptide/pituitary adenylate cyclase-activating peptide receptors in human benign hyperplastic prostate. *Endocrinology*, 137(7), 2815–2822. <https://doi.org/10.1210/endo.137.7.8770902>

- Somiya, M., & Kuroda, S. (2020). [DDS Nanocarriers Mimicking Early Infection Machinery of Viruses]. *Yakugaku Zasshi : Journal of the Pharmaceutical Society of Japan*, 140(2), 147–152. <https://doi.org/10.1248/yakushi.19-00187-2>
- Song, C., Al-Mehdi, A. B., & Fisher, A. B. (2001). An immediate endothelial cell signaling response to lung ischemia. *American Journal of Physiology-Lung Cellular and Molecular Physiology*, 281(4), L993–L1000. <https://doi.org/10.1152/ajplung.2001.281.4.L993>
- Srimanee, A., Regberg, J., Hällbrink, M., Vajragupta, O., & Langel, Ü. (2016). Role of scavenger receptors in peptide-based delivery of plasmid DNA across a blood–brain barrier model. *International Journal of Pharmaceutics*, 500(1–2), 128–135. <https://doi.org/10.1016/j.ijpharm.2016.01.014>
- Stavropoulos, P., Blobel, G., & Hoelz, A. (2006). Crystal structure and mechanism of human lysine-specific demethylase-1. *Nature Structural & Molecular Biology*, 13(7), 626–632. <https://doi.org/10.1038/nsmb1113>
- Stazi, G., Zwergel, C., Valente, S., & Mai, A. (2016). LSD1 inhibitors: a patent review (2010-2015). *Expert Opinion on Therapeutic Patents*, 26(5), 565–580. <https://doi.org/10.1517/13543776.2016.1165209>
- Steiner, D. F., Nagpal, K., Sayres, R., Foote, D. J., Wedin, B. D., Pearce, A., Cai, C. J., Winter, S. R., Symonds, M., Yatziv, L., Kapishnikov, A., Brown, T., Flament-Auvigne, I., Tan, F., Stumpe, M. C., Jiang, P.-P., Liu, Y., Chen, P.-H. C., Corrado, G. S., ... Mermel, C. H. (2020). Evaluation of the Use of Combined Artificial Intelligence and Pathologist Assessment to Review and Grade Prostate Biopsies. *JAMA Network Open*, 3(11), e2023267. <https://doi.org/10.1001/jamanetworkopen.2020.23267>
- Stenmark, H., & Olkkonen, V. M. (2001). The Rab GTPase family. *Genome Biology*, 2(5), REVIEWS3007. <https://doi.org/10.1186/gb-2001-2-5-reviews3007>
- Stephenson, A. J., Scardino, P. T., Eastham, J. A., Bianco, F. J., Dotan, Z. A., DiBlasio, C. J., Reuther, A., Klein, E. A., & Kattan, M. W. (2005). Postoperative Nomogram Predicting the 10-Year Probability of Prostate Cancer Recurrence After Radical Prostatectomy. *Journal of Clinical Oncology*, 23(28), 7005–7012. <https://doi.org/10.1200/JCO.2005.01.867>
- Stevens, J. W., Palechek, P. L., Griebeling, T. L., Midura, R. J., Rokhlin, O. W., & Cohen, M. B. (1996). Expression of CD44 isoforms in human prostate tumor cell lines. *The Prostate*, 28(3), 153–161. [https://doi.org/10.1002/\(SICI\)1097-0045\(199603\)28:3<153::AID-PROS2>3.0.CO;2-G](https://doi.org/10.1002/(SICI)1097-0045(199603)28:3<153::AID-PROS2>3.0.CO;2-G)
- Stewart, C. R., Stuart, L. M., Wilkinson, K., van Gils, J. M., Deng, J., Halle, A., Rayner, K. J., Boyer, L., Zhong, R., Frazier, W. A., Lacy-Hulbert, A., Khoury, J. El, Golenbock, D. T., & Moore, K. J. (2010). CD36 ligands promote sterile inflammation through assembly of a Toll-like receptor 4 and 6 heterodimer. *Nature Immunology*, 11(2), 155–161. <https://doi.org/10.1038/ni.1836>
- Stopeck, A. T., Lipton, A., Body, J.-J., Steger, G. G., Tonkin, K., de Boer, R. H., Lichinitser, M., Fujiwara, Y., Yardley, D. A., Viniegra, M., Fan, M., Jiang, Q., Dansey, R., Jun, S., & Braun, A. (2010). Denosumab Compared With

- Zoledronic Acid for the Treatment of Bone Metastases in Patients With Advanced Breast Cancer: A Randomized, Double-Blind Study. *Journal of Clinical Oncology*, 28(35), 5132–5139. <https://doi.org/10.1200/JCO.2010.29.7101>
- Sugahara, K. N., Teesalu, T., Karmali, P. P., Kotamraju, V. R., Agemy, L., Girard, O. M., Hanahan, D., Mattrey, R. F., & Ruoslahti, E. (2009). Tissue-Penetrating Delivery of Compounds and Nanoparticles into Tumors. *Cancer Cell*, 16(6), 510–520. <https://doi.org/10.1016/j.ccr.2009.10.013>
- Sumanasuriya, S., & De Bono, J. (2018). Treatment of Advanced Prostate Cancer—A Review of Current Therapies and Future Promise. *Cold Spring Harbor Perspectives in Medicine*, 8(6), a030635. <https://doi.org/10.1101/cshperspect.a030635>
- Sun, J., Hsu, F.-C., Turner, A. R., Zheng, S. L., Chang, B.-L., Liu, W., Isaacs, W. B., & Xu, J. (2006). Meta-analysis of association of rare mutations and common sequence variants in theMSR1 gene and prostate cancer risk. *The Prostate*, 66(7), 728–737. <https://doi.org/10.1002/pros.20396>
- Sun, L.-C., & Coy, D. (2011). Somatostatin Receptor-Targeted Anti-Cancer Therapy. *Current Drug Delivery*, 8(1), 2–10. <https://doi.org/10.2174/156720111793663633>
- Sung, H., Ferlay, J., Siegel, R. L., Laversanne, M., Soerjomataram, I., Jemal, A., & Bray, F. (2021). Global Cancer Statistics 2020: GLOBOCAN Estimates of Incidence and Mortality Worldwide for 36 Cancers in 185 Countries. *CA: A Cancer Journal for Clinicians*, 71(3), 209–249. <https://doi.org/10.3322/caac.21660>
- Surintranont, J., & Zhou, M. (2023). Prostate Pathology: What is New in the 2022 WHO Classification of Urinary and Male Genital Tumors? *Pathologica*, 1–16. <https://doi.org/10.32074/1591-951X-822>
- Suzuki, H., Emi, M., Komiya, A., Fujiwara, Y., Yatani, R., Nakamura, Y., & Shimazaki, J. (1995). Localization of a tumor suppressor gene associated with progression of human prostate cancer within a 1.2 Mb region of 8p22-p21.3. *Genes, Chromosomes and Cancer*, 13(3), 168–174. <https://doi.org/10.1002/gcc.2870130306>
- Suzuki, H., Kurihara, Y., Takeya, M., Kamada, N., Kataoka, M., Jishage, K., Ueda, O., Sakaguchi, H., Higashi, T., Suzuki, T., Takashima, Y., Kawabe, Y., Cynshi, O., Wada, Y., Honda, M., Kurihara, H., Aburatani, H., Doi, T., Matsumoto, A., ... Kodama, T. (1997). A role for macrophage scavenger receptors in atherosclerosis and susceptibility to infection. *Nature*, 386(6622), 292–296. <https://doi.org/10.1038/386292a0>
- Swanson, J. A., & Watts, C. (1995). Macropinocytosis. *Trends in Cell Biology*, 5(11), 424–428. [https://doi.org/10.1016/S0962-8924\(00\)89101-1](https://doi.org/10.1016/S0962-8924(00)89101-1)
- Sweeney, C., Bracarda, S., Sternberg, C. N., Chi, K. N., Olmos, D., Sandhu, S., Massard, C., Matsubara, N., Alekseev, B., Parnis, F., Atduev, V., Buchschacher, G. L., Gafanov, R., Corrales, L., Borre, M., Stroyakovskiy, D., Alves, G. V., Bournakis, E., Puente, J., ... de Bono, J. S. (2021). Ipatasertib plus abiraterone and prednisolone in metastatic castration-resistant prostate

cancer (IPATential150): a multicentre, randomised, double-blind, phase 3 trial. *The Lancet*, 398(10295), 131–142. [https://doi.org/10.1016/S0140-6736\(21\)00580-8](https://doi.org/10.1016/S0140-6736(21)00580-8)

- Sweeney, C. J., Chen, Y.-H., Carducci, M., Liu, G., Jarrard, D. F., Eisenberger, M., Wong, Y.-N., Hahn, N., Kohli, M., Cooney, M. M., Dreicer, R., Vogelzang, N. J., Picus, J., Shevrin, D., Hussain, M., Garcia, J. A., & DiPaola, R. S. (2015). Chemohormonal Therapy in Metastatic Hormone-Sensitive Prostate Cancer. *New England Journal of Medicine*, 373(8), 737–746. <https://doi.org/10.1056/NEJMoa1503747>
- Swiecicki, J.-M., Bartsch, A., Tailhades, J., Di Pisa, M., Heller, B., Chassaing, G., Mansuy, C., Burlina, F., & Lavielle, S. (2014). The Efficacies of Cell-Penetrating Peptides in Accumulating in Large Unilamellar Vesicles Depend on their Ability To Form Inverted Micelles. *ChemBioChem*, 15(6), 884–891. <https://doi.org/10.1002/cbic.201300742>
- Taban, Q., Mumtaz, P. T., Masoodi, K. Z., Haq, E., & Ahmad, S. M. (2022). Scavenger receptors in host defense: from functional aspects to mode of action. *Cell Communication and Signaling* 2021 20:1, 20(1), 1–17. <https://doi.org/10.1186/S12964-021-00812-0>
- Tai, S., Sun, Y., Squires, J. M., Zhang, H., Oh, W. K., Liang, C.-Z., & Huang, J. (2011). PC3 is a cell line characteristic of prostatic small cell carcinoma. *The Prostate*, 71(15), 1668–1679. <https://doi.org/10.1002/pros.21383>
- Tai, W., Shukla, R. S., Qin, B., Li, B., & Cheng, K. (2011). Development of a Peptide–Drug Conjugate for Prostate Cancer Therapy. *Molecular Pharmaceutics*, 8(3), 901–912. <https://doi.org/10.1021/mp200007b>
- Tanaka, G., Nakase, I., Fukuda, Y., Masuda, R., Oishi, S., Shimura, K., Kawaguchi, Y., Takatani-Nakase, T., Langel, Ü., Gräslund, A., Okawa, K., Matsuoka, M., Fujii, N., Hatanaka, Y., & Futaki, S. (2012). CXCR4 Stimulates Macropinocytosis: Implications for Cellular Uptake of Arginine-Rich Cell-Penetrating Peptides and HIV. *Chemistry & Biology*, 19(11), 1437–1446. <https://doi.org/10.1016/j.chembiol.2012.09.011>
- Tang, D. G., Patrawala, L., Calhoun, T., Bhatia, B., Choy, G., Schneider-Broussard, R., & Jeter, C. (2007). Prostate cancer stem/progenitor cells: Identification, characterization, and implications. *Molecular Carcinogenesis*, 46(1), 1–14. <https://doi.org/10.1002/mc.20255>
- Tannock, I. F., de Wit, R., Berry, W. R., Horti, J., Pluzanska, A., Chi, K. N., Oudard, S., Théodore, C., James, N. D., Turesson, I., Rosenthal, M. A., & Eisenberger, M. A. (2004). Docetaxel plus Prednisone or Mitoxantrone plus Prednisone for Advanced Prostate Cancer. *New England Journal of Medicine*, 351(15), 1502–1512. <https://doi.org/10.1056/NEJMoa040720>
- Tashima, T. (2017). Intelligent substance delivery into cells using cell-penetrating peptides. *Bioorganic & Medicinal Chemistry Letters*, 27(2), 121–130. <https://doi.org/10.1016/j.bmcl.2016.11.083>
- Taylor, A., Kosoff, D., Emamekhoo, H., Lang, J. M., & Kyriakopoulos, C. E. (2023). PARP inhibitors in metastatic prostate cancer. *Frontiers in Oncology*, 13. <https://doi.org/10.3389/fonc.2023.1159557>

- Taylor, B. N., Mehta, R. R., Yamada, T., Lekmine, F., Christov, K., Chakrabarty, A. M., Green, A., Bratescu, L., Shilkaitis, A., Beattie, C. W., & Das Gupta, T. K. (2009). Noncationic Peptides Obtained From Azurin Preferentially Enter Cancer Cells. *Cancer Research*, 69(2), 537–546. <https://doi.org/10.1158/0008-5472.CAN-08-2932>
- Teesalu, T., Sugahara, K. N., & Ruoslahti, E. (2013). Tumor-penetrating peptides. *Frontiers in Oncology*, 3 AUG, 216. <https://doi.org/10.3389/FONC.2013.00216/BIBTEX>
- Terpe, H. J., Stark, H., Prehm, P., & Günthert, U. (1994). CD44 variant isoforms are preferentially expressed in basal epithelial of non-malignant human fetal and adult tissues. *Histochemistry*, 101(2), 79–89. <https://doi.org/10.1007/BF00269353>
- Terrone, D., Sang, S. L. W., Roudaia, L., & Silviu, J. R. (2003). Penetratin and Related Cell-Penetrating Cationic Peptides Can Translocate Across Lipid Bilayers in the Presence of a Transbilayer Potential. *Biochemistry*, 42(47), 13787–13799. <https://doi.org/10.1021/bi035293y>
- Testa, U., Castelli, G., & Pelosi, E. (2019). Cellular and Molecular Mechanisms Underlying Prostate Cancer Development: Therapeutic Implications. *Medicines*, 6(3), 82. <https://doi.org/10.3390/medicines6030082>
- Theart, R. P., Loos, B., Powrie, Y. S. L., & Niesler, T. R. (2018). Improved region of interest selection and colocalization analysis in three-dimensional fluorescence microscopy samples using virtual reality. *PLOS ONE*, 13(8), e0201965. <https://doi.org/10.1371/journal.pone.0201965>
- Thennarasu, S., Tan, A., Penumatchu, R., Shelburne, C. E., Heyl, D. L., & Ramamoorthy, A. (2010). Antimicrobial and Membrane Disrupting Activities of a Peptide Derived from the Human Cathelicidin Antimicrobial Peptide LL37. *Biophysical Journal*, 98(2), 248–257. <https://doi.org/10.1016/j.bpj.2009.09.060>
- Thériault, J. R., Adachi, H., & Calderwood, S. K. (2006). Role of Scavenger Receptors in the Binding and Internalization of Heat Shock Protein 70. *The Journal of Immunology*, 177(12), 8604–8611. <https://doi.org/10.4049/jimmunol.177.12.8604>
- Thundimadathil, J. (2012). Cancer Treatment Using Peptides: Current Therapies and Future Prospects. *Journal of Amino Acids*, 2012, 1–13. <https://doi.org/10.1155/2012/967347>
- Timms, B. G. (2008). Prostate development: a historical perspective. *Differentiation*, 76(6), 565–577. <https://doi.org/10.1111/j.1432-0436.2008.00278.x>
- Tindall, D., & Lonergan, P. (2011). Androgen receptor signaling in prostate cancer development and progression. *Journal of Carcinogenesis*, 10(1), 20. <https://doi.org/10.4103/1477-3163.83937>
- Tortorici, M., Borrello, M. T., Tardugno, M., Chiarelli, L. R., Pilotto, S., Ciossani, G., Vellore, N. A., Bailey, S. G., Cowan, J., O'Connell, M., Crabb, S. J., Packham, G., Mai, A., Baron, R., Ganesan, A., & Mattevi, A. (2013). Protein Recognition by Short Peptide Reversible Inhibitors of the Chromatin-Modifying

- LSD1/CoREST Lysine Demethylase. *ACS Chemical Biology*, 8(8), 1677–1682. <https://doi.org/10.1021/cb4001926>
- Tossi, A., Sandri, L., & Giangaspero, A. (2000). Amphipathic, alpha-helical antimicrobial peptides. *Biopolymers*, 55(1), 4–30. [https://doi.org/10.1002/1097-0282\(2000\)55:1<4::AID-BIP30>3.0.CO;2-M](https://doi.org/10.1002/1097-0282(2000)55:1<4::AID-BIP30>3.0.CO;2-M)
- Tossi, A., Tarantino, C., & Romeo, D. (1997). Design of Synthetic Antimicrobial Peptides Based on Sequence Analogy and Amphipathicity. *European Journal of Biochemistry*, 250(2), 549–558. <https://doi.org/10.1111/j.1432-1033.1997.0549a.x>
- Tousignant, K. D., Rockstroh, A., Taherian Fard, A., Lehman, M. L., Wang, C., McPherson, S. J., Philp, L. K., Bartonicek, N., Dinger, M. E., Nelson, C. C., & Sadowski, M. C. (2019). Lipid Uptake Is an Androgen-Enhanced Lipid Supply Pathway Associated with Prostate Cancer Disease Progression and Bone Metastasis. *Molecular Cancer Research*, 17(5), 1166–1179. <https://doi.org/10.1158/1541-7786.MCR-18-1147>
- Trabulo, S., Cardoso, A. L., Mano, M., & de Lima, M. C. P. (2010). Cell-Penetrating Peptides-Mechanisms of Cellular Uptake and Generation of Delivery Systems. *Pharmaceuticals (Basel, Switzerland)*, 3(4), 961–993. <https://doi.org/10.3390/PH3040961>
- Tran, C., Ouk, S., Clegg, N. J., Chen, Y., Watson, P. A., Arora, V., Wongvipat, J., Smith-Jones, P. M., Yoo, D., Kwon, A., Wasielewska, T., Welsbie, D., Chen, C. D., Higano, C. S., Beer, T. M., Hung, D. T., Scher, H. I., Jung, M. E., & Sawyers, C. L. (2009). Development of a Second-Generation Antiandrogen for Treatment of Advanced Prostate Cancer. *Science*, 324(5928), 787–790. <https://doi.org/10.1126/science.1168175>
- Traugher, C. A., Opoku, E., Brubaker, G., Major, J., Lu, H., Lorkowski, S. W., Neumann, C., Hardaway, A., Chung, Y.-M., Gulshan, K., Sharifi, N., Brown, J. M., & Smith, J. D. (2020). Uptake of high-density lipoprotein by scavenger receptor class B type 1 is associated with prostate cancer proliferation and tumor progression in mice. *Journal of Biological Chemistry*, 295(24), 8252–8261. <https://doi.org/10.1074/jbc.RA120.013694>
- Trofimenko, E., Grasso, G., Heulot, M., Chevalier, N., Deriu, M. A., Dubuis, G., Arribat, Y., Serulla, M., Michel, S., Vantomme, G., Ory, F., Dam, L. C., Puyal, J., Amati, F., Lüthi, A., Danani, A., & Widmann, C. (2021b). Genetic, cellular, and structural characterization of the membrane potential-dependent cell-penetrating peptide translocation pore. *ELife*, 10. <https://doi.org/10.7554/eLife.69832>
- Trofimenko, E., Homma, Y., Fukuda, M., & Widmann, C. (2021a). The endocytic pathway taken by cationic substances requires Rab14 but not Rab5 and Rab7. *Cell Reports*, 37(5), 109945. <https://doi.org/10.1016/j.celrep.2021.109945>
- Trybus, K. M. (2008). Myosin V from head to tail. *Cellular and Molecular Life Sciences*, 65(9), 1378–1389. <https://doi.org/10.1007/s00018-008-7507-6>

- Tsugita, M., Morimoto, N., Tashiro, M., Kinoshita, K., & Nakayama, M. (2017). SR-B1 Is a Silica Receptor that Mediates Canonical Inflammasome Activation. *Cell Reports*, 18(5), 1298–1311. <https://doi.org/10.1016/j.celrep.2017.01.004>
- Tsuzuki, S., Kimoto, Y., Lee, S., Sugawara, T., Manabe, Y., & Inoue, K. (2018a). A novel role for scavenger receptor B1 as a contributor to the capture of specific volatile odorants in the nasal cavity. *Biomedical Research (Tokyo, Japan)*, 39(3), 117–129. <https://doi.org/10.2220/biomedres.39.117>
- Tsuzuki, S., Lee, S., Kimoto, Y., Sugawara, T., Manabe, Y., & Inoue, K. (2018b). A role for scavenger receptor B1 as a captor of specific fatty acids in taste buds of circumvallate papillae. *Biomedical Research (Tokyo, Japan)*, 39(6), 295–300. <https://doi.org/10.2220/biomedres.39.295>
- Tucci, M., Scagliotti, G. V., & Vignani, F. (2015). Metastatic castration-resistant prostate cancer: time for innovation. *Future Oncology*, 11(1), 91–106. <https://doi.org/10.2217/fon.14.145>
- Tung, C.-H., & Weissleder, R. (2003). Arginine containing peptides as delivery vectors. *Advanced Drug Delivery Reviews*, 55(2), 281–294. [https://doi.org/10.1016/S0169-409X\(02\)00183-7](https://doi.org/10.1016/S0169-409X(02)00183-7)
- Tünnemann, G., Martin, R. M., Haupt, S., Patsch, C., Edenhofer, F., & Cardoso, M. C. (2006). Cargo-dependent mode of uptake and bioavailability of TAT-containing proteins and peptides in living cells. *The FASEB Journal*, 20(11), 1775–1784. <https://doi.org/10.1096/fj.05-5523com>
- Twiddy, A. L., Cox, M. E., & Wasan, K. M. (2012). Knockdown of scavenger receptor Class B Type I reduces prostate specific antigen secretion and viability of prostate cancer cells. *The Prostate*, 72(9), 955–965. <https://doi.org/10.1002/pros.21499>
- Tzakos, A. G., Briasoulis, E., Thalhammer, T., Jäger, W., & Apostolopoulos, V. (2013). Novel Oncology Therapeutics: Targeted Drug Delivery for Cancer. *Journal of Drug Delivery*, 2013, 1–5. <https://doi.org/10.1155/2013/918304>
- Uhlen, M., Oksvold, P., Fagerberg, L., Lundberg, E., Jonasson, K., Forsberg, M., Zwahlen, M., Kampf, C., Wester, K., Hober, S., Wernerus, H., Björling, L., & Ponten, F. (2010). Towards a knowledge-based Human Protein Atlas. *Nature Biotechnology*, 28(12), 1248–1250. <https://doi.org/10.1038/nbt1210-1248>
- Ullrich, O., Reinsch, S., Urbé, S., Zerial, M., & Parton, R. G. (1996). Rab11 regulates recycling through the pericentriolar recycling endosome. *The Journal of Cell Biology*, 135(4), 913–924. <https://doi.org/10.1083/jcb.135.4.913>
- Urandur, S., & Sullivan, M. O. (2023). Peptide-Based Vectors: A Biomolecular Engineering Strategy for Gene Delivery. *Annual Review of Chemical and Biomolecular Engineering*, 14, 243–264. <https://doi.org/10.1146/annurev-chembioeng-101121-070232>
- van Bokhoven, A., Varella-Garcia, M., Korch, C., Johannes, W. U., Smith, E. E., Miller, H. L., Nordeen, S. K., Miller, G. J., & Lucia, M. S. (2003). Molecular characterization of human prostate carcinoma cell lines. *The Prostate*, 57(3), 205–225. <https://doi.org/10.1002/pros.10290>

- Van der Steen, T., Tindall, D., & Huang, H. (2013). Posttranslational Modification of the Androgen Receptor in Prostate Cancer. *International Journal of Molecular Sciences*, 14(7), 14833–14859. <https://doi.org/10.3390/ijms140714833>
- Van Leenders, G. J. L. H., & Schalken, J. A. (2003). Epithelial cell differentiation in the human prostate epithelium: Implications for the pathogenesis and therapy of prostate cancer. *Critical Reviews in Oncology/Hematology*, 46(SUPPL.), 3–10. [https://doi.org/10.1016/S1040-8428\(03\)00059-3](https://doi.org/10.1016/S1040-8428(03)00059-3)
- van Leenders, G. J. L. H., van der Kwast, T. H., Grignon, D. J., Evans, A. J., Kristiansen, G., Kweldam, C. F., Litjens, G., McKenney, J. K., Melamed, J., Mottet, N., Paner, G. P., Samaratunga, H., Schoots, I. G., Simko, J. P., Tsuzuki, T., Varma, M., Warren, A. Y., Wheeler, T. M., Williamson, S. R., & Iczkowski, K. A. (2020). The 2019 International Society of Urological Pathology (ISUP) Consensus Conference on Grading of Prostatic Carcinoma. *American Journal of Surgical Pathology*, 44(8), e87–e99. <https://doi.org/10.1097/PAS.0000000000001497>
- van Schouwenburg, P. A., Bartelds, G. M., Hart, M. H., Aarden, L., Wolbink, G. J., & Wouters, D. (2010). A novel method for the detection of antibodies to adalimumab in the presence of drug reveals “hidden” immunogenicity in rheumatoid arthritis patients. *Journal of Immunological Methods*, 362(1–2), 82–88. <https://doi.org/10.1016/j.jim.2010.09.005>
- Váňová, J., Číhařová, B., Hejtmánková, A., Epperla, C. P., Škvára, P., Forstová, J., Hubálek Kalbáčová, M., & Španielová, H. (2022). VirPorters: Insights into the action of cationic and histidine-rich cell-penetrating peptides. *International Journal of Pharmaceutics*, 611, 121308. <https://doi.org/10.1016/j.ijpharm.2021.121308>
- Varadi, A., Tsuboi, T., & Rutter, G. A. (2005). Myosin Va Transports Dense Core Secretory Vesicles in Pancreatic MIN6 β -Cells. *Molecular Biology of the Cell*, 16(6), 2670–2680. <https://doi.org/10.1091/mbc.e04-11-1001>
- Varkouhi, A. K., Scholte, M., Storm, G., & Haisma, H. J. (2011). Endosomal escape pathways for delivery of biologicals. *Journal of Controlled Release*, 151(3), 220–228. <https://doi.org/10.1016/j.jconrel.2010.11.004>
- Varma, M. (2023). An update on atypical large glandular proliferations of the prostate. *Diagnostic Histopathology*, 29(6), 283–293. <https://doi.org/10.1016/j.mpdhp.2023.03.003>
- Veiman, K.-L., Mäger, I., Ezzat, K., Margus, H., Lehto, T., Langel, K., Kurrikoff, K., Arukuusk, P., Suhorutšenko, J., Padari, K., Pooga, M., Lehto, T., & Langel, Ü. (2013). PepFect14 Peptide Vector for Efficient Gene Delivery in Cell Cultures. *Molecular Pharmaceutics*, 10(1), 199–210. <https://doi.org/10.1021/mp3003557>
- Veldhoen, S., Laufer, S. D., Trampe, A., & Restle, T. (2006). Cellular delivery of small interfering RNA by a non-covalently attached cell-penetrating peptide: quantitative analysis of uptake and biological effect. *Nucleic Acids Research*, 34(22), 6561–6573. <https://doi.org/10.1093/nar/gkl941>

- Vellky, J. E., & Ricke, W. A. (2020). Development and prevalence of castration-resistant prostate cancer subtypes. *Neoplasia*, 22(11), 566–575. <https://doi.org/10.1016/j.neo.2020.09.002>
- Ventimiglia, E., Seisen, T., Abdollah, F., Briganti, A., Fonteyne, V., James, N., Roach, M., Thalmann, G. N., Touijer, K., Chen, R. C., & Cheng, L. (2019). A Systematic Review of the Role of Definitive Local Treatment in Patients with Clinically Lymph Node-positive Prostate Cancer. *European Urology Oncology*, 2(3), 294–301. <https://doi.org/10.1016/j.euo.2019.02.001>
- Verze, P., Cai, T., & Lorenzetti, S. (2016). The role of the prostate in male fertility, health and disease. Nature Publishing Group. <https://doi.org/10.1038/nrurol.2016.89>
- Vhora, I., Patil, S., Bhatt, P., Gandhi, R., Baradia, D., & Misra, A. (2014). Receptor-targeted drug delivery: current perspective and challenges. *Therapeutic Delivery*, 5(9), 1007–1024. <https://doi.org/10.4155/tde.14.63>
- Via, M. A., Del Pópolo, M. G., & Wilke, N. (2018). Negative Dipole Potentials and Carboxylic Polar Head Groups Foster the Insertion of Cell-Penetrating Peptides into Lipid Monolayers. *Langmuir*, 34(9), 3102–3111. <https://doi.org/10.1021/acs.langmuir.7b04038>
- Vietri, M. T., D'Elia, G., Caliendo, G., Resse, M., Casamassimi, A., Passariello, L., Albanese, L., Cioffi, M., & Molinari, A. M. (2021). Hereditary Prostate Cancer: Genes Related, Target Therapy and Prevention. *International Journal of Molecular Sciences*, 22(7), 3753. <https://doi.org/10.3390/ijms22073753>
- Violet, J., Jackson, P., Ferdinandus, J., Sandhu, S., Akhurst, T., Irvani, A., Kong, G., Kumar, A. R., Thang, S. P., Eu, P., Scalzo, M., Murphy, D., Williams, S., Hicks, R. J., & Hofman, M. S. (2019). Dosimetry of 177 Lu-PSMA-617 in Metastatic Castration-Resistant Prostate Cancer: Correlations Between Pretherapeutic Imaging and Whole-Body Tumor Dosimetry with Treatment Outcomes. *Journal of Nuclear Medicine*, 60(4), 517–523. <https://doi.org/10.2967/jnumed.118.219352>
- Visakorpi, T., Hyytinen, E., Koivisto, P., Tanner, M., Keinänen, R., Palmberg, C., Palotie, A., Tammela, T., Isola, J., & Kallioniemi, O.-P. (1995). In vivo amplification of the androgen receptor gene and progression of human prostate cancer. *Nature Genetics*, 9(4), 401–406. <https://doi.org/10.1038/ng0495-401>
- Vishnyakova, T. G., Bocharov, A. V., Baranova, I. N., Chen, Z., Remaley, A. T., Csako, G., Eggerman, T. L., & Patterson, A. P. (2003). Binding and Internalization of Lipopolysaccharide by Cla-1, a Human Orthologue of Rodent Scavenger Receptor B1. *Journal of Biological Chemistry*, 278(25), 22771–22780. <https://doi.org/10.1074/jbc.M211032200>
- Vivès, E., Brodin, P., & Lebleu, B. (1997). A Truncated HIV-1 Tat Protein Basic Domain Rapidly Translocates through the Plasma Membrane and Accumulates in the Cell Nucleus. *Journal of Biological Chemistry*, 272(25), 16010–16017. <https://doi.org/10.1074/jbc.272.25.16010>

- Vivès, E., Schmidt, J., & Pèlegri, A. (2008). Cell-penetrating and cell-targeting peptides in drug delivery. *Biochimica et Biophysica Acta (BBA) - Reviews on Cancer*, 1786(2), 126–138. <https://doi.org/10.1016/j.bbcan.2008.03.001>
- Vlieghe, P., Lisowski, V., Martinez, J., & Khrestchatsky, M. (2010). Synthetic therapeutic peptides: science and market. *Drug Discovery Today*, 15(1–2), 40–56. <https://doi.org/10.1016/j.drudis.2009.10.009>
- Vo, T.-T. T., Kong, G., Kim, C., Juang, U., Gwon, S., Jung, W., Nguyen, H., Kim, S.-H., & Park, J. (2023). Exploring scavenger receptor class F member 2 and the importance of scavenger receptor family in prediagnostic diseases. *Toxicological Research*. <https://doi.org/10.1007/s43188-023-00176-2>
- Volante, M., Rosas, R., Allia, E., Granata, R., Baragli, A., Muccioli, G., & Papotti, M. (2008). Somatostatin, cortistatin and their receptors in tumours. *Molecular and Cellular Endocrinology*, 286(1–2), 219–229. <https://doi.org/10.1016/j.mce.2007.12.002>
- Voltà-Durán, E., Parladé, E., Serna, N., Villaverde, A., Vazquez, E., & Unzueta, U. (2023). Endosomal escape for cell-targeted proteins. Going out after going in. *Biotechnology Advances*, 63, 108103. <https://doi.org/10.1016/j.biotechadv.2023.108103>
- von Klot, C. A., Kuczyk, M. A., & Merseburger, A. S. (2014). No Androgen Withdrawal Syndrome for Enzalutamide: A Report of Disease Dynamics in the Postchemotherapy Setting. *European Urology*, 65(1), 258–259. <https://doi.org/10.1016/j.eururo.2013.09.036>
- Votyakova, T. V., & Reynolds, I. J. (2008). $\Delta\Psi$ m-Dependent and -independent production of reactive oxygen species by rat brain mitochondria. *Journal of Neurochemistry*, 79(2), 266–277. <https://doi.org/10.1046/j.1471-4159.2001.00548.x>
- Vrettos, E. I., Mező, G., & Tzakos, A. G. (2018). On the design principles of peptide-drug conjugates for targeted drug delivery to the malignant tumor site. *Beilstein Journal of Organic Chemistry*, 14, 930–954. <https://doi.org/10.3762/BJOC.14.80>
- Wadia, J. S., Stan, R. V., & Dowdy, S. F. (2004). Transducible TAT-HA fusogenic peptide enhances escape of TAT-fusion proteins after lipid raft macropinocytosis. *Nature Medicine*, 10(3), 310–315. <https://doi.org/10.1038/nm996>
- Wadosky, K. M., & Koochekpour, S. (2016). Molecular mechanisms underlying resistance to androgen deprivation therapy in prostate cancer. *Oncotarget*, 7(39), 64447–64470. <https://doi.org/10.18632/oncotarget.10901>
- Wagh, A., Song, H., Zeng, M., Tao, L., & Das, T. K. (2018). Challenges and new frontiers in analytical characterization of antibody-drug conjugates. *MAbs*, 10(2), 222–243. <https://doi.org/10.1080/19420862.2017.1412025>
- Wagner, B. A., Evig, C. B., Reszka, K. J., Buettner, G. R., & Burns, C. P. (2005). Doxorubicin increases intracellular hydrogen peroxide in PC3 prostate cancer cells. *Archives of Biochemistry and Biophysics*, 440(2), 181–190. <https://doi.org/10.1016/j.abb.2005.06.015>

- Walker-Daniels, J., Hess, A. R., Hendrix, M. J. C., & Kinch, M. S. (2003). Differential Regulation of EphA2 in Normal and Malignant Cells. *The American Journal of Pathology*, 162(4), 1037–1042. [https://doi.org/10.1016/S0002-9440\(10\)63899-0](https://doi.org/10.1016/S0002-9440(10)63899-0)
- Wan, F., Qin, X., Zhang, G., Lu, X., Zhu, Y., Zhang, H., Dai, B., Shi, G., & Ye, D. (2015). Oxidized low-density lipoprotein is associated with advanced-stage prostate cancer. *Tumor Biology*, 36(5), 3573–3582. <https://doi.org/10.1007/s13277-014-2994-6>
- Wandinger-Ness, A., & Zerial, M. (2014). Rab proteins and the compartmentalization of the endosomal system. *Cold Spring Harbor Perspectives in Biology*, 6(11), a022616. <https://doi.org/10.1101/cshperspect.a022616>
- Wang, J., Hevi, S., Kurash, J. K., Lei, H., Gay, F., Bajko, J., Su, H., Sun, W., Chang, H., Xu, G., Gaudet, F., Li, E., & Chen, T. (2009). The lysine demethylase LSD1 (KDM1) is required for maintenance of global DNA methylation. *Nature Genetics*, 41(1), 125–129. <https://doi.org/10.1038/ng.268>
- Wang, J., Kobayashi, T., Floc'h, N., Kinkade, C. W., Aytes, A., Dankort, D., Lefebvre, C., Mitrofanova, A., Cardiff, R. D., McMahon, M., Califano, A., Shen, M. M., & Abate-Shen, C. (2012). B-Raf Activation Cooperates with PTEN Loss to Drive c-Myc Expression in Advanced Prostate Cancer. *Cancer Research*, 72(18), 4765–4776. <https://doi.org/10.1158/0008-5472.CAN-12-0820>
- Wang, J., Lu, Y., Wang, J., Koch, A. E., Zhang, J., & Taichman, R. S. (2008). CXCR6 Induces Prostate Cancer Progression by the AKT/Mammalian Target of Rapamycin Signaling Pathway. *Cancer Research*, 68(24), 10367–10377. <https://doi.org/10.1158/0008-5472.CAN-08-2780>
- Wang, J., Scully, K., Zhu, X., Cai, L., Zhang, J., Prefontaine, G. G., Krones, A., Ohgi, K. A., Zhu, P., Garcia-Bassets, I., Liu, F., Taylor, H., Lozach, J., Jayes, F. L., Korach, K. S., Glass, C. K., Fu, X.-D., & Rosenfeld, M. G. (2007). Opposing LSD1 complexes function in developmental gene activation and repression programmes. *Nature*, 446(7138), 882–887. <https://doi.org/10.1038/nature05671>
- Wang, J., Telese, F., Tan, Y., Li, W., Jin, C., He, X., Basnet, H., Ma, Q., Merkurjev, D., Zhu, X., Liu, Z., Zhang, J., Ohgi, K., Taylor, H., White, R. R., Tazearslan, C., Suh, Y., Macfarlan, T. S., Pfaff, S. L., & Rosenfeld, M. G. (2015). LSD1n is an H4K20 demethylase regulating memory formation via transcriptional elongation control. *Nature Neuroscience*, 18(9), 1256–1264. <https://doi.org/10.1038/nn.4069>
- Wang, L., McDonnell, S. K., Cunningham, J. M., Hebring, S., Jacobsen, S. J., Cerhan, J. R., Slager, S. L., Blute, M. L., Schaid, D. J., & Thibodeau, S. N. (2003). No association of germline alteration of MSR1 with prostate cancer risk. *Nature Genetics*, 35(2), 128–129. <https://doi.org/10.1038/ng1239>
- Wang, M., Liu, X., Chen, Z., Zhang, L., & Weng, X. (2020). Downregulation of lysine specific demethylase 1 enhances the sensitivity of hormone sensitive

- prostate cancer cells to androgen deprivation therapy. *Oncology Letters*, 21(2), 93. <https://doi.org/10.3892/ol.2020.12354>
- Wang, M., Liu, X., Guo, J., Weng, X., Jiang, G., Wang, Z., & He, L. (2015). Inhibition of LSD1 by Pargyline inhibited process of EMT and delayed progression of prostate cancer in vivo. *Biochemical and Biophysical Research Communications*, 467(2), 310–315. <https://doi.org/10.1016/j.bbrc.2015.09.164>
- Wang, T., Ming, Z., Xiaochun, W., & Hong, W. (2011). Rab7: Role of its protein interaction cascades in endo-lysosomal traffic. *Cellular Signalling*, 23(3), 516–521. <https://doi.org/10.1016/j.cellsig.2010.09.012>
- Wang, Y., Cheetham, A. G., Angacian, G., Su, H., Xie, L., & Cui, H. (2017). Peptide–drug conjugates as effective prodrug strategies for targeted delivery. *Advanced Drug Delivery Reviews*, 110–111, 112–126. <https://doi.org/10.1016/j.addr.2016.06.015>
- Wang, Y., Chen, J., Wu, Z., Ding, W., Gao, S., Gao, Y., & Xu, C. (2021). Mechanisms of enzalutamide resistance in castration-resistant prostate cancer and therapeutic strategies to overcome it. *British Journal of Pharmacology*, 178(2), 239–261. <https://doi.org/10.1111/bph.15300>
- Wang, Y., Zhang, H., Chen, Y., Sun, Y., Yang, F., Yu, W., Liang, J., Sun, L., Yang, X., Shi, L., Li, R., Li, Y., Zhang, Y., Li, Q., Yi, X., & Shang, Y. (2009). LSD1 is a Subunit of the NuRD Complex and Targets the Metastasis Programs in Breast Cancer. *Cell*, 138(4), 660–672. <https://doi.org/10.1016/j.cell.2009.05.050>
- Wang, Z., Gao, S., Han, D., Han, W., Li, M., & Cai, C. (2019). LSD1 Activates PI3K/AKT Signaling Through Regulating p85 Expression in Prostate Cancer Cells. *Frontiers in Oncology*, 9. <https://doi.org/10.3389/fonc.2019.00721>
- Wartosch, L., Bright, N. A., & Luzio, J. P. (2015). Lysosomes. *Current Biology*, 25(8), R315–R316. <https://doi.org/10.1016/j.cub.2015.02.027>
- Watson, P. (2009). Live cell imaging for target and drug discovery. *Drug News & Perspectives*, 22(2), 69–79. <https://doi.org/10.1358/dnp.2009.22.2.1334450>
- Watt, K. W., Lee, P. J., M'Timkulu, T., Chan, W. P., & Loo, R. (1986). Human prostate-specific antigen: structural and functional similarity with serine proteases. *Proceedings of the National Academy of Sciences*, 83(10), 3166–3170. <https://doi.org/10.1073/pnas.83.10.3166>
- Weckbecker, G., Raulf, F., Stolz, B., & Bruns, C. (1993). Somatostatin analogs for diagnosis and treatment of cancer. *Pharmacology & Therapeutics*, 60(2), 245–264. [https://doi.org/10.1016/0163-7258\(93\)90009-3](https://doi.org/10.1016/0163-7258(93)90009-3)
- Wei, C., Wan, L., Yan, Q., Wang, X., Zhang, J., Yang, X., Zhang, Y., Fan, C., Li, D., Deng, Y., Sun, J., Gong, J., Yang, X., Wang, Y., Wang, X., Li, J., Yang, H., Li, H., Zhang, Z., ... Zhong, H. (2020). HDL-scavenger receptor B type 1 facilitates SARS-CoV-2 entry. *Nature Metabolism*, 2(12), 1391–1400. <https://doi.org/10.1038/s42255-020-00324-0>
- Wei, Y., Wu, J., Gu, W., Wang, J., Lin, G., Qin, X., Dai, B., Gan, H., Ye, D., & Zhu, Y. (2020). Prognostic Value of Germline DNA Repair Gene Mutations in De

- Novo Metastatic and Castration-Sensitive Prostate Cancer. *The Oncologist*, 25(7), e1042–e1050. <https://doi.org/10.1634/theoncologist.2019-0495>
- Weiss, G. A., & Chamberlin, R. (2003). Bridging the Synthetic and Biopolymer Worlds with Peptide-Drug Conjugates. *Chemistry & Biology*, 10(3), 201–202. [https://doi.org/10.1016/S1074-5521\(03\)00056-5](https://doi.org/10.1016/S1074-5521(03)00056-5)
- Welcker, M., & Clurman, B. E. (2008). FBW7 ubiquitin ligase: a tumour suppressor at the crossroads of cell division, growth and differentiation. *Nature Reviews Cancer*, 8(2), 83–93. <https://doi.org/10.1038/nrc2290>
- Whyte, W. A., Bilodeau, S., Orlando, D. A., Hoke, H. A., Frampton, G. M., Foster, C. T., Cowley, S. M., & Young, R. A. (2012). Enhancer decommissioning by LSD1 during embryonic stem cell differentiation. *Nature*, 482(7384), 221–225. <https://doi.org/10.1038/nature10805>
- Wicker-Planquart, C., Tacnet-Delorme, P., Preisser, L., Dufour, S., Delneste, Y., Housset, D., Frachet, P., & Thielens, N. M. (2021). Insights into the ligand binding specificity of SREC-II (scavenger receptor expressed by endothelial cells). *FEBS Open Bio*, 11(10), 2693–2704. <https://doi.org/10.1002/2211-5463.13260>
- Willmann, D., Lim, S., Wetzel, S., Metzger, E., Jandausch, A., Wilk, W., Jung, M., Forne, I., Imhof, A., Janzer, A., Kirfel, J., Waldmann, H., Schüle, R., & Buettner, R. (2012). Impairment of prostate cancer cell growth by a selective and reversible lysine-specific demethylase 1 inhibitor. *International Journal of Cancer*, 131(11), 2704–2709. <https://doi.org/10.1002/ijc.27555>
- Wilson, R. L., Taaffe, D. R., Newton, R. U., Hart, N. H., Lyons-Wall, P., & Galvão, D. A. (2022). Obesity and prostate cancer: A narrative review. *Critical Reviews in Oncology/Hematology*, 169, 103543. <https://doi.org/10.1016/j.critrevonc.2021.103543>
- Wissmann, M., Yin, N., Müller, J. M., Greschik, H., Fodor, B. D., Jenuwein, T., Vogler, C., Schneider, R., Günther, T., Buettner, R., Metzger, E., & Schüle, R. (2007). Cooperative demethylation by JMJD2C and LSD1 promotes androgen receptor-dependent gene expression. *Nature Cell Biology*, 9(3), 347–353. <https://doi.org/10.1038/ncb1546>
- Wombacher, R., & Cornish, V. W. (2011). Chemical tags: Applications in live cell fluorescence imaging. *Journal of Biophotonics*, 4(6), 391–402. <https://doi.org/10.1002/jbio.201100018>
- Worm, D. J., Els-Heindl, S., & Beck-Sickinger, A. G. (2020). Targeting of peptide-binding receptors on cancer cells with peptide-drug conjugates. *Peptide Science*, 112(3). <https://doi.org/10.1002/pep2.24171>
- Xiao, H., Verdier-Pinard, P., Fernandez-Fuentes, N., Burd, B., Angeletti, R., Fiser, A., Horwitz, S. B., & Orr, G. A. (2006). Insights into the mechanism of microtubule stabilization by Taxol. *Proceedings of the National Academy of Sciences*, 103(27), 10166–10173. <https://doi.org/10.1073/pnas.0603704103>
- Xu, J., Khan, A. R., Fu, M., Wang, R., Ji, J., & Zhai, G. (2019). Cell-penetrating peptide: a means of breaking through the physiological barriers of different

tissues and organs. *Journal of Controlled Release*, 309, 106–124.
<https://doi.org/10.1016/J.JCONREL.2019.07.020>

- Xu, J., Zheng, S. L., Komiya, A., Mychaleckyj, J. C., Isaacs, S. D., Chang, B., Turner, A. R., Ewing, C. M., Wiley, K. E., Hawkins, G. A., Bleecker, E. R., Walsh, P. C., Meyers, D. A., & Isaacs, W. B. (2003). Common Sequence Variants of the Macrophage Scavenger Receptor 1 Gene Are Associated with Prostate Cancer Risk. *The American Journal of Human Genetics*, 72(1), 208–212. <https://doi.org/10.1086/345802>
- Xu, J., Zheng, S. L., Komiya, A., Mychaleckyj, J. C., Isaacs, S. D., Hu, J. J., Sterling, D., Lange, E. M., Hawkins, G. A., Turner, A., Ewing, C. M., Faith, D. A., Johnson, J. R., Suzuki, H., Bujnovszky, P., Wiley, K. E., DeMarzo, A. M., Bova, G. S., Chang, B., ... Meyers, D. A. (2002). Germline mutations and sequence variants of the macrophage scavenger receptor 1 gene are associated with prostate cancer risk. *Nature Genetics*, 32(2), 321–325. <https://doi.org/10.1038/ng994>
- Xu, S., Laccotripe, M., Huang, X., Rigotti, A., Zannis, V. I., & Krieger, M. (1997). Apolipoproteins of HDL can directly mediate binding to the scavenger receptor SR-BI, an HDL receptor that mediates selective lipid uptake. *Journal of Lipid Research*, 38(7), 1289–1298.
- Yamayoshi, S., Ohka, S., Fujii, K., & Koike, S. (2013). Functional Comparison of SCARB2 and PSGL1 as Receptors for Enterovirus 71. *Journal of Virology*, 87(6), 3335–3347. <https://doi.org/10.1128/JVI.02070-12>
- Yamayoshi, S., Yamashita, Y., Li, J., Hanagata, N., Minowa, T., Takemura, T., & Koike, S. (2009). Scavenger receptor B2 is a cellular receptor for enterovirus 71. *Nature Medicine*, 15(7), 798–801. <https://doi.org/10.1038/nm.1992>
- Yang, C., Wang, W., Liang, J.-X., Li, G., Vellaisamy, K., Wong, C.-Y., Ma, D.-L., & Leung, C.-H. (2017). A Rhodium(III)-Based Inhibitor of Lysine-Specific Histone Demethylase 1 as an Epigenetic Modulator in Prostate Cancer Cells. *Journal of Medicinal Chemistry*, 60(6), 2597–2603. <https://doi.org/10.1021/acs.jmedchem.7b00133>
- Yang, J., Huang, J., Dasgupta, M., Sears, N., Miyagi, M., Wang, B., Chance, M. R., Chen, X., Du, Y., Wang, Y., An, L., Wang, Q., Lu, T., Zhang, X., Wang, Z., & Stark, G. R. (2010). Reversible methylation of promoter-bound STAT3 by histone-modifying enzymes. *Proceedings of the National Academy of Sciences*, 107(50), 21499–21504. <https://doi.org/10.1073/pnas.1016147107>
- Yang, J., Luo, Y., Shibu, M. A., Toth, I., & Skwarczynska, M. (2019). Cell-penetrating Peptides: Efficient Vectors for Vaccine Delivery. *Current Drug Delivery*, 16(5), 430–443. <https://doi.org/10.2174/1567201816666190123120915>
- Yang, L., Harroun, T. A., Weiss, T. M., Ding, L., & Huang, H. W. (2001). Barrel-Stack Model or Toroidal Model? A Case Study on Melittin Pores. *Biophysical Journal*, 81(3), 1475–1485. [https://doi.org/10.1016/S0006-3495\(01\)75802-X](https://doi.org/10.1016/S0006-3495(01)75802-X)
- Yang, M., Culhane, J. C., Szewczuk, L. M., Gocke, C. B., Brautigam, C. A., Tomchick, D. R., Machius, M., Cole, P. A., & Yu, H. (2007b). Structural basis of histone demethylation by LSD1 revealed by suicide inactivation. *Nature*

Structural & Molecular Biology, 14(6), 535–539.
<https://doi.org/10.1038/nsmb1255>

- Yang, M., Culhane, J. C., Szewczuk, L. M., Jalili, P., Ball, H. L., Machius, M., Cole, P. A., & Yu, H. (2007a). Structural Basis for the Inhibition of the LSD1 Histone Demethylase by the Antidepressant trans -2-Phenylcyclopropylamine ., Biochemistry, 46(27), 8058–8065. <https://doi.org/10.1021/bi700664y>
- Yang, S., Park, Y. S., Cho, J. H., Moon, B., An, H., Lee, J. Y., Xie, Z., Wang, Y., Pocalyko, D., Lee, D. C., Sohn, H. A., Kang, M., Kim, J. Y., Kim, E., Park, K. C., Kim, J., & Yeom, Y. II. (2017). Regulation of hypoxia responses by flavin adenine dinucleotide-dependent modulation of <sc>HIF</sc> -1 α protein stability. The EMBO Journal, 36(8), 1011–1028.
<https://doi.org/10.15252/embj.201694408>
- Yang, S.-T., Zaitseva, E., Chernomordik, L. V., & Melikov, K. (2010). Cell-Penetrating Peptide Induces Leaky Fusion of Liposomes Containing Late Endosome-Specific Anionic Lipid. Biophysical Journal, 99(8), 2525–2533.
<https://doi.org/10.1016/j.bpj.2010.08.029>
- Yang, X. L., Xie, J., Niu, B., Hu, X. N., Gao, Y., Xiang, Q., Zhang, Y. H., Guo, Y., & Zhang, Z. G. (2005). Structure analysis of the protein transduction domain of human Period1 and its mutant analogs. Journal of Molecular Graphics & Modelling, 23(5), 389–394. <https://doi.org/10.1016/j.jmglm.2004.11.008>
- Yang, X., Okamura, D. M., Lu, X., Chen, Y., Moorhead, J., Varghese, Z., & Ruan, X. Z. (2017). CD36 in chronic kidney disease: novel insights and therapeutic opportunities. <https://doi.org/10.1038/hrneph.2017.126>
- Yang, Y. A., & Yu, J. (2015). Current perspectives on FOXA1 regulation of androgen receptor signaling and prostate cancer. Genes & Diseases, 2(2), 144–151. <https://doi.org/10.1016/j.gendis.2015.01.003>
- Yang, Z., Jiang, J., Stewart, D. M., Qi, S., Yamane, K., Li, J., Zhang, Y., & Wong, J. (2010). AOF1 is a histone H3K4 demethylase possessing demethylase activity-independent repression function. Cell Research, 20(3), 276–287.
<https://doi.org/10.1038/cr.2010.12>
- Yap, C. C., Digilio, L., McMahon, L. P., Garcia, A. D. R., & Winckler, B. (2018). Degradation of dendritic cargos requires Rab7-dependent transport to somatic lysosomes. The Journal of Cell Biology, 217(9), 3141–3159.
<https://doi.org/10.1083/jcb.201711039>
- Yarden, Y., & Pines, G. (2012). The ERBB network: at last, cancer therapy meets systems biology. Nature Reviews Cancer, 12(8), 553–563.
<https://doi.org/10.1038/nrc3309>
- Yates, M., Kolmakova, A., Zhao, Y., & Rodriguez, A. (2011). Clinical impact of scavenger receptor class B type I gene polymorphisms on human female fertility. Human Reproduction, 26(7), 1910–1916.
<https://doi.org/10.1093/humrep/der124>
- Ye, J., Pei, X., Cui, H., Yu, Z., Lee, H., Wang, J., Wang, X., Sun, L., He, H., & Yang, V. C. (2018). Cellular uptake mechanism and comparative in vitro cytotoxicity studies of monomeric LMWP-siRNA conjugate. Journal of

Industrial and Engineering Chemistry, 63, 103–111.
<https://doi.org/10.1016/j.jiec.2018.02.005>

- Yeh, C.-Y., Hsiao, J.-K., Wang, Y.-P., Lan, C.-H., & Wu, H.-C. (2016). Peptide-conjugated nanoparticles for targeted imaging and therapy of prostate cancer. *Biomaterials*, 99, 1–15. <https://doi.org/10.1016/j.biomaterials.2016.05.015>
- Yoshioka, Y., Konishi, Y., Kosaka, N., Katsuda, T., Kato, T., & Ochiya, T. (2013). Comparative marker analysis of extracellular vesicles in different human cancer types. *Journal of Extracellular Vesicles*, 2(1), 20424. <https://doi.org/10.3402/jev.v2i0.20424>
- Yu, G., Tseng, G. C., Yu, Y. P., Gavel, T., Nelson, J., Wells, A., Michalopoulos, G., Kokkinakis, D., & Luo, J.-H. (2006). CSR1 Suppresses Tumor Growth and Metastasis of Prostate Cancer. *The American Journal of Pathology*, 168(2), 597–607. <https://doi.org/10.2353/ajpath.2006.050620>
- Yu, X., Guo, C., Fisher, P. B., Subjeck, J. R., & Wang, X.-Y. (2015). Scavenger Receptors: Emerging Roles in Cancer Biology and Immunology. *Advances in Cancer Research*, 128, 309–364. <https://doi.org/10.1016/bs.acr.2015.04.004>
- Yuhanna, I. S., Zhu, Y., Cox, B. E., Hahner, L. D., Osborne-Lawrence, S., Lu, P., Marcel, Y. L., Anderson, R. G. W., Mendelsohn, M. E., Hobbs, H. H., & Shaul, P. W. (2001). High-density lipoprotein binding to scavenger receptor-BI activates endothelial nitric oxide synthase. *Nature Medicine*, 7(7), 853–857. <https://doi.org/10.1038/89986>
- Zaazouee, M. S., Hamdallah, A., Helmy, S. K., Hasabo, E. A., Sayed, A. K., Gbreel, M. I., Elmegeed, A. A., Aladwan, H., Elshanbary, A. A., Abdel-Aziz, W., Elshahawy, I. M., Rabie, S., Elkady, S., Ali, A. S., Ragab, K. M., & Nourelden, A. Z. (2022). Semaglutide for the treatment of type 2 Diabetes Mellitus: A systematic review and network meta-analysis of safety and efficacy outcomes. *Diabetes & Metabolic Syndrome: Clinical Research & Reviews*, 16(6), 102511. <https://doi.org/10.1016/j.dsx.2022.102511>
- Zahid, M., & Robbins, P. D. (2015). Cell-Type Specific Penetrating Peptides: Therapeutic Promises and Challenges. *Molecules*, 20(7), 13055. <https://doi.org/10.3390/MOLECULES200713055>
- Zani, I. A., Stephen, S. L., Mughal, N. A., Russell, D., Homer-Vanniasinkam, S., Wheatcroft, S. B., & Ponnambalam, S. (2015). Scavenger Receptor Structure and Function in Health and Disease. *Cells* 2015, Vol. 4, Pages 178-201, 4(2), 178–201. <https://doi.org/10.3390/CELLS4020178>
- Zeisel, M. B., Koutsoudakis, G., Schnober, E. K., Haberstroh, A., Blum, H. E., Cosset, F.-L., Wakita, T., Jaeck, D., Doffoel, M., Royer, C., Soulier, E., Schvoerer, E., Schuster, C., Stoll-Keller, F., Bartenschlager, R., Pietschmann, T., Barth, H., & Baumert, T. F. (2007). Scavenger receptor class B type I is a key host factor for hepatitis C virus infection required for an entry step closely linked to CD81. *Hepatology*, 46(6), 1722–1731. <https://doi.org/10.1002/hep.21994>
- Zeng, Y., Wodzinski, D., Gao, D., Shiraishi, T., Terada, N., Li, Y., Vander Griend, D. J., Luo, J., Kong, C., Getzenberg, R. H., & Kulkarni, P. (2013). Stress-Response Protein RBM3 Attenuates the Stem-like Properties of Prostate

- Cancer Cells by Interfering with CD44 Variant Splicing. *Cancer Research*, 73(13), 4123–4133. <https://doi.org/10.1158/0008-5472.CAN-12-1343>
- Zhang, H., Gao, Q., Tan, S., You, J., Lyu, C., Zhang, Y., Han, M., Chen, Z., Li, J., Wang, H., Liao, L., Qin, J., Li, J., & Wong, J. (2019). SET8 prevents excessive DNA methylation by methylation-mediated degradation of UHRF1 and DNMT1. *Nucleic Acids Research*. <https://doi.org/10.1093/nar/gkz626>
- Zhang, L., & Bulaj, G. (2012). Converting Peptides into Drug Leads by Lipidation. *Current Medicinal Chemistry*, 19(11), 1602–1618. <https://doi.org/10.2174/092986712799945003>
- Zhang, P., Cheetham, A. G., Lock, L. L., & Cui, H. (2013). Cellular Uptake and Cytotoxicity of Drug–Peptide Conjugates Regulated by Conjugation Site. *Bioconjugate Chemistry*, 24(4), 604–613. <https://doi.org/10.1021/bc300585h>
- Zhang, X., Lin, Y., & Gillies, R. J. (2010). Tumor pH and its measurement. *Journal of Nuclear Medicine : Official Publication, Society of Nuclear Medicine*, 51(8), 1167–1170. <https://doi.org/10.2967/jnumed.109.068981>
- Zhang, X., Tanaka, K., Yan, J., Li, J., Peng, D., Jiang, Y., Yang, Z., Barton, M. C., Wen, H., & Shi, X. (2013). Regulation of estrogen receptor α by histone methyltransferase SMYD2-mediated protein methylation. *Proceedings of the National Academy of Sciences*, 110(43), 17284–17289. <https://doi.org/10.1073/pnas.1307959110>
- Zhang, Z., Zhou, C., Li, X., Barnes, S. D., Deng, S., Hoover, E., Chen, C.-C., Lee, Y. S., Zhang, Y., Wang, C., Metang, L. A., Wu, C., Tirado, C. R., Johnson, N. A., Wongvipat, J., Navrazhina, K., Cao, Z., Choi, D., Huang, C.-H., ... Mu, P. (2020). Loss of CHD1 Promotes Heterogeneous Mechanisms of Resistance to AR-Targeted Therapy via Chromatin Dysregulation. *Cancer Cell*, 37(4), 584–598.e11. <https://doi.org/10.1016/j.ccell.2020.03.001>
- Zhao, D., Cai, L., Lu, X., Liang, X., Li, J., Chen, P., Ittmann, M., Shang, X., Jiang, S., Li, H., Meng, C., Flores, I., Song, J. H., Horner, J. W., Lan, Z., Wu, C.-J., Li, J., Chang, Q., Chen, K.-C., ... DePinho, R. A. (2020). Chromatin Regulator CHD1 Remodels the Immunosuppressive Tumor Microenvironment in PTEN-Deficient Prostate Cancer. *Cancer Discovery*, 10(9), 1374–1387. <https://doi.org/10.1158/2159-8290.CD-19-1352>
- Zhao, D., Lu, X., Wang, G., Lan, Z., Liao, W., Li, J., Liang, X., Chen, J. R., Shah, S., Shang, X., Tang, M., Deng, P., Dey, P., Chakravarti, D., Chen, P., Spring, D. J., Navone, N. M., Troncoso, P., Zhang, J., ... DePinho, R. A. (2017). Synthetic essentiality of chromatin remodelling factor CHD1 in PTEN-deficient cancer. *Nature*, 542(7642), 484–488. <https://doi.org/10.1038/nature21357>
- Zhao, F., Zhao, Y., Liu, Y., Chang, X., Chen, C., & Zhao, Y. (2011). Cellular Uptake, Intracellular Trafficking, and Cytotoxicity of Nanomaterials. *Small*, 7(10), 1322–1337. <https://doi.org/10.1002/sml.201100001>
- Zhao, K. H., Hernandez, D. J., Han, M., Humphreys, E. B., Mangold, L. A., & Partin, A. W. (2008). External Validation of University of California, San Francisco, Cancer of the Prostate Risk Assessment Score. *Urology*, 72(2), 396–400. <https://doi.org/10.1016/j.urology.2007.11.165>

- Zhao, S., Chen, C., Chang, K., Karnad, A., Jagirdar, J., Kumar, A. P., & Freeman, J. W. (2016). CD44 Expression Level and Isoform Contributes to Pancreatic Cancer Cell Plasticity, Invasiveness, and Response to Therapy. *Clinical Cancer Research*, 22(22), 5592–5604. <https://doi.org/10.1158/1078-0432.CCR-15-3115>
- Zhen, J. T., Syed, J., Nguyen, K. A., Leapman, M. S., Agarwal, N., Brierley, K., Llor, X., Hofstatter, E., & Shuch, B. (2018). Genetic testing for hereditary prostate cancer: Current status and limitations. *Cancer*, 124(15), 3105–3117. <https://doi.org/10.1002/cncr.31316>
- Zheng, Y. C., Yu, B., Jiang, G. Z., Feng, X. J., He, P. X., Chu, X. Y., Zhao, W., & Liu, H. M. (2016). Irreversible LSD1 Inhibitors: Application of Tranylcyproamine and Its Derivatives in Cancer Treatment. *Current Topics in Medicinal Chemistry*, 16(19), 2179–2188. <https://doi.org/10.2174/1568026616666160216154042>
- Zhou, M. (2018). High-grade prostatic intraepithelial neoplasia, PIN-like carcinoma, ductal carcinoma, and intraductal carcinoma of the prostate. *Modern Pathology*, 31, 71–79. <https://doi.org/10.1038/modpathol.2017.138>
- Zhu, Y.-S., Tang, K., & Lv, J. (2021). Peptide–drug conjugate-based novel molecular drug delivery system in cancer. *Trends in Pharmacological Sciences*, 42(10), 857–869. <https://doi.org/10.1016/j.tips.2021.07.001>
- Zi, H., He, S.-H., Leng, X.-Y., Xu, X.-F., Huang, Q., Weng, H., Zhu, C., Li, L.-Y., Gu, J.-M., Li, X.-H., Ming, D.-J., Li, X.-D., Yuan, S., Wang, X.-H., He, D.-L., & Zeng, X.-T. (2021). Global, regional, and national burden of kidney, bladder, and prostate cancers and their attributable risk factors, 1990–2019. *Military Medical Research*, 8(1), 60. <https://doi.org/10.1186/s40779-021-00354-z>
- Ziegler, A. (2008). Thermodynamic studies and binding mechanisms of cell-penetrating peptides with lipids and glycosaminoglycans. *Advanced Drug Delivery Reviews*, 60(4–5), 580–597. <https://doi.org/10.1016/j.addr.2007.10.005>
- Zlotta, A. R., Egawa, S., Pushkar, D., Govorov, A., Kimura, T., Kido, M., Takahashi, H., Kuk, C., Kovylyna, M., Aldaoud, N., Fleshner, N., Finelli, A., Klotz, L., Sykes, J., Lockwood, G., & van der Kwast, T. H. (2013). Prevalence of Prostate Cancer on Autopsy: Cross-Sectional Study on Unscreened Caucasian and Asian Men. *JNCI: Journal of the National Cancer Institute*, 105(14), 1050–1058. <https://doi.org/10.1093/jnci/djt151>
- Zorko, M., Jones, S., & Langel, Ü. (2022). Cell-penetrating peptides in protein mimicry and cancer therapeutics. *Advanced Drug Delivery Reviews*, 180, 114044. <https://doi.org/10.1016/j.addr.2021.114044>
- Zorko, M., & Langel, Ü. (2022). Cell-Penetrating Peptides. In *Methods in Molecular Biology* (Vol. 2383, pp. 3–32). Humana Press Inc. https://doi.org/10.1007/978-1-0716-1752-6_1